

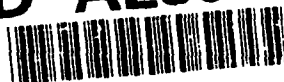


US Army Corps  
of Engineers  
Waterways Experiment  
Station

Technical Report CERC-94-9  
August 1994



AD-A285 542

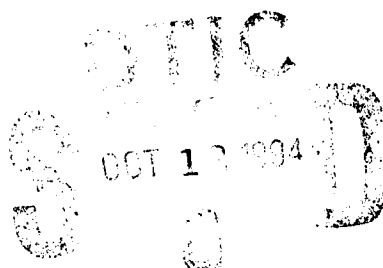


# Kings Bay Coastal and Estuarine Physical Monitoring and Evaluation Program: Coastal Studies

## Volume I: Main Text and Appendix A

by Nicholas C. Kraus, Laurel T. Gorman, Joan Pope

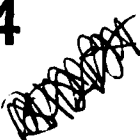
DTIC QUALITY INSPECTED 2



Approved For Public Release; Distribution Is Unlimited

308P

94-32014



94

Prepared for Office of the Chief of Naval Operations

# Kings Bay Coastal and Estuarine Physical Monitoring and Evaluation Program: Coastal Studies

## Volume I: Main Text and Appendix A

by Nicholas C. Kraus, Laurel T. Gorman, Joan Pope

U.S. Army Corps of Engineers  
Waterways Experiment Station  
3909 Halls Ferry Road  
Vicksburg, MS 39180-6199

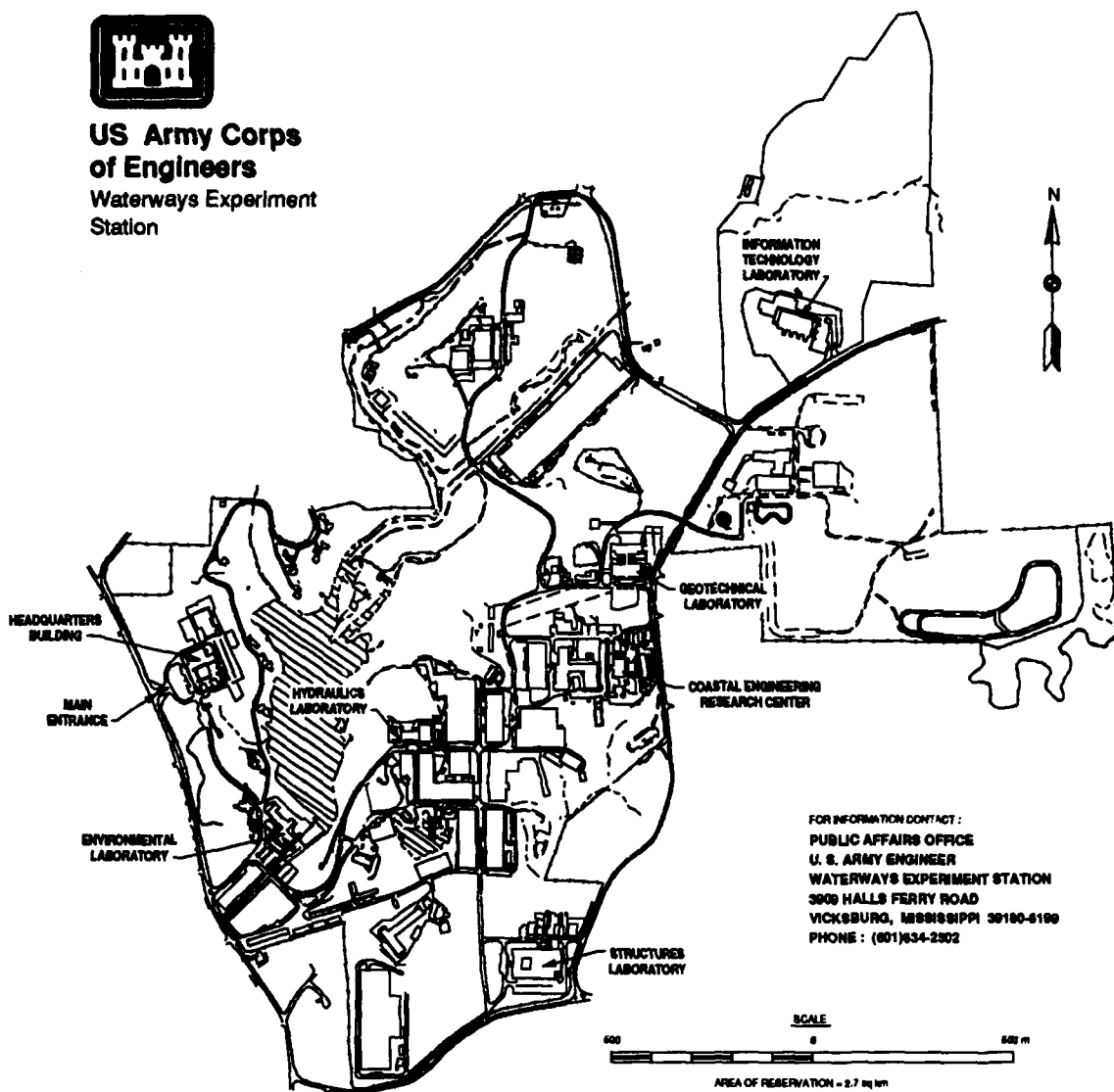
Accession For	
NTIS	CRA&I <input checked="checked" type="checkbox"/>
DTIC	TAB <input type="checkbox"/>
Unannounced <input type="checkbox"/>	
Justification	
By	
Distribution /	
Availability Codes	
Dist	Avail and/or Special
A-1	

Final report

Approved for public release; distribution is unlimited



**US Army Corps  
of Engineers**  
Waterways Experiment  
Station



**Waterways Experiment Station Cataloging-In-Publication Data**

Kraus, Nicholas C.

Kings Bay Coastal and Estuarine Physical Monitoring and Evaluation Program: Coastal studies. Volume I, Main text and appendix A / by Nicholas C. Kraus, Laurel T. Gorman, Joan Pope ; prepared for Office of the Chief of Naval Operations.

310 p. : ill. ; 27 cm. — (Technical report ; CERC-94-8 v. 1)

Includes bibliographic references.

1. Coast changes — Georgia — Kings Bay. 2. Dredging — Environmental aspects. 3. Channels (Hydraulic engineering) — Environmental aspects. 4. Kings Bay (Ga.) I. Gorman, Laurel T. II. Pope, Joan. III. United States. Army. Corps of Engineers. IV. U.S. Army Engineer Waterways Experiment Station. V. Coastal Engineering Research Laboratory (U.S.) VI. United States. Office of the Chief of Naval Operations. VII. Title. VIII. Title: Coastal studies. IX. Series: Technical report (U.S. Army Engineer Waterways Experiment Station) ; CERC-94-9 v. 1. TA7 W34 no. CERC-94-9 v. 1

# Contents

---

Preface . . . . .	xvii
Conversion Factors, Non-SI to SI Units of Measurement . . . . .	xxi
1 Introduction . . . . .	1
Study Background . . . . .	1
Site Description . . . . .	2
Purpose and Structure of Study . . . . .	3
Coastal Monitoring Program . . . . .	5
Report Structure . . . . .	8
2 Regional, Physical, and Engineering Setting . . . . .	9
Introduction . . . . .	9
Physiography . . . . .	10
Regional Geologic Setting . . . . .	12
Coastal Processes . . . . .	18
Local Geomorphology and Geology . . . . .	25
Engineering History of St. Marys Entrance . . . . .	41
Coastal Response to Inlet Stabilization . . . . .	48
Organization of the Coastal Morphologic Compartments . . . . .	58
3 Shoreline Position and Nearshore Bathymetric Change . . . . .	61
Introduction . . . . .	61
Shoreline Position Change . . . . .	64
Nearshore Bathymetric Change . . . . .	101
4 Dredging Activities and Shoaling Analysis . . . . .	145
Introduction . . . . .	145
Dredging History . . . . .	145
Shoaling Analysis . . . . .	147
Summary . . . . .	152

5	Profile Surveys, Sediments, and Beach Fills . . . . .	155
	Introduction . . . . .	155
	Profile Volume Change . . . . .	164
	Shoreline Position Change from Profiles . . . . .	171
	Seasonal Variability . . . . .	175
	Sediment Samples . . . . .	179
	Morphologic Compartments . . . . .	186
	Trend Analysis and Implications of Recent Engineering Activities . . .	195
6	Tides and Waves . . . . .	211
	Introduction . . . . .	211
	Tides . . . . .	211
	Waves . . . . .	221
7	Shoreline Change Extrapolation . . . . .	229
	General Approach . . . . .	229
	Wave Database . . . . .	229
	Wave Model . . . . .	231
	Wave Transformation Analysis . . . . .	232
	Shoreline Change Model . . . . .	238
	Shoreline Response Model Application . . . . .	243
	Shoreline Response Calibration/Verification . . . . .	244
	Shoreline Position Extrapolation . . . . .	249
	Historical Sand Transport Rates . . . . .	251
	Effect of TRIDENT-Related Channel Deepening . . . . .	257
8	Conclusions . . . . .	261
	Study Background . . . . .	261
	Conclusions . . . . .	263
	Consistency of Results . . . . .	267
	References . . . . .	269
	Appendix A: Notation . . . . .	A1

## List of Figures

---

Figure 1.	Location of study area . . . . .	3
Figure 2.	Authorized channel dimensions for St. Marys Entrance . . . . .	4
Figure 3.	Regional physiography . . . . .	10

Figure 4.	Barrier island response to Holocene sea level change . . . . .	12
Figure 5.	Regional sedimentary basins and major structural features in the southeastern United States. . . . .	13
Figure 6.	Regional drainage pattern of Satilla-St. Marys River Basins .	14
Figure 7.	Depositional shorelines classified by tidal range . . . . .	15
Figure 8.	Model of mesotidal inlet . . . . .	16
Figure 9.	Regional inlet models . . . . .	17
Figure 10.	Regional inlet model in response to jetty construction . . . . .	19
Figure 11.	Hindcast Atlantic hurricane wave heights for WIS Station 57 .	21
Figure 12.	Yearly mean sea level values during 1939-1988 period for Fernandina Beach Station . . . . .	24
Figure 13.	Summary of estimates of local relative sea level changes along the U.S. Coast . . . . .	24
Figure 14.	Geology of Cumberland Island . . . . .	27
Figure 15.	Beach face of Cumberland Island . . . . .	28
Figure 16.	Dunes migrating along southern Cumberland Island . . . . .	28
Figure 17.	Backbarrier <i>Spartina</i> marshes along the western side of Cumberland Island . . . . .	29
Figure 18.	Classification of Georgia salt marshes . . . . .	29
Figure 19.	Composite geologic column of Cumberland Island . . . . .	30
Figure 20.	Cross section of lower Cumberland Sound and inlet throat area . . . . .	32
Figure 21.	Cross section of channel through jetties and ebb delta . . . . .	33
Figure 22.	Geology of Amelia Island . . . . .	36
Figure 23.	View of northern Amelia Island beach . . . . .	37
Figure 24.	Composite geologic column of Amelia Island . . . . .	37
Figure 25.	Regional bathymetry and associated morphologic features based on 1974 bathymetry (NGVD) . . . . .	39

Figure 26. Representative offshore cross section, perpendicular to shore . . . . .	40
Figure 27. Map of St. Marys Entrance channel in 1875 . . . . .	41
Figure 28. Position of navigation channels and ebb shoal bar complex, 1856. Contours based on MLW. . . . .	42
Figure 29. Typical section of north and south jetties . . . . .	46
Figure 30. Position of channel alignments after jetty construction . . . . .	46
Figure 31. Location of authorized disposal areas for St. Marys Entrance channel material . . . . .	49
Figure 32. Net shoreline change map, 1843 or 1871 to 1974 . . . . .	51
Figure 33. Volume changes computed by Olsen . . . . .	55
Figure 34. Areas and volume of sand movement calculated postjetty construction, 1902-1907 . . . . .	57
Figure 35. Location diagram showing morphologic compartments for the Kings Bay study area . . . . .	59
Figure 36. Coastal monitoring program GIS strategy . . . . .	63
Figure 37. Civilian use of Global Positioning System . . . . .	66
Figure 38. Well-defined scarp along northern Cumberland Island formed at high tide . . . . .	68
Figure 39. Shoreline position change for the Kings Bay study area from 1857/71 to 1991 . . . . .	72
Figure 40. Cumulative change in shoreline position relative to the 1857/71 shoreline . . . . .	76
Figure 41. Change in historical shoreline position for central Cumberland Island . . . . .	77
Figure 42. Trends in rates of shoreline position change for Cumberland Island . . . . .	78
Figure 43. Change in historical shoreline position near St. Marys Entrance . . . . .	79
Figure 44. Change in historical shoreline position along southern Amelia Island . . . . .	80

Figure 45. Trends in rates of shoreline position change for Amelia Island . . . . .	81
Figure 46. Trend of change in shoreline position for Cumberland and Amelia Islands . . . . .	82
Figure 47. Spatial and temporal trends in shoreline position change, 1857/71 to 1924 . . . . .	86
Figure 48. Spatial and temporal trends in shoreline position change, 1857/71 to 1933 . . . . .	87
Figure 49. Spatial and temporal trends in shoreline position change, 1857/71 to 1957 . . . . .	88
Figure 50. Spatial and temporal trends in shoreline position change, 1857/71 to 1973/74 . . . . .	89
Figure 51. Spatial and temporal trends in shoreline position change, 1857/71 to 1991 . . . . .	90
Figure 52. Spatial and temporal trends in shoreline position change, 1924 to 1933 . . . . .	91
Figure 53. Spatial and temporal trends in shoreline position change, 1924 to 1957 . . . . .	92
Figure 54. Spatial and temporal trends in shoreline position change, 1924 to 1973/74 . . . . .	93
Figure 55. Spatial and temporal trends in shoreline position change, 1924 to 1991 . . . . .	94
Figure 56. Spatial and temporal trends in shoreline position change, 1933 to 1957 . . . . .	95
Figure 57. Spatial and temporal trends in shoreline position change, 1933 to 1973/74 . . . . .	96
Figure 58. Spatial and temporal trends in shoreline position change, 1933 to 1991 . . . . .	97
Figure 59. Spatial and temporal trends in shoreline position change, 1957 to 1973/74 . . . . .	98
Figure 60. Spatial and temporal trends in shoreline position change, 1957 to 1991 . . . . .	99

Figure 61. Spatial and temporal trends in shoreline position change, 1973/74 to 1991 . . . . .	100
Figure 62. Bathymetric data coverage for the 1855/75 composite . . . . .	103
Figure 63. Bathymetric data coverage for the 1910 survey . . . . .	104
Figure 64. Bathymetric data coverage for the 1915 and 1924 surveys . . .	105
Figure 65. Bathymetric data coverage for the 1934/35 survey . . . . .	106
Figure 66. Bathymetric data coverage for the 1953/55 surveys . . . . .	107
Figure 67. Bathymetric data coverage for the 1953/79 composite . . . . .	108
Figure 68. Bathymetric data coverage for the 1988 survey . . . . .	109
Figure 69. Bathymetric data coverage for the 1992 survey . . . . .	110
Figure 70. Reference vertical datums for the Kings Bay study area (1960-1978 tidal epoch) . . . . .	113
Figure 71. Polygon boundaries defined for the regional study area . . . . .	115
Figure 72. Polygon boundaries defined for the regional study area based on 1924 data . . . . .	116
Figure 73. Regional bathymetric contour map for the period 1855/75 . . .	118
Figure 74. Regional bathymetric contour map for the 1924 data set . . . . .	120
Figure 75. Regional bathymetric contour map for the period 1953/79 . . .	121
Figure 76. Change in position of the 6-m- (NGVD) depth contour for the period of record . . . . .	122
Figure 77. Color-fill contour map of regional changes in bathymetry between 1855/75 and 1924 . . . . .	124
Figure 78. Color-fill contour map of regional changes in bathymetry between 1924 and 1953/79 . . . . .	125
Figure 79. Color-fill contour map of regional changes in bathymetry between 1855/75 and 1953/79 . . . . .	126
Figure 80. Bathymetric contour map for St. Marys Tidal Inlet Complex, 1870/75 . . . . .	129

Figure 81. Bathymetric contour map for St. Marys Tidal Inlet Complex, 1934/55 . . . . .	129
Figure 82. Bathymetric contour map for St. Marys Tidal Inlet Complex, 1954/79 . . . . .	130
Figure 83. Bathymetric change map for St. Marys Tidal Inlet Complex, 1870/75-1934/55 . . . . .	131
Figure 84. Bathymetric change map for St. Marys Tidal Inlet Complex, 1934/55-1954/79 . . . . .	132
Figure 85. Bathymetric change map for St. Marys Tidal Inlet Complex, 1870/75-1954/79 . . . . .	132
Figure 86. Bathymetric contour map for St. Marys ebb-tidal delta, 1870/75 . . . . .	133
Figure 87. Bathymetric contour map for St. Marys ebb-tidal delta, 1910/24 . . . . .	133
Figure 88. Bathymetric contour map for St. Marys ebb-tidal delta, 1934/55 . . . . .	134
Figure 89. Bathymetric contour map for St. Marys ebb-tidal delta, 1954/79 . . . . .	134
Figure 90. Bathymetric contour map for St. Marys ebb-tidal delta, 1988 . . . . .	135
Figure 91. Bathymetric contour map for St. Marys ebb-tidal delta, 1992 . . . . .	135
Figure 92. Bathymetric change map for St. Marys ebb-tidal delta, 1870/75-1910/24 . . . . .	136
Figure 93. Bathymetric change map for St. Marys ebb-tidal delta, 1910/24-1934/55 . . . . .	137
Figure 94. Bathymetric change map for St. Marys ebb-tidal delta, 1934/55-1954/79 . . . . .	138
Figure 95. Bathymetric change map for St. Marys ebb-tidal delta, 1954/79-1988 . . . . .	138
Figure 96. Bathymetric change map for St. Marys ebb-tidal delta, 1988-1992 . . . . .	139

Figure 97.	Bathymetric change map, with 0.1 m added to the 1992 data, for St. Marys ebb-tidal delta, 1988-1992 . . . . .	140
Figure 98	Bathymetric change map for St. Marys ebb-tidal delta, 1870/75-1992 . . . . .	141
Figure 99.	Cumulative changes in sediment volume at St. Marys ebb-tidal delta with a +0.1-m adjustment to 1993 bathymetry data . .	143
Figure 100.	Channel depth and average annual maintenance dredged volumes for St. Marys Entrance channel for the period 1870-1992 . . . . .	147
Figure 101.	Maintenance dredging location for Epoch 7 (1988-1992) . . .	149
Figure 102.	Channel reaches based on shoaling characteristics after the 1987-1988 channel deepening . . . . .	151
Figure 103.	Maintenance dredging event channel reach, volume, and sediment type with respect to channel configuration and ebb-tidal delta profile (1988-1992) . . . . .	153
Figure 104.	Location map of Jul 1988 profile survey lines and sediment sampling along Cumberland Island . . . . .	157
Figure 105.	Location map of Jul 1988 profile survey lines and sediment sampling along Amelia Island . . . . .	158
Figure 106.	Location map of Apr/May 1992 profile survey lines and sediment sampling along Cumberland Island . . . . .	159
Figure 107.	Location map of Apr/May 1992 profile survey lines and sediment sampling along Amelia Island . . . . .	160
Figure 108.	Location map of survey lines for the ebb-tidal delta survey of Jun/Jul 1988 and Apr 1992 . . . . .	162
Figure 109.	Definition sketch of profile computational parameters . . . .	163
Figure 110.	Net volume change for elevation 2.5 to 0.0 m (NGVD), Jul 1988 - Apr/May 1992, Cumberland Island . . . . .	166
Figure 111.	Net volume change for elevation 4.0 to 0.0 m (NGVD), Jul 1988 - Apr/May 1992, Amelia Island . . . . .	167
Figure 112.	Locations of beach fill placements along Amelia Island . . .	168
Figure 113.	Profile comparison of Line A79, Aug 1990 - Apr/May 1992, Amelia Island . . . . .	170

Figure 114. Shoreline change rates, Jul 1988 - Apr/May 1992, Cumberland Island . . . . .	173
Figure 115. Shoreline positions relative to the Jul 1988 shoreline, Cumberland Island . . . . .	174
Figure 116. Shoreline change rates, Jul 1988 - Apr/May 1992, Amelia Island . . . . .	175
Figure 117. Shoreline positions relative to the Jul 1988 shoreline, Amelia Island . . . . .	176
Figure 118. An example of berm crest (about elevation 2.2 m NGVD) and escarpment during winter in the Stafford Shoal compartment . . . . .	177
Figure 119. An example of bar formation in the winter and welding onto the beach (advancing the berm) in the summer . . . . .	177
Figure 120. Dune escarpment and retreat along Line A73 in the Nassau Sound Tidal Inlet Complex compartment . . . . .	178
Figure 121. Mean grain size for MHW sediment samples . . . . .	180
Figure 122. Mean grain size for 4.5-m (NGVD) depth sediment samples . . . . .	181
Figure 123. Scatter plot of standard deviation versus mean grain size for Cumberland Island, 1992 . . . . .	181
Figure 124. Beach composites, Jul 1988, Cumberland Island . . . . .	182
Figure 125. Beach composites, Apr/May 1992, Cumberland Island . . . . .	183
Figure 126. Scatter plot of standard deviation versus mean grain size for Amelia Island, Apr/May 1992 . . . . .	184
Figure 127. Beach composites, Jul 1988, Amelia Island . . . . .	184
Figure 128. Beach composites, Apr/May 1992, Amelia Island . . . . .	185
Figure 129. Distance to inner bar from elevation 0.0 m (NGVD) and inner bar crest elevation, Apr/May 1992, Cumberland Island . . . . .	189
Figure 130. Distance to inner bar from elevation 0.0 m (NGVD) and inner bar elevation, Apr/May 1992, Amelia Island . . . . .	189
Figure 131. Mean grain size versus beach slope . . . . .	190

Figure 132. Representative profile comparison, Stafford Shoal . . . . .	190
Figure 133. Representative profile comparison, Cumberland Embayment . . . . .	191
Figure 134. Representative profile comparison, north fillet of St. Marys Entrance . . . . .	192
Figure 135. Representative profile, south fillet of St. Marys Entrance . .	192
Figure 136. Representative profile comparison, North Amelia Platform .	193
Figure 137. Representative profile comparison, Amelia Embayment . . .	194
Figure 138. Representative profile comparison, Nassau Sound Tidal Inlet Complex . . . . .	195
Figure 139. Comparison of shoreline change rates . . . . .	199
Figure 140. Profile comparison of Line A19 in beach fill Zone A illustrating the sequential retreat of the placed beach fill (Jul 1988) through the monitoring period . . . . .	200
Figure 141. Profile comparison of Line A31 in the northern portion of beach fill Zone B illustrating profile accretion between Jul 1988 and Oct 1989 . . . . .	201
Figure 142. Profile comparison of Line A43 in the southern portion of beach fill Zone B illustrating profile accretion between Oct 1989 and Sep 1991 . . . . .	201
Figure 143. Profile comparison of Line A49 in beach fill Zone C illustrating the retreat of fill placed prior to the Jul 1988 survey . . . . .	202
Figure 144. Profile comparison of Line A55 in the northern portion of beach fill Zone D illustrating the relative stability of the beach fill since Oct 1989 . . . . .	203
Figure 145. Profile comparison of Line A58 in the southern portion of beach fill Zone D illustrating minor erosion of the placed fill since Oct 1989 . . . . .	204
Figure 146. Profile comparison of Line A64 in beach fill Zone E . . . . .	204
Figure 147. Recent shoreline change rate response as a function of Amelia Island beach-fill placement operations . . . . .	206

Figure 148.	Profile comparison of Line A10 north of beach fill Zone A illustrating accretionary trend of the fillet south of the south jetty since Jul 1988 . . . . .	208
Figure 149.	Kings Bay tide gage location map . . . . .	213
Figure 150.	Kings Bay ARTTES observed tide and nonastronomical residual . . . . .	215
Figure 151.	Comparison of ARTTES and stilling well gage measurements . . . . .	217
Figure 152.	Comparison of ARTTES and offshore gage G1 during spring tide . . . . .	218
Figure 153.	Comparison of ARTTES and offshore gage G1 during neap tide . . . . .	218
Figure 154.	Location of wave gages relative to St. Marys Entrance . . .	222
Figure 155.	Plot of wave spectra for 4 May 1989 at 0200 hr GMT . . .	227
Figure 156.	Number of days per month where wave heights exceeded 2 m based on NDBC buoy data . . . . .	228
Figure 157.	Location of nested grids used in STWAVE modeling . . . .	233
Figure 158.	Contour map of Grid 1 (1,854 m) for STWAVE modeling	234
Figure 159.	Contour map of Grid 2 (457 m) for STWAVE modeling . .	235
Figure 160.	Three-dimensional perspective of Grid 2 (457 m) for STWAVE modeling . . . . .	237
Figure 161.	Contour map of Grid 3 (91.4 m) for STWAVE modeling .	238
Figure 162.	Flow of shoreline change calculation . . . . .	240
Figure 163.	Shoreline model reaches and grids . . . . .	245
Figure 164.	Cumberland Island model shoreline change calibration results . . . . .	248
Figure 165.	Sand transport rates for Cumberland Island during calibration period . . . . .	249
Figure 166.	Amelia Island model shoreline change calibration results . .	250

Figure 167.	Sand transport rates for Amelia Island during calibration period . . . . .	251
Figure 168.	Amelia Island model shoreline change verification results .	252
Figure 169.	Transport rates for Amelia Island verification period . . . .	253
Figure 170.	Cumberland Island shoreline 17-year extrapolation, 1974-1991 . . . . .	253
Figure 171.	Amelia Island shoreline 11-year extrapolation, 1974-1985 .	254
Figure 172.	Cumberland Island sand transport rates during the 1870s . .	255
Figure 173.	Cumberland Island sand transport rates during the 1920s . .	255
Figure 174.	Amelia Island sand transport rates during the 1870s . . . . .	256
Figure 175.	Amelia Island sand transport rates during the 1920s . . . . .	256

## List of Tables

---

Table 1.	Description of Services (DOS): Kings Bay Coastal and Estuarine Physical Monitoring and Evaluation Program . . . . .	6
Table 2.	Changes Made to the Description of Services (DOS) During Program Execution . . . . .	7
Table 3.	Characteristics of Regional Inlet Systems, Charleston, South Carolina, to Nassau Sound, Florida . . . . .	18
Table 4.	Predicted Mean Tide Levels and Tidal Range at Selected NOS Subordinate Stations in South Georgia and North Florida, 1992 . . . . .	22
Table 5.	Engineering Epochs of St. Marys Entrance and Cumberland Sound . . . . .	43
Table 6.	Chronology of Significant Engineering Events, St. Marys Entrance and Vicinity . . . . .	44
Table 7.	St. Marys Entrance Channel Dimensions . . . . .	47
Table 8.	Longshore Sediment Transport and Ebb-Delta Volume: Summary of Previous Study Results . . . . .	58

Table 9.	Summary of Shoreline Source Data Characteristics for the Study Area . . . . .	67
Table 10.	Estimates of Potential Error Associated with Shoreline Position Surveys . . . . .	70
Table 11.	Maximum Root-Mean-Square Potential Error for Shoreline Change Data . . . . .	71
Table 12.	Average Shoreline Position Change for Cumberland Island . .	74
Table 13.	Average Shoreline Position Change for Amelia Island . . . . .	75
Table 14.	Shoreline Position Change at Transects Along Cumberland and Amelia Islands . . . . .	82
Table 15.	Spatial and Temporal Trends in Shoreline Position Change for Cumberland Island . . . . .	84
Table 16.	Spatial and Temporal Trends in Shoreline Position Change for Amelia Island . . . . .	85
Table 17.	Maximum Root-Mean-Square Potential Error for Bathymetry Change Data . . . . .	112
Table 18.	Historical Changes in Sediment Volume for Polygons Defining the Nearshore Bathymetry Based on the 1924 Data Limits . . . . .	127
Table 19.	Historical Changes in Sediment Volume for Polygons Defining Nearshore Bathymetry . . . . .	128
Table 20.	Historical Changes in Sediment Volume for St. Marys Tidal Inlet Complex . . . . .	131
Table 21.	Historical Changes in Sediment Volume for St. Marys Ebb-Tidal Delta . . . . .	137
Table 22.	Historical Changes in Sediment Volume by Geomorphic Subset for St. Marys Ebb-Tidal Delta . . . . .	142
Table 23.	Schedule of Field Data Collection for Coastal Monitoring . . .	155
Table 24.	Survey and Sediment Field Data Collection for Monitoring Program . . . . .	161
Table 25.	Net Volume Change for Cumberland Island . . . . .	165
Table 26.	Net Volume Change for Amelia Island . . . . .	167

Table 27. Beach Fill Placements on Amelia Island . . . . .	169
Table 28. Shoreline Change for Cumberland Island . . . . .	172
Table 29. Shoreline Change for Amelia Island . . . . .	172
Table 30. Selected Seasonal Change in Contour Position at Elevations 1.3 and 0.0 m (NGVD) . . . . .	179
Table 31. Summary of Sediment Grain Size and Profile Parameters for Cumberland Island . . . . .	1
Table 32. Summary of Sediment Grain Size and Profile Parameters for Amelia Island . . . . .	188
Table 33. Comparison of Dredged Material Quantities Placed on Amelia Island to Net Beach Volume Change (Jul 1988 - Apr/May 1992) . . . . .	198
Table 34. Shoreline Change Rates Per Beach-Fill Compartment for Amelia Island . . . . .	205
Table 35. Regional Tides . . . . .	214
Table 36. Tidal Constituents for ARTTES and Stilling Well Gage . . . . .	215
Table 37. Tidal Constituents for ARTTES and Offshore Gage G1 . . . . .	217
Table 38. Temporary Tide Gage Locations and Dates of Operation . . . . .	219
Table 39. Tidal Constituents for South Amelia TDR 3 and ARTTES . . . . .	220
Table 40. Observed Water-Level Differences Between South Amelia Island and Fernandina Beach . . . . .	220
Table 41. Tidal Constituents for Cumberland Island TDR1 and 2 and ARTTES . . . . .	221
Table 42. Mean and Largest Wave Height Summary . . . . .	225
Table 43. WIS Hindcast Direction Bands and Percent Occurrence . . . . .	231
Table 44. Annual Transport Rates at 1.8-km-Long Increments Along Cumberland Island Based Upon a 20-Year Wave Hindcast . . . . .	258
Table 45. Annual Transport Rates at 1.8-km-Long Increments Along Amelia Island Based Upon a 20-Year Wave Hindcast . . . . .	259

# Preface

---

The coastal processes physical monitoring and evaluation study described in this report was performed by elements of the U.S. Army Corps of Engineers (USACE) for the Department of the Navy, Office of the Chief of Naval Operations, through the Naval Facilities Engineering Command (NAVFAC). The study was conducted over the 5-year period 1 November 1987 to 30 September 1992. The U.S. Army Engineer Division, South Atlantic (SAD), was the lead Corps element and responsible for overall conduct of the study and coordination with the NAVFAC. The U.S. Army Engineer District (USAED), Jacksonville, and USAED, Savannah, conducted the majority of hydrographic and topographic surveys for the study, and the U.S. Army Engineer Waterways Experiment Station's (WES) Coastal Engineering Research Center (CERC) and Hydraulics Laboratory (HL), respectively, conducted the coastal studies and estuarine studies. In the final 15 months of the project, CERC was assisted through a contract with the Coastal Studies Institute, Louisiana State University (LSU), in analysis of shoreline position and bathymetry change, and in development of a Geographic Information System for the study, and by Offshore Coastal Technology, Inc., - East Coast, (OCTI-EC) in numerical modeling and in a sled hydrographic survey made in April 1992. The study was reviewed by and received guidance from a Technical Review Committee (TRC) reporting to an Interagency Steering Committee (ISC) representing the Department of the Navy and the Department of the Interior (DOI).

This report consists of two volumes. Volume I presents the main narrative, including study objectives, background information, procedures, and principal results. The purpose of Volume I is to present the study results. Volume II describes the historical and field data sets and products generated and analyzed in the study. Each major data set is documented in an appendix in Volume II, in which detailed information is given on data sources and collection methods, properties of the data, data tabulations and plots, and photographs of the study site.

The study was directed by the ISC, whose members were Mr. Thomas J. Peeling, representing the Office of the Chief of Naval Operations as Special Assistant for Environmental Planning, and Drs. Albert G. Greene, Jr. (1988-1990) and Dennis B. Fenn (1991-1992) from the DOI. The ISC was responsible for overseeing and reviewing TRC actions and appointment of TRC members. Members of the TRC were: Mr. Darrell Molzan, representing South

Division, NAVFAC, as the U.S. Navy study manager; Dr. Stephen Cofer-Shabica, representing the National Park Service (NPS), DOI as its study manager; Dr. James A. Baillard, formerly of the Naval Civil Engineering Laboratory (1988); Mr. John R. Headland, formerly NAVFAC (1989-1992); the late Dr. William Odum, University of Virginia, NPS representative (1988-1990); Dr. Robert G. Dean, University of Florida, NPS representative; and Dr. Vernon J. Henry, Georgia State University, NPS representative (1991-1992). Mr. Mark Leadon, Florida Department of Natural Resources, represented the State of Florida in TRC study reviews. The USACE study coordinator was Mr. James Robinson, SAD, and USACE District points of contact were Ms. Susan Brinson, USAED, Savannah, and Mr. Thomas Martin, USAED, Jacksonville. Ms. Joan Pope, Chief, Coastal Structures and Evaluation Branch (CSEB), Engineering Development Division (EDD), CERC, was principal WES contact for the study and coordinator of the coastal studies for 1988-1990. Dr. Nicholas C. Kraus, Senior Scientist, CERC, was coordinator of the coastal studies for 1991-1992. Mr. Thomas W. Richardson, Chief, EDD, CERC, participated in preproject planning and assisted throughout the study. Mr. George Fisackerly (HL) was the point of contact for the USACE estuarine studies. Ms. Laurel T. Gorman, CSEB, CERC, coordinated the historical and coastal monitoring substudies (1989-1992).

This report was written over the period October 1991 through March 1993. Chapter 1 was written by Ms. Pope and Mr. Richardson. Chapter 2 was written by Ms. Gorman and Pope. Chapter 3 was written by Dr. Mark R. Byrnes and Mr. Matteson W. Hiland, LSU. Chapter 4 was written by Mr. J. Bailey Smith, CSEB, CERC, and Ms. Pope and Gorman. Chapter 5 was written by Ms. Gorman, Pope, and Karen R. Pitchford, CSEB, CERC. Chapter 6 was written by Messrs. John W. McCormick, CSEB, CERC, William D. Corson, Prototype Measurement and Analysis Branch (PMAB), CERC, and W. Jeff Lillycrop, CSEB, CERC. Chapter 7 was written by Mr. William G. Grosskopf, OCTI-EC, and Dr. Kraus. Chapter 8 was written by Drs. Kraus and Byrnes, with input from all authors. Appendix B was written by Dr. Byrnes and Mr. Hiland. Appendix C was written by Mr. Smith and Ms. Pope and Gorman, Mr. Martin, and Ms. Brinson. Appendix D was written by Ms. Gorman and Pitchford, Dr. Donald K. Stauble, and Mr. James T. Langston, CSEB, CERC. Appendix E was written by Mr. Corson. Appendix F was written by Ms. Jane McKee Smith, Coastal Processes Branch (CPB), Research Division (RD), CERC. Appendix G was written by Dr. Kraus and Ms. Allison Abbe, CPB, CERC. Dr. Kraus and Ms. Gorman and Pope were technical editors for the report.

Mr. Stephen C. Knowles, formerly CSEB, CERC, and Dr. S. Rao Vemulakonda, CPB, CERC, participated in the early stages of the project. Mr. Randolph A. McBride, LSU, and Mr. Greg Forrester, NPS, assisted with the global positioning system shoreline survey (October 1991). The following individuals assisted in sample and data analysis, file handling, and figure and text preparation: Ms. Mary C. Allison, Mr. Lee A. Cheney, Ms. Margaret V. Edris and Jackie J. Johnston, Mr. Corey L. Kindhart, Ms. Michelle K. Kindhart, Mr. M. Danny Marshall, Ms. Yvette L. McGowen, and Mr. Brian N. Williams

all of CSEB, CERC; Meses. Abbe and J. Holley Messing, CPB, CERC; Ms. Robin Hoban, Coastal Oceanography Branch, RD, CERC; and Ms. Rhonda M. Lofton, PMAB, CERC. Ms. Pitchford contributed substantially in coordinating inter-agency data transfer and in developing final presentations of text and figures for both volumes of this report.

This study was performed under the administrative supervision of Dr. James R. Houston, Director, CERC; Mr. Charles C. Calhoun, Jr., Assistant Director, CERC; Mr. Richardson, Mr. H. Lee Butler, Chief, RD, CERC; Mr. Bruce A. Ebersole, Chief, CPB, RD, CERC; Ms. Pope, and Mr. William L. Preslan, Chief, PMAB, EDD, CERC.

At the time of publication of this report, Director of WES was Dr. Robert W. Whalin. Commander was COL Bruce K. Howard, EN.

*The contents of this report are not to be used for advertising, publication, or promotional purposes. Citation of trade names does not constitute an official endorsement or approval of the use of such commercial products.*

# Conversion Factors, Non-SI to SI Units of Measurement

---

Non-SI units of measurement used in this report can be converted to SI units as follows:

<b>Multiply</b>	<b>By</b>	<b>To Obtain</b>
cubic yards	0.7645549	cubic meters
degrees (angle)	0.01745329	radians
feet	0.3048006	meters
inches	25.40005	millimeters
miles (U.S. statute)	1.6093472	kilometers
miles (U.S. nautical)	1.85325	kilometers
yards	0.9144018	meters

# 1 Introduction<sup>1</sup>

---

## Study Background

In the early 1980s, Kings Bay, Georgia, was selected as a U.S. Navy home port for TRIDENT submarines. In upgrading the Kings Bay base for this fleet, the navigation channels in Cumberland Sound and through St. Marys Entrance into the Atlantic Ocean had to be deepened and widened and the entrance channel lengthened.

At the request of the U.S. Navy Officer-in-Charge TRIDENT, in support of the Naval Submarine Base Kings Bay (NSB Kings Bay) expansion, mathematical and physical model studies were conducted during the late 1970s and early 1980s by the U.S. Army Engineer Waterways Experiment Station (WES) (Vemulakonda et al. 1988, Granat et al. 1989). The purpose of these studies was to assess the potential impact of proposed modifications on physical processes in Cumberland Sound and to evaluate the possible range of channel maintenance requirements.

During review of the Environmental Impact Statement (EIS) for the Kings Bay upgrade, the State of Florida raised concerns about the potential for adverse physical impacts on Amelia Island to the south, and objected to the proposed dredged material disposal plan which provided for placement of 1.1 million cu m of beach-quality sand on northern Amelia Island and an additional 2.4 million cu m of beach-quality sand to be placed in a nearshore disposal area. As a result, on 19 December 1986, the U.S. Navy signed a Memorandum of Understanding (MOU) with the State of Florida, agreeing to cost-share the placement on the beaches of central and southern Amelia Island all or a portion of the beach-quality material originally designated to be placed in the nearshore disposal area. Furthermore, the MOU provided for placement on Amelia Island of that portion of beach-quality sand resulting from routine maintenance operations attributable to the U.S. Navy, if the present study should conclude, "...based upon actual data..., that significant additional erosion of the southern end of Amelia Island is being directly caused by the dredging of the St. Marys channel for Navy purposes...."

In addition, the Department of the Interior (DOI) raised concerns to the U.S. Navy about potential impacts of channel modifications to the Cumberland Island National Seashore located immediately north of St. Marys Entrance. Specific areas of concern included the ocean coast of Cumberland Island and the bay shore and adjacent wetlands in the Cumberland Sound estuary.

---

<sup>1</sup> Written by Joan Pope and Thomas W. Richardson.

An MOU between the U.S. Navy and DOI, dated 17 November 1987, established the subject study to evaluate the physical and ecological impacts associated with the channel modification.

## Site Description

St. Marys Entrance is a Federally stabilized and maintained inlet which provides access between the Atlantic Ocean and the Intracoastal Waterway (ICWW) for fishing, commercial, and military fleets at the ports of Fernandina Beach, Florida, St. Marys, Georgia, and NSB Kings Bay, Georgia (Figure 1). The Entrance is located at latitude 30°43' N and longitude 81°26' W and lies about 50 km north-northeast of Jacksonville, Florida, and 50 km south of Brunswick, Georgia. This tidal inlet separates Amelia Island, Florida, to the south from Cumberland Island, Georgia, to the north. Amelia Island includes many residential and commercial developments, paper manufacturing and fishing industries, and Fort Clinch State Park. Cumberland Island National Seashore, which includes most of Cumberland Island, is administered by the National Park Service (NPS), DOI. The backbarrier estuary, Cumberland Sound, contains extensive salt marsh and sand flats, and receives small quantities of fresh water from the St. Marys and Crooked Rivers.

After initial jetty construction and inlet stabilization started in the 1880s, St. Marys Entrance has served as a navigation route to the Atlantic Ocean for boats harbored at Fernandina Beach on the Amelia River and the town of St. Marys on St. Marys River. Since completion of the jetties in 1905, incremental deepening of the navigation channels was periodically authorized by Congress in response to commercial boat traffic demands (civil works authorization). However, the inlet also has been used by military vessels since the 1950s in support of an emergency Army Munitions Operation Transport Facility and, since 1978, by fleet ballistic missile submarines with the development of NSB Kings Bay (military authorization). The authorized channel, now serving a combined military and civil works mission, was deepened from 10.4 m to 12.2 m below mean low water (MLW) in the 1970s to accommodate use by POSEIDON submarines. Further development of the NSB Kings Bay to accommodate use by TRIDENT submarines has resulted in construction during the period 1987-1988 to increase project channel depth, width, and length.

The present civil-works-authorized channel is 122 m wide and 9.8 m deep relative to MLW, and it extends offshore to the 9.8-m National Geodetic Vertical Datum (NGVD) contour. The military-authorized portion of the entrance channel widened the civil works channel by 30 m (on the north side of the preproject channel) resulting in a 152-m width, added 5.7 m of depth, resulting in a maximum depth of 15.5 m (14.0 m project depth plus 0.9 m advance maintenance and 0.6 m to allow for dredging inaccuracies), and extended the channel seaward of the 9.8-m contour for a total entrance channel length of approximately 22.2 km (only the shoreward 19.8 km have required dredging). Figure 2 depicts the authorized changes in St. Marys Entrance channel dimensions since 1955. Both the civil-works- and military-authorized project channel dimensions are maintained on an as-needed basis by the U.S. Army Corps of Engineers (USACE) with U.S. Navy sponsorship of the military portion. The channel is used by a varied fleet representing fishing, recreational, commercial shipping, and military needs.

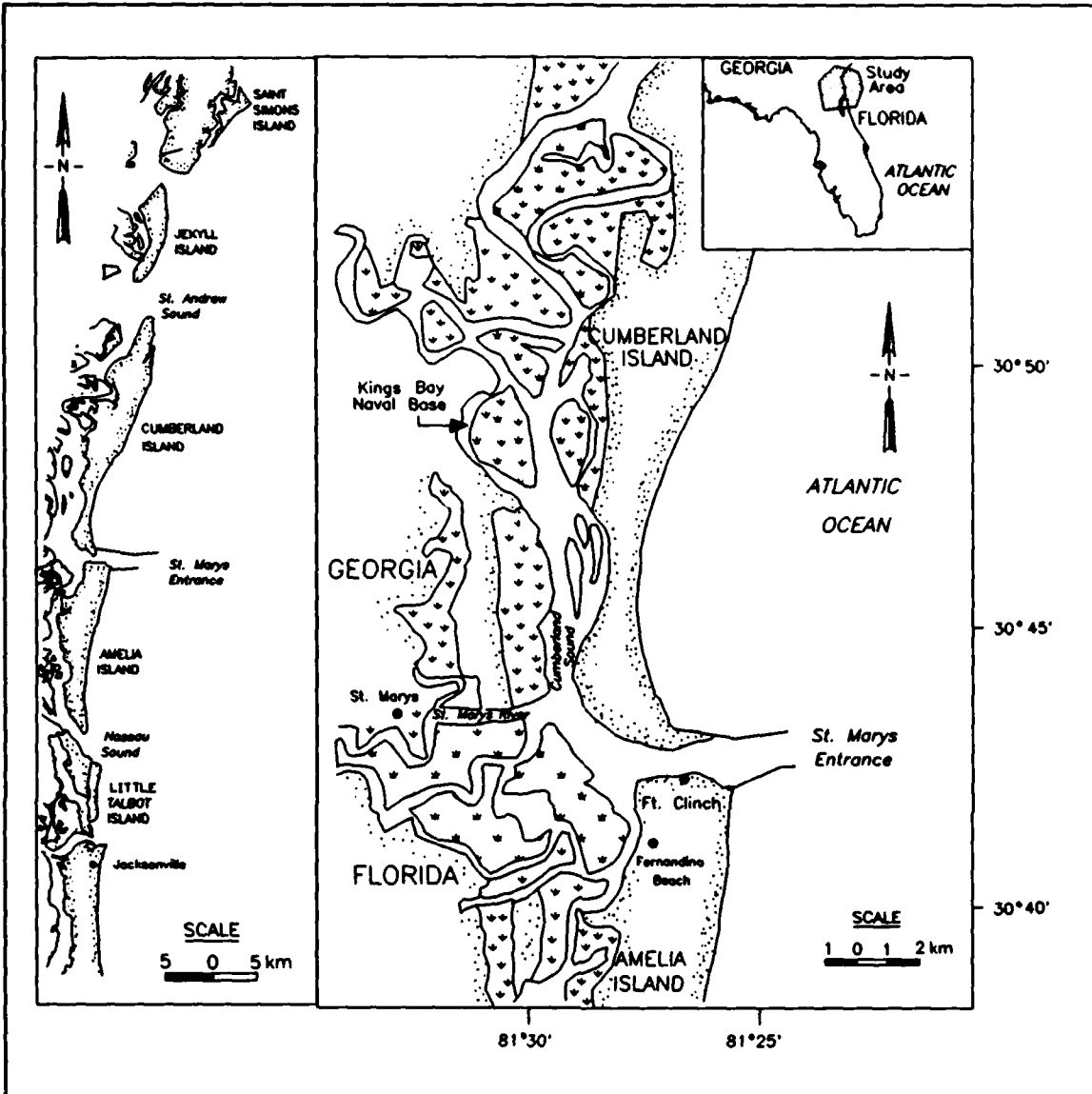


Figure 1. Location of study area

## Purpose and Structure of Study

In the Military Construction Appropriation Act of 1988, the U.S. Congress authorized the Departments of the Navy and Interior to "...establish a long-term environmental monitoring program to examine the impact of the U.S. Navy dredging on the Cumberland Island National Seashore and the waters of the Cumberland Sound and the St. Marys River." As a result, representatives of the Departments of the Navy and Interior developed a 5-year monitoring and evaluation program. The ecological aspects of the program are the responsibility of the DOI with the NPS as the implementing agency. The Department of the Navy is responsible for the physical aspects of the study with the Naval Facilities Engineering Command (NAVFAC) as the coordinating organization.

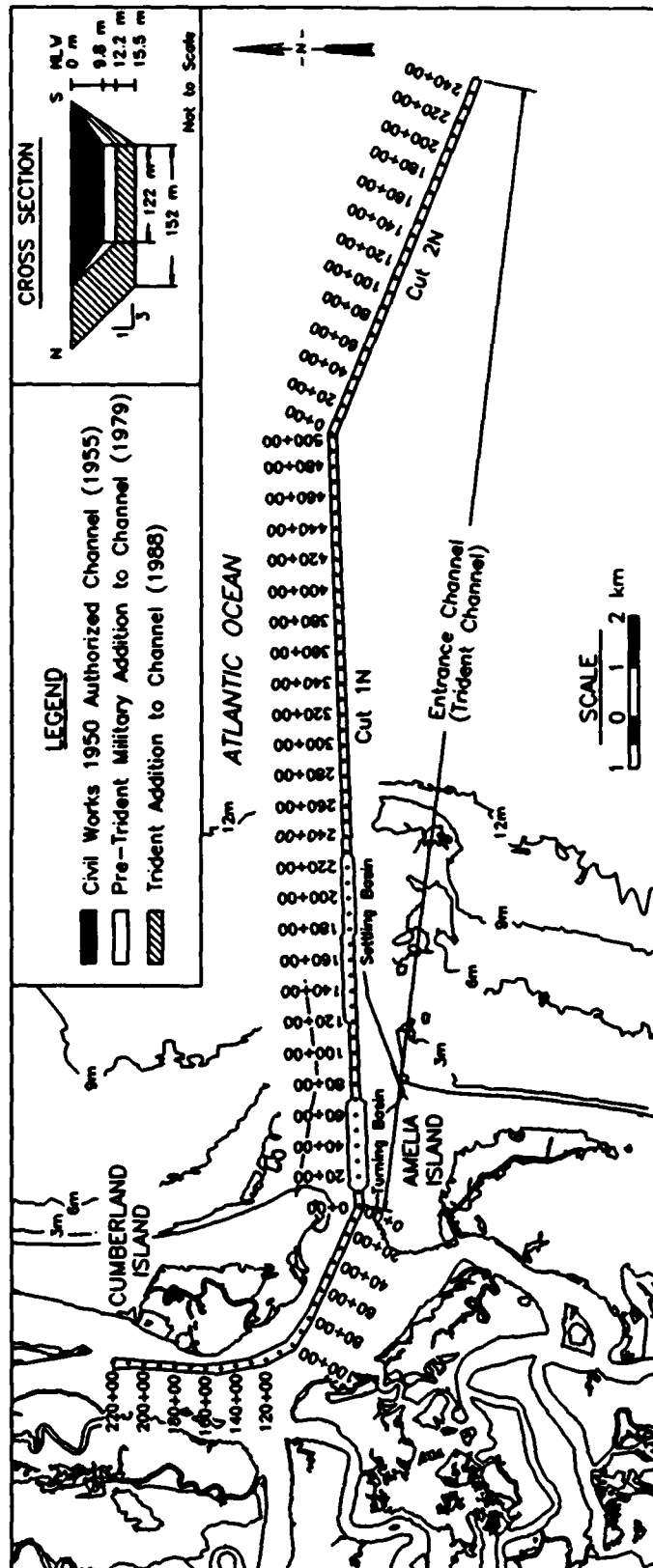


Figure 2. Authorized channel dimensions for St. Marys Entrance

In March 1988, the Commander of the U.S. Army Engineer Division, South Atlantic (CESAD), agreed to perform the physical monitoring and evaluation aspects of the program, through a negotiated Description of Services (DOS) with the NAVFAC. This DOS is the scope of work that describes the tasks, schedule, and products which are the responsibility of the USACE and is summarized in Table 1. A Technical Review Committee (TRC), including representatives of the U.S. Navy and NPS and consultants from the academic community, was established to periodically review study progress and provide recommendations to the U.S. Navy and DOI Interagency Steering Committee.

The physical monitoring and evaluation program involved the support of many USACE organizational elements. The U.S. Army Engineer District (USAED), Jacksonville, and USAED, Savannah, were responsible for conducting hydrographic and topographic surveys. The physical monitoring and evaluation program included both coastal and estuarine studies (Table 1). The WES Coastal Engineering Research Center (CERC) conducted the coastal studies. The estuarine studies (including long-term data collection, short-duration physical measurements, numerical model testing, and the conduct of several data analysis studies) were conducted by the WES Hydraulics Laboratory, and are reported elsewhere (Granat 1990; Fagerburg, Coleman, and Parman 1991a, 1991b; Fagerburg et al. 1992a, 1992b, 1992c). The CESAD was responsible for coordination among the Corps elements and with the U.S. Navy.

The monitoring and evaluation study included several components which continued throughout the 5-year period and some components which were of limited duration. Each year, the original monitoring plan was re-evaluated by the TRC as experience was gained and preliminary results were compiled. Consequently, the implemented monitoring plan was modified from that shown in Table 1. Table 2 lists some of the more significant modifications. These modifications usually involved streamlining the survey plan, rescheduling activities between fiscal years, or adding or revising specific tasks. None of these changes amended the structure or focus of the study specified in the DOS. In each case, the U.S. Navy, NPS, and TRC reviewed and approved study changes.

## **Coastal Monitoring Program**

The primary purpose of the coastal monitoring program was to assess the impacts of U.S. Navy-sponsored channel modification and maintenance activities on shoreline behavior in the vicinity of St. Marys Entrance. In order to address this issue within the 5-year monitoring period, a three-tiered approach was adopted (Table 1). The study included a review of the regional setting and historical data used to document the long-term evolution of the project area (Historical Substudy), data collection during the 5-year program designed to monitor coastal processes and responses (Monitoring Substudy), and numerical modeling activities designed to simulate ocean shoreline responses for Amelia Island and the southern half of Cumberland Island for a range of physical conditions (called "scenarios" in the DOS) (Extrapolation Substudy). The basic approach was to define predeepening conditions for St. Marys Entrance and adjacent beach and nearshore systems, document any trends within the monitoring period which may indicate changes in the coastal processes and responses, and evaluate any potential impacts of the channel modification to the coastal system.

**Table 1**  
**Description of Services (DOS): Kings Bay Coastal and Estuarine Physical Monitoring and Evaluation Program**

Substudy/Task	FY 88	FY 89	FY 90	FY 91	FY 92
<b>Coastal</b>					
History					
Collect and screen data	X X X				
Reduce and analyze data	X X	X X			
Draft technical report		X			
Monitoring					
Arrange for NDBC gage	X				
Operate NDBC gage	X X X	X X X X	X X X X	X X X X	X X
Begin nearshore station work		X X			
Operate short-term nearshore station		X X	X X		
Conduct Cumberland and Amelia Islands profile surveys	X	X	X	X	X
Conduct Cumberland Sound profile surveys	X	X	X	X	X
Conduct additional selected profile surveys		X	X		
Conduct St. Marys ebb delta bathymetric survey	X				X
Fly aerial photography	X	X	X	X	X
Collect beach/channel sediment samples	X	X	X		X
Begin data analysis and draft interim miscellaneous paper		X X X X	X X	X X	
Shoreline Evolution Modeling					
Develop bathymetry grid	X X				
Set up response model		X X			
Perform initial calibration		X X			
Incorporate interim results		X	X X	X X	
Incorporate final results					X
Develop scenarios			X	X	X X
Assess scenario effects					X X
Final Report					X X X X
<b>Estuarine</b>					
Long-term Field	X X X X	X X X X	X X X X	X X X X	X X X
Collect equipment	X	X	X	X	X
Initiate reporting		X	X	X	X
Salinity Impact				X X	
Initiate reporting				X	
Sediment Impact	X X				
Intensive Field			X		
Initiate reporting			X		
Fernandina Tide				X X	
Bottom Change	X	X	X	X	X

**Table 2**  
**Changes Made to the Description of Services (DOS) During Program Execution**

Substudy/Task	As Implemented
<b>Coastal</b>	
History	Continuing throughout study period.
Monitoring	
NDBC gage	Gage operational entire 5-year study period.
Nearshore gage	Unchanged from DOS.
Surveys and sediment samples	
Cumberland Beach	Reduced number of profile lines in FY 89. Dropped sediment sampling in FY 91.
Cumberland Sound	Dropped 2 lines, added 2 lines in FY 89. Not surveyed in 1992.
Amelia Island	Reduced number of profile lines in FY 89, combined surveys with required permit surveys in FY 90. Dropped sediment samples in FY 91.
Winter	Winter surveys conducted only in FY 89 and 91.
Ebb Delta	Unchanged from DOS.
Aerial photography	Used NPS aerals.
Data analysis	Added real-time tide datum control system FY 90, continuing throughout study period.
GIS Database	Added to program in FY 91 for database management.
Shoreline Evolution Modeling	Unchanged from DOS.
Final Report	Unchanged from DOS.
<b>Estuarine</b>	
Long-term Monitoring	Unchanged from DOS.
Salinity Impact	Not conducted in a physical model, impact analysis based on review of field data (FY 92).
Sediment Impact	Unchanged from DOS.
Intensive Sampling	Schedule modified, reporting moved to FY 91.
Fernandina Tide	Initial analysis conducted in FY 89, follow-up in FY 92.
Bottom Change	Conducted by USAED, Savannah, part of Coastal Report.

During the Historical Substudy survey, shoreline position, bathymetry, geologic, sedimentologic, engineering, photographic, and hydrodynamic data were compiled from numerous sources and analyzed. The bulk of this substudy concentrated on evaluating the historic changes in shoreline position and bathymetry in order to identify regional and local trends. A morphodynamic evaluation based on the historic changes was used to assess the effect of the hydrodynamic processes and construction activities on the shoreline and bathymetry of the study site. This work is reported in Chapters 2 and 3.

Monitoring Substudy activities, which are discussed in Chapters 5 and 6, included: 4-year operation of a National Data Buoy Center (NDBC) offshore directional wave gage and short-term installation of nearshore directional wave gages off Cumberland and Amelia Islands; annual profile surveys for the beach and nearshore of Cumberland and Amelia Islands; winter or 6-month surveys for about 15 percent of these lines; annual profile surveys of the wetlands, shore, and nearshore on the sound side of Cumberland Island; first-year (1988) and final-year (1992) surveys of St. Marys ebb-tidal delta; sediment sampling; and continuing data analysis and interpretation. During the process of data analysis and interpretation, information was compiled and an additional assessment made of the pre- and during-monitoring period dredging and beach fill operations. These are reported in Chapters 4 and 5. The Shoreline Evolution Modeling (or Extrapolation) Substudy utilized the Historical and Monitoring Substudy results to develop input data sets, calibrate and verify the model parameters, and define various cause-and-effect relationships for testing. Several integrated numerical models were used, as discussed in Chapter 7. Ocean shoreline position change was simulated for the southern half of Cumberland Island and for Amelia Island, providing estimates of longshore transport rates. Wave transformation modeling, based on Wave Information Study (WIS) hindcasts and wave data collected during this study, was conducted using the STWAVE model (Resio 1987, 1988a, 1988b). Transformed inshore waves were then used to drive two shoreline change models (a separate model for each island) using CERC's Generalized Model for Simulating Shoreline Change (GENESIS) (Hanson and Kraus 1989; Graves, Kraus, and Hanson 1991).

## **Report Structure**

This report is structured according to the basic study elements that supported each major work effort, as shown in Table 1. Major report sections presented in Volume I describe the background information and regional setting (Chapter 2), the historical data analysis (Chapter 3), the analysis of dredging and shoaling data (Chapter 4), the monitoring data analysis and beach fill assessment (Chapter 5), the tide and wave data collection activities conducted during this study (Chapter 6), shoreline change extrapolation results (Chapter 7), and conclusions of the study (Chapter 8). Volume II provides detailed information on historical and field data sets such as data sources, collection methods, summary tables and plots, and a collection of photographs of the study area.

## 2 Regional, Physical, and Engineering Setting<sup>1</sup>

---

### Introduction

This chapter presents the regional, physical, and engineering setting in which navigation channel modifications were made at St. Marys Entrance and summarizes previous work and available data for the Cumberland Island, Georgia, and Amelia Island, Florida, study area. Chapter 2 contains seven sections that cover physiography, regional geologic setting, coastal processes, local geomorphology and geology, engineering history of St. Marys Entrance, studies of the coastal response to inlet stabilization, and the organization of the coast into morphologic compartments.

Regional and local studies are reviewed in the first four sections to document coastal and geological processes. These sections provide background information on the processes and their effect on shoreline and ebb-tidal delta development. The geologic framework of the study area is the foundation upon which coastal processes act and the regional and local geomorphology evolves. Long- and short-term geologic events create, destroy, and modify sediment bodies and erosional forms, influencing the resultant shoreline configuration and nearshore bathymetry. Coastal morphology responds to hydrodynamic and meteorological processes and their variability. The shoreline and associated beach and offshore bathymetric features migrate laterally and vertically in response to waves, currents, winds, and tides.

The *Engineering History of St. Marys Entrance* section summarizes the history of inlet modifications and related engineering activities based on Federal documents. This section also presents the temporal periods (i.e. engineering epochs) which are used in this report to identify sequential phases of inlet modification. The few published analytical studies of the shoreline and bathymetric changes in the study area are reviewed in the *Coastal Response to Inlet Stabilization* section. The last section defines the spatial limits used to assess the beach and nearshore zones of the study area based on information from studies presented in this chapter and preliminary project results.

The shoreline position and nearshore morphology changes discussed in Chapter 3 and any assessment of the impacts of the incremental deepening, widening, and lengthening of an existing navigation channel are best understood when assessed relative to the project setting. Entrance

---

<sup>1</sup> Written by Laurel T. Gorman and Joan Pope.

channel modifications sponsored by the U.S. Navy in 1987-1988 were inserted into an evolving and variable coastal system comprised of Cumberland Island, St. Marys Entrance, and Amelia Island. This system had already experienced several engineered modifications including construction of jetties, placement of dredged material on the beach, and construction and maintenance of a civil-works and military-authorized channel. Additive effects of the 1987-1988 TRIDENT channel modifications should be viewed from the perspective of the responses associated with initial inlet stabilization and previous engineering activities.

## Physiography

The study area is located in the Southeast Atlantic Coastal Plain, a region of plains and low hills that extends inland to the foothills of the Appalachian Mountains (Figure 3). The Coastal Plain and submerged continental shelf together are about 400 km wide and extend from Cape Cod, Massachusetts, to Georgia. The Southeast Atlantic Plain includes the coastal lowlands ranging from sea level to about 40 m above sea level. Further subdivision of the coastal lowlands includes the regional compartment known as the Sea Islands Downwarp between Cape Fear Arch and Peninsular Arch (Figure 3) (Cooke 1945, Hunt 1974). The coastline of the study area is located in the Sea Islands Downwarp which consists of a series of short, curved barrier islands with well-developed backbarrier marshes. The Sea Islands includes 180 km of barrier islands extending from Bulls Island, South Carolina, to Little Talbot Island, Florida (Brown 1977) (Figure 1).

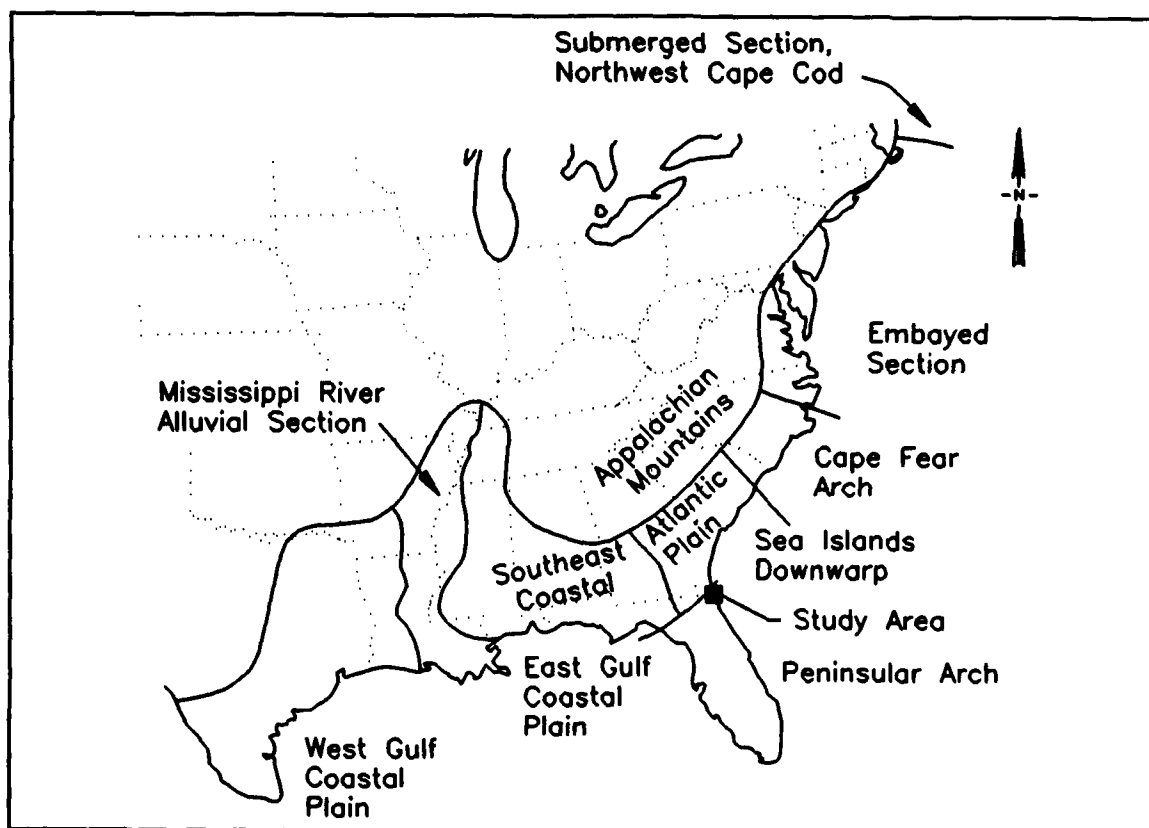


Figure 3. Regional physiography (modified after Hunt (1974))

Recent barrier islands are clastic geological features with a morphology shaped by present oceanographic and climatic processes. About 50,000 years before present (BP), during the Late Pleistocene Epoch, a modern beach system developed along the entire U.S. East Coast. Subsequently, rising seas flooded behind the dune lines, forming lagoonal and estuarine environments. Evidence of this lagoonal flooding is found on Cumberland and Amelia Islands where parallel dune ridges of Pleistocene and Holocene age are separated by thick marsh deposits. The entire sequence of barrier island environments, including previous shoreline positions, dune systems, woodlands, and backbarrier marshes was formed throughout this time (McLemore et al. 1981). The Pleistocene barrier island remnants in the region range from 9 to 19 km in length and 1 to 3 km in width (DePratter and Howard 1977).

Three regional shoreline terrace deposits are recognized as former high sea level stands along the Georgia and Florida coasts. These terraces include the Pamlico shoreline with a maximum elevation of approximately 8 m relative to present mean sea level (MSL),<sup>1</sup> Princess Anne shoreline with an elevation of approximately 4.5 m (MSL), and the youngest or most seaward shoreline with an elevation of about 2 m (MSL). The chronology of terrace positions was defined based on measurements of fossil burrows that form in beach and shallow water environments (Weimer and Hoyt 1964). The earliest documented coastal shoreline submergence has been assigned to the Sangamon Interglacial period which ended about 70,000 to 80,000 years ago (Flint 1964). The remaining shoreline submergences were dated based on the radiocarbon content of shell material from the Georgia coast deposits as reported by Hoyt, Henry, and Weimer (1968). A submergence represented by the Princess Anne shoreline about 48,000 to 40,000 years BP and the last submergence represented by the Silver Bluff shoreline about 30,000 to 25,000 years BP are recognized as the high sea level stands during the Wisconsin Glaciation.

During the early part of the Holocene Epoch (15,000 years BP to present), melting ice sheets resulted in global sea level rise. Pleistocene barrier islands were submerged and covered with marine, estuarine, and reworked terrestrial deposits. A transgressive sequence reflecting the landward migration of the shoreline was preserved in the regional stratigraphic record. About 6,000 years BP, sea level rise slowed and modern-day barrier island environments evolved. Figure 4 depicts the typical response of East Coast barrier islands to sea level rise in a landward and upward migration through time (Leatherman 1983a). Holocene coastal sediments are found in the upper unit of the barrier island facies (Huddleston 1988). During the past 5,000 years, cycles of erosion and deposition have resulted in an irregular coastline consisting of beach ridge complexes and erosional remnants. Except for the area immediately south of the Savannah and Altamaha Rivers, where the shoreline has prograded about 10 and 5.5 km, respectively, the coastline along the Sea Islands exhibits little net Holocene accretion (Howard, DePratter, and Frey 1980).

---

<sup>1</sup> At present, MSL at Fernandina Beach is 0.14 m above National Geodetic Vertical Datum (NGVD); mean high water (MHW) is 1.02 m above NGVD, and MLW is 0.82 m below NGVD. See Chapter 3 for a discussion of the relative displacement between vertical datums.

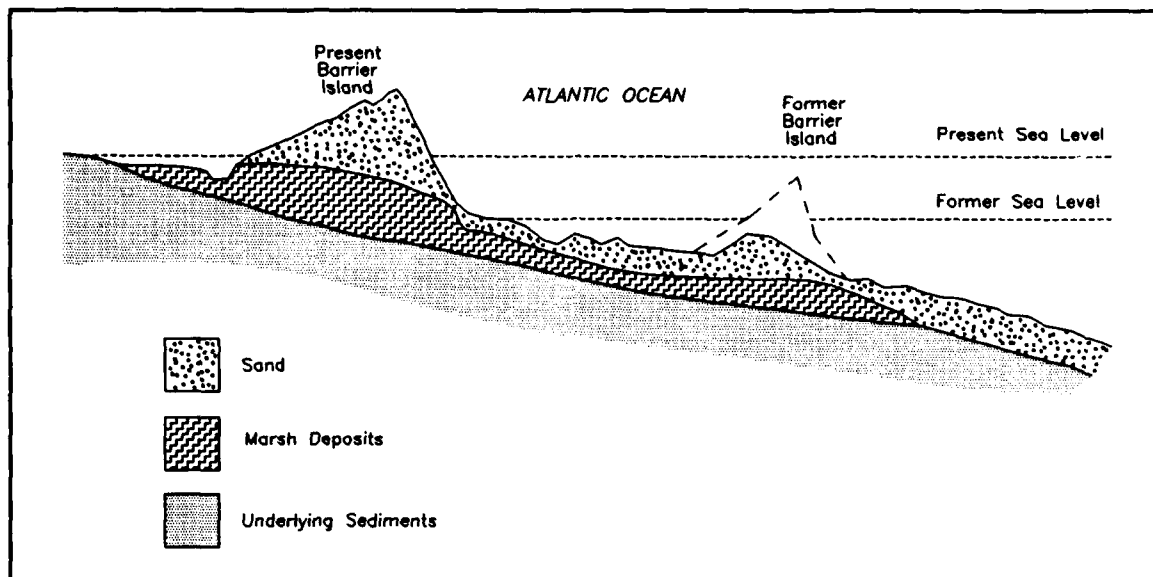


Figure 4. Barrier island response to Holocene sea level change (modified after Leatherman (1983a))

## Regional Geologic Setting

### Satilla-St. Marys River Basins

The South Carolinian and Georgian sea island barrier system (called the Sea Islands) is situated within the Southeast Georgia Embayment (Figure 5), which consists of soft, reworkable marine and fluvial sediment. Over many thousands of years, longshore currents transported sediment away from the mouth of the ancestral Piedmont rivers (Savannah and Altamaha Rivers, Georgia) and to the south, building up the Coastal Plain to its present configuration (Giles and Pilkey 1965). The vertical thickness of the regional sediment basin, which extends from mid-South Carolina, to northeast Florida, varies between 30 and 300 m (Leve 1961). This basin dips toward the coast at a gradient of about 0.4 m per km.

The drainage basin influencing the study area is part of the Satilla-St. Marys River Basins (Figure 6) between 30 and 300 m (Leve 1961). The basins comprise about 14,290 sq km, of which the St. Marys River Basin encompasses 3,909 sq km including the Okefenokee Swamp and 9,138 sq km are in the Satilla River Basin (U.S. Study Commission, Southeast River Basins 1963). The coastal portion of this basin is located in an area of low relief with the streams and rivers traversing wetlands and tidal marshes.

Most of the Sea Islands are classified based on their origin and are referred to as beach-ridge barrier islands. These islands are characterized by high dunes and parallel beach ridges extending the length of the islands as a result of seaward island growth. The Sea Islands are generally recessive at the updrift or northern ends, prograding at the downdrift or southern ends, and stable or slightly accretional in the central portion with numerous vegetated beach ridges aligned parallel to the shoreline (Hubbard, Barwis, and Nummedal 1977). The center of the islands includes a zone of overlap that is influenced by inlets on either end. On average, the alongshore length of

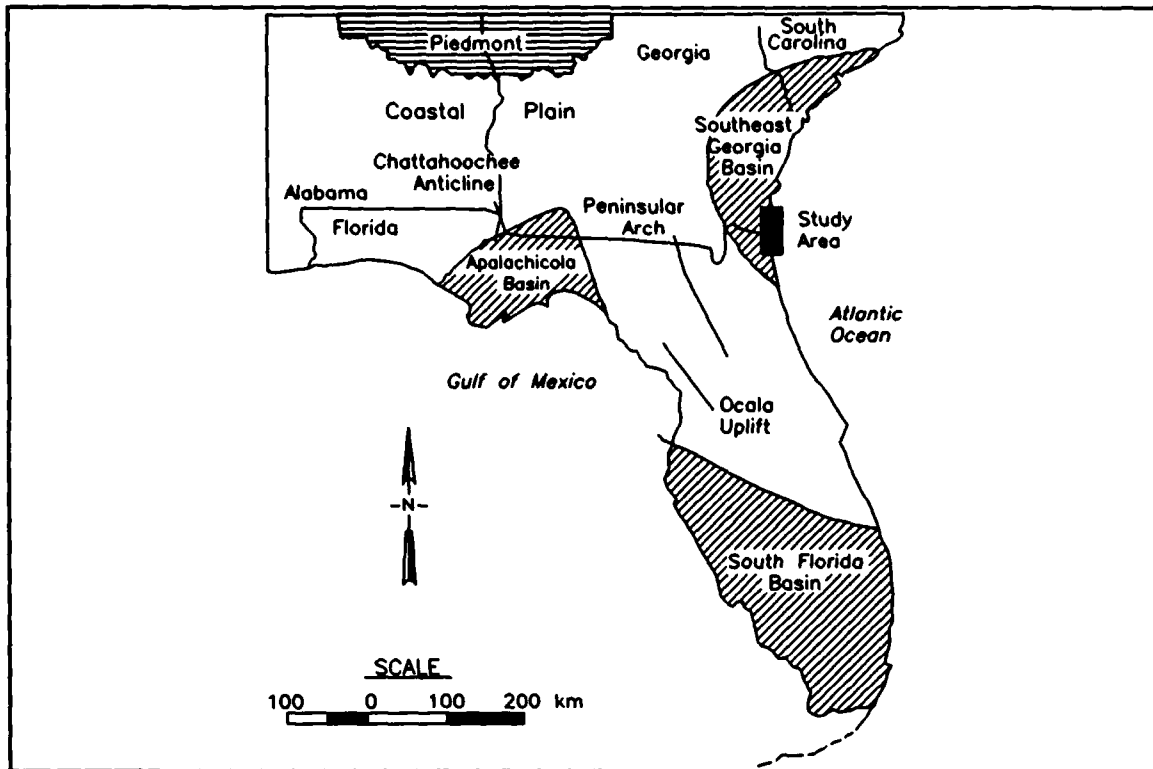


Figure 5. Regional sedimentary basins and major structural features in the southeastern United States (modified after Stringfield (1966))

the Sea Islands is 11 km with fine-grained, well-sorted sediments and gently sloped beaches. The beach slopes range between 1.5 and 2.5 deg (Brown 1977).

### Inlet geology and morphodynamics

Typical inlet morphology for the region, particularly along the southern portion of the Sea Islands, is characterized by a well-developed ebb-tidal delta and a small or absent flood delta (Nummedal et al. 1977, Oertel 1988). Figure 7 illustrates the variation in morphology of the three dominant types of depositional shorelines with respect to tidal range. The tidal inlets and ebb-tidal delta features along the southeastern South Carolina and Georgia coastlines are classified as mesotidal coasts (tidal range of 2-4 m (Davies 1973, Hayes 1975)). Mesotidal environments are recognized by distinct, well-developed, ebb-tidal deltas forming seaward of the inlet (Figure 8). In contrast, microtidal environments (less than 2-m tidal range) have more wave-dominated, smaller inlets, with poorly developed ebb-tidal deltas.

Several regional inlets have slightly less than 2-m tidal range including St. Marys Entrance. These inlets are located on the flanks of the regional embayment with the morphology and inlet characteristics resembling a classical mesotidal coast. Adjacent shorelines along Georgia and South Carolina can be further classified as mixed-energy shorelines that are affected by varying degrees of tidal and wave energies (Hayes 1979). The Sea Islands coastline is dominated by tidal processes with moderate wave energy across a wide shelf. As a result, local geomorphology is characterized by short, wide barrier islands with deep main channels flanked by extensive channel

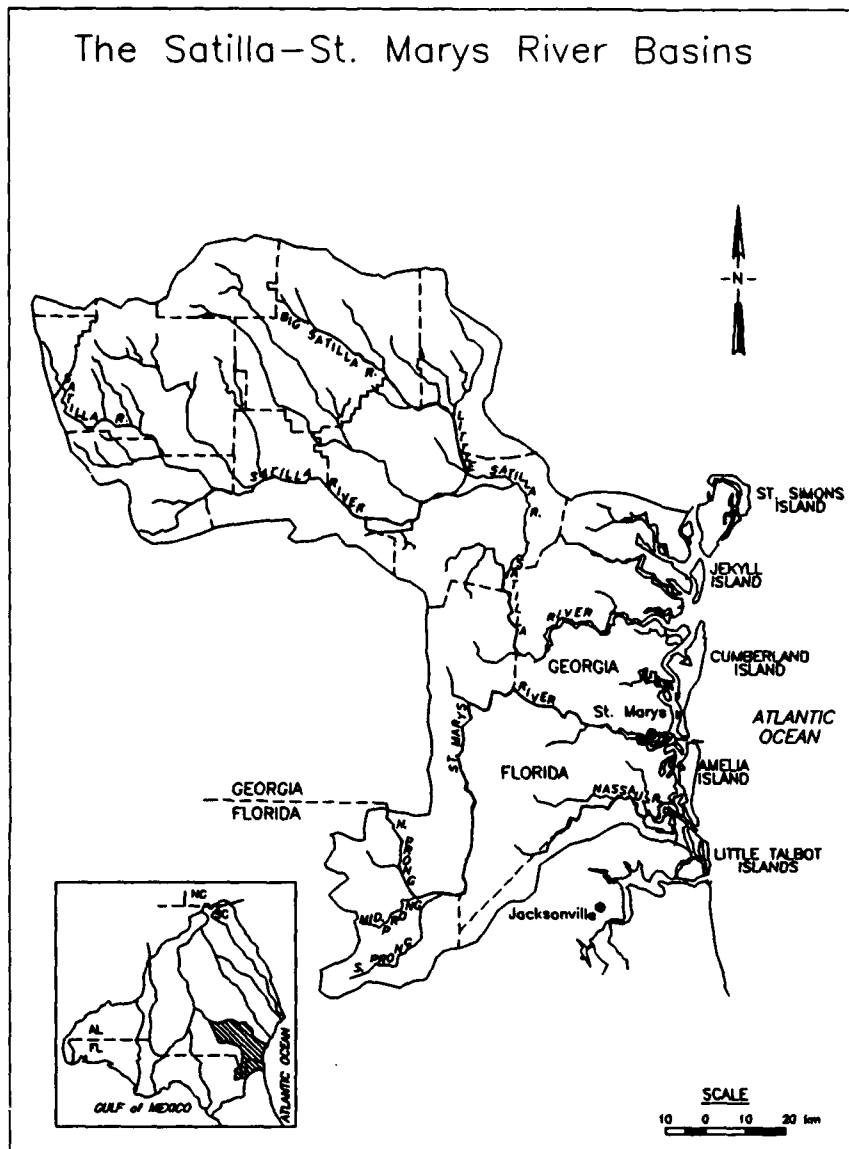


Figure 6. Regional drainage pattern of Satilla-St. Marys River Basins (modified after U.S. Study Commission, Southeast River Basins (1963))

margins (Figure 7). The main ebb channel is usually split at its seaward end to form multiple lobes along the edge of the terminal lobe. In addition, extensive marshes and small tidal point bars occur on the backside of the barrier islands (Barwis 1978). The drumstick-shaped barrier islands are distinctive, with the updrift recurved spit generally accreting and the downdrift side eroding (Hayes 1977). St. Marys tidal inlet system exhibits these shoreline features and ebb-tidal delta geometry.

FitzGerald (1988) proposed three regional inlet models: (a) inlet migration, (b) ebb-tidal delta breaching, and (c) stable inlet (Figure 9). The pre-jetty construction natural inlet at St. Marys behaved most like FitzGerald's ebb-tidal delta breaching model (Figure 9b). Large bar complexes would form north of the main ebb channel, pinching the main ebb channel toward the

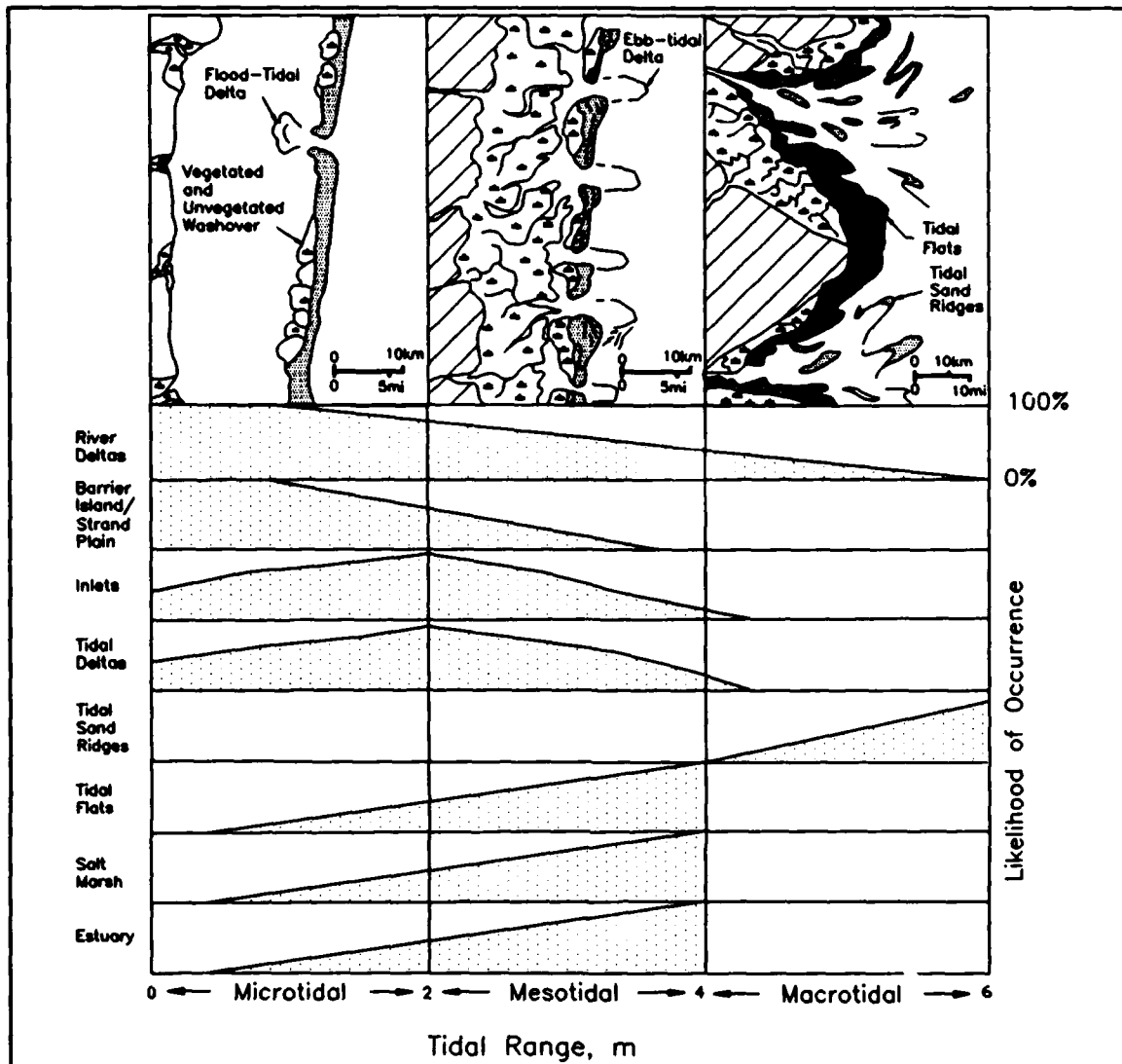


Figure 7. Depositional shorelines classified by tidal range (modified after Hayes (1975))

south. The channel would become hydraulically inefficient and a new channel would open further to the north. The swash bar platform then would be driven onshore by the waves, welding onto the beach south of the inlet. However, since jetty construction, the inlet has become geomorphically stable, with a single main ebb channel which does not migrate. Therefore, the present inlet behaves more like a stable inlet (Figure 9c).

Several regional studies (Walton and Adams 1976, Nummedal et al. 1977, and Oertel 1988) were conducted in the southern part of the Georgia barrier islands in support of FitzGerald's model. Key measurements of the Southern Sea Islands inlet systems between Charleston, South Carolina, and Nassau Sound, Florida, were obtained from these previous studies and are summarized in Table 3. The main channel of these inlets is dominated by strong ebb currents, and the deepest portions of the channels usually have scour holes with coarse lag deposits or large sand waves migrating through the inlet throat (Hubbard, Barwis, and Nummedal 1977).

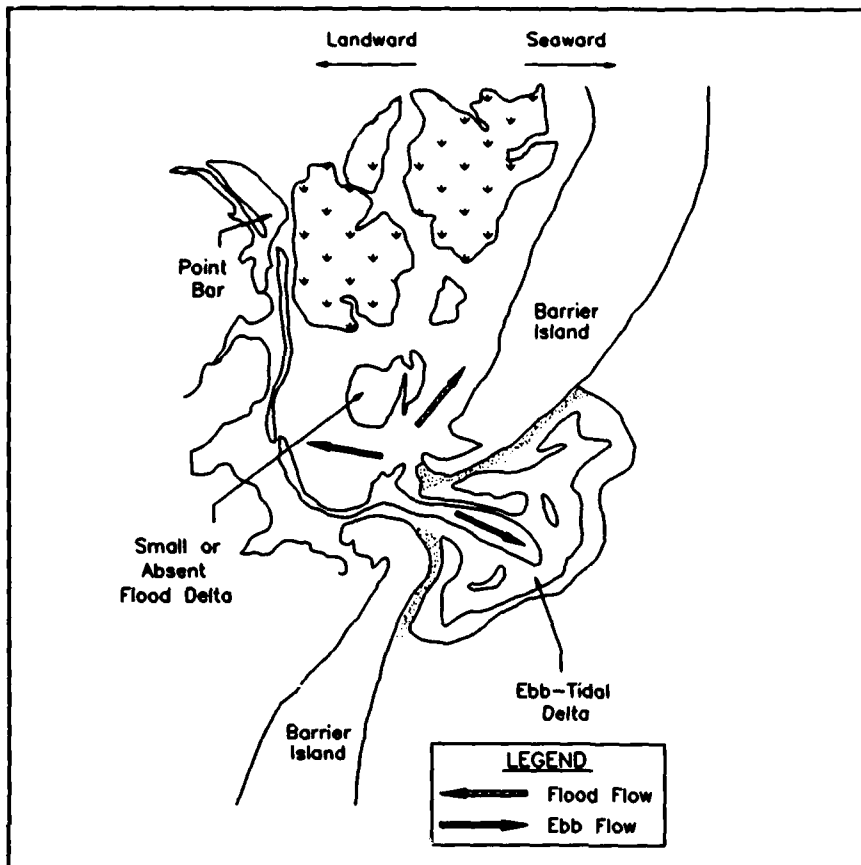


Figure 8. Model of mesotidal inlet (modified after Hayes (1975))

Comparison of the shoreline changes within the region shows a mixed pattern of accretion and erosion on the updrift (north) and downdrift (south) shoreline (Table 3). An important controlling factor of sand supply to the adjacent shorelines is the growth and size of the ebb-tidal delta (FitzGerald and Hayes 1980). Hubbard, Barwis, and Nummedal (1977) noted that the morphology at the terminus of the barrier islands is a function of the size and spacing of the inlets. Generally, ebb-tidal delta features for the Sea Island area extend seaward many kilometers onto the shelf, in some instances as far as 12 km. Large amounts of sediment are transferred and stored on the ebb-tidal delta. Hence, sand bypassing to the adjacent shoreline and nearshore zone is controlled by growth and migration cycles of the ebb delta. Another common feature of these regional inlets is the downdrift orientation of the ebb-tidal delta (Hayes, Goldsmith, and Hobbs 1970). The barrier beach on the updrift side is usually composed of multiple recurved spits, indicating sediment transport directed toward the inlet.

A final consideration in studying regional inlet morphodynamics is the effects of jetty structures on ebb-tidal delta morphology and natural bypassing mechanisms. Morphologic features are altered as the channel flow is confined between jetty structures. The general response and adjustment of the ebb shoal area to jetties are similar for most downdrift inlet systems. However, differences occur based on tidal range, wave climate, local sediment supply, and direction. The most applicable regional example of the impacts induced by jetties on an inlet

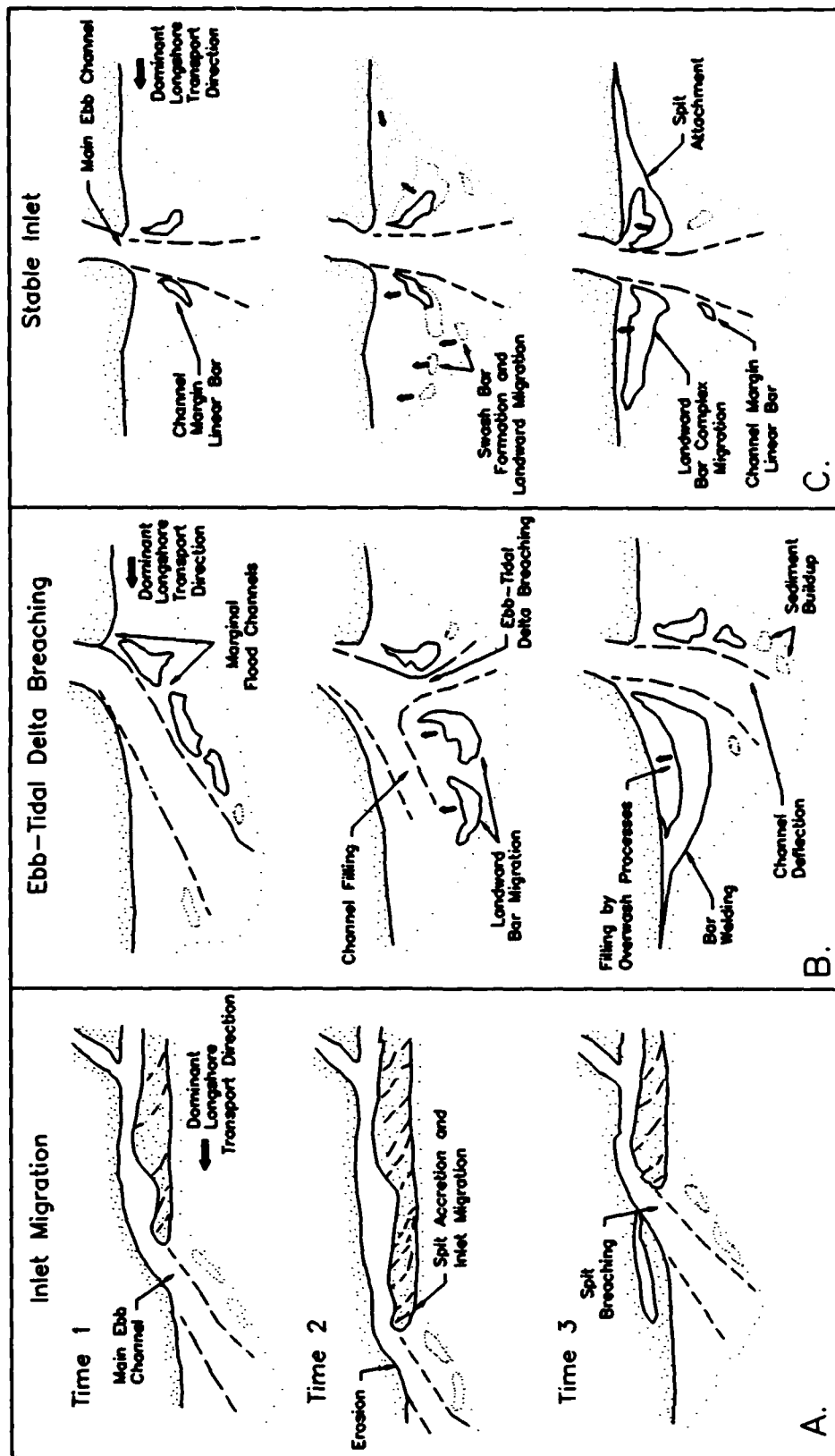


Figure 9. Regional inlet models (FitzGerald 1988)

**Table 3**  
**Characteristics of Regional Inlet Systems, Charleston, South Carolina, to**  
**Nassau Sound, Florida**

Inlet	Tidal Range <sup>1</sup> m		Tidal Prism <sup>2</sup> x10 <sup>6</sup> cu m	Maximum Depth, m	Ebb Delta Volume <sup>3</sup> x10 <sup>6</sup> cu m	Updrift Shoreline Rate <sup>4</sup> m/year	Downdrift Shoreline Change Rate <sup>4</sup> m/year
	Mean	Spring					
Charleston, SC	1.6	1.9	135	15	253	1.9	-2.9
St. Helena Sound, SC	1.8	2.1	-- <sup>5</sup>	15	218	1.2	0.2
Port Royal Sound, SC	2.0	2.4	--	19	209	0.5	-0.4
Calibogue Sound, SC	2.2	2.6	100	15	60	3.3	-1.6
Savannah River, GA/SC	2.1	2.4	--	11	59	2.2	-0.9
St. Catherine's Sound, GA	2.2	2.5	198	20	116	3.9	3.7
Sapelo Sound, GA	2.2	2.4	208	26	115	-7.6	1.5
Doboy Sound, GA	2.0	2.6	110	16	62	6.3	-8.2
St. Simons Sound, GA	1.9	2.3	180	21	87	2.3	-2.8
St. Andrew Sound, GA	2.0	2.3	280	23	168	4.9	0.6
St. Marys Entrance, GA/FL	1.8	2.1	158	20	95	4.5	4.3
Nassau Sound, FL	1.6	1.9	--	11	40	-2.4	2.3

<sup>1</sup> Source: NOAA (1991b).

<sup>2</sup> Source: Oertel (1988).

<sup>3</sup> Sources: Nummedal et al. (1977), Oertel (1988), and Marino and Mehta (1988).

<sup>4</sup> Sources: Anders, Reed, and Meisburger (1990), Knowles and Gorman (1991), Stauble et al. (1993).  
 Shoreline change rate is based on 150-m distance from the inlet. Updrift is north,  
 downdrift is south of the inlet.

<sup>5</sup> No data available.

system and adjacent beaches is Charleston Harbor, South Carolina. Major changes in the geomorphic configuration of the ebb-tidal delta occurred shortly after completion of jetty construction (FitzGerald, Hubbard, and Nummedal 1978; Hansen and Knowles 1988; Pope 1991). Figure 10 illustrates the typical inlet and adjacent shoreline response to jetties, which includes abandonment of the marginal flood channels (Dean 1988, Hansen and Knowles 1988). On a regional scale, the post-jetty ebb delta can impact a significant length of the shore by storing and trapping sediment (Hansen and Knowles 1988, Knowles and Gorman 1991, Pope 1991) and by reorienting the inshore wave climate as waves move over the readjusted deeper ebb delta platform (Kana and Mason 1988).

## Coastal Processes

### Climate

The south Georgia-north Florida climate is characterized by short, mild winters and long, humid summers. The St. Marys area lies within a subtropical zone where 60 percent of the

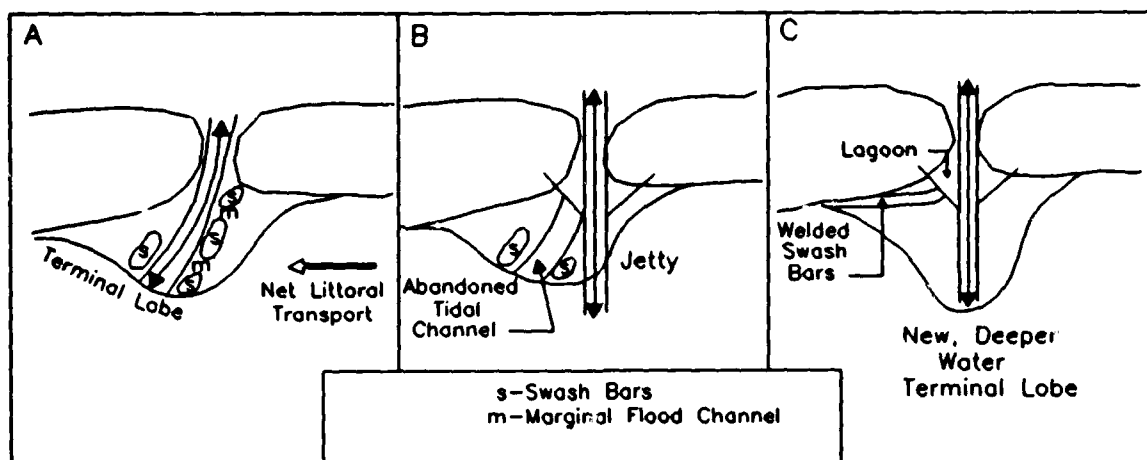


Figure 10. Regional inlet model in response to jetty construction (Hansen and Knowles 1988)

annual rainfall occurs from June through September and 60 percent of the annual evapotranspiration occurs from April through September (National Oceanic and Atmospheric Administration (NOAA) 1987a). The temperature generally ranges between 4.4 and 32.2 °C, with an average annual temperature of 19.8 °C. Normal average monthly precipitation ranges between 6.7 cm in January and 17.8 cm in August, with an average annual total of 107.4 cm/year. During January and February, temperatures occasionally fall below freezing. Snow accumulation of 3.8 cm occurred in February 1987; however, snow is rare in this region (NOAA 1976, 1982).

## Winds

Local wind direction, intensity, and duration influence water circulation, current patterns, and local waves. Wind information is available from the National Weather Service for the nearest station, Jacksonville, Florida. The dominant winds are from the south and southeast. In the fall (September-November), winds are from the northeast and north-northeast and in the winter (December-February) winds are frequently directed offshore. Consequently, the highest waves and strongest southerly littoral currents occur during the fall when stronger northeast winds dominate (Oertel and Howard 1972).

## Waves and littoral transport

The wave climate along the U.S. Atlantic coast is estimated from 20 years (1956-1975) of hindcast wave information produced as part of USACE WIS (Jensen 1983a). This information is supplemented by measurements from NOAA buoys along the coast. The revised Atlantic hindcast station, WIS Station 28 (30.75 °N, 81.25 °W), at a depth of 11 m (Hubertz et al. 1992), and NOAA Buoy 41008 at a depth of 18 m are near the Kings Bay site. Hindcast data from WIS Station 28 and measured data from NOAA Buoy 41008 indicate the mean wave height and peak period in this location are 1.0 m and 7 to 8 sec, respectively, with most waves coming from the northeast to the southeast. The wave climate for south Georgia and north Florida is seasonally variable in height, direction, and period. Waves are higher and have longer periods during the winter months and are more likely to approach from directions north of east. Heights and

periods are smaller in the summer months with directions mainly from south of east. Maximum wave height and period in the hindcast are 4.5 m and 20 sec, respectively.

Breaking waves produce longshore currents which establish the sediment transport direction and rates in the surf zone. Parchure (1982) and Griffin and Henry (1984) discussed the seasonal variation in wave and longshore current regime at the site, and concluded that the predominant transport is from north to south. Richards and Clausner (1988) documented potential trends in longshore transport, based on the WIS hindcast. They found a seasonal variance where monthly net sediment transport was toward the north from March through July. During September through January, dominant transport was toward the south. Average net yearly sediment transport potential for St. Marys Entrance and the adjacent areas was computed as approximately 416,000 cu m toward the south, and average yearly gross transport potential was approximately 765,000 cu m. Independent estimates of transport rates along Cumberland and Amelia Islands are given in the *Coastal Response to Inlet Stabilization* section.

Although the regional dominant longshore transport is toward the south, there is a localized reversal on Amelia Island just south of the south jetty, where structure sheltering (diffraction) and wave refraction over the ebb-tidal delta can produce a local dominant transport toward the north. The result is a tendency for littoral sand to be driven toward the inlet from both Cumberland and Amelia Islands. As littoral sand moves through and across the low and permeable sections of the jetties, tidal currents move significant amounts of sand from the upper inlet throat area seaward to the ebb-tidal delta and offshore bar area (Dean 1988, Pope 1991).

## Storms

Storms can impact a barrier island system in several ways, including sand redistribution in the surf zone, migration of dunes, washover into the backbarrier, and changes to the beach and nearshore profile shape. Some of these impacts are short-lived, such as bar migration and episodic beach erosion. Other impacts may persist over many years and be semipermanent modifications to the system, such as overwash fans, dune erosion, inlet formation, chronic erosion, and channel migration. Several studies (McLemore et al. 1981, Griffin and Henry 1984) have documented shoreline recession on Cumberland and Amelia Islands produced by major storms.

Winter storms in this region tend to form outside of the tropics (extratropical storms or "northeasters") and derive energy primarily from differences in temperature and humidity associated with a cold or warm front resulting in barometric lows. These storms tend to be regional events with a duration lasting up to several days and are more common in the late fall through early spring. Summer storms tend to form in the tropics and can evolve into squall lines, thunderstorms, or well-developed storms or hurricanes. They are more localized and of shorter duration at a given location than extratropical storms. Fully developed summer storms, or hurricanes, however, are characterized by destructive winds, torrential rains, and coastal storm surges 3-7 m or more above the normal tide in extreme cases. These storms occur primarily from late June through mid-October. The most common storms affecting this area are convectively driven summer tropical storms. These are generally short-lived and localized. Summer tropical storms tend to produce minimal changes to the beach.

Hurricanes have been documented since 1871 (NOAA 1987b). There is little available storm information prior to 1871 except for newspaper accounts. The study area was impacted by

significant hurricanes in 1881, 1893, 1896, and 1898, which caused property damage and shoreline erosion. The major hurricane of October 1898 resulted in the southern end of Cumberland Island breaching, connecting the ocean with Beach Creek which drains into Cumberland Sound (USACE 1948). Recent hurricanes of 1944, 1964 (Dora and Cleo), and 1984 (Isidore) also caused shoreline recession. Generally, a storm of hurricane intensity passes within 50 km of St. Marys Entrance approximately every 5 years (Florida Coastal Engineers, Inc. 1976). Abel et al. (1989) hindcast 43 hurricanes which passed the Atlantic seaboard during the period 1956-1975, and developed wave statistics for the various WIS stations. Figure 11 summarizes the maximum wave heights computed for each Atlantic hurricane at the WIS Phase II Station 57. Hurricanes have not been re-evaluated using the revised Atlantic hindcast grid at the time of this publication. The highest hurricane wave hindcast at this station was 7.1 m (Figure 11, Storm 31). This occurred on 18 October 1968 with the arrival of Gladys, which passed across St. Marys toward the east and away from shore.

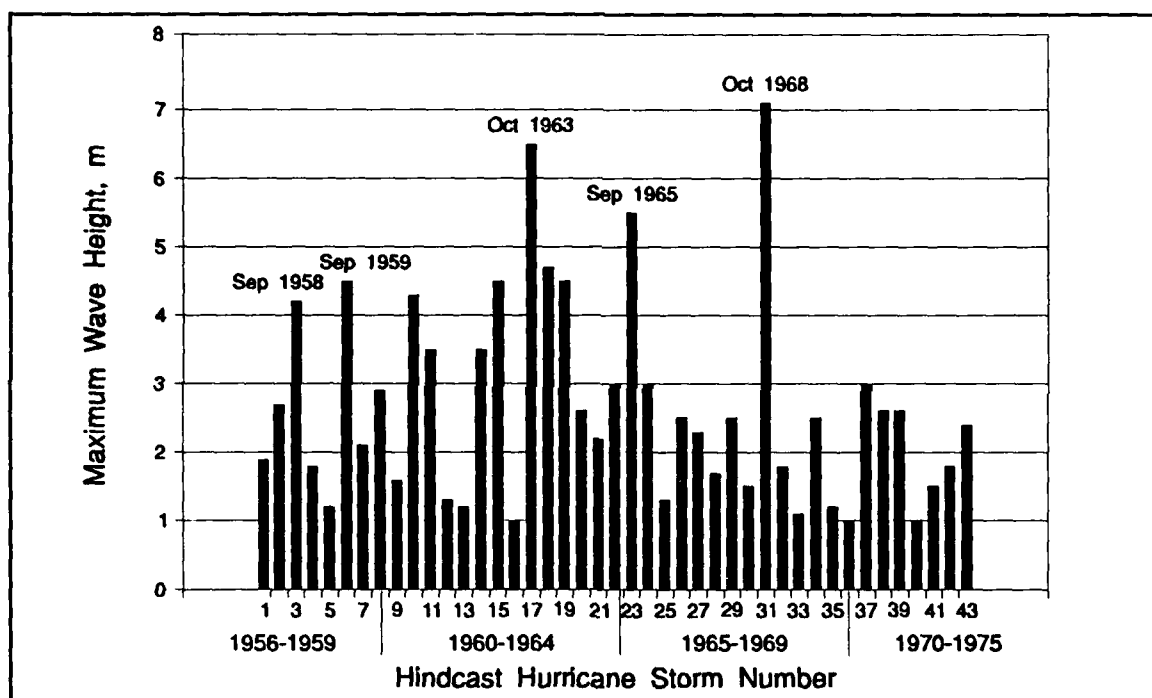


Figure 11. Hindcast Atlantic hurricane wave heights for WIS Station 57

Extratropical storms can also seriously damage beaches, buildings, and coastal structures. High erosion rates and heavy damage were reported for the following extratropical storms: November 1932 (tides were 0.6 m above normal); 24 September - 7 October 1947 (high tides and waves caused the beach to lose 1.5 m of elevation); 8 and 9 March 1962 (estimated maximum deep-water wave height was 12.2 m with wave periods up to 23 sec); 9-13 February 1973; and 24 November 1984 (Parchure 1982, USAED, Jacksonville 1984a).

During the monitoring period, several hurricanes and northeasters moving offshore of the study area caused varying degrees of shoreline erosion and large volumes of shoaling in the entrance channel. Among the most significant events to affect Cumberland and Amelia Islands were Hurricane Hugo on 17 September 1989 and the "Halloween" storm (northeaster) on 30 October

1991. Other hurricanes and tropical storms which affected the area to a lesser degree were Hurricanes Alberto, Chris, and Keith in 1988, Gabrielle in 1989, and Bob in 1991 (USAED, Jacksonville 1993).

### Tides and currents

Tides in the study area are semidiurnal, which is typical for the Atlantic coast. The mean annual astronomical tidal range at the project area is 1.8 m, and the spring range is 2.1 m. This relatively large tidal range dominates the inlet morphology, making it a mesotidal inlet (Figure 7).

Several National Ocean Service (NOS) subordinate tide stations are present along the south Georgia and north Florida coastal region. Table 4 lists the 1992 predicted mean tide level (relative to mean lower low water (MLLW)) and tidal ranges for select south Georgia and north Florida tide stations. The mean annual tide range at the Fernandina Beach gage (located on the northwestern end of Amelia Island) varies over an 18.6-year cycle. The mean tide range is 1.9 m and the maximum spring tide is 2.1 m (NOAA 1991b).

**Table 4**

**Predicted Mean Tide Levels<sup>1</sup> and Tidal Range at Selected NOS Subordinate Stations in South Georgia and North Florida, 1992**

Location	Tidal Range <sup>2</sup>		Mean Tide Level m
	Mean m	Spring m	
St. Simons Light, GA	2.0	2.4	1.0
Jekyll Point, GA	2.0	2.3	1.1
Crooked River Entrance, GA	2.1	2.4	1.1
St. Marys Entrance, (North Jetty), GA/FL	1.8	2.1	0.9
Fernandina Beach (outer coast), FL	1.7	2.0	0.9
Fernandina Beach (Amelia River), FL	1.8	2.1	1.0
Nassau Sound, FL	1.6	1.9	0.8
Mayport, FL	1.4	1.6	0.7

<sup>1</sup> Datum is MLLW.

<sup>2</sup> Source: Tide Tables 1992 (NOAA, 1991b).

A multidirectional current field exists throughout the estuary and the inlet system. Tidal current tables (NOAA 1991a) for the Fernandina Beach Station (0.56 km north of Fort Clinch) indicate that the average velocity during maximum flood is 0.72 m/sec at 275 deg and for maximum ebb is 0.82 m/sec at 87 deg. Measurements made during the Kings Bay Monitoring Study of the physical parameters in the estuary have greatly added to the previously sparse database. Over a tidal cycle, ebb and flood tidal currents through the inlet tend to be balanced with a peak value of 1.2 m/sec and an average speed of 0.64 m/sec (Fisackerly, Fagerburg, and Knowles 1991). The spring tidal prism at St. Marys Entrance had been estimated with a range of 170 to 270 million cu m based on previous studies (Parchure 1982). Fisackerly, Fagerburg, and Knowles (1991) have recomputed the spring prism at 300 million cu m.

## Sea level change

Relative sea level (RSL) change is the combination of global (eustatic) sea level change of the oceanic water level and tectonic or geologic controls which may cause either an uplift or subsidence of the local earth's surface. Sea level changes are highly variable; however, at most of the East Coast tide gages, relative mean sea level has maintained a steady rise over the past century. Eigenfunction analysis of East Coast tide gage records between 1940 and 1979 reveals three distinct regions with a consistent sea level trend (Braatz and Aubrey 1987). The study area is located in the southern region from Cape Hatteras, North Carolina, to Pensacola, Florida. For this area, the rates of RSL rise range between  $2.8 \pm 0.5$  and  $1.8 \pm 0.3$  mm/year, which are moderate rates in comparison with the central and northeastern regions of the Atlantic Coast.

Regional RSL curves show that the last glacial warming epoch began about 16,000 years BP and continued until sea level reached its present stand about 3,000 years BP (Redfield 1967, Scholl and Stuvier 1967, Gornitz and Seeber 1990). Recent studies of global sea level change suggest that there has been a gradual, long-term rise with short-term fluctuations, probably not exceeding 2 m during the past 1,500 years (National Research Council (NRC) 1987). Published predictions for a future rate of eustatic mean sea level rise range significantly. After reviewing the various hypotheses, the NRC (1987) concluded that a reasonable eustatic component of RSL rise was 1.2 mm/year. This value is consistent with previous studies (e.g., Lisitzin 1974; Gornitz, Lebedeff, and Hansen 1982; Barnett 1983, 1984) and provides additional independent support for unpredicted increase in sea level.

The apparent secular trend of the local tide gage, based on the Fernandina Beach tide gage station, indicates a relative rise of 1.7 mm/year (Lyles, Hickman, and Debaugh 1988). Figure 12 shows yearly mean sea level values for the Fernandina Beach gage during the period 1939 to 1988. Yearly mean sea level represents the arithmetic mean of a calendar year of hourly heights. Several studies show slight variations in RSL movement values at the Fernandina Beach gage, such as Braatz and Aubrey (1987) who calculated a rate of RSL rise of  $1.8 \pm 0.3$  mm/year (eigenfunction analysis of tide gage records, 1920-1983). The NRC (1987) adopted a value of 1.6 mm/year for the 1940-1980 Fernandina Beach tide gage data (Figure 13).

As can be seen in Figure 13, the RSL rate in the vicinity of Fernandina Beach is a regional low. Local tide gage records and apparent RSL may be influenced by subsurface stratigraphy and basement structure (Braatz and Aubrey 1987). The project area is located on the flank of the Southeast Georgia Embayment in a geologic structure which may slow local subsidence.

## Salinity and suspended sediments

Salinity in St. Marys Entrance and Cumberland Sound ranges from 26.2 to 35.0 g/kg (Radtke 1985). Study results showed salinity did not vary appreciably within and between the vertical measurement columns. However, at ebb and flood, small differences were detected throughout the project area. Generally, the estuary is a well-mixed system that has only minor freshwater discharge influences. Influx of freshwater from the St. Marys River accounts for some spatial and tidal variation in salinity.

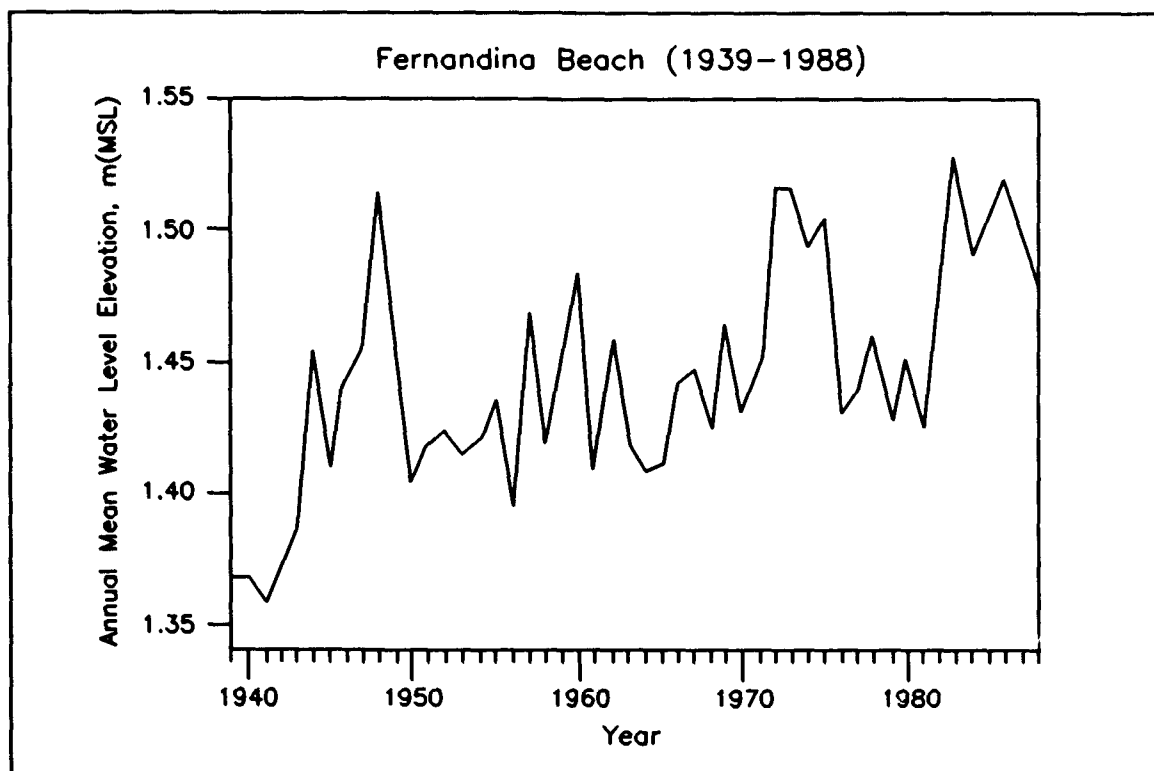


Figure 12. Yearly mean sea level values during 1939-1988 period for Fernandina Beach Station (after Lyles, Hickman, and Debaugh (1988))

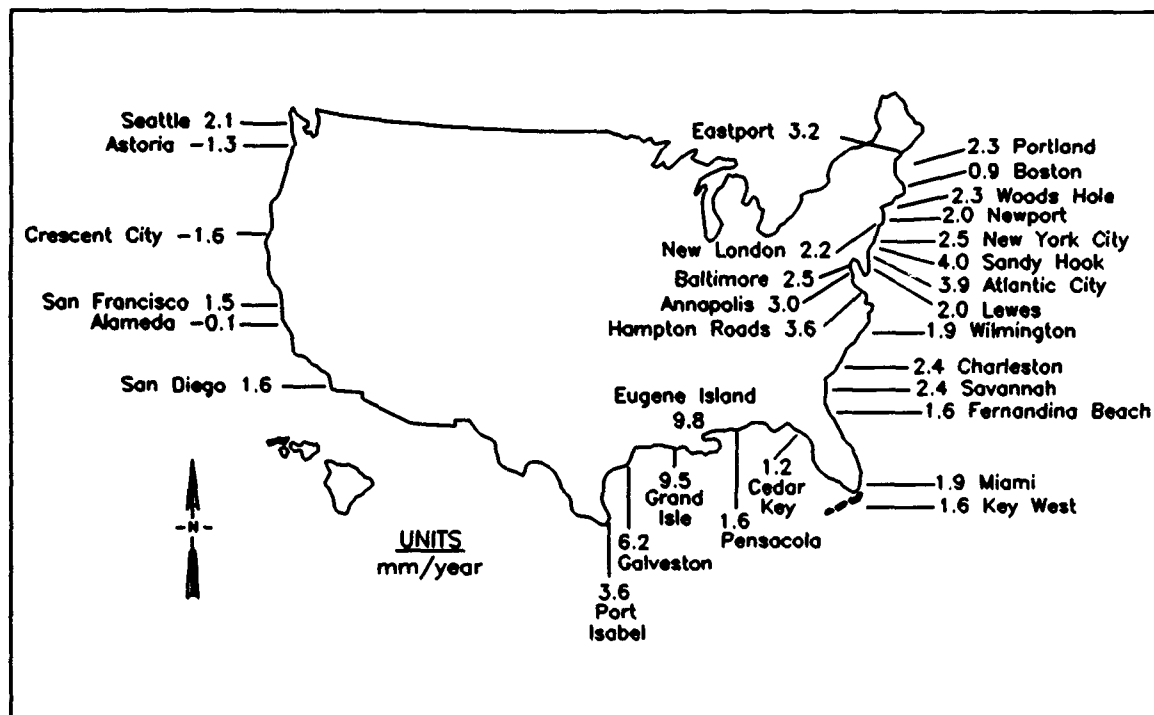


Figure 13. Summary of estimates of local relative sea level changes along the U.S. Coast (NRC 1987, adapted from Stevenson, Ward, and Kearney (1986))

Fisackerly, Fagerburg, and Knowles (1991) found the maximum salinity (mean of 32.9 g/kg) at St. Marys Entrance and minimum salinity (mean of 28.1 g/kg upstream of Kings Bay) as distance from the entrance increased. They identified vertical salinity gradients in locations where the navigation channel is significantly deeper than the surrounding bathymetry, suggesting that the channel acts as a conduit by which higher salinity ocean water flows into the estuary with limited vertical mixing or lateral spreading.

Significant volumes of suspended sediment are transported within the estuary and through the entrance channel. Gross transport of approximately 4,700 cu m (assuming a specific gravity of 1.25) for a measured tidal cycle has been reported. More of the suspended sediment was carried on the ebb than on the flood, resulting in an estimated yield of approximately 459,000 cu m/year of suspended sediment transported seaward through the inlet (Fisackerly, Fagerburg, and Knowles 1991).

## **Local Geomorphology and Geology**

Examination of the long-term record of coastal and shoreline evolution provides information on the spatial and temporal trends of accretion and erosion. Subsurface characteristics exert strong control on the migration of barrier islands and inlet position through time. Geologic cross sections reveal the material and conditions encountered during channel deepening and maintenance of St. Marys navigation channel. A crucial construction factor during deepening has been the occurrence of bedrock which is close to the surface and exposed in some areas of the inlet throat. Core borings were made for both the POSEIDON (1978) and TRIDENT (1988) channel projects. In this report, material is generally presented by location from north to south. The study area geomorphology and geology are subdivided into two barrier islands (Cumberland Island on the north side and Amelia Island to the south), St. Marys Inlet, an extensive wetland and estuary system (Cumberland Sound), the two adjacent inlets at the study limits (St. Andrew Sound, Georgia, and Nassau Sound, Florida), and the nearshore and offshore zones, as presented below.

### **St. Andrew Sound**

St. Andrew Sound separates Jekyll Island from Cumberland Island and is about 4 km wide at its narrowest point. The Sound and adjacent ebb-tidal delta are the largest on the Georgia coast (Table 3). Estimated ebb delta volume is 168 million cu m (Nummedal et al. 1977), which is 43 percent more volume than the St. Marys ebb delta (Table 3). Unlike the jettied main channel at St. Marys Entrance, this inlet exhibits two distinct parallel channels separated by a large shoal (Horseshoe Shoal). The southern predominant channel adjacent to Cumberland Island extends on the shelf to the 15-m depth contour. The northern channel has a thalweg depth of 10.3 m (MSL), whereas the southern channel is considerably deeper with a thalweg depth of 20.4 m. The volume of littoral material transported into the channel appears to be small relative to the ability of the inlet current to remove sediment and scour deeper. The St. Andrew Sound is typical of Georgia's tide-dominated inlets (Oertel 1988).

Similar to the St. Marys Entrance, St. Andrew Sound ebb-tidal delta is asymmetrically skewed toward the downdrift side. On the updrift side, an extensive system of marginal and distal shoals continues 12 km seaward of the inlet. The northern marginal shoals are essentially stable, whereas the shoals on the downdrift side are erosional (McLemore et al. 1981). Dominant

sediment transport is to the south with little seasonal variation. Olsen Associates, Inc. (1990) calculated the average net longshore transport rate along the southern end of Jekyll Island to be 249,000 cu m/year to the south.

### Cumberland Island

Cumberland Island is the southernmost barrier island along the Georgia coastline. The surface of the island includes areas of high relief. However, most of the island is dominated by low-relief features with elevations less than 6 m above MSL. Cumberland Island is approximately 30 km long and 0.8 to 6.4 km wide. The major geologic units within the island include a beach/dune system, interior dune ridge system, barrier island core, and backbarrier salt marshes. Figure 14 shows the boundaries of these zones and their respective geologic time periods. The fine-grained Holocene beach zone is variable in width reaching a maximum of 100 m on the south end of Cumberland Island. The nearshore includes a pronounced ridge and runnel system as a result of the high tidal range (Figure 15). Cumberland Island beach sediments are typically fine quartz sands. Sediments on the foreshore consist of light gray, fine-to-medium sands with a shell content of 5-10 percent (Roberts 1975). Sediment analysis by Giles and Pilkey (1965) identified the heavy mineral fraction to include ilmenite, magnetite, epidote, hornblende, and sillimanite. Origins of the sands and heavy minerals are attributed to marine and terrigenous sediment from the Piedmont (Giles and Pilkey 1965).

Parallel dune ridges up to 17 m high are located adjacent to the backshore area of Cumberland Island. Historical surveys and aerial photographs show a general widening of the dune system along most of the island (McLemore et al. 1981). As a result, these migrating dunes cover inland environments (e.g., meadows, ponds, and forests) and become a sink for beach sand (Figure 16).

The primary subenvironment on the western side of Cumberland Island is the extensive salt marsh, which varies in width from about 0.8 to 2.6 km (Figure 17). This subenvironment exhibits unique vegetative-sediment characteristics. Typical vegetation includes *Spartina alterniflora*, *Spartina patens*, *Juncus* sp., *Distichlis spicata*, and *Salicornia virginica* which is supported by a clay and silt substrate (McLemore et al. 1981). Minor amounts of quartz sand collect along the channel banks and higher elevated areas within the marsh plain, as shown in Figure 18 (Frey and Basan 1985). The woodland subenvironment is situated between 1.5 and 12.2 m above MLW and overlies Pleistocene deposits. Predominant flora includes pine species, live oaks, and palmettos (Hillestad et al. 1975). Woodlands encompass the central portion of Cumberland Island and are the dominant landform on the island.

Subsurface characteristics typical of Cumberland Island are summarized in Figure 19. Several publications including Cooke (1943, 1945), Herrick and Vorhis (1963), Huddlestun (1988), McLemore et al. (1981), and Markewich, Hacke, and Huddlestun (1992) describe the local and regional stratigraphy, as summarized below. Surficial sediments on Cumberland Island are geologically young deposits of Late Pleistocene (50,000-15,000 years BP) and Holocene (15,000 years BP-present) age. These sediments represent both modern and ancient barrier island systems which migrated in response to worldwide sea level changes. Upper Holocene sediments are distinguished by the presence of a soil profile and shell debris. The underlying Pleistocene deposits are characterized by unstained fine-grained, quartz sand found in the central core of the

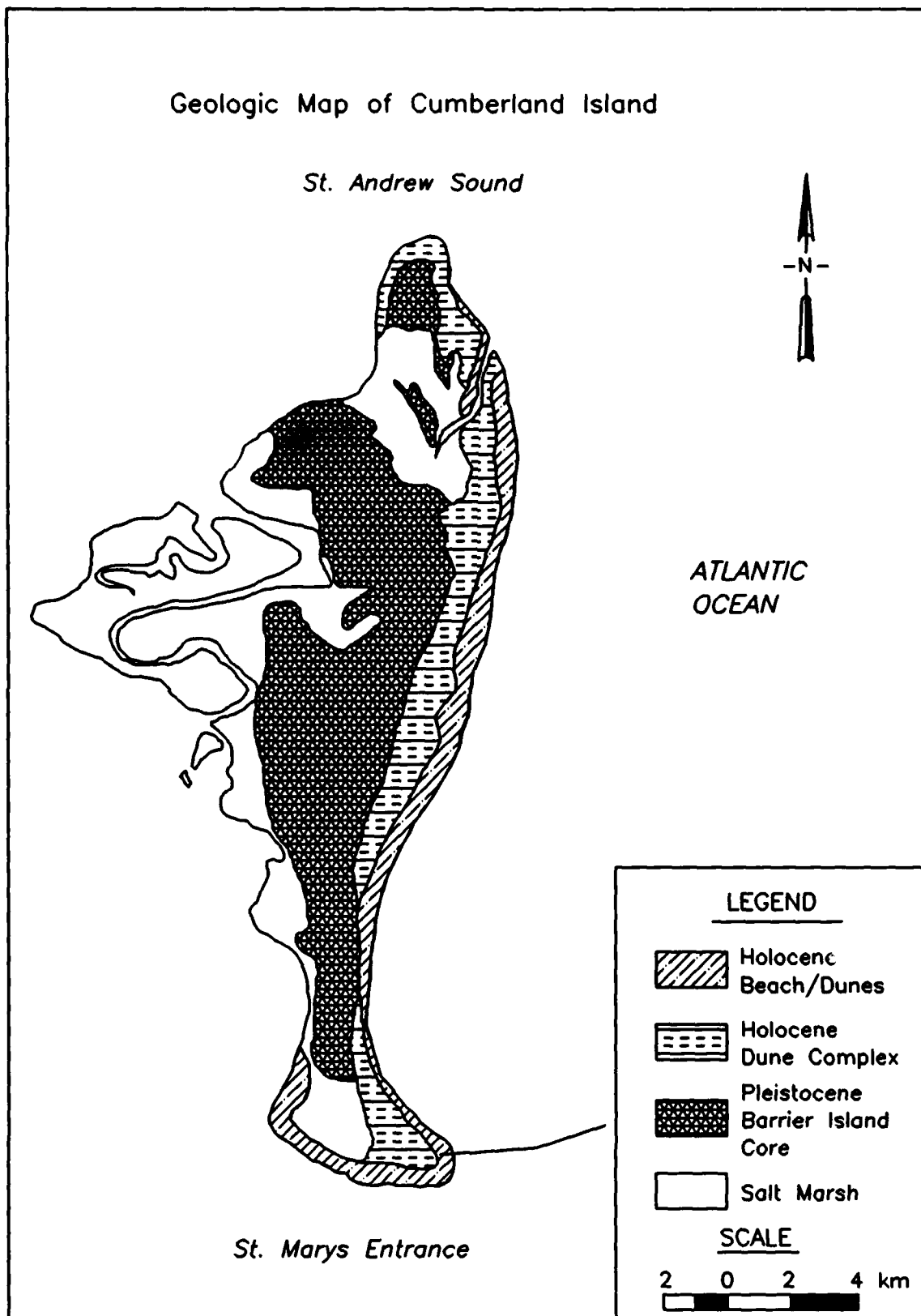


Figure 14. Geology of Cumberland Island (modified after McLemore et al. (1981))

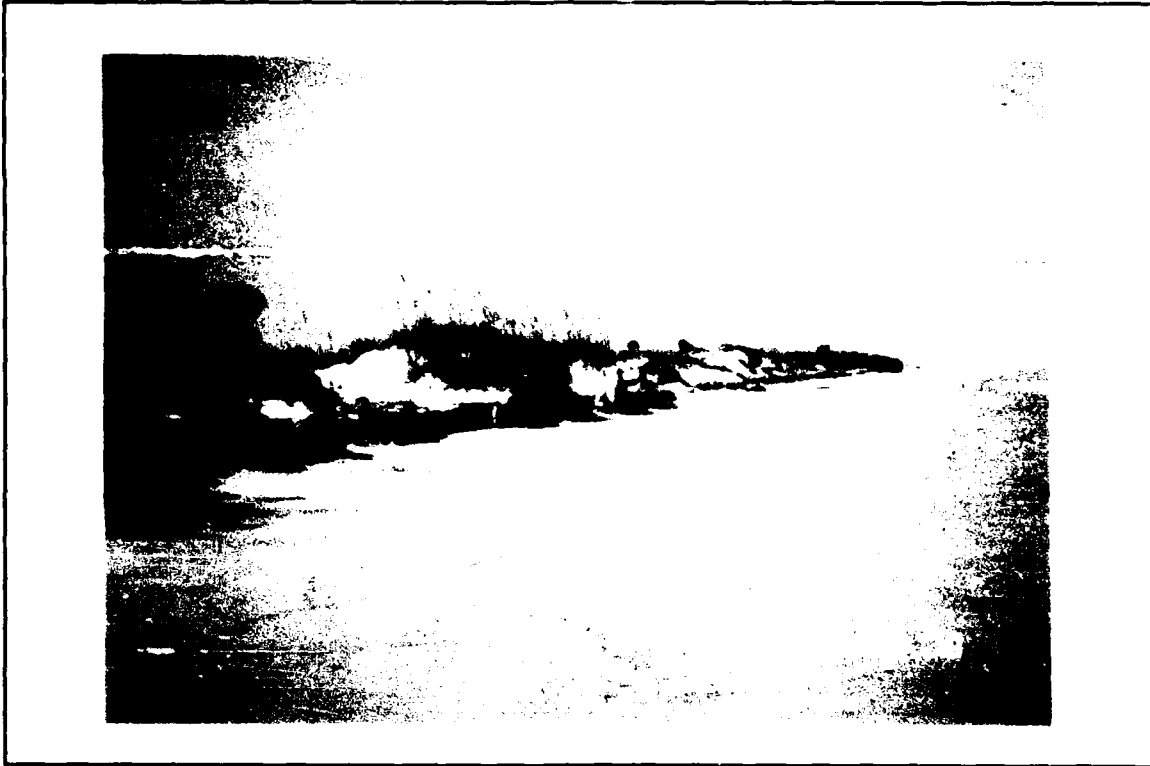


Figure 15. Beach face of Cumberland Island



Figure 16. Dunes migrating along southern Cumberland Island



Figure 17. Backbarrier *Spartina* marshes along the western side of Cumberland Island

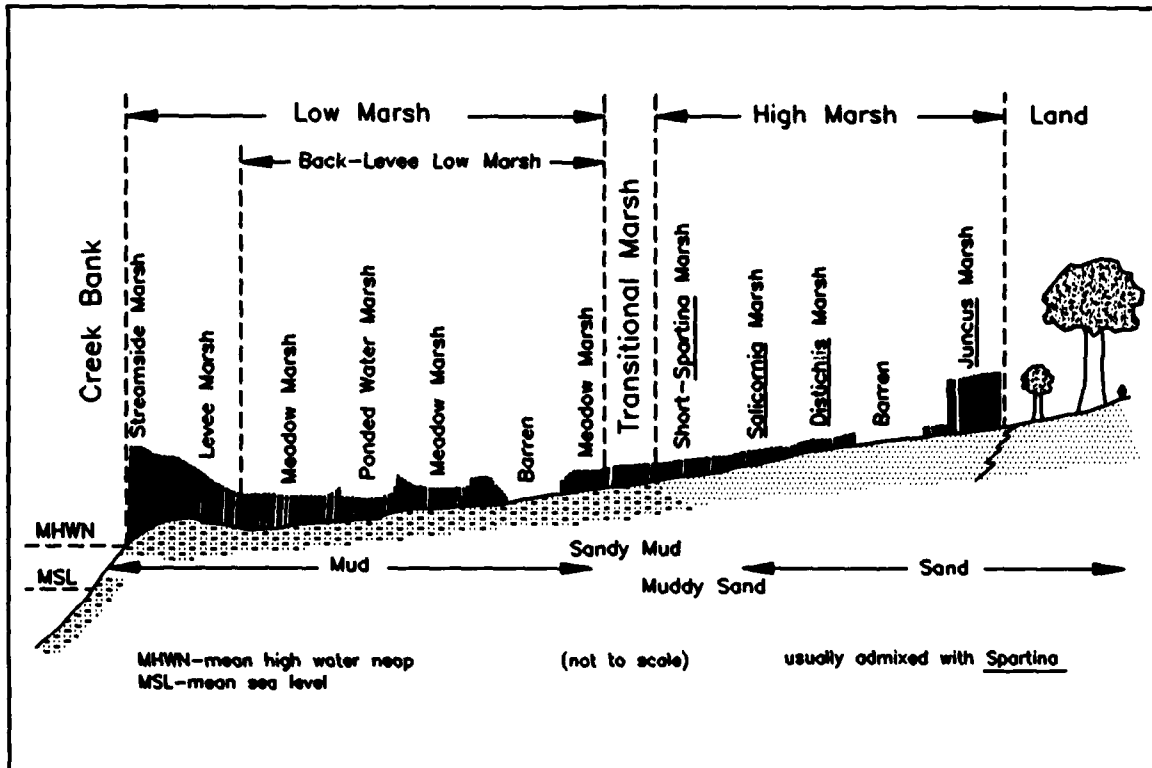


Figure 18. Classification of Georgia salt marshes (Frey and Basan 1985)

GEOLOGIC SECTION - CUMBERLAND ISLAND					
Age	Strat. Unit <sup>1</sup>		Thickness	Section	Lithology
Pleistocene	Satilla		9 m		Sand, fine to medium, dark heavy minerals
Pleistocene	Undifferentiated		11 m		Clay, silty, sandy, micaceous, fossiliferous
Pliocene	Duplin		7 m		Sand, fine to coarse, subangular, fossiliferous
Miocene	middle	Charlton Member	30 m		Dolostone, fine to very coarse, argillaceous, fossiliferous, phosphatic with clay lenses
		Ebenezer Member	31 m		Marl, sand, and limestone, greenish-gray, sandy calcareous, phosphatic, and porous limestone
		Berryville Member	26 m		Silt, dolostone, and sandstone, sandy, argillaceous
	early	Marks Head	12 m		Limestone and clay, phosphatic, calcareous
		Parachucla	32 m		Limestone and clay, sandy, very fine to medium
Eocene	late	Ocala Group	Crystal River	34 m	Limestone, cream-colored, soft to hard, finely crystalline, dense dolomite

<sup>1</sup>Stratigraphic Unit.

Figure 19. Composite geologic column of Cumberland Island (modified after McLemore et al. (1981))

island, and backbarrier marsh deposits consisting of silts and clays. Beneath the Pleistocene sediments is the Duplin Formation of Pliocene Age (6-3 million years BP). This unit consists of heterogenous sediments of shallow marine origin which include fine-to-medium, fossiliferous marine sands with clay and dark mineral lenses (McLemore et al. 1981).

Underlying the unconsolidated sediments is the Miocene Charlton member consisting of an upper calcareous, well-cemented limestone unit. Beneath the Charlton is the Hawthorn Formation described as a gray to blue-green, clastic, phosphatic, fossiliferous carbonate limestone. Based on core data these two units have a total thickness of 100 m (McLemore et al. 1981). Underlying the Miocene sediment sequence are Eocene age sediments known as the Jackson and Claiborne Group. The upper Eocene, Ocala Limestone, consists of fossiliferous limestones that are unconformable beneath the Miocene Series. A deep well in southern Cumberland Island penetrated through the top of the Ocala Group to a depth of 157 m (MSL). Further subdivision of the Ocala Group includes three formations (ascending order): the Lower Inglis, the Williston, and the Upper Crystal River Formations. Well logs indicate the thickness of the Ocala Group is about 145 m.

## Cumberland Sound/St. Marys Tidal Inlet Complex

Cumberland Sound is located on the western side of Cumberland Island and is classified as a bar-built estuary in a coastal lagoon environment characterized by shallow bars, exposed at low tide, and enclosed by backbarrier islands. Extensive marshlands are situated adjacent to Cumberland Sound as well as tidal creeks and inlets. An intricate system of channels and creeks contributes sediment during flood periods and allows tidal exchange of sound and ocean water. On the ocean side, St. Marys Entrance connects the Atlantic Ocean to Cumberland Sound and St. Marys River.

A distinctive surficial sediment texture was described by McLemore et al. (1981) for the backbarrier marshes. In this estuarine subenvironment, fine materials in the silt and clay range are found in the immediate subsurface together with high organic matter derived from decomposed marsh plants and animals. Clays are classified as a mixed layer of kaolinite and montmorillonite. The local stratigraphic sequence consists of an upper unit of dark green, clayey fines and clay with interbedded units of sand ranging from thin lenses up to 3.0 m thick. Generally silt and clay beds grade laterally into silty clay and clayey sand, which probably represent quiet deposition interrupted by high-energy wave conditions from storms. Marsh sediment of Cumberland Sound typically consists of an average sediment composition of 44 percent silt and clay, 29 percent sand, and 27 percent silty sand (McLemore et al. 1981).

Just prior to TRIDENT channel deepening, a large-scale geotechnical investigation of the lower Cumberland Sound (Station 220+00) to St. Marys inlet throat (Station 0+00) was conducted by USAED, Savannah. The USAED, Jacksonville, conducted a geotechnical investigation from the inlet throat (Station 0+00) seaward to the end of the channel (Station 250+00, Cut 2N) (Figure 2). Cores were taken in order to characterize the subsurface using American Society for Testing Materials (ASTM) standards and the *Unified Soil Classification System* (USAEWES 1960). A series of cross sections constructed from boring logs by USAED, Jacksonville, in 1981 and available seismic records were used to develop the stratigraphy of St. Marys Tidal Inlet Complex (Figures 20 and 21). Quaternary deposits are rarely present due to the deepening of the channel. Where dredging has not occurred, cores indicate a relatively thin layer of undifferentiated Holocene and Pleistocene fine sands (about 4 m thick) and soft, low plasticity clays and silts overlying cross-bedded Pliocene quartz sands and, in places, Miocene limestone outcrops on the channel floor. A lack of thick Quaternary deposits and fossil material is indicative of an erosional unconformity (an interruption or missing depositional sequence of sediments).

Surface expression of the Tertiary bedrock is an important consideration in dredging and maintaining the channel. Two types of rock are common: a foraminiferal, calcareous-cemented limestone and a dolomitic siltstone. The Pliocene-age unit has an erosional surface separating the *unconsolidated* sediments of Quaternary age from the older Tertiary sediments. Due to the dip angle of the underlying older strata, the Tertiary dips to the north and northeast. Core logs for borings through the inlet throat show the Tertiary surface varies from -12.5 to -18 m MLW. Variability in the surface is attributed to erosional processes that occurred as sea level changed. Geologic and seismic cross sections indicate a carbonate mound and karst topography located in the inlet throat (Figure 20). In addition, seismic records show sand waves up to 2.3 m high through the inlet throat. Hence, surface channel sediments range from fine sands, and silty sands, to silty clays. Similar sediments are found along the adjacent channel side slopes. Materials from sand bypassing, channel side slopes, and flood-ebb shoals are deposited along the

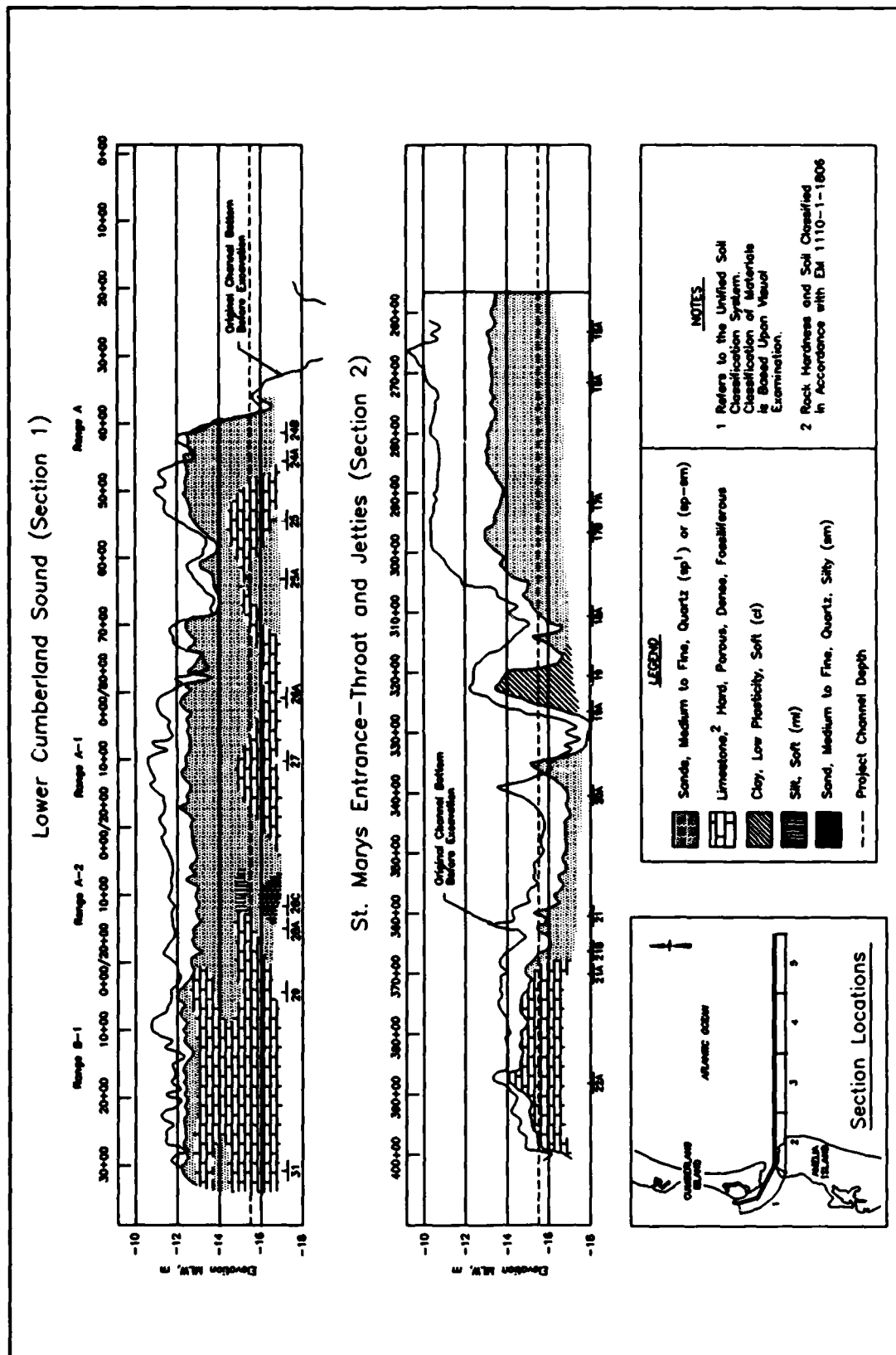


Figure 20. Cross section of lower Cumberland Sound and inlet throat area (unpublished map USAED, Jacksonville (1981))

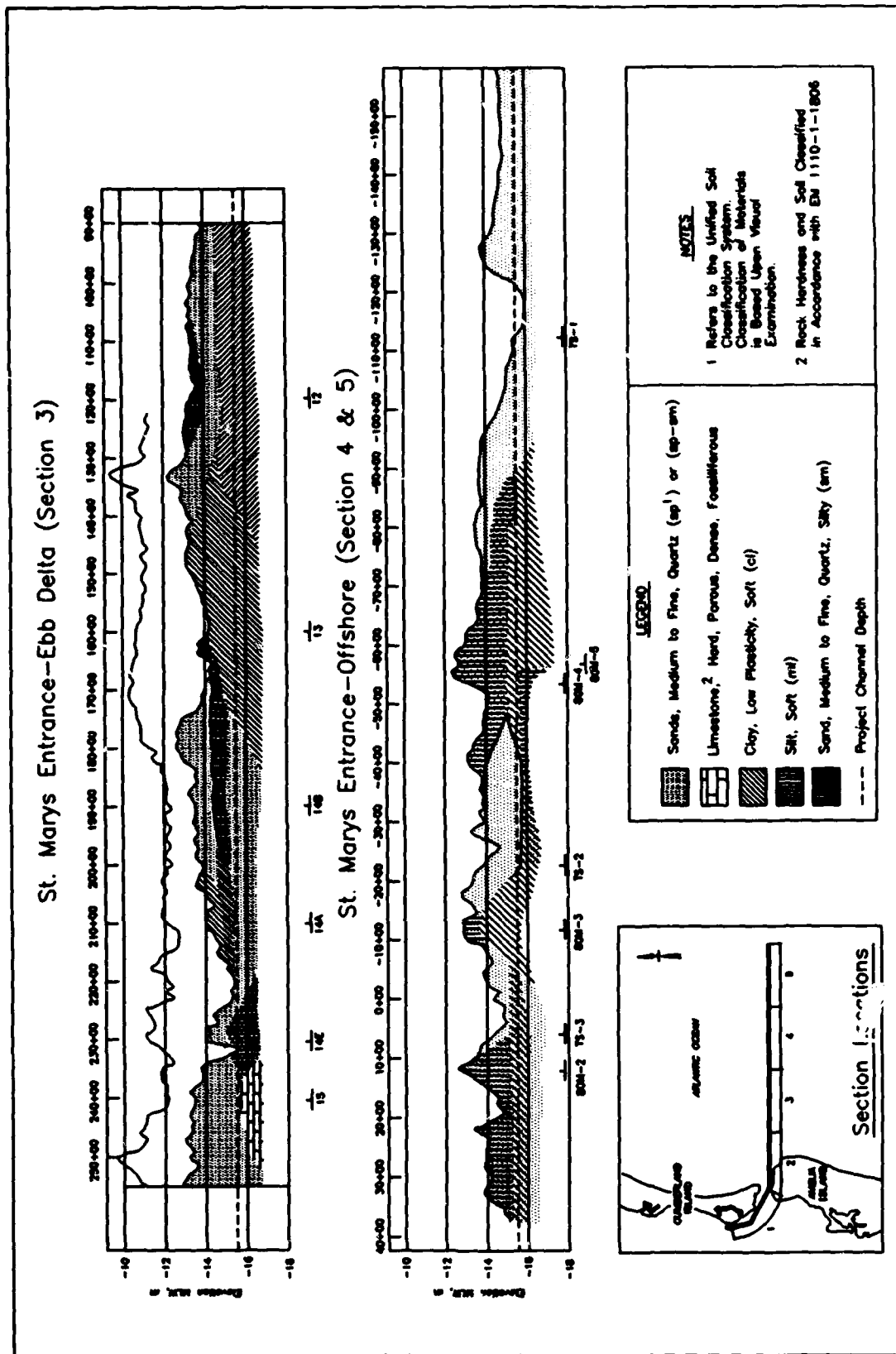


Figure 21. Cross section of channel through jetties and ebb delta (unpublished map USAED, Jacksonville (1981))

channel bottom. Other anthropogenic factors that may influence the described channel bottom characteristics include turbidity, disturbances from vessels, and the coring equipment (jackup rig) used to collect the borings. Further discussion of the type of material dredged along the ocean entrance channel can be found in Appendix C.

Material composition along the channel walls varies slightly from the centerline channel sections of St. Marys Entrance seaward to the offshore zone. As part of the geotechnical investigation for the TRIDENT channel deepening, core borings were drilled along the north (left) bank, centerline, and south (right) bank of the navigation channel. The logs of these cores indicate that most of the sediment is fine-to-medium clean sands and fine silty sands. The thick deposits of clean sands are part of the Pliocene aquifer sands. The upper fine silty sands as found along the inlet throat area (Figure 20, Section 2) represent Recent or Holocene littoral sands. An exception to these sands occurs on the north bank of the throat section where massive clay units represent mudflat deposition. Along the jetty section (Figure 20, Section 3), the clean fine sands continue to occur along both channel walls between elevation 13 and 18 m (MLW). The presence of clay and silt material represents the former position of the offshore zone beyond the historic platform (Station 320+00,<sup>1</sup> Figure 20, Section 3). Beyond the jetties, the new ebb-tidal delta feature (Stations 230+00 to 160+00) consists of massive, planar sands about 1.5 m thick with occasional lag deposits of clay material (Figure 21, Section 4). At the edge of the ebb-tidal delta, the silty sands are distributed along the lobe (Figure 21, Section 5). Just seaward of Station 160+00, the offshore zone consists of clays (Stations 160+00 to 145+00), and fine silty sands and clean sands (seaward of Station 145+00).

### **Amelia Island**

Amelia Island is the northernmost barrier island in Florida. It is situated between Cumberland Island and Little Talbot Island and bounded by St. Marys River on the north and Nassau River on the south. There have been limited unpublished reports<sup>2</sup> and USACE reports (USAED, Jacksonville 1984a, 1984b, 1993) describing the local geology and physical setting of Amelia Island. The interpretation presented herein is primarily based on available maps, channel and borrow area borings, and sediment beach and nearshore grab samples taken by USAED, Jacksonville, in support of channel modifications and erosion control projects. Amelia Island lies within the northern or proximal zone of Florida where the dominant features are high, broad uplands pot-marked and intersected by dry sinkholes and intermittent streams and lakes (Cooke 1945). East of Amelia River, the land surface is part of the coastal lowlands which slope gently seaward. The island is approximately 21 km long with a maximum width of about 3 km. Land surface elevation is less than 12 m (MSL). Cross-sectional zonation of Amelia Island is similar to Cumberland Island and includes the following geomorphic features: a gentle-sloping beach zone backed by a series of irregular dunes 9-12 m high, landward of a low ridge adjacent to a sandy plain extending landward for about 600 m, and marshlands on the backside of the island.<sup>2</sup> Within the marshlands, tidal creeks and mesotidal marshes are separated by small channels.

---

<sup>1</sup> Station numbers established prior to TRIDENT channel deepening.

<sup>2</sup> Wallace, McHarg, Roberts, and Todd (1971). "A report on the master planning process for a new recreational community," unpublished report for Amelia Island Property of the Sea Pines Company, Hilton Head Island, South Carolina.

Amelia Island is characterized by moderate-relief, barrier and backbarrier deposits, and a slightly arcuate shoreline. Figure 22 shows the geologic environments of Amelia Island. The formation and extent of the landforms are very similar to Cumberland Island except that the southern end of Amelia Island displays pronounced overwash features. The beach zone is moderately developed with residential and commercial buildings. The beach geometry and sedimentary characteristics are influenced by beach fills and engineering structures, as discussed in the next section of this chapter. Figure 23 is a typical view of the northern end of Amelia Island with a wide beach-fill berm.

Based on premonitoring studies, the native beach material as assessed by USAED, Jacksonville (1984a) consisted of fine-to-medium quartz sands with abundant shell material. Along the northern and central beaches, native sands were classified as fine grained with a mean of 0.28 mm and a standard deviation of 0.48 mm. The narrow beaches along the Fort Clinch shoreline were much finer with a mean grain size of 0.20 mm and standard deviation of 0.71 mm. Other mineral constituents of the native beach material included ilmenite, monazite, rutile, zircon, epidote, and magnetite (Bludgett 1956). The presence of these minerals in the beach and dune deposits indicated that sediment originated from the Piedmont rivers and historical transport has been to the south. Since 1978, the characteristics of the beach material, particularly along the northern end of Amelia Island, have been influenced by beach fills using only beach-quality sand, sometimes containing shell material, dredged from the St. Marys navigation channel. Sediment characteristics and statistical parameters were studied as part of the Coastal Monitoring Program and are summarized in Chapter 3 and Appendix D. A detailed discussion of the native and post-beach fill sediment grain sizes is also contained in Appendix D.

The subsurface characteristics of Amelia Island were reported by Cooke (1945) and Leve (1961, 1966) in several Florida Geological Survey reports. Core logs, electric logs, and rock cuttings were analyzed to define subsurface units in Nassau County. Figure 24 represents the composite geologic column of Amelia Island based on core logs collected by USAED, Jacksonville (1984b) and water well logs (Leve 1966). The upper surface is composed of undifferentiated Recent and Pleistocene Age, yellowish, fine-to-medium quartz sand and clayey sands. Thickness of this unit is about 10 m (Figure 24). Below the relatively shallow Quaternary sediments and Pliocene sands is the Upper Miocene Hawthorn Formation. These sediments are characterized by interbedded, gray-green calcareous silts and fine-to-medium, friable limestone and marl (Figure 21). This unit, about 6 m thick, appears to be gradational. With depth, the Hawthorn Formation is distinctive due to the presence of phosphate. Other lithologic properties include gray to blue-green, calcareous, phosphatic sands, clays, clayey sands, and interbedded, discontinuous lenses of sandy phosphate, limestone, and dolomite. Beneath the Hawthorn Formation, more massive, fossiliferous, and crystalline marine limestone of Eocene age are found. The underlying limestone is part of the Ocala Limestone, which is the principal artesian aquifer in Florida (Stringfield 1966).

Higher in the geologic column near ground surface is a freshwater lens with a maximum depth of 20 m (McLemore et al. 1981). Groundwater is withdrawn both regionally and locally for municipal, industrial, and agricultural use by the town of Fernandina Beach, privately owned Amelia Plantation community, and the pulp mills located in Fernandina Beach. Further evaluation of the hydrogeological system for the study area is contained in Cofer-Shabica and Hargrove (1991), Herndon and Cofer-Shabica (1991), and Wilson, Rose, and Cofer-Shabica (1991) which is part of the Kings Bay Environmental Monitoring Study being conducted by NPS.

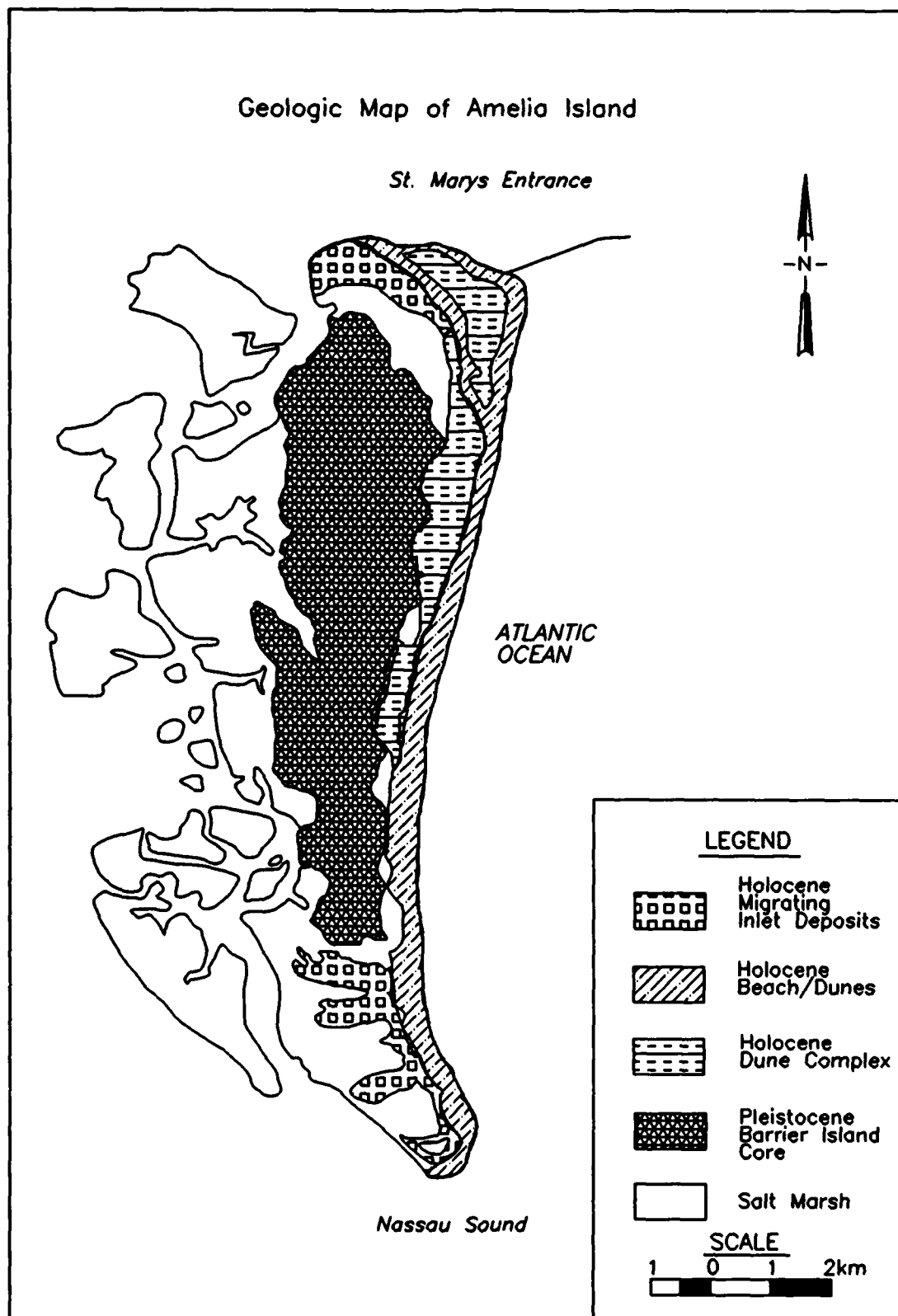


Figure 22. Geology of Amelia Island (modified after Wallace et al. (1971))



Figure 23. View of northern Amelia Island beach

UPPER GEOLOGIC SECTION - AMELIA ISLAND				
Age	Strat. Unit'	Thickness	Section	Lithology
Quaternary	Undifferentiated	6 m		Sand, gray, fine quartz, slightly shelly
				Sand, grayish tan, fine to medium, very shelly
				Sand, gray, less shelly
		4 m		Sand, gray, silty, slightly plastic, slightly shelly
				Sand, fine, no silt or clay
Pliocene	Duplin	1.5 m		Sand, gray, clean
'Stratigraphic Unit				

Figure 24. Composite geologic column of Amelia Island (based on USAED, Jacksonville (1984a))

## **Nassau Sound**

Nassau Sound, located at the southern end of the study area, is considerably smaller than St. Andrew Sound and Cumberland Sound. The inlet there is about 2 km wide, with depths ranging between 6 and 10 m (MLW). This inlet has not been extensively studied and available scientific information is limited. Nassau Sound inlet is classified as a natural downdrift offset inlet with two inlet channels separated by large shoals. The ebb-tidal delta contains 40.5 million cu m of material based on bathymetric change during 1871-1970 (Marino and Mehta 1988). On both sides of the inlet, shoals have typically migrated to the south following the trend of the main channel. Available current tables for Nassau Sound (mid-Sound, 1.6 km north of Sawpit Creek) indicate that the average current during maximum flood is 0.9 m/sec at 312 deg and for maximum ebb is 0.9 m/sec at 135 deg (NOAA 1991a).

## **Inner shelf zone**

Much of the study area lies within the submerged coastal zone and is part of the South Atlantic Inner Continental Shelf (Meisburger and Field 1975). The immediate surface is a broad, low-relief shelf with relict Pleistocene and Holocene terraces, and submerged beach sand ridges. The nearshore zone is defined as extending from the water line seaward to about the 12-m depth contour based on available data sets and the seaward limit of ebb-tidal delta features. Offshore features are inlet related and based on bathymetric morphology and local seismic records (McLemore et al. 1981, Henry and Kellam 1988) (Figure 25).

Typically, sedimentary deposits consist of thin, discontinuous Quaternary sands overlying Tertiary sands and limestone. Surficial sediment ranges from quartzitic to subarkosic (contains feldspar) sands (Milliman, Pilkey, and Ross 1972). A reconnaissance study of the inner shelf by Meisburger and Field (1975) identified the nearshore sediment distribution as very fine-to-medium, poorly sorted sands ranging from 0.09 to 0.35 mm. These shoreface sands extend offshore 7.4 km or to about the 15-m depth contour. Beyond the 15-m depth contour, the inner shelf is dominated by fine-to-coarse, moderately well-sorted quartz sands. Across the outer shelf, sediments are predominantly Tertiary quartz-foraminiferal, very fine sands, and dolomitic and phosphatic sands.

Several investigators (Pilkey and Field 1972, Meisburger and Field 1975, Henry and Kellam 1988, Huddleston 1988) conducted regional geophysical studies of the inner shelf. Seismic reflection profiles, similar to the representative seismic cross section in Figure 26, show sedimentary structures and historical inlet channelization. The upper surface or Quaternary deposits are characterized by weak, discontinuous horizontal reflectors except where cut and fill fluvial channels incise into the underlying Pliocene deposits. The Pliocene sands are the thickest and most extensive along the Sea Islands. Along the east coast, the Pliocene section is characterized by cross-bedded foreset sand bodies indicative of a high sedimentation rate as found in the vicinity of St. Andrew Sound and St. Marys Entrance. Underlying these unconsolidated sediments is the prominent reflector of the middle Miocene erosion surface. The strong reflectors exhibit parallel "banding" which is traceable throughout the continental shelf (Woolsey 1977, Kellam and Henry 1986, Henry and Kellam 1988).

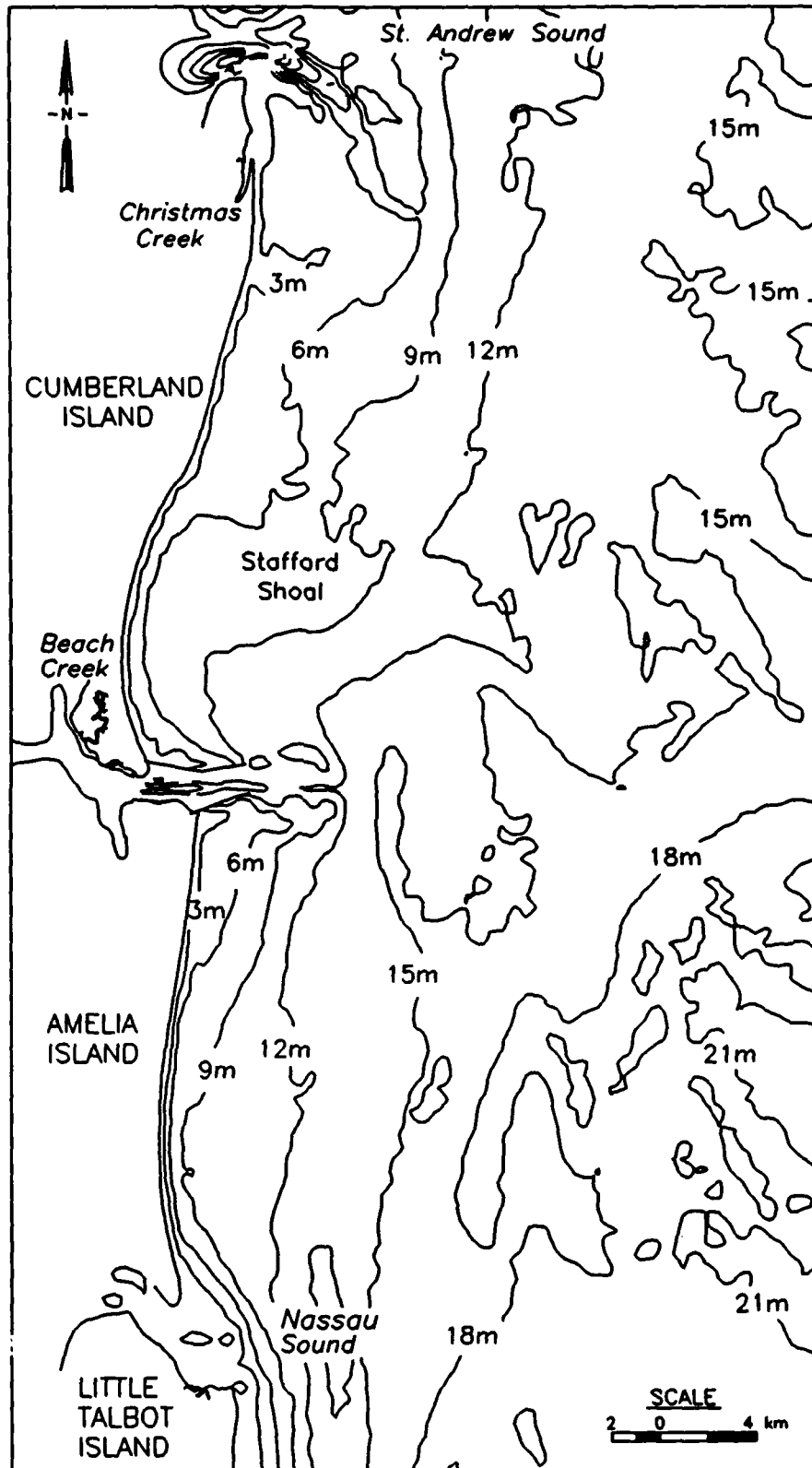


Figure 25. Regional bathymetry and associated morphologic features based on 1974 bathymetry (NGVD)

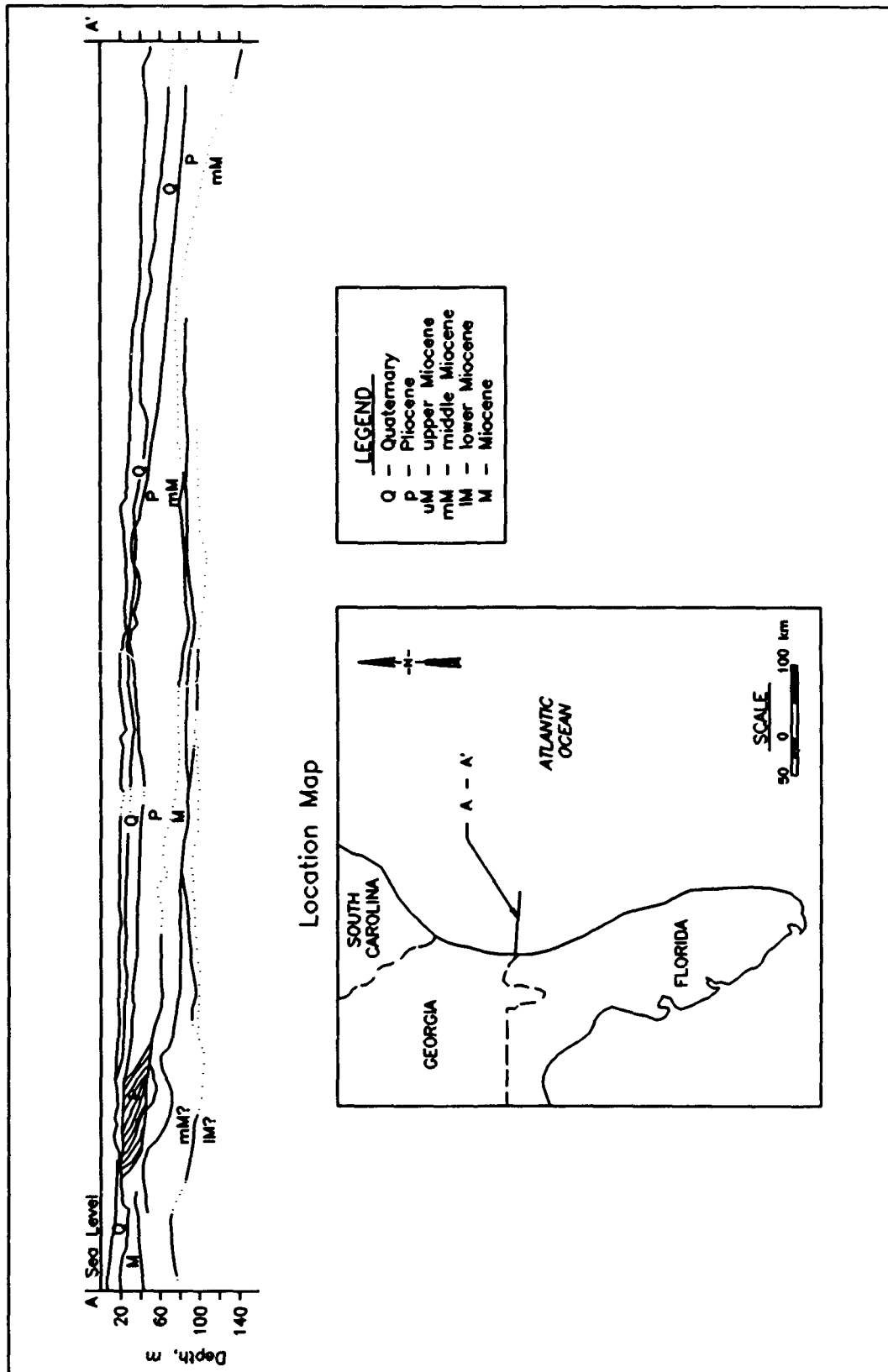


Figure 26. Representative offshore cross section, perpendicular to shore (modified after Henry and Kellam (1988))

## Engineering History of St. Marys Entrance

### Natural inlet

St. Marys Inlet has remained navigable throughout its recorded history, beginning in 1567 when the harbor town of Fernandina was established. Fernandina later served as an unpoliced free port until 1817 (Parchure 1982). St. Marys Entrance was fronted on its seaward side by a large bar formation incised by two relatively stable channels. Figure 27 is an 1875 map of the inlet area; however, features illustrated here coincide with a pictorial description of St. Marys Inlet prepared in 1779 by French navigators (Parchure 1982).

These early records and maps document a main S-shaped tidal channel which cuts through the ebb-tidal delta close to the north shore of Amelia Island and empties into the Atlantic Ocean (Figure 28). This was the deeper channel and probably was the primary navigation access into Cumberland Sound. The more northerly channel was a shorter and shallower secondary channel which extended north-northeast close to the shoreline of Cumberland Island. The northern channel was probably flood-flow dominated, and the better defined southern channel was probably ebb dominated, based on the tidal delta model of Hayes (1979) and documentation from other ebb-dominated inlet systems along the Southeast Atlantic seaboard (Hayes 1980, FitzGerald and Nummedal 1983, Hansen and Knowles 1988, Kana 1989, and Pope 1991).



Figure 27. Map of St. Marys Entrance channel in 1875 (unpublished map, U.S. Coast Survey, (1875))

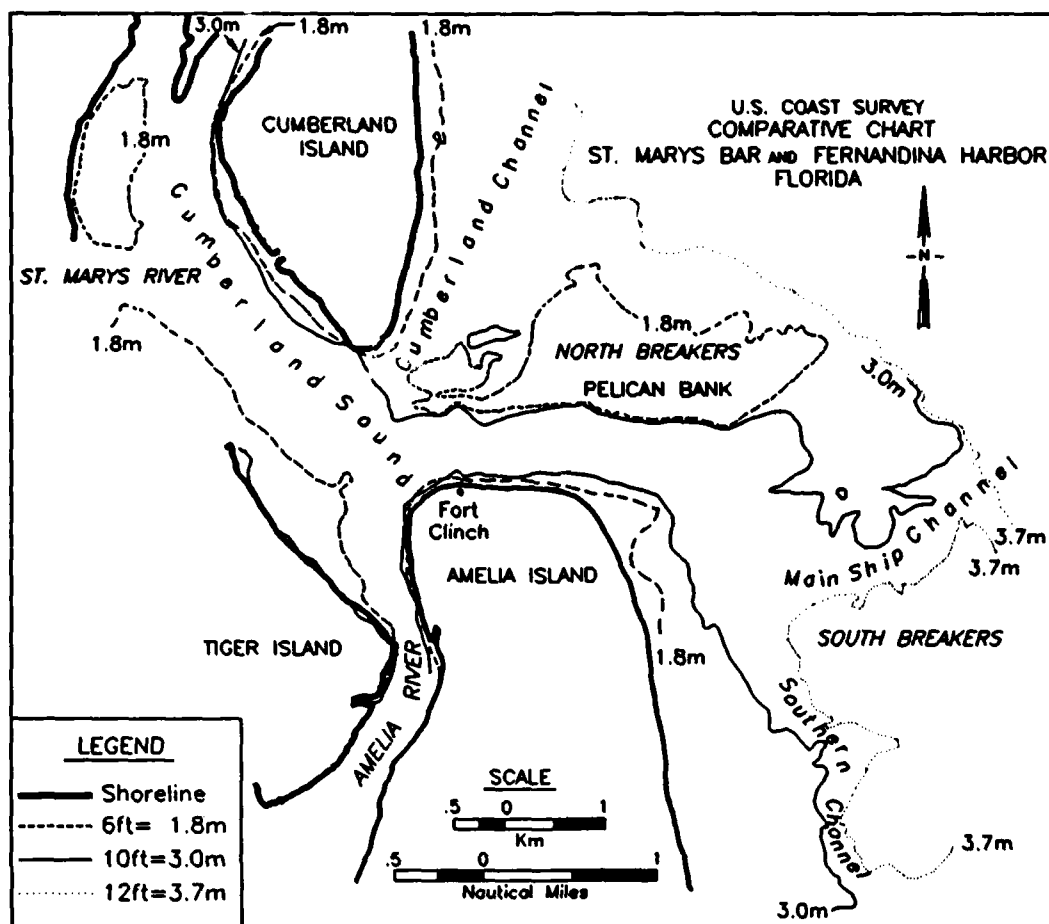


Figure 28. Position of navigation channels and ebb shoal bar complex, 1856.  
Contours based on MLW

By the 1870s, the southern channel bifurcated a long sandbar located approximately 3 km offshore at the 2.4-m-depth contour. The controlling depth in the channel at the bar was approximately 3 m below MLW. The deepest section of the inlet throat was opposite the Fort Clinch shoreline, where the subsurface had been scoured to a depth in excess of 20 m (Figure 28).

The extensive ebb-tidal delta and shoal system seaward of St. Marys Inlet influence both sediment supply and inshore wave patterns at adjacent beaches. The result is a complicated littoral transport system that is highly interactive between the beaches and the tidal inlet. Flood currents in St. Marys Inlet flow into the adjacent estuarine salt marsh through a zone of sandy point bars without a definable flood delta form.

The natural inlet exhibited some distinctive, consistent morphology in the early maps and charts. However, the seaward opening of the main channel frequently shifted, bifurcated, and/or shoaled. This behavior was accompanied by extensive migration of the ebb-tidal delta shoal system. Navigation of the preproject channel was frequently impossible and dangerous, prompting the Federal Government to authorize inlet stabilization.

## Engineering epochs and activities

**Engineering epochs.** A chronology of significant engineered modifications to St. Marys Entrance can be used to define temporal epochs (Table 5). The preproject natural channel, initial jetty construction, and incremental increases in the channel dimensions each define an engineering event in the evolutionary history of the inlet. The implementation of an engineered modification to the system has the potential to modify hydrodynamic and sediment transport characteristics. A step-by-step review of these changes allows for analysis of system impacts associated with each modification. These engineering epochs group common conditions which may alter the coastal morphology and are used to incrementally analyze the St. Marys dredging and shoaling data (Chapter 4).

<b>Table 5</b> <b>Engineering Epochs of St. Marys Entrance and Cumberland Sound</b>		
<b>Number</b>	<b>Epoch</b>	<b>Event</b>
1	Pre-1880	Natural inlet; channel bifurcated.
2	1881-1904	Jetty constructed and channel realigned.
3	1905-1923	Jetty repair work completed. Channel deepened to 5.8 m.
4	1924-1953	North jetty-Crest elev increased to 2.1 m MLW. South jetty-Crest elev increased to 1.8 m MLW. Channel deepened to 8.5 m MLW.
5	1954-1973	Channel deepened to 10.4 m MLW. Channel realigned.
6	1974-1986	Channel deepened to 12.2 m MLW, widened to 122 m, and lengthened to 8.3 km.
7	1987-1992	TRIDENT channel constructed and maintained. Channel deepened to 15.5 m MLW, widened to 152 m, and lengthened to 19.8 km.

Various engineering activities have been implemented during the past 110 years which have significantly modified the natural inlet, estuary, and coastal system. These activities included: construction and modification of the rubble-mound jetties; channel deepening and maintenance; groin construction at Fort Clinch; and coastal armoring, and nearshore and beach fill placement on Amelia Island. A chronology of the significant engineering events in the study area has been developed based on project authorization, documents, and USAED, Jacksonville, project reports (Table 6).

**The jetties.** Congressional authorization to stabilize St. Marys Inlet was granted in 1880, resulting in the construction of massive rock jetties and a Federally maintained navigation channel. Stabilization of the inlet began in 1881 with the start of construction of the north jetty. The original jetty design specified rubble-mound over a core of logs and small stones with a foundation mattress of logs and brush. Initially, the jetty crests were to be at MLW, except for the outer 1,000 m, which was to crest at midtide. The River and Harbor Act of 1896 provided for raising the jetties to MHW (USACE 1961). The revised project also included a core of small

**Table 6**  
**Chronology of Significant Engineering Events, St. Marys Entrance and Vicinity**

Date	Inlet Modification/Engineering Work
<b>Pre-1880</b>	
1875	U.S. Congress authorized a report on St. Marys inlet and soundside. Natural inlet; channel bifurcated with depths ranging between 3.3 to 3.8 m MLW.
1879	Plan was presented to Congress recommending an increase in channel depth to 5.8 m MLW and construction of two stone jetties.
1880	Congress approved a survey of Cumberland Sound.
<b>1881-1904</b>	
1881	Construction began on the north jetty in June. Five spur groins were constructed adjacent to Fort Clinch.
1882-1883	North jetty extended 2,194 m (7,200 ft). Construction of south jetty began in June 1882.
1883-1886	About 100 m of accretion occurred along the shoreline in south fillet area.
1886-1888	Work continued on both jetties. Noticeable increase in water depth within channel occurred as a result of south jetty extension.
1898	Hurricane breached across outer beach of Cumberland Island north of inlet.
1902	Channel opened through the seaward inlet shoal adjacent to the north jetty.
1904	Jetty construction completed. Breach in Cumberland Island deepened and widened; emergency improvements made by constructing a 2,103-m-long (6,900-ft) dike.
<b>1905-1923</b>	
1905-1913	Jetty repair work was required to maintain jetties.
1916	Jetty crests raised to MHW.
1905-1923	16,700 cu m of maintenance dredging performed annually.
<b>1924-1953</b>	
1924-1953	Channel depth increased to 8.5 m MLW.
1924-1953	12,700 cu m of maintenance dredging performed annually.
1927	Crest elevations of the north jetty increased to 2.1 m (MLW) and of the south jetty to 1.8 m (MLW).
1940	189,650 cu m of new work dredging performed.
<b>1954-1973</b>	
1955-1956	Entrance channel realigned near south jetty where former natural channel was located and channel depth increased to 10.4 m MLW. 2.0 million cu m of new work dredging performed.
1954-1973	81,000 cu m maintenance dredging performed annually.
<i>(Continued)</i>	

<b>Table 6 (Concluded)</b>	
<b>Date</b>	<b>Inlet Modification/Engineering Work</b>
<b>1974-1986</b>	
<b>1978-1979</b>	Authorized channel depth increased to 12.2 m MLW. 1.4 million cu m of new work dredging performed. 767,000 cu m of beach fill <sup>1</sup> placed on north end of Amelia Island (Survey Lines 12-22).
<b>1982</b>	302,000 cu m of beach fill placed on central Amelia Island (Survey Lines 19-25).
<b>1984</b>	57,000 cu m of privately funded fill used for dune restoration at south end of Amelia Island (Survey Lines 60-71).
<b>1974-1986</b>	272,000 cu m of maintenance dredging performed annually.
<b>1987-1992</b>	
<b>1987-1988</b>	Authorized channel depth increased to 15.5 m MLW. 693,000 cu m of beach fill placed on north end of Amelia Island (Survey Lines 13-22) and 405,000 cu m placed on central Amelia Island (Survey Lines 48-54). 460 m of landward portion of south jetty sand tightened.
<b>1987-1988</b>	6.5 million cu m of new work dredging performed.
<b>1988-1989</b>	826,000 cu m of beach fill placed on south central Amelia Island (Survey Lines 54-60).
<b>1989</b>	38,000 cu m of privately funded fill placed on south end of Amelia Island (Survey Lines 60-71).
<b>1990</b>	113,000 cu m of beach fill placed on north end of Amelia Island (Survey Lines 13-16).
<b>1991</b>	9,900 cu m of privately funded fill placed on south end of Amelia Island (Survey Lines 60-71).
<b>1991-1992</b>	Fort Clinch groins repaired.
<b>1988-1992</b>	616,200 cu m of maintenance dredging performed annually.
<b>1992</b>	148,000 cu m of beach fill placed on north end of Amelia Island (Survey Lines 13-16).
<sup>1</sup> Beach fill quantities are based on pre- and post-dredging surveys of the channel.	

stone and cover stone ranging from 450 kg at the shore end to 5 metric tons at depths of 4 m with larger stones placed farther seaward (Figure 29). The distance between the seaward ends of the jetties was set at about 1,200 m; channel depths of 6 m were planned. In 1904, an emergency pile and stone dike, 2,100 m long, was built from the shore end of the north jetty tying it to high ground to the northwest (Figure 30). This was done to prevent flanking of the jetty and breaching of the outer beach along the south end of Cumberland Island. The jetties were completed by 1905; the north jetty was 5,841 m long and the south jetty 3,416 m long, with their crests at MHW (USACE 1961).

The main tidal currents and deepest channel were confined between the jetties. Flows which had previously maintained the natural north and south channels were partially cut off, resulting in shoaling of these prestabilization channels. Because the St. Marys jetties were constructed without a solid core and with a low crest elevation, some passage of flood tidal flow and sediment

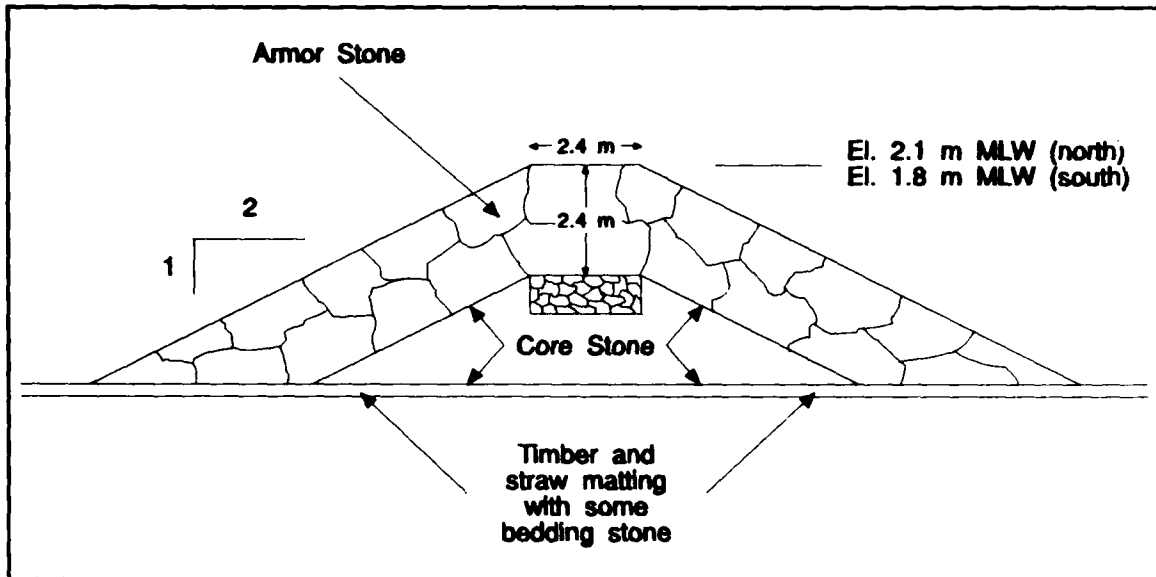


Figure 29. Typical section of north and south jetties (unpublished map USAED, Jacksonville (1987))

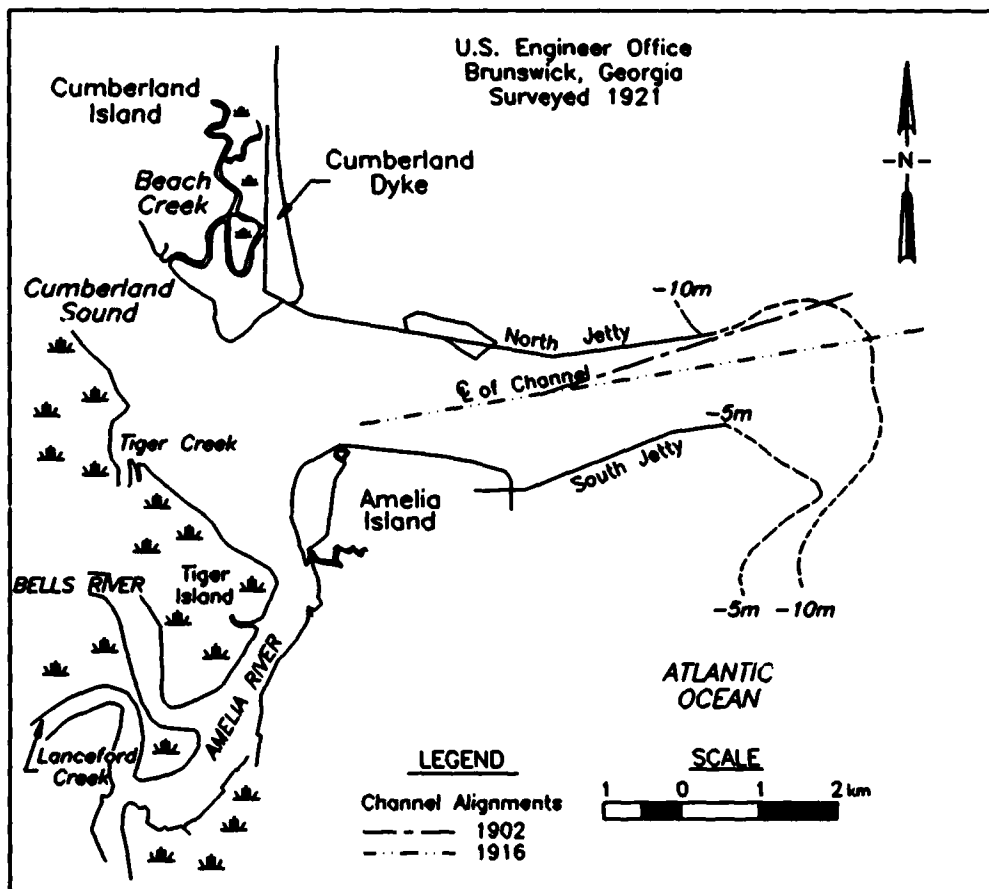


Figure 30. Position of channel alignments after jetty construction (modified after unpublished map U.S. Engineer Office, Brunswick, Georgia (1921))

occurs through and over the structures and into the inlet. This characteristic of St. Marys Entrance contributes to an ebb-dominance of the main navigation channel and also allows some littoral material to be transported into the protected inter-jetty area from both north and south. In 1927, as part of major repair work on the jetties, the crest elevation of the north jetty was increased to 2.1 m MLW and of the south jetty to 1.8 m MLW. Although periodic repairs were made to the jetties, they remained virtually unchanged until 1988, when a contract was let to sand-tighten the landward 460 m of the south jetty using precast concrete units (Sargent 1988). Actual construction started in the summer of 1987 and continued intermittently over the summer months until October 1988.

**The channel.** The original channel depth was authorized as 5.8 m below MLW. During jetty construction the main navigation channel was aligned toward the south jetty. As a result of the north jetty construction during 1881-1895, the north channel opened naturally through the large ebb shoal bar located between the jetties. By May 1902, the channel adjacent to the north jetty was used entirely for shipping (Figure 30).

The initial channel dredging in 1903-1904 removed 417,500 cu m from the vicinity of the north jetty. A channel realignment toward the middle of the inlet was made in May 1916 (Figure 30). The present channel alignment was established during the 1955-1956 excavation of the 1950 authorized civil works channel. Additional improvements were made to maintain the channel as a navigation route. These included significant channel deepening in 1924, 1955-1956, and 1975-1979, and the most recent deepening from 1982-1988. A summary of channel dimensions from 1955-1956 to the present is presented in Table 7. A discussion of the channel deepening and maintenance history is presented in Chapter 4 and Appendix C.

<b>Table 7</b> <b>St. Marys Entrance Channel Dimensions</b>			
Channel Characteristics	Civil Works Channel (1955-1956)	Pre-TRIDENT Civil Works Plus Military (1978-1979)	TRIDENT Channel <sup>1</sup> (1988-1989)
Depth (MLW)	9.8, 10.4 m	12.2 m	15.5 m
Width	122 m	122 m	152 m <sup>2</sup>
Seaward Limit	Sta 270 + 73 Cut 1N	--	Sta 148 + 00 Cut 2N
Length (Offshore from Sta 0 + 00)	8.3 km	--	19.8 km
Auxiliary Elements	--	--	Turning Basin Settling Basin
<sup>1</sup> Dimensions given are as constructed and maintained. <sup>2</sup> Additional width added onto north side of existing channel.			

The Federal civil-works-authorized project depth is 9.8 m below MLW. As part of the construction for the Kings Bay Army Terminal, the project channel depth was increased to 10.4 m below MLW in 1955-1956. Since the 1970s, continued development of the NSB Kings Bay has required deepening the St. Marys approach and entrance channel and the navigation channel within Cumberland Sound. By 1980, the channel depth had been increased from 10.4 to 12.2 m below MLW to allow for safe passage of the POSEIDON submarine fleet. In order

to accommodate the TRIDENT submarines, modification of the project channel dimensions began in the mid-1980s to create a channel depth of 15.5 m below MLW (14 m project depth plus 0.9 m advance maintenance plus 0.6 m to allow for dredging inaccuracies), a channel width of 152 m, and channel length of 19.8 km. Final design side slopes were 3H:1V (Figure 2).

**Dredged material disposal and Federal beach fill placements.** Prior to the 1970s, most of the entrance channel dredged material was placed via side-casting along the flanks of the channel (Figure 31). Between 1970 and 1985, Offshore Disposal Area #1 was used as the authorized disposal area, although disposal of beach-quality dredged material on northern Amelia Island started in 1978. During the 1987-1988 TRIDENT deepening of the ocean channel, dredged material was placed in four locations: Offshore Disposal Area #2, 4.2 million cu m; Amelia Island North Beach (2.7 km long), 693,000 cu m; the Nearshore Disposal Area, 1.2 million cu m; and the South Beach Disposal Area, 530,000 cu m.

Between 1978 and 1992, approximately 3.4 million cu m of dredged material from St. Marys Entrance were placed along the shoreline of Amelia Island. Most of this material has been placed along the northern and south-central portions of the island. The quantity and location of beach fill operations, including material obtained from sources other than St. Marys Entrance, are listed in Table 6 and are discussed in more detail in Chapter 5.

**Other engineering activities.** Several projects have been constructed to reduce erosion on Amelia Island. The first was in 1881, when five spur groins were constructed along the westernmost wall of Fort Clinch to prevent undermining of the fortification walls. Two additional groins were added in 1883. In 1953, the City of Fernandina Beach constructed eight asphalt groins along the Atlantic Ocean shore, north of Atlantic Avenue. As a temporary protective measure following Hurricane Dora (1964), 5.8 km of granite revetment were placed along portions of Fort Clinch, Fernandina Beach, and American Beach (USAED, Jacksonville 1984a).

Private interests have performed small-scale erosion control efforts and dune enhancement projects along the southern portion of Amelia Island. In the 1970s, and in June 1980, sand was scraped from the beach intertidal area and placed at the dune toes. In 1984, approximately 57,000 cu m of sand were trucked from an ICWW dredged material disposal site and placed along the dune toe at the southern end of Amelia Island. An additional 4,200, 38,000, and 9,900 cu m were trucked in from an ICWW disposal site in the spring of 1985, fall of 1989, and 1991, respectively (Olsen Associates, Inc. 1990).

## **Coastal Response to Inlet Stabilization**

### **Shoreline movement**

Historical trends of shoreline change have been studied by several Federal agencies and the States of Georgia and Florida. Three previous studies, Roberts (1975), Nash (1977), and Griffin and Henry (1984), describe historical shoreline movements for Cumberland Island. McLemore et al. (1981) summarized the comprehensive shoreline study conducted by Nash (1977) and the work of Roberts (1975) for the NPS as part of their land-use management plan for Cumberland

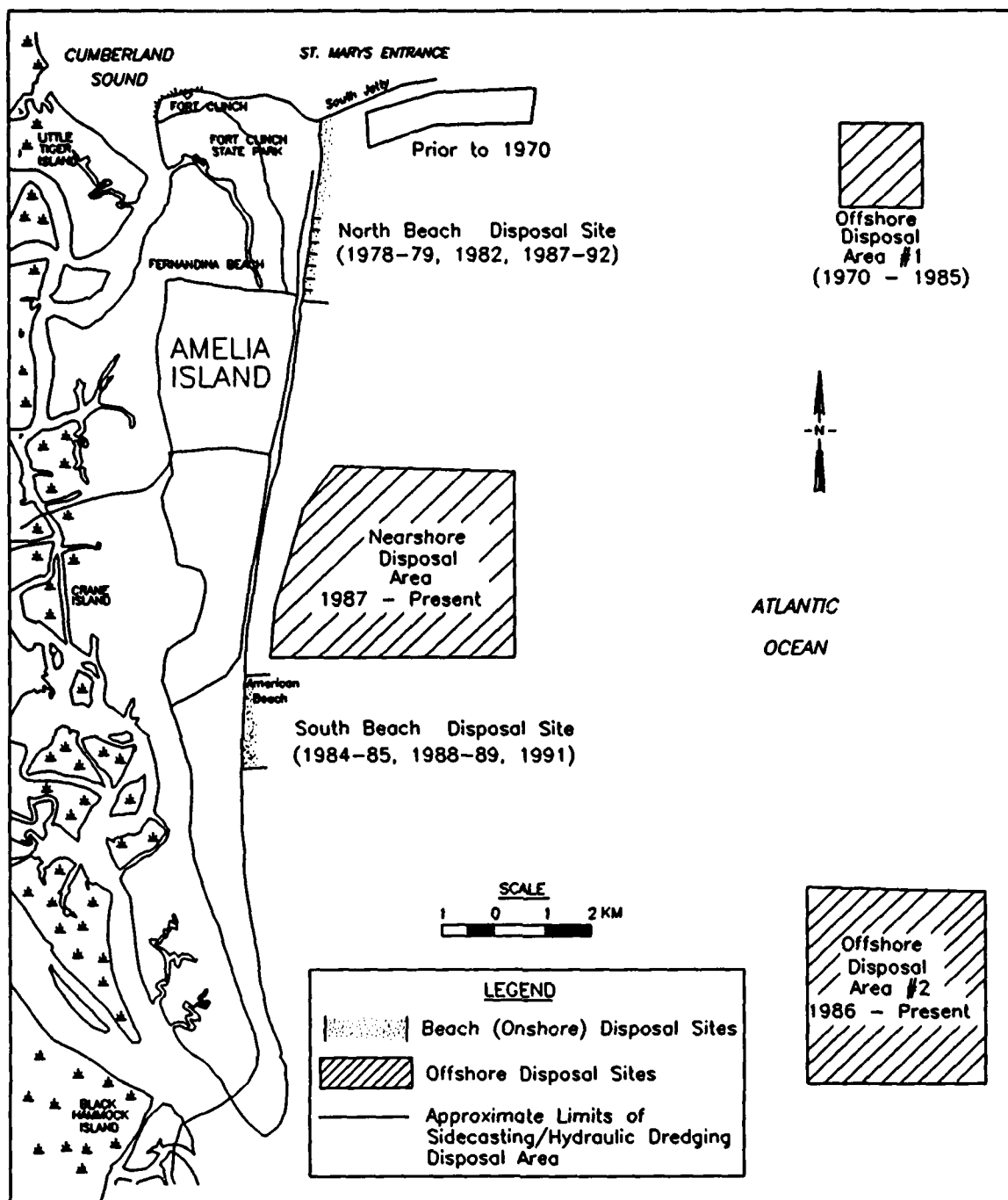


Figure 31. Location of authorized disposal areas for St. Marys Entrance channel material

Island National Seashore. Shoreline change rates for Amelia Island were also reported by USAED, Jacksonville, (USACE 1961; Florida Coastal Engineers, Inc. 1976; USAED, Jacksonville 1984a) as part of beach erosion control studies. Preliminary shoreline change rates for the Kings Bay historical study subtask were calculated and published by Knowles and Gorman (1991). Chapter 3 discusses shoreline change analysis for the period 1857-1991 and Chapter 5 discusses shoreline change analysis for the monitoring period conducted as part of this study.

The trends and rates of shoreline movement for the various published studies are summarized here. Most shoreline change data were based on NOS topographic survey sheets (T-sheets) and aerial photographs. However, the methods used to compile and analyze the shoreline data were different, and study periods varied. All referenced studies describe the shoreline as the MHW line; however, the shoreline as defined on NOS topography survey sheets and as interpreted from aerial photography is actually the high water line captured in that data set. In order to conform with the convention of these previous studies, shorelines will continue to be described as MHW throughout this section. These shoreline change studies generally conclude that the region has been remarkably stable except for beaches adjacent to inlets. Most of the shoreline either showed no movement or showed slightly recessional or progradational trends. An exception to this relative stability is the recession of the shoreline along a 2-km section of Amelia Island located from 3 to 5 km south of the south jetty. Also, the southern 5 km of Amelia Island have exhibited a persistent trend of shoreline retreat since the 1870s.

**Cumberland Island.** According to previous studies, the Cumberland Island shoreline has prograded over most of its length. The earliest study that described geographic variability at the southern end of Cumberland Island was conducted by Roberts (1975). In addition to beach profile and coring information, a composite map of shoreline position extending 2.3 km north of the north jetty was compiled for the 1857-1972 period. Roberts (1975) calculated a shoreline recession rate of 3.0 m/year for the prejetty construction period (1857-1898) along the same shoreline segment. Immediately after jetty construction this recession increased to an average rate of 35.3 m/year between 1903 and 1907. Once the jetties were in place and the ebb-tidal delta had shifted (post-1922), the Cumberland Island shoreline began prograding at an average rate of 10.3 m/year (Roberts 1975).

Nash (1977) used the combined 1843 and 1871 shorelines, along with the combined 1973 and 1974 MHW shorelines from U.S. Coast and Geodetic Survey (USC&GS) and U.S. Geological Survey (USGS) topographic survey sheets to conduct a shoreline change analysis (Figure 32). The 1843 shoreline was interpreted from a hydrographic survey reported in the Annual Report of the Chief of Engineers, U.S. Army, June 1888 and is a limited data set which is only available for the southern end of Cumberland Island. McLemore et al. (1981) updated this work with 1979 aerial photography. Because these photographs were taken 1 day after Hurricane David (3 September 1979), they are of limited value in quantifying long-term shoreline change trends. Nash (1977) measured shoreline changes for Cumberland Island and northern Amelia Island along transects perpendicular to the shoreline. Maximum net change occurred at the southern end of Cumberland Island, where the shoreline prograded approximately 4 km from 1843 to 1974. In terms of shoreline trends, Nash (1977) identified three geographic sections along Cumberland Island: (a) the northern end of Cumberland Island bounded on the south by Christmas Creek, (b) a central segment including the shoreline adjacent to Stafford Shoal and the northern portion of the arc-shaped shoreline, and (c) the southern end of Cumberland Island, including the fillet area of the north jetty. Nash (1977) summarized the following trends for these sections (Figure 32):

- a. Northern section: The northwestern portion of Cumberland Island (Transects C1-C3) had an average of 1.5 m/year of shoreline retreat during the 1871-1974 period. During the same period, the shoreline south of Transect C7 prograded 430 m, largely as the result of the formation of a tidal delta by Christmas Creek.

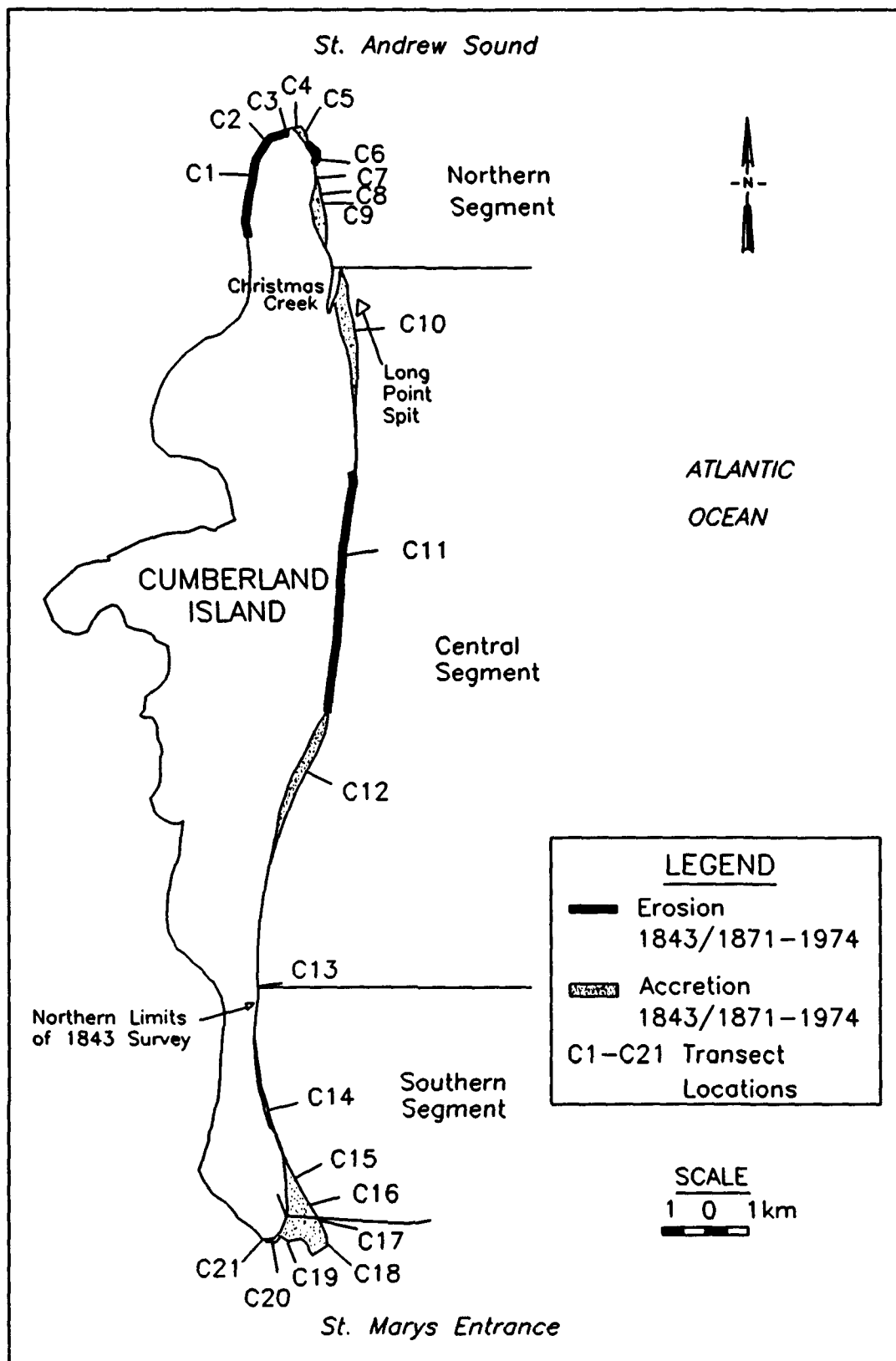


Figure 32. Net shoreline change map, 1843 or 1871 to 1974 (Nash 1977)

- b. Central section: A majority of the shoreline segment adjacent to Stafford Shoal (Transect C11) retreated an average of 50 m prior to 1924. However, since 1924 this segment experienced gradual accretion. Further south, in the vicinity of Transect C12, a depositional trend was dominant, resulting in a net gain of approximately 0.8 sq km of land. Net rates of retreat or advance along the central areas did not exceed  $\pm 1$  m/year. The long-term trend over the 1871-1974 period was one of stability for the middle portion of this section.
- c. Southern section: The shoreline along the southern end of Cumberland Island has been influenced by inlet morphology and jetty construction. The greatest rate of shoreline advancement was 18 m/year at Transect C18 from 1876 through 1974. Nearly 2 sq km of land accreted to the southern end of Cumberland Island since jetty construction.

Localized erosion was attributed to jetty construction, a gradual increase in sea level, and the occurrence of severe storms and hurricanes (Nash 1977). Based on aerial photos taken before and after Hurricane Dora (1964), the entire central section of Cumberland Island retreated, but recovered by 1965. Hurricane Dora also caused a maximum shoreline recession of approximately 200 m at Transect C15 along the southern section (Nash 1977).

In 1982, the Georgia Geological Survey funded a regional shoreline change study (Griffin and Henry 1984) to develop a broad and comprehensive database for the Georgia coast. The authors used conventional map sources, i.e., USGS 15- and 7-1/2-min topographic and orthophotographic quadrangle sheets, and NOS hydrographic and topographic survey sheets and low-altitude controlled photographs from the Georgia Department of Transportation to compile a shoreline change history based on the MHW position from 1857 through 1982. All maps and shoreline surveys were brought to a common scale of 1:24,000. Shoreline position maps were generated for five periods: 1857/1868, 1924, 1957, 1974, and 1982. Major shoreline trend conclusions of the Griffin and Henry (1984) study are summarized, according to the geographic sections defined by Nash (1977) and referenced to Figure 32:

- a. Northern section: Frequent reversals of recession and progradation occurred along Little Cumberland Island (Transects C1-C9). Long Point spit at Christmas Creek inlet accreted toward the north (Transect C10).
- b. Central section: Along the south-central portion where the shoreline is arc-shaped, the shoreline was stable to slightly accretional for all time periods (Transect C13).
- c. Southern section: Maximum accretion of Cumberland Island occurred in the vicinity of the north jetty. Northward of the jetty, the shoreline advanced at a rate of 12.6 m/year during the 1957-1974 period (Transect C16). The shoreline south of the jetty also accreted during the same time period.

Although several previous studies presented shoreline change rates for the study area, the Kings Bay Coastal Monitoring Program is the first to establish a comprehensive shoreline change analysis using computer mapping and Geographical Information System (GIS) technology (Chapter 3). Preliminary project shoreline change statistics (Knowles and Gorman 1991) were generated for transects having a 150-m alongshore spacing. An overall accretion rate of 1.5 m/year was calculated for the entire shoreline of Cumberland Island from 1857/70 through 1973. If accretion adjacent to the north jetty is excluded, the rate of progradation is 0.9 m/year.

During the postjetty construction period (1924-1974), south-central and southern Cumberland Island continually advanced at a rate of 7.1 m/year. Erosion (1.3 m/year) occurred chiefly along northern Cumberland Island adjacent to the St. Andrew ebb-tidal delta for the same period. Central Cumberland Island was stable with accretion (7.1 m/year) near the southern end of Stafford Shoal.

**Amelia Island.** Shoreline change studies for Amelia Island are reported in USACE (1948, 1961), Nash (1977), Olsen (1977), and Knowles and Gorman (1991). The earliest analyses were included in two beach erosion control reports submitted to the U.S. Congress (USACE 1948, 1961). Both reports were prepared in response to concerns raised by local interests that the "...entrance jetties are partially or wholly responsible for shore erosion on Amelia Island..." (USACE 1948). USACE (1948) concluded that "...the entrance jetties have no deleterious effect on adjacent shorelines...." However, USACE (1961) recognized that "The problem is primarily one of starvation of the beach...caused by the littoral barrier created by the ocean inlet to Cumberland Sound and its jetties." Both studies found significant changes adjacent to the north and south jetties. USACE (1961) reported shoreline advancements of 12.2 m/year and 10.7 m/year in the north and south fillet areas, respectively, for the period 1857-1945. The report also recognized there had been 1.1 m/year of recession from 1.2 to 6.2 km south of the south jetty.

In the earlier study, USACE (1948) accredited the local erosion 4 to 5 km south of the south jetty to unusually severe storm action. Storm events, particularly local northeasters, can cause temporary shoreline recession (Florida Coastal Engineers, Inc. 1976; USAED, Jacksonville 1984a, 1993). USAED, Jacksonville (1984a) reported severe erosion ranging between 9.1 and 18.3 m along Fernandina Beach caused by Hurricane Dora in 1964.

A comprehensive ecological planning and land use study was conducted by Wallace et al. (1971)<sup>1</sup> for the development of Amelia Island Plantation. This private development includes about 665 hectares and 6.4 km of beachfront. Multi-disciplinary studies were designed to determine the local physical and biological characteristics of the entire island. In addition to determining the geology and water resources, rates of erosion and storm tide elevations were investigated. Wallace et al. (1971) quoted a coastal recession rate of 7 to 8 ft/year (2.1-2.4 m/year) for Amelia Island Plantation beaches based on vegetation line movement from 1943 to 1970. This relatively high rate was attributed to an unusually high occurrence of storms over that time period. The report also stated that the average erosion rate should not exceed 3 ft/year (0.9 m/year). Evaluation of storm wave heights indicated that a 15-ft (4.6-m) elevation for structures would be safe, within a 1- in 80-year probability for wave uprushes above 5 to 6 ft (1.5-1.8 m/year) above the general tide elevation.

Nash (1977) evaluated shoreline change along Amelia Island. He noted a shift in shoreline orientation along the northern part of Amelia Island following jetty construction. Based on shoreline transects of the high-water line for the 1962-1975 period contained in Nash (1977), the USAED, Jacksonville (1984a) calculated shoreline recession rates ranging between 1.2 and 9.2 m/year for the shore located between 0.8 and 6.4 km south of the south jetty. Olsen (1977)

---

<sup>1</sup> Wallace, McHarg, Roberts, and Todd, Inc. (1971). "A report on the master planning process for a new recreational community," unpublished report for Amelia Island Property of the Sea Pines Company, Hilton Head Island, South Carolina.

reported shoreline recession at Fernandina Beach and steepening of the nearshore slopes, which he attributed to inlet stabilization and jetty construction at St. Marys Entrance.

Shoreline change analysis by Olsen Associates, Inc. (1990) for Amelia Island was based on values interpreted from the State of Florida, DNR beach profile surveys (see Appendix D for a profile location map). Olsen Associates, Inc. computed shoreline change rates along the southern end of Amelia Island from February 1974 to April 1990. MHW line recession varied from 0.3 m/year at Florida DNR Line 61 to 3.7 m/year at Line 72, located 5.5 and 2.5 km north of the southern end of Amelia Island, respectively. Olsen also found that the rate of shoreline and dune erosion has increased in recent years despite dune/beach restoration.

Knowles and Gorman (1991) found spatial and temporal shoreline trends similar to those previously published. If the south jetty fillet area is excluded, Amelia Island showed a net recessional trend of 0.5 m/year for the 100-year period (1857/1870 to 1974). During the post-jetty construction period (1924-1974), the Amelia Island shoreline, including the south jetty fillet area, receded at 0.2 m/year.

### **Bathymetric change**

In addition to quantifying shoreline change, many of the reports cited in the previous section also analyzed nearshore changes in terms of sediment volumes and estimated sediment transport directions and rates. Previous studies of volume change in the St. Marys tidal inlet system concentrated primarily on the fillet areas, inlet throat, and ebb-tidal delta. The principal study of nearshore morphologic change was completed by Florida Coastal Engineers, Inc., under contract to USAED, Jacksonville. Results of this study were published in Florida Coastal Engineers, Inc. (1976), Olsen (1977), and USAED, Jacksonville (1984a).

The volumetric analysis by Olsen (1977) incorporated 1870s through 1970s bathymetry data. Data analysis covered an area extending 13.7 km north and 12.1 km south of the St. Marys Entrance Channel, and 14 km offshore. Some areas of significant accretion were excluded, such as Stafford Shoal and the nearshore zone adjacent to central Amelia Island. The analysis was based on computer-generated grids from digitized NOS hydrographic survey sheets (H-sheets). Net volumetric changes were calculated based on the difference between the depth grids. A datum correction factor of 0.2 m was used to account for the effect of changes in relative sea level during this 100-year period. Figure 33 is a summary of volume changes calculated by Olsen (1977). The net volume change indicated erosion in excess of 94 million cu m from the nearshore area, and 92 million cu m of material stored in the ebb delta since the 1870s. There is a near balance (less than 3 percent difference) between the total volumes of erosion and accretion. Olsen (1977) was based on a comparison of bathymetry sets separated by about 100 years, rather than on an examination of the shoreline and bathymetry data before and after jetty construction. An important clarification of reported volumetric change and calculated littoral transport rates for the St. Marys inlet system is that the bathymetry sets used by this and previous studies represent composites of individual hydrographic surveys taken over several years. The available bathymetric surveys and data coverage within the study area are described in Chapter 3.

Additional analyses conducted by Olsen (1977) showed that the present inlet throat cross-sectional area of 12,540 sq m has not reached his predicted equilibrium value of 13,750 sq m. Since 1855, the minimum cross-sectional area of the inlet has increased over 30 percent. Furthermore, Olsen (1977) identified offshore movement of ebb-jetted material as an important

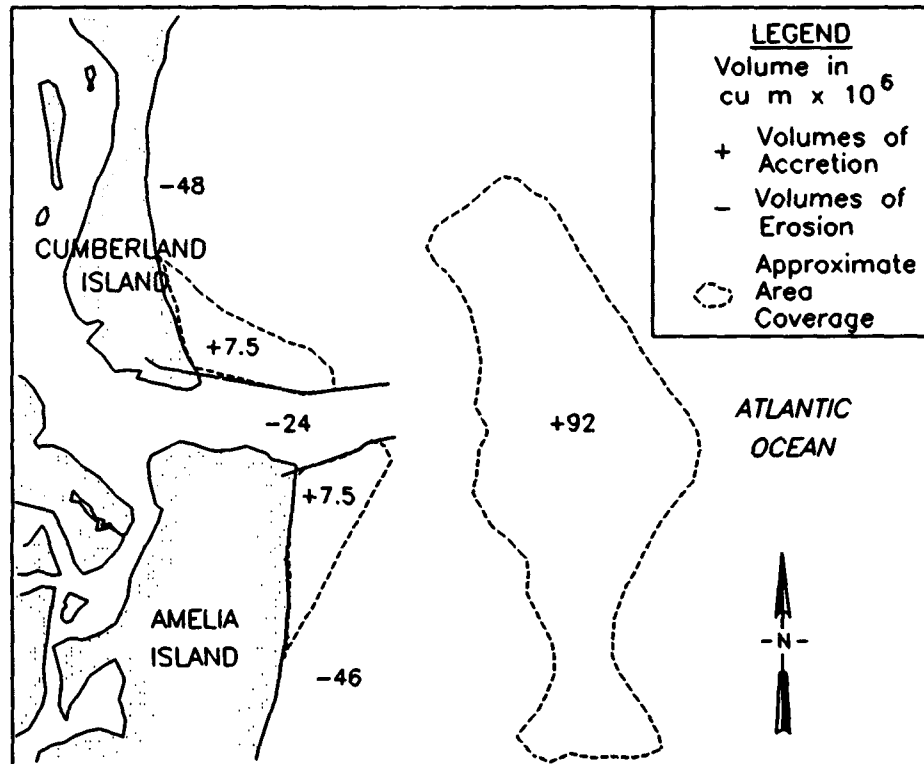


Figure 33. Volume changes computed by Olsen (1977)

factor in the postjetty development of the ebb-tidal delta fronting St. Marys Entrance. Specifically, he suggested that littoral sediment enters the dredged channel from both Cumberland and Amelia Islands through the relatively permeable jetty structures, and that most of this material is then jetted seaward by ebb-tidal currents and deposited in the ebb-tidal delta. This mechanism led Olsen (1977) to describe St. Marys Entrance as a complete littoral trap. Pertinent findings and conclusions from the Olsen (1977) analysis of the St. Marys inlet system are:

- a. The broad natural ebb-tidal delta platform was altered as a result of jetty construction and was translated seaward, with steepening of the nearshore profile along Cumberland Island from 3.5 to 11 km north of the north jetty.
- b. Sediment transport on Amelia Island between the south jetty and Fernandina Beach is to the north, which is opposite to the regional trend of southerly longshore transport.
- c. Despite improved hydraulic characteristics of the inlet channel, sedimentation in the channel still occurred.
- d. St. Marys Entrance is a complete littoral trap.
- e. Nearshore and offshore erosion occurred at both Fernandina Beach and along a section of Cumberland Island 4-10 km north of the north jetty.

Other studies of volume change, in most cases, were confined to the immediate vicinity of St. Marys Entrance. The earliest documented volume changes were calculated by the U.S. Engineer Office, Brunswick, Georgia, for the postjetty construction period (1902-1907). Figure 34 shows the areas of accretion (fill) and erosion (scour) in the vicinity of St. Marys Entrance. Because of continuous construction activity associated with the jetties during this period, including channel alignment and disposal of dredged material, it is difficult to determine annual transport rates. However, the patterns of fill and scour are similar to those of the modern system.

Preliminary bathymetric analyses reported by Knowles and Gorman (1991) were derived from volumetric grids extending from the MHW shoreline out to the 9-m depth (NGVD) contour. The net volume change for the fillet areas, inlet channel, and ebb-tidal delta was estimated as a gain of 12.4 million cu m for the prejetty period (1870s-1924) and 58.8 million cu m during the post-jetty period (1924-1974). This resulted in a net change of 74.2 million cu m during the 100-year period of record. The volume change from the 1870s to the 1970s for the two polygon areas, which defined the new ebb-tidal delta crest and its flanks, was computed as a gain of 90.4 million cu m.

One of the most documented parameters of the St. Marys inlet system has been the ebb-tidal delta (ebb shoal) volumes. A comparison of the published literature (Olsen 1977; USAED, Jacksonville 1984a; Dean 1988; Knowles and Gorman 1991) gives similar ebb-tidal delta shoal volume change for the period 1857/1870s to the 1970s, ranging between 90 and 95 million cu m, with some variation in the definition of the ebb-delta polygon per investigator (Table 8). Marino and Mehta (1988) conducted an analysis of the sediment volumes associated with the tidal shoals, adjacent beaches, and dredging operations for 19 tidal inlets along the east coast of Florida. For St. Marys Entrance, they calculated a total volume of 89.2 million cu m in the prejetty ebb-tidal shoal in 1870s, whereas postjetty volume increased to a total volume of 95.1 million cu m, resulting in a residual of 5.9 million cu m of material gained to the ebb shoal. Because St. Marys inlet system does not have a well-developed back-bay delta, no flood shoal volume was calculated.

Other parameters relevant to littoral processes in the study area are the longshore transport direction and rates of gross and net transport. Long-term dominance of sediment transport to the south has been well established for the study area based on the deposition and erosion pattern of the nearshore zone, channel position, and the ebb-tidal delta orientation (USACE 1961, Olsen 1977, Dean 1988, Knowles and Gorman 1991). Annual net sediment transport rates are subject to short-term variability and inaccuracies in determining the northerly and southerly transport components. Table 8 lists the net annual longshore transport rates computed by various studies. Olsen (1977) and Knowles and Gorman (1991) computed comparable net rates of 380,000 and 300,000 cu m/year to the south, respectively, using volumetric changes from bathymetry maps with similar measured areas.

Dean (1988) summarized net longshore sediment rates at coastal inlets along the eastern coast of Florida. He found the highest transport rate of 459,000 cu m, at St. Marys Entrance, with transport rates decreasing toward the southern portion of the state (Dean 1988). Dean also noted that ebb flow is constrained between the jetties, whereas a substantial portion of flood flow occurs over the jetties. Consequently, there is a seaward bias to the channel flow resulting in significant littoral material being deposited on the ebb shoal.

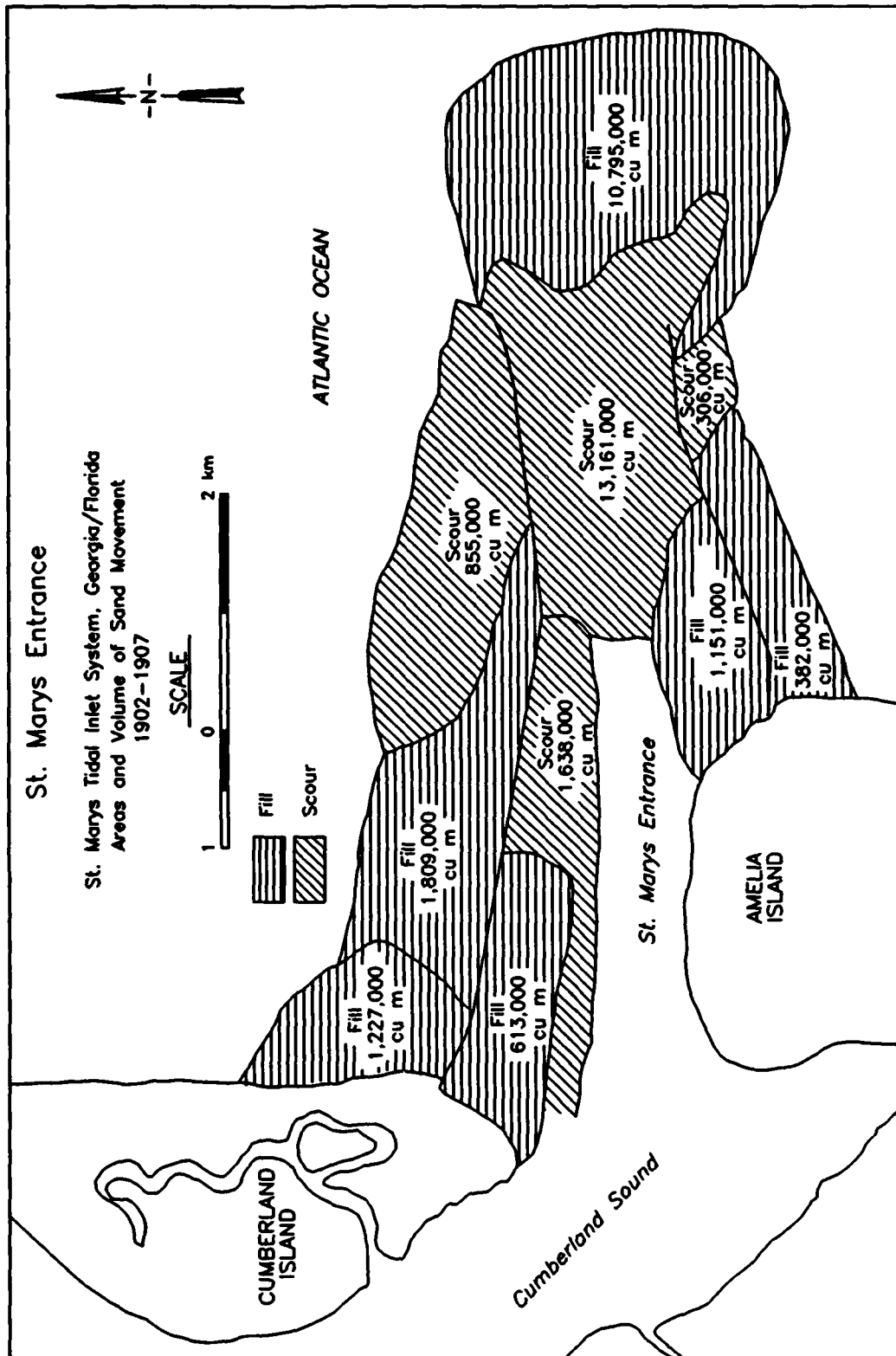


Figure 34. Areas and volume of sand movement calculated postjetty construction, 1902-1907 (unpublished map U.S. Engineer Office, Brunswick, Georgia (1907))

**Table 8**  
**Longshore Sediment Transport and Ebb-Delta Volume: Summary of Previous Study Results**

Cited Report	Net Sediment Transport cu m/year	Gross Sediment Transport cu m/year	Ebb Delta Volume million cu m
Florida Coastal Engineers, Inc. (1976), USAED, Jacksonville (1984a), Olsen (1977)	380,000	700,000- 800,000	91.7
Parchure (1982)	182,000	400,000	.. <sup>1</sup>
Richards and Clausner (1988)	416,000	765,000	--
Marino and Mehta (1988)	--	--	95.1
Dean (1988)	459,000	--	90.4
Knowles and Gorman (1991)	300,000	900,000	90.4
<sup>1</sup> No data available.			

## Organization of the Coastal Morphologic Compartments

Based on preliminary results of this study (Knowles and Gorman 1991, Gorman 1991) and other geologic and coastal inlet investigations (Olsen 1977, McLemore et al. 1981), the study area was subdivided into morphologic compartments which encompass the dune/beach zone seaward to the limits of data coverage. The location and boundaries of the morphologic compartments are illustrated in Figure 35. These compartments are the spatial framework which was used for defining the nearshore volume polygons used in the long-term bathymetry change analysis (Chapter 3) and profile surveys and sediment data analysis (Chapter 5, Appendix D). The geomorphology of the dune complex and subaerial beaches, the nearshore morphologic features, littoral transport pattern, and local physical processes were used to define the alongshore boundaries. Based on inlet and shoal namesakes used on navigational charts and additional new features, the following compartments were designated from north to south within the study limits: St. Andrew Sound Tidal Inlet Complex, Stafford Shoal, Cumberland Embayment, St. Marys Tidal Inlet Complex, North Amelia Platform, Amelia Embayment, and Nassau Sound Tidal Inlet Complex. A brief description of the primary features and relative alongshore distance (based on profile location) within each morphologic compartment is provided below.

The northern boundary of the study area, St. Andrew Sound Tidal Inlet Complex, is located between Jekyll Island and Cumberland Island, Georgia. Data analysis for this project includes only the downdrift portion of the ebb-tidal delta because it is an important sediment source for the Cumberland Island barrier island and nearshore system. The Stafford Shoal compartment consists of a large, dynamic shoal oriented northeast-southwest seaward of central Cumberland Island. This compartment (9.3 km long) included the northern limit of the field data collection for the coastal monitoring program. Cumberland Embayment (9.6 km long) located along south central Cumberland Island is distinctive because of the concave arc-shaped shoreline and relatively smooth seafloor devoid of large sand bodies. The focal point of the study is the St. Marys Tidal Inlet Complex (4.5 km long) which encompasses the updrift fillet area adjacent

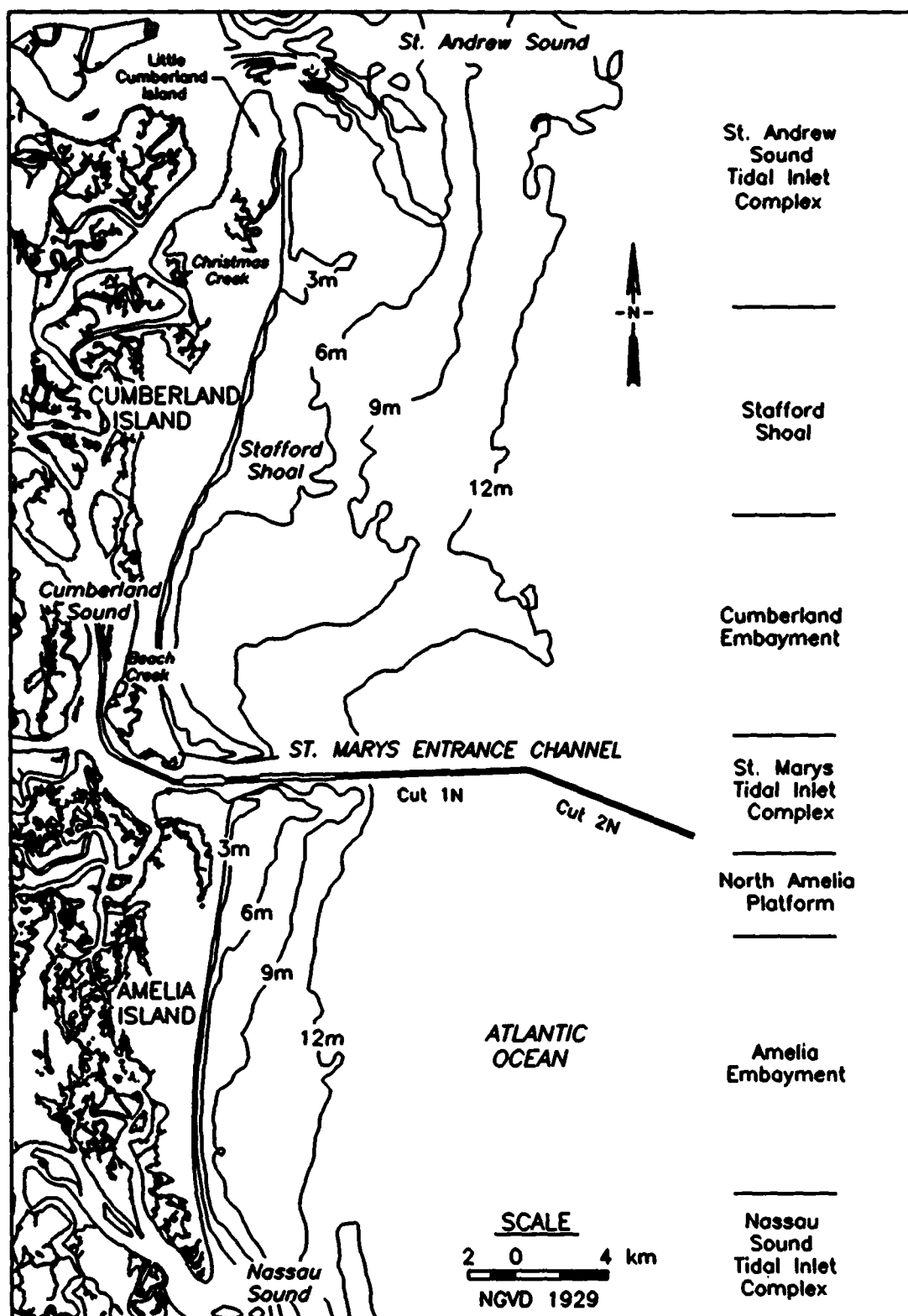


Figure 35. Location diagram showing morphologic compartments for the Kings Bay study area (after Gorman (1991))

to the north jetty, the navigational channel and ebb-tidal delta, and the downdrift fillet area adjacent to the south jetty. The North Amelia Platform (4.0 km long) compartment includes the shoreline and nearshore where the topography follows the pre-inlet stabilization ebb-delta platform. South of the influence of historic and modern inlet processes is the centrally located Amelia Embayment (11.4 km long) where the beach and nearshore area is slightly concave arc-shaped. At the southern limits of the study area is the Nassau Sound Tidal Inlet Complex (3.0 km long) consisting of a shallow, wave-dominated ebb delta between Amelia Island and Little Talbot Island, Florida. The analysis of the long-term bathymetry change and field data collection was limited to the updrift part on the Nassau Sound Tidal Inlet Complex.

### 3 Shoreline Position and Nearshore Bathymetric Change<sup>1</sup>

---

#### Introduction

This chapter summarizes results from shoreline position and bathymetric change analyses performed as part of the historical and coastal monitoring studies. The purpose of these analyses was to evaluate long- and short-term changes in coastal response to physical processes in the nearshore zone of the Cumberland and Amelia barrier island system, particularly as it relates to tidal-influenced sedimentation patterns associated with St. Marys Entrance. In order to make this assessment, historical and recent field data sets were compiled and analyzed. Historical information summarized in this chapter includes shoreline position surveys (from maps and near-vertical aerial photographs) and bathymetric surveys (from NOAA maps and digital data). Field measurements consisted of a shoreline position survey (1991) using global positioning system (GPS) data and bathymetric surveys of St. Marys ebb-tidal delta (1988 and 1992) conducted by the USAED, Jacksonville. The data sets were compiled to characterize individual components of the littoral system. These data were integrated and analyzed to evaluate coastal and nearshore response to natural processes and engineering activities in the study area.

Shoreline position and bathymetric surveys, collected as part of the monitoring program, enhanced existing historical information. These data, along with the short-term analysis of beach profile surveys (Chapter 5), were used to quantify spatial and temporal changes in beach and shoreface morphology, and as input for numerical shoreline change simulations (Chapter 7). Based on nearshore morphology and change characteristics of the historical databases, morphologic compartments were assigned to specific longshore segments of coast as positions of common reference for presenting results and conclusions (Chapter 2). Morphologic compartments refer to the beach and nearshore zones from the shoreline to the 12-m-depth (NGVD) contour or the limit of data coverage.

#### Coastal GIS strategy

In light of the immense quantity of geographic data assembled for quantifying changes in the study area, an integrated approach was applied for compiling and storing digital databases and analyzing magnitudes of change. Geographic data describe objects in terms of their position with respect to a known coordinate system, their spatial relationship with each other (topological

---

<sup>1</sup> Written by Mark R. Byrnes and Matteson W. Hiland.

information describing spatial units and their boundaries), and their attributes that are unrelated to position (e.g., geomorphic characteristics). For accurate assessment of position and topology, an integrated approach includes computer-aided drafting and design (CADD), computer cartography, and spatial analysis software within a GIS framework. A relational database was an integral component of the GIS used in this study to organize and store attribute information for processing. The capability of a GIS to perform spatial analyses is a primary factor that distinguishes it from CADD, computer cartography, and computer graphics display software. In addition to analysis benefits provided by a GIS, a number of practical considerations also are addressed. First, map data are more secure and better organized; second, redundant map information is eliminated; third, map revisions can be completed much faster and more accurately; and fourth, map data are easier to search, analyze, and present (Korte 1991). Most important, a GIS provides a standardized framework for consistent data capture and analysis.

The GIS strategy adopted in this study for data capture, analysis, and storage is shown in Figure 36. It includes six basic components: (a) source data, (b) data input, (c) interactive application modules, (d) geographic database, (e) spatial analyses, and (f) data output. The initial step in the strategy is compilation and evaluation of available source data. Within this procedure, it is imperative that all inherent errors be evaluated thoroughly to gauge the significance of measured change and whether this level of error will affect study objectives. Data input for this study includes compiling maps, field observations, electronically sensed data, textual attributes, and information stored on magnetic media. Digitizing points and lines (vector method) from maps and importing existing digital data files were the primary methods used for data compilation. A component of data capture procedures involves application-specific software modules for the type of geographic information being processed. For example, map data have certain cartographic parameters that must be retained during data capture. CADD systems are designed for digitizing but computerized cartographic procedures also are needed for accurate representation of map data within a GIS. Geographic queries include retrieval of data by location and attributes, whereas geographic processing involves calculation of distances, areas, and perimeters for quantifying change. Other related application software modules accept engineering surveys and GPS data for horizontal control.

The geographic database component in Figure 36 describes the structure and organization of digital data with regard to position, spatial relationships (topology), and attributes of geographical elements. This is discussed in detail in Appendix B under the *Organization of Geographic Data* section. Spatial analysis functions allow one to examine cause and effect relationships to develop models for describing the response of a coastal system to existing and expected changes. Finally, data output is related to the way in which information is displayed and results are reported to a user. Data may be displayed as maps, tables, reports, and text on a computer terminal or as a hardcopy. By utilizing this procedure for the coastal monitoring program tasks, present and future data sets used for analysis of morphologic changes at St. Marys Entrance and in adjacent offshore areas may be maintained in a common format. The data compiled and analyzed for Chapter 3 were performed and stored within a GIS framework. Much of the data presented in Chapters 4 and 5 are stored in a GIS for potential future application.

## Scope

Chapter 3 describes specific laboratory and field analyses and results associated with the shoreline position and bathymetric change component of the coastal monitoring program. Data sources, methodology of processing and analysis, and results are summarized and a discussion

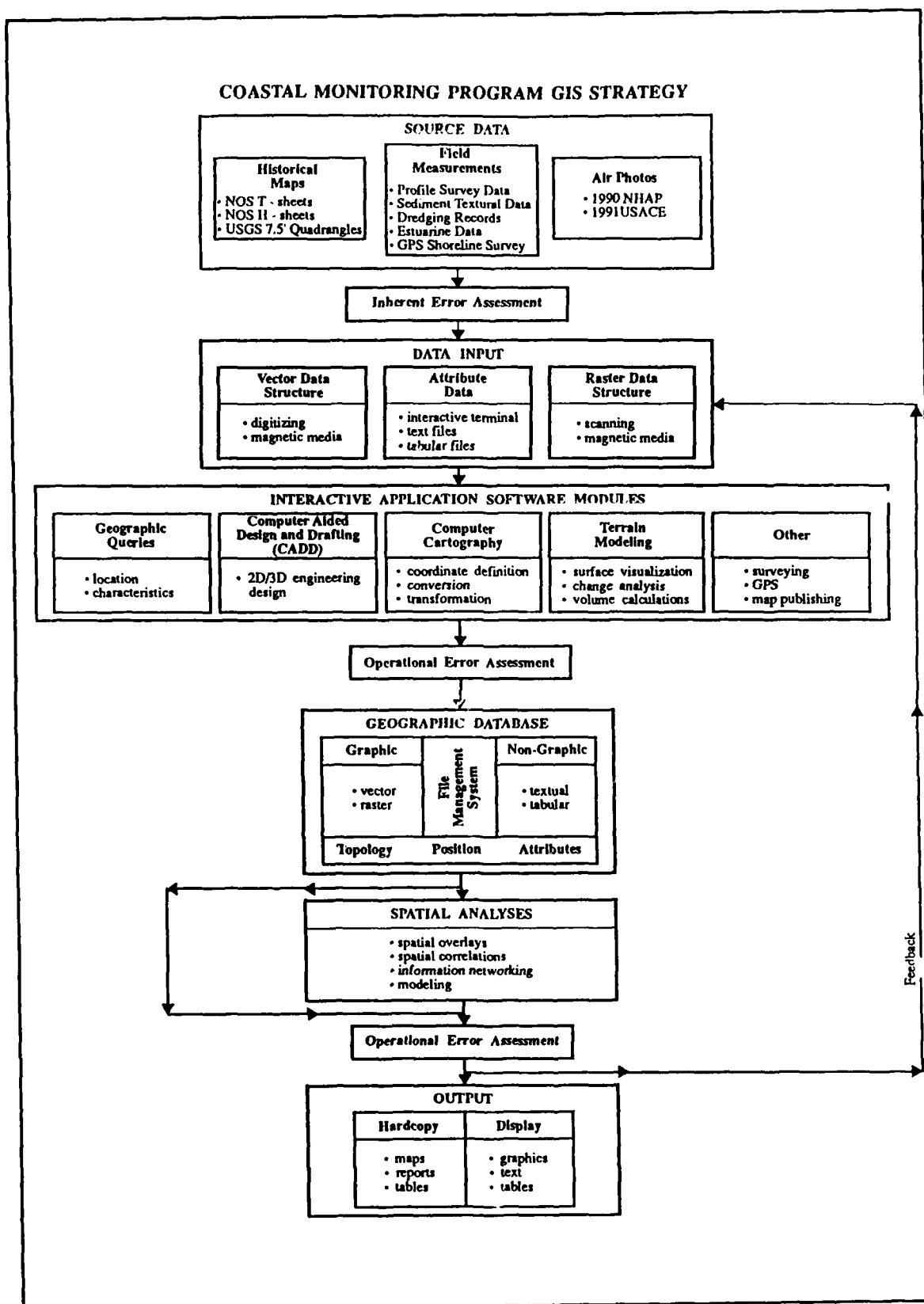


Figure 36. Coastal monitoring program GIS strategy (after Byrnes, McBride, and Hiland 1991)

of methods for analysis of cartographic data and the potential problems that must be considered when comparing map data for quantifying change is provided in Appendix B. A critical component of Appendix B is the section on organization of geographic data that provides details about mapping and GIS software applications as well as database structure and design for the study.

## Shoreline Position Change

Repetitive surveys of historical shoreline position have been recognized as a primary data source for quantifying rates of erosion and accretion (e.g., Morgan and Larimore 1957; Caldwell 1966; Langfelder, Stafford, and Amein 1970; Dolan et al. 1979; Morton 1979; Everts, Battley, and Gibson 1983; Leatherman 1984; Anders, Reed, and Meisburger 1990; Byrnes et al. 1991; McBride et al. 1991). Coastal scientists, engineers, and planners often use this information for estimating the magnitude and direction of sediment transport (Headland, Vallianos, and Sheldon 1987), monitoring engineering modifications to a beach (Dean 1988), examining geomorphic variations in the coastal zone (Hosier and Cleary 1977), establishing coastal erosion setback lines (Shows 1978), and verifying shoreline change numerical models (Kraus 1989). For the present study, these data are used to characterize shoreline response to natural and anthropogenic processes, provide baseline input requirements for predicting future changes in shoreline position using a numerical shoreline change model (Chapter 7), and establish a landward boundary for quantifying changes in nearshore bathymetry (this chapter).

Because mapping shoreline position has employed a variety of techniques since the mid-1800s (topographic surveys, aerial photographic interpretation, GPS surveys), it is necessary to determine the characteristics of the position being monitored for quantifying change. Shalowitz (1964) discusses the line being monitored, as documented in instructions to USC&GS (now called NOS of NOAA) topographic field parties, and states that the high-water shoreline is "determined from the physical appearance of the beach" rather than a position associated with a precise vertical tidal datum. He further states, "What the topographer actually delineated are the markings left on the beach by the preceding high water." From this explanation, it is clear the operative definition for *high-water line or shoreline* for early topographic surveys is the horizontal position associated with wave runup at high tide (Anders and Byrnes 1991). This shoreline generally is associated with features on the beach such as a dune scarp, berm crest, debris line, or tonal difference between wet and dry beach, below which the foreshore is smooth (most of these features can be identified on aerial photography as well). Whether planned or fortuitous, the high-water shoreline delineated from photography is consistent with historical field survey measurements because rectification procedures in most cases are planimetric (vertical position relative to a datum is not considered) (Stafford and Langfelder 1971, Dolan et al. 1980, Leatherman 1983b). Finally, a similar interpretation procedure was used for delineating high-water shoreline position with the GPS survey carried out during the monitoring study. This symmetry of interpretation among various data sources enables a reasonably accurate assessment of historical shoreline position change.

A computer-based shoreline mapping methodology, within a GIS framework, was used to compile and analyze changes in historical shoreline position between 1857/71 and 1991 for Cumberland and Amelia Islands. The purpose of this task was to quantify changes in shoreline position using the most accurate data sources and compilation procedures to characterize the

morphological evolution of the Cumberland-Amelia barrier island system as influenced by human modifications and natural processes. Because this information addresses a critical component of the study and provides baseline data for other study tasks, emphasis was placed on data accuracy and potential error estimates for gaging the significance of results. The following discussion focuses on available data sources, potential error estimates, a synthesis of regional trends, and spatial and temporal variability associated with shoreline position change.

### **Data sources**

Five potential data sources exist for assessing spatial and temporal changes in shoreline position. These include USGS topographic quadrangles, NOS topographic sheets, local engineering surveys, near-vertical aerial photographs, and GPS surveys. Each data source addresses a specific need that dictates use for a given project. Maps and charts are classified as either metric or nonmetric based on quality of construction. A metric-quality map contains a graticule (grid) of meridians and parallels (Ellis 1978). It represents all map features in precise relation to one another and to the grid. Only the most accurate metric maps were used in this study to ensure data quality.

**USGS topographic maps.** The most common maps used for documenting changes along the coast are USGS topographic quadrangle maps. These maps are created at a range of scales from 1:24,000 to 1:250,000 (Ellis 1978). The primary purpose of these maps is to portray the shape and elevation of the terrain above the shoreline. Accurate delineation of the shoreline was not a primary concern on these land-oriented maps. However, high-water shoreline position routinely is revised on 1:24,000 topographic maps using aerial photographic surveys. Many shoreline mapping studies have used these data for quantifying changes in position, but more accurate and appropriate sources should be employed if available.

**NOS topographic maps.** Another type of topographic map is that produced by NOS. Because this agency is responsible for surveying and mapping topographic information along the coast, topographic map products (T-sheets) have been used in the study of coastal erosion and protection, and frequently in courts in the investigation of land ownership (Shalowitz 1964). Most of these maps are planimetric in that only horizontal position of selected features is recorded; the primary mapped feature is the high-water shoreline. From 1835 to 1927, almost all topographic surveys were made by plane table; most post-1927 maps were produced using aerial photographs (Shalowitz 1964). NOS shoreline position data are often used on USGS topographic quadrangles, suggesting that T-sheets are the primary source for accurate shoreline surveys. Scales of topographic surveys are generally 1:10,000 or 1:20,000, although others exist. These larger scale products provide the most accurate representation of shoreline position other than direct field measurements using engineering methods.

**Large-scale engineering surveys.** In areas of significant human activity, engineering site maps often exist for specific coastal regions. Project planning and design demands this level of accuracy. However, surveyed areas often are quite limited by the scope of the project; regional mapping at large scale (greater than 1:5,000) is sparse. If these data do exist, they potentially provide the most accurate estimates of high-water shoreline position and should be used. These data are valuable for rectifying aerial photography for mapping shoreline position.

**Near-vertical aerial photography.** Since the 1920s, aerial photography has been used to record shoreline characteristics in many coastal regions. However, these data cannot be used

directly to produce a map. Aircraft tilt and relief may cause serious distortions that have to be removed by rectification. A number of graphical methods and computational routines exist for removing distortions inherent in photography (Leatherman 1983b, Anders and Byrnes 1991). Orthophotoquads and orthophotomosaics are photomaps made by applying differential rectification techniques (stereoplotters) to remove photographic distortions. Ease of data collection and the synoptic nature of this data source provide a significant advantage over most standard surveying techniques.

**GPS surveys.** During the late 1970s through the 1980s, significant advances in satellite surveying were made with the development of the Navigation Satellite Timing and Ranging (NAVSTAR) GPS. The system was developed to support military navigation and timing needs; however, many other applications are possible with the current level of technology (Figure 37). This surveying technique can be very accurate under certain conditions; however, signal degradation through selective availability causes significant positional errors if only one station is being used (Leick 1990). Differencing the satellite signals at two stations eliminates most of the error. Differential GPS provides the capability for accurately delineating high-water shoreline position from ground surveys.

**Shoreline position data for coastal monitoring study.** The two primary data sources used in compiling shoreline positions in this study were NOS T-sheets and a differential GPS survey. Shoreline position data for the period 1857/71 represent the earliest surveys on record for quantitative evaluation. Another field survey was conducted in 1924, and the 1933 and 1974 T-sheets were compiled by NOS from rectified aerial photography. A USGS topographic survey

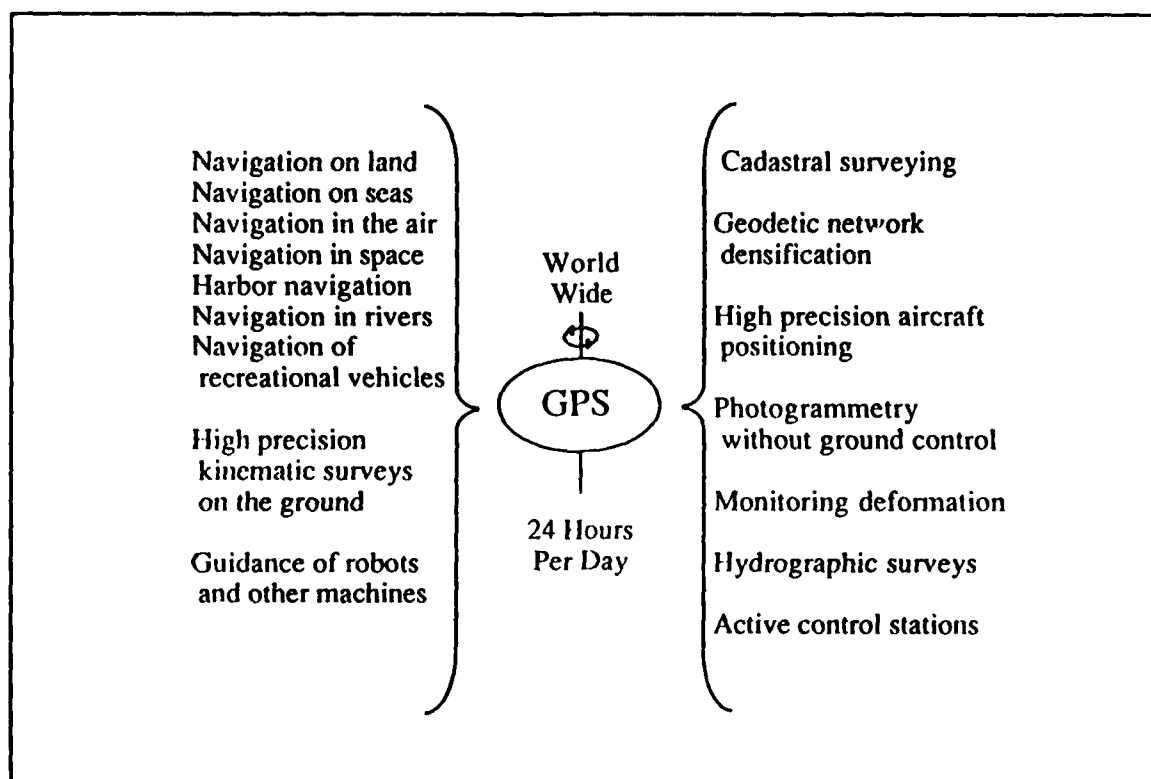


Figure 37. Civilian use of Global Positioning System (from Leick (1990))

based on aerial photography flown in 1957 also was used in the study because shoreline position information was lacking between 1933 and 1974, and the survey was temporally consistent with process data for shoreline numerical modeling efforts. The most recent and most accurate continuous shoreline position data were collected in October 1991 as part of a GPS field survey. After evaluating the merit of potential sources of information, it was evident that these data would provide the most accurate and complete summary of historical shoreline change for the coastline of Cumberland and Amelia Islands. Table 9 lists data sources used in the study, and the last section in Appendix B details specific characteristics associated with source data and digital compilation procedures. High-altitude aerial photography (flown in 1990), rectified with recent USGS topographic maps, provided a physiographic framework of the study area. However, photographic scale (1:62,500) precluded using the interpreted shoreline position along the outer coast for analytical purposes.

**Table 9**  
**Summary of Shoreline Source Data Characteristics for the Study Area**

Date	Data Source	Comments
1857/71	USC&GS Topographic Sheet (1:10,000 and 1:20,000)	First surveyed shoreline using standard engineering techniques; 1857 survey (1:10,000 scale) - southern 5 km of Cumberland Island and northern 7.5 km of Amelia Island; 1870 survey - northern 25 km of Cumberland Island; 1871 survey - southern 14 km of Amelia Island.
Aug-Nov 1924	USC&GS Topographic Sheet (1:20,000)	Field survey taken in conjunction with 1924 bathymetric survey.
Nov-Dec 1933	USC&GS Topographic Sheet (1:10,000)	First photo-interpreted shoreline; position of high-water shoreline appears in error (see Appendix B).
March 1957	USGS 7.5' Topographic Quadrangle (1:24,000)	Data source inconsistent relative to other surveys (see text and Appendix B).
Oct 1973/ Apr 1974	NOS Topographic Sheet (1:20,000)	Only seaward shoreline is delineated from photography; Oct 1973 survey - Cumberland Island; Apr 1974 survey - Amelia Island.
Oct 1991	GPS Survey (1:1); one stationary unit and one roving unit	Differential corrections were applied for accurate estimates of high-water shoreline position.

### Mapping shoreline position using GPS

The most recent shoreline position survey completed for this study was obtained by modern field survey techniques using GPS technology. Many advantages exist with this technique over traditional data sources, not the least of which is a rapid and accurate field measurement of high-water shoreline position. Two six-channel Trimble Navigation Pathfinder Professional GPS receivers were deployed for this effort. One unit was referenced with a first-order leveled benchmark at the southern end of Cumberland Island (USACE marker PAUL-ST). The other unit was used to collect shoreline position information from a four-wheel All-Terrain Vehicle (ATV) and four-wheel-drive pickup. The base station collected a data point every 10 sec while the mobile unit collected information at a 1-sec interval. Base station data were used to differentially correct shoreline position data for signal degradation by selective availability and differences in signal transmission (Leick 1990). Numerous secondary benchmarks (third-order

leveled) along the length of the Cumberland and Amelia Islands were used to gage the accuracy of shoreline measurements ( $\pm 1$  to 3 m) relative to the base station.

The horizontal position of the high-water shoreline as recognized on the beach was determined visually using a hierarchy of criteria dependent on morphologic features present on the subaerial beach. The primary criterion was a well-marked limit of uprush by waves associated with high tide. This generally was recognized as a dune or beach scarp, marking the upper limit of the foreshore (Figure 38). If a scarp did not exist, a debris line usually could be identified. Sometimes a debris line existed landward and at a lower elevation than the berm crest. When this was encountered, the position of the berm crest was tracked as the high-water shoreline because different physical processes affect the location of the debris line relative to those associated with a scarp or upper foreshore demarcation. The criteria adopted are consistent with those used by field topographers and photo interpreters (Shalowitz 1964).

The shoreline was surveyed in about 2 hr for each island. Data were collected only when a minimum of four satellite signals were being received simultaneously. This kept the accuracy of surveys high and had minimal effect on the timing of data collection. More important, the procedure provided a means of obtaining a direct field measurement of shoreline position without having to consider cartographic parameters and limitations. Field data collection using this technique encompasses interpretation and digitizing, thus increasing accuracy and streamlining the processes of data compilation and analysis.



Figure 38. Well-defined scarp along northern Cumberland Island formed at high tide

## Quantifying shoreline change

Once shoreline position data are compiled accurately, spatial and temporal changes can be quantified using manual or automated procedures. The manual technique involves making measurements at regular intervals from overlay maps or from the computer screen and tabulating this information for assessing trends. Not only is this approach time-consuming, but, if analog map overlays are used, another level of inherent errors is included in the measurements because the composite map is a second-generation product at scale. Most current procedures applied for quantifying changes in shoreline position involve some method of digital data comparison.

For this study, the Automated Shoreline Analysis Program (ASAP) was used to quantify shoreline change at a 50-m longshore interval. The first step of the procedure is to identify segments of the coast with similar shoreline orientations. Next, digital data stored in an Intergraph MicroStation design file are imported by a software routine that prepares the information for temporal comparison. Because digital shoreline position data are stored in a design file in the order in which shorelines were compiled, sorting of points by location (Universal Transverse Mercator (UTM) x- and y-coordinates) must be done upon export from the design file to ensure spatial consistency for temporal comparisons. Once the points are in order, the average orientation angle of the shoreline is used as a reference for calculating discrete positions for a user-defined interval. Cubic spline interpolation procedures are used to obtain these positions because a curve-fitted shoreline boundary defined by multiple points is considered more representative of natural conditions than one produced by linear interpolation techniques. This step organizes randomly spaced information for a systematic comparison of spatial and temporal changes. Because the original data vary in distance between data points, the average of five equally spaced points within each 50-m segment represents change for any given time interval.

Three primary statistics are calculated for characterizing change. They include the sample mean, sample standard deviation, and 95 percent confidence limits. The sample mean is defined as a measure of central tendency for a set of sample observations and is expressed as follows:

$$\bar{x} = \frac{\sum_{i=1}^n x_i}{n} \quad (1)$$

where  $x_i$  = sample observations for  $i = 1$  to  $n$  and  $n$  = total number of observations. The sample standard deviation  $s$  is a measure of sample variability about the mean.

$$s = \sqrt{\frac{\sum_{i=1}^n (x_i - \bar{x})^2}{n - 1}} \quad (2)$$

The 95-percent confidence limit is an estimate of the probability that the sample mean is within a calculated number of units of the population mean. It is expressed as:

$$\pm t_f \frac{s}{\sqrt{n}} \quad (3)$$

where  $t_f$  represents the percentage points of Student's  $t$ -distribution for a given level of significance and is obtained as a function of the number of unrestricted variables associated with the sample standard deviation (Anderson and Sclove 1978).

Comparisons of temporal trends are made using these statistics. In addition, spatial trends are evaluated using a blocking technique where regions exhibiting a similar direction of change are grouped for variable-length shoreline cells. This approach provides a natural segregation of shoreline segments, rather than more subjectively chosen boundaries, for assessing temporal and spatial trends. Sample mean, standard deviation, 95-percent confidence limit, and percentage of shoreline represented by the statistics were tabulated for each cell.

### Cumulative potential error

When considering all the potential errors discussed in Appendix B, it should be recognized that these apply to each individual map or air photo. In making comparisons of shoreline position, error is additive because separate maps and air photos are being used. Worst-case error estimates can be made by summing the maximum error values for each data source being compared. If it is assumed that individual errors represent standard deviations, a root-mean-square (rms) approach can be applied to provide a more realistic assessment of combined potential errors (Merchant 1987; Crowell, Leatherman, and Buckley 1991). Table 10 summarizes estimates of potential error for the primary data sources used in this study. The rms errors for 1857/71 and

**Table 10**  
**Estimates of Potential Error Associated with Shoreline Position Surveys**

Traditional Engineering Field Surveys (1857/71 and 1924 shorelines)		
Location of rodded points	± 1 m	
Location of plane table	± 2 to 3 m	
Interpretation of high-water shoreline position at rodded points	± 3 to 4 m	
Error due to sketching between rodded points	up to ± 5 m	
Cartographic Errors (all maps for this study)	Map Scale	
	1:10,000	1:20,000
Inaccurate location of control points on map relative to true field location	up to ± 3 m	up to ± 6 m
Placement of shoreline on map	± 5 m	± 10 m
Line width for representing shoreline	± 3 m	± 6 m
Digitizer error	± 1 m	± 2 m
Operator error	± 1 m	± 2 m
Aerial Surveys (1933 and 1973/74 shorelines)	Map Scale	
	1:10,000	1:20,000
Delineating high-water shoreline position	± 5 m	± 10 m
GPS Survey (1991 shoreline)		
Delineating high-water shoreline	± 1 to 3 m	
Position of measured points	± 2 to 5 m (specified); ± 1 to 3 m (field tests)	
Sources: Shalowitz 1984; Ellis 1978; Kruczynski and Lange 1990; Anders and Byrnes 1991; Crowell, Leatherman, and Buckley 1991		

1924 T-sheets (1:20,000 scale) are about  $\pm 15.2$  m, whereas the 1933 (1:10,000) and 1973/74 (1:20,000) cartographic data sources contain about  $\pm 8.4$  and  $\pm 16.7$  m of potential error, respectively. Although it seems unlikely that potential error associated with newer data sources could be greater than historical field surveys, interpretation of high-water shoreline position from remotely sensed data rectified using base maps or points from base maps at a scale of 1:20,000 is less accurate than direct field measurements. The GPS survey provided the most accurate measurement of shoreline position with an estimated maximum rms error of  $\pm 5.8$  m. Table 11 provides a summary of maximum rms errors for available shoreline change data for the study area.

<b>Table 11</b> <b>Maximum Root-Mean-Square (rms) Potential Error for Shoreline Change Data</b>					
<b>Date</b>	<b>1924</b>	<b>1933<sup>1</sup></b>	<b>1957</b>	<b>1973/74</b>	<b>1991</b>
<b>1857/71</b>	$\pm 21.5^2$	$\pm 17.3$	$\pm 25.2$	$\pm 22.6$	$\pm 16.3$
	$(\pm 0.3/\pm 0.4)^3$	$(\pm 0.2/\pm 0.3)$	$(\pm 0.3/\pm 0.3)$	$(\pm 0.2/\pm 0.2)$	$(\pm 0.1/\pm 0.1)$
<b>1924</b>		$\pm 17.3$	$\pm 25.2$	$\pm 22.6$	$\pm 16.3$
		$(\pm 1.9)$	$(\pm 0.8)$	$(\pm 0.5)$	$(\pm 0.2)$
<b>1933<sup>1</sup></b>			$\pm 21.7$	$\pm 18.7$	$\pm 10.2$
			$(\pm 0.9)$	$(\pm 0.5)$	$(\pm 0.2)$
<b>1957</b>				$\pm 26.1$	$\pm 20.9$
				$(\pm 1.5)$	$(\pm 0.6)$
<b>1973/74</b>					$\pm 17.7$
					$(\pm 1.0)$
<sup>1</sup> Interpreted high-water shoreline position appears to be in error (see Table 10). <sup>2</sup> Magnitude of potential error associated with high-water shoreline position change (m). <sup>3</sup> Rate of potential error associated with high-water shoreline position change (m/year).					

## Results

The magnitude and direction of shoreline position change were evaluated for Cumberland and Amelia Islands using six different surveys (1857/71, 1924, 1933, 1957, 1973/74, 1991). Patterns of shoreline movement for the period of record were described qualitatively to provide a regional perspective of change for the study area. Quantitative estimates also were tabulated for gaging temporal and spatial trends in the magnitude and rate of shore response. Cumulative and incremental rates of change were summarized for evaluating temporal trends, and spatial variability was assessed by averaging rates of change for coastal segments having similar response characteristics (retreat versus advance) for each time interval. Sample standard deviation and 95-percent confidence limits also were calculated to estimate sample variability around mean shoreline change rates. The following discussion outlines these results for addressing historical geomorphic response to natural and human-induced impacts in the study area.

**Synthesis of regional shoreline change trends.** Regional changes in high-water shoreline position for surveys in the study area are illustrated in Figure 39. Although a number of significant changes in shoreline position are identified for local areas of the study region, the

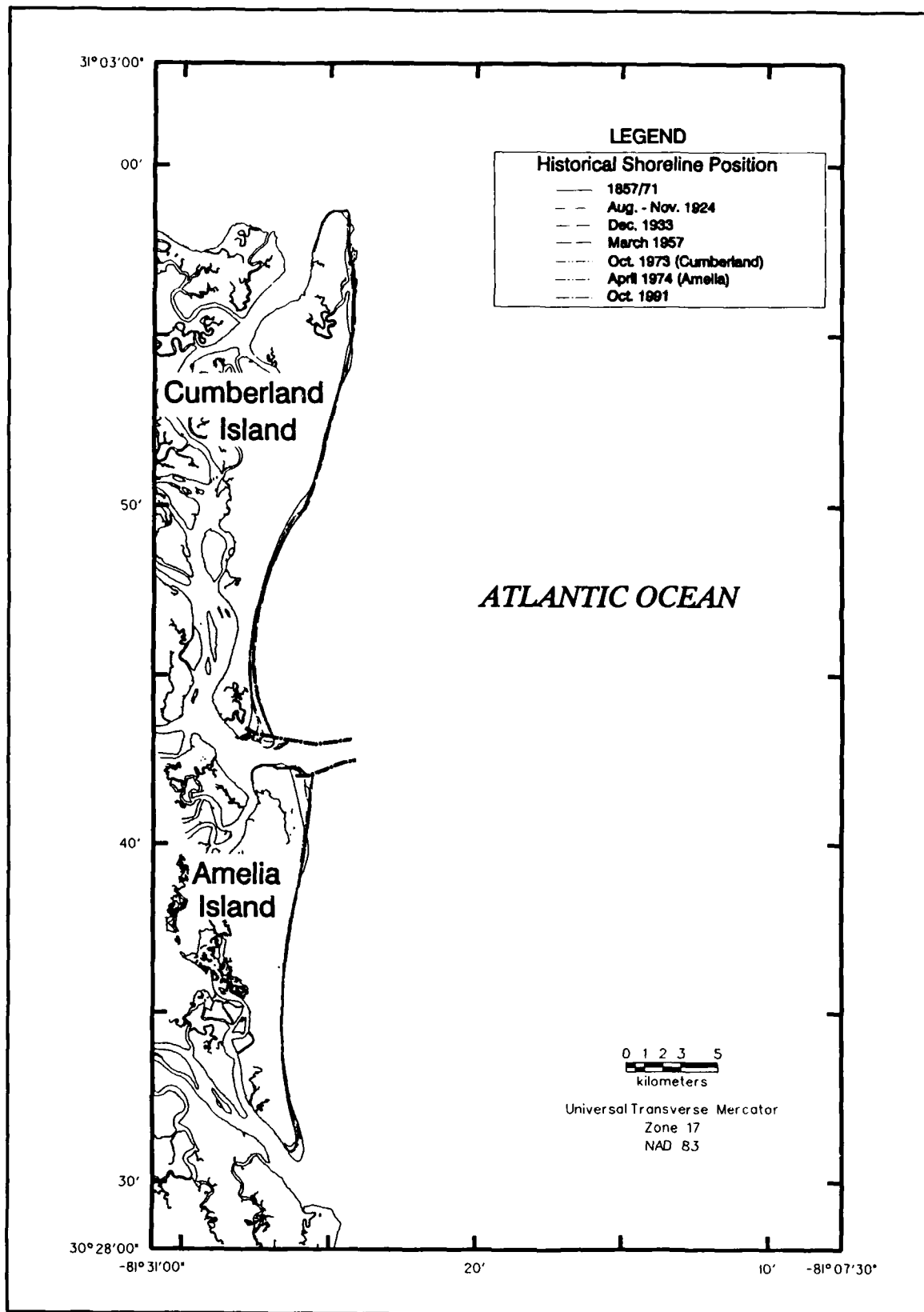


Figure 39. Shoreline position change for the Kings Bay study area from 1857/71 to 1991

dominant trend for all time periods is relative stability to progradation for the Cumberland-Amelia barrier island system. The greatest amount of change occurred between 1857/71 and 1924, apparently in response to jetty construction (Figure 39). Shorelines adjacent to the jetties on southern Cumberland and northern Amelia Islands indicate transport of sand toward the inlet at both sites. This trend is most noticeable on Amelia Island where approximately 68 percent of historical shoreline movement occurred during the first 53 years (44 percent of total record) of shoreline surveys. It should be noted that the northern third of Amelia Island was first surveyed in 1857, 14 years prior to the rest of the island. Although shoreline rates of change were computed using this date, it is assumed that minimal change occurred in this area between 1857 and 1871 for the analysis presented above. A similar assumption was used for Cumberland Island where the southern 5 km of shoreline were initially surveyed in 1857 and the rest of the coast was surveyed in 1870. The rate of change is more gradual for Cumberland Island than Amelia Island, and shoreline response between 1857/70 and 1924 represents about 37 percent of total historical shoreline movement.

Cumulative and incremental changes in position of the high-water shoreline were calculated to estimate historical trends for Cumberland and Amelia Islands. As shown in Figure 39, the general pattern that evolved for both coastlines was regional consistency in the direction of shoreline movement. Table 12 illustrates the magnitude and direction of the rate of change for Cumberland Island, indicating shoreline progradation for all time periods relative to the 1857/70 survey. Net shoreline advance predominates at an average rate of 1.5 m/year for the period 1857/70 to 1991. In fact, all combinations within the change matrix for Cumberland Island (Table 12) show average coastal progradation for the 134-year time period. Average rates of change for Amelia Island (Table 13) show the same general characteristics as those for Cumberland. Net shoreline progradation is dominant between 1857/71 and 1991, and the long-term net rate of change is 0.4 m/year. However, one primary difference exists between the two islands; some incremental rates of change for Amelia Island show periods of retreat. For both areas, the rate of shoreline position change is not constant in direction or magnitude for the historical record.

Because the information provided in the tables represents averages for each island, sample standard deviations are large relative to mean change rates. The variation in historical trend along Amelia Island has larger sample standard deviation values than those for Cumberland Island, suggesting greater longshore variability in direction and magnitude of change. In fact, the predominant direction of change switches from progradation along the northern coast to retreat for the southern 6 km of the island. Only small sections of Cumberland exhibit retreat for any time interval, resulting in lower variability. However, because the number of points sampled was large for each shoreline (calculated at 50-m intervals), the 95-percent confidence limit was relatively small for both islands. This suggests that the computed sample mean provides a reasonable estimate of the population mean for both shorelines.

Overall trends in cumulative shoreline position change for both islands present similar patterns of movement, although the magnitude of change varies (Figure 40). Minor deviations in trend are associated with change rates for Cumberland Island (except for a slight increase in shoreline progradation to 1957), although the rate of shoreline advance for the entire time period is lower than any other historical time interval. The fact that the rate of shoreline change has remained relatively constant and progradational indicates a surplus in sand supply to the subaerial beach.

**Table 12**  
**Average Shoreline Position Change for Cumberland Island**

Year	1924	1933	1957	1973	1991
1857/70	1.6 <sup>1</sup>	1.6	1.8	1.7	1.5
	2.3 <sup>2</sup>	2.4	2.1	2.0	1.9
	0.2 <sup>3</sup>	0.2	0.2	0.2	0.2
	24.4 <sup>4</sup>	24.7	24.8	24.8	24.8
1924		0.5	1.8	1.6	1.2
		4.6	2.4	2.4	2.3
		0.4	0.2	0.2	0.2
		24.95	24.95	24.95	24.95
1933			2.3	1.8	1.3
			2.4	2.5	2.4
			0.2	0.2	0.2
			25.4	25.45	25.45
1957				1.4	0.8
				3.5	2.9
				0.3	0.3
				25.8	25.9
1973					0.1
					3.3
					0.3
					26.2

<sup>1</sup> Average shoreline change rate (m/year).

<sup>2</sup> Sample standard deviation ( $\pm$  m/year).

<sup>3</sup> 95-percent confidence limit ( $\pm$  m/year).

<sup>4</sup> Length of analyzed shoreline (km).

Based on observations of shoreline movement presented in Figure 39, sediment supply is from the north. Cumulative changes for Amelia Island show a different trend in that the magnitude of change in shoreline advance is decreasing for most time periods. Incremental changes in average shoreline position emphasize this trend (shoreline retreat), but rates of change for most intermediate time intervals are insignificant relative to inherent potential errors (Tables 11 and 13). Thus, cumulative change since 1857/71 is most appropriate for quantifying trends. By 1991, the average cumulative rate of progradation had decreased by about 60 percent relative to the value in 1924. Since 1957, both islands have shown the same direction and magnitude of change in rates of shoreline advance, but long-term reduction in the average rate of shoreline progradation along Amelia Island appears more chronic since 1924.

**Site-specific shoreline response.** Although net shoreline movements over the period of record indicate a stable to prograding system for both islands, five areas of substantial localized change have had significant influence on average system response. The following regions and characteristics are identified: (a) the Cumberland Embayment morphologic compartment (Figure 35) shows persistent progradation in response to southerly directed sand transport; (b) southern Cumberland Island shows net shoreline advance of about 1.0 km since 1857 as a fillet against the north jetty of St. Marys Entrance; (c) northern Amelia Island exhibits net shoreline advance of

**Table 13**  
**Average Shoreline Position Change for Amelia Island**

Year	1924	1933	1957	1974	1991
1857/71	1.1 <sup>1</sup>	0.6	0.7	0.5	0.4
	3.0 <sup>2</sup>	3.1	2.6	2.1	1.9
	0.3 <sup>3</sup>	0.3	0.3	0.2	0.2
	19.25 <sup>4</sup>	19.25	19.25	19.25	19.25
1924		-2.8	0.1	-0.2	-0.2
		5.9	2.9	1.8	1.6
		0.6	0.3	0.2	0.2
		19.4	19.4	19.4	19.4
1933			1.2	0.4	0.2
			3.0	1.9	1.6
			0.3	0.2	0.2
			19.4	19.4	19.4
1957				-0.8	-0.5
				2.6	1.9
				0.3	0.2
				19.5	19.5
1974					-0.3
					1.8
					0.2
					19.5

<sup>1</sup> Average shoreline change rate (m/year).  
<sup>2</sup> Sample standard deviation ( $\pm$  m/year).  
<sup>3</sup> 95 percent confidence limit ( $\pm$  m/year).  
<sup>4</sup> Length of analyzed shoreline (km).

about 0.75 km since 1857 for approximately 3 km south of the south jetty at St. Marys Entrance; (d) the headland just south of the fillet along northern Amelia Island retreated in response to jetty construction, resulting in a straightened shoreline; and (e) the southern terminus of Amelia Island eroded rapidly between 1871 and 1924, and the shoreline has continued retreating landward since this time. The greatest magnitudes of historical shoreline change are associated with these areas.

The southern half of Cumberland Island exhibits shoreline progradation between 1857/70 and 1924. Two areas of substantial change include the northern coast of the Cumberland Embayment and the southern prograding shoreline near the jetty. Figure 41 illustrates historical shoreline response for central Cumberland Island (the northern half of the Cumberland Embayment and the southern 4 km of the Stafford Shoal morphologic compartments) where accretion of sand on the subaerial beach caused shoreline advance for most of the area. Only the northern 2 km of coast in this area have experienced shore retreat since 1870, and this occurred after the 1957 survey. Just south of this zone of erosion is a 2-km reach of rapid shoreline progradation. Most of the change recorded for this area occurred between 1870 and 1924. However, this stretch of coast continued to prograde to the south and east between 1924 and 1991 at a slower rate. Figure 42 is a plot of rate of change versus alongshore distance for Cumberland Island, showing that the rate of shoreline advance for the Cumberland Embayment (starting at an alongshore distance of about 14 km) has been persistent since 1924.

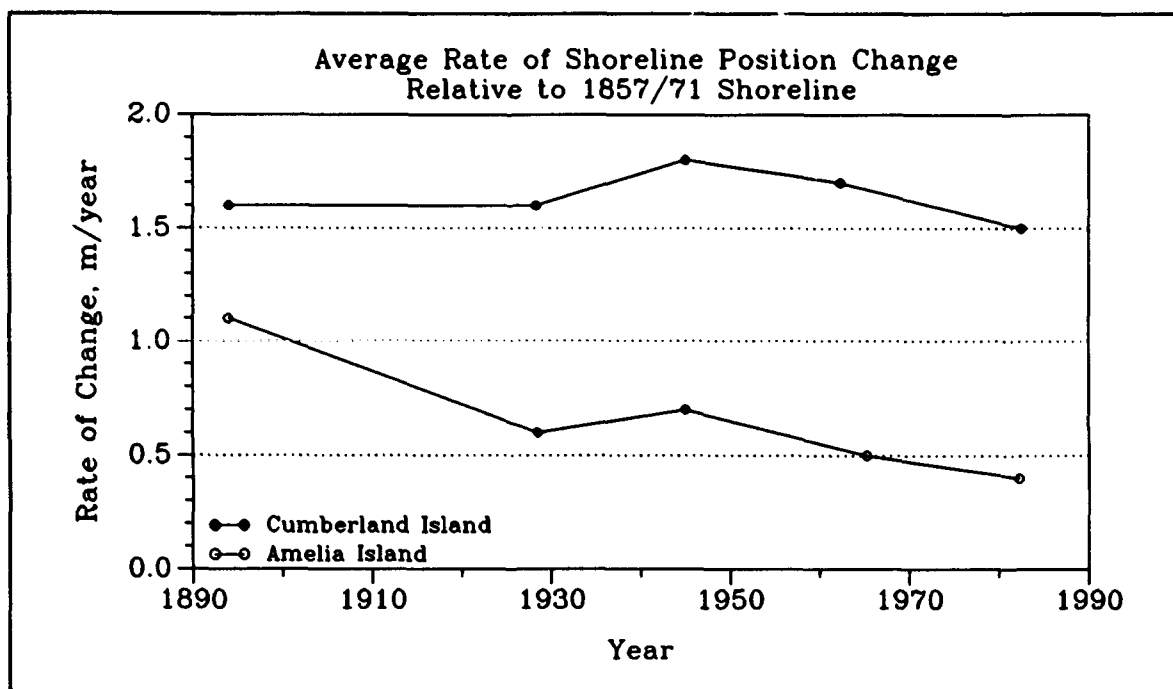
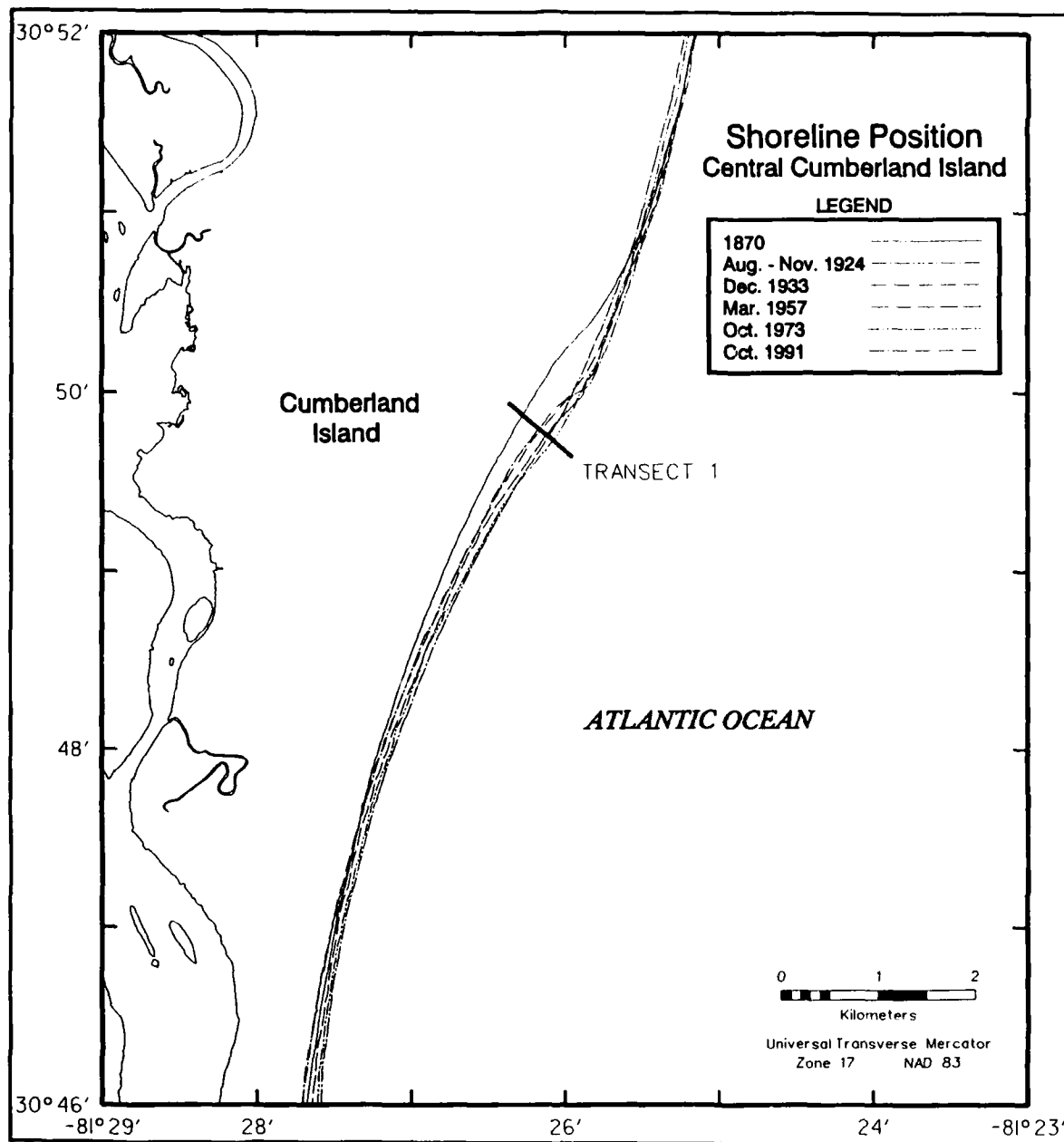


Figure 40. Cumulative change in shoreline position relative to the 1857/71 shoreline

The shorelines adjacent to St. Marys Entrance show the greatest amount of change for the study area. The magnitude of change for the period 1857 to 1991 is illustrated in Figure 43 (the boundaries for this figure represent the limits of data coverage for the 1857 shoreline). Shoreline response for southern Cumberland Island was progradational for the period of record except for the northern 3 km of this area between 1857 and 1924. The rate of shoreline advance for southern Cumberland Island has been relatively constant throughout the period of record (Figure 42). Northern Amelia Island shows the same general trend at the sand fillet just south of the jetty. The most significant change in shoreline position for this area occurred between 1857 and 1924. However, unlike southern Cumberland Island, shoreline retreat occurred between 1957 and 1974 from the south entrance jetty to the seawall at Fernandina Beach, Florida. Consequently, this stretch of shore has been replenished since the late 1970s (Chapter 5).

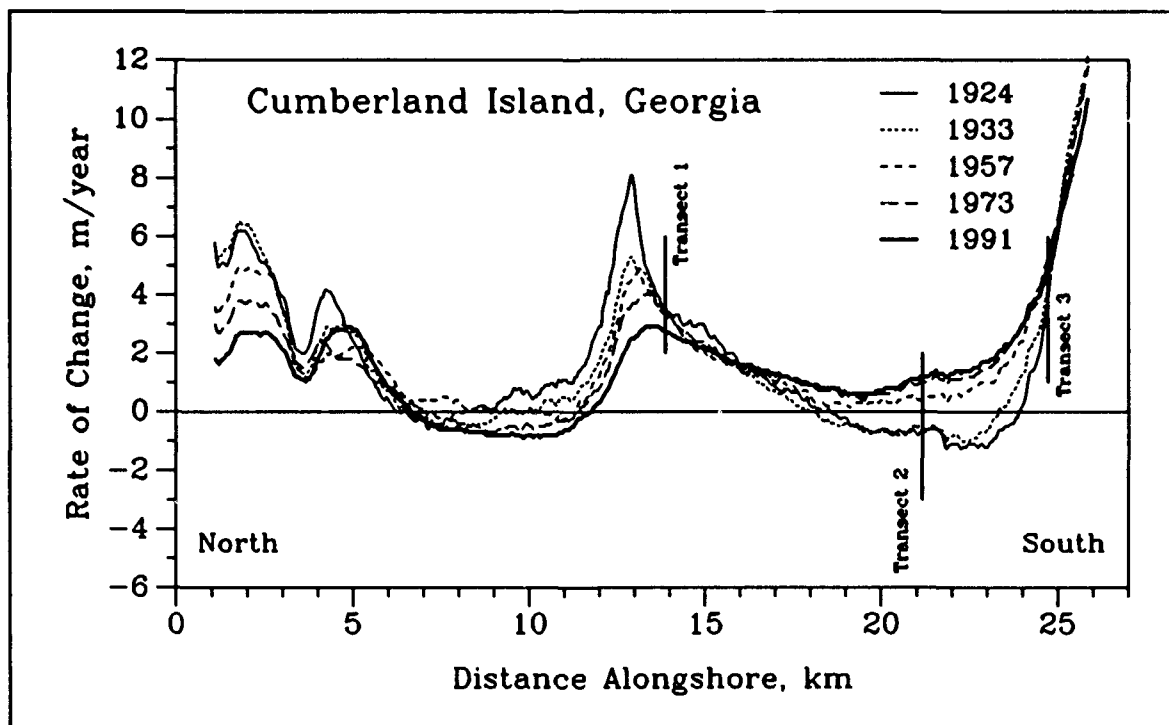
Another area of significant change is located near the revetment east of the city of Fernandina Beach. In 1857, the shoreline was approximately 300 m seaward of its present location. Practically all of this change occurred between 1857 and 1924 as the northern end of Amelia Island realigned in response to jetty construction. Since this time, little change in shoreline position has occurred, although a revetment was constructed in 1964 after Hurricane Dora.

The final region of significant shoreline movement for the study area is southern Amelia Island. Figure 44 shows a trend of decreasing change with distance north of the Nassau Sound Tidal Inlet Complex. At American Beach, nearly stable conditions have persisted historically. Similar to trends identified in Figures 41 and 43, most of the change at the southern terminus of Amelia Island occurred by 1924. However, this is not the case updrift of this area where rates of retreat have increased steadily between 1871 and 1991. Figure 45 shows this trend most clearly when comparing historical shoreline positions with the 1991 survey.

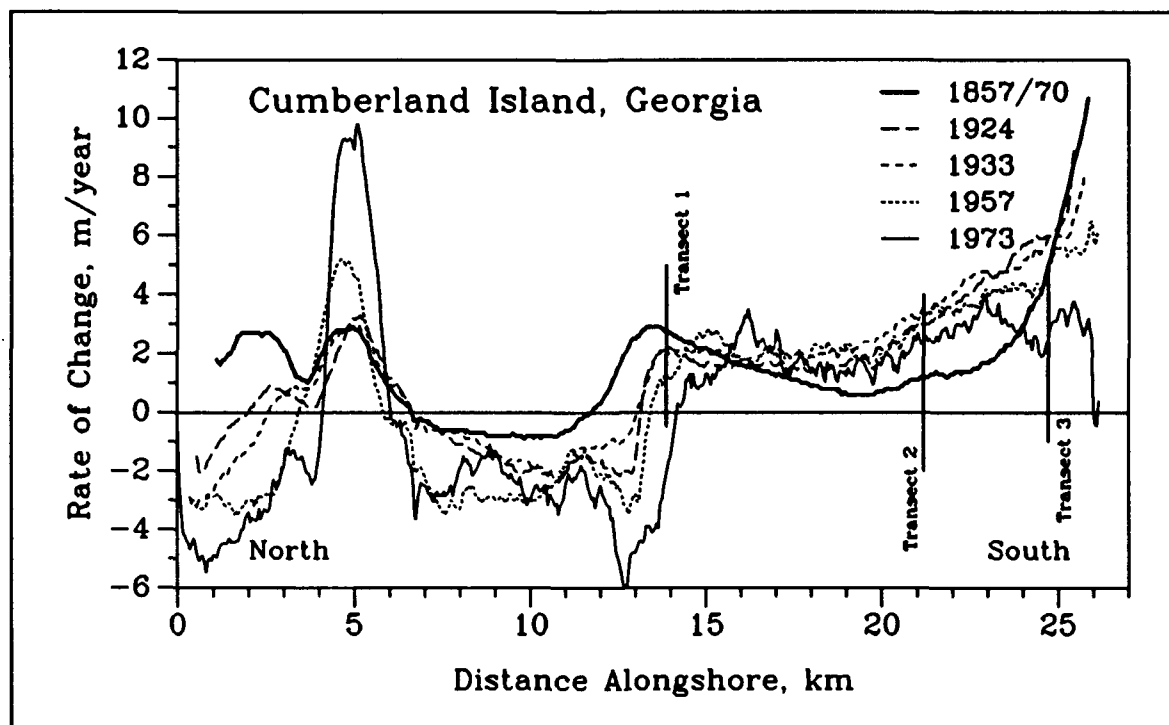


**Figure 41. Change in historical shoreline position for central Cumberland Island**

One recurring trend for shoreline response at these five localized regions is rapid change in shoreline position between 1857/71 and 1924. Besides shoreline change maps, two additional approaches were used to document this and other historical trends. Figures 42 and 45 illustrate alongshore variations in rates of shoreline movement for cumulative and incremental changes. For the five identified areas of localized change, the magnitude of shoreline response associated with the 1857/71 to 1924 time interval generally was dramatic relative to other time intervals. Exceptions do exist for the Cumberland Embayment and the coast south of American Beach, where rates of change have been increasing at a constant rate since 1924. Figure 46 summarizes



a. Shoreline position change relative to 1857/70



b. Shoreline position change relative to 1991

Figure 42. Trends in rates of shoreline position change for Cumberland Island

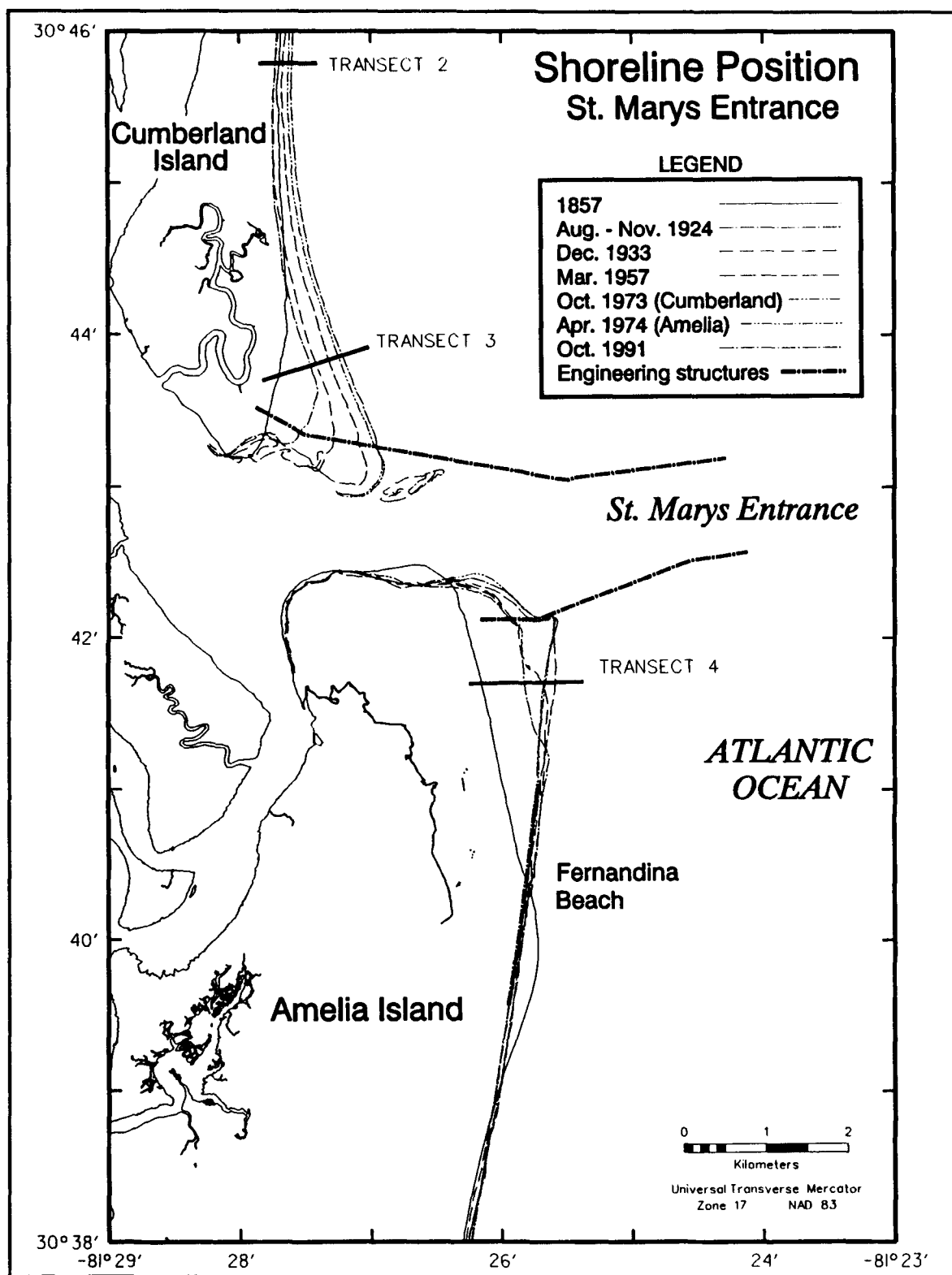


Figure 43. Change in historical shoreline position near St. Marys Entrance

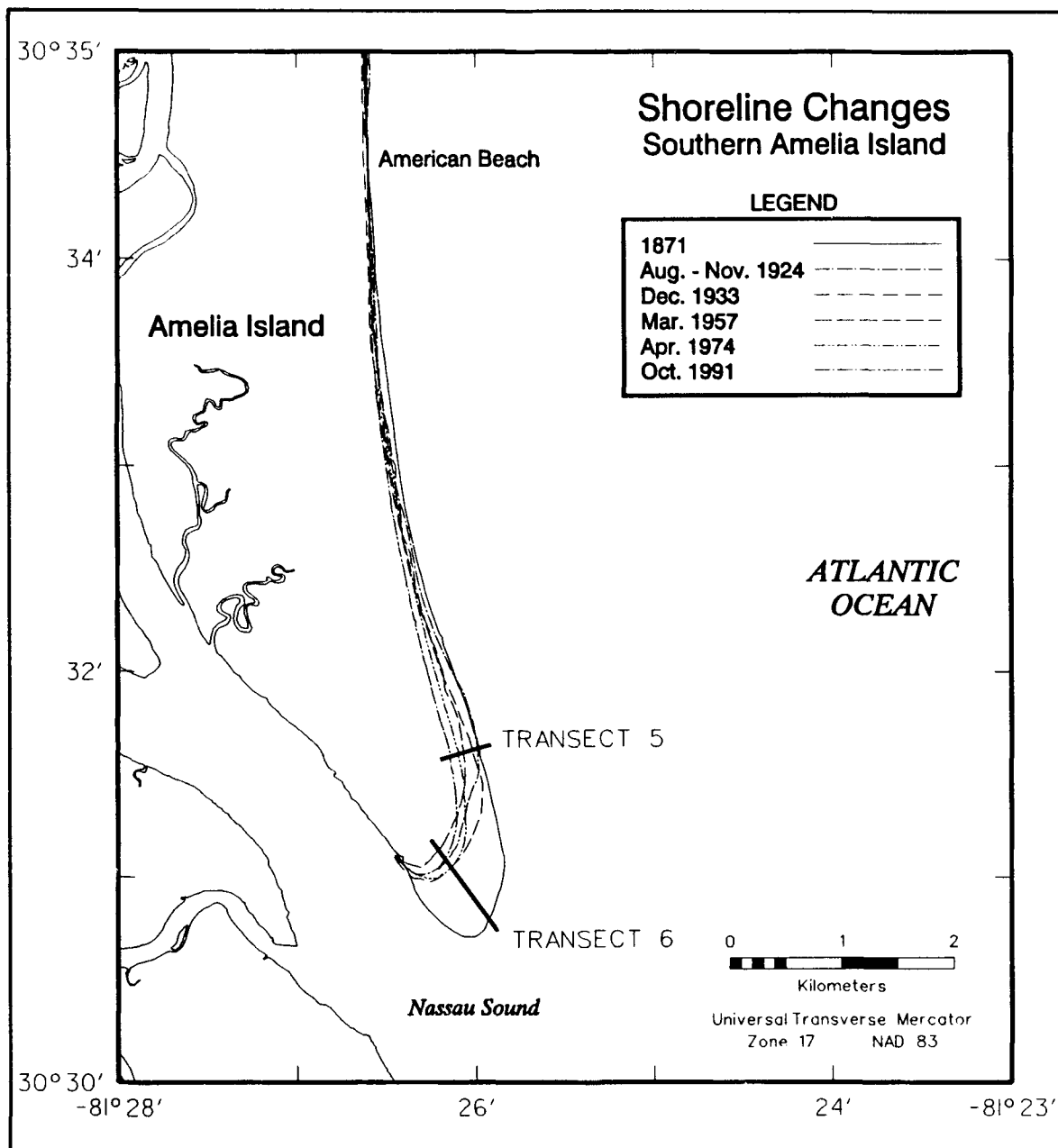
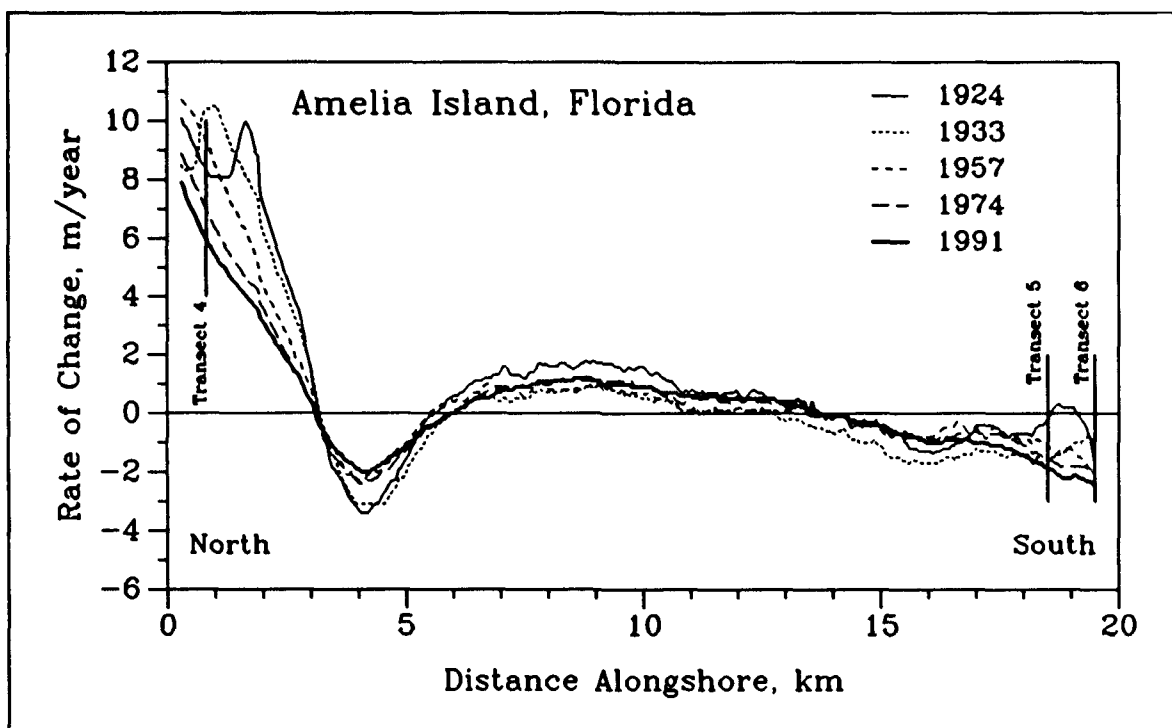
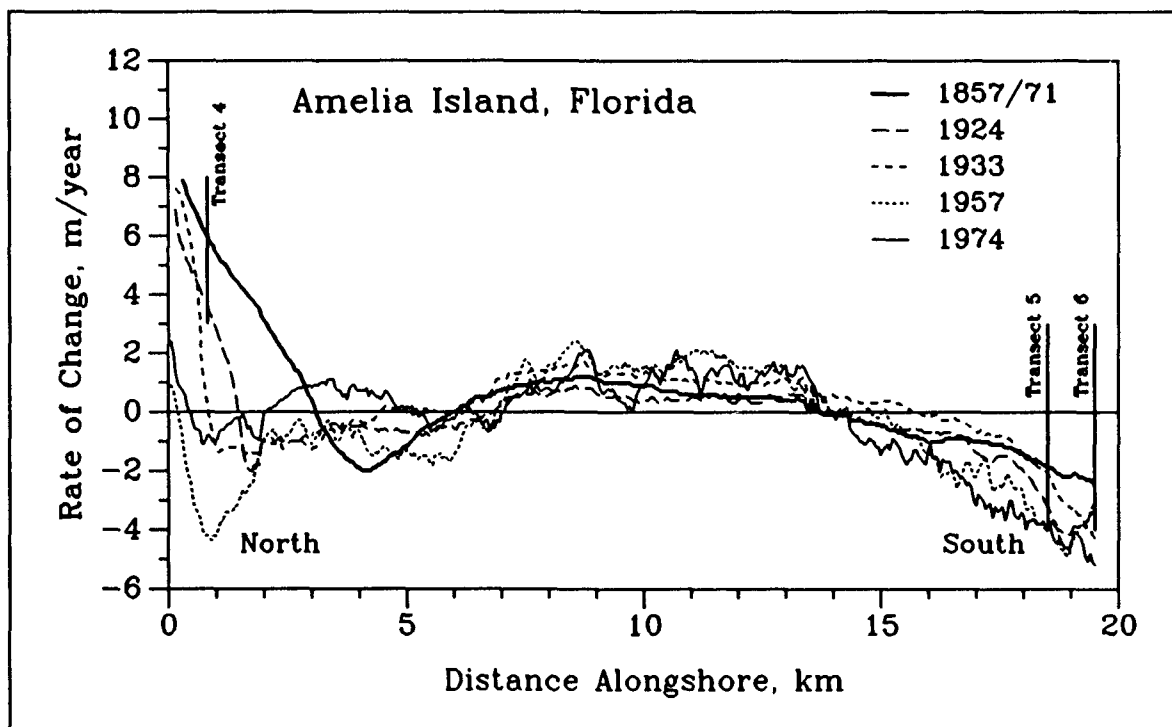


Figure 44. Change in historical shoreline position along southern Amelia Island

these trends for the six transects identified in Figures 41, 43, and 44. Shoreline change measurements were taken at each transect relative to the 1857/71 shoreline to document long-term trends and illustrate spatial variability in shore response at natural and human-influenced coastal systems. Table 14 summarizes shoreline position change for all transects. Areas showing greatest amounts of movement (Transects 1, 3, 4, and 6) generally have maintained similar rates of change since 1924, except for the southern terminus of Amelia Island (Transect 6) where shoreline position has remained relatively constant since 1924, reflecting a decrease in the rate of change since 1871. Transects 2 and 5 show opposite trends; the rate of shoreline progradation (Transect 2) and retreat (Transect 5) has increased at a constant rate since 1924.



a. Shoreline position change relative to 1857/71



b. Shoreline position change relative to 1991

Figure 45. Trends in rates of shoreline position change for Amelia Island

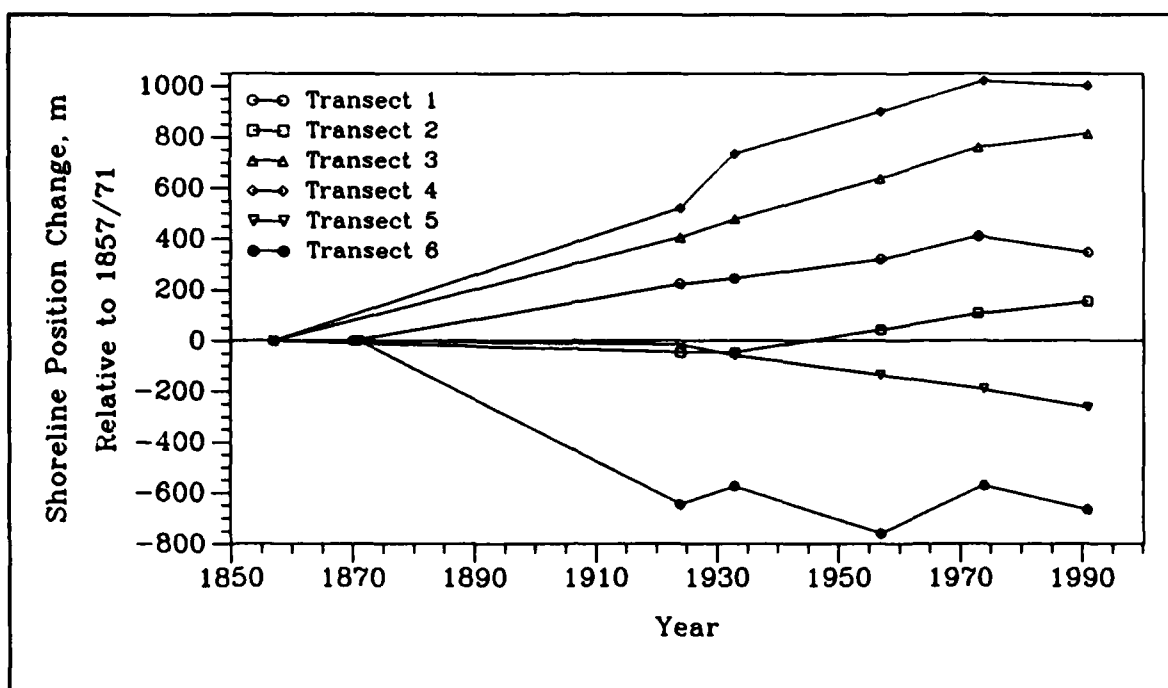


Figure 46. Trend of change in shoreline position for Cumberland and Amelia Islands

Although northern Amelia Island, from the jetty to the revetment, has been eroding in recent years, only two of the six transects indicate net long-term losses from the system since 1857/71 (south Amelia Island), and only one indicates chronic losses (Transect 5). The shoreline along the southern 4 km of Amelia Island appears to be responding to a persistent deficit in sediment supply since 1871, possibly associated with inlet processes at Nassau Sound. Conversely, data in Table 14 indicate the majority of change at the southern terminus of Amelia happened between 1871 and 1924, encompassing the period of jetty construction at St. Marys Entrance. Although it is plausible to employ this cause and effect relationship to explain change, data for Transect 1 (Cumberland Embayment) show the same trend of rapid change, and this area is located updrift of jetty influences.

Table 14

Shoreline Position Change (m) at Transects Along Cumberland and Amelia Islands

Year	Transect	1924	1933	1957	1973	1974	1991
1857	2	-47	-46	43	108	-- <sup>1</sup>	154
	3	406	478	638	760	--	814
	4	505	731	894	--	759	743
1870	1	223	245	320	411	--	346
1871	5	-15	-59	-136	--	-191	-263
	6 <sup>2</sup>	-645	-574	-759	--	-571	-666

<sup>1</sup> No data available.

<sup>2</sup> Measurements taken at the southern terminus of Amelia Island; negative value denotes shoreline retreat to the north.

**Spatial variability.** To this point, general trends have been used to characterize the regional scope of shoreline position change for the study area. A method for evaluating spatial changes in coastal response for each time interval is to analyze change for segments of coast with similar patterns of movement. The benefit of this analysis is that it defines natural breaks in coastal response to incident processes, providing important data for quantifying historical longshore sediment transport rates and depositional patterns. The following discussion emphasizes cumulative change patterns for each island, but the details of all time intervals are summarized for assessing temporal and spatial trends. Tables 15 and 16 contain quantitative estimates of shoreline change by island and shoreline cell. Figures 47-61 graphically present average shoreline change rate and sample standard deviation for all defined shoreline cells. These provide a regional perspective of change (magnitude and extent) for the study area. The primary focus here will be on cumulative changes since 1857/71 (Figures 47-51).

Along Cumberland Island, the length of shoreline occupied by Cell 1 remained relatively constant for all time intervals referenced to the 1857/70 shoreline (Table 15, Figures 47-51). Concurrently, the rate of change consistently decreased from 3.2 to 1.9 m/year for the period of record. With this net decrease in the rate of shoreline progradation in this region, it might be expected that shorelines to the south would benefit from this net transfer of sand. Cumulative shoreline position change data for 1957, 1974, and 1991 do support this transport mechanism. Shoreline Cell 3 exhibits a net increase in the rate of progradation (1.9 to 2.1 m/year) and the extent of the segment becomes larger with time (43.5 to 57.4 percent of total shoreline). Figure 41 graphically depicts these trends. In addition, bathymetric change analysis shows offshore deposition seaward and south of Cell 1 for the same general time period (*Nearshore Bathymetric Change* section). Although a small segment of the Cumberland Island shoreline exhibits net retreat (Cell 2), the magnitude and extent of change is small relative to updrift and downdrift trends. However, the position of this zone is consistent throughout the period of record and is expanding laterally.

Spatial trends along Amelia Island are similar for all time intervals referenced to the 1857/71 shoreline, although the magnitude of change varies (Table 16, Figures 47-51). Cell 1 illustrates a consistent decrease in the rate of shoreline progradation (6.9 to 3.9 m/year) while shoreline Cell 2 shows a net decrease in the rate of shoreline retreat for the same time period (-2.0 to -1.1 m/year). Both cells essentially remained constant in shoreline length. Cell 3 depicts a small decrease in the rate of shoreline progradation whereas the rate of retreat along southern Amelia Island increased over the period of record (Figures 44 and 45). These trends are different than those found along Cumberland Island in that the area experiencing shoreline retreat is a more significant component of the entire system. For the entire study area, shoreline change measurements suggest a net drift of sediment to the south.

## Summary

Six shoreline surveys were used to quantify changes in shoreline position between 1857/71 and 1991. Potential error estimates were calculated to gauge the significance of shoreline change measurements. In most cases, measurements of change exceeded potential errors; however, in some cases, areas showing small amounts of change over short time intervals were considered insignificant. Four primary results can be used to summarize the findings of the historical shoreline change study. First, average long-term shoreline position change is net progradational

**Table 15**  
**Spatial and Temporal Trends in Shoreline Position Change for Cumberland Island**

1857/70 to					1924 to				1933 to			1957 to		1973 to
1924	1933	1957	1973	1991	1933	1957	1973	1991	1957	1973	1991	1973	1991	1991
<b>SHORELINE CELL 1<sup>1</sup></b>														
3.2 <sup>2</sup>	2.9	1.7	2.0	1.9	6.4	-0.5	-0.7	-1.0	-2.1	-1.3	-1.9	-1.8	-2.7	-3.4
1.9 <sup>3</sup>	2.1	1.6	1.2	0.8	2.5	0.4	0.3	0.7	1.0	0.8	0.9	0.7	0.8	1.3
0.4 <sup>4</sup>	0.4	0.2	0.2	0.1	0.7	0.3	0.2	0.3	0.4	0.3	0.3	0.2	0.2	0.3
22.4 <sup>5</sup>	24.2	36.5	24.6	22.3	10.4	1.8	1.8	5.8	4.5	7.2	8.8	11.0	11.8	15.6
<b>SHORELINE CELL 2</b>														
-0.3	-0.4	-0.2	-0.4	-0.6	-3.3	2.6	1.0	1.2	2.2	0.9	1.5	2.9	2.9	6.2
0.2	0.1	0.1	0.2	0.2	1.7	1.3	0.6	1.0	1.3	0.7	0.9	2.2	1.8	3.2
0.1	0.0	0.0	0.0	0.0	0.6	0.4	0.1	0.2	0.4	0.1	0.2	0.7	0.5	1.0
5.3	8.5	4.4	16.2	20.3	6.0	10.4	26.2	18.8	9.4	22.5	15.9	6.7	9.2	7.4
<b>SHORELINE CELL 3</b>														
1.9	1.6	2.0	2.2	2.1	2.6	-1.1	-1.4	-1.5	-0.4	-1.1	-1.2	-2.2	-2.3	-2.7
1.9	1.5	2.3	2.2	1.9	1.7	0.6	0.4	0.6	0.2	0.5	0.5	1.5	0.9	1.2
0.3	0.2	0.3	0.2	0.2	0.5	0.2	0.1	0.1	0.1	0.1	0.1	0.2	0.1	0.2
43.5	36.2	59.1	59.0	57.4	10.4	4.6	21.7	26.0	3.7	17.2	25.3	31.8	29.4	31.2
<b>SHORELINE CELL 4</b>														
-0.7	-0.6				-4.1	1.5	3.2	2.9	1.7	3.6	3.2	4.1	3.0	2.2
0.3	0.2				2.4	1.1	2.0	1.7	1.0	2.0	1.6	2.2	1.4	0.9
0.1	0.0				0.4	0.2	0.3	0.2	0.2	0.2	0.2	0.3	0.2	0.1
22.4	21.2				23.8	17.2	50.3	49.4	19.6	53.1	50.0	50.5	49.6	45.8
<b>SHORELINE CELL 5</b>														
4.0	4.5				1.7	-1.4			-1.1					
2.9	3.7				1.1	0.5			0.7					
1.0	1.1				0.4	0.1			0.2					
6.4	9.9				5.6	16.0			7.6					
<b>SHORELINE CELL 6</b>														
					-0.8	3.0			3.5					
					0.6	2.3			2.1					
					0.3	0.3			0.2					
					5.4	50.0			55.2					
<b>SHORELINE CELL 7</b>														
					0.9									
					0.7									
					0.5									
					1.8									
<b>SHORELINE CELL 8</b>														
					-1.2									
					0.8									
					0.2									
					17.2									
<b>SHORELINE CELL 9</b>														
					4.8									
					4.8									
					1.0									
					19.4									

<sup>1</sup> Each shoreline cell was determined by directional changes in the rate of shoreline position change (shoreline cell numbers increase from north to south). <sup>2</sup> Average shoreline change rate (m/year). <sup>3</sup> Sample standard deviation ( $\pm$  m/year). <sup>4</sup> 95-percent confidence interval ( $\pm$  m/year). <sup>5</sup> Percent of analyzed shoreline covered by each cell.

**Table 16****Spatial and Temporal Trends in Shoreline Position Change for Amelia Island**

1857/71 to					1924 to				1933 to			1957 to		1974 to	
1924	1933	1957	1974	1991	1933	1957	1974	1991	1957	1974	1991	1974	1991	1991	
<b>SHORELINE CELL 1<sup>1</sup></b>															
6.9 <sup>2</sup>	6.7	5.7	4.5	3.9	12.4	9.3	4.8	3.5	7.2	6.6	5.0	-3.1	-1.5	0.3	
2.7 <sup>3</sup>	2.9	3.1	2.4	2.1	12.2	3.6	2.3	1.8	7.1	3.6	2.5	1.9	1.1	0.7	
0.7 <sup>4</sup>	0.7	0.8	0.6	0.6	4.7	1.4	0.9	0.7	2.5	2.0	1.5	0.3	0.2	0.1	
15.7 <sup>5</sup>	15.7	15.4	15.1	14.5	7.4	7.4	6.9	7.0	8.4	3.8	3.6	35.1	34.9	26.5	
<b>SHORELINE CELL 2</b>															
-2.0	-1.9	-1.4	-1.4	-1.1	-4.0	-0.9	-1.1	-0.7	-1.2	-1.4	-0.9	1.6	1.3	-0.3	
1.1	1.0	0.7	0.8	0.6	2.3	0.5	0.5	0.4	0.5	0.5	0.4	0.9	0.7	0.2	
0.3	0.3	0.2	0.2	0.2	0.2	0.1	0.1	0.1	0.2	0.1	0.1	0.1	0.1	0.1	
12.3	14.2	12.0	14.6	14.7	92.6	13.7	26.8	26.9	11.3	19.9	18.5	45.2	40.8	8.9	
<b>SHORELINE CELL 3</b>															
1.0	0.4	0.5	0.7	0.7		0.1	0.3	0.4	1.1	0.9	0.8	-2.2	-2.3	1.0	
0.5	0.3	0.3	0.4	0.3		0.2	0.2	0.2	0.7	0.5	0.5	1.3	1.3	0.6	
0.1	0.0	0.1	0.1	0.0		0.1	0.0	0.0	0.1	0.1	0.1	0.3	0.3	0.1	
40.5	35.3	41.8	40.3	40.8		10.4	38.7	38.7	75.2	66.6	58.6	19.7	24.3	35.9	
<b>SHORELINE CELL 4</b>															
-0.6	-1.1	-0.7	-0.8	-1.1		-0.7	-1.2	-1.6	-2.3	-1.9	-1.6			-2.6	
0.4	0.5	0.4	0.6	0.7		1.0	1.3	1.3	1.7	1.2	1.4			1.7	
0.1	0.1	0.1	0.1	0.1		0.1	0.2	0.2	0.8	0.4	0.3			0.3	
31.5	34.8	30.8	30.0	30.0		68.5	27.6	27.4	5.1	9.7	19.3			28.7	

<sup>1</sup> Each shoreline cell was determined by directional changes in the rate of shoreline position change (shoreline cell numbers increase from north to south).

<sup>2</sup> Average shoreline change rate (m/year).

<sup>3</sup> Sample standard deviation ( $\pm$  m/year).

<sup>4</sup> 95-percent confidence interval ( $\pm$  m/year).

<sup>5</sup> Percent of analyzed shoreline covered by each cell.

for the Cumberland-Amelia barrier island systems. In other words, the magnitude of shoreline advance exceeded retreat for the study area. Between 1857/70 and 1991, Cumberland Island prograded at a net rate of 1.5 m/year; Amelia Island prograded 0.4 m/year between 1857/71 and 1991. Second, five areas of substantial shoreline movement were identified for the study area. The northern margin of the Cumberland Embayment, southern Cumberland Island at the jetty, and the northern end of Amelia Island at the jetty show large shoreline advances since 1857/71. The historical pronuberance near Fernandina Beach and the southern 6 km of Amelia Island show net shoreline retreat. Third, only one area of long-term chronic erosion is identified. This includes the southern 4 km of Amelia Island where the rate of shoreline retreat has steadily increased since 1871. Finally, for the five areas of significant change, most movement took place between 1857/71 and 1924. This time period encompasses jetty construction at St. Marys Entrance that is related to deposition on adjacent shorelines. However, direct association between retreat along southern Amelia Island and jetty placement is not as straightforward because inlet processes at Nassau Sound also influence adjacent shoreline response.

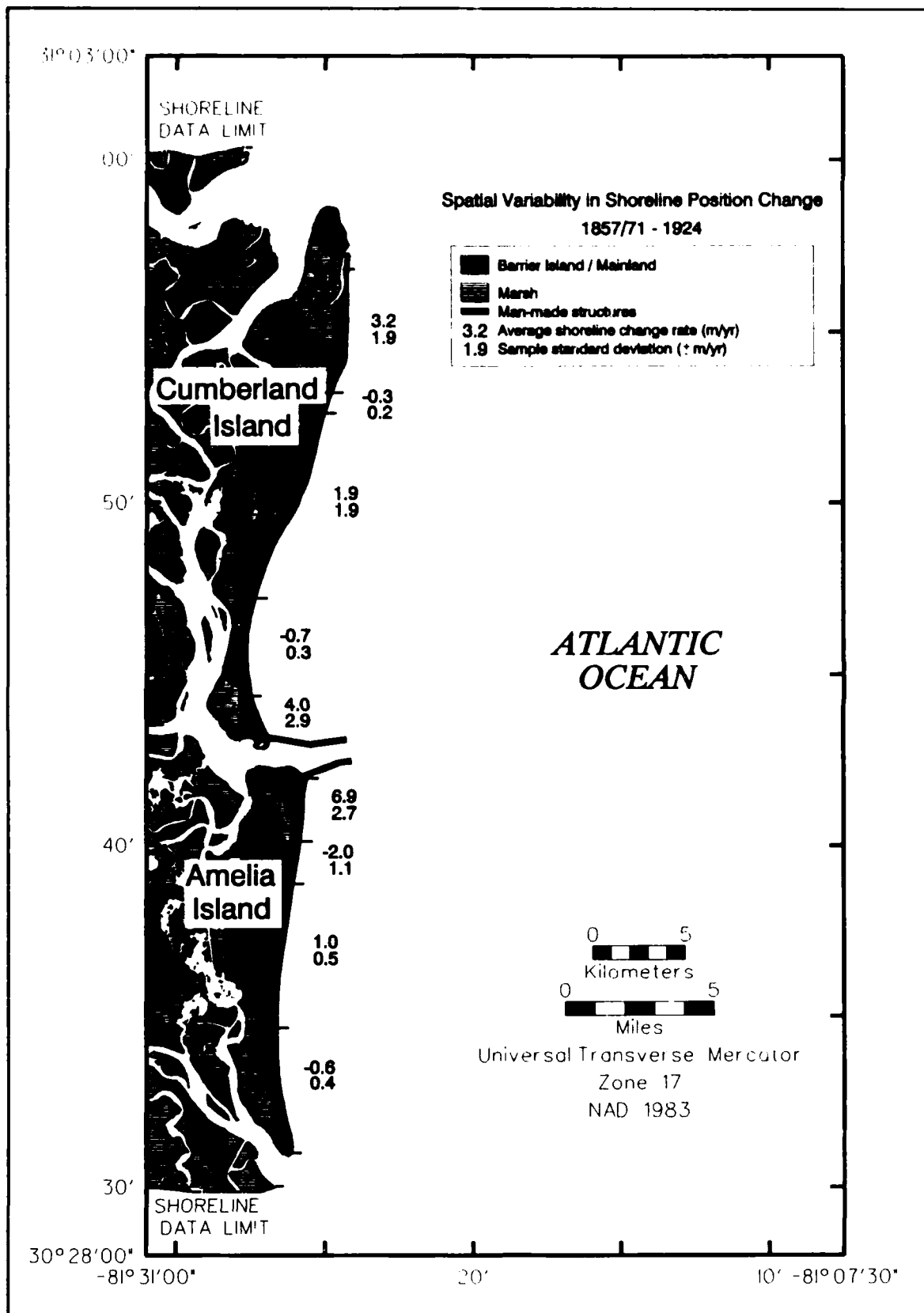


Figure 47. Spatial and temporal trends in shoreline position change, 1857/71 to 1924

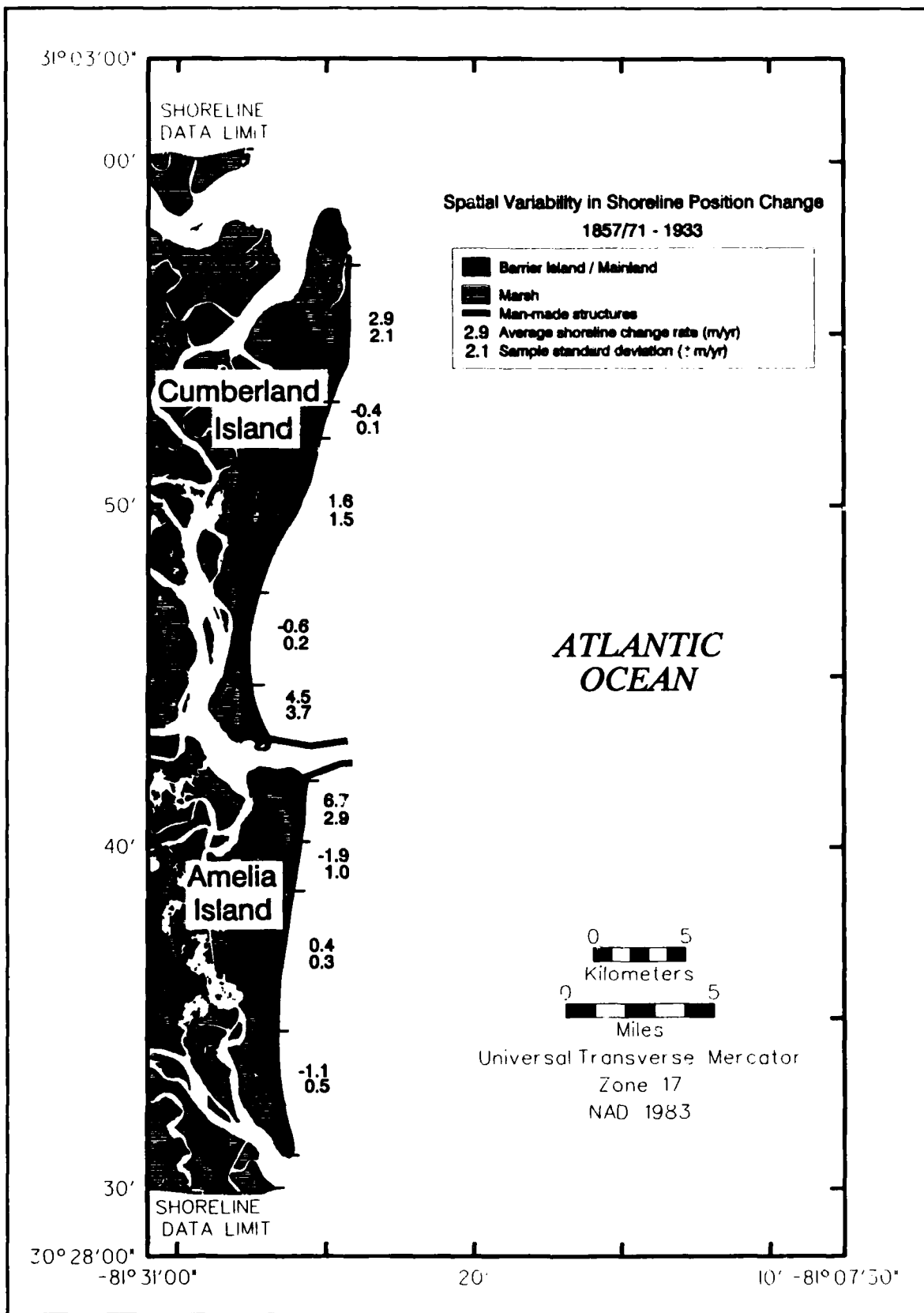


Figure 48. Spatial and temporal trends in shoreline position change, 1857/71 to 1933

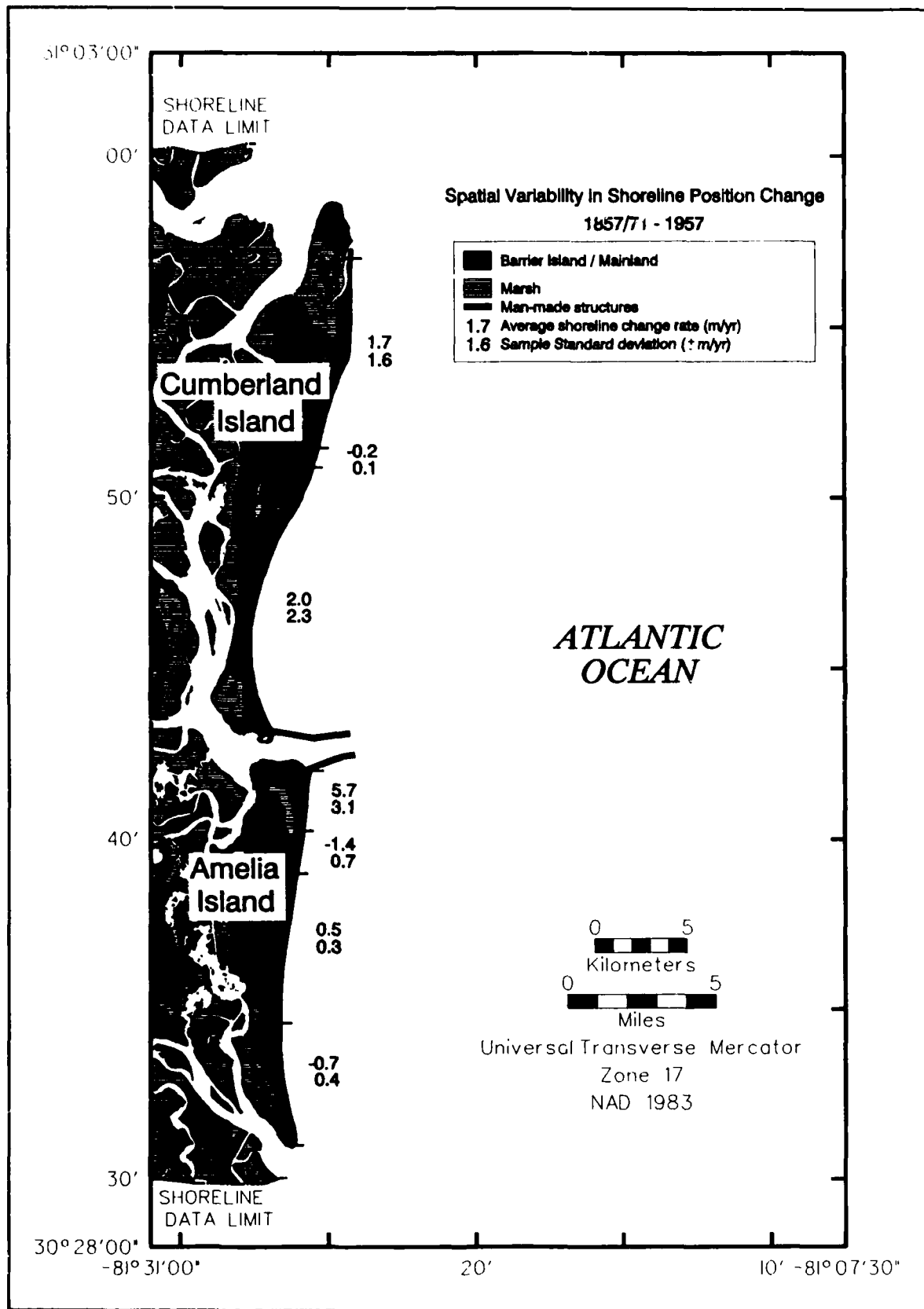


Figure 49. Spatial and temporal trends in shoreline position change, 1857/71 to 1957

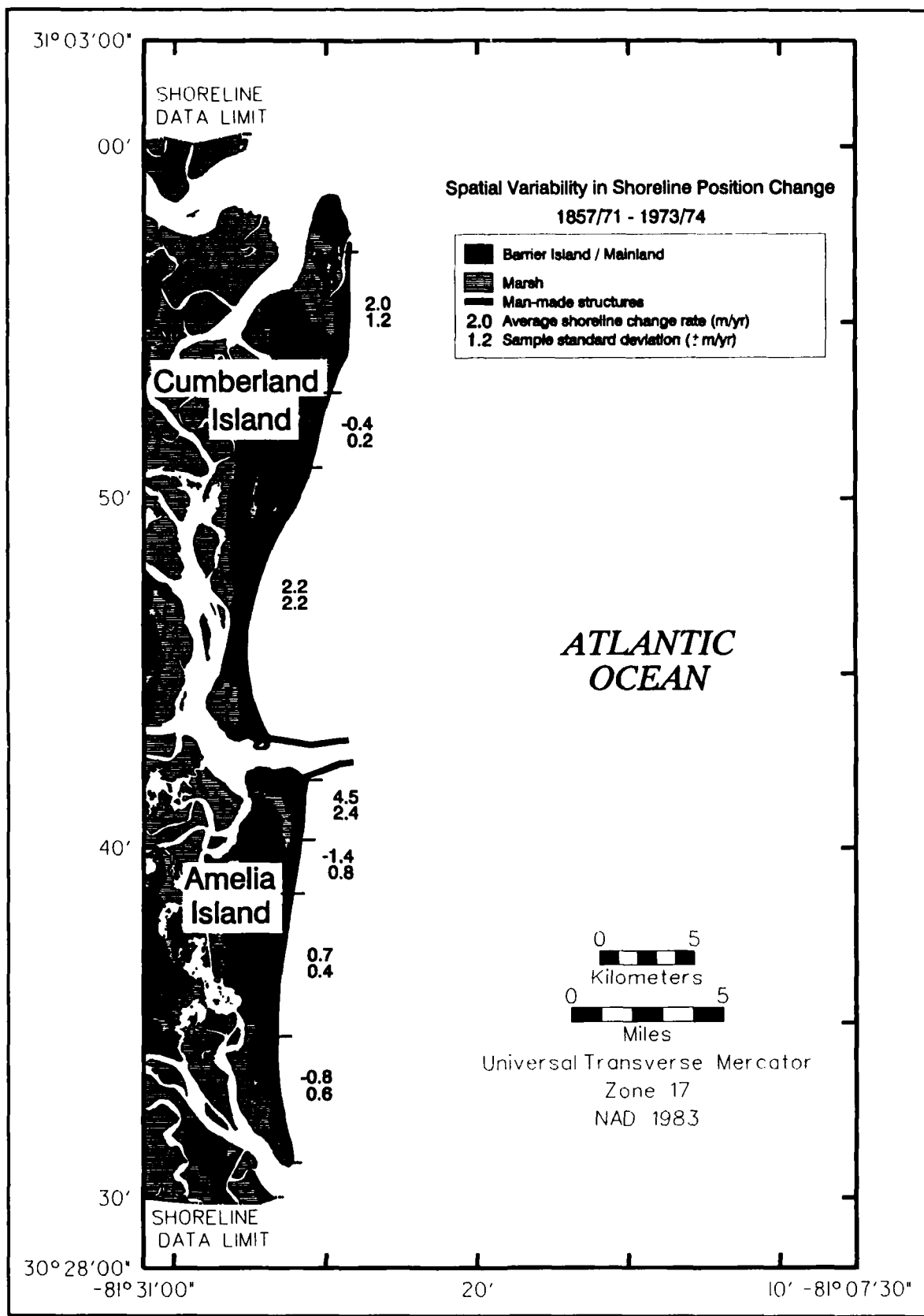


Figure 50. Spatial and temporal trends in shoreline position change, 1857/71 to 1973/74

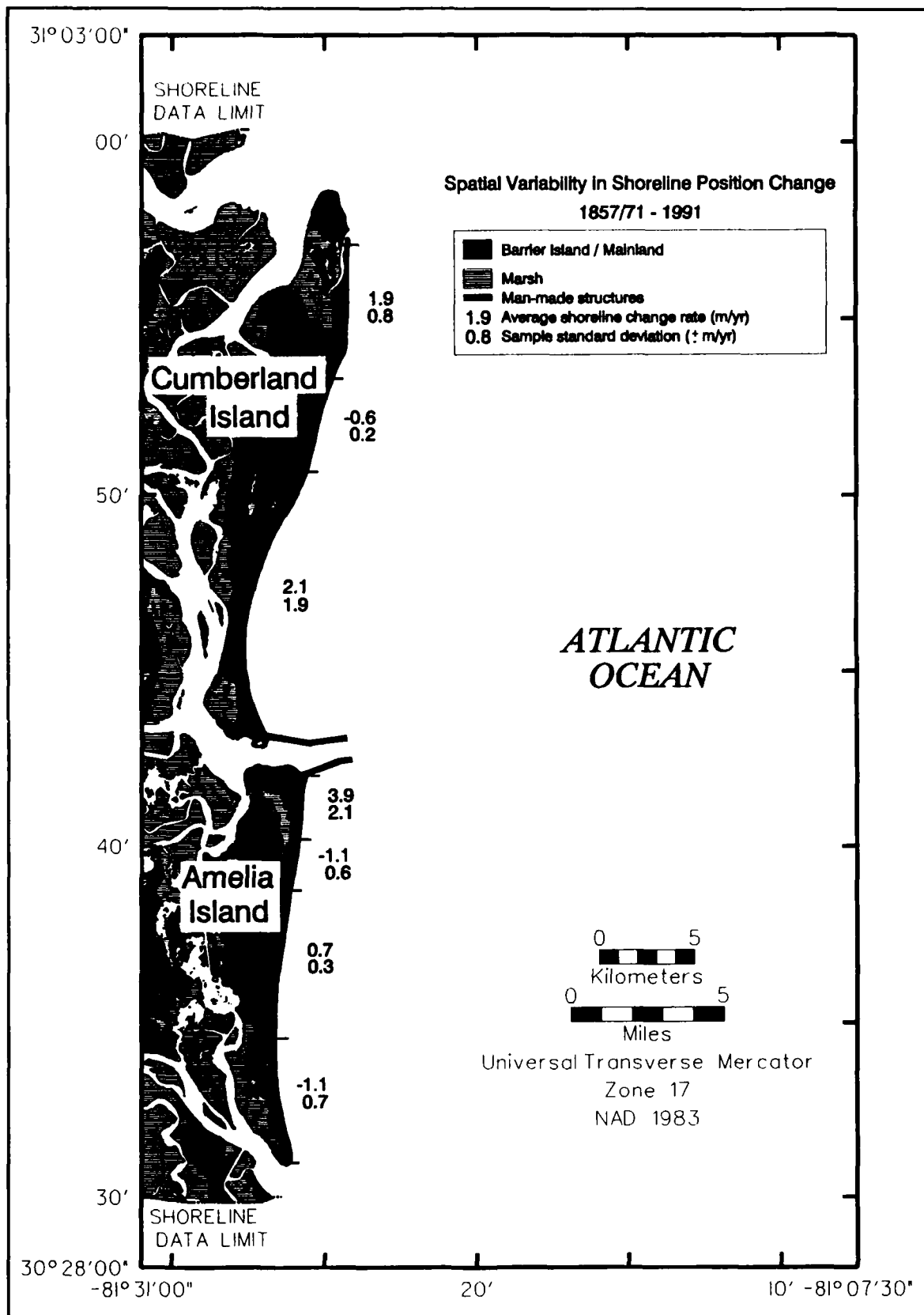


Figure 51. Spatial and temporal trends in shoreline position change, 1857/71 to 1991

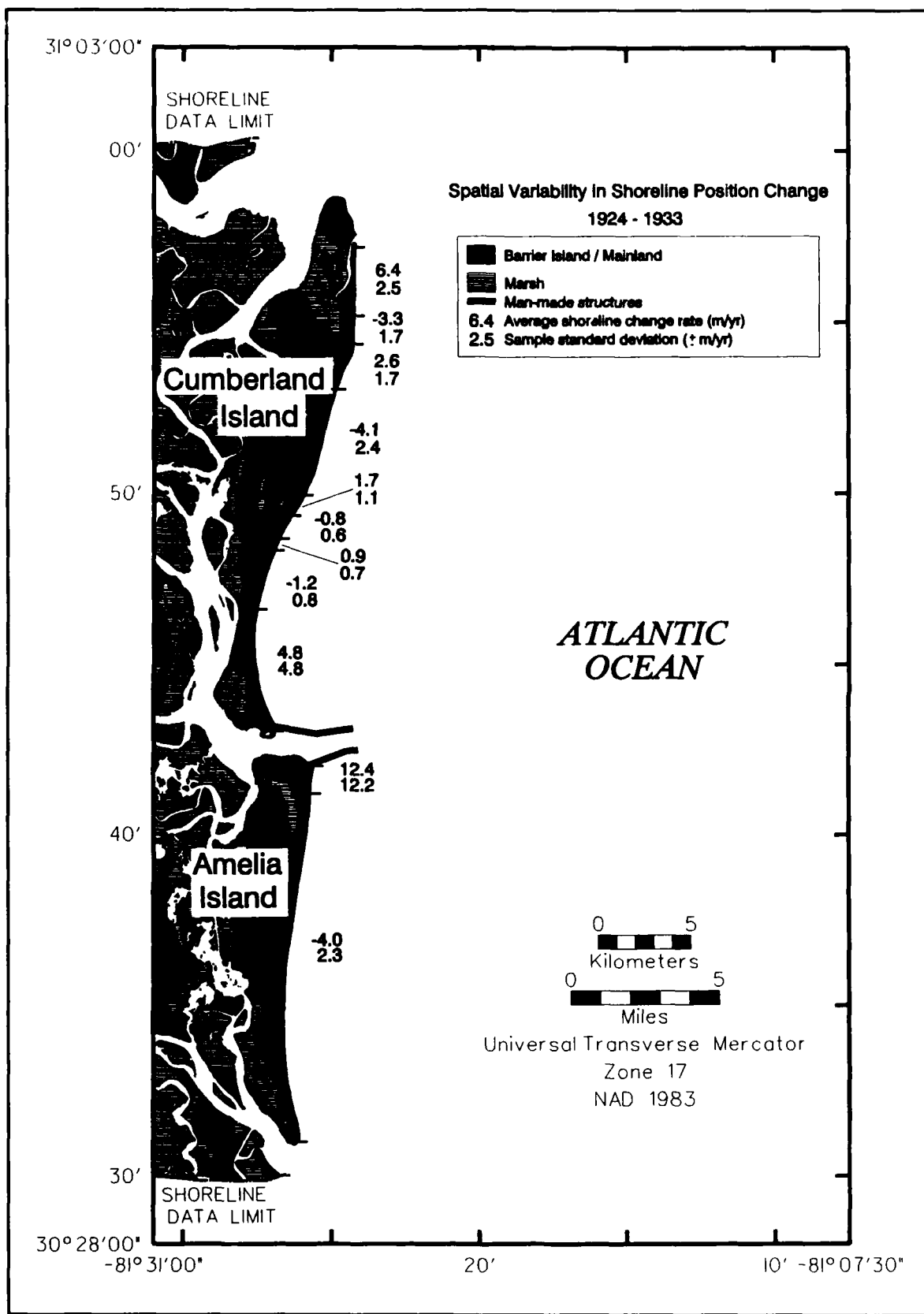


Figure 52. Spatial and temporal trends in shoreline position change, 1924 to 1933

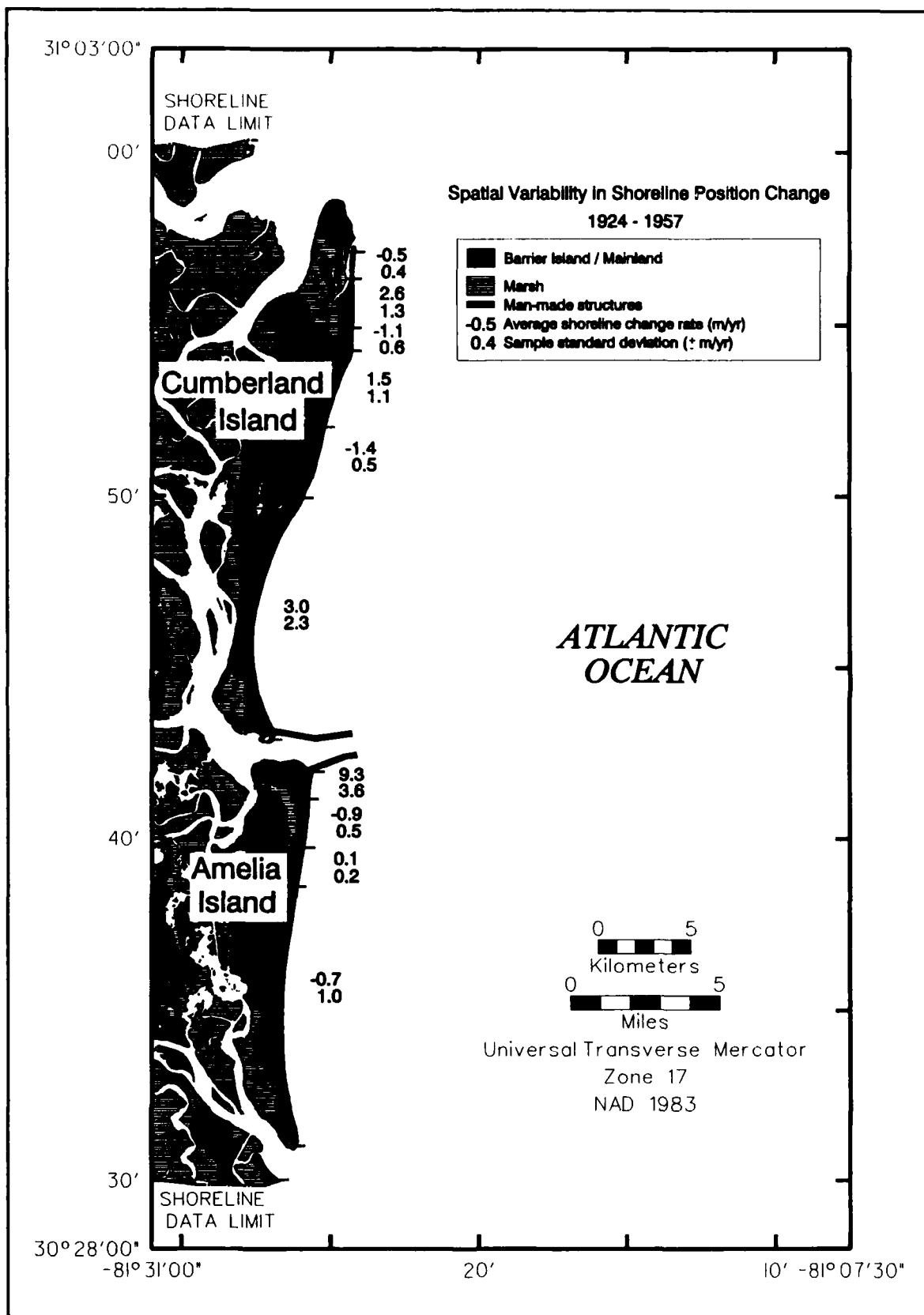


Figure 53. Spatial and temporal trends in shoreline position change, 1924 to 1957

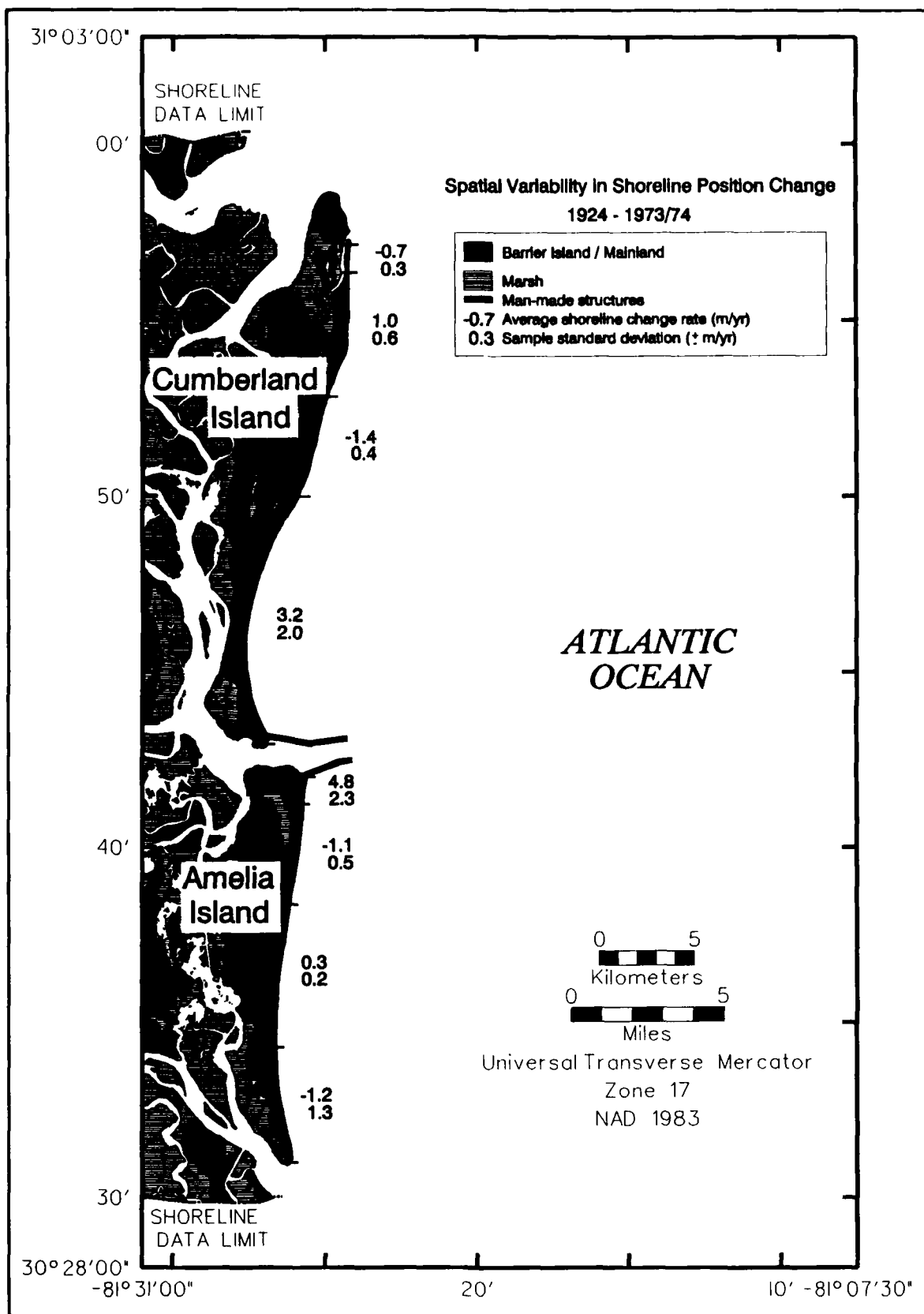


Figure 54. Spatial and temporal trends in shoreline position change, 1924 to 1973/74

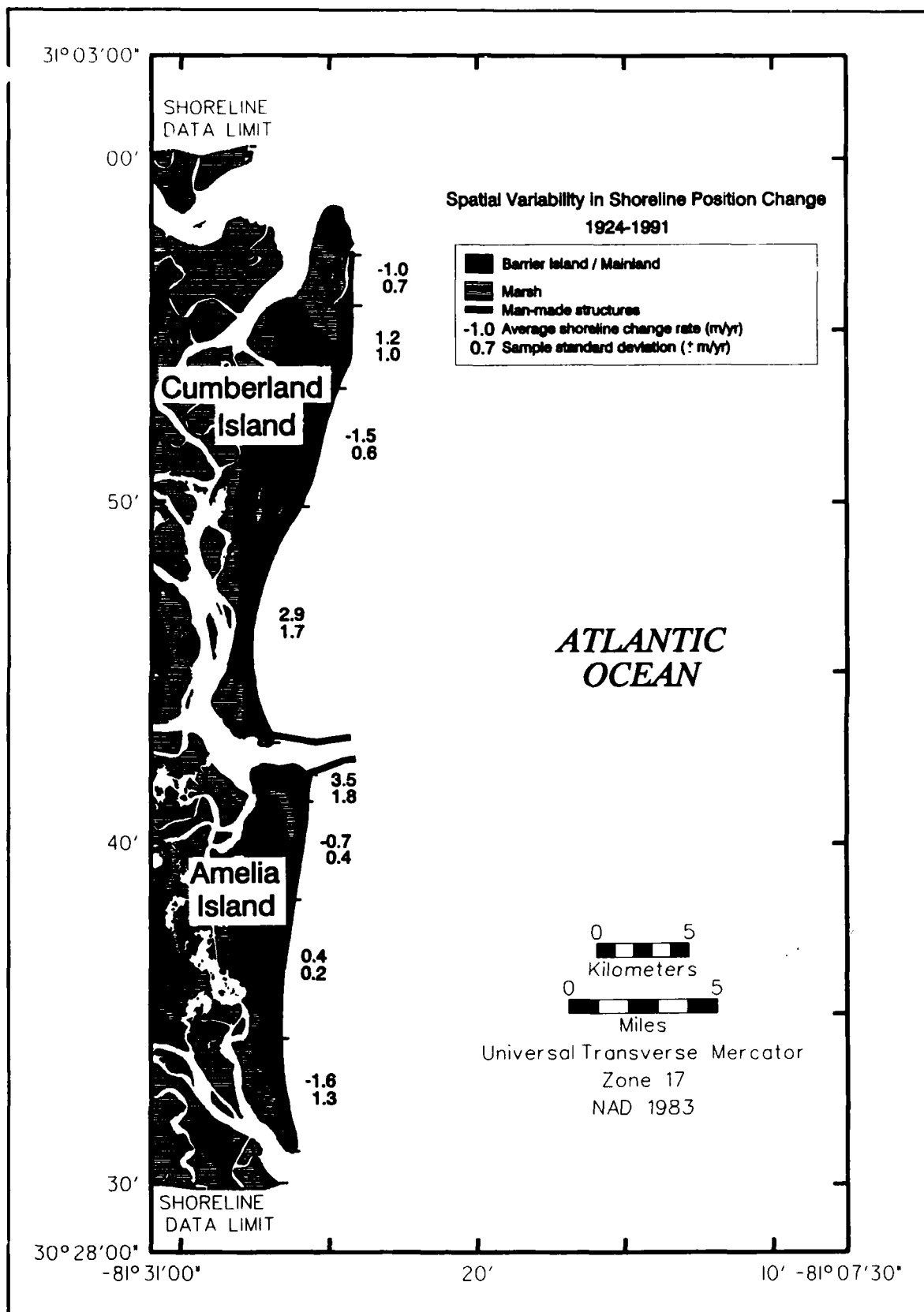


Figure 55. Spatial and temporal trends in shoreline position change, 1924 to 1991

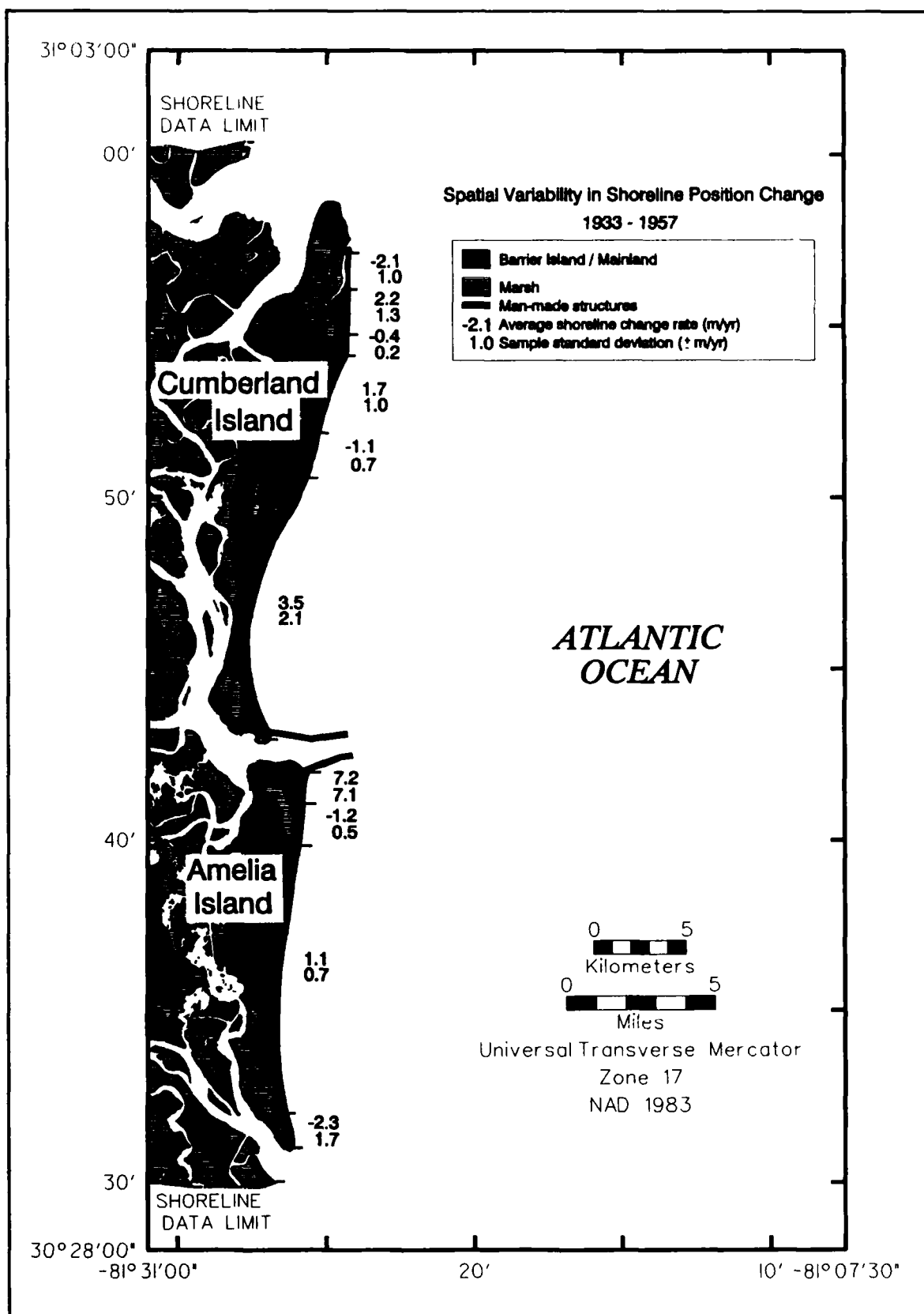


Figure 56. Spatial and temporal trends in shoreline position change, 1933 to 1957

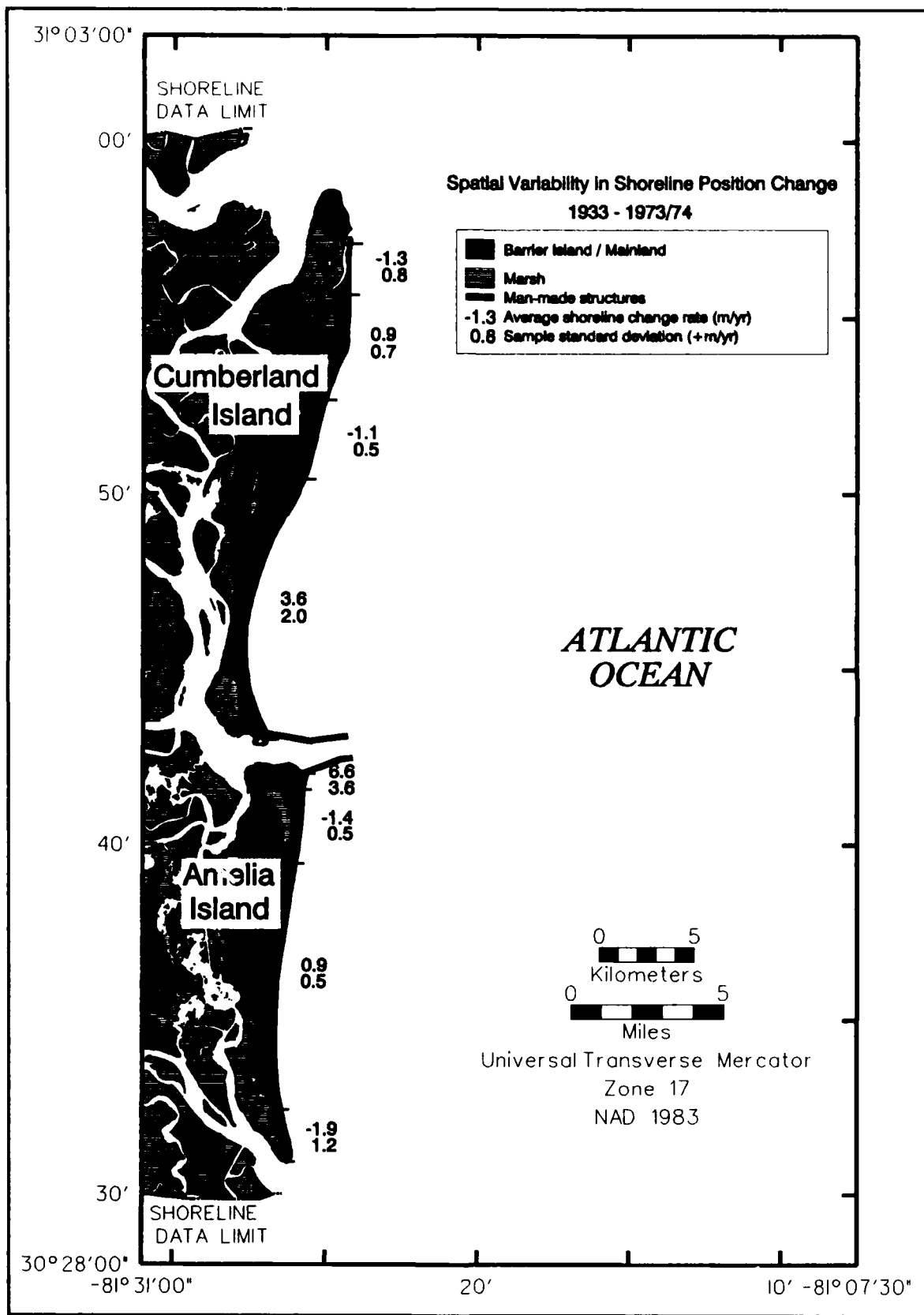


Figure 57. Spatial and temporal trends in shoreline position change, 1933 to 1973/74

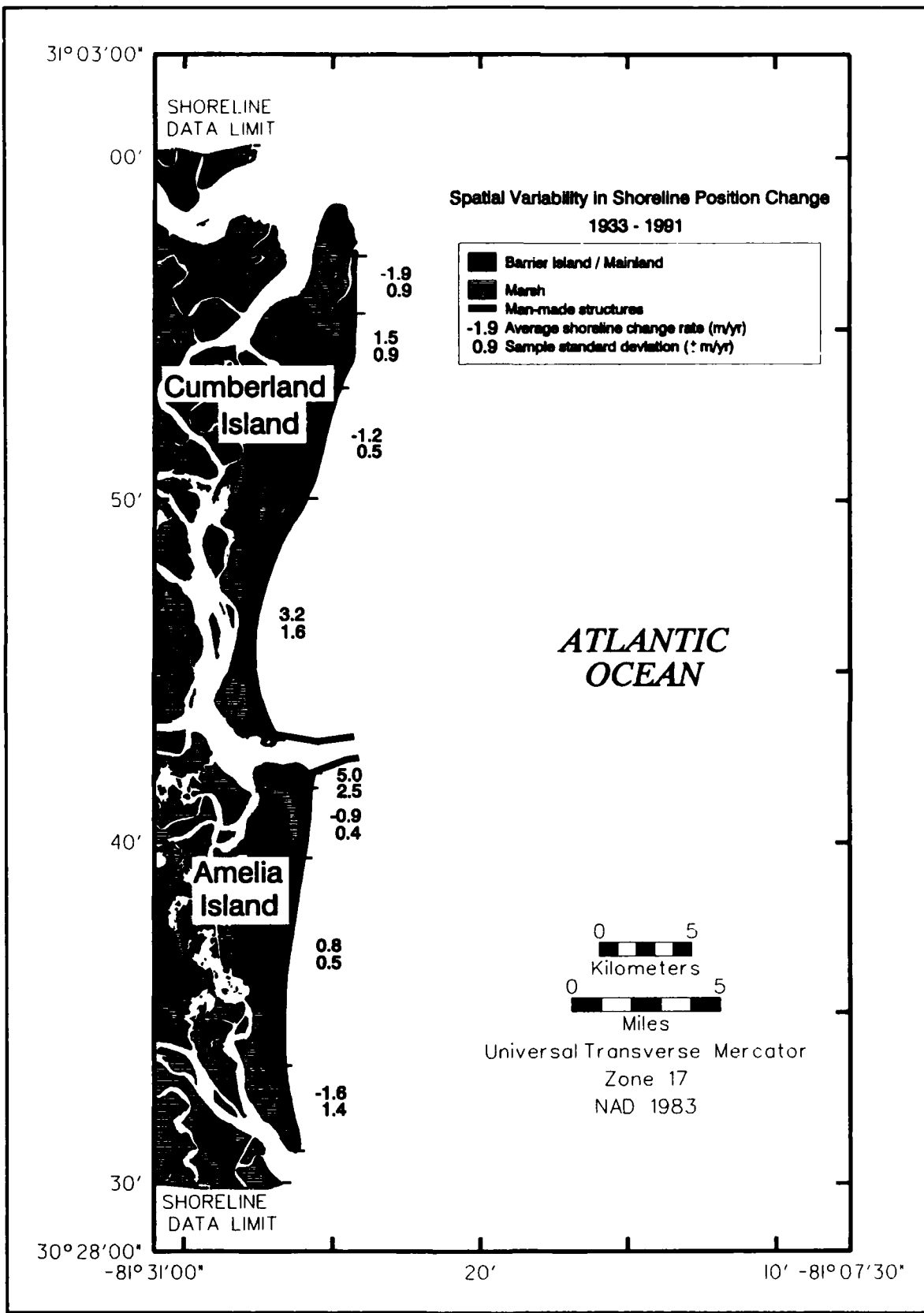


Figure 58. Spatial and temporal trends in shoreline position change, 1933 to 1991

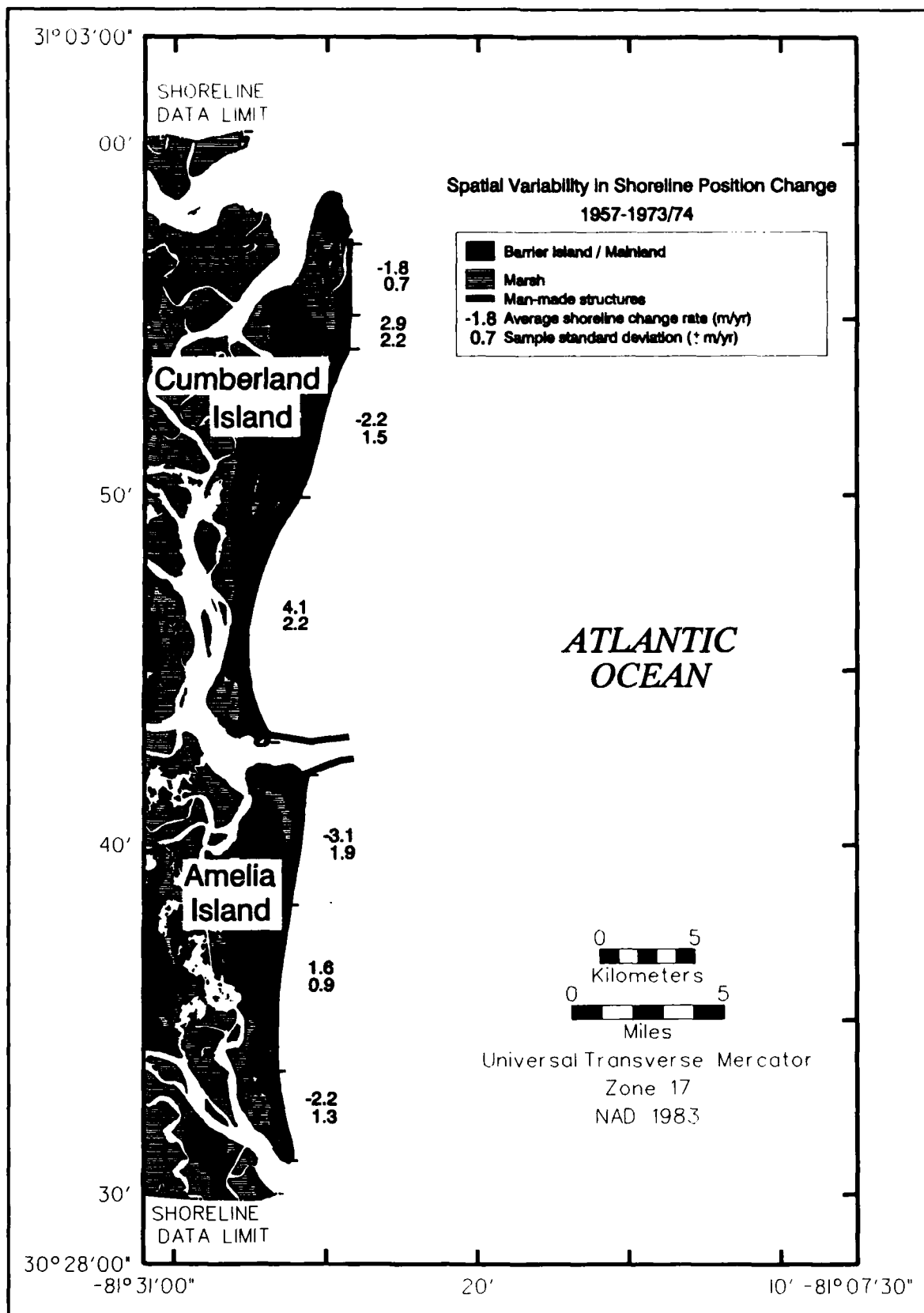


Figure 59. Spatial and temporal trends in shoreline position change, 1957 to 1973/74

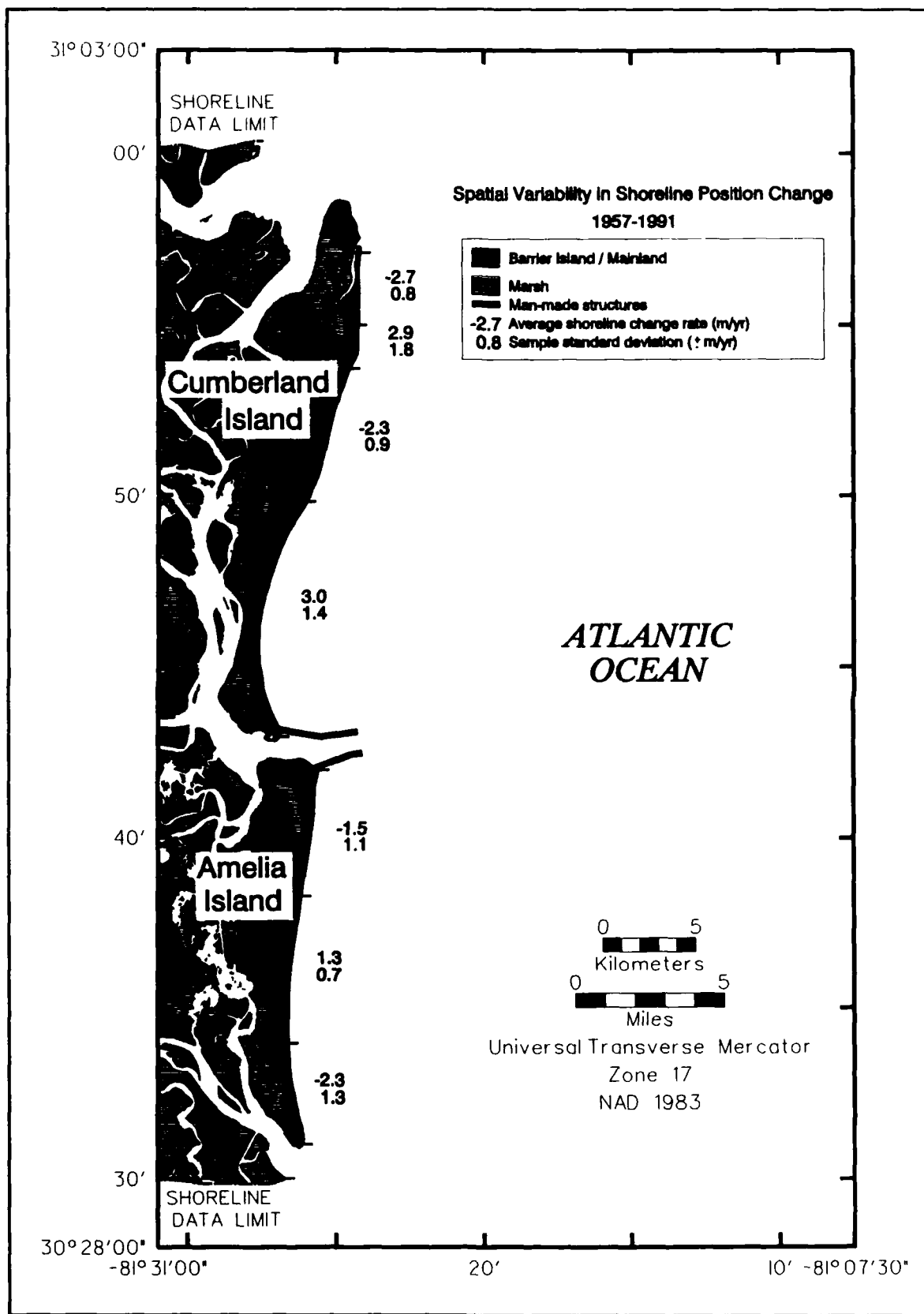
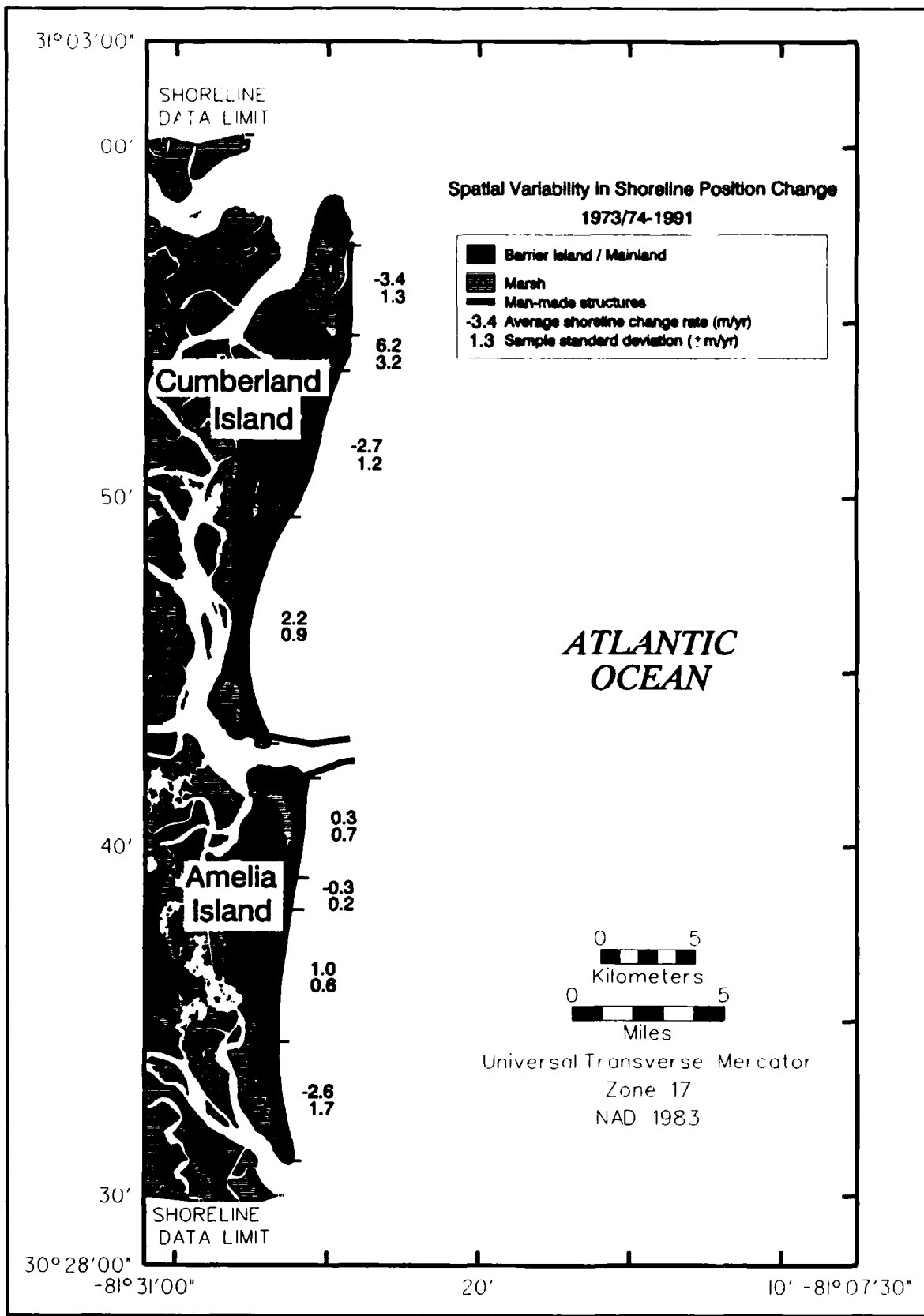


Figure 60. Spatial and temporal trends in shoreline position change, 1957 to 1991



**Figure 61. Spatial and temporal trends in shoreline position change, 1973/74 to 1991**

## Nearshore Bathymetric Change

Hydrographic surveys of regional nearshore morphology provide a direct source of data for quantifying changes in seafloor elevation. Historically, these data have been collected in conjunction with regional shoreline position surveys by the NOS. However, bathymetric data are often overlooked as a primary source of information for assessing small-scale (large areas) coastal evolution or site-specific response to natural and human-induced processes. This neglect may be related to the amount of analysis necessary to attain an accurate result. Comparison of digital bathymetric data for the same region but different time periods provides a method for calculating net movements of sediment into (accretion) and out of (erosion) an area of study. Several manual and automated techniques have been used for making quantitative estimates of change. Moody (1964) superimposed contour data from charts of different time periods to identify change. Pierce (1969) used data point comparisons for exact geographic positions on charts of different time periods to calculate volumetric changes. Until the 1980s, these two procedures were standard practice (primarily contour overlay) for evaluating historical changes in nearshore bathymetry (e.g. Stauble and Warnke 1974), particularly those related to inlet systems (Dean and Walton 1973, Olsen 1977). However, in recent years, bathymetric data have been processed using commercially available surface modeling software (Hansen and Knowles 1988; List, Jaffe, and Sallenger 1991).

The purposes of this task are to quantify changes in nearshore bathymetry to identify trends in large-scale coastal evolution, and to evaluate the impact of natural processes and human influences on the study area. Digital data for the area between St. Andrew Sound, Georgia, and Nassau Sound, Florida, and seaward from the high-water shoreline to the 12-m depth (NGVD) contour or the limit of data were used to assess change between 1855/75 and 1953/79. In addition, site-specific data collected as part of the coastal monitoring program were used to evaluate long- and short-term trends for St. Marys ebb-tidal delta. Because this information is critical to understanding the historical response of a system to nearshore processes, data accuracy and potential error estimates were assessed for gaging the significance of results. The following discussion presents information on available data sources, potential error estimates, regional patterns of change, and historical evolution of the ebb-tidal delta at St. Marys Entrance as influenced by jetty construction and channel dredging.

### Data sources

Three primary sources of data were available for assessing changes in nearshore bathymetry for the study area. These include NOS hydrographic maps (H-sheets), digital bathymetric data from the National Geophysical Data Center (NGDC), and digital bathymetric data from the USACE.

**NOS hydrographic maps:** H-sheets are the result of surveys performed in response to the act of 10 February 1807, establishing a national "Survey of the Coast" (Shalowitz 1964). Generally used for construction of navigation charts, H-sheets are considered the most accurate source of historical bathymetric data. Prior to the 1930s, surveys were performed using a graduated pole or a lead weight and graduated line. In the 1930s, a change was made to echo soundings, and more recent surveys use digital data collection methods. Hydrographic surveys were often preceded by a topographic survey to establish control points along the shoreline. Thus, T-sheets and H-sheets are usually available for similar dates, providing a useful and

consistent data set for studies of coastal change. Bathymetry data from the mid-1800s to the 1950s were digitized from H-sheets. Figures 62-66 summarize the H-sheets that were digitized using CADD and computer mapping software, the geographic areas covered by each survey, and the year in which the survey was completed.

**Digital bathymetry data.** The NGDC in Boulder, Colorado, maintains a digital database of the most recent NOS hydrographic surveys for U.S. coastal areas. These data are delivered as standard ASCII files and contain information including sounding depths, longitude and latitude of soundings, the map number from which the soundings originated, and the date of the map. For newer maps, these files contain all positions collected by a digital fathometer. Published maps are somewhat generalized and contain fewer points than digital files. Maps produced prior to digital data collection are digitized at NGDC and contain all points on the published map. The 1953/79 data were imported to design files for comparison with other bathymetry data sets. The corresponding map boundaries and dates are shown in Figure 67.

**USACE bathymetric surveys.** Two bathymetric surveys were performed by the USAED, Jacksonville, in conjunction with the Kings Bay Coastal Monitoring Program. Bathymetry data were collected in 1988 and 1992 for the area covering the ebb-tidal delta at St. Marys Entrance. These data were collected in digital and analog (depth traces on paper) form, and the original files were processed for tidal corrections prior to temporal comparisons. For the 1988 survey (25 June - 8 July), digital data were used to characterize morphology of the ebb-tidal delta; however, digital data files from the 1992 survey (15-17 April) were not used because of data acquisition difficulties. Instead, analog recordings were interpreted and manually digitized by USAED, Jacksonville, personnel for comparison with data from earlier surveys. Survey locations are shown in Figures 68 and 69.

**Composite data sets.** Due to various factors, including the time and cost required to perform a bathymetric survey, complete data coverages over large areas generally are not available for a single date. In the earlier surveys, map dates were separated by a year or two for most areas, indicating the slow process of manual methods employed. Also, although large areas were surveyed in the 1870s, previous surveys for small areas were not replaced with new ones. Generally, areas of greater change and commercial importance were updated more frequently. For the earliest data set, the dates range from 1855 to 1875 (Figure 62). However, the 1855 data set covers a small backbarrier area that is relatively stable. The majority of the study area was surveyed between the years 1869 and 1871, and a portion of the ebb-tidal delta at St. Marys Entrance was updated in 1875. All of these data were collected prior to commencement of jetty construction at St. Marys Entrance. This data set is used for regional, local, and detailed analyses of seafloor changes, and it is referred to as the 1855/75 data set.

In 1910, the jetties at St. Marys Entrance were completed and a bathymetric survey was conducted for the area just seaward of the ends of the jetties (Figure 63). Map H-3555 covers a portion of the realigned ebb-tidal delta, although most of the survey was conducted seaward of the present position of the deposit.

Another regional nearshore bathymetric survey of the study area was executed in 1924 (Figure 64). Although the soundings are relatively sparse and only cover the area between the shoreline and the 6-m depth contour, this data set provides consistent coverage for the entire area. Map H-3770 from 1915 contains a very small-scale (1:80,000) offshore survey of Cumberland and Amelia Islands (Figure 64). It was envisaged at the start of this study that these data would

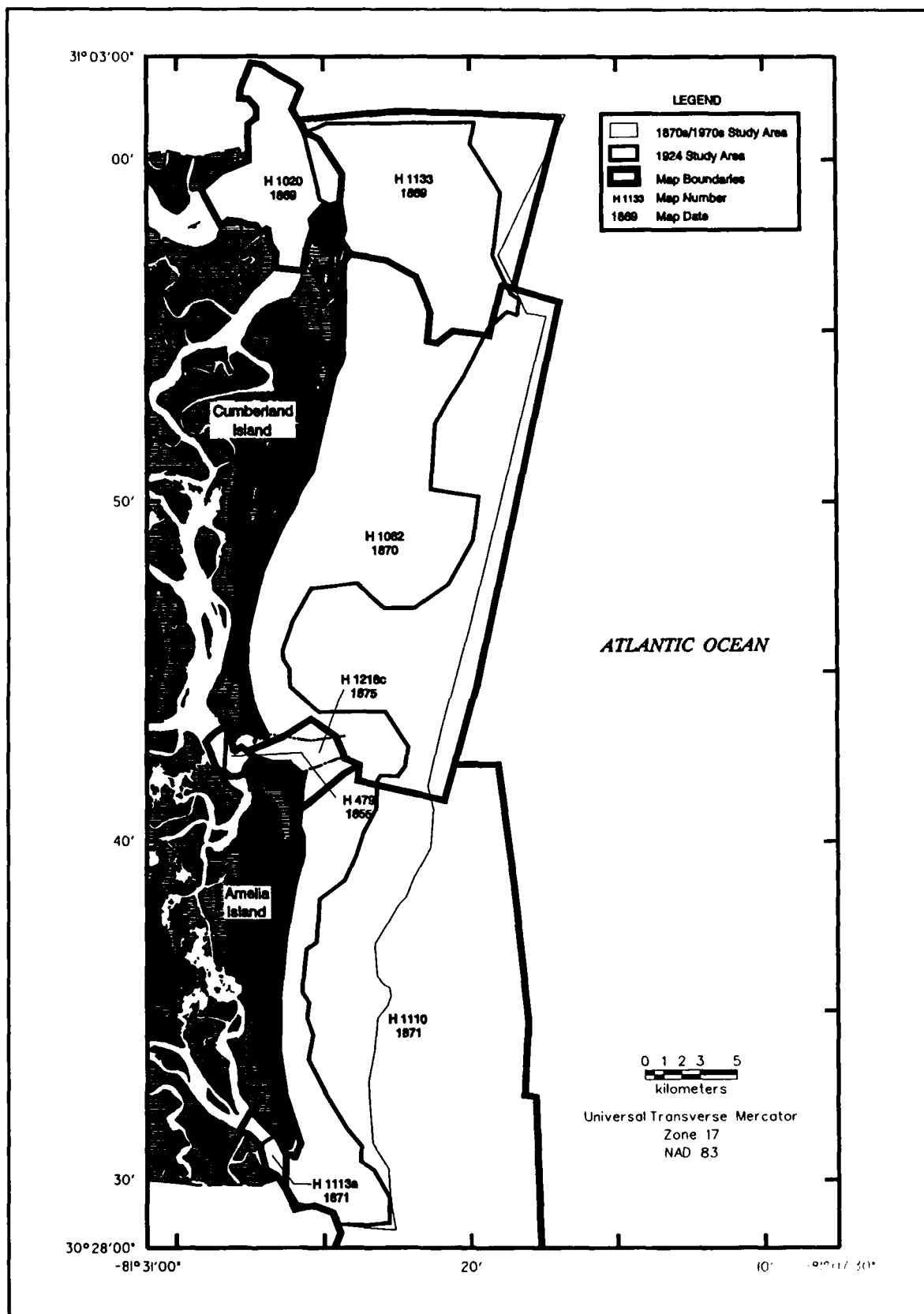


Figure 62. Bathymetric data coverage for the 1855/75 composite

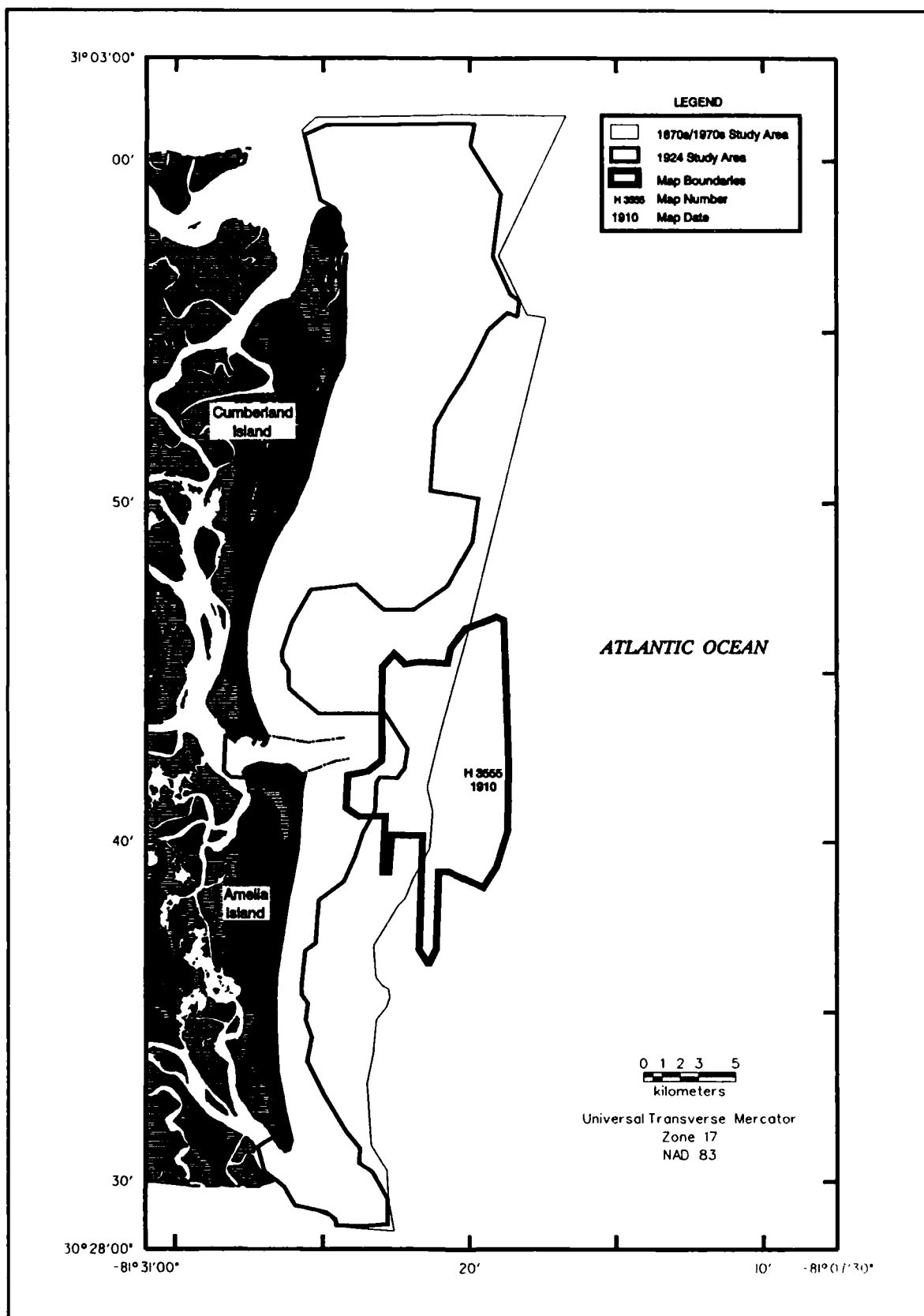


Figure 63. Bathymetric data coverage for the 1910 survey

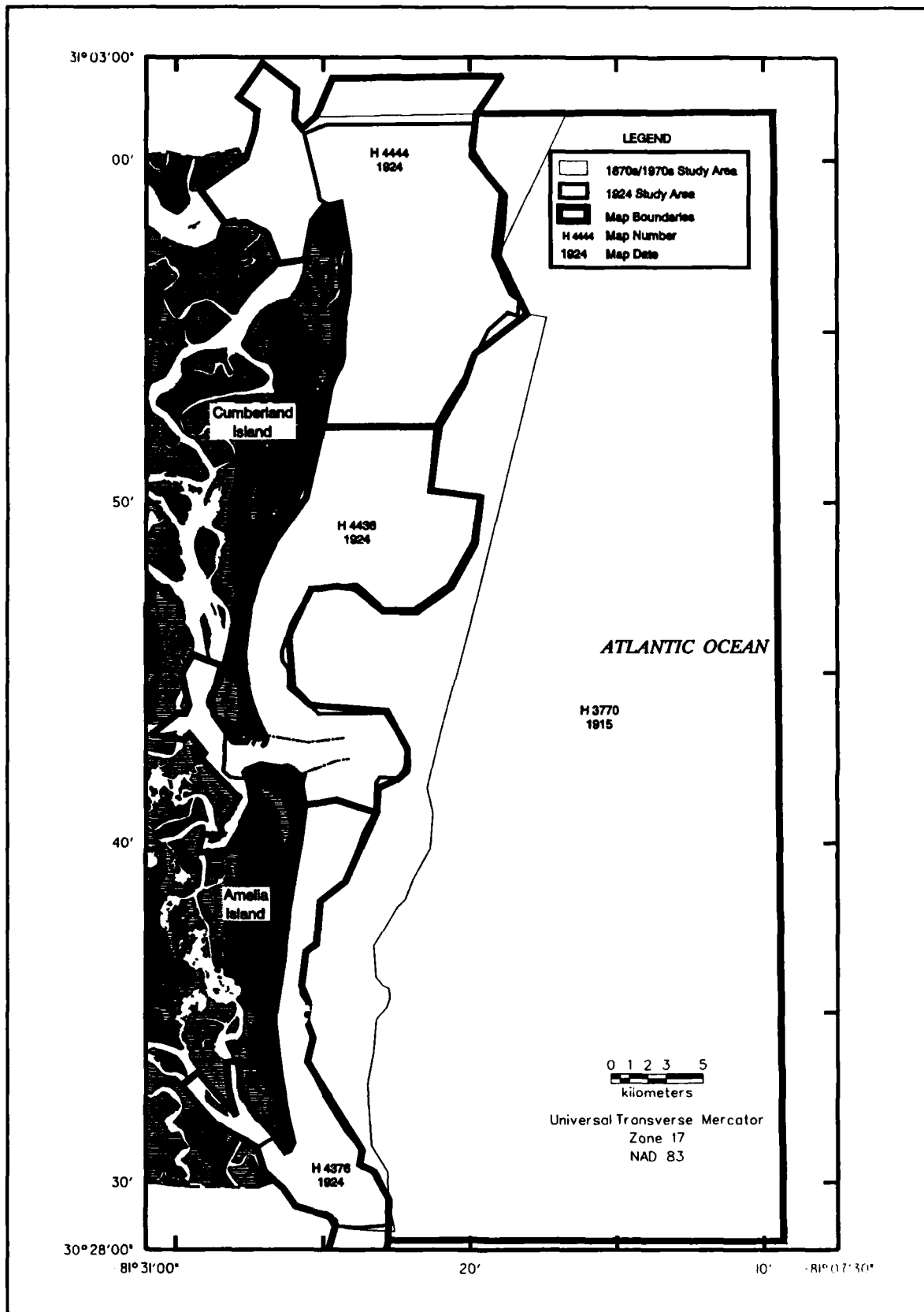


Figure 64. Bathymetric data coverage for the 1915 and 1924 surveys

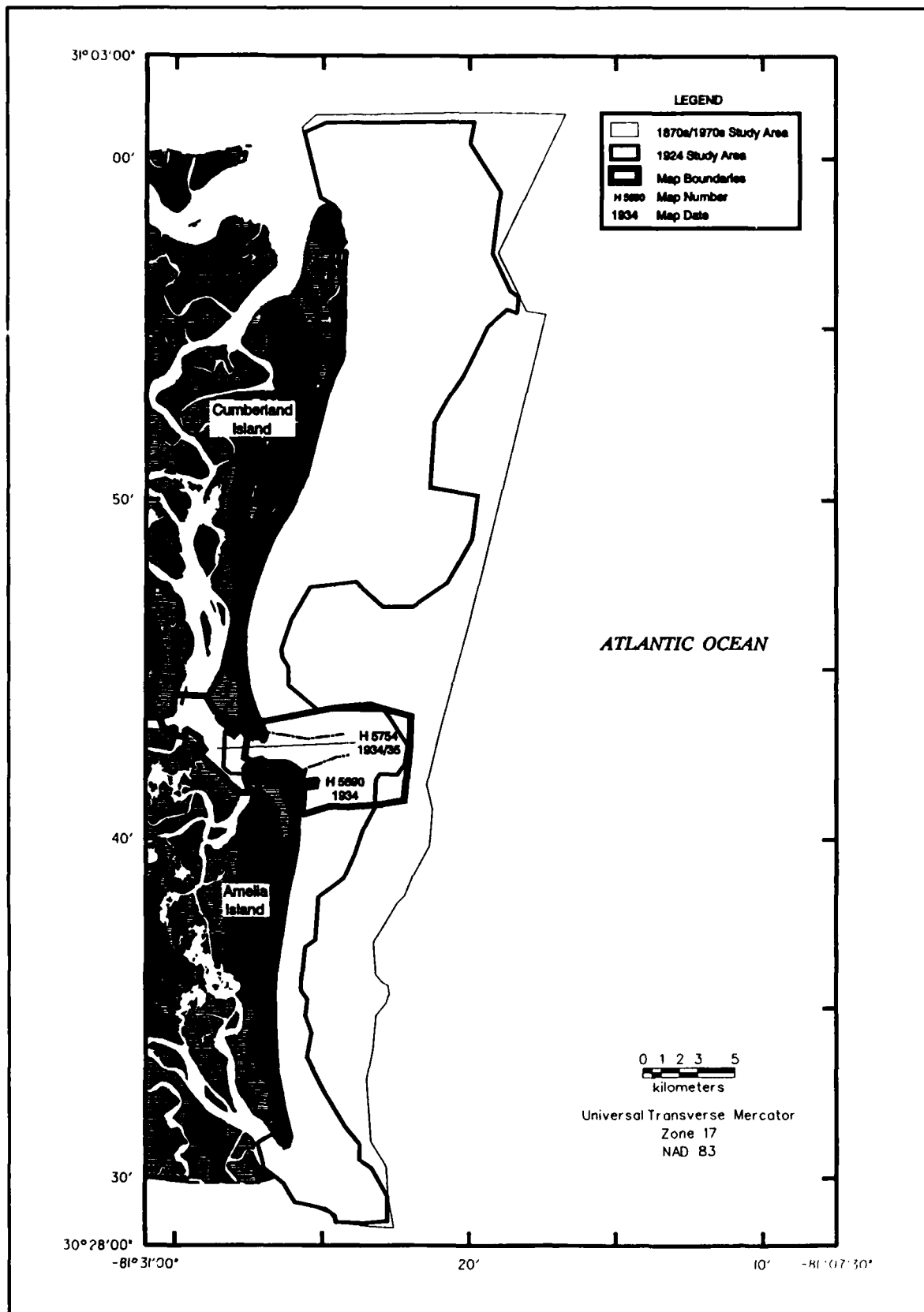


Figure 65. Bathymetric data coverage for the 1934/35 survey

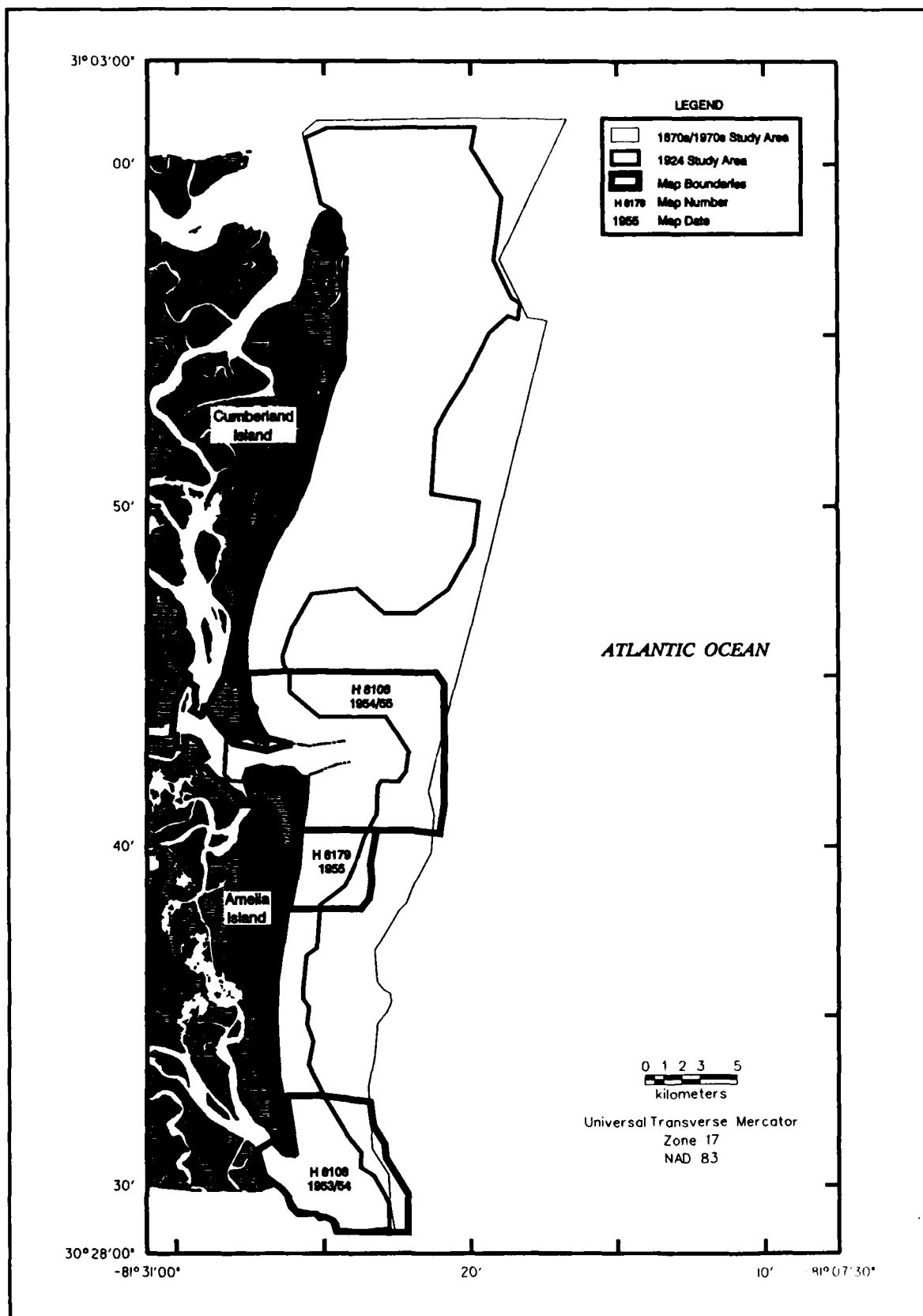


Figure 66. Bathymetric data coverage for the 1953/55 surveys

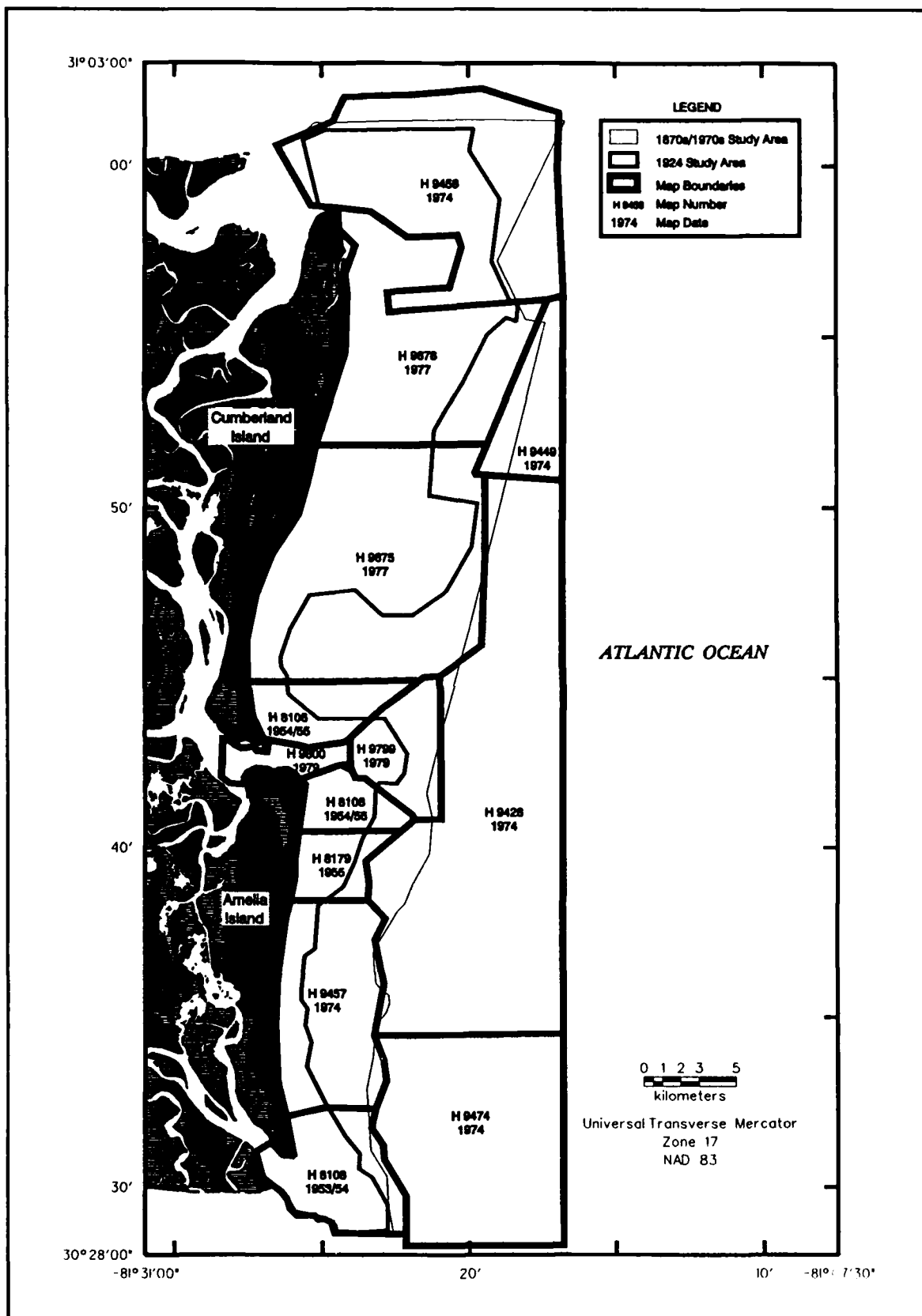


Figure 67. Bathymetric data coverage for the 1953/79 composite

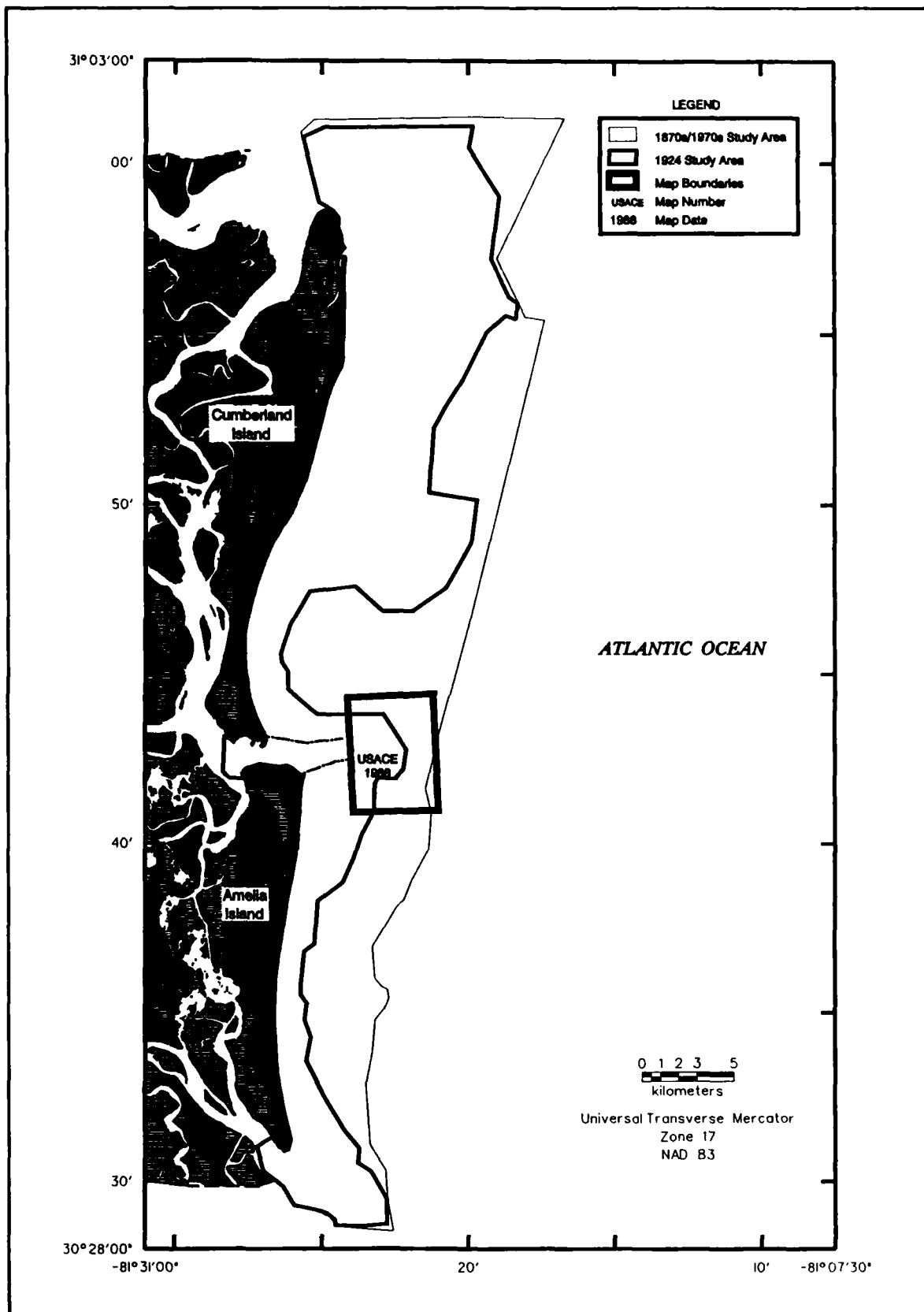


Figure 68. Bathymetric data coverage for the 1988 survey

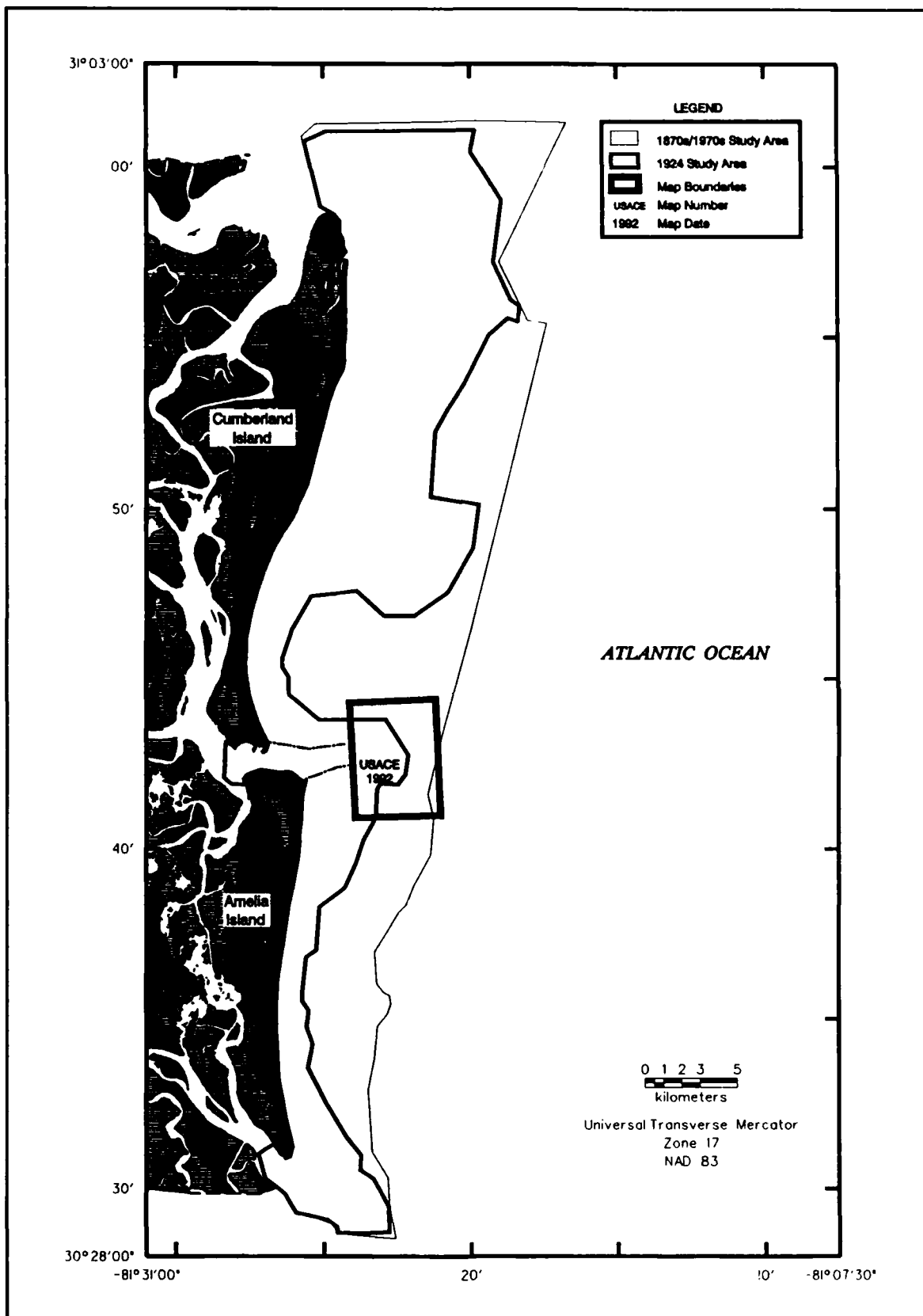


Figure 69. Bathymetric data coverage for the 1992 survey

be used to create a composite regional summary (1915/24). However, sparseness of soundings, map scale, and datum inaccuracies made the 1915 survey unsuitable for accurate analysis of seafloor change. Therefore, only the 1924 data set was used for assessing regional morphology and change affected by littoral processes. It is also used for detailed analysis at St. Marys Entrance by combining the 1924 data covering a majority of the ebb-tidal delta with the 1910 data extending to the seaward edge of the polygon. This is referred to as the 1910/24 data set. Because very little change is shown seaward of the limits of the delta, the time difference should introduce minimal ambiguity in the quality of results.

In 1934/35, a detailed survey was performed at St. Marys Entrance. The area covered is small and does not extend to the limits of the ebb-tidal delta (Figure 65). In 1954/55, another survey was completed at St. Marys Entrance that covered a much larger area (Figure 66). However, a portion of the ebb-tidal delta was not surveyed, leaving a gap in the data set. A composite of the 1934/35 and 1954/55 data (1934/55) was used for analysis of change at the inlet area, including adjacent shorelines, as well as detailed analysis of ebb-tidal delta evolution.

Surveys performed in the 1970s for this study area were numerous, widespread, and detailed (Figure 67). Dates range from 1974 to 1979. These data were collected digitally and were imported into map files. However, three regions were not surveyed during this time: the Nassau Sound area, northern Amelia Island including Fernandina Beach, and the area just north of the jetties at St. Marys Entrance. Therefore, the most recent data (1953/55) were inserted to create a composite regional summary. The resulting 1953/79 data set was used for regional, local, and detailed analyses.

The 1988 (Figure 68) and 1992 (Figure 69) surveys of the ebb-tidal delta at St. Marys Entrance defined the area of analysis for detailed examination of shoal evolution for the period of record. The corresponding polygon defined the limits for historical data sets (1870/75, 1910/24, 1934/55, and 1954/79) for temporal comparisons of change.

### **Potential error estimates**

When comparing bathymetric data digitized from maps, the potential error sources for horizontal location of points are identical to those for shoreline surveys (Table 11). Data sets recorded digitally and imported directly (1970s, 1988) contain less inherent error due to the elimination of cartographic inaccuracies and digitization procedure. Although it is difficult to quantify potential errors in elevation due to inaccurate horizontal positioning, conservative estimates range between  $\pm 0.3$  and  $0.5$  m based on USC&GS, NOAA, and USACE hydrographic manuals (e.g. Adams 1942). Corrections to soundings for tides and sea level change introduce additional errors in vertical position of  $\pm 0.1$  to  $0.3$  m. Finally, the accuracy of the depth measurement itself adds errors that are variable depending on the measurement method.

For the 1870s data, measurements were required to coincide within 3 percent of the water depth at sounding line crossings (Shalowitz 1964). Accuracy of the measurements for this time period was approximately  $\pm 0.5$  m for offshore areas where the lead line was employed and  $\pm 0.2$  m for nearshore areas surveyed using a graduated pole. For the 1924 and later surveys, all soundings have a measurement accuracy of  $\pm 0.3$  m. For the 1992 survey, bathymetry measurements were interpreted and digitized from analog fathometer records, resulting in added potential error of approximately  $\pm 0.1$  to  $0.2$  m. In comparisons of model surfaces made between two time periods, potential errors are additive. The rms potential errors were calculated for all

data set comparisons and are presented in Table 17. All volume change plots use these ranges to mark areas of no significant change.

<b>Table 17</b>					
<b>Maximum Root-Mean-Square (rms) Potential Error for Bathymetry Change Data (m)</b>					
<b>Date</b>	<b>1924</b>	<b>1934/55</b>	<b>1953/79</b>	<b>1988</b>	<b>1992</b>
<b>1855/75</b>	$\pm 0.6$	$\pm 0.6$	$\pm 0.6$	$\pm 0.6$	$\pm 0.6$
<b>1924</b>		$\pm 0.5$	$\pm 0.5$	$\pm 0.5$	$\pm 0.5$
<b>1934/55</b>			$\pm 0.5$	$\pm 0.5$	$\pm 0.5$
<b>1953/79</b>				$\pm 0.4$	$\pm 0.4$
<b>1988</b>					$\pm 0.4$

### **Cartographic data capture**

The same set of guidelines presented for digitization of T-sheets (Appendix B) applies for digitizing H-sheets. Scale, projection, ellipsoid, and horizontal datum are considered in assessing each map. Files are created matching specific cartographic parameters for each map, and text strings (sounding values) are placed in the file in their appropriate position. Generally, sounding text on a map is centered on the point representing the position at which the sounding was taken (Shalowitz 1964). Therefore, the center point of text on the map was digitized as the sounding location unless other indications of sounding location were present. For example, on some H-sheets, a dot is drawn at the sounding location. In this case, the location of the dot was digitized. After digitization, the files were converted to a common coordinate system (UTM Zone 17, NAD 83) for further analysis.

Digital data from the NGDC for the most recent NOS surveys included longitude and latitude, map number, date, depth, and depth units for each sounding. A computer program was written to place these data in a file for processing by MicroStation and Terrain Modeler. A map file was created in NAD 27, and text strings were placed according to locations provided in the original file. This file then was converted to a coordinate system common to other data sets.

### **Vertical adjustments**

Because ocean elevations are temporally and spatially inconsistent, adjustments to depth measurements must be made to bring all data to a common point of reference. These corrections include changes in relative sea level over time, adjustment to compensate for tidal fluctuations for different surveys, and differences in reference vertical datums (Figure 70).

All bathymetry data were adjusted to the NGVD 1929 and projected average sea level for 1992. The 1992 depths were collected relative to MLW, then corrected for tides and adjusted to the NGVD. Changes in relative sea level were calculated for each previous survey according to the time elapsed and the rate of sea level change at the respective reference tide gages. Also, the relationships between MLW and NGVD were obtained for each tide gage. Because relative sea level has been rising and MLW is a lower elevation than NGVD, the corrections to all elevation values were applied such that the resulting water depth was increased. In other words,

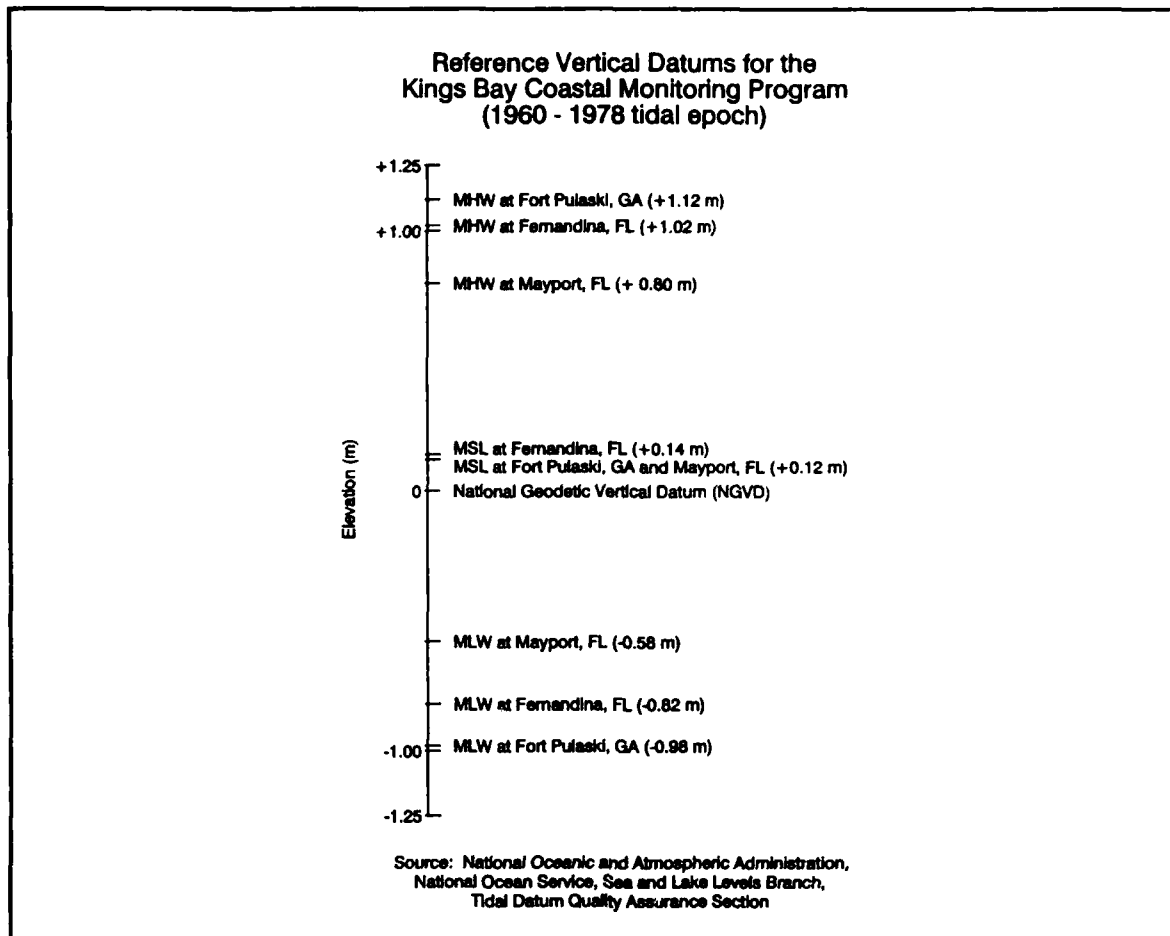


**Figure 70. Reference vertical datums for the Kings Bay study area (1960-1978 tidal epoch)**

depths were entered as negative numbers and the vertical adjustment was subtracted from the depth. The exact adjustment values for all maps and digital data from NGDC are given in Appendix B on the Hydrographic Information Sheets. The 1988 survey required the same corrections as the 1992 survey because the change in relative sea level between 1988 and 1992 was negligible.

Vertical adjustments were made after digitization of maps or importing of digital data, and after the map files were brought to a common horizontal reference. Older maps often had values in feet, fathoms, and fractions of fathoms, whereas newer maps were in feet. An interactive program was written in MicroStation Development Language to read the digitized values, convert feet or fathoms to meters, and apply the appropriate vertical adjustment. The finest resolution of depth was 0.5 ft (approximately 0.1 m). Therefore, after corrected water depths were converted to meters, all final values were rounded to one decimal place.

### **Analysis of bathymetric data**

Bathymetric data were analyzed using Intergraph's MGE Terrain Modeler (Modeler), which operates within the framework of the Modular GIS Environment. This means that simultaneous access to shorelines, engineering structures, bathymetry, annotation, and other data is possible.

The interactive nature of the software allows incorporation of shoreline and structure information into the established terrain model, providing an accurate and complete representation of the seafloor and adjacent boundaries. Polygon boundaries, defined in terms of physical processes, were established for the study area, though bathymetric data limits controlled the position of boundaries in some areas. The landward boundary condition was determined by overlaying all digitized shoreline position data and creating a composite edge on most landward positions. This method ensures that all areas that show change over the period of record are included in the analysis.

Unlike shoreline change analysis, where horizontal position is the only variable necessary to quantify change, terrain modeling requires a vertical measurement at each point to create a model surface for temporal and spatial comparisons. Because the landward boundary was defined as the position of a composite landward high-water shoreline, an elevation for this position was estimated using WIS hindcast data and beach profile information. As discussed in Appendix B, the position monitored by topographers and photo-interpreters during shoreline surveys is defined visually as the line associated with wave uprush during high tide. This elevation is known as the active subaerial beach profile height. Larson, Kraus, and Byrnes (1990) defined this zone in terms of  $Z_R$ , wave runup above a given datum. Runup height is estimated as

$$Z_R = 1.47 \xi^{0.79} \quad (4)$$

where the surf scaling parameter  $\xi$  is given by

$$\xi = \tan \beta (H_o/L_o)^{-0.5} \quad (5)$$

in which  $\tan \beta$  is the average beach slope in the surf zone, and  $H_o$  and  $L_o$  are deepwater wave height and wavelength. The elevation of the HWL was estimated to be 1.3 m above NGVD using this procedure.

Similar logic was used for defining boundaries in the nearshore zone (Figure 71). The offshore boundary for the study area was estimated using the criterion Hallermeier (1981) defined as the seaward limit for the initiation of sand motion for average annual waves,  $d_i$ . Average annual wave statistics from the WIS database also were used to estimate  $d_i$ , which was approximately 12 m below NGVD. In some areas, data coverage was not inclusive to this depth, in which case data coverage limits defined the boundary. Another cross-shore zone was defined by the seaward limiting depth  $d_l$  of significant sand transport due to steady wave action (Hallermeier 1981). This region defines the littoral zone for the study area and is consistent with procedures used to define this zone for shoreline change simulations (Chapter 7). The depth  $d_l$  associated with littoral processes was estimated at 6 m (NGVD) using this criterion.

The northern and southern boundaries of the study area were chosen to include St. Andrew Sound and Nassau Sound Tidal Inlet Complexes. Longshore divisions in Figure 71 were based primarily on the distribution of long-term seafloor change and were consistent with the boundaries of morphologic compartments defined in Figure 35. For regional comparisons with the 1924 data set, the seaward boundary coincides with the limits of the 1924 data (Figure 72); all other boundaries are the same as those identified for Figure 71.

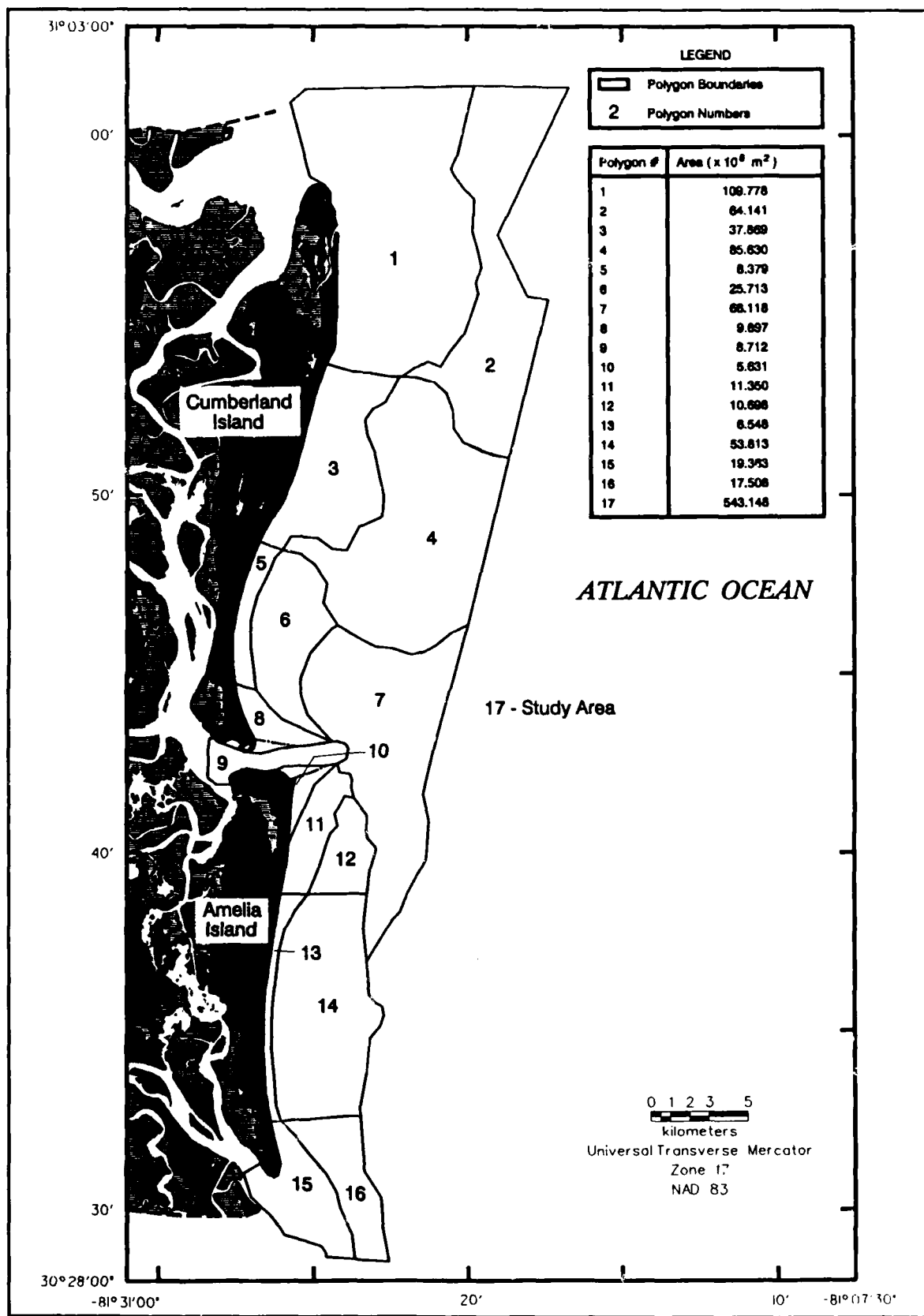


Figure 71. Polygon boundaries defined for the regional study area

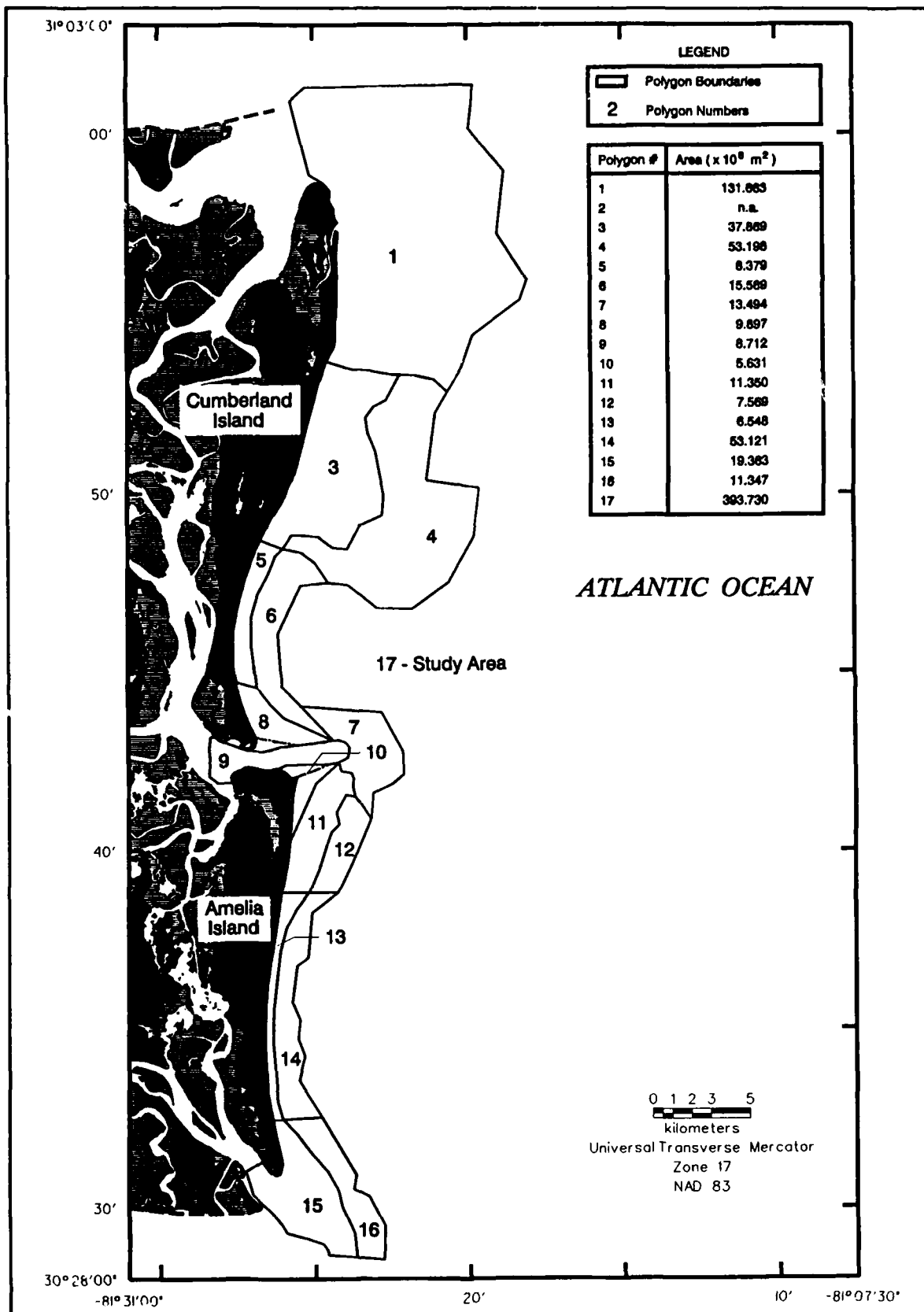


Figure 72. Polygon boundaries defined for the regional study area based on 1924 data

Digitized soundings, shorelines, structures, and compartment polygons were used to create digital elevation models of the seafloor for each time period. The Triangulated Irregular Network (TIN) was the terrain modeling routine used in this study to form a surface of continuous connected triangular planes based on irregular points. The elevation of each point is determined by solving equations for its horizontal location on the triangulated surface. Therefore, only points existing in the original data sources are used to create the surface model, as opposed to grid models which interpolate evenly spaced points from original data. TIN models were used for all calculations of bathymetry change; however, grid surfaces were generated for graphic display purposes.

MGE Terrain Modeler software provides a mechanism for loading digital elements from MicroStation files into a TIN model by specifying the type of terrain feature these elements represent. Soundings are imported as regular  $x$ ,  $y$ ,  $z$  locations. The shoreline corresponding to the date of the soundings is loaded as a 1.3-m-elevation contour. Jetty positions at St. Marys Entrance are used as breaklines, meaning that no triangles may cross the boundary. The compartment polygons are loaded as edges, creating models that vary in date and elevation, but are identical in horizontal coverage. These models are created in random access memory and then saved to disk in a Triangulated Topological Network (TTN) file, a special binary data storage format used by Modeler. TIN models can then be retrieved into memory from TTN files for display and analysis.

To calculate volume change, TIN models representing two different dates were compared using the Compute Volume function within MGE Terrain Modeler software. Primary and secondary surfaces are identified prior to differencing. Every data point from the primary surface is projected onto the secondary surface and the  $z$ -value of the secondary surface is subtracted from the  $z$ -value of the original point. Likewise, every data point from the secondary surface is projected onto the primary surface and the  $z$ -values subtracted. The resultant TIN model then contains a point corresponding to each point from the primary and secondary surfaces, with the  $z$ -value representing the differences in elevation between the two. Volume change is calculated by summing the volume of each triangle region. In addition to resultant TIN models showing bathymetric change, text files are output that summarize volume changes. Values for cut (erosion), fill (accretion), absolute volume change, and net change are included. Eighty-eight bathymetry change calculations were made: three for the entire study area, three for each of the 16 polygons (except Polygon 2 for 1924 data comparisons), three for the St. Marys Entrance tidal inlet complex, and 36 for the ebb-tidal delta at St. Marys Entrance.

### **Regional bathymetry and change**

Prior to jetty construction, the morphology of ebb-tidal delta sand deposits at St. Marys Entrance appeared much like those associated with other natural inlet systems separating offset barrier islands (Hayes and Kana 1976, Hayes 1991). Figure 73 illustrates the regional characteristics of nearshore morphology in the study area for the period 1855/75. Several important features are recognized. First, the orientation of contours defining shoals is skewed to the south, suggesting a net southerly directed transport of sediment for the entire region. The tidal channel at all three inlet systems (St. Andrew Sound to the north, St. Marys Entrance, and Nassau Sound to the south) exits the coast with a southeast orientation. The shoals associated with St. Andrew Sound appear to be oriented to the southeast as well. In addition, the ebb-tidal

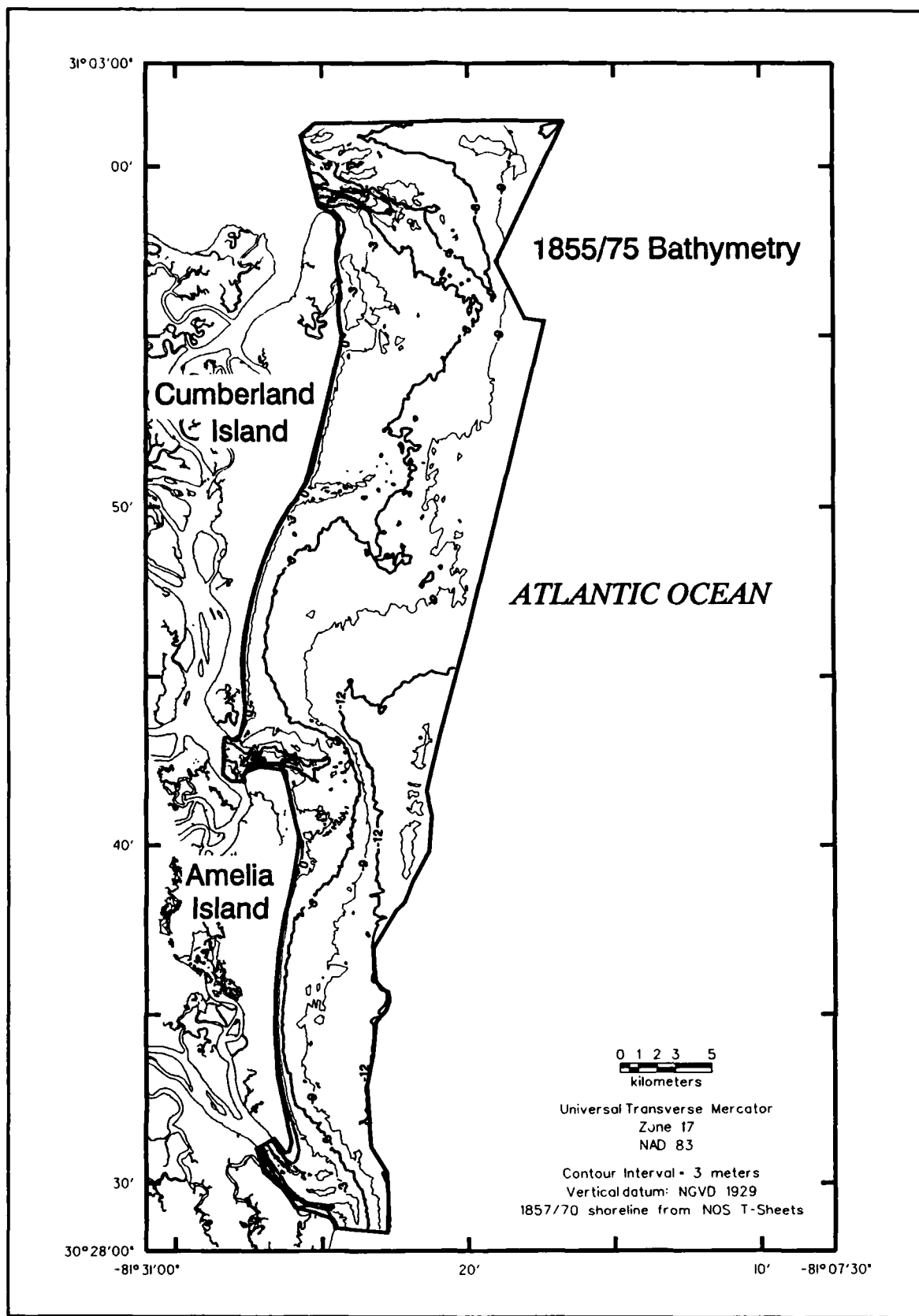


Figure 73. Regional bathymetric contour map for the period 1855/75

delta identified with St. Marys Entrance is well defined by the 6-m (NGVD) depth contour and is strongly skewed to the south. Second, the shoal complex associated with St. Andrew Sound is by far the most extensive subaqueous feature in the study area, and the channel is greater than 15 m deep in some places. Sand deposits defined by the 6-m (NGVD) depth contour extend approximately 8 km offshore and at least 10 km south along Cumberland Island. Third, Stafford Shoal, a sand deposit located midway along Cumberland Island, is approximately the same size as the ebb-tidal delta at St. Marys Entrance and extends 4 to 5 km offshore. Fourth, the ebb shield associated with St. Marys ebb-tidal delta is well defined by the 6-m (NGVD) depth contour. The ebb-tidal delta extends about 4.5 km seaward from the coast adjacent to the entrance and connects with the shoreline approximately 5 km south of the main channel where a headland existed. The deposit appears to provide an efficient conduit for sediment bypassing from Cumberland to Amelia Islands. Fifth, Nassau Sound has the smallest shoal deposits, primarily confined to within 2 km of the coast. The general decrease in sand storage in ebb-tidal deltas from north to south correlates well with a decrease in tidal prism in backbarrier environments. Sixth, the inner shelf area north of St. Marys Entrance is broader and more gently sloping than that associated with Amelia Island to the south. Finally, the 6-m (NGVD) depth contour away from tidal inlets and Stafford Shoal is located within 1 km of the shoreline and within 0.5 km of the coast along central Amelia Island.

Nearshore bathymetry for 1924 shows no major deviation from that described for 1855/75 except along the seaward margin of Stafford Shoal and at St. Marys Entrance (Figure 74). Stafford Shoal, as outlined by the 6-m (NGVD) depth contour, decreased in size since 1855/75. A more pronounced regional change is that associated with jetty construction at St. Marys Entrance at the turn of the century. The ebb-tidal delta is located approximately 2 km seaward of its prejetty configuration and defined by the 9-m (NGVD) depth contour. In addition, the southern half of the historical ebb-tidal delta is eroding, as indicated by landward translation of the 6-m (NGVD) depth contour. However, the location of the 6-m (NGVD) depth contour in the Cumberland and Amelia Embayments has not changed since 1855/75.

The most recent regional bathymetric survey (1953/79) shows significant changes at St. Marys Entrance and some minor changes elsewhere (Figure 75). Compared with the earliest survey, the position of the 6-m (NGVD) depth contour defining the ebb-tidal delta at St. Andrew Sound has shifted landward by about 1 km. Approximately half of this change occurred by 1924. Stafford Shoal remained in the same general location between 1924 and 1953/79, although the shallow platform at the landward margin of the shoal (0-m NGVD contour) has decreased in size significantly. Major changes in the extent of deposition at St. Marys Entrance occurred relative to both earlier time periods. By 1953/79 the ebb-tidal delta and entrance channel were well defined by the 9- and 12-m (NGVD) depth contours, respectively. The ebb-tidal delta shifted approximately 3 km seaward since 1855/75, and water depth over the shoal increased by about 3 m. These two factors limit (if not eliminate) sand bypassing around the shoal and wave sheltering of the shoreline. Finally, the position of the 6-m (NGVD) depth contour in the Cumberland and Amelia Embayments showed no significant change for the entire period of record, indicating remarkable stability in these regions and a reasonable depth estimate for the littoral zone (Figure 76). However, the 9-m (NGVD) depth contour in these areas has shifted, apparently as a result of continental shelf processes.

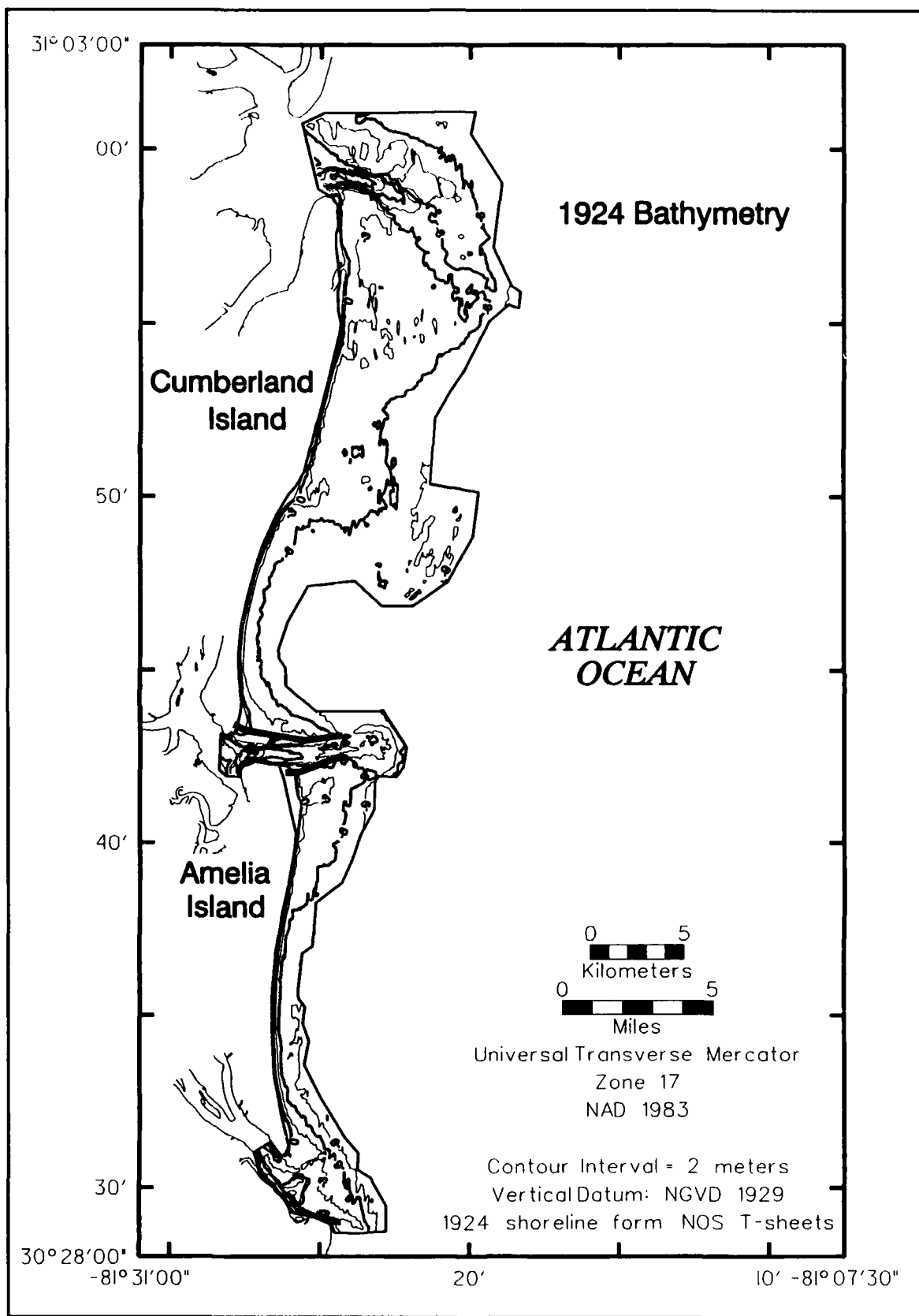


Figure 74. Regional bathymetric contour map for the 1924 data set

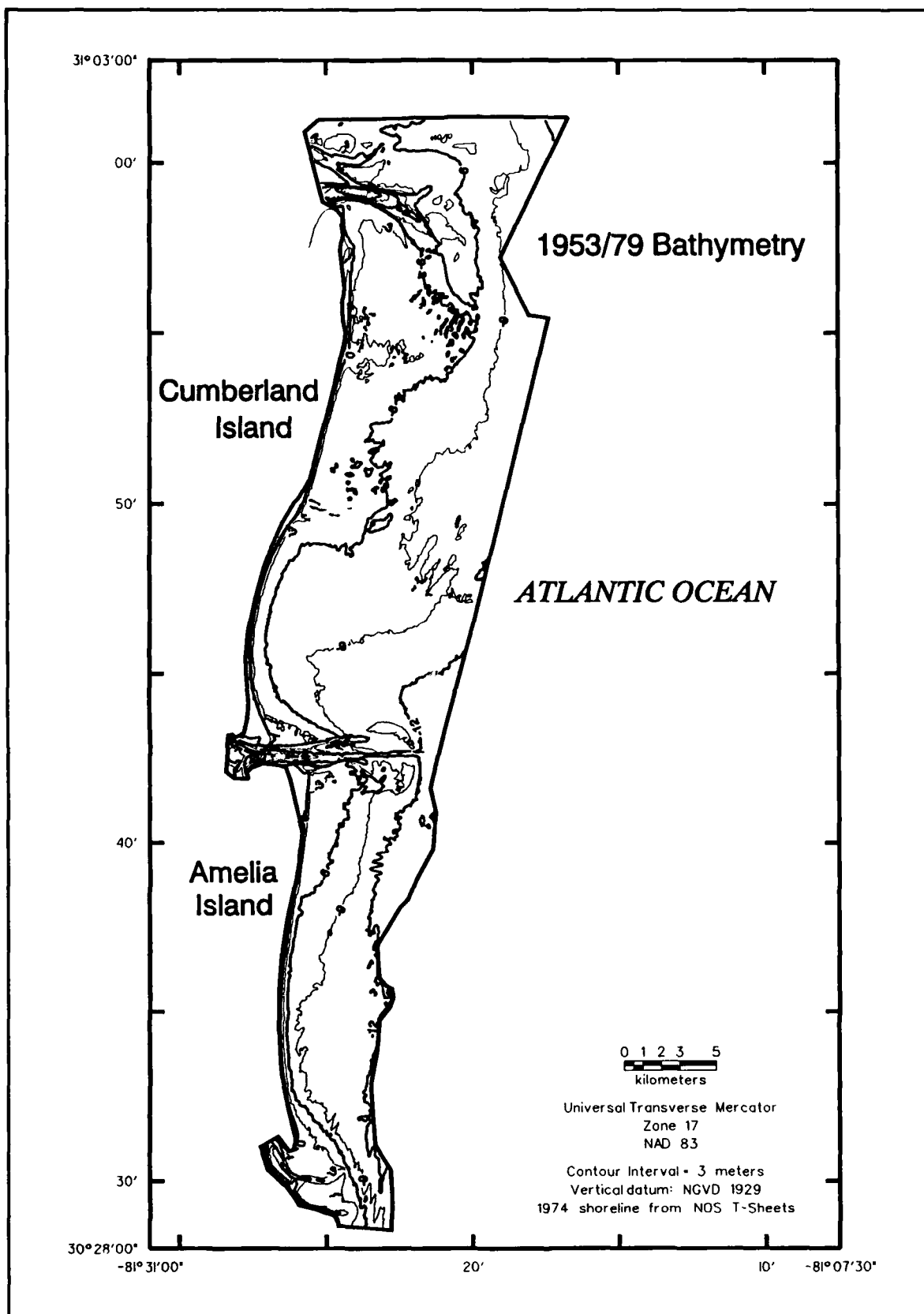


Figure 75. Regional bathymetric contour map for the period 1953/79

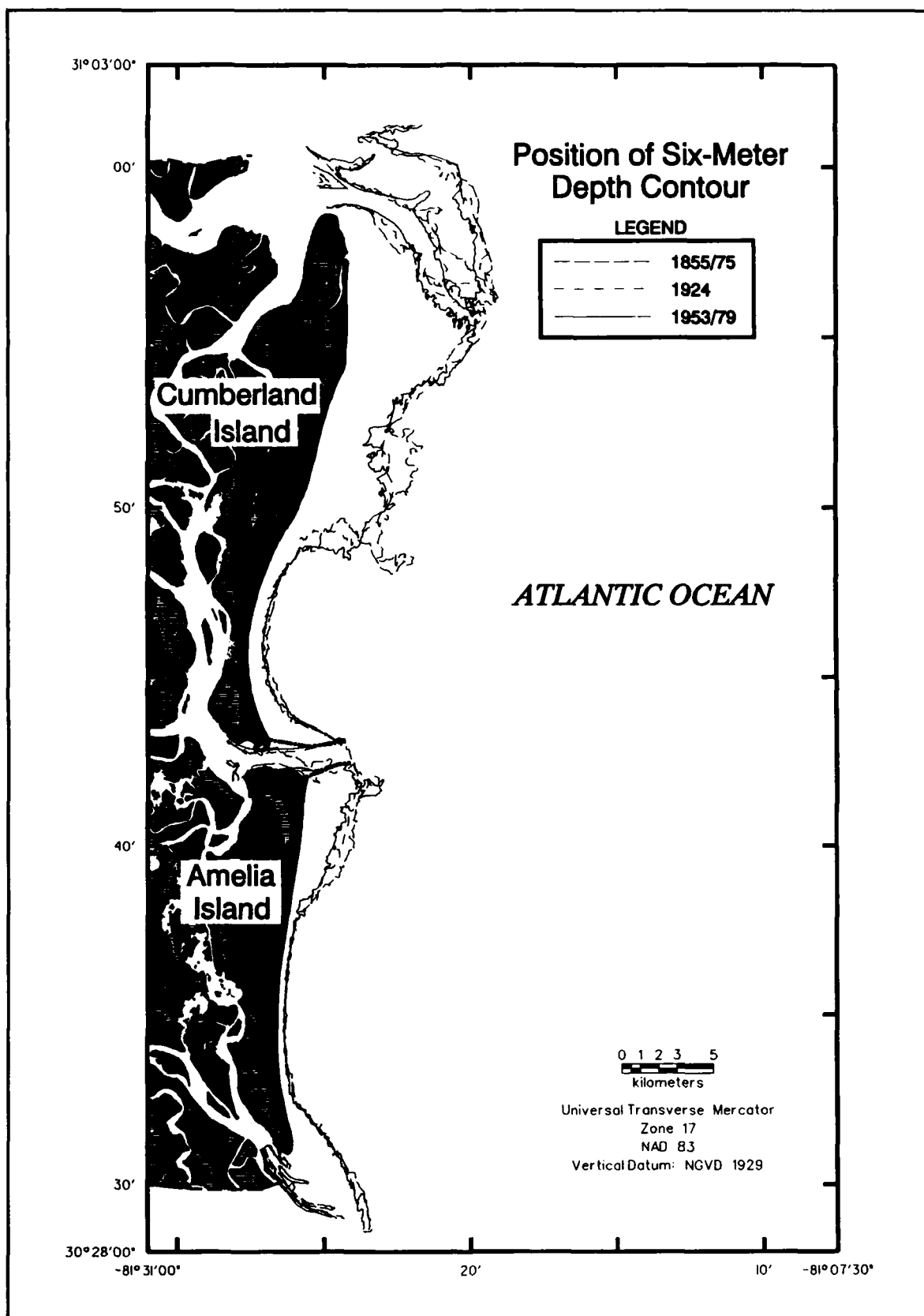


Figure 76. Change in position of the 6-m (NGVD) depth contour for the period of record

Volumetric changes associated with the three time periods are illustrated on Figures 77-79. Between 1855/75 and 1924, evidence of net southerly drift throughout the study area is indicated where deposition occurs downdrift of regions of erosion (Figure 77). This is most pronounced at St. Andrew Sound and Stafford Shoal. At St. Marys Entrance, the ebb-tidal delta associated with jetty construction is well-defined as a center of deposition seaward of the entrance channel (Figure 77, Polygon 7 in Table 18). At the same time, the area between the jetties has scoured significantly. In addition, the area seaward of the south jetty tip has eroded as the channel attempts to redirect its flow to the southeast. Deposition along the north and south jetties created large fillets on both shorelines. Erosion of the historical ebb-tidal delta is indicated seaward of Fernandina Beach as the system adjusts to placement of the jetties. Finally, a long band of deposition is indicated along central Amelia Island, and erosion at the southern terminus of Amelia is pronounced.

Between 1924 and 1953/79, shoal migration to the south-southeast continued, and deposition along the Cumberland Embayment shoreline was significant (Figure 78). Translation of the ebb-tidal delta seaward beyond the data coverage for 1924 was associated with erosion of an earlier stage of shoal development. This is the reason for net loss of sediment from Polygon 7 in Table 18. The remnant historical ebb-tidal delta continued to erode and shoreline deposition adjacent to the jetties persisted. The nearshore area off southern Amelia Island showed a small amount of erosion with subaqueous deposition occurring seaward of the southern terminus of the island.

Regional trends for the entire period of record provide the most complete summary of change for the entire study area. The 1924 data set only provided a limited assessment of large-scale coastal evolution. Figure 79 provides a detailed survey of elevation changes between 1855/75 and 1953/79. The most pronounced change is that associated with the ebb-tidal delta at St. Marys Entrance. Approximately 90 million cu m of sediment are associated with the development of this feature (Polygon 7 in Table 19). Conversely, the channel entrance between the jetties shows a net loss of approximately 40 million cu m (Polygon 9). As in previous discussions, net southerly drift of sediment is illustrated for the St. Andrew Sound ebb-tidal delta and Stafford Shoal. Regions of deposition are situated downdrift (south) of zones of erosion. In addition, the orientation of deposition associated with the modern ebb-tidal delta at St. Marys Entrance is to the south. Erosion on the southern half of the historical ebb-tidal delta and adjacent coastline of Amelia Island is associated with deposition along northern Amelia Island at the fillet and along the Amelia Embayment. Deposition along the northern 4 km of Amelia Island is related to a reversal in sand transport associated with localized wave refraction across the historical ebb-tidal delta. The nearshore region associated with the southern 6 km of Amelia Island indicates erosion; however, nearshore deposition along the southern 3 km of the island, particularly at the northern margin of the inlet, also is shown.

Overall, the littoral zone along Cumberland Island is accretional whereas that associated with Amelia Island is erosional. Cumberland shows a net surplus of sand (5,538,000 cu m) for areas influenced primarily by littoral processes (Polygons 3, 5, and 8) for the period of record, whereas Amelia has a deficit of 7,034,000 cu m for a similar zone along its coast (Polygons 9, 11, and 13). The entire study area shows a net deficit of 51,236,000 cu m between 1855/75 and 1953/79, but most of this change (78 percent) is associated with areas involving a multitude of nearshore shelf and inlet processes, and not just littoral processes.

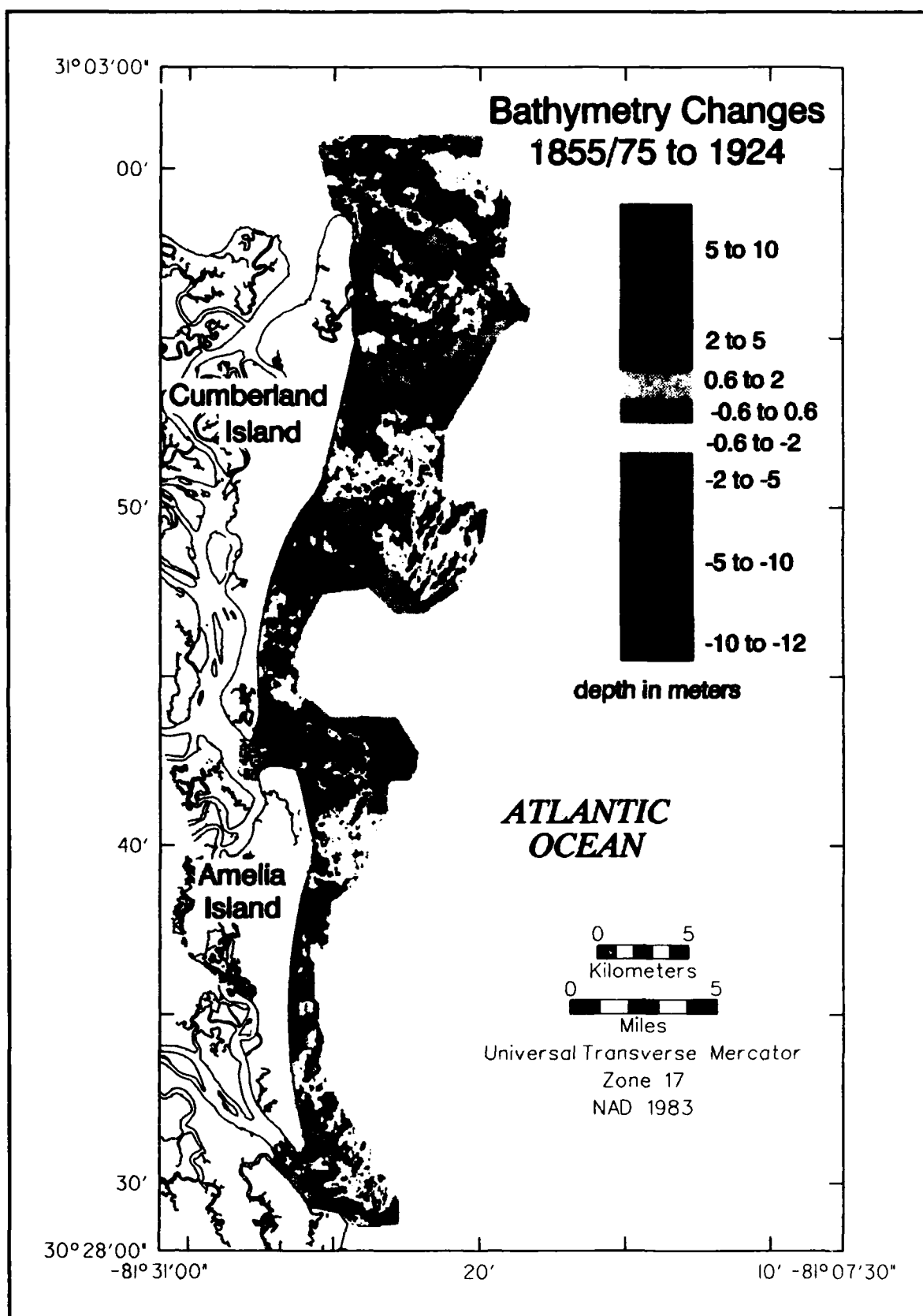


Figure 77. Color-fill contour map of regional changes in bathymetry between 1855/75 and 1924

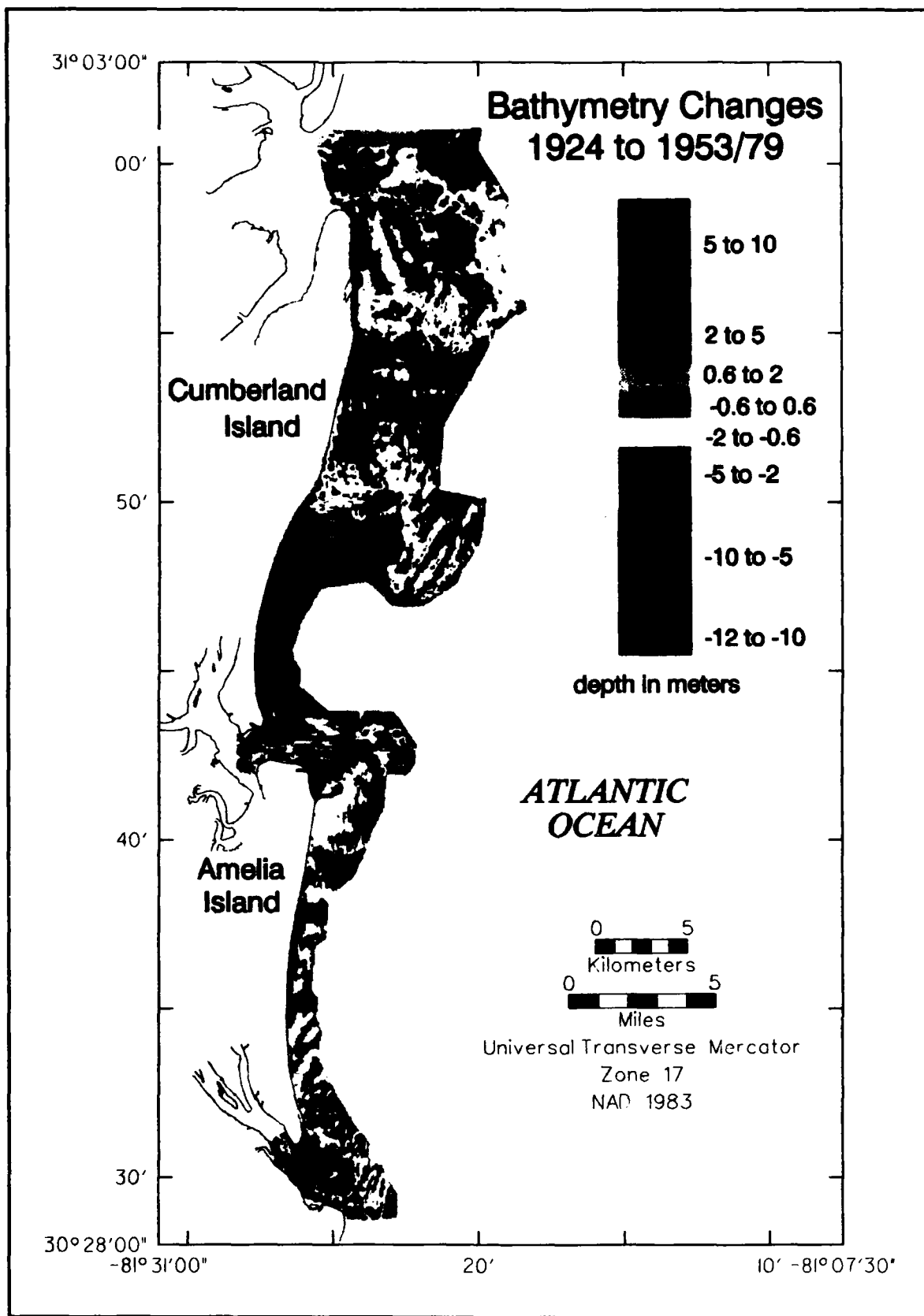


Figure 78. Color-fill contour map of regional changes in bathymetry between 1924 and 1953/79

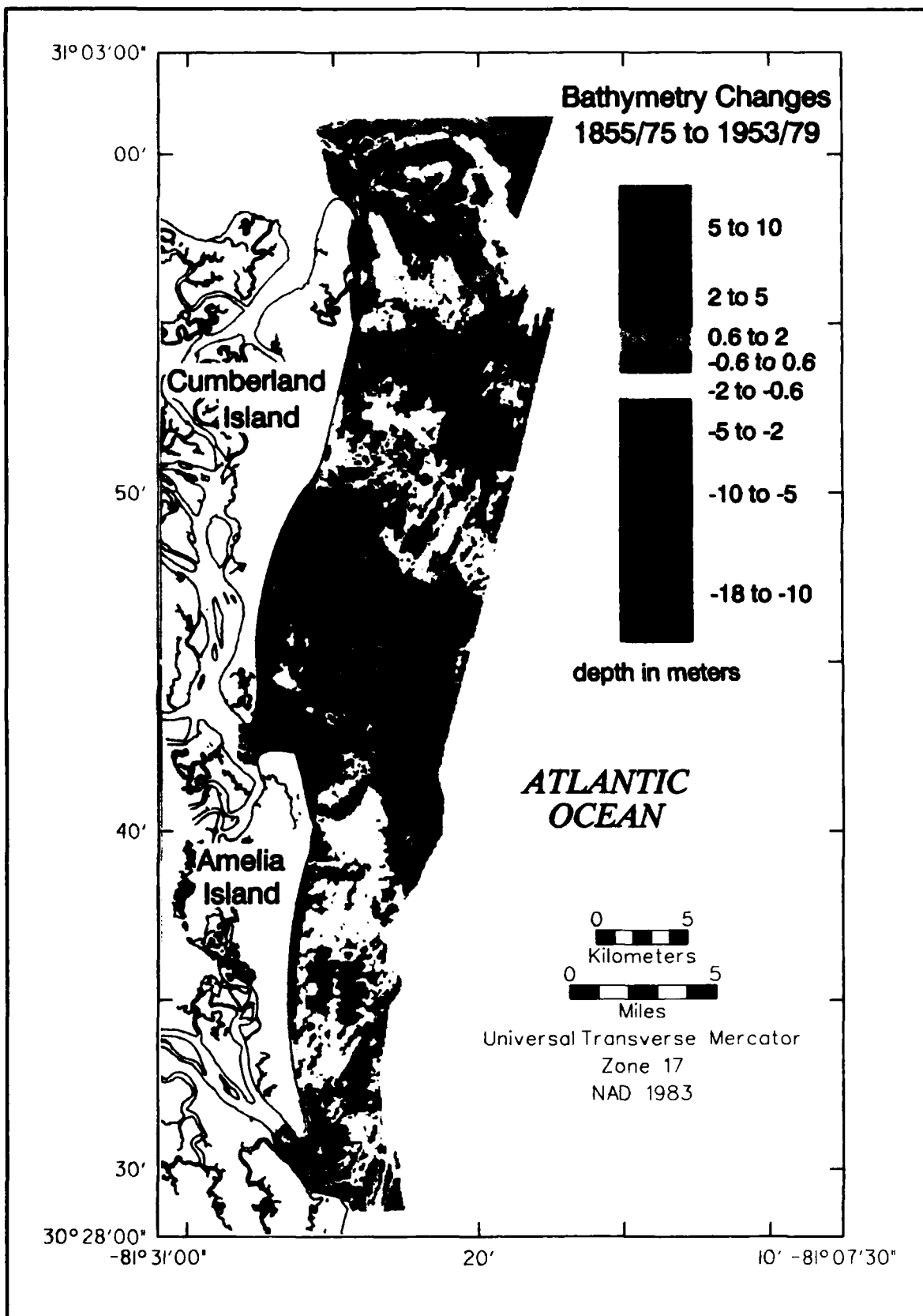


Figure 79. Color-fill contour map of regional changes in bathymetry between 1855/75 and 1953/79

**Table 18**  
**Historical Changes in Sediment Volume (cu m) for Polygons Defining the**  
**Nearshore Bathymetry Based on the 1924 Data Limits (Figure 72)**

Polygon	Date	Cut	Fill	Absolute	Net
1	1855/75-1924	-45,987,000	68,297,000	114,284,000	22,310,000
	1924-1953/79	-70,253,000	53,814,000	124,067,000	-16,439,000
2	1855/75-1924				
	1924-1953/79				
3	1855/75-1924	-14,099,000	11,901,000	26,000,000	-2,198,000
	1924-1953/79	-15,056,000	8,917,000	23,973,000	-6,139,000
4	1855/75-1924	-36,849,000	8,961,000	45,810,000	-27,888,000
	1924-1953/79	-18,912,000	9,852,000	28,764,000	-9,061,000
5	1855/75-1924	-3,444,000	513,000	3,957,000	-2,930,000
	1924-1953/79	-131,000	5,449,000	5,580,000	5,317,000
6	1855/75-1924	-4,940,000	1,185,000	6,126,000	-3,755,000
	1924-1953/79	-544,000	2,431,000	2,976,000	1,887,000
7	1855/75-1924	-1,173,000	31,391,000	32,564,000	30,219,000
	1924-1953/79	-9,036,000	8,362,000	17,398,000	-674,000
8	1855/75-1924	-1,660,000	10,630,000	12,290,000	8,970,000
	1924-1953/79	-2,625,000	5,116,000	7,742,000	2,491,000
9	1855/75-1924	-31,151,000	814,000	31,965,000	-30,337,000
	1924-1953/79	-12,832,000	2,617,000	15,545,000	-10,216,000
10	1855/75-1924	-2,496,000	9,162,000	11,659,000	6,666,000
	1924-1953/79	-1,689,000	5,281,000	6,970,000	3,592,000
11	1855/75-1924	-11,509,000	2,535,000	14,044,000	-8,973,000
	1924-1953/79	-8,995,000	270,000	9,265,000	-8,726,000
12	1855/75-1924	-6,512,000	51,000	6,564,000	-6,461,000
	1924-1953/79	-2,333,000	199,000	2,533,000	-2,134,000
13	1855/75-1924	-1,004,000	3,906,000	4,910,000	2,901,000
	1924-1953/79	-2,735,000	577,000	3,311,000	-2,158,000
14	1855/75-1924	-5,697,000	567,000	6,264,000	-5,130,000
	1924-1953/79	-6,654,000	441,000	7,096,000	-6,213,000
15	1855/75-1924	-16,068,000	13,945,000	30,014,000	-2,213,000
	1924-1953/79	-15,291,000	12,770,000	28,061,000	-2,521,000
16	1855/75-1924	-7,954,000	1,152,000	9,106,000	-6,802,000
	1924-1953/79	-5,630,000	1,195,000	6,825,000	-4,434,000
17	1855/75-1924	-191,741,000	165,471,000	357,211,000	-26,270,000
	1924-1953/79	-172,296,000	117,588,000	289,885,000	-54,708,000

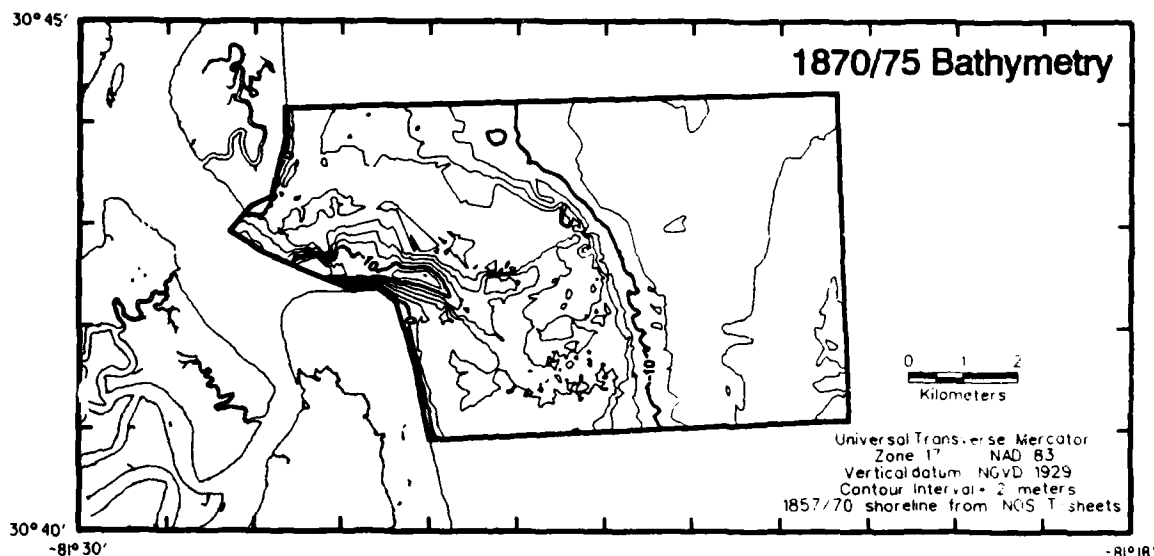
**Table 19**  
**Historical Changes in Sediment Volume (cu m) for Polygons Defining**  
**Nearshore Bathymetry (Figure 71)**

Polygon	Date	Cut	Fill	Absolute	Net
1	1855/75-1953/79	-55,800,000	77,333,000	133,133,000	21,534,000
2	1855/75-1953/79	-27,861,000	5,600,000	33,461,000	-22,260,000
3	1855/75-1953/79	-21,892,000	13,574,000	35,466,000	-8,319,000
4	1855/75-1953/79	-56,212,000	24,163,000	80,374,000	-32,049,000
5	1855/75-1953/79	-1,437,000	3,868,000	5,306,000	2,431,000
6	1855/75-1953/79	-4,236,000	4,199,000	8,435,000	-37,000
7	1855/75-1953/79	-7,072,000	96,816,000	103,888,000	89,743,000
8	1855/75-1953/79	-2,354,000	13,780,000	16,134,000	11,423,000
9	1855/75-1953/79	-41,329,000	830,000	42,159,000	-40,499,000
10	1855/75-1953/79	-2,039,000	12,184,000	14,223,000	10,145,000
11	1855/75-1953/79	-18,484,000	592,000	19,076,000	-17,892,000
12	1855/75-1953/79	-12,003,000	139,000	12,142,000	-11,864,000
13	1855/75-1953/79	-2,431,000	3,144,000	5,575,000	713,000
14	1855/75-1953/79	-36,025,000	984,000	37,009,000	-35,041,000
15	1855/75-1953/79	-19,172,000	14,629,000	33,801,000	-4,543,000
16	1855/75-1953/79	-16,175,000	1,147,000	17,322,000	-15,028,000
17	1855/75-1953/79	-324,176,000	272,940,000	597,117,000	-51,236,000

#### **Bathymetry and change at St. Marys Entrance and vicinity**

After documenting regional trends, a detailed analysis of changes at the St. Marys Tidal Inlet Complex was performed to assess the patterns of ebb-tidal delta evolution at larger scale and for finer increments of time. As shown in the *Data sources* subsection, information is available for St. Marys Entrance on intermediate time intervals not recorded on a regional scale. The following discussion is intended to summarize these data for two areas: (a) a majority of the inlet system, including the channel, the ebb-tidal delta, and adjacent shorelines (referred to as the tidal inlet complex); and (b) a region encompassing the modern ebb-tidal delta. Data for the tidal inlet complex polygon shows only one new time period of change (1934/55), but these data provide a more detailed view of spatial change than the regional summary maps. Six time periods are used to document the evolution of the ebb-tidal delta between 1870/75 and 1992. Consequently, the most detailed analysis of change was performed for this region.

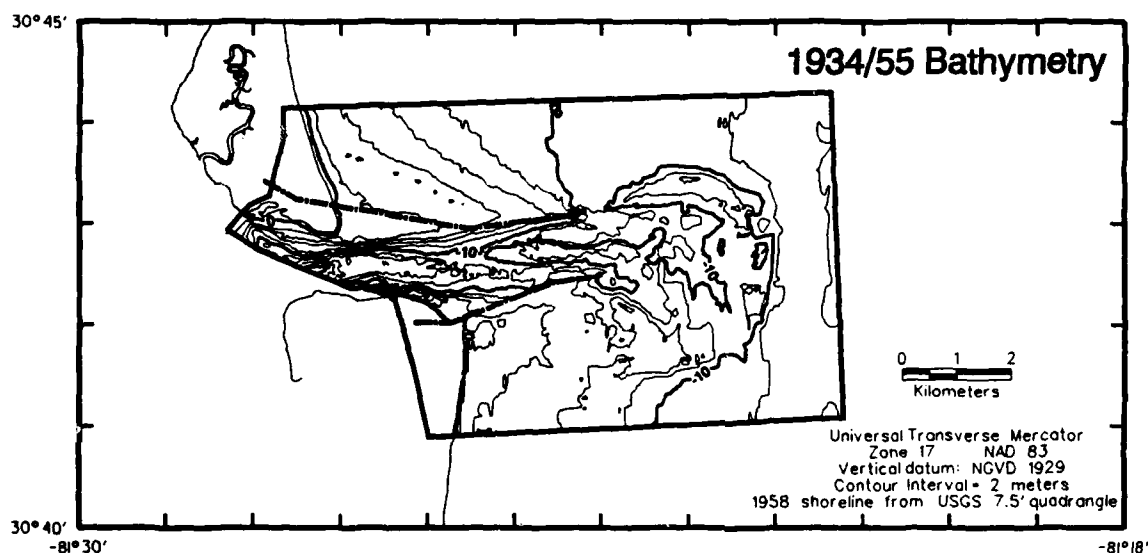
**St. Marys Tidal Inlet Complex.** The morphology of St. Marys Tidal Inlet Complex, as indicated from the 1870/75 survey, shows a well-developed channel up to 14 m deep along the southern margin of the inlet and extending southeast onto the shelf after exiting the coast between Cumberland and Amelia Islands (Figure 80). An extensive ebb-tidal delta projects seaward from the coast approximately 4 km and is skewed to the south. Although the 4- through 10-m (NGVD) depth contours show the arcuate pattern of the delta seaward of southern Cumberland Island, it appears the 6-m (NGVD) depth contour best reflects the seaward margin of the delta



**Figure 80. Bathymetric contour map for St. Marys Tidal Inlet Complex, 1870/75**

south of the inlet along Amelia Island. This pattern was also shown in the regional bathymetry (Figure 73).

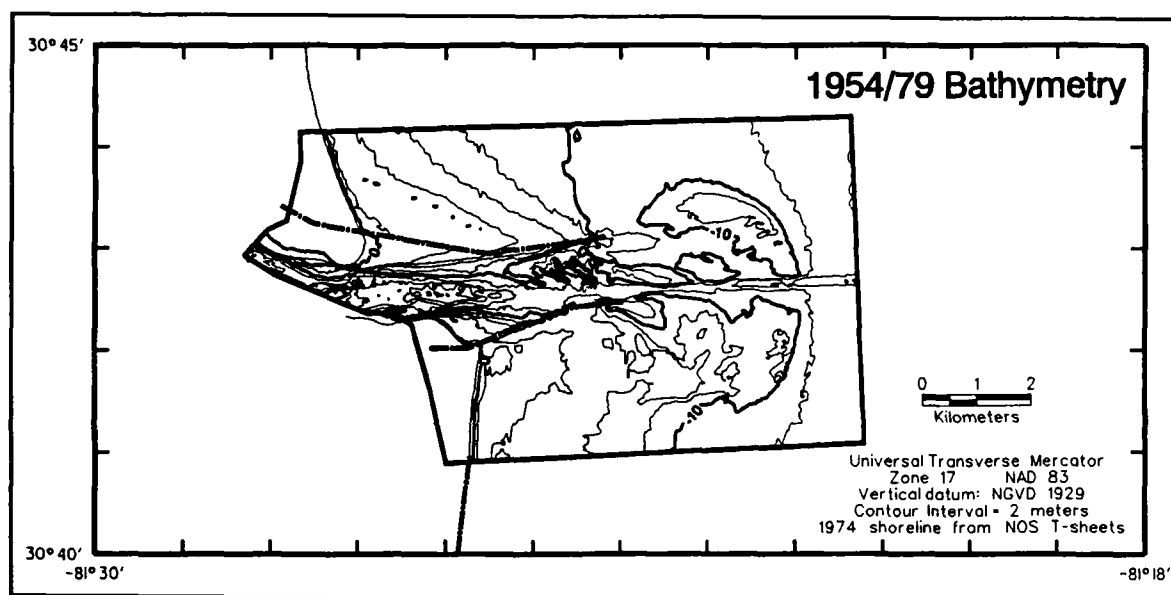
By 1934/55, the jetties had been constructed, and the configuration of the channel and ebb-tidal delta was noticeably different (Figure 81). The lobe of the ebb-tidal delta, as defined by the 10-m (NGVD) depth contour, was located in deeper water on the shelf about 3 km seaward of its position in 1870/75. For the 1934/55 bathymetry, the 10-m (NGVD) depth contour denotes the outer margin of the delta quite well, unlike what was shown in 1870/75. The channel remains oriented along the southern margin of the inlet and south jetty, and after exiting the seaward side of the jetties, channel position reorients to the southeast. Shoreline progradation



**Figure 81. Bathymetric contour map for St. Marys Tidal Inlet Complex, 1934/55**

adjacent to the jetties was significant between 1870/75 and 1934/55, creating subaerial fillets and subaqueous shallowing seaward of these areas.

The most recent bathymetry data set for the tidal inlet complex was collected between 1954 and 1979. For this time period, the ebb-tidal delta was well-developed, and a linear dredged channel 12 m deep separated the north and south lobes of the delta (Figure 82). Although flow from the inlet is directed out this channel, a small ebb-channel extending to the southeast from the seaward end of the south jetty is well-defined. Conversely, sand deposition near the seaward end of the north jetty and into the channel is indicated by extension of the 6- and 8-m (NGVD) depth contours into an area 10.7 m or deeper. The outer margin of the ebb shield translated seaward approximately 0.1 km since 1934/55, and the ebb-tidal delta, as indicated by the 10-m (NGVD) depth contour, is better defined.



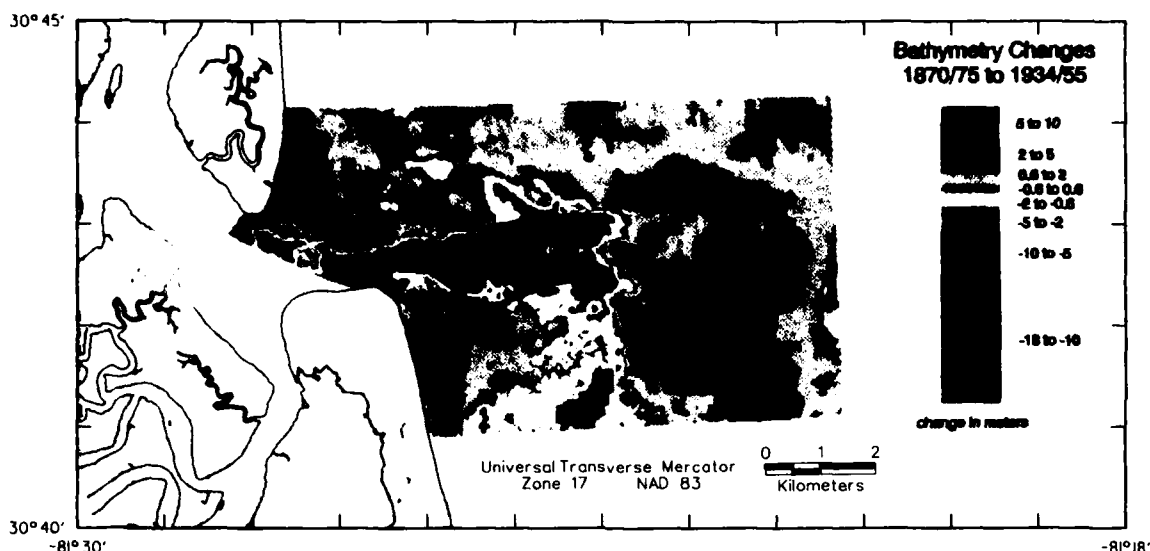


Figure 83. Bathymetric change map for St. Marys Tidal Inlet Complex, 1870/75-1934/55

Therefore, changes in the entrance channel, on part of the ebb-tidal delta, and at adjacent shorelines are all that can be included for comparison with the 1954/79 time period, and volume changes shown for this time period in Table 20 should be viewed cautiously. In addition to growth of that portion of the ebb-tidal delta having different data coverages, the area between the jetties continued to scour, and a dredged channel can be recognized through the center of the delta. Also, a large area of deposition persists southeast of the north jetty near the channel and a lobe of deposition is situated to the southeast of a small channel off the end of the south jetty. The shoreline along northern Amelia Island has eroded, and shoreline progradation along southern Cumberland Island persists.

Table 20

Historical Changes in Sediment Volume (cu m) for St. Marys Tidal Inlet Complex

Date	Cut	Fill	Absolute	Net
1870/75-1934/55	-42,129,000	90,921,000	133,050,000	48,792,000
1934/55-1954/79	-17,404,000	15,607,000	33,012,000	-1,797,000
1870/75-1954/79	-48,475,000	95,483,000	143,958,000	47,008,000

Changes for the entire period of record (Figure 85) show the same general patterns as those for the period 1870/75 to 1934/55. A few basic differences exist. First, the area between the jetties shows a greater magnitude of scour, including some areas where at least 10 m of vertical change occurred. Second, the ebb-tidal delta has evolved to a well-defined arcuate shape. The greatest amount of deposition continues to be located on the southern lobe of the delta. Third, a linear dredged channel can be identified through the central portion of the delta; however, only a small segment of the channel is excavated deeper than the 1870/75 surface.

**St. Marys ebb-tidal delta.** Because the ebb-tidal delta would be the first feature likely to exhibit potential adverse impacts of channel dredging, a detailed evaluation of spatial and

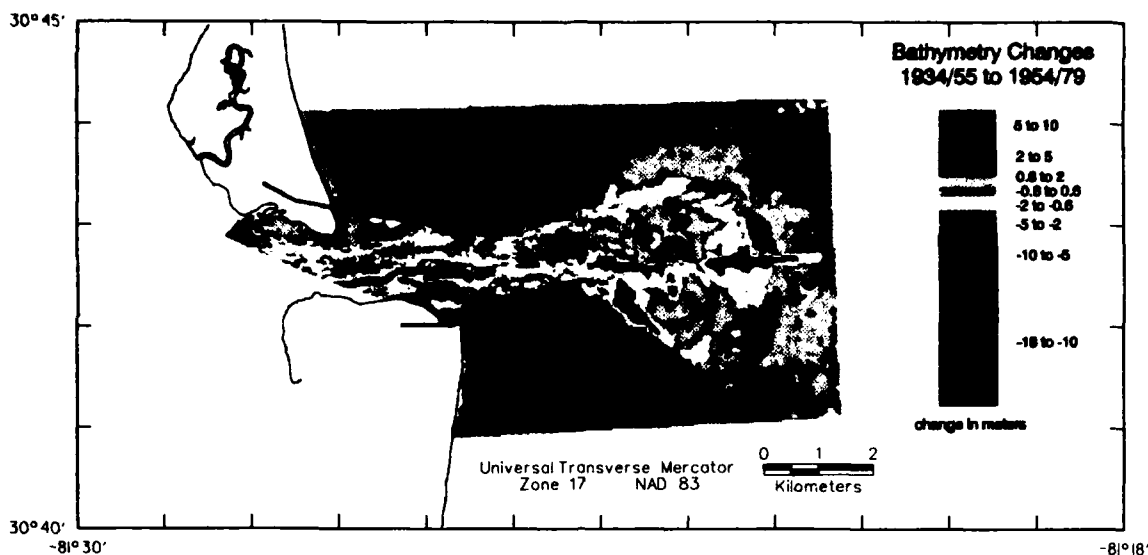


Figure 84. Bathymetric change map for St. Marys Tidal Inlet Complex, 1934/55-1954/79

temporal changes for an area defined by the 1988 and 1992 bathymetric surveys was completed. Three additional time periods were available for making comparisons (1910/24, 1988, 1992). Figures 86-91 detail the evolution of the modern ebb-tidal delta between 1870/75 and 1992. For the initial time period (prejetty construction), a small portion of the seaward margin of the ebb-tidal delta extended into the western side of the area of coverage. Most of the area consisted of inner-shelf morphology between the 10- and 15-m (NGVD) depth contours (Figure 86). By the 1910/24 time period (postjetty construction), a large lobe of sediment had been deposited on the shelf surface, bound on its seaward margin by the 10-m (NGVD) depth contour (Figure 87). By 1934/55, the ebb-tidal delta was large in extent and had prograded farther seaward by about 0.5 km (Figure 88). The 1954/79 data show a well-defined ebb-tidal delta, outlined by the 10-m

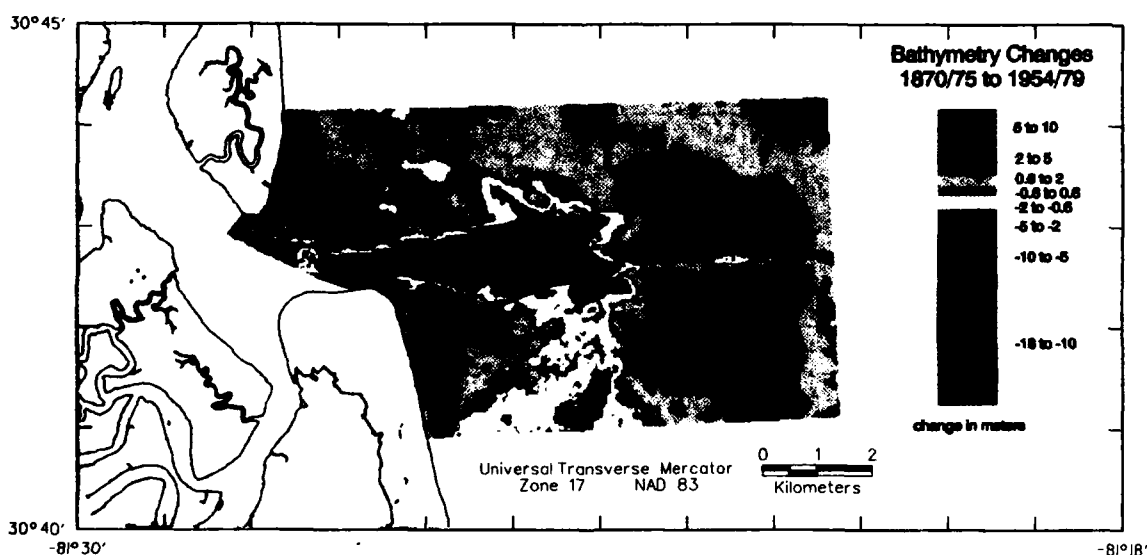
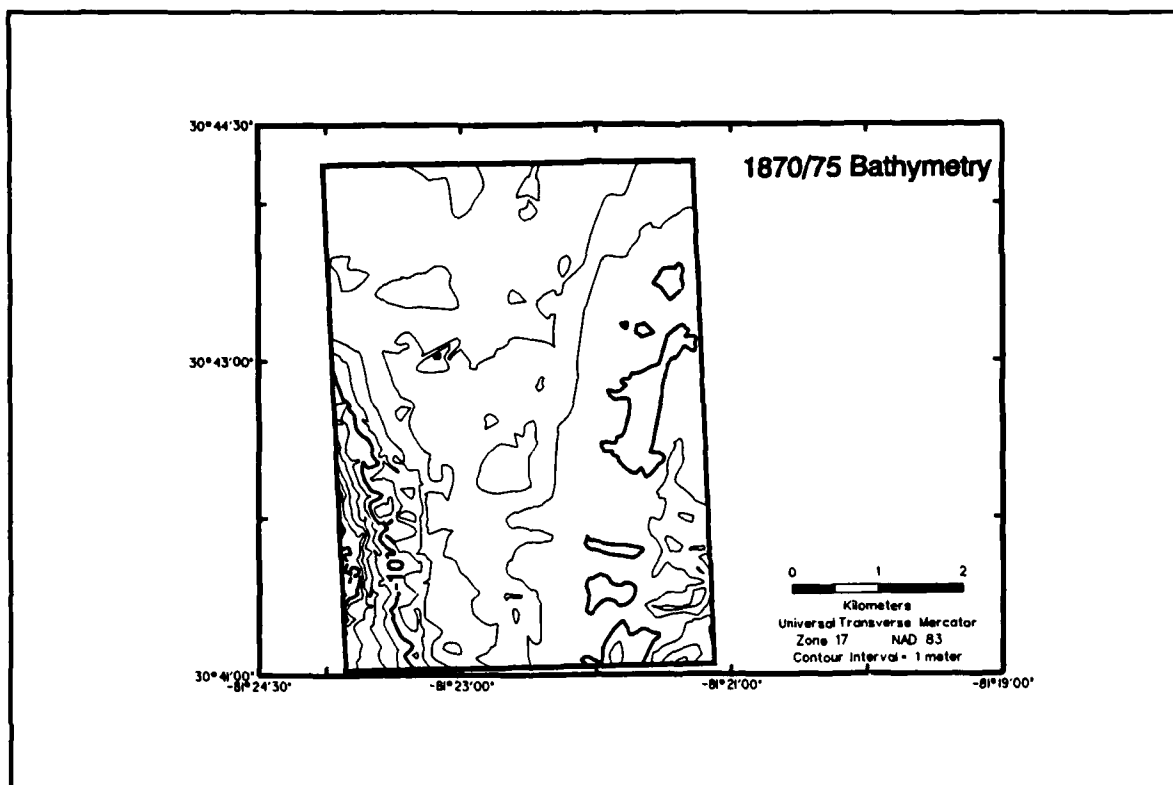
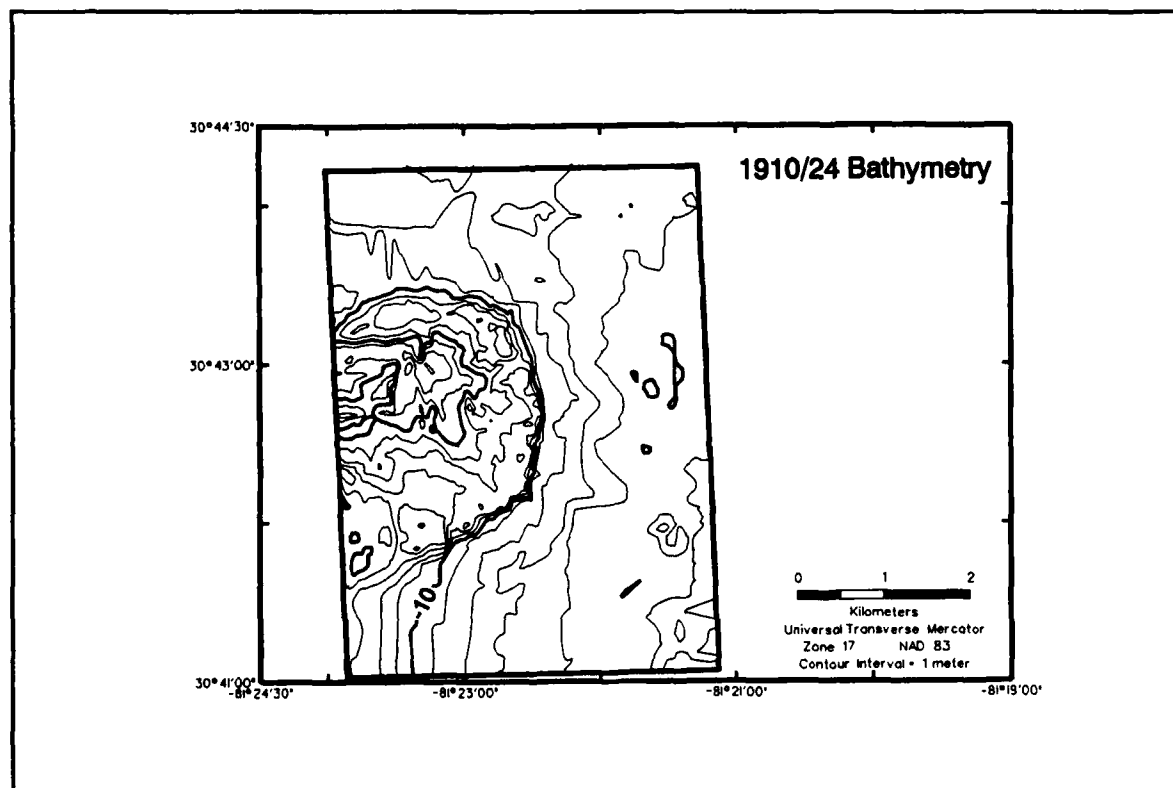


Figure 85. Bathymetric change map for St. Marys Tidal Inlet Complex, 1870/75-1954/79



**Figure 86. Bathymetric contour map for St. Marys ebb-tidal delta, 1870/75**



**Figure 87. Bathymetric contour map for St. Marys ebb-tidal delta, 1910/24**

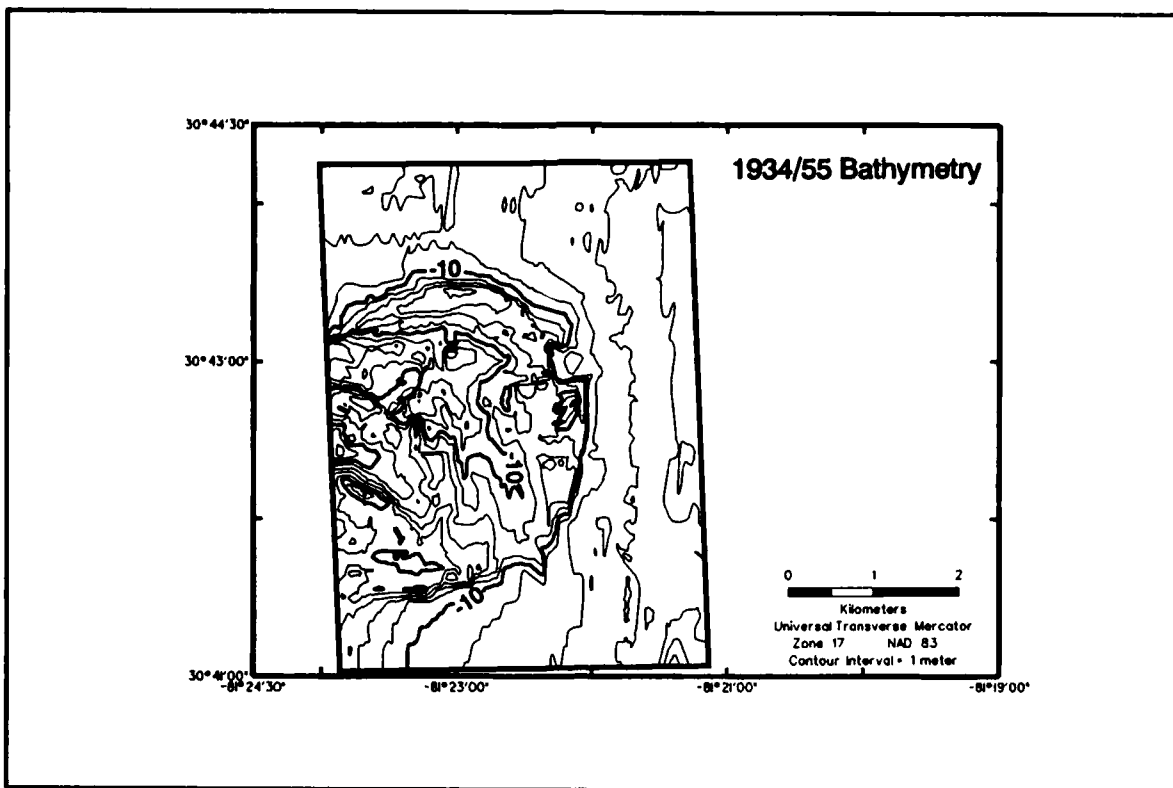


Figure 88. Bathymetric contour map for St. Marys ebb-tidal delta, 1934/55

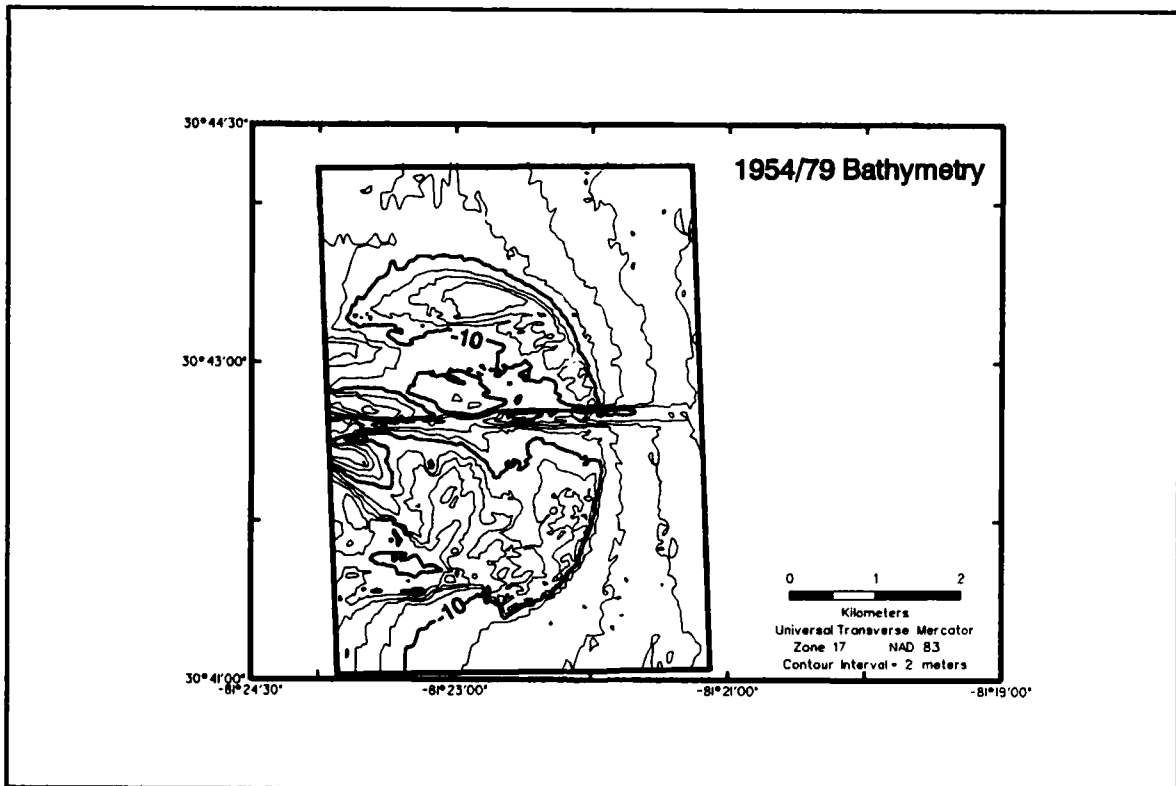


Figure 89. Bathymetric contour map for St. Marys ebb-tidal delta, 1954/79

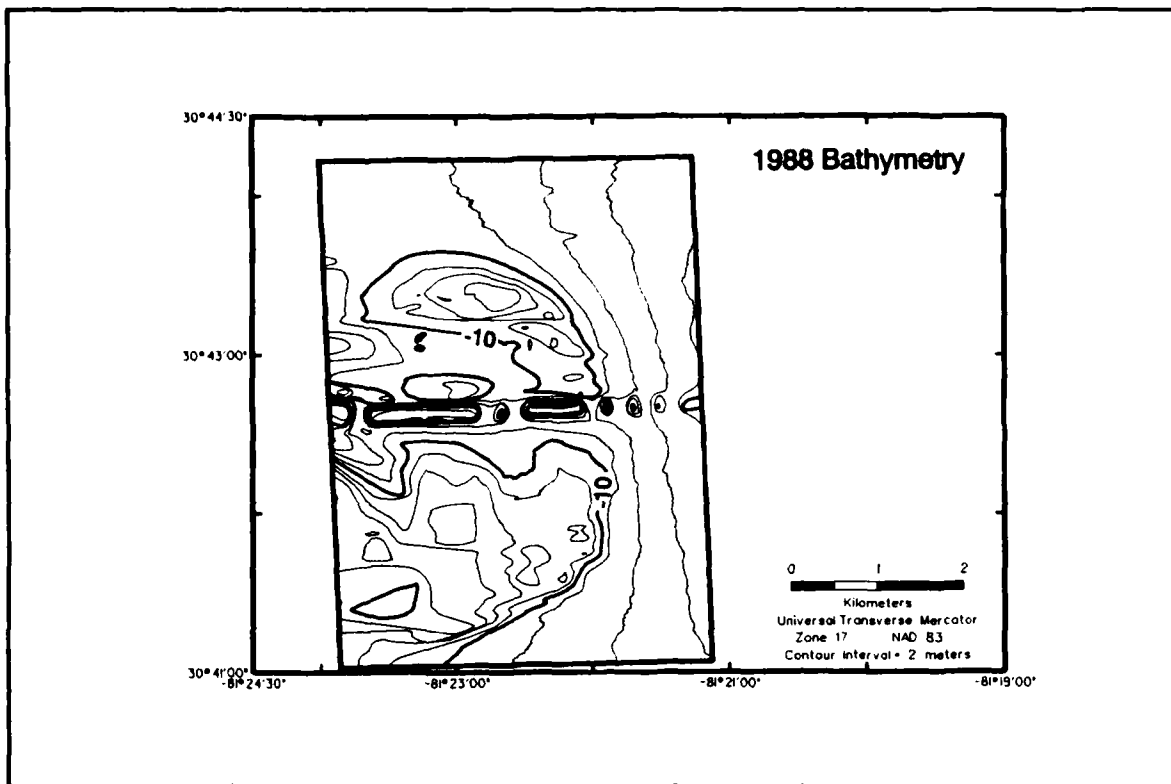


Figure 90. Bathymetric contour map for St. Marys ebb-tidal delta, 1988

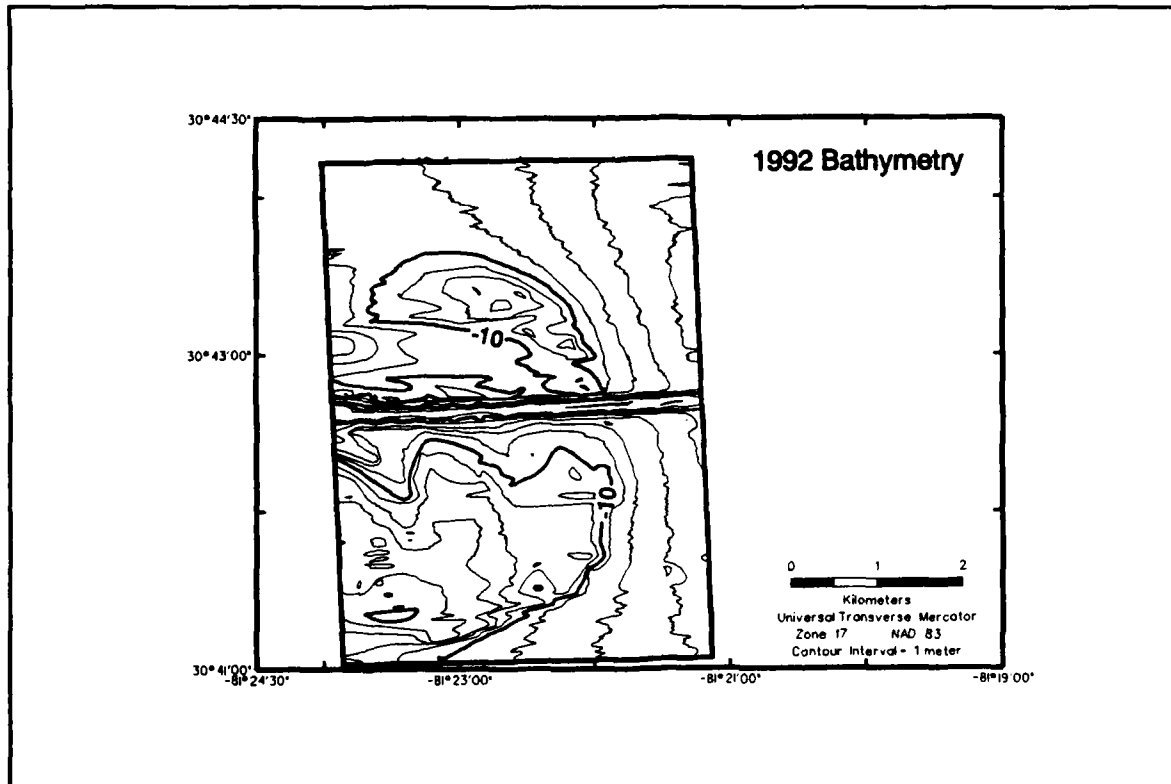


Figure 91. Bathymetric contour map for St. Marys ebb-tidal delta, 1992

(NGVD) depth contour (Figure 89). Although the ebb delta had enlarged laterally and increased in elevation slightly, its general position relative to the coast remained unchanged since the previous time period. The navigation channel was well-defined at this time and was 10 to 15 m deep. A secondary channel oriented to the southeast off the end of the south jetty likely enhanced deposition on the south lobe of the delta. This small channel persists through 1992 and is similar in orientation to the natural inlet channel in 1870/75. The 1988 and 1992 contour maps (Figures 90 and 91) indicate a less well-developed feature than the previous data. The difference in level of detail is an artifact of the way in which the bathymetric surveys were conducted (many longshore-oriented survey lines and few cross-shore-directed lines). In 1988, channel depths were quite variable, possibly related to shoaling at certain points. However, by 1992, channel dredging created consistent depths, and an unobstructed linear feature is shown. For both times, the configuration of the ebb delta is comparable to the 1954/79 data; however, significant changes in contour shape are shown on the southern lobe of the delta.

Patterns of bathymetric change for St. Marys ebb-tidal delta document the magnitude of change associated with morphologic adjustments. The dominant pattern of change between 1870/75 and 1910/24 was initial formation of the modern ebb-tidal delta on the shelf (Figure 92). Approximately 35 million cu m of sediment were deposited in this area (Table 21), in many places, showing 2 to 10 m of vertical gradation. This trend of rapid deposition continued from 1910/24 to 1934/55 as the delta translated seaward. Erosion on the original ebb-tidal delta was accompanied by deposition offshore to form a new outer margin to the delta (Figure 93). The shoal continued to grow in elevation and extent as net change estimates showed an addition of 25 million cu m of sediment. Between 1934/55 and 1954/79, relatively small amounts of net change were occurring. Sediment was still being deposited seaward of the previous position of

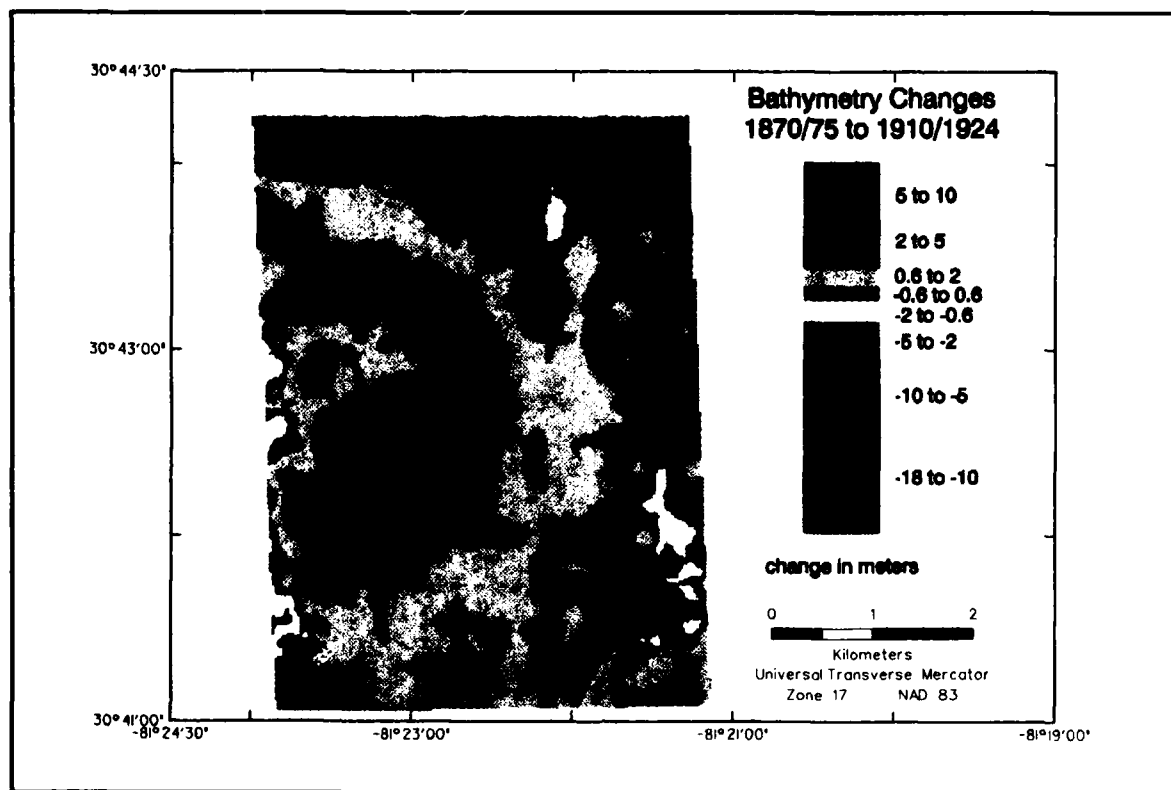


Figure 92. Bathymetric change map for St. Marys ebb-tidal delta, 1870/75-1910/24

**Table 21****Historical Changes in Sediment Volume (cu m) for St. Marys Ebb-Tidal Delta**

Date	Cut	Fill	Absolute	Net
1870/75-1910/24	-1,516,000	36,440,000	37,955,000	34,924,000
1910/24-1934/55	-6,216,000	31,067,000	37,283,000	24,851,000
1934/55-1954/79	-7,459,000	11,176,000	18,635,000	3,717,000
1954/79-1988	-6,429,000	8,623,000	15,052,000	2,195,000
1988-1992	-2,951,000 (-4,394,000)	3,552,000 (2,394,000)	6,503,000 (6,788,000)	601,000 (-2,000,000)
1870/75-1934/55	-1,270,000	61,017,000	62,287,000	59,746,000
1870/75-1954/79	-1,919,000	65,467,000	67,385,000	63,548,000
1870/75-1988	-2,884,000	68,485,000	71,369,000	65,602,000
1870/75-1992	-3,219,000 (-3,381,000)	69,370,000 (67,065,000)	72,589,000 (70,446,000)	66,151,000 (63,684,000)

Note: Numbers in parentheses represent change prior to +0.1-m adjustment to 1992 bathymetry data.

the ebb-tidal delta, and erosion on the ebb delta and excavation of the navigation channel continued (Figure 94). However, net change was an order of magnitude less than changes shown in previous comparisons (Table 21). Although changes were shown in comparisons of the 1954/79 and 1988 bathymetry, most of the deposition was related to an area of no data coverage on the southeast lobe of the ebb-tidal delta between 1954 and 1979 (Figures 94 and 95). Removal

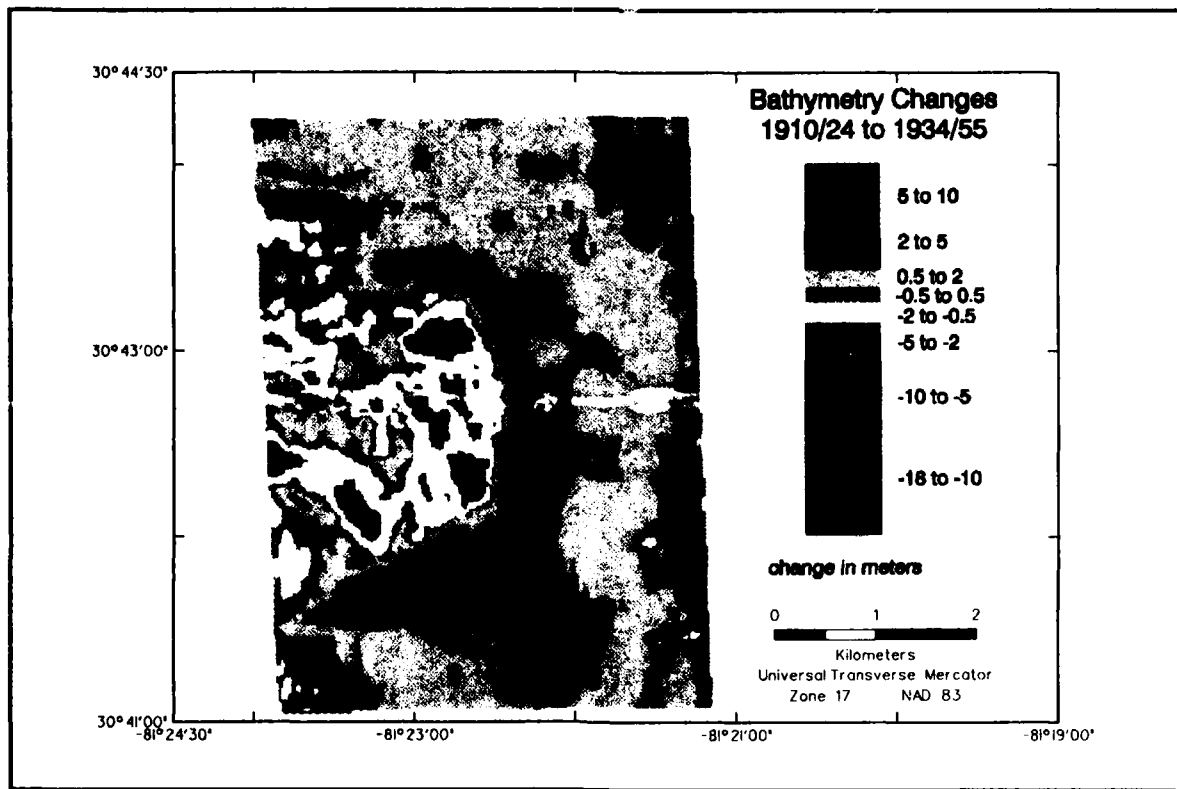
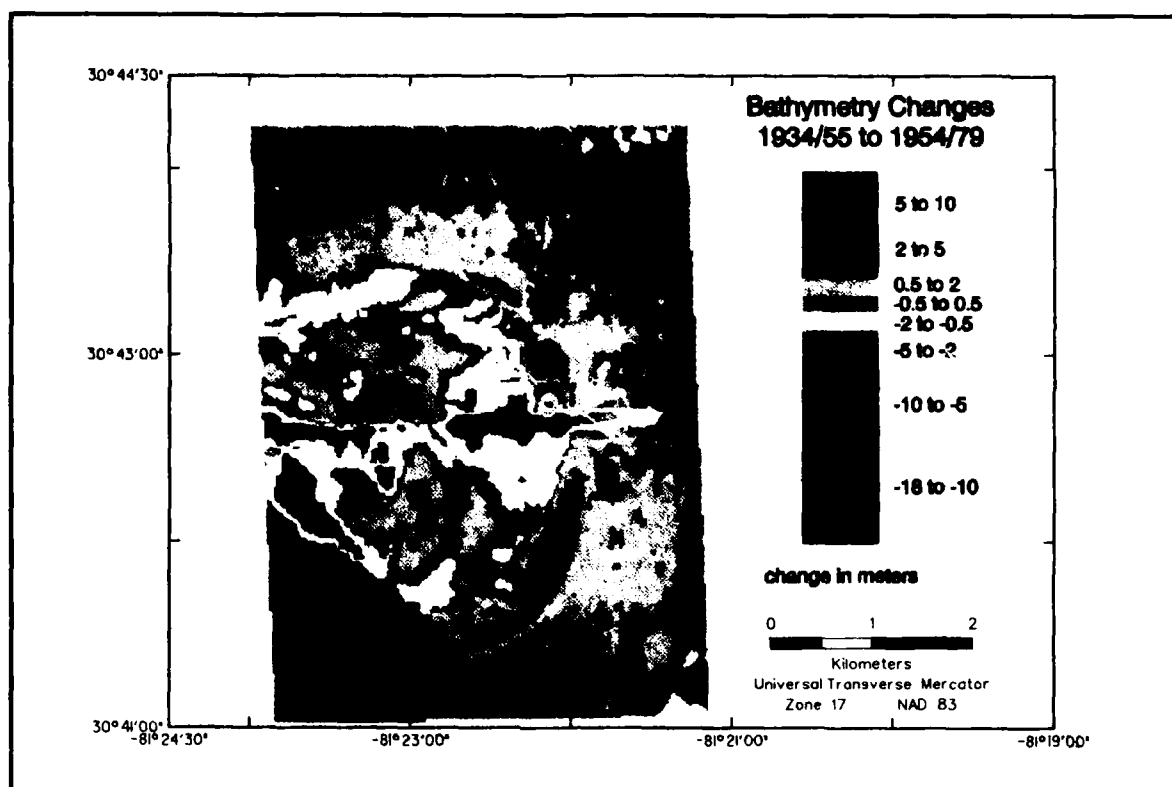
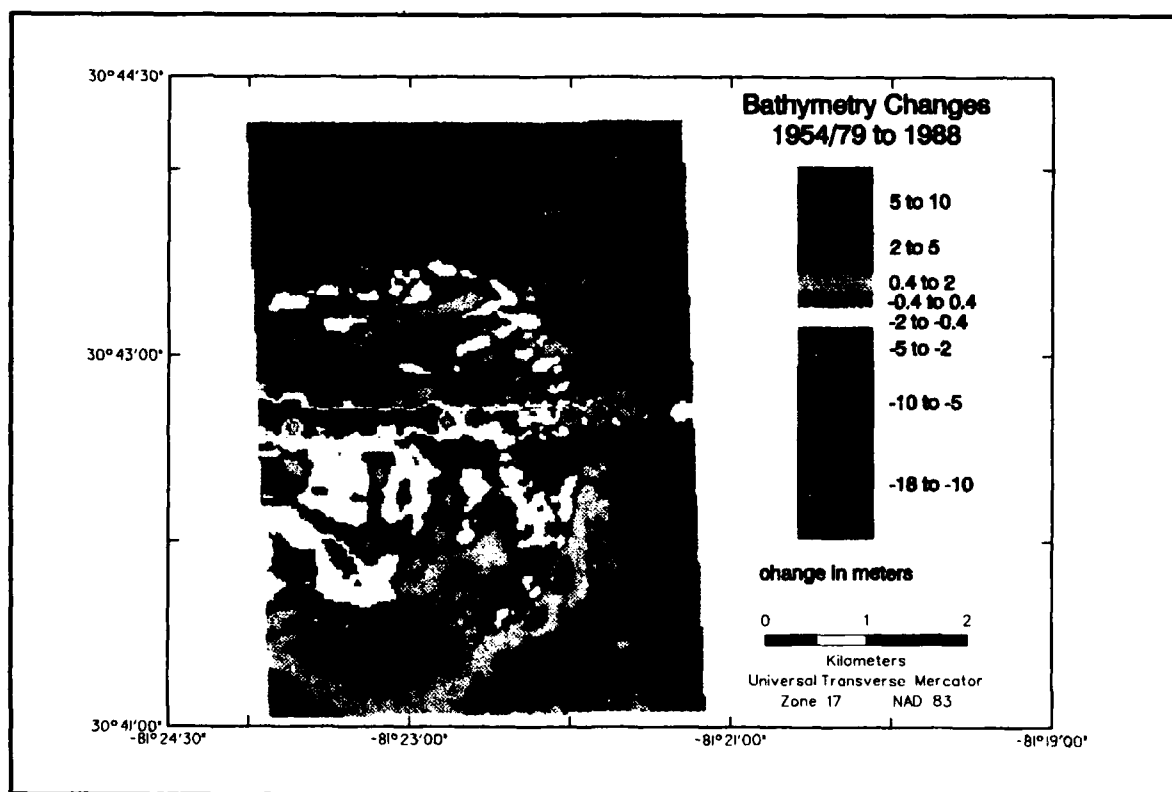


Figure 93. Bathymetric change map for St. Marys ebb-tidal delta, 1910/24-1934/55



**Figure 94. Bathymetric change map for St. Marys ebb-tidal delta, 1934/55-1954/79**



**Figure 95. Bathymetric change map for St. Marys ebb-tidal delta, 1954/79-1988**

of this artifact of change most likely would result in a decrease in the magnitude of net sediment deposition for the period 1954/79 to 1988 and an increase in sediment accumulation for the period 1934/55 to 1954/79.

In contrast to other time periods, bathymetric data collected in 1992 suggest that 2 million cu m of sediment were eroded from the ebb-tidal delta between 1988 and 1992. Although it is possible, there is reason to doubt this finding. The 1988 to 1992 bathymetry comparison indicates a region of erosion along the seaward margin of the model in the 12- to 14-m water depth (shown as yellow in Figure 96). It is unlikely that erosion took place in this area between 1988 and 1992 when an arcuate zone just landward of this area shows no change. Instead, a shift in vertical datum seems likely, similar to but of less magnitude than that found in the 1915 data. After reviewing procedures performed prior to surface modeling, a number of factors influencing data collection and analysis are believed to have contributed to this anomalous result. First, although the method of bathymetry data collection was consistent for both surveys, the method of raw data compilation was not. Digital bathymetry data comprised the 1988 data set; however, digital data from the 1992 cruise were not usable due to adverse weather conditions that caused rapid changes in apparent seafloor elevation over short distances. Second, as an alternative to the 1992 digital data set, analog recordings (fathometer traces) obtained for the exact same period of time as the 1992 digital bathymetry acquisition effort were manually digitized for comparison with the 1988 survey. These different data compilation procedures add greater uncertainty for comparison of change, particularly for short time intervals. Finally, manual digitizing implies that a line was interpreted on the fathometer trace by field office personnel (USAED, Jacksonville, Survey Section). It is estimated that this procedure adds approximately  $\pm 0.1$  to

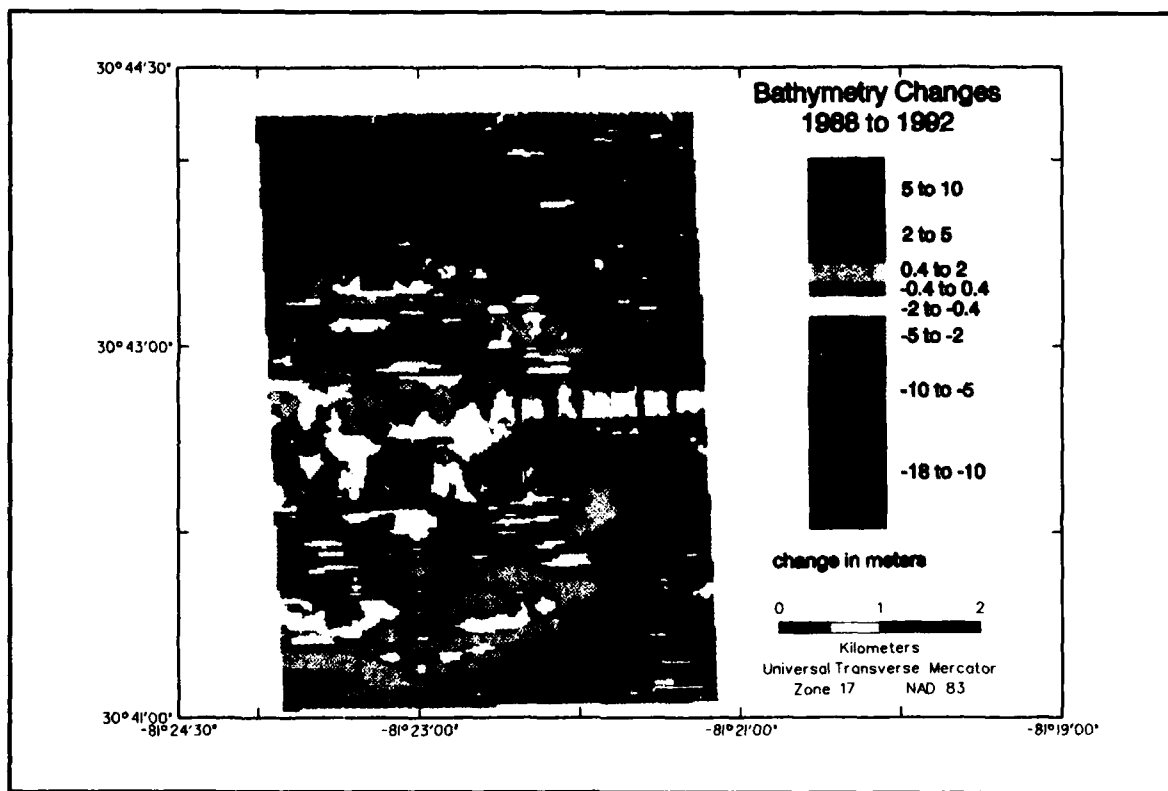


Figure 96. Bathymetric change map for St. Marys ebb-tidal delta, 1988-1992

0.2 m difference in seabed elevation as compared with digital bathymetry acquisition.<sup>1</sup> Furthermore, because digital fathometers record depths at the water-seafloor interface, interpretations of that depth from analog records (the white/black contrast signifying the contact) are likely overestimates (deeper than expected), and the datum difference will be biased rather than random. Discussions with USAED, Jacksonville, personnel confirmed a bias toward deeper seafloor elevation estimates for the 1992 survey in digitization from analog records.<sup>1</sup> This phenomenon is illustrated in Figure 96, where greater water depths in 1992 along the western portion of the model created a zone of erosion that would be expected to show no change (see Figure 95 for the period 1954/79 to 1988 for comparison).

With the information presented above, 0.1- and 0.2-m elevation additions were made to the 1992 bathymetry data for comparison with data presented in Figure 96 and Table 21. Figure 97 illustrates bathymetric change between 1988 and 1992 with a +0.1-m adjustment to all depths on the 1992 survey. A comparison of Figures 96 and 97 illustrates the absence of a zone of erosion along the seaward margin of the area and retention of the characteristics of change throughout other areas of the model. Also, volume change calculations indicate a net addition of sediment to the ebb-tidal delta of approximately 601,000 cu m. Converted to a rate, this amount of change is consistent with the trend for the previous time periods. If 0.2 m is added to the 1992 bathymetry data, the change distribution appears similar to that shown in Figure 97, but the magnitude of change is about 2.5 million cu m. This amount is significantly higher than

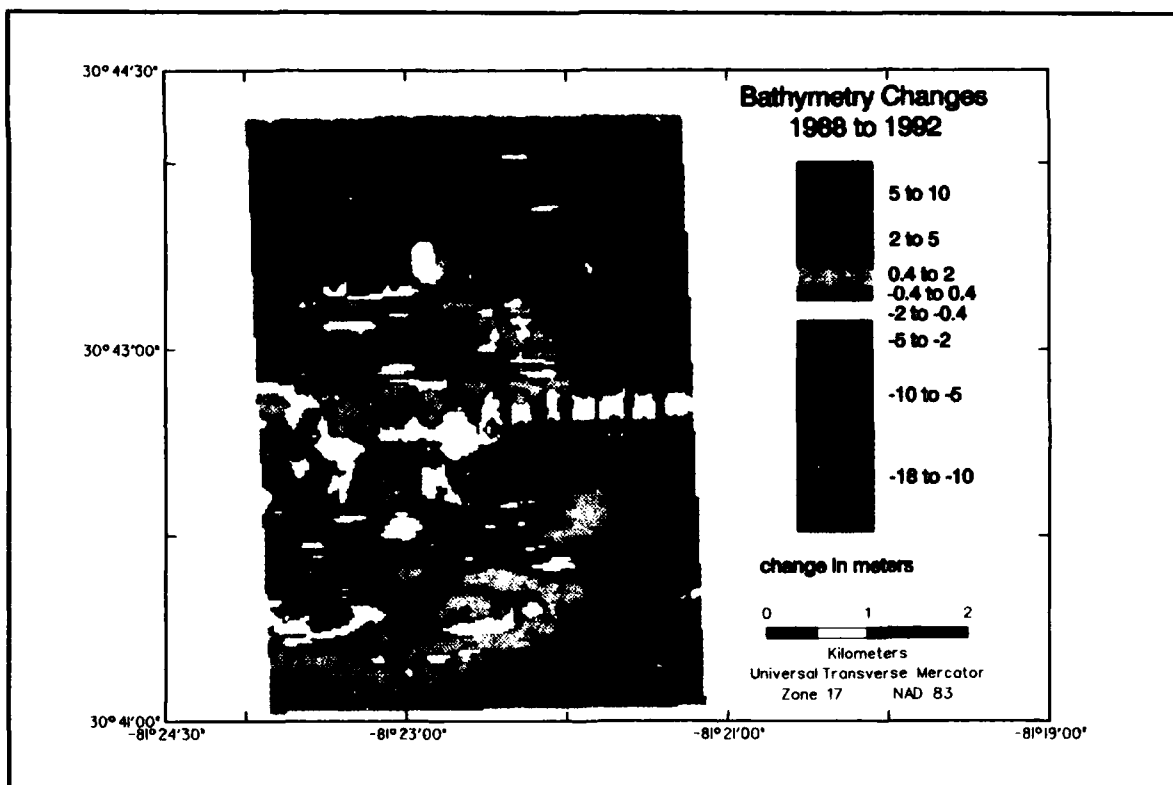


Figure 97. Bathymetric change map, with 0.1 m added to the 1992 data, for St. Marys ebb-tidal delta, 1988-1992

<sup>1</sup> Personal communication with Mr. Hank Remmer, Chief, Survey Section, USAED, Jacksonville, 29 January 1993.

the trend for other time periods and was judged to be unreasonable. Consequently, a +0.1-m adjustment to bathymetry data for the 1992 survey was accepted as the most reasonable representation of seafloor elevation for evaluating long- and short-term volume changes.

Net change from 1870/75 to 1992 shows a large area of accretion, many parts of which indicate 5 to 10 m of deposition (Figure 98). Sediment volume change for this period of time is estimated at 66 million cu m. The navigation channel dredged through the center of the ebb delta and erosion from a secondary channel formed off the south jetty are the primary areas of erosion. The 1992 survey was the first time the entire navigation channel was excavated below the ambient shelf surface of 1870/75.

Because the navigation channel dissects the ebb-tidal delta as a potential barrier for sediment transport from the north, trends in volume change also were evaluated for the north and south lobes of the delta and the channel, separately. Table 22 provides a quantitative summary of change for these features. Most change associated with the ebb delta took place by the 1950s. Although net deposition on the ebb delta continued through 1992, the rate of change was reduced slightly (Figure 99). Between 1954/79 and 1992, the north lobe of the ebb-tidal delta exhibited no net change. In addition, the rate of volume change as erosion in the channel and deposition on the south lobe of the ebb-tidal delta decreased by about a factor of two for the period 1988 to 1992 relative to the previous time interval (Table 22). Overall, net change on the ebb-tidal delta is consistent for the period 1954/79 to 1992 (Table 21, Figure 99). In addition, even though the rates of change varied across the ebb delta for the two intervals encompassing this time period, the trend for a decrease in the rate of accretion was found to be consistent.

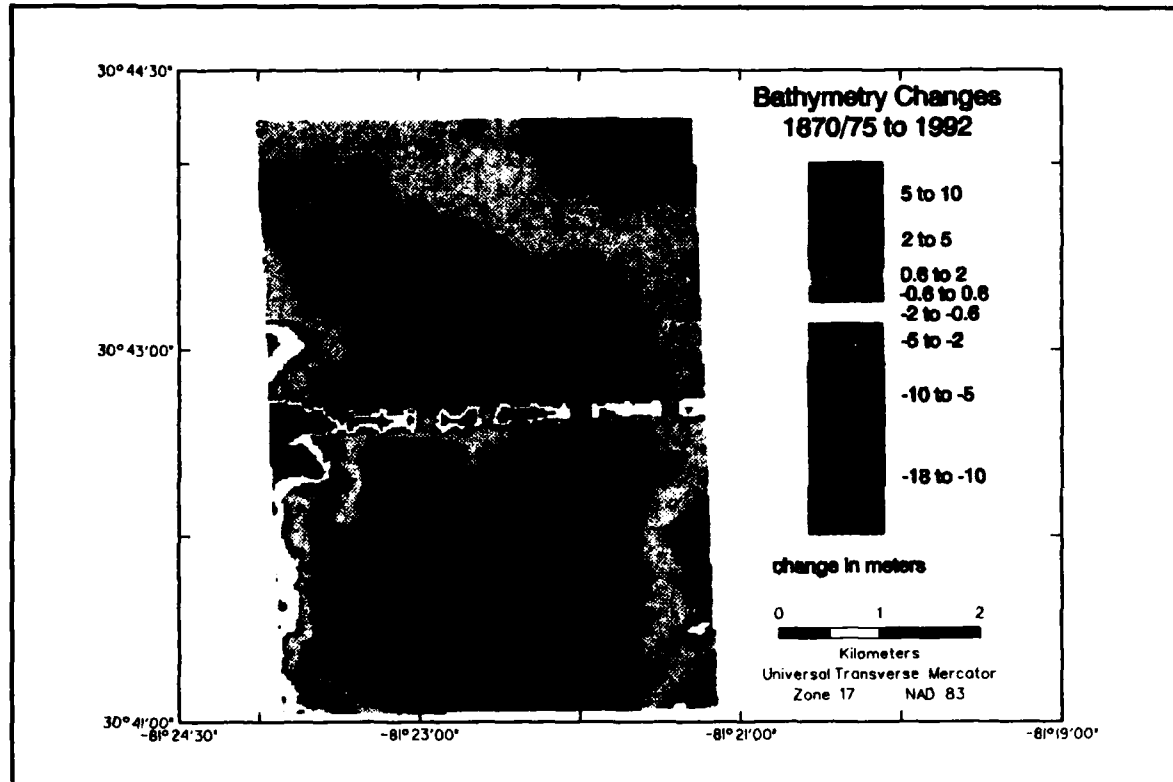


Figure 98. Bathymetric change map for St. Marys ebb-tidal delta, 1870/75-1992

**Table 22**  
**Historical Changes in Sediment Volume (cu m) by Geomorphic Subset for**  
**St. Marys Ebb-Tidal Delta**

Date	Cut	Fill	Absolute	Net
<b>North Lobe</b>				
1870/75-1910/24	-707,000	14,926,000	15,633,000	14,220,000
1910/24-1934/55	-2,717,000	12,111,000	14,828,000	9,393,000
1934/55-1954/79	-1,928,000	5,340,000	7,268,000	3,412,000
1954/79-1988	-1,853,000	1,648,000	3,502,000	-205,000
1988-1992	-1,085,000 (-2,496,000)	1,290,000 (518,000)	2,374,000 (3,014,000)	205,000 (-1,023,000)
1870/75-1934/55	-251,000	23,803,000	24,054,000	23,552,000
1870/75-1954/79	-300,000	27,284,000	27,584,000	26,984,000
1870/75-1988	-287,000	27,096,000	27,382,000	26,809,000
1870/75-1992	-323,000 (-495,000)	27,361,000 (25,351,000)	27,684,000 (25,846,000)	27,038,000 (25,832,000)
<b>Channel</b>				
1870/75-1910/24	-65,000	3,054,000	3,119,000	2,988,000
1910/24-1934/55	-534,000	1,221,000	1,755,000	687,000
1934/55-1954/79	-2,648,000	81,000	2,729,000	-2,567,000
1954/79-1988	-1,902,000	243,000	2,145,000	-1,658,000
1988-1992	-443,000 (-615,000)	147,000 (92,000)	590,000 (707,000)	-296,000 (-432,000)
1870/75-1934/55	-114,000	3,788,000	3,902,000	3,674,000
1870/75-1954/79	-514,000	1,602,000	2,116,000	1,088,000
1870/75-1988	-1,312,000	1,033,000	2,345,000	-279,000
1870/75-1992	-1,466,000 (-1,619,000)	861,000 (706,000)	2,327,000 (2,325,000)	-605,000 (-657,000)
<b>South Lobe</b>				
1870/75-1910/24	-649,000	18,298,000	18,946,000	17,649,000
1910/24-1934/55	-2,852,000	17,477,000	20,330,000	14,625,000
1934/55-1954/79	-2,808,000	5,708,000	8,517,000	2,900,000
1954/79-1988	-2,564,000	6,626,000	9,190,000	4,062,000
1988-1992	-1,313,000 (-2,578,000)	2,093,000 (1,199,000)	3,405,000 (3,777,000)	780,000 (-411,000)
1870/75-1934/55	-757,000	33,051,000	33,808,000	32,294,000
1870/75-1954/79	-932,000	36,201,000	37,133,000	35,269,000
1870/75-1988	-881,000	40,062,000	40,943,000	39,181,000
1870/75-1992	-943,000 (1,088,000)	40,910,000 (38,928,000)	41,853,000 (40,015,000)	39,967,000 (38,769,000)
Note: Numbers in parentheses represent change prior to +0.1-m adjustment to 1992 bathymetry data.				

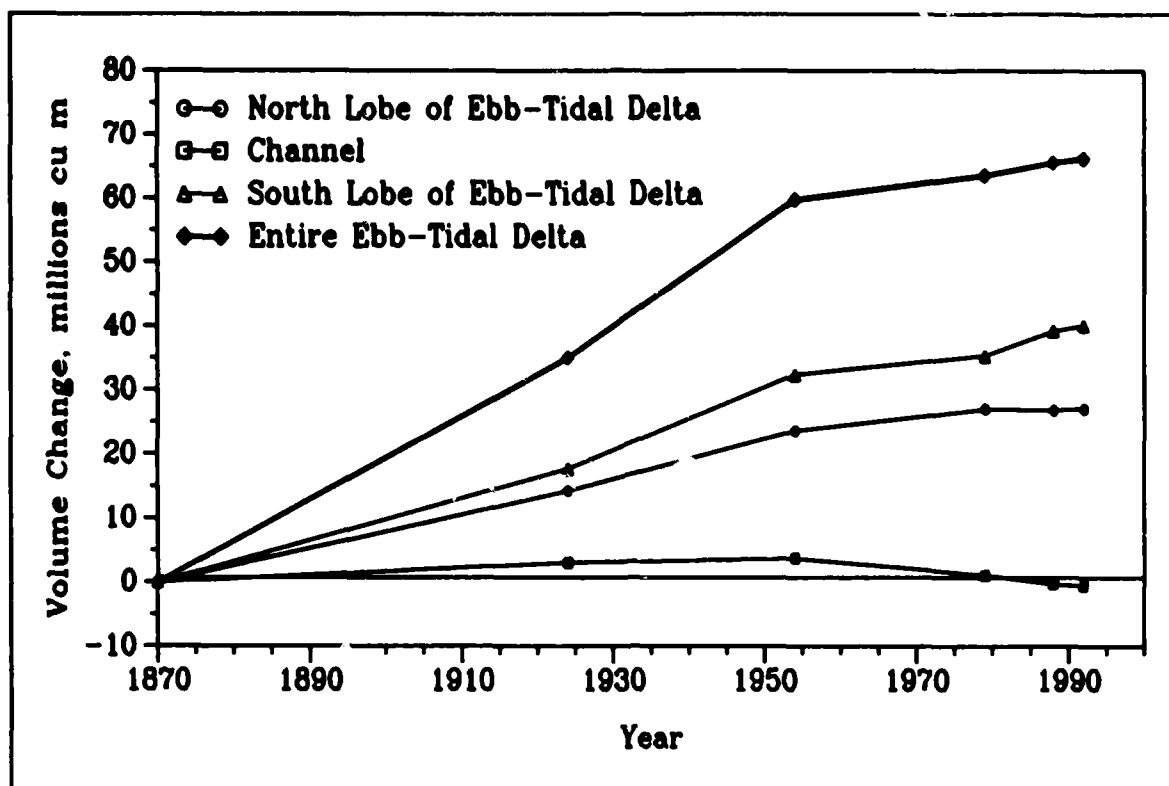


Figure 99. Cumulative changes in sediment volume at St. Marys ebb-tidal delta with a +0.1-m adjustment to 1992 bathymetry data

Increased channel dredging between 1979 and 1992 apparently has had little influence on ebb-tidal delta evolution.

### Summary

Most change occurring in the study area is associated with tidal inlet systems and areas affected by nearshore shelf processes. Net change in the littoral zone along Cumberland and Amelia Islands between 1855/75 and 1953/79 is a loss of 1.5 million cu m. The modern ebb-tidal delta at St. Marys Entrance has formed since the early 1900s, after jetty construction was completed. The present position of the delta is about 4 km seaward of the original natural feature shown on the 1870/75 bathymetry. Consequently, the depth of water in which this deposit exists has increased. The combination of these two factors makes it unlikely that sand bypassing could function as it might have in 1870/75. The volume of sediment comprising the modern ebb delta is approximately 90 million cu m. Losses from the channel area between the jetties only contributed about 40 million cu m to this total, suggesting that the delta has been a net sink of littoral and nearshore shelf sediment since the time of jetty construction. However, much of the deposition associated with ebb-tidal delta evolution occurred by the 1950s (Tables 21 and 22, Figure 99), and the amount of change since that time has decreased. For changes that have occurred throughout the period of record, the only direct connections that can be made between delta evolution and shoreline change are the large adjustments that were shown everywhere in the system between the mid-1800s and 1924. Since then, most system changes associated with the channel and ebb-tidal delta appear decoupled from shoreline response.

# 4 Dredging Activities and Shoaling Analysis<sup>1</sup>

---

## Introduction

This chapter documents the history of channel improvement and maintenance (i.e., dredging volumes and locations) for St. Marys Entrance and Cumberland Sound channels since 1881. In addition, the recent pattern of shoaling characteristics is discussed. Since 1904, deepening and maintenance dredging of the navigation channel have been performed to provide safe passage for various classes of commercial and military vessels, including submarines, which have required different channel dimensions over the years. Maintenance of the most recent channel dimensions of 150-m width and 15.5-m depth (below MLW), with side slopes of 3H:1V, during the period 1988 through 1992 (Epoch 7) to accommodate TRIDENT (Ohio-class) submarines, has required increased dredging compared to earlier channel usage (Chapter 1).

Characterization of shoaling rates and patterns for St. Marys Entrance and Cumberland Sound channel is based on maintenance dredging records, bathymetric condition surveys, pre- and post-maintenance dredging core borings, and channel bottom sediment classification. Shoaling of material in the navigation channel is introduced by wave activity, including longshore and storm-induced cross-shore transport, and by ebb- and flood-tidal currents. At St. Marys Entrance Channel, two areas of significant shoaling are defined at the ebb-tidal delta terminal lobe and in the vicinity of the jetty tips. Cumberland Sound is characterized by two areas of moderate shoaling.

This review of dredging data and shoaling patterns is used to analyze any impact of the TRIDENT channel modification on the quantity and location of channel maintenance requirements. While Chapters 3 and 5 review the potential regional impacts of channel modification to the shoreline and nearshore zone, this chapter focuses on the direct impacts to the navigation channel.

## Dredging History

Historical dredging volumes and locations and sediment shoaling patterns have been documented for St. Marys Entrance channel and sections of Cumberland Sound through analysis

---

<sup>1</sup> Written by J. Bailey Smith, Joan Pope, and Laurel T. Gorman.

of coastal charts, bathymetric condition surveys, side-scan sonar records, dredging records, and channel bottom sediment characteristics. These data are described in Appendix C, and an overview is given here.

Dredging histories of St. Marys Entrance and Cumberland Sound channels are based on USAED, Savannah, and USAED, Jacksonville, dredging location and volume summaries, miscellaneous unpublished dredging activity reports, and volumetric changes of channel cross sections determined from survey data. Dredging at St. Marys Entrance channel for the period 1955 to 1983 was performed by U.S. Government hopper dredges on all but two occasions, when U.S. Government cutterhead pipeline and clamshell dredges were used. From 1984 to the present, dredging was performed by U.S. Government dredges and private companies utilizing hopper, clamshell, and cutterhead pipeline dredges. Dredging in the Cumberland Sound portion of the channel was performed by private companies utilizing cutterhead pipeline dredges.

### **St. Marys Entrance channel**

The dredging history of St. Marys Entrance channel, as summarized in Figure 100, indicates a continuous increase of annual maintenance dredging over the engineered history of the channel from 16,700 cu m during Epoch 3 (1905-1923) to 616,200 cu m during Epoch-7 TRIDENT channel conditions (1988-1992). (Authorized and natural channel depths of Figure 100 are placed at actual dates of channel depth conditions. Maintenance dredged volumes are placed in the center of the epochs as maintenance dredging occurs, not as one event, but over a period of time.) New work dredging at St. Marys Entrance channel also increased as channel parameters such as depth, width, and length were increased. The maximum new work dredging amount was 6,507,100 cu m during Epoch 7. Detailed analysis of the dredging history of St. Marys Entrance channel prior to the 1987-1988 TRIDENT channel expansion is difficult because of limited dredging records which do not distinguish between dredging estimates and actual dredged volumes.

Dredging volumes and shoaling patterns used throughout this report are referenced to channel stations established by USAED, Savannah, and USAED, Jacksonville (Figure 102). Channel stationing (presented in feet according to customary surveying practice) of St. Marys Entrance channel starts at Station 0+00 of Cut 1N (approximate location at the inlet throat), and increases to the east to Station 501+23.68 of Cut 1N. Station 0+00 of Cut 2N continues seaward to Station 250+00. In this section, stationing of Cumberland Sound channel, discussed herein, starts at Station 0+00 and increases to the west and north to Station 220+00. There is an overlap of 33.5 m (i.e. 110 ft) between the Cumberland Sound channel and Cut 1N of the St. Marys Entrance channel.

### **Cumberland Sound**

The dredging history of Cumberland Sound (Station 0+00 to 220+00) for the two most recent epochs is dominated by new work channel-deepening events. For Epoch 6 (1979-1984) and Epoch 7 (1985-1992), new work dredging volumes were calculated to be 466,200 cu m and 3,132,600 cu m, respectively. Maintenance dredging volumes for Epoch 6 and Epoch 7 were 103,200 cu m (17,200 cu m/year) and 29,300 cu m (3,700 cu m/year), respectively.

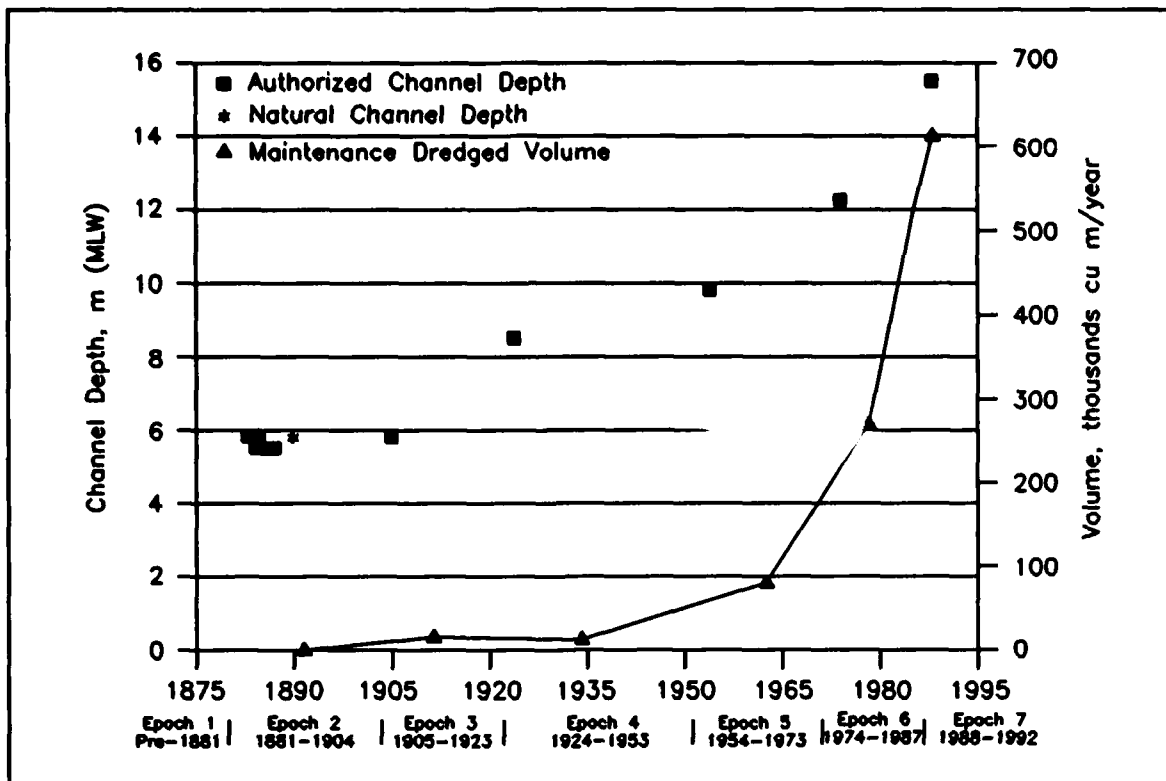


Figure 100. Channel depth and average annual maintenance dredged volumes for St. Marys Entrance channel for the period 1870-1992

## Shoaling Analysis

### St. Marys Entrance channel

The shoaling rate for the entire length of St. Marys Entrance channel during Epoch 7 (1988-1992) has been calculated at 616,200 cu m/year. This value was derived from the total maintenance dredged volume per year for both cohesive and noncohesive sediments. However, because 99 percent of the maintenance dredging took place in Cut 1N of the Entrance channel, this rate is indicative of a dredging (and shoaling rate) only for Cut 1N (a length of 15,300 m). This rate is comparable to a rate of 602,500 cu m/year for noncohesive sediments only as determined by Vemulakonda and Scheffner (1987) and Vemulakonda et al. (1988) for a 12,300-m section of the channel, Cut 1N from Station 77+00 to 481+00. These shoaling rates are much lower than a maximum potential shoaling rate of 1,032,100 cu m/year determined from the cumulative maximum shoaling rates of several channel reaches as presented in a Kings Bay EIS (1986).<sup>1</sup>

<sup>1</sup> Kings Bay Environmental Impact Statement. (1986). "Final third supplement to the Environmental Impact Statement for the preferred alternative location for a fleet ballistic missile submarine support base, Kings Bay, Georgia (St. Marys Entrance channel)," unpublished report, U.S. Department of the Navy, Officer in Charge of Construction, Trident, St. Marys, Georgia.

Shoaling patterns in the Entrance channel, which are identified primarily through dredging locations and volumes, and sediment volume differences between condition surveys for Epoch 7 are known to result from two processes. Introduction of littoral sands into the system produces shoals from Station 0+00 to 230+00 of Cut 1N. An area of significant shoaling occurs in the vicinity of the jetty tips from Station 110+00 to 180+00 of Cut 1N. Shoaling rates for this portion of the channel, based on the amount of material shoaled between dredging events, have been approximated at 31,000 cu m/1,000-m section of channel. Aubrey, McSherry, and Spencer (1990) documented sand waves between Stations 72+00 and 220+00 inside the channel with wavelengths between 1.0 and 3.6 m.

The second shoaling process in the channel is the transport and deposition of clay and silt-sized material from Station 230+00 to 350+00 of Cut 1N. Shoaling rates between Station 240+00 and 285+00 of Cut 1N are 200,000 cu m/1,000-m section of channel as determined through analysis of pre- and post-dredge channel cross sections.

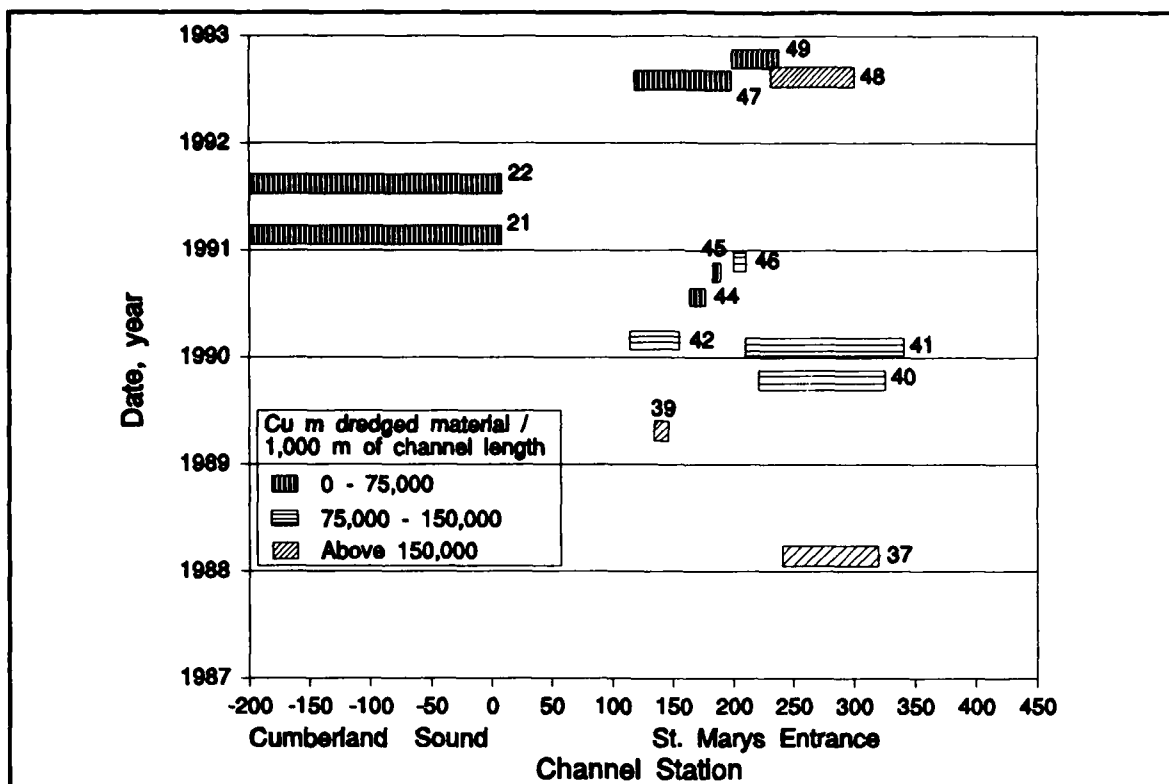
St. Marys Entrance channel maintenance dredging during Epoch 7 was performed mainly between Stations 120+00 and 350+00 of Cut 1N. Dredging Events 37, 39, and 48 are the most significant dredging events of Cut 1N with values of 226,000, 827,000, and 200,000 cu m of dredged material/1,000 m of channel length, respectively (Figure 101). Two of these events (Events 37 and 48), as well as two other events with values above 90,000 cu m of dredged volume/1,000 m of channel length (Events 40 and 41), took place between Station 240+00 and 300+00 of Cut 1N. Another area of frequent dredging during Epoch 7, with nine dredging events, three of which were above 90,000 cu m dredged volume/1,000 m of channel length (Events 39, 42, and 46), was located between Stations 115+00 and 210+00 of Cut 1N. Relatively small quantities of maintenance dredged material were removed from the Cumberland Sound channel.

Shoaling locations estimated by Vemulakonda et al. (1988), utilizing a system of numerical models, concerned only noncohesive sediment (sand) transport support shoaling rates (Appendix C). Vemulakonda and Scheffner (1987) and Vemulakonda et al. (1988) determined that the majority of the shoaling occurs between Stations 110+00 and 310+00 with maximum shoaling rates occurring between Stations 130+00 and 230+00.

Shoaling rates with respect to type of material (i.e., fine-grained material [clay and silt from estuarine and offshore sources] versus littoral sandy material) were estimated for the entire length of Cut 1N for Epoch 7. Shoaling rates for the Entrance channel during Epoch 7 were  $493,400 \pm 55,600$  cu m/year for clay and silt and  $108,300 \pm 41,100$  cu m/year for sand introduced by littoral processes. These rates represent averaged rates determined by two methods: (a) identification of channel bottom sediment type of pre-maintenance dredging core borings (1989-1991) and (b) field analysis of sediments during maintenance dredging events. Error range per shoaling rate was determined by considering the difference between the two rates and halving that amount. These shoaling rates indicate that the majority of shoaling at St. Marys Entrance channel is a result of the introduction of clay and silt into the channel between Stations 225+00 and 340+00.

### **Cumberland Sound**

Shoaling patterns in Cumberland Sound channel from Station 0+00 to 220+00 are based on volumetric changes of channel cross sections from survey data. This portion of the channel is



Dredging Event No. <sup>1</sup>	Total Dredged Amount cu m	Cu m Dredged Material/1,000 m of Channel Length	Dredging Event No.	Total Dredged Amount cu m	Cu m Dredged Material/1,000 m of Channel Length
37	550,500	226,000	45	2,800	16,000
38	116,200	NA <sup>2</sup>	46	35,500	116,000
39	252,300	827,000	21 <sup>4</sup>	28,700	5,000
40	324,300	101,000	22 <sup>4</sup>	600	100
41	386,900	98,000	47	147,800	57,000
42	112,900	93,000	48	489,500	200,000
43 <sup>3</sup>	13,300	24,000	49	27,500	45,000
44	5,100	13,000			

<sup>1</sup> Refers to dredging event number in Table C2 - Dredging History at St Marys Entrance.

<sup>2</sup> Cu m dredged material/1,000 m of channel length cannot be determined as channel reach of dredging event was not available.

<sup>3</sup> Dredging event was not included in above graph as dredging was performed at three sections of channel, 60-300 m in length, between Stations 67 + 00 and 148 + 00.

<sup>4</sup> Dredging event number refers to dredging event number in Table C3 - Dredging History of Cumberland Sound between Stations 0 + 00 and 220 + 00.

Figure 101. Maintenance dredging location for Epoch 7 (1988-1992)

naturally scoured as is inferred from pre- (September 1983 - January 1985) and post- (January 1989 - August 1990 and April/May 1991 - October 1991) TRIDENT channel condition surveys, which indicate average sediment volume scouring of 378,800 cu m/year and 31,200 cu m/year, respectively. These figures suggest scouring rates of 56,500 and 4,700 cu m/year/1,000-m section of channel, respectively. However, two reaches of shoaling associated with the introduction of littoral sand occur from Station 50+00 to 100+00 and from Station 150+00 to 200+00. The annual shoaling volume rates for post-TRIDENT channel conditions for each of these 1,500-m-long reaches are 26,000 cu m and 35,800 cu m, respectively.

Shoaling rate and pattern comparisons between epochs for the St. Marys Entrance channel cannot be determined from the available database. The near-equilibrium configuration of the ebb-tidal delta and eventual adjustment of the channel side slopes toward equilibrium indicate that the average shoaling rate at St. Marys Entrance channel for Epoch 7 of 616,200 cu m/year represents a realistic, but probably high, estimate of the future average annual dredging requirement. However, the rate of shoaling experienced during Epoch 7 is expected to continue if the present channel dimensions are maintained (Figure 100). Shoaling rate comparisons for Cumberland Sound channel indicate that from Station 50+00 to 100+00 and from Station 150+00 to 200+00, the channel scoured during pre-TRIDENT channel conditions but shoaled during post-TRIDENT channel conditions. Average annual volume differences for this combined approximately 3,000-m-long section of channel are 140,900 cu m of scour (or 46,200 cu m of scour/1,000-m section of channel) for pre-TRIDENT channel conditions and 61,800 cu m (or 20,300 cu m of shoaling/1,000-m section of channel) for post-TRIDENT channel conditions.

#### **Channel shoaling reaches**

For the present analysis, the navigation channel was divided into six reaches of differential shoaling patterns (Figure 102) based on channel bottom sediment characteristics. Maintenance dredging core borings performed from 1989 to 1991, new work core borings<sup>1</sup> performed from 1985 to 1986 obtained prior to the TRIDENT channel deepening, and geological cross sections<sup>2</sup> were used to define the following reaches:

- a. Reach 1 (Station 220+00 to 50+00 of Cumberland Sound channel) is devoid of significant shoaling. An area of moderate shoaling associated with the transport of littoral sands into the backbarrier channels exists from Station 50+00 to 100+00 and from Station 150+00 to 200+00. Sediment type in this reach is moderately to poorly sorted fine- to medium-grained sand.
- b. Reach 2 (Station 50+00 of Cumberland Sound channel to Station 75+00 of St. Marys Entrance channel, Cut 1N), located in the vicinity of the inlet throat, experiences minor shoaling because strong currents tend to keep the channel scoured. Sediment type in this reach seaward of Station 0+00 is fine- to medium-grained sand with some silt and shell matter.

---

<sup>1</sup> U.S. Army Corps of Engineers. (1992). "Kings Bay core boring logs," unpublished report, U.S. Army Engineer District, Jacksonville, Florida.

<sup>2</sup> U.S. Army Corps of Engineers. (1981). "Kings Bay geological cross sections," unpublished report, U.S. Army Engineer District, Jacksonville, Florida.

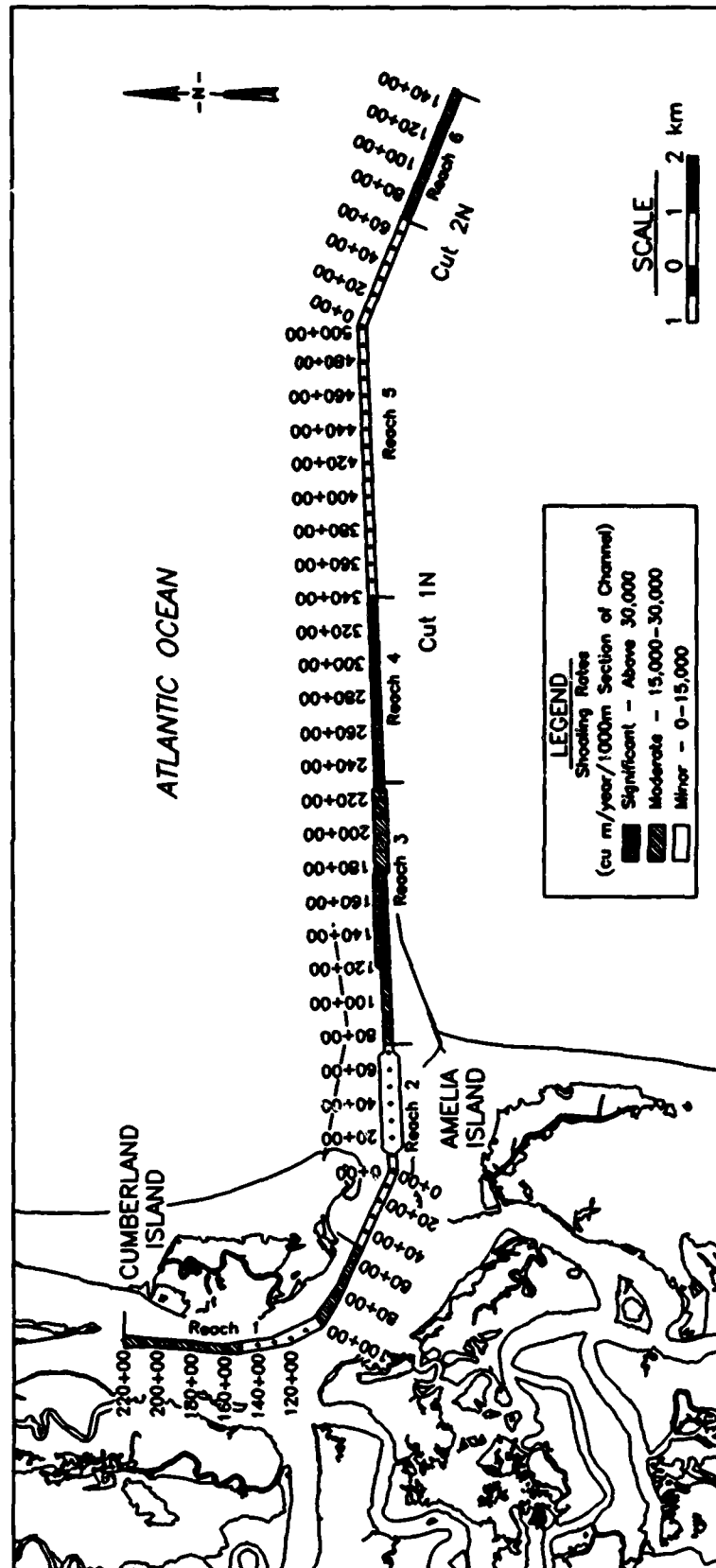


Figure 102. Channel reaches based on shoaling characteristics after the 1987-1988 channel deepening

- c. Reach 3 (Station 75+00 to 230+00 of St. Marys Entrance channel, Cut 1N) includes significant shoaling rates from Station 110+00 to 180+00 of St. Marys Entrance channel, Cut 1N, associated with the migration of shoals and bed forms at the tips and slightly landward of the jetties into the navigation channel. Sediment type in this reach is also moderately to poorly sorted, fine- to medium-grained sand with some silt and shell matter.
- d. Reach 4 (Station 230+00 to 340+00 of St. Marys Entrance channel, Cut 1N) has the most significant shoaling rates, particularly at locations where ebb-tidal delta shoals migrate into the channel. Sediment type in this portion of the channel is primarily silt and clay with traces of sand and shell matter.
- e. Reach 5 (Station 340+00 of St. Marys Entrance channel, Cut 1N, to Station 65+00 of St. Marys Entrance channel, Cut 2N) experiences minor shoaling. Silt and clay from Station 340+00 to 355+00 of St. Marys Entrance channel, Cut 1N, and moderately to poorly sorted fine- to medium-grained sand and shell from Station 355+00 of St. Marys Entrance channel, Cut 1N, to Station 65+00 of St. Marys Entrance channel, Cut 2N, are the dominant sediment types.
- f. Reach 6 (Station 65+00 to 150+00 of St. Marys Entrance channel, Cut 2N) experiences moderate shoaling problems associated with significant storms. Sediment type is moderately to poorly sorted fine- to medium-grained sand and shell.

## Summary

The identification of shoaling patterns in St. Marys Entrance channel is based on sediment volume differences as determined from bathymetric condition surveys and dredging locations and dredging volumes during Epoch 7 post-TRIDENT channel conditions. Figure 101 shows that maintenance dredging has taken place between Station 115+00 and 340+00 of St. Marys Entrance channel, Cut 1N, with the majority of these dredging events occurring between Station 120+00 and 340+00 of St. Marys Entrance channel, Cut 1N. At the Cumberland Sound portion of the channel, two areas of moderate shoaling exist from Station 50+00 to 100+00 and from Station 150+00 to 200+00.

The most significant shoaling rate, 200,000 cu m/1,000 m section of channel, occurs in St. Marys Entrance channel, Cut 1N, between Station 240+00 and 285+00 at the location of the ebb-tidal delta. Another area of significant shoaling occurs between Station 110+00 and 180+00 of St. Marys Entrance channel, Cut 1N, in the vicinity of the tips of the jetties where the shoaling rate is estimated at 31,000 cu m/1,000-m section of channel.

The average maintenance dredged volume during Epoch 7 (1988-1992) for the entire length of the St. Marys Entrance channel, indicative of an estimated average shoaling rate, was 616,200 cu m/year. Of the total 616,200 cu m/year of shoaling, 71 percent (437,800 cu m/year) (Table C9) of the dredged material consisted of fine-grained silt and clay material of estuarine or offshore origin, dredged between Station 210+00 and 340+00 inclusive of the ebb-tidal delta terminal lobe. Figure 103 illustrates the dredging event channel reach, volume and sediment type, reaches of channel shoaling material type (sand shoaling from Stations 125+00 to 225+00,

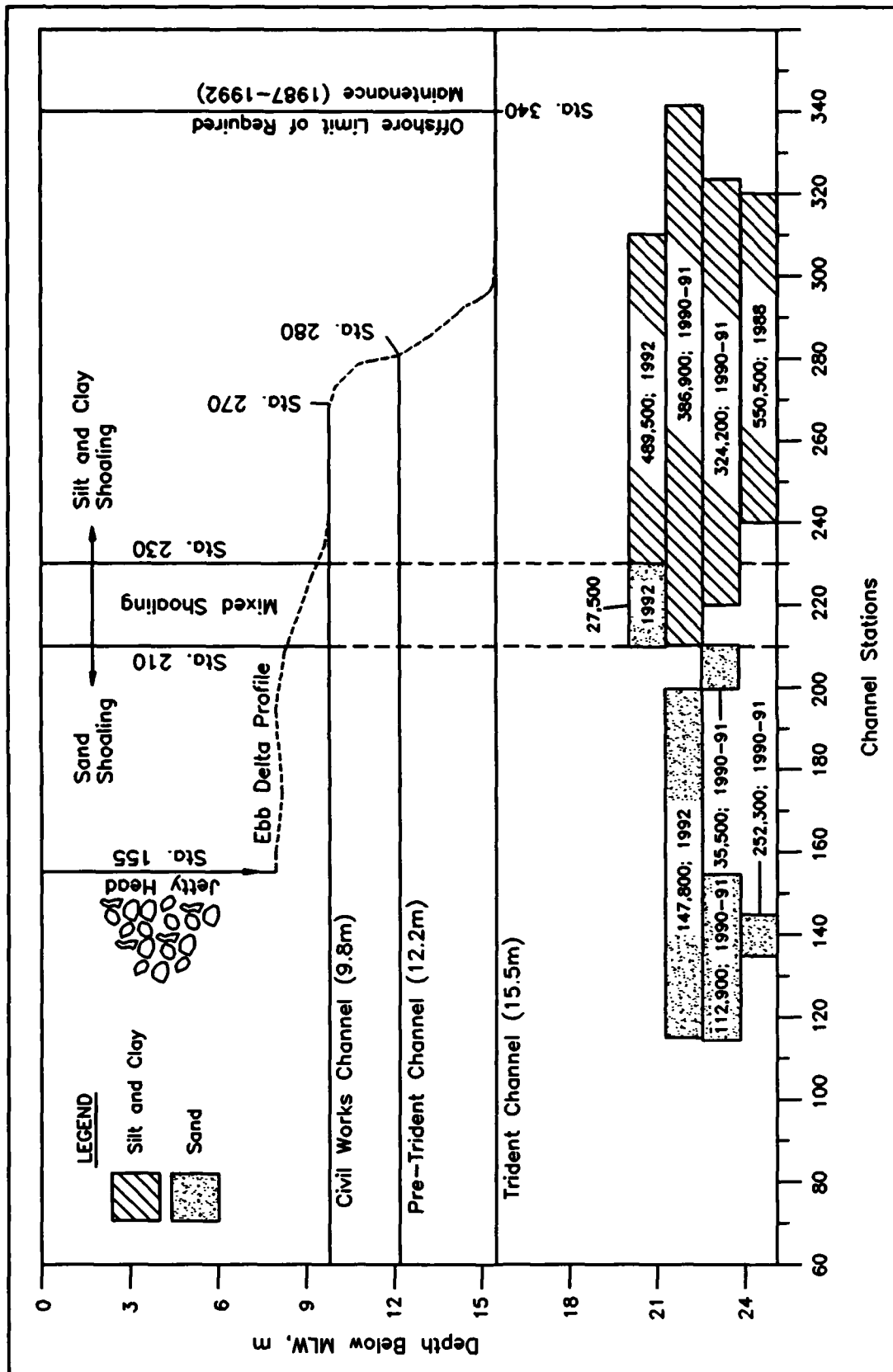


Figure 103. Maintenance dredging event channel reach, volume, and sediment type (1988-1992) with respect to channel configuration and ebb-tidal delta profile (1988-1992)

Cut 1N, and silt and clay shoaling seaward of Station 225+00), and channel configuration (depth and length). Littorally introduced sand constituted 24 percent (149,300 cu m/year) of Epoch 7 maintenance dredging. This dredging of littoral sands occurred in the vicinity of the ends of the jetties between Stations 67+00 to 230+00, Cut 1N, with predominant dredging performed between Stations 110+00 and 180+00. Sediment type of the remaining 5 percent of the 616,200 cu m/year of Epoch 7 maintenance dredging (29,100 cu m/year) was unclassifiable.

Areas of minor shoaling during Epoch 7 occurred between Stations 345+00 and 375+00 of St. Marys Entrance channel, Cut 1N, with rates of 9,400 cu m/1,000-m section of channel. Two sections of the Cumberland Sound portion of the channel from Station 0+00 to 50+00, and from Station 100+00 to 150+00 experienced scouring on the order of 48,700 cu m/1,000-m section of channel and scouring of 19,900 cu m/1,000-m section of channel, respectively.

# 5 Profile Surveys, Sediments, and Beach Fills<sup>1</sup>

## Introduction

This chapter summarizes results from the coastal monitoring portion of the study. The purpose of the coastal monitoring activities was to measure and evaluate changes in coastal response to physical processes in the littoral zone of Cumberland and Amelia Islands for the period July 1988 through April/May 1992. Field measurements consisted of beach and nearshore profiles and sediment samples, bathymetric surveys of St. Marys ebb delta, offshore and nearshore waves, and tidal elevations. The ebb delta surveys are discussed in Chapter 3 and the wave and tide data are discussed in Chapter 6. The sampling schedule for collected field data sets for the period of coastal monitoring and wave gage operations is shown in Table 23.

Profile surveys and sediment sampling conducted during the coastal monitoring period were integrated and analyzed to evaluate the response of the beach to natural processes and engineering activities during the monitoring period. The purpose of collecting and analyzing profile and sediment data was to document changes in the shoreline position, beach topography, and near-shore bathymetric features during the monitoring period. Quantitative and qualitative results of the profile survey analysis are used to determine alongshore (spatial) and incremental (temporal) variability of the beach and nearshore. The monitoring profile surveys are also compared with

**Table 23**  
**Schedule of Field Data Collection for Coastal Monitoring**

Data	FY 88				FY 89				FY 90				FY 91				FY 92			
Aerial Survey			*							*				*						
Beach Profile Survey			*		*	*				*			*						*	
Ebb Delta Bathymetric Survey			*																*	
Sediment Samples			*			*				*								*		
NDBC Gage			*	*	*	*	*	*	*	*	*	*	*	*	*	*	*	*	*	*
Nearshore Gage						*	*	*	*											

Note: Locations of asterisks denote approximate time (quarter) of data collection.

<sup>1</sup> Written by Laurel T. Gorman, Joan Pope, and Karen R. Pitchford.

the historical data, allowing examination of the short-term, intensive monitoring data set relative to the long-term record. This chapter also includes an analysis of beach change trends documented during the monitoring period relative to the background data presented in Chapter 3. The recent history (1978-present) of dredged material placement on Amelia Island and the implication of these engineering activities to the beach response is discussed in the last section of this chapter.

The spatial trends are defined based upon the morphologic compartments introduced in Chapter 2 (Figure 35). These compartments are alongshore sections of the study area which have a consistent character across the backbeach, beach, nearshore, and offshore zones. Three compartments are directly influenced by tidal inlet morphology and processes: St. Andrew Sound, St. Marys Tidal Inlet Complex, and Nassau Sound. Other coastal compartments within the study area are Stafford Shoal (located along central Cumberland), Cumberland Embayment (at the southern end of Cumberland), North Amelia Platform (beyond the south fillet area), and Amelia Embayment (along central Amelia Island). Within each compartment, distinctive trends in local geomorphology, shoreline position, and bathymetric features were identified. Analysis of the temporal profile and sediment trends per compartment is based principally on the net surveyed changes between July 1988 and April/May 1992 and also on a review of the intermediate year data (i.e., 1989, 1990, and 1991). Some modifications and reductions in the number of profiles surveyed were made each year. These intermediate partial data sets are used to evaluate the variability during the monitoring period and to assess the representativeness of the end point (i.e., July 1988 and April/May 1992) data results.

This chapter describes the field data collection methods, the analytical results, the topography, and beach characteristics of each of the morphologic compartments and the implications of beach fill placement activities to the monitoring period beach response. Beach and nearshore changes were evaluated based on geomorphic interpretation and analysis of measurements from the coastal monitoring program for each island and for each compartment. The following sections summarize individual field measurements including profile volumetric change, shoreline position change, inner bar position, and sediment grain size. More detailed information on the profile survey and sediment data sets including data collection, processing methods, and results are presented in Appendix D, *Survey and Sediment Grain Size Data* section.

### **Surveying plan**

As described in the DOS (Chapter 1), the coastal monitoring program included annual summer beach profile surveys supplemented by two winter surveys. These data were collected to quantify the beach and nearshore topography of the study area and its variability. The July 1988 profile survey and sediment (marked by S) sampling lines for Cumberland and Amelia Island are shown in Figures 104 and 105, respectively. Individual profile lines are numbered in consecutive order from north to south and prefaced in the text by a C or an A denoting whether the profile line pertains to Cumberland or Amelia Island, respectively. Spacing between survey lines varied slightly, with an average of approximately 0.9 km. The lines extended offshore to the approximate 10-m (NGVD) depth contour. After the July 1988 survey, the alongshore profile variability was appraised. The annual survey plan was revised to reduce study costs, while still assuring that adequate coverage was maintained to represent the individual morphologic compartments. Locations of the April/May 1992 profile survey lines are shown in Figures 106 and 107. A few survey lines were excluded in the quantitative analysis presented here due to

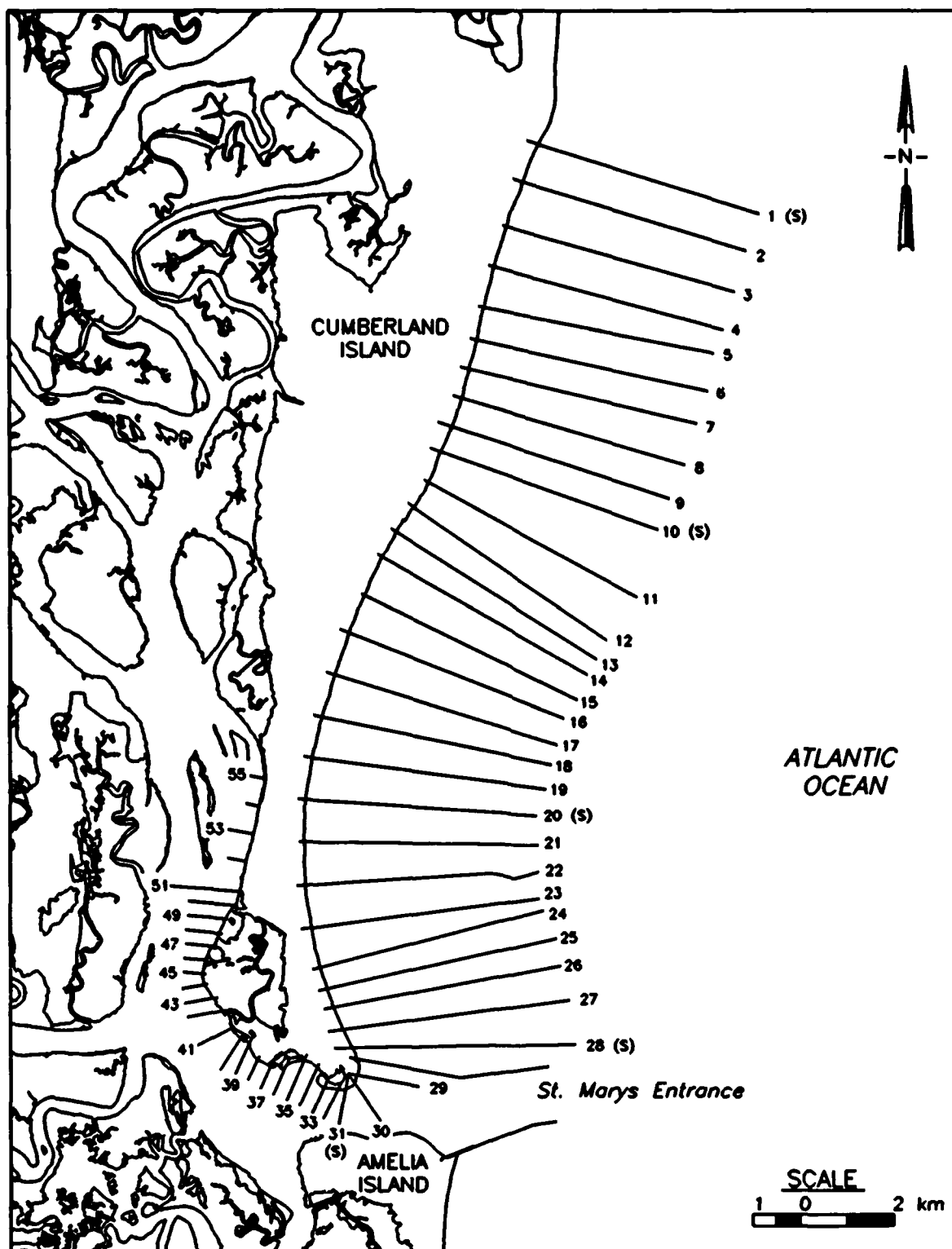


Figure 104. Location map of Jul 1988 profile survey lines and sediment sampling (S) along Cumberland Island

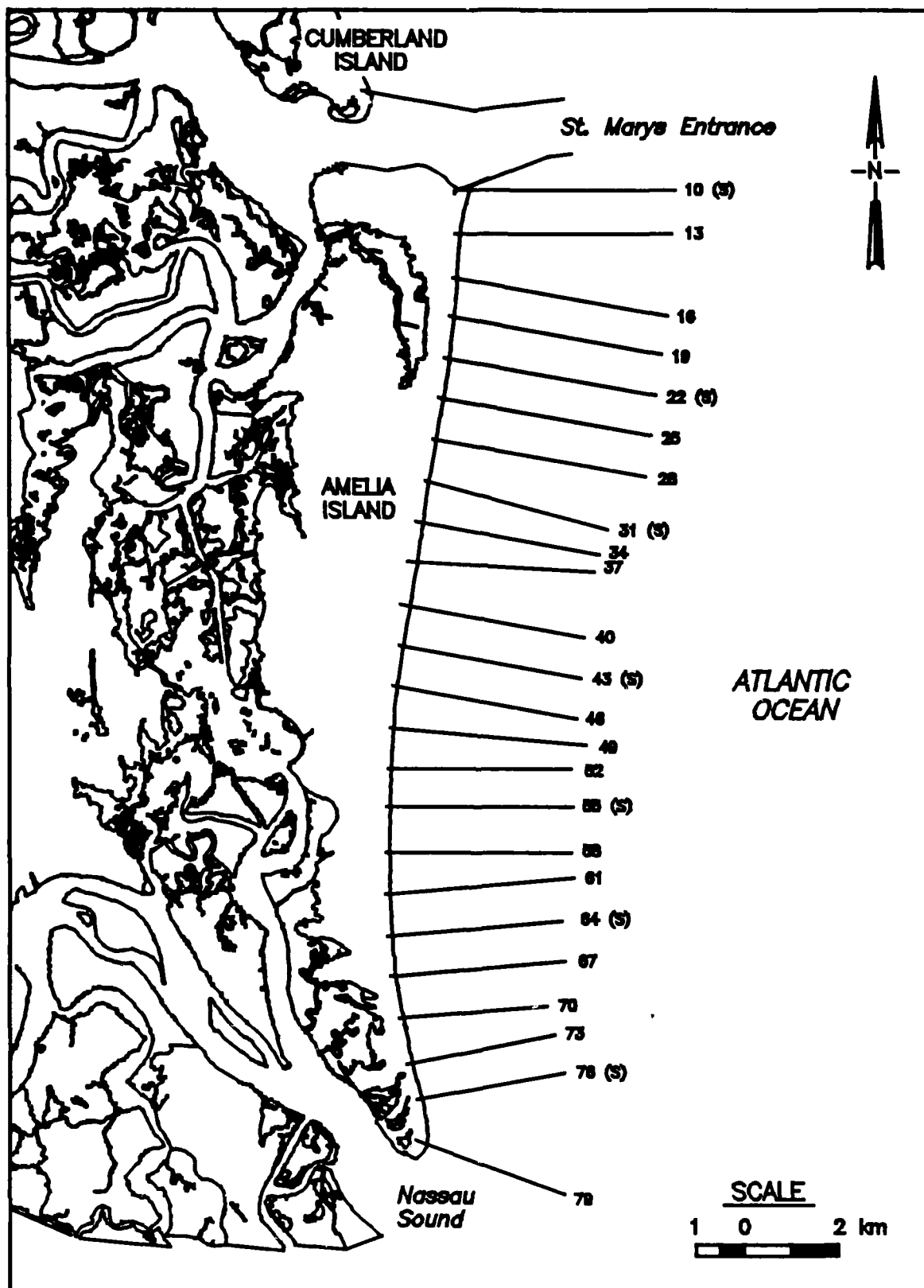


Figure 105. Location map of Jul 1988 profile survey lines and sediment sampling (S) along Amelia Island

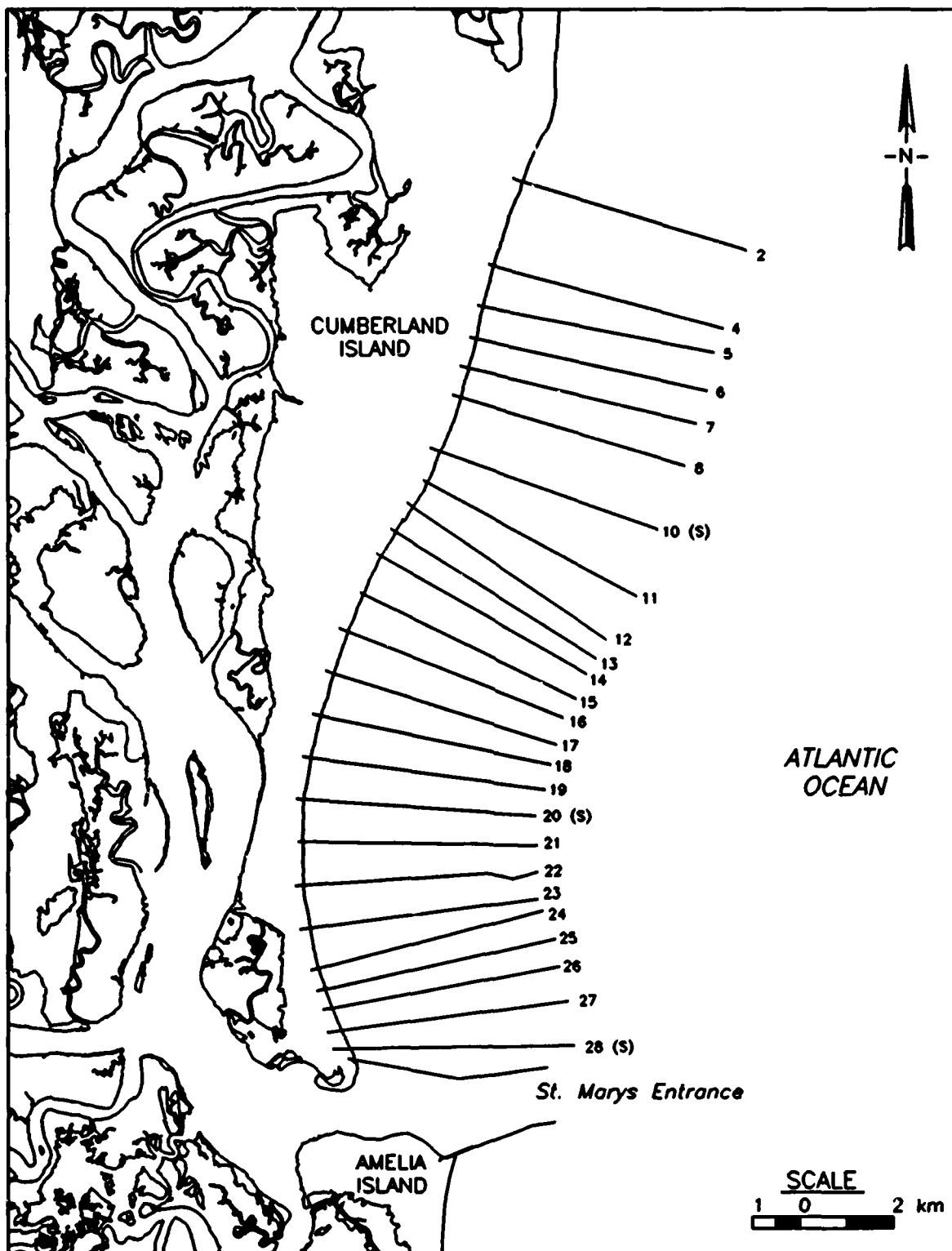


Figure 106. Location map of Apr/May 1992 profile survey lines and sediment sampling (S) along Cumberland Island

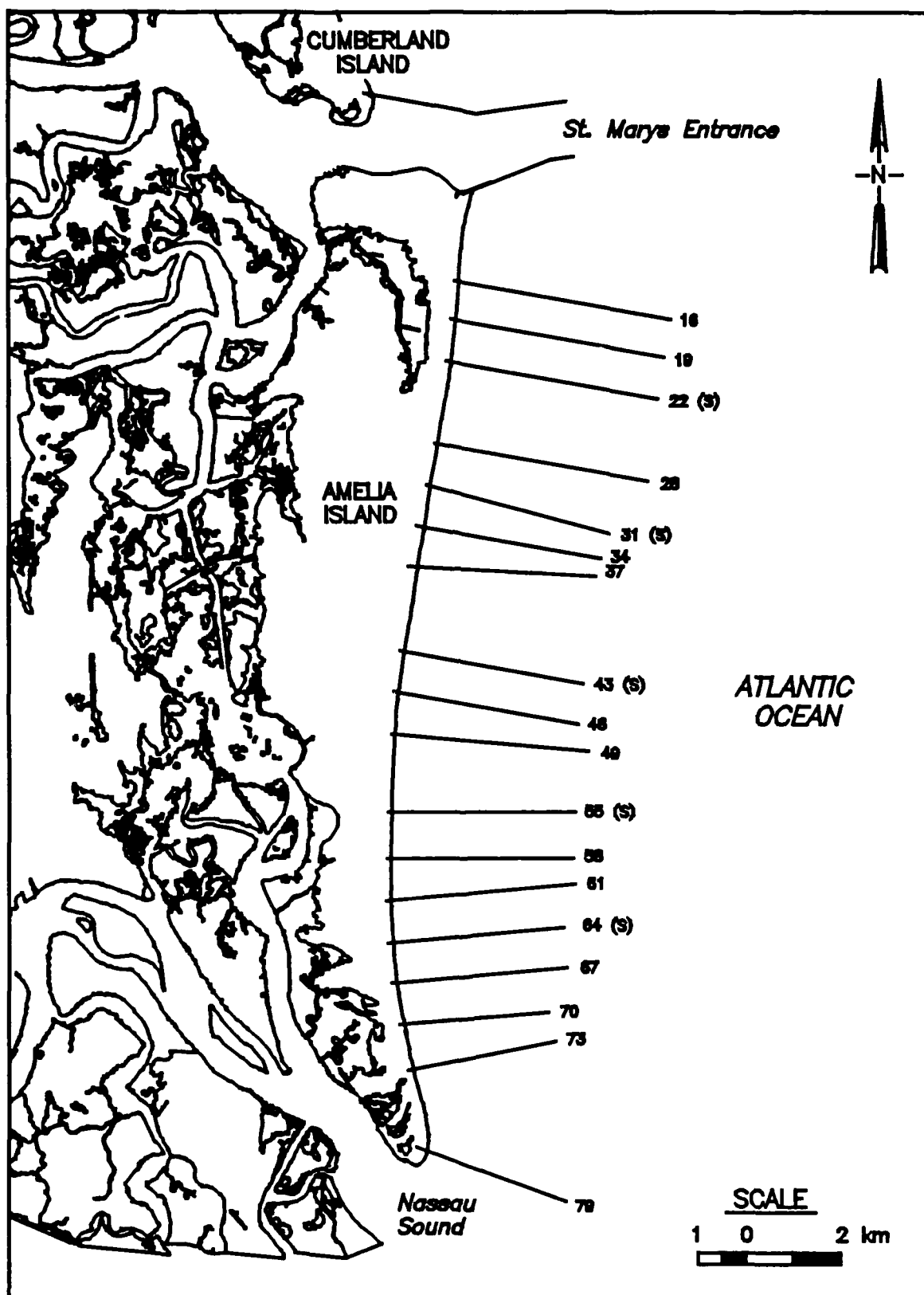


Figure 107. Location map of Apr/May 1992 profile survey lines and sediment sampling (S) along Amelia Island

vertical or horizontal datum control ambiguities. The schedule and number of profile surveys and sediment samples are listed in Table 24.

Offshore bathymetry surveys were conducted in June/July 1988 and April 1992 to assess the morphology and movement of the ebb-tidal delta (Figure 108). A rectangular grid, consisting of 16 north-south lines and 6 east-west lines, was surveyed seaward of the jetties. Discussion and comparison of the ebb delta surveys are presented in Chapter 3.

**Table 24**  
**Survey and Sediment Field Data Collection for Monitoring Program**

Date	Jul 1988	Aug/Oct 1989 <sup>1</sup>	Dec 1989	Aug 1990	Aug 1991	Apr/May 1992
<b>Number of Survey Lines</b>						
Cumberland Ocean	28	18	4	18	18	18
Cumberland Sound	27	23	-- <sup>2</sup>	23	23	23
Amelia Ocean	24	16	6	16	16	16
Ebb Delta	22	--	--	--	--	22
<b>Total</b>	<b>101</b>	<b>57</b>	<b>10</b>	<b>57</b>	<b>57</b>	<b>79</b>
<b>Number of Sediment Samples</b>						
Cumberland Ocean	30	12	--	12	--	12
Cumberland Sound	5	4	--	4	--	4
Amelia Ocean	48	30	--	30	--	30
<b>Total</b>	<b>83</b>	<b>46</b>	<b>--</b>	<b>46</b>	<b>--</b>	<b>46</b>
<sup>1</sup> Cumberland Island sampled in Aug 1989. Amelia Island sampled in Oct 1989.						
<sup>2</sup> No data available.						

### Data collection methods

Profile surveys to wading depth were accomplished using conventional land-based survey equipment, and subaqueous surveys were done using a boat-towed sled or a boat-mounted fathometer. Boats were utilized for the offshore surveys during the 1988-1990 period, whereas only land-based data were collected for 1991. The April/May 1992 survey was conducted using a sled. A baseline located behind the dune system was established along both islands for long-term monitoring by USAED, Savannah, on Cumberland Island in 1988 and by the State of Florida, Department of Natural Resources, on Amelia Island in 1974. Each profile was surveyed relative to vertical and horizontal control monuments along the baseline. Measurements were made at 7.6-m intervals or major breaks in topography along both the subaerial and offshore portions of the individual profile lines. Both Districts followed the operational standards required for Class 2 survey standards as described in the USACE Hydrographic Surveying Engineer Manual (USACE 1991).

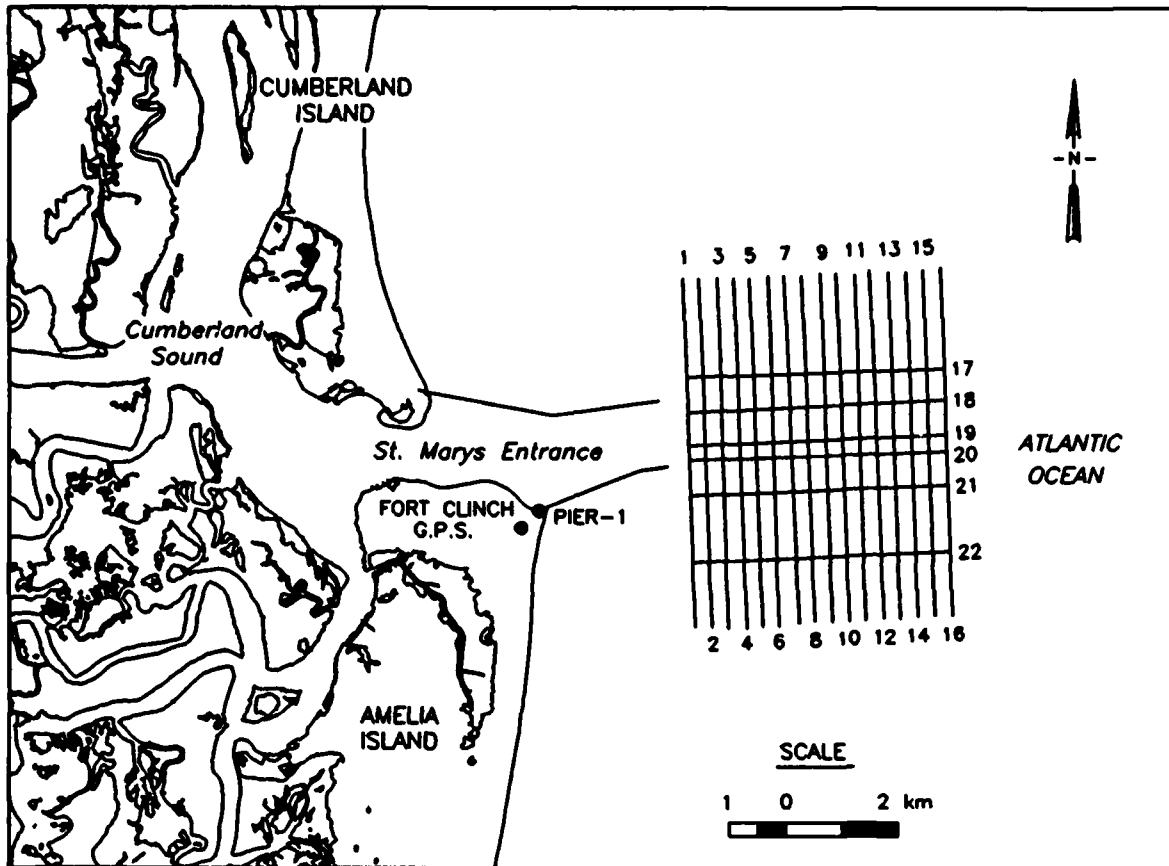


Figure 108. Location map of survey lines for the ebb-tidal delta survey of Jun/Jul 1988 and Apr 1992

An important consideration in using the shoreline position and volumetric computations is the amount of error associated with the profile survey measurements. According to USACE standards for conducting Class 2 hydrographic surveys (USACE 1991), the maximum allowable error is  $\pm 6.0$  m horizontal and  $\pm 0.3$  m vertical. These criteria are based on the attainable positional accuracy and instrument precision, assuming typical USACE survey equipment, procedures, and project conditions. However, after comparing several annual nearshore surveys for this project, it was apparent that the vertical error exceeded  $\pm 0.3$  m for the boat-mounted fathometer portions of some of the surveys. This conclusion was based on the vertical offsets along the offshore portion of the monitoring survey lines which is also considered as a depth of relative topographic stability (i.e. profile closure depth). Assuming all standard operational procedures as defined by USACE (1991) were followed, the probable source of this vertical error is the difficulty in attaining consistent tidal datum control over such a large region. Examples of this vertical error are shown in Appendix D. Because the vertical error associated with the fathometer surveys in many cases exceeded the expected natural variability of the offshore portions of these profiles, only the land-based surveys are used for quantitative analysis. The offshore surveys were used to qualitatively describe the bathymetric topography and identify dynamic features in the offshore. In April/May 1992, a sled survey was conducted in order to obtain accurate profile measurements in the offshore. Properly conducted sled surveys are accurate to  $\pm 0.05$  m in the vertical (Clausner, Birkemeier, and Clark 1986). The April/May

1992 sled surveys provided continuous, accurate coverage through the surf zone and accurate assessment of bar-trough features.

The profile data were analyzed using the Interactive Survey Reduction Program (ISRP), (Birkemeier 1984). ISRP plots and analyzes data pairs representing the distance in meters from the baseline and the elevation in meters relative to NGVD, respectively. Profile volume change was computed based on elevation intervals and distances along profile line (Figure 109), allowing the analysis to be sensitive to the variable morphology of the active beach envelope and the range of beach widths (ranging from 30 to 200 m) found throughout the study area. The lower limit of the active beach used for computing volume changes is the midtide elevation of 0.0 m (NGVD). The elevation selected to represent the upper limit of the active foreshore was 2.5 m (NGVD) for Cumberland Island and 4.0 m (NGVD) for Amelia Island. The lower limit of 0.0 m (NGVD) is the most seaward point on the land-based portions of the profiles for which data were consistently available. The selected upper limit was different for each island because the base of the dune field on Cumberland Island is at approximately 2.5 m (NGVD) and the top of the berm of the placed beach fill on Amelia Island is at a maximum of 4.0 m (NGVD), as determined by the characteristics of the plotted beach profiles. These elevational limits used in the volume analysis define the active foreshore and represent the subaerial beach. Volume changes are presented as a net change for the entire monitoring period in this section to represent alongshore trends and for comparison with other beach condition indicators. Appendix D contains the volumetric summary for individual survey lines.

Additional calculations with the profile survey data were made to obtain beach and nearshore parameters, including shoreline position change, beach and nearshore slope angle, and inner bar position (Figure 109). Discussion of shoreline position follows the *Profile Volume Change* section. Shoreline position change was calculated at the high-water line, elevation 1.3 m

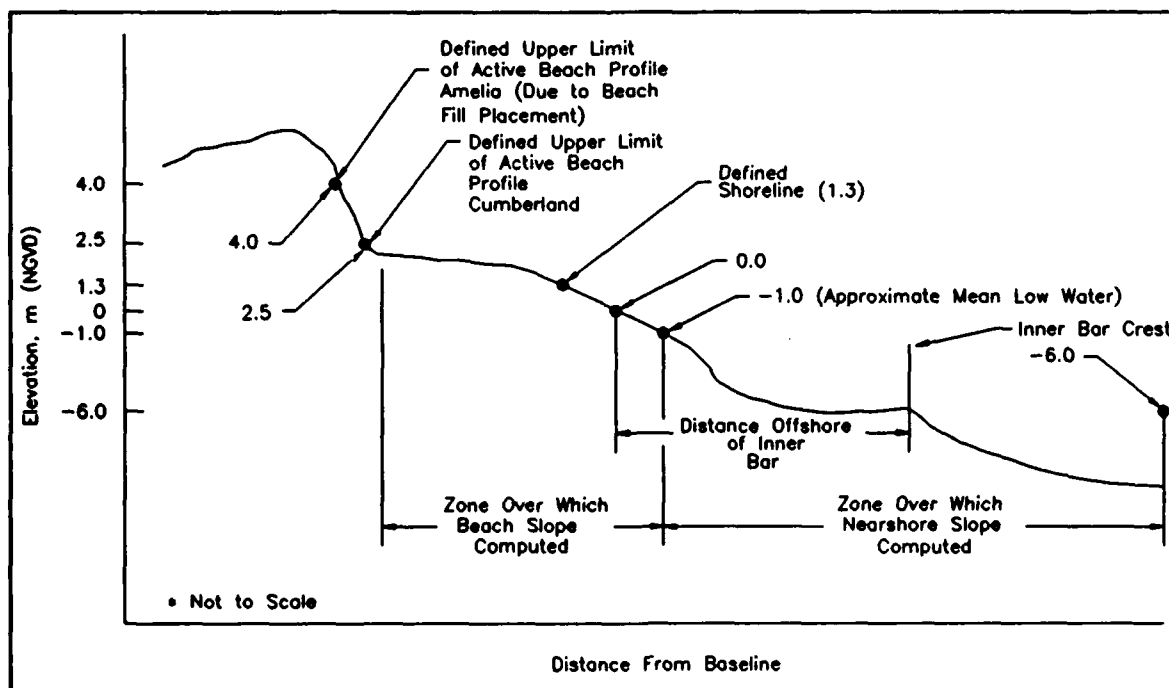


Figure 109. Definition sketch of profile computational parameters

(NGVD) from the profile surveys. The 1.3-m (NGVD) elevation is the approximate high-water line as defined in Chapter 3. Shoreline position rates of change (m/year) were computed as a net value for the entire monitoring period and as interim values representing the 1989, 1990, and 1991 surveys. Additional statistical analysis of the shoreline is contained in the *Shoreline Position Change from Profiles* section. Slope angle was defined for the subaerial beach between elevation 2.5 and -1.0 m (NGVD) and for the nearshore from -1.0 to the slope break (about -6.0 m) (Figure 109). Alongshore variations in the position (relative to NGVD) and crest elevation of the inner bar were measured from the April/May 1992 sled survey. The occurrence of an outer bar was sporadic. In some areas, the profile seaward of the inner bar crossed shoal complexes. These secondary profile parameters of the slope and inner bar are discussed in the *Morphologic Compartments* section. Averaged volumes, shorelines, and other profile-related measurements compiled per compartment or island were determined by a procedure which weighted each profile according to the distance between survey lines (Appendix D). All values except seasonal surveys and sediment samples presented within the tables contained in this chapter were weighted based on data available per time period and do not represent a simple average.

Sediment samples were collected along selected profiles within the individual morphological compartments to determine if changes in sediment texture occurred during the monitoring period (Figures 104-107). Surface grab samples were taken at the following measured positions or elevations: berm or dune crest, mean high water, mean low water, trough of nearshore bar, nearshore bar crest, and 4.5-, 8.1-, and 11.8-m depths. Statistical parameters used to discuss the spatial and temporal trends are the mean grain size and standard deviation (sorting), computed using the method of moments (Friedman and Sanders 1978). To determine the cross-shore variability in grain-size change, a mathematical beach composite was computed from the berm or dune crest to MLW. Additional background information on sediment sampling methods and processing is presented in Appendix D.

## Profile Volume Change

Net volumetric change trends and profile variability are computed from the active beach portions of the July 1988 and April/May 1992 surveys. These two surveys represent different periods of the beach's natural seasonal cycle (*Seasonal Variability* section). The April/May survey would tend to characterize a beach which is still in its narrower, steeper winter cycle, and the July survey would represent the wider, more gently sloping summer beach. Intermediate-year profiles were evaluated and the geometry of the 1988 and 1992 profiles was compared to ascertain the extent of the seasonal variability. Although the April/May 1992 survey did capture certain seasonal characteristics, they were considered and judged to be minor relative to the entire monitoring period which was the focus of this study.

For this study, the active subaerial beach is defined as the beach between elevations 2.5 and 0.0 m (NGVD) for Cumberland Island and between elevations 4.0 and 0.0 m (NGVD) for Amelia Island (Figure 109). Volumetric changes across this active subaerial beach profile reveal distinctive spatial trends within the morphologic compartments on both Cumberland and Amelia Islands.

## Cumberland Island

During the monitoring period, the overall average net volume change for Cumberland Island was a gain of 9.3 cu m/m (2.5 to 0.0 m NGVD), as listed in Table 25. At the northern limit of the study area (Line C2), there was a maximum net accretion of 79.9 cu m/m between July 1988 and April/May 1992 (Figure 110). Most of the Stafford Shoal compartment (between Lines C3-C14) experienced net erosion with a maximum loss at Line C12 of 36.4 cu m/m. An exception to the dominant erosion in the Stafford Shoal compartment is the relative net stability at Lines C10 and C11 (Figure 110). This particular section of shore is sheltered by the main body of Stafford Shoal and is referred to in this report as the "Stafford Shoal axis," as it appears to function as a stable point about which the shoreline changes to the north and south. At the northern end of the Cumberland Embayment (Line C15) there is a prominent change from a net volume loss to the north (averaging 14.2 cu m/m) to gains south of Line C15 (averaging 28.4 cu m/m). This net accretional trend increases to the south along the entire Cumberland Embayment compartment. Profile gains along the Cumberland Embayment compartment increased from 19.8 cu m/m at Line C18 to 42.2 cu m/m at Line C25. The southernmost compartment along Cumberland Island, the north fillet of St. Marys Tidal Inlet Complex, continued its historical accretional trend (average net volumetric change 35.8 cu m/m). However, the profile immediately north of the north jetty (Line C28) exhibited minimal accretion (1.7 cu m/m), which may indicate sediment transport through the jetty or localized scour.

**Table 25**  
**Net Volume Change for Cumberland Island<sup>1</sup>**

	Stafford Shoal C1-C14	Cumberland Embayment C15-C26	St. Marys Tidal Inlet Complex C27-C28	Cumberland Island Average C1-C28
Net Volume Change, cu m/m				
Jul 1988- Apr/May 1992	-14.2	28.4	35.8	9.3
Incremental Volume Change, cu m/m				
Jul 1988- Aug/Sep 1989	0.5	12.9	26.0	7.7
Aug/Sep 1989- Jul 1990	-1.7	7.2	2.4	3.0
Jul 1990- Aug 1991	2.1	15.1	30.5	9.6
Aug 1991- Apr/May 1992	-9.1	-11.2	-9.5	-10.1
<sup>1</sup> Volume change is defined from elevation 2.5 to 0.0 (NGVD). Reference Appendix D.				

In general, the intermediate-year surveys (listed in Appendix D) exhibited little variability relative to the monitoring period trend. The greatest variability occurred in Stafford Shoal (Appendix D), along the northern limit of the study area (Line C1), along the axis of Stafford Shoal (Line C11), and adjacent to the north jetty (Line C28) in the St. Marys Tidal Inlet Complex (Appendix D). Intermediate-year survey data from Line C20 exhibited reversals in trend.

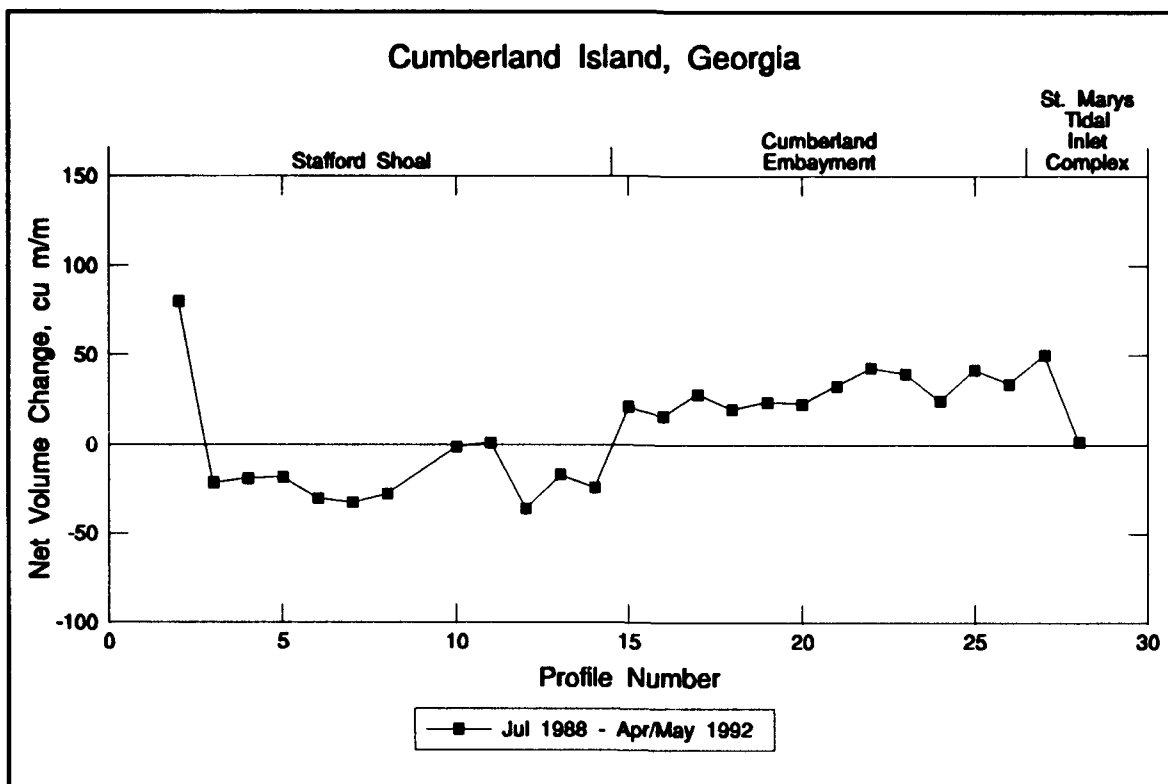


Figure 110. Net volume change for elevation 2.5 to 0.0 m (NGVD), Jul 1988 - Apr/May 1992, Cumberland Island

### Amelia Island

Volume change was more variable along Amelia Island than along Cumberland Island. Net volume changes and beach fill construction operations extending between Lines A16 and A73 are shown in Figure 111. The dominant trend during the monitoring period was near stability with an average net volume gain of 0.6 cu m/m for the July 1988 - April/May 1992 period (Table 26). The natural volume and shoreline change trends were masked by multiple and overlapping beach disposal operations of beach-quality sand dredged from St. Marys Entrance channel. These activities began before the study started (i.e. 1978) and extended through the entire study period for Amelia Island (Figure 112). A typical section of beach placement consisted of dredged material hydraulically placed between the face of the dune (berm elevation is variable but generally less than 4.0 m NGVD) and approximately 0.0 m (NGVD). Table 27 summarizes the known Federal and privately funded beach fill events along Amelia Island by profile number and year. Unfortunately, records specifying beach disposal construction dates and volume placed per profile line are not available. This limits direct comparison of the volume of material placed to the measured profile volume change. Therefore, the net beach fill affect to the Amelia Island data is described based on the July 1988 - April/May 1992 profile volume change.

At the northern end of Amelia Island (North Amelia Platform), Lines A16-A22 were surveyed after the June 1987 - February 1988 beach fill placement. Comparison of the July 1988 postfill

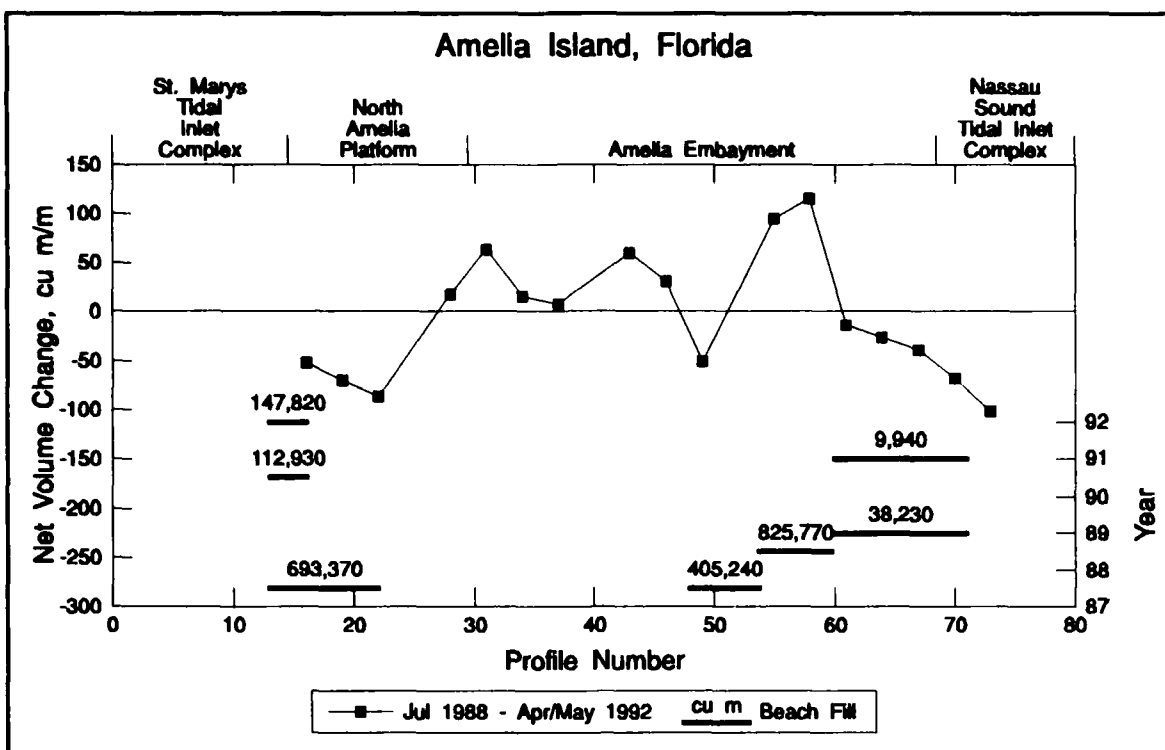


Figure 111. Net volume change for elevation 4.0 to 0.0 m (NGVD), Jul 1988 - Apr/May 1992, Amelia Island

Table 26 Net Volume Change for Amelia Island <sup>1</sup>					
	St. Marys Tidal Inlet Complex A10-A13	North Amelia Platform A16-A28	Amelia Embayment A31-A67	Nassau Sound Tidal Inlet Complex A70-A79	Amelia Island Summary A10-A79 <sup>2</sup>
Net Volume Change, cu m/m					
Jul 1988- Apr/May 1992	-- <sup>3</sup>	-44.3	24.8	-79.3	0.6
Incremental Volume Change, cu m/m					
Jul 1988- Oct 1989	-5.0	-16.8	17.0	-11.9	4.7
Oct 1989- Aug 1990	2.9	1.9	16.0	8.9	11.1
<sup>1</sup> Volume change is defined from elevation 4.0 to 0.0 m (NGVD). Reference Appendix D. <sup>2</sup> Range of profile surveys actually used is Lines A16-A70. <sup>3</sup> No data available.					

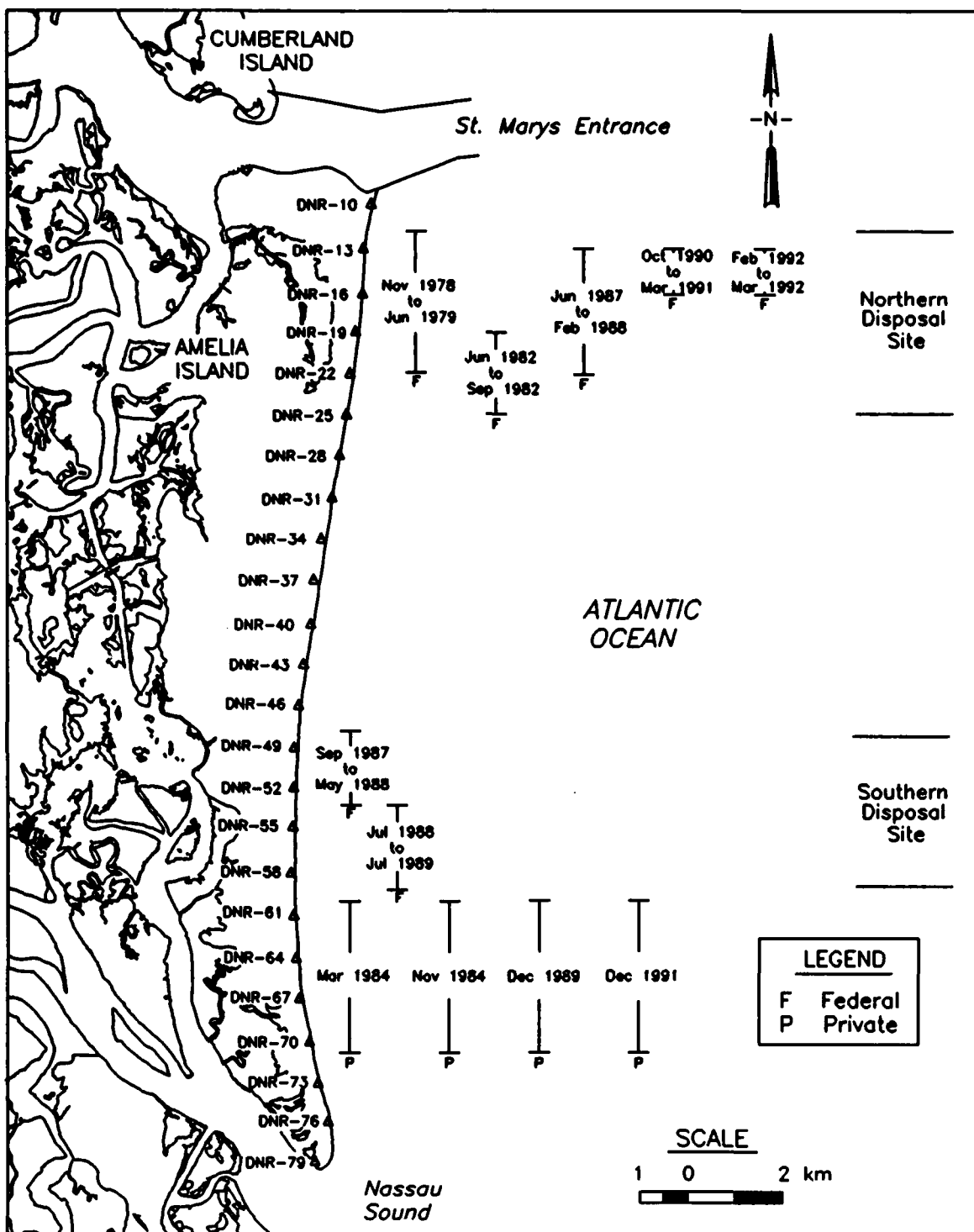


Figure 112. Locations of beach fill placements along Amelia Island

**Table 27**  
**Beach Fill Placements on Amelia Island<sup>1</sup>**

Year	Authority	Profile Number	Quantity, <sup>2</sup> cu m
Nov 1978 to Jun 1979	Federal	DNR-12 to DNR-22	765,000
Jun 1982 to Sep 1982	Federal	DNR-19 to DNR-25	302,000
Mar 1984	Private	DNR-60 to DNR-71	57,340
Nov 1984	Private	DNR-60 to DNR-71	4,200
Jun 1987 to Feb 1988 <sup>3</sup>	Federal	DNR-13 to DNR-22	693,370
Sep 1987 to May 1988 <sup>3</sup>	Federal	DNR-48 to DNR-53.7	405,240
<b>Total Federal fill, prior to Kings Bay monitoring period</b>			<b>2,165,610</b>
<b>Total private fill, prior to Kings Bay monitoring period</b>			<b>61,540</b>
Jul 1988 to Jul 1989	Federal	DNR-53.7 to DNR-59.8	825,770
Dec 1989	Private	DNR-60 to DNR-71	38,230
Oct 1990 to Mar 1991	Federal	DNR-13 to DNR-16	112,930
Dec 1991	Private	DNR-60 to DNR-71	9,940
Feb 1992 to Mar 1992	Federal	DNR-13 to DNR-16	147,820
<b>Total Federal fill, during Kings Bay monitoring period</b>			<b>1,086,520</b>
<b>Total private fill, during Kings Bay monitoring period</b>			<b>48,170</b>
<sup>1</sup> Source: USAED, Jacksonville (1993).			
<sup>2</sup> Quantity represents volume dredged from the channel which was designated for beach disposal. The actual volume placed on the beach will be less due to losses during the dredging and disposal operations.			
<sup>3</sup> Fill placement occurred as part of the TRIDENT channel deepening, before the monitoring period (Jul 1988 to Apr/May 1992) of this study.			

and April/May 1992 postfill data indicates net volume losses that increased toward the south, from 52.5 (Line A16) to 87.1 (Line A22) cu m/m, across the 4.0 to 0.0 m NGVD envelope. This trend of net erosion reverses south of Line A22, where Line A28 exhibits a 17.8-cu m/m gain over the same envelope. This apparent reversal in the alongshore trend could be explained by the existence of the historical shoreline change node (erosion to the north and minor accretion to the south) which was close to Line A22, or more likely, is due to the relative timing of the 1988 beach fill placement and survey schedule. A freshly placed and surveyed beach fill will appear to lose material before the next survey as the beach adjusts to an equilibrium (Stauble and Hoel 1986), whereas an adjacent unfilled section of the beach may gain, particularly if beach fill is placed after the first survey. See *Trend Analysis and Implication of Recent Engineering Activities* section for a more detailed discussion of the beach fill activities and shoreline response.

The data for the central compartment known as Amelia Embayment exhibit alternating patterns of erosion and accretion (Figure 111), although the dominant pattern was one of increasing accretion toward the south. Most of the accretion along the upper beach profile represents beach fill disposal operations. Based on the elevation interval 4.0 to 0.0 m (NGVD), the average net volume gain was 24.8 cu m/m for this compartment, probably reflecting the effect of a major beach fill operation between July 1988 and July 1989 (Table 27). A maximum amount of

accretion occurred along Line A58, where the net beach accretion was 115.5 cu m/m. Seventy percent of this volume gain occurred across the upper portion of the beach (between 4.0 and 2.5 m NGVD). Lower rates of accretion, and even losses, occurred from Lines A34 (15.3 cu m/m) through A49 (-51.1 cu m/m) which were in an area where no fill was placed during the monitoring period.

At the southern end of Amelia Embayment and along the Nassau Sound Tidal Inlet Complex compartment, there is a well-defined trend of increasing volume loss to the south (Lines A61-A73). Within the profile envelope, small volume gains occurred between 1.5 and -1.0 m (NGVD) possibly representing private beach fills (December 1989 and December 1991) (Table 27). The profile envelope for Nassau Sound Tidal Inlet Complex, between elevation 4.0 and 0.0 m (NGVD), shows an average net volume loss of 79.3 cu m/m (July 1988 - April/May 1992), which represents the highest volumetric loss for any of the study area compartments. The dunes in this area are frequently eroded by storm waves, as evidenced by the steepness of the upper portion of the profile and volumetric losses of the dune between elevation 4.0 and 0.0 m (NGVD). Along the southern tip of Amelia Island (Line A79), the profile is gently sloping and undulating as shoals form and migrate due to tidal inlet processes (Figure 113).

Volume change trends are variable from year to year for Amelia Island, reflecting the multiple beach fills. Intermediate-year data (presented in Appendix D) illustrate the alternating cycles of gains and losses associated with beach fill placement. The main value of the intermediate-year data is in providing a picture of the general trends and in supplementing some survey lines which could not be revisited during the April/May 1992 survey. The April/May 1992 survey coverage was reduced at the northern end of Amelia Island because storm damage disturbed several baseline benchmarks, including Lines A10 and A13 in the south fillet area of St. Marys Entrance.

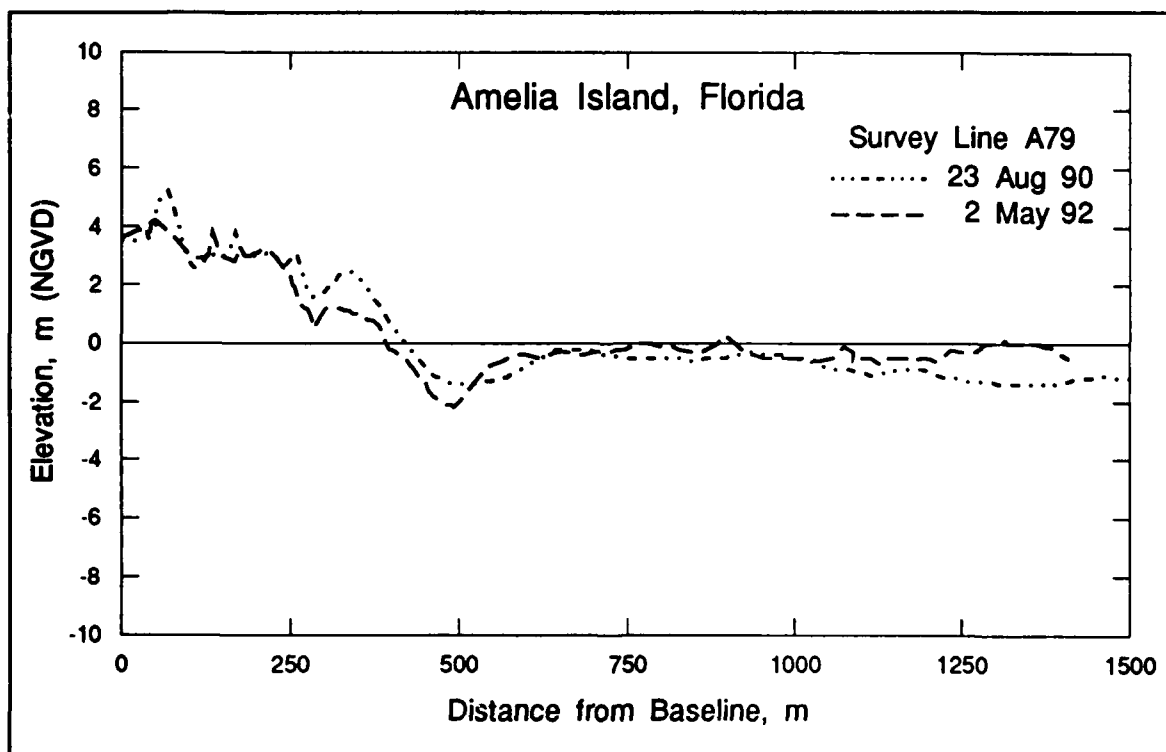


Figure 113. Profile comparison of Line A79, Aug 1990 - Apr/May 1992, Amelia Island

Survey data (presented in Appendix D) included 1988-1990 or 1991 coverage of Lines A10 and A13 across the south fillet area. Line A10 exhibited a cumulative gain from 1988-1991 (116.3 cu m/m), whereas Line A13 experienced a loss (22.3 cu m/m) from 1988-1990. The sediment gains along Line A10 (located immediately south of the south jetty) may be due to the sand tightening of the south jetty which was conducted in July 1988 (Table 6) while the sediment losses along Line A13 are probably due to the adjustment of a fill placed prior to the July 1988 survey.

## Shoreline Position Change from Profiles

The shoreline position change rates discussed in this section were calculated based on the most seaward location of the 1.3-m (NGVD) elevation on each individual profile line. The alongshore pattern of shoreline recession and advancement is a convenient indicator of coastal process variability. Analysis of short-term and long-term shoreline change is frequently used as a technique to assess the impacts of engineering works on the adjacent coastline. Shoreline change is a key measurement from the July 1988 - April/May 1992 monitoring period, as it represents the only parameter common to the long-term historic trend analysis. The July 1988 shoreline represents the baseline to which subsequent monitoring period data are compared. It is also the data set which links the monitoring period with the shorelines of the historical analysis. Direct comparison of these data with results presented in Chapter 3 is complicated by the following limitations: (a) the data were extracted from individual profile lines at a periodic spacing of approximately 0.9 km, thus a continuous shoreline is not documented; (b) changes in shoreline position may be a reasonable measure of profile translation but not necessarily a good indicator of changes in profile slope; and (c) the use of the 1.3-m contour as a definition of the high-water level is mathematically derived but may not necessarily be directly translatable to a shoreline position extracted from planform information (i.e. aerial photography) which will be influenced by the alongshore variability in wave run-up over the different sloping beach faces. Average shoreline position change for each morphologic compartment for the intermediate-year surveys represents the annual variability within the monitoring period for Cumberland Island (Table 28) and Amelia Island (Table 29).

### Cumberland Island

The net shoreline position change during the monitoring period revealed a trend in which recession dominated the northern portion and advancement dominated the southern portion of Cumberland Island (Figure 114). This longshore trend of shoreline retreat or advance during the monitoring period is a distinctive parameter for demarking each compartment. During the July 1988 - April/May 1992 period, the average shoreline recession rate was 1.4 m/year along the Stafford Shoal compartment while the Cumberland Embayment shore advanced 1.6 m/year (Table 28).

Even though the Stafford Shoal Compartment was generally recessional (Table 28), the northern profile (Line C2) shoreline advanced 4.3 m/year during the monitoring period (Figure 114). This suggests that this northerly profile is influenced by sand released from the St. Andrew ebb-tidal delta. Lines C10-12 in the central portion of the Stafford Shoal compartment are relatively stable with significant recession both north and south of this area (Appendix D). Note that this zone of shoreline stability is the same as the zone of volumetric

**Table 28**  
**Shoreline Change for Cumberland Island<sup>1</sup>**

Date	Stafford Shoal C1-C14	Cumberland Embayment C15-C26	St. Marys Tidal Inlet Complex C27-C28	Cumberland Island Average C1-C28
Shoreline Change Rate, m/year				
Jul 1988- Apr/May 1992	-1.4	1.6	3.9	0.3
Shoreline Position Relative to Jul 1988, m				
Aug/Sep 1989	4.8	6.0	16.1	5.8
Jul 1990	0.2	5.6	6.8	3.2
Aug 1991	3.9	12.6	13.2	8.6
Apr/May 1992	-5.5	6.2	15.2	1.2
<sup>1</sup> Shoreline is defined as the 1.3-m (NGVD) intersect with the profile. Reference Appendix D.				

**Table 29**  
**Shoreline Change for Amelia Island<sup>1</sup>**

Date	St. Marys Tidal Inlet Complex A10-A13	North Amelia Platform A16-A28	Amelia Embayment A31-A67	Nassau Sound Tidal Inlet Complex A70-A79	Amelia Island Average A10-A79 <sup>2</sup>
Shoreline Change Rate, m/year					
Feb 1974- Sep/Nov 1981	-- <sup>3</sup>	1.0	-0.3	-1.1	0.0
Sep/Nov 1981- Jul 1988	--	3.6	1.6	-3.6	1.9
Jul 1988- Apr/May 1992	--	-3.2	1.6	-4.6	0.2
Feb 1974- Apr/May 1992	--	1.1	0.7	-2.8	0.7
Shoreline Position Relative to Jul 1988, m					
Oct 1989	--	-10.5	3.0	-2.5	0.6
May 1990	--	6.8	7.8	3.4	7.3
Apr/May 1992	--	-5.8	6.1	-17.1	2.3
<sup>1</sup> Shoreline is defined as the 1.3-m (NGVD) intersect with the profile. Reference Appendix D.					
<sup>2</sup> Profile surveys actually used are Lines A16-A70.					
<sup>3</sup> No data available.					

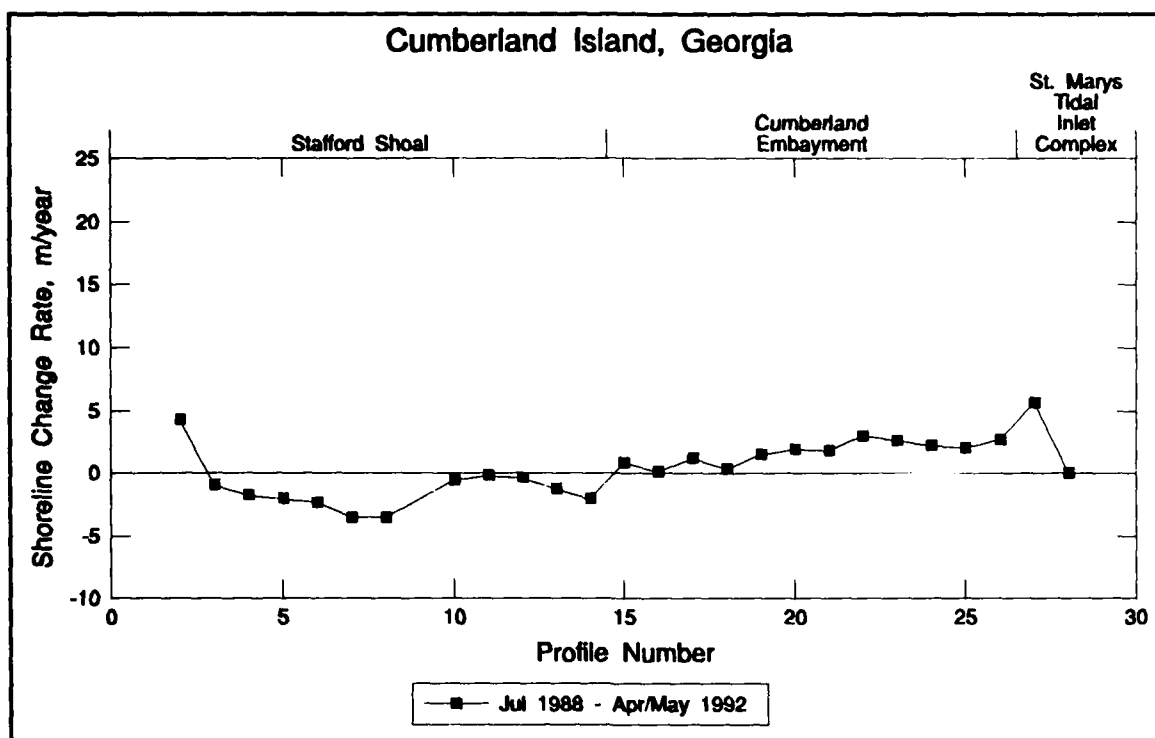


Figure 114. Shoreline change rates (m/year), Jul 1988 - Apr/May 1992, Cumberland Island

stability as discussed in the previous section. However, Lines C14 and C15, located at the southern end of Stafford Shoal, serve as a distinctive transition between the erosion to the north and accretion to the south for both the shoreline change and the volumetric analysis data sets. Lines C14 and C15 are the boundary between the Stafford Shoal and Cumberland Embayment compartments, and when evaluated relative to the historical shoreline change data (Chapter 3), can be considered as the morphodynamic rotation point for the island.

The trend of shoreline position advancement gradually increased toward the south within the Cumberland Embayment compartment (Figure 114). Maximum shoreline advance (5.6 m/year) was measured on Line C27, which is in the northern fillet of the St. Marys Tidal Inlet Complex. Adjacent to the jetty structure (Line C28), the shoreline position was stable at a calculated change rate of 0.0 m/year. The average shoreline position change along the entire monitored section of Cumberland Island was 0.3 m/year of progradation.

The shoreline position for each annual survey relative to the July 1988 shoreline is presented in Figure 115 and Table 28. There is a trend of alternating advancement and recession for the Stafford Shoal compartment. During the August 1991 - April/May 1992 period, an absolute recession of 9.4 m resulted in a shoreline position 5.5 m landward of the July 1988 shoreline and an average rate over the entire monitoring period of -1.4 m/year. There is also an alongshore undulation in the shoreline position. Within any given year a one- or two-profile sequence will advance, while the zone immediately south (downdrift) is recessional (Figure 115, Appendix D). Local zones of short-term shoreline advancement occurred at Lines C1, C2, C7, C11, and C12 in 1990; Lines C1, C2, C6, and C11 in 1991; and Line C2 in 1992 in the Stafford Shoal compartment. This trend is characteristic of a shore which receives its primary littoral supply

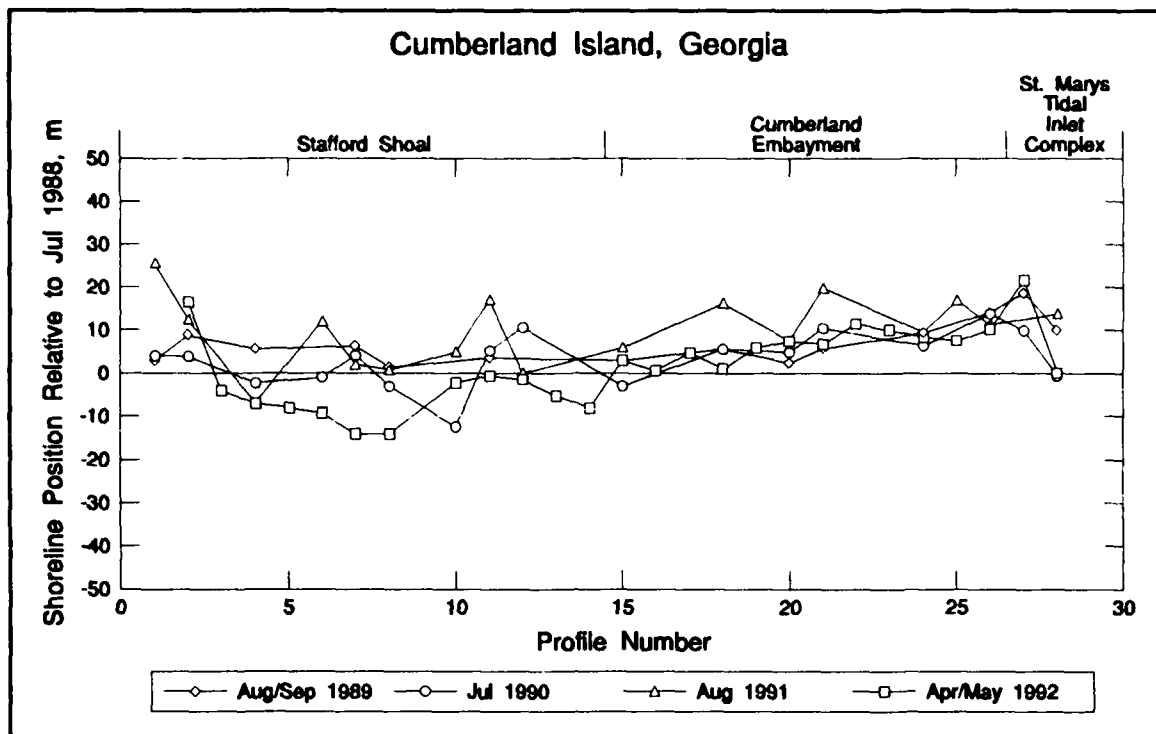


Figure 115. Shoreline positions relative to the Jul 1988 shoreline, Cumberland Island

through the periodic influx of sand masses which then migrate alongshore as a salient or bulge in the shoreline. Sediment storage and release cycles of shoals in the ebb delta complex at St. Andrew Sound influence the Stafford Shoal compartment littoral supply and morphodynamic character (Chapter 3). The annual trend of shoreline movement for the Cumberland Embayment is very uniform, with gradual and consistent advance.

### Amelia Island

The shoreline position change pattern along Amelia Island is inconsistent, as are the volume changes, due to the influence of the many beach fill placements during the monitoring period (Figure 116, Table 29). The North Amelia Platform compartment (Lines A16-A28) shoreline position retreated at an average rate of 3.2 m/year from July 1988 to April/May 1992, while in the Amelia Embayment the shoreline advanced seaward at a rate of 1.6 m/year during the monitoring period. However, within both compartments there were local zones of significant shoreline advance and retreat. An example of this alongshore reversal occurred in Amelia Embayment between Lines A49 and A55, where the shoreline position change shifted from 3.2 m/year of retreat to 7.7 m/year of advance, respectively (Figure 116, Table D14). The high rate of shoreline advance in the southern portion of Amelia Embayment (Lines A55-A58) was the result of a major beach fill (up to 825,770 cu m) placed July 1988 - July 1989 (Table 27). Near the southern boundary of Amelia Embayment, the shoreline position trend reversed again to continuous retreat through the Nassau Sound Tidal Inlet Complex compartment (Lines A60-A73). The highest average annual recession in the entire study area occurred in the Nassau Sound Tidal Inlet Complex compartment with a rate of 4.6 m/year (Table 29). The average shoreline position change rate for Amelia Island was 0.2 m/year during the monitoring

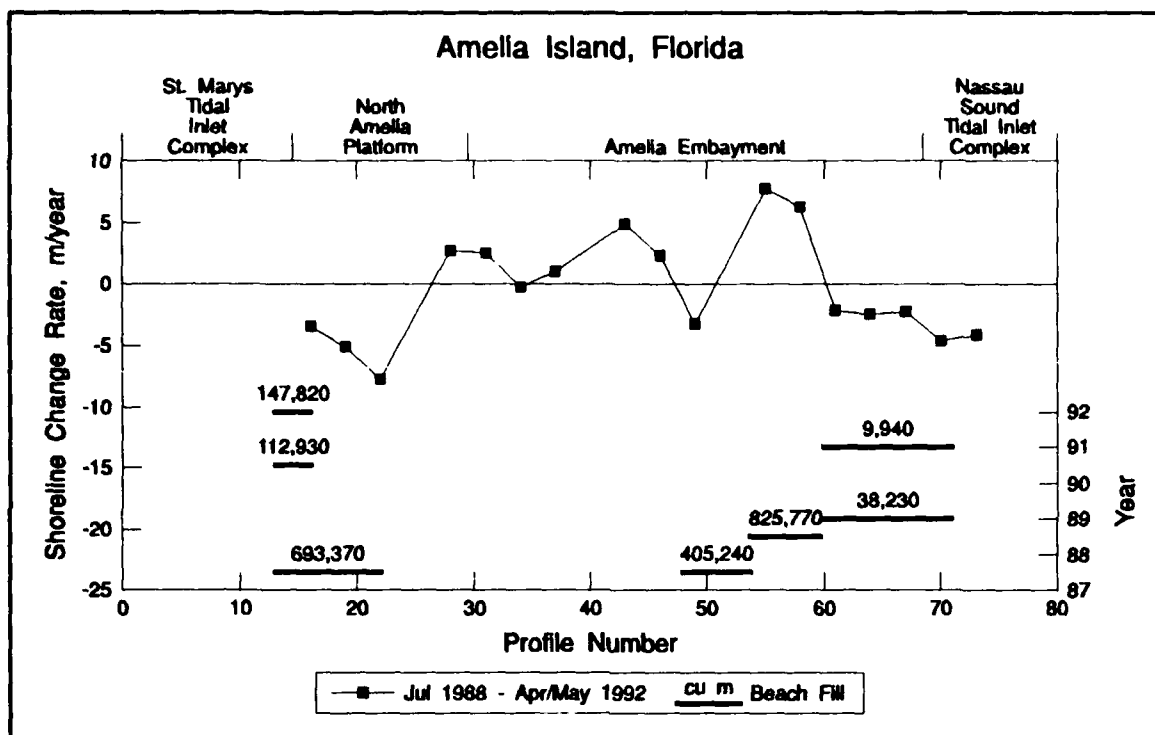


Figure 116. Shoreline change rates (m/year), Jul 1988 - Apr/May 1992, Amelia Island

period, which is comparable to the 0.3 m/year advance on Cumberland Island. In comparison to the historical trends (Chapter 3), the shoreline change rates during the monitoring period were similar for Cumberland Island, but Amelia Island showed advance instead of the historical recession.

Major patterns of annual advance or retreat of the shore are primarily controlled by the timing of the survey relative to beach fill placement operations, resulting in alongshore fluctuations of the shoreline position (Figure 117). See *Trend Analysis and Implications of Recent Engineering Activities* section for additional discussion on beach fill activities.

## Seasonal Variability

Changes to the beach brought about by seasonal variations in wave climate must be considered in interpreting and quantifying trends in the shoreline and beach profile characteristics. Variations in wind and wave forcing produce a cyclical change in the shoreline position throughout the year. In calculating shoreline position change over time, most reliable results are obtained by comparing surveys made in the same season, particularly if the time interval between surveys is relatively short (less than approximately 10 years). Shoreline position may also be strongly influenced by storms. As discussed in Chapter 6, the study area was influenced by varying sequences of storm events, with the last year of the monitoring period (1991) having the highest occurrence of storm events (waves exceeding 2 m).

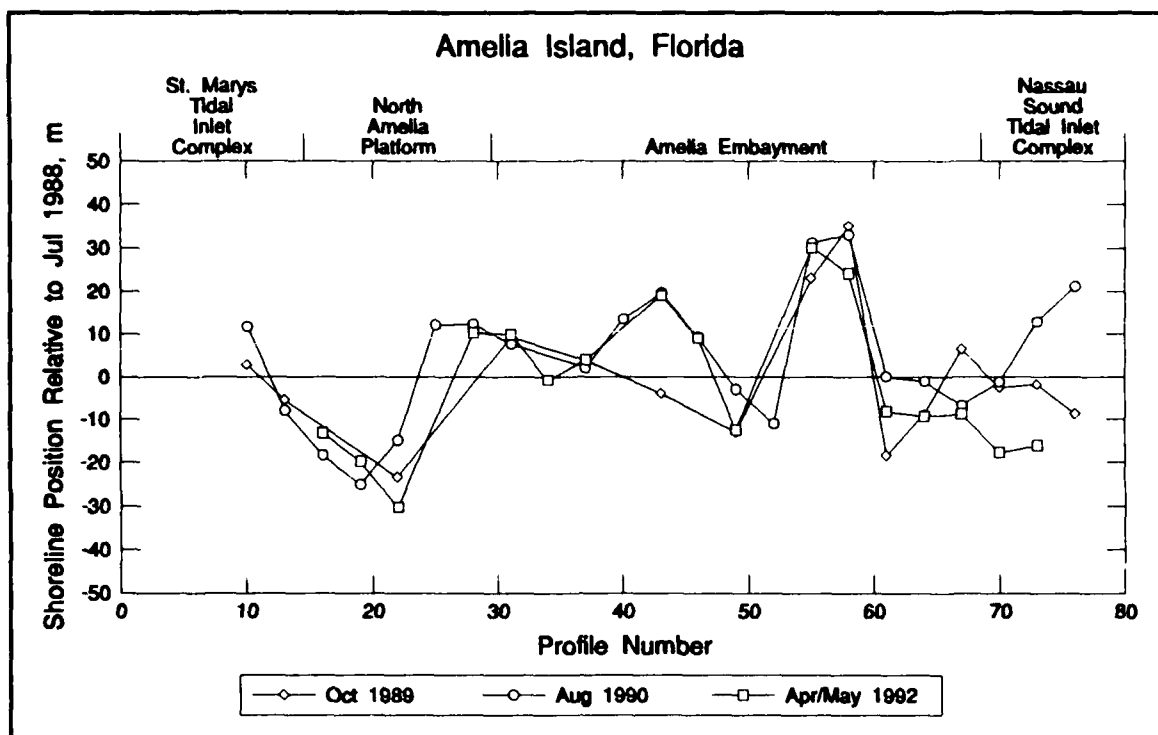


Figure 117. Shoreline positions relative to the Jul 1988 shoreline, Amelia Island

As is typical of most open-coast beaches, sediment at the project site moves offshore during winter months of higher and steeper waves, and may be stored in bars in the subtidal zone. During summer months of lower and less steep waves, sediment migrates onshore from the surf zone, welding onto the berm. In addition to cross-shore sediment movement, seasonal-dependent longshore movement also occurs due to shifts in incident wave direction, causing longshore transport rates and direction to change. Seasonal changes on the beaches along Cumberland and Amelia Islands include berm building during the summer and escarpment of the berm and dune during the winter months, as shown in Figures 118 (Line C8) and 119 (Line A43). In particular, along the Nassau Sound Tidal Inlet Complex, dune escarpment is prevalent, as illustrated in Figure 120 (Line A73), during fall and winter storms when higher water levels cause the waves to reach the base of the dunes.

The berm crest represents the approximate limit of storm wave runup. At about elevation 2.0 m (NGVD), a pronounced berm crest typically appears along the Cumberland Island beach (Figure 118), except at the southern terminus of the island where a wide, relatively flat upper beach with no distinct berm is prevalent. Because of repeated beach-fill placement, the natural berm crest on Amelia Island is difficult to identify. During the monitoring period, the berm crest, which follows the edge of the beach fill, was located between 3.0 and 4.0 m (NGVD). In areas without beach fill, the natural berm crest appears to be between 2.0 and 3.0 m (NGVD) (Figures 119 and 120). On the lower part of the profile in the surf zone, sandbars typically migrate onshore and offshore between the summer and winter profiles.

Seasonal variability was calculated as the winter (later) shoreline position minus the summer (earlier) shoreline position. Examples of calculated shoreline change between winter and summer

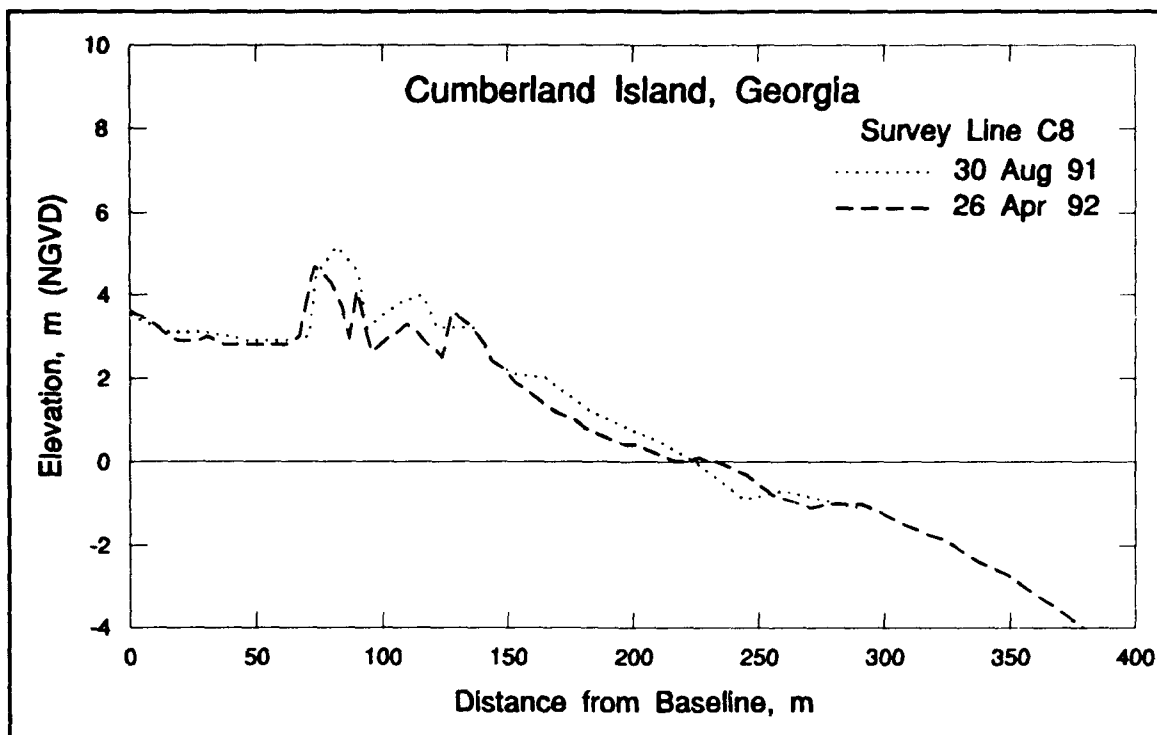


Figure 118. An example of berm crest (about elevation 2.2 m NGVD) and escarpment during winter in the Stafford Shoal compartment

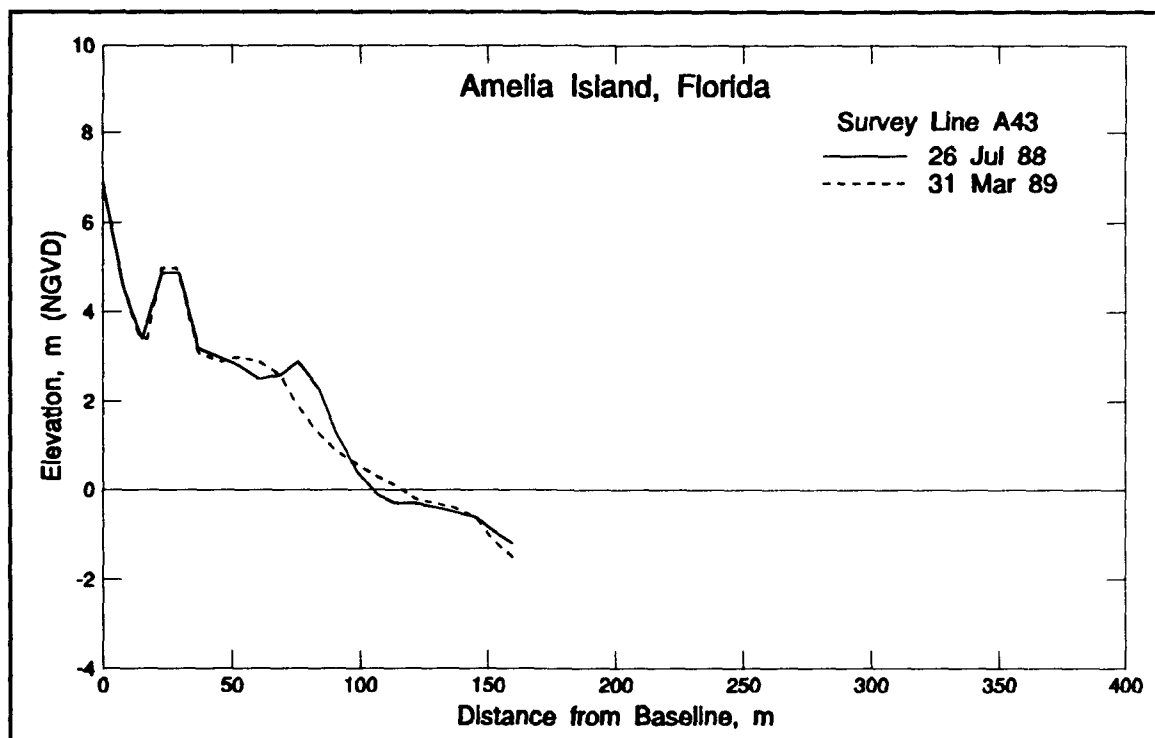


Figure 119. An example of bar formation in the winter and welding onto the beach (advancing the berm) in the summer

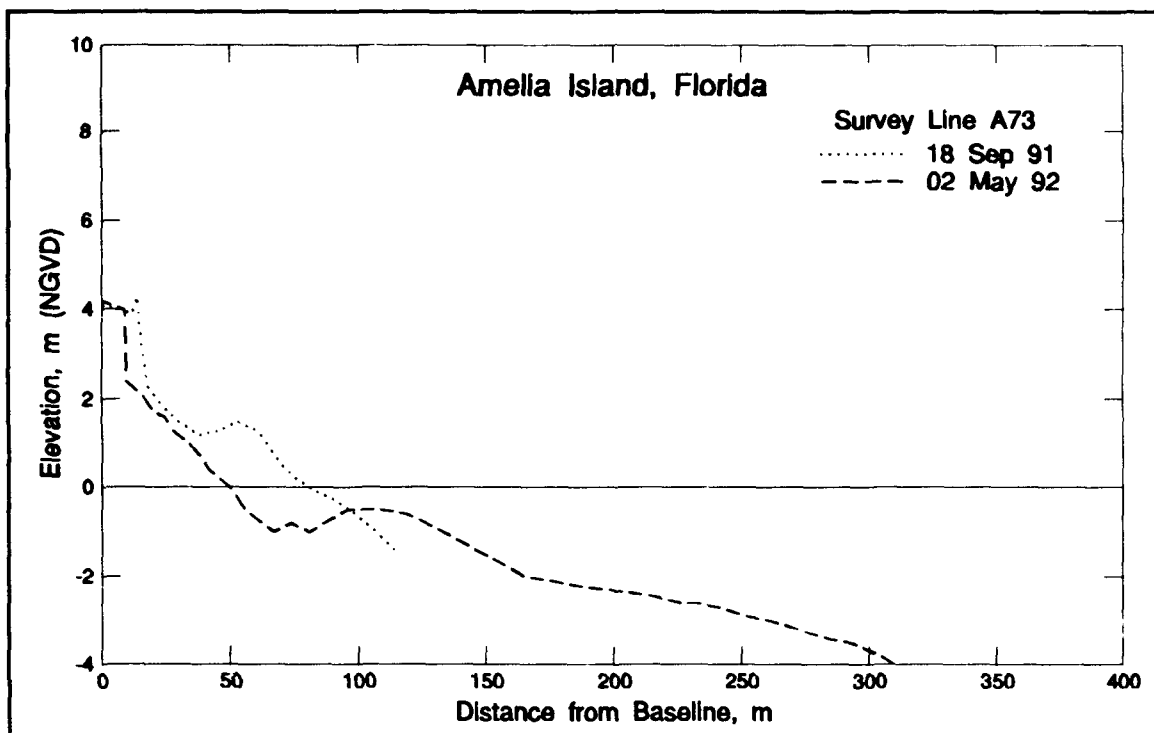


Figure 120. Dune escarpment and retreat along Line A73 in the Nassau Sound Tidal Inlet Complex compartment

pairs of surveys for the 1.3- and 0.0-m (NGVD) contours are listed in Table 30. Differences in contour position for the 1.3-m shoreline and the NGVD intercept varies in magnitude and direction, indicating change in beach profile slope between seasons. The beach face in Figure 118 moved approximately in parallel with itself, with a crossing point near the NGVD intercept. In comparison, the beach face in Figure 119 crossed above the NGVD intercept, with the summer profile having a prominent berm, while the winter profile was steeper and included a distinctive bar. These profiles exhibit typical seasonal morphologic behavior. Shoreline position change for the Cumberland Island profile (Figure 118) is calculated as -14.8 and -6.7 m for the 1.3- and 0.0-m elevations, respectively, during the August 1991 to April/May 1992 comparison. Shoreline position change for the two Amelia Island profiles (Figures 119 and 120) is calculated as -7.0 and 11.3 m and as -33.0 and -31.3 m for the 1.3- and 0.0-m elevations, respectively, during the July 1988 to May 1989 comparison. A summary of all winter-summer profile survey pairs is given in Appendix D, Table D19.

Generally, values of average shoreline position change are predominantly negative, indicating the expected recession of the profile from summer to winter (Table 30). In considering this seasonal variability, it is often observed that the profile does not translate landward and seaward in parallel to itself, but typically changes slope across the beach face. The average absolute variability in the shoreline position due to short-term seasonal fluctuations, considering the limited number of comparable surveys, is calculated as 13.6 m (Table D19).

**Table 30****Selected Seasonal Change in Contour Position at Elevations 1.3 and 0.0 m (NGVD)<sup>1</sup>**

Profile Line No.	Elev. 1.3 m	Elev. 0.0 m	Elev. 1.3 m	Elev. 0.0 m
<b>Cumberland Island</b>				
	<b>Jul 1988 - Mar 1989</b>		<b>Aug 1991 - Apr/May 1992</b>	
C8	-- <sup>2</sup>	--	-14.8	-6.7
C11	15.7	-25.0	-17.7	-33.0
C15	--	--	-3.0	2.0
C20	-2.0	-14.0	-0.2	-9.0
<b>Amelia Island</b>				
	<b>Jul 1988 - May 1989</b>		<b>Sep/Nov 1991 - Apr/May 1992</b>	
A13	-7.7	-6.0	--	--
A19	-12.3	-8.4	--	--
A43	-7.0	11.3	17.0	-2.7
A73	-33.0	-31.3	--	--
A79	-100.0	-30.0	--	--

<sup>1</sup> See Table D19 for a complete listing of survey pairs exhibiting seasonal change.<sup>2</sup> No data available.

## Sediment Samples

The July 1988 and April/May 1992 beach and nearshore sediments consist of predominantly well-sorted, fine to medium sands for Cumberland and Amelia Islands. There are distinct grain-size differences between the fine sands along Cumberland Island (mean of 0.18 mm) and the medium sands along Amelia Island (mean of 0.31 mm). Cross-shore textural variations from the dune line to the nearshore zone exhibit typical trends, where the grain size becomes finer landward of MHW and also seaward of the surf zone or nearshore bar (Bascom 1959, Davis 1989). The coarsest material was found on the lower foreshore along MLW. Sorting (as calculated from the standard deviation of the grain size distribution) follows the same pattern as the dune sands which are predominantly better sorted than those on the beach (between berm and MLW). The nearshore is generally better sorted and finer than the beach. However, the nearshore has samples that are poorly sorted due to coarse sand patches and shell debris. In addition, the cross-shore sediment distribution, within each morphologic compartment, is variable as described below for each island.

### Cumberland Island

Cumberland Island, a natural barrier island system, is characterized by a flat beach face and a shallow, gentle cross-shore bathymetric gradient. Surficial sediments for Cumberland Island

consist of uniform, well- to very well-sorted, unimodal, positively skewed sands. Figures 121 and 122 show the spatial trends for representative beaches sampled at MHW and nearshore sediments sampled at 4.5-m depth, respectively. Temporally, the mean grain size of the beach (berm crest, MHW, and MLW) was relatively uniform for Cumberland Island. The overall mean grain size of the beach for Cumberland Island is 0.16 mm for 1988 and 0.18 mm for 1989, 1990, and 1992. The mean grain size along Cumberland Island decreases slightly from north to south within the Stafford Shoal compartment. From the Cumberland Embayment to the north jetty the mean grain size increases slightly. A surface lag deposit of slightly coarser, poorly sorted sediments may be trapped adjacent to the north jetty (Line C28). The beach mean grain size of Line C28 was 0.19 mm (April/May 1992 sample). Along northern and central Cumberland Island, the beach and nearshore zone sediments exhibited no major cross-shore trends within the morphologic compartments. Other grain-size parameters, such as standard deviation, skewness, and kurtosis, were also evaluated (Appendix D). Samples across the profile and alongshore showed a weak grouping, as evidenced by the scatter plot of standard deviation (sorting) versus mean grain size shown in Figure 123 for the April/May 1992 sample set. The beach sands were coarser and more coarsely skewed than the nearshore sands. Coarser (i.e. MLW) samples were more poorly sorted than finer (i.e. berm) samples. Nearshore samples had no such relationship to sorting, probably due to the shell lag deposits on the nearshore shelf.

As with most of the southeastern coast, the subaerial beach along Cumberland Island is fine-grained and well-sorted, which is indicative of a stable beach. No beach fills have been placed on Cumberland Island, and the only structure is the jetty adjacent to St. Marys Entrance. The primary sources of beach sand are the St. Andrew ebb-tidal delta located offshore of the northern end of the island and the dune headland area located near central Cumberland Island. Winds and

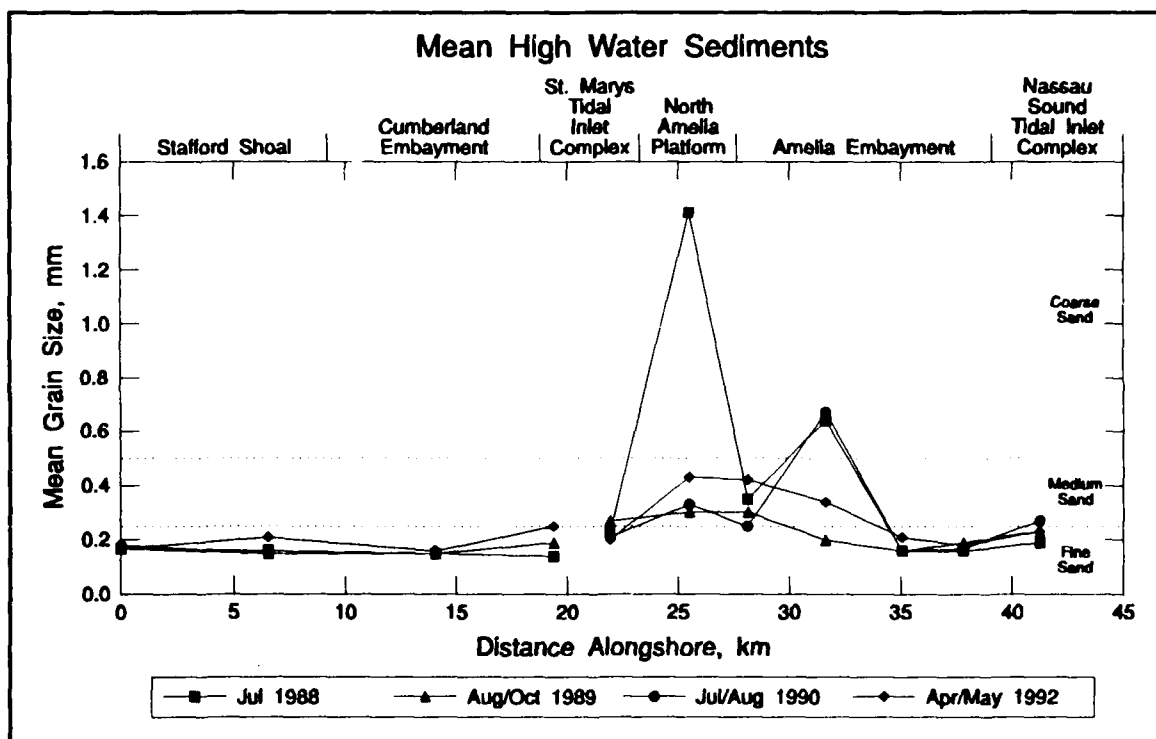


Figure 121. Mean grain size for MHW sediment samples

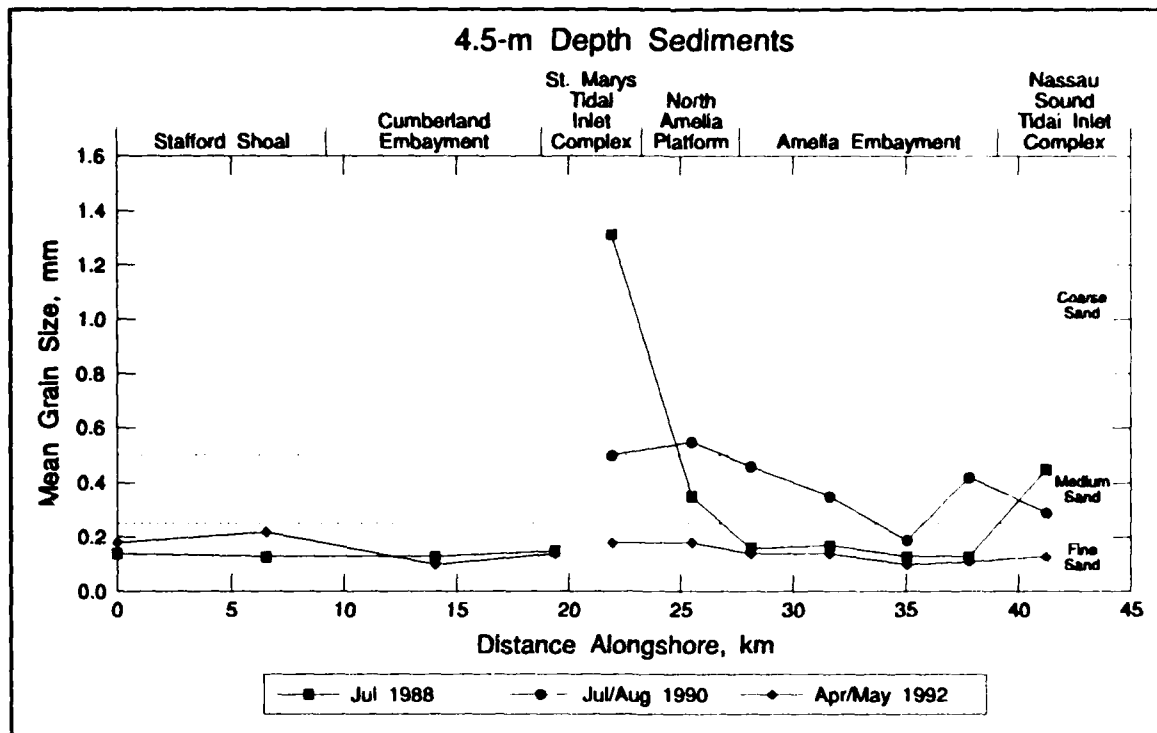


Figure 122. Mean grain size for 4.5-m (NGVD) depth sediment samples

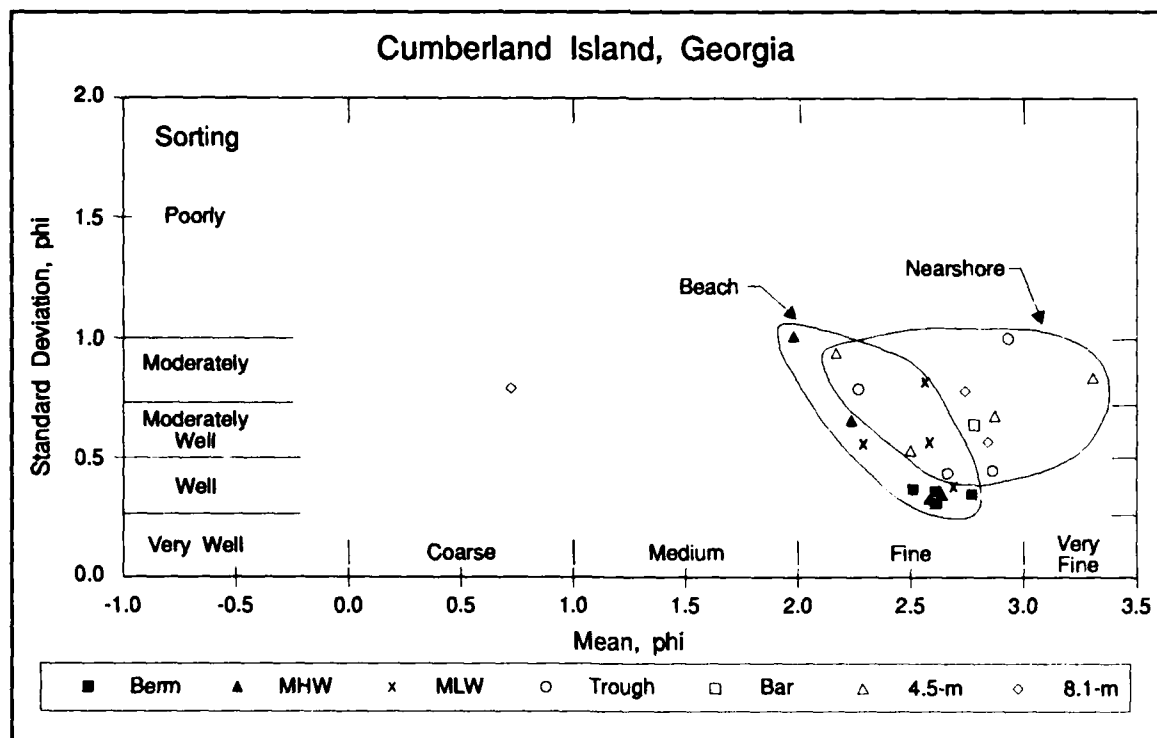


Figure 123. Scatter plot of standard deviation (sorting) versus mean grain size for Cumberland Island, 1992

winter storms remove material from the dune area and transport the sediment to the adjacent beach zone. The nearshore along Cumberland Island is shallow and gently sloping which is typical of a fine-grained, low-energy environment. Longshore currents in the nearshore zone move large quantities of sediment south (Chapter 3) from the St. Andrew ebb-tidal delta and Stafford Shoal.

Beach composites were compiled based on berm crest to MLW, as plotted in Figures 124 and 125 for Cumberland Island. The samples are predominantly fine with minor amounts of medium to coarse sands. The medium to coarse sand size fraction is derived in large part from sands sampled at MLW where medium and coarse material settles from the interaction of backwash with incoming surf. Comparison of the 1988 and 1992 beach composites verifies the uniformity of the fine beach sands. An exception to this uniformity occurred at Line C28, where the average varied between a mean grain size of 0.13 mm in 1988 and 0.19 mm in 1992.

### Amelia Island

Amelia Island sediments have a more variable grain size than those of Cumberland Island, being moderately to poorly sorted, coarser grained, and less skewed. For the sampled years, the overall mean grain size for the beach on Amelia Island is 0.35, 0.31, 0.37, and 0.31 mm for 1988, 1989, 1990, and 1992, respectively. The alongshore trends of the beach using MHW and of the nearshore zone using a 4.5-m (NGVD) depth are shown in Figures 121 and 122. The narrower nearshore platform and the exposure to a slightly higher wave energy contribute to the coarser and more varied sediment distribution pattern on Amelia Island. Alongshore trends of natural grain-size variability within the defined morphologic compartments are masked by

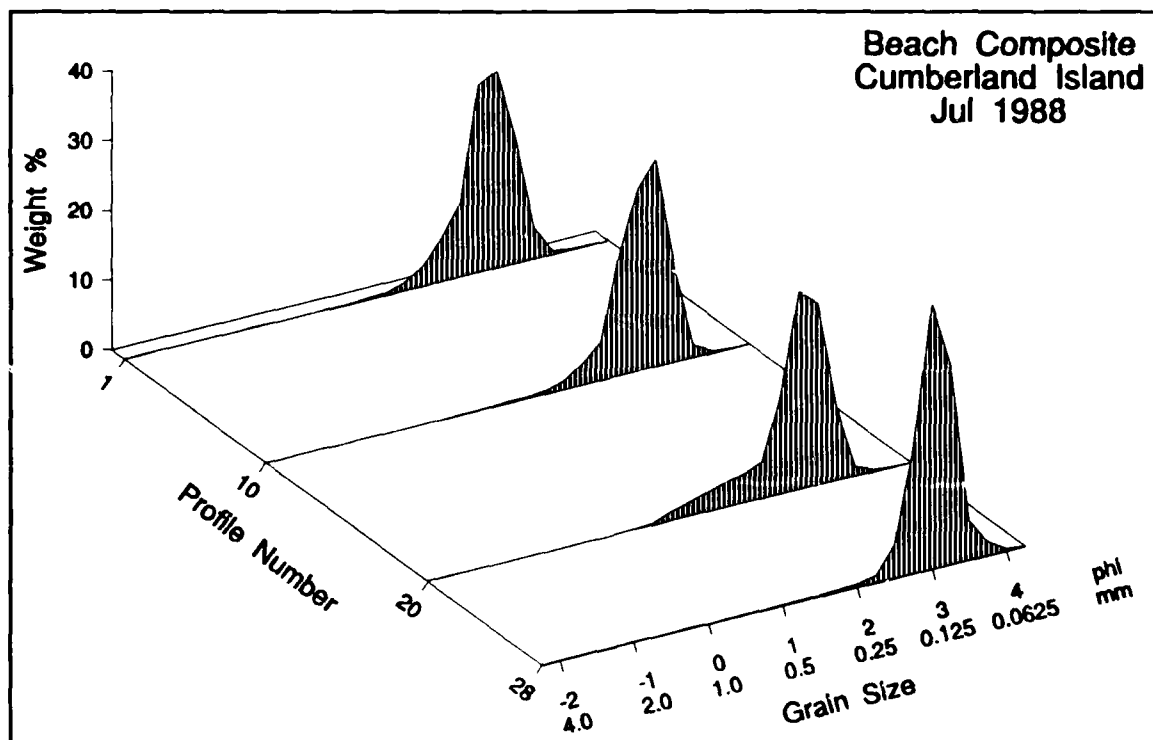


Figure 124. Beach composites, Jul 1988, Cumberland Island

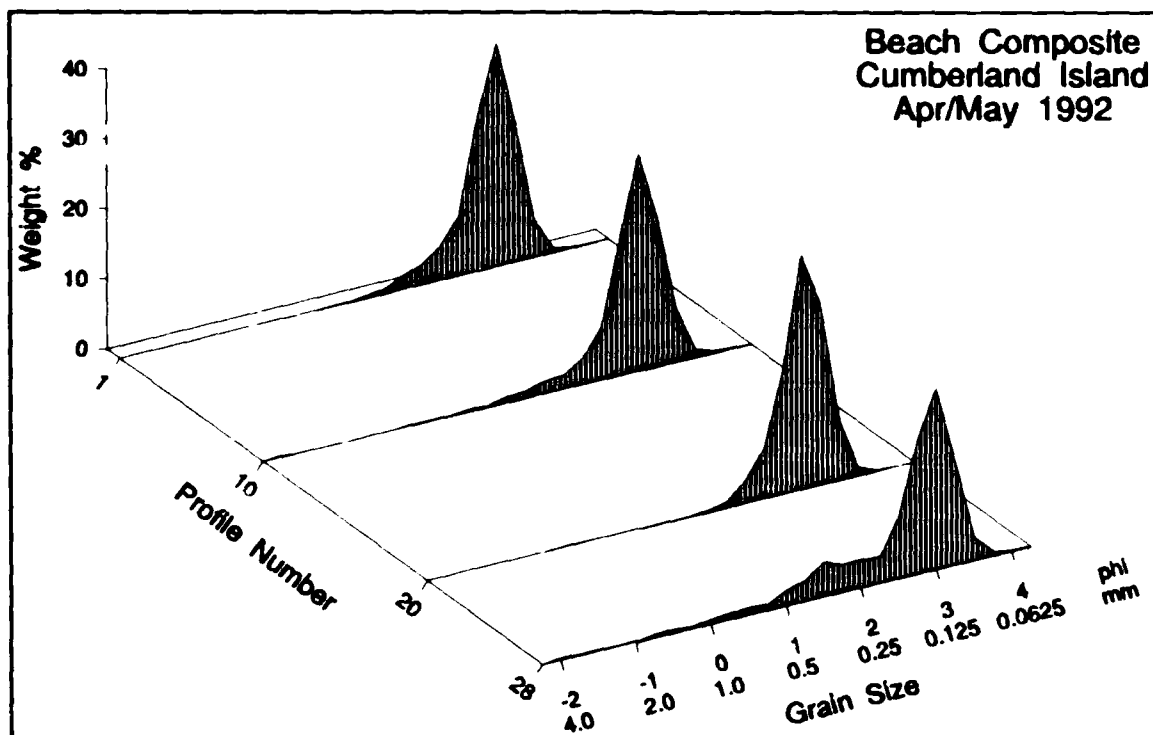


Figure 125. Beach composites, Apr/May 1992, Cumberland Island

11 beach fills placed at different times and locations between 1978 and 1992 in three separate zones of Amelia Island. Hence, the sediment distribution pattern is highly variable along the sampled profile survey lines. A comparison of mean grain size and sorting for the April/May 1992 sediment sample set shows wide variance in beach data (berm, MHW, and MLW), due to the addition of beach fills in the north (Lines A13-A22), south-central (Lines A48-A60), and south (Lines A60-A71) areas prior to sampling. The coarser means correspond generally to the more poorly sorted fill material which included shell. The nearshore samples cover a finer range in means with a wide range of sorting values (Figure 126).

Along Amelia Island, the beach composites have a large range in grain-size distribution. As shown in Figures 127 and 128, most samples have a multi-modal distribution. Samples with a distinct coarse fraction included Lines A22, A31, and A43. Sampling of these lines in July 1988 occurred just after two major beach fill placements. At both ends of the island, the sediments are finer, although the alongshore trend is variable.

An additional five beach fills were placed along Amelia Island prior to the April/May 1992 sediment sampling. Fills from maintenance dredging of the channel were more poorly sorted, multi-modal sediment which contained coarse-grained shell material, as is evident in the beach composite samples from the north and central lines on Figure 128. Again, Lines A10 and A76 at both ends of the island have a better sorted, finer beach composite distribution than the samples collected from the central part of Amelia Island (Lines A22-A55).

In several areas, atypical coarse sands were found in the nearshore (trough, 4.5- and 8.1-m depths). The samples along Lines A22, A31, and A43 show an abundance of whole and

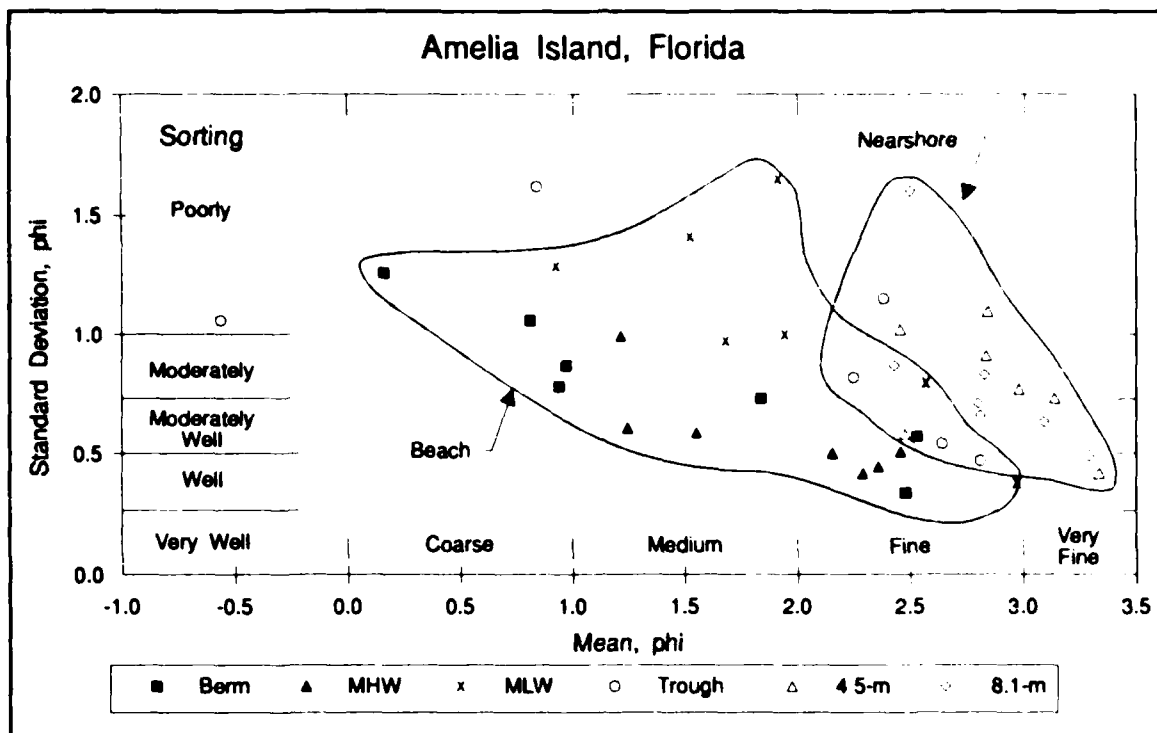


Figure 126. Scatter plot of standard deviation (sorting) versus mean grain size for Amelia Island, Apr/May 1992

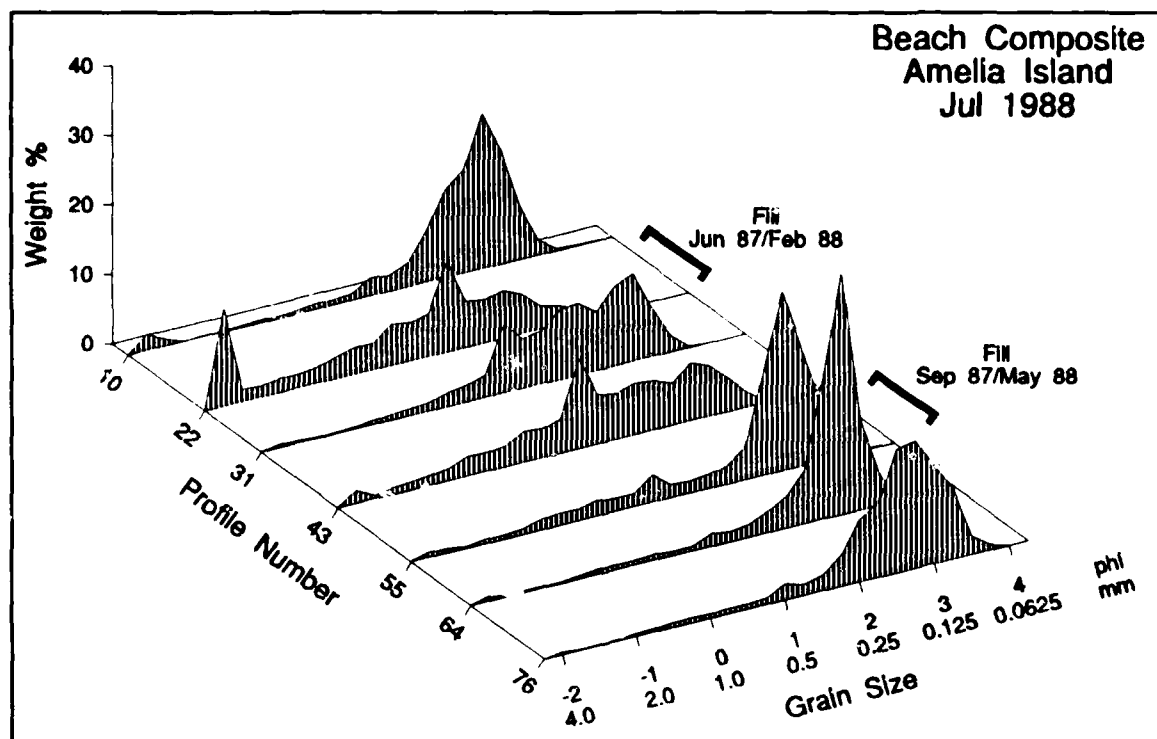


Figure 127. Beach composites, Jul 1988, Amelia Island

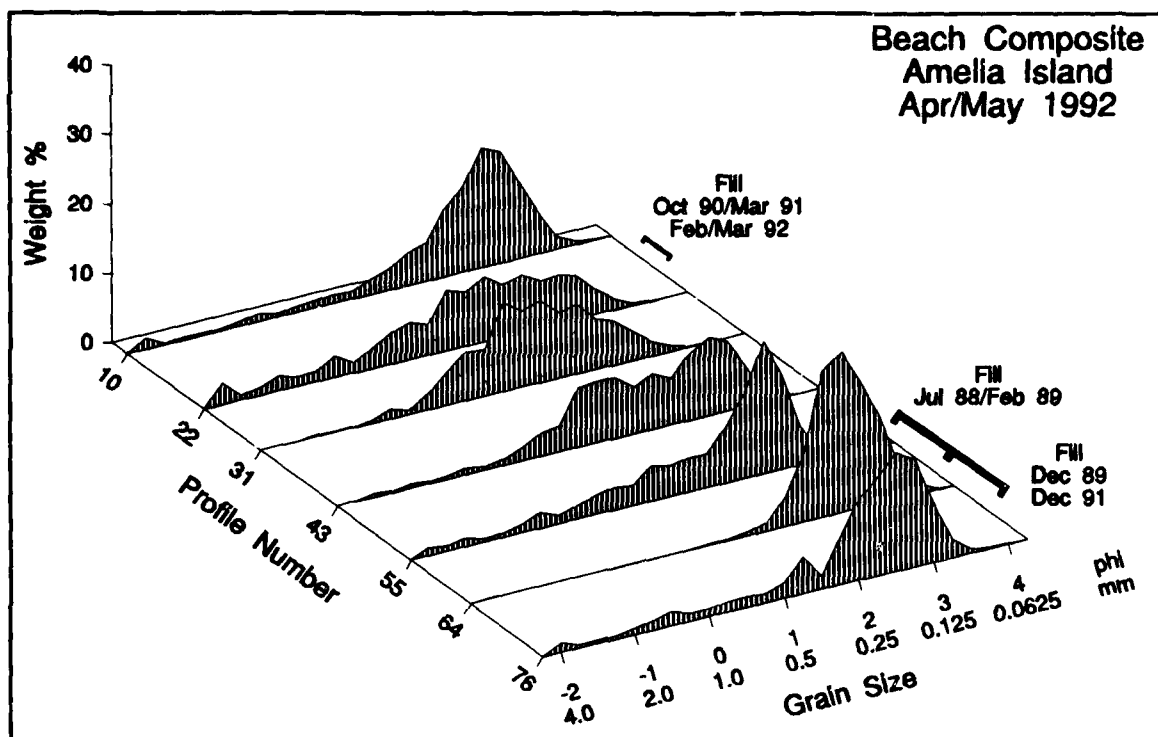


Figure 128. Beach composites, Apr/May 1992, Amelia Island

fragmented shells. The lithologic fraction of these samples is micaceous, dark grey, fine-to-very fine quartz sands and silts, which is the dominant texture of the inner shelf. The biogenic fraction appears to be from several shallow-water mollusk species (ranging from 1 to 6 mm in width) and in some cases are relict shells reworked from previous deposits. Shoal bars along the southern end of Amelia Island (Line A76 at 4.5-m depth) consist of light tan, medium sands with abundant shell fragments indicative of high wave energy conditions. Typically, the relict shells are black as a result of burial under reducing conditions in fine sediments. These shells originated in nearshore and estuarine environments formed during the last transgression (Pilkey et al. 1969).

Since 1978, 11 beach fills placed along Amelia Island contributed to the presence of medium and coarse material in the multimodal grain-size distribution (Table 27). Most of the native beach has been influenced by sand from beach disposal of dredged material from the navigation channel. The majority of beach fill material was placed along the northern and central portion of Amelia beginning in November 1978. Similar to the surficial beach samples, grain-size analysis of core borings of the dredged sections of St. Marys Entrance channel characterized the inlet material as poorly graded, fine-to-medium quartz sands with abundant shells (USAED, Jacksonville 1993). Silt content ranged from 1 to 7 percent. Field observations and grain-size analysis indicate the fill material is responding to local wave and storm conditions with a dominant fining offshore.

In summary, the beach and nearshore sediments along Cumberland and Amelia Islands are predominantly fine-to-medium sands with varying amounts of shell fragments. Along the Cumberland Island coast, the beach zone (berm to MLW) consists of uniform, fine, well-sorted

sand. St. Marys Tidal Inlet Complex and Amelia Island have moderately to poorly sorted, medium sands along the beach zone. The beach fill material on Amelia Island consists of medium sands and abundant shell material dredged from St. Marys Entrance channel. The fill generally appears to adjust with a dominant fining offshore. Alongshore there was significant variability because of the multiple beach fills (1978-1992) before and during the monitoring period. The coarser sediments were found along northern Cumberland Island and Amelia Island and in sporadic patches offshore in depths ranging between 4.5 and 8.1 m (NGVD). These medium and occasionally coarse sands are dominated by abundant shell material from shallow-water and relict mollusk shells. Nearshore samples consist of predominantly fine, quartz sands and silts.

## Morphologic Compartments

This section summarizes the general geomorphic features and measurable characteristics for the beach and nearshore areas of each morphologic compartment (Figure 35), including the beach and subbottom topography, inner bar position, and slope gradient (Tables 31 and 32). Figures 129 and 130 present the inner bar position and crest elevation for each island, and Figure 131 presents the relationship between mean grain size (mm) and beach slope. Beach and nearshore measurements in the following discussion represent primarily averages from the July 1988 and April/May 1992 data sets.

### Stafford Shoal (Lines C1-C14)

The Stafford Shoal compartment is dominated by a large dune complex and a broad offshore shoal platform (Figure 132). The beach is backed by a three-ridged barrier dune. Dune crest elevations range from 3.8 to 7.5 m (NGVD). The highest dunes of the study area are found in this compartment. The most seaward set of dunes, or foredunes, are linear with steep windward and leeward slopes. Prevailing south-southeast winds developed these rapidly migrating transgressive dunes. This local dune ridge complex is a significant sediment source and sink for this compartment. Beach width varies seasonally although the average beach width of the compartment is consistent, ranging between 79.5 m during the summer (July 1988) and 80.4 m during late winter (April/May 1992) (Table 31). The gently sloping beach face is fine-grained, with an average beach grain size of 0.18 mm and an average gradient of 1.4 to 1.7 deg over the monitoring period (Table 31).

The 1992 sled survey data revealed significant variability in the inner bar position and crest elevation along this compartment. Noteworthy is the lack of an inner bar near Stafford Shoal, a zone of volumetric and shoreline position stability (i.e. the Stafford Shoal axis) (Lines C10-C11). There is a trend for the bar crest elevation to become shallower from the north to the axis, and then the trend reverses to an increase in bar depth south to Line C24 (Figure 129). The inner bar distance averages 64.6 m seaward from the 0.0-m NGVD elevation.

The nearshore bathymetry of this compartment is extremely variable due to the Stafford Shoal complex. Seismic records indicate that Stafford Shoal is underlain by thick sand deposits which may represent antecedent headland topography (McLemore et al. 1981, Hayes 1980, McBride and Moslow 1991). Multiple sand ridges, separated by fine-grained swale features, dominate the surface bed forms. The shoal bars have a relief above the seafloor ranging from 0.5 to 3.0 m

**Table 31**  
**Summary of Sediment Grain Size and Profile Parameters for Cumberland Island<sup>1</sup>**

Date	Stafford Shoal C1-C14	Cumberland Embayment C15-C26	St. Marys Tidal Inlet Complex C27-C28	Cumberland Island Summary C1-C28
Distance, km				
	9.3	9.6	1.7	20.6
Beach Width, m				
Jul 1988	79.5	111.7	148.0	98.2
Apr/May 1992	80.4	102.0	192.2	95.0
Beach Grain Size, mm				
Jul 1988	0.18	0.17	0.13	0.16
Apr/May 1992	0.18	0.16	0.19	0.18
Nearshore Grain Size, mm				
Jul 1988	0.15	0.13	0.15	0.14
Apr/May 1992	0.17	0.10	0.28	0.18
Beach Face Slope, deg				
Jul 1988	1.4	1.1	0.9	1.2
Apr/May 1992	1.7	1.3	0.7	1.5
Nearshore Beach Slope, deg				
Jul 1988	0.7	0.5	0.6	0.6
Inner Bar Distance, m				
Apr/May 1992	64.6	123.0	47.7	101.6
Inner Bar Crest Elevation, m (NGVD)				
Apr/May 1992	-1.0	-1.6	-0.3	-1.4

<sup>1</sup> See Appendix D for information on number of survey lines used in developing parameters shown.

and parallel the dominant wave direction, with a northeast-southwest orientation. Six nearshore bars and shoal features were surveyed on Line C10 between 0.0 and the 9.0-m depth (NGVD) contour (Figure 132). The nearshore bathymetry along the northern end of Stafford Shoal (Lines C1-C5) contains no large bed forms and is relatively flat (average nearshore slope of 0.7 deg).

#### **Cumberland Embayment (Lines C15-C26)**

Cumberland Embayment is characterized by a fine-grained, arc-shaped shoreline which also has fairly flat beach face slopes averaging between 1.1 and 1.3 deg. In general, the beaches of Cumberland Island have milder slopes and finer sediments than Amelia Island (Figure 133). This compartment contains the finest sediment and is the most gently sloping in comparison with the

**Table 32****Summary of Sediment Grain Size and Profile Parameters for Amelia Island<sup>1</sup>**

Date	St. Marys Tidal Inlet Complex A10-A13	North Amelia Platform A16-A28	Amelia Embayment A31-A67	Nassau Sound Tidal Inlet Complex A70-A79	Amelia Island Summary A10-A79
<b>Distance, km</b>					
	2.0	4.3	11.4	3.0	20.7
<b>Beach Width, m</b>					
Jul 1988	-- <sup>2</sup>	30.4	57.3	68.2	51.9
Apr/May 1992	--	28.3	46.9	58.0	43.4
<b>Beach Grain Size, mm</b>					
1988	0.26	0.81	0.30	0.21	0.35
1992	0.25	0.47	0.30	0.28	0.31
<b>Nearshore Grain Size, mm</b>					
1988	0.74	0.30	0.17	0.29	0.29
1992	0.23	0.16	0.14	0.13	0.15
<b>Beach Slope, deg</b>					
1988	--	3.4	2.2	1.8	2.4
1992	--	4.1	2.8	2.3	3.1
<b>Nearshore Slope, deg</b>					
1988	0.7	1.1	0.6	0.4	0.7
<b>Inner Bar Distance, m</b>					
1992	--	50.6	103.8	96.8	101.3
<b>Inner Bar Crest Elevation, m (NGVD)</b>					
1992	--	-1.1	-1.9	-1.6	-1.8
<sup>1</sup> See Appendix D for information on number of survey lines used in developing parameters shown.					
<sup>2</sup> No data available.					

other compartments. Cumberland Embayment has remained the most stable of all the compartments, with the least amount of change along the profile envelope and between profiles. The coastline in this compartment follows a distinctive arc. This type of beach planform develops typically in the lee of a prominent shoal area, such as Stafford Shoal.

The nearshore portion of the profile consists generally of a featureless bottom (Figure 133) except towards the north jetty. The nearshore slope in this region is the mildest in the study area with an average of 0.5 deg for the compartment. The distance offshore to the inner bar increases toward the central part of the embayment at Line C21 and then decreases to Line C25 (Figure 129). Compared to the rest of the study area, the Cumberland Embayment inner bar is

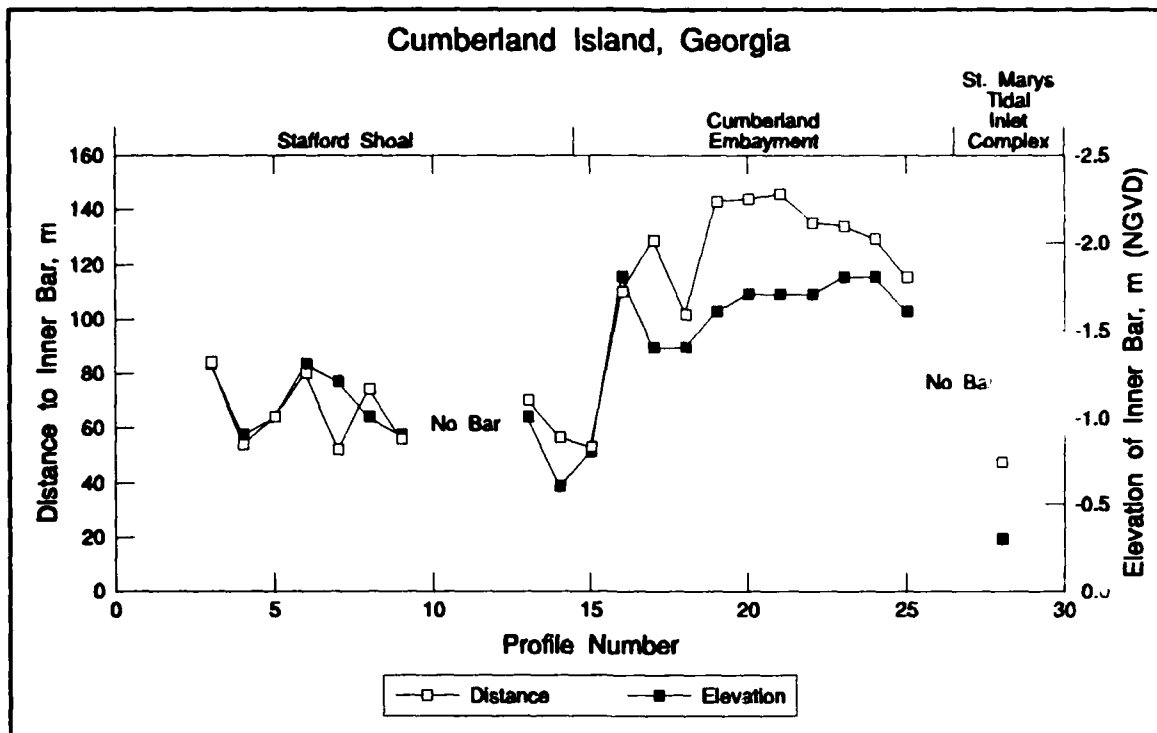


Figure 129. Distance to inner bar from elevation 0.0 m (NGVD) and inner bar crest elevation, Apr/May 1992, Cumberland Island

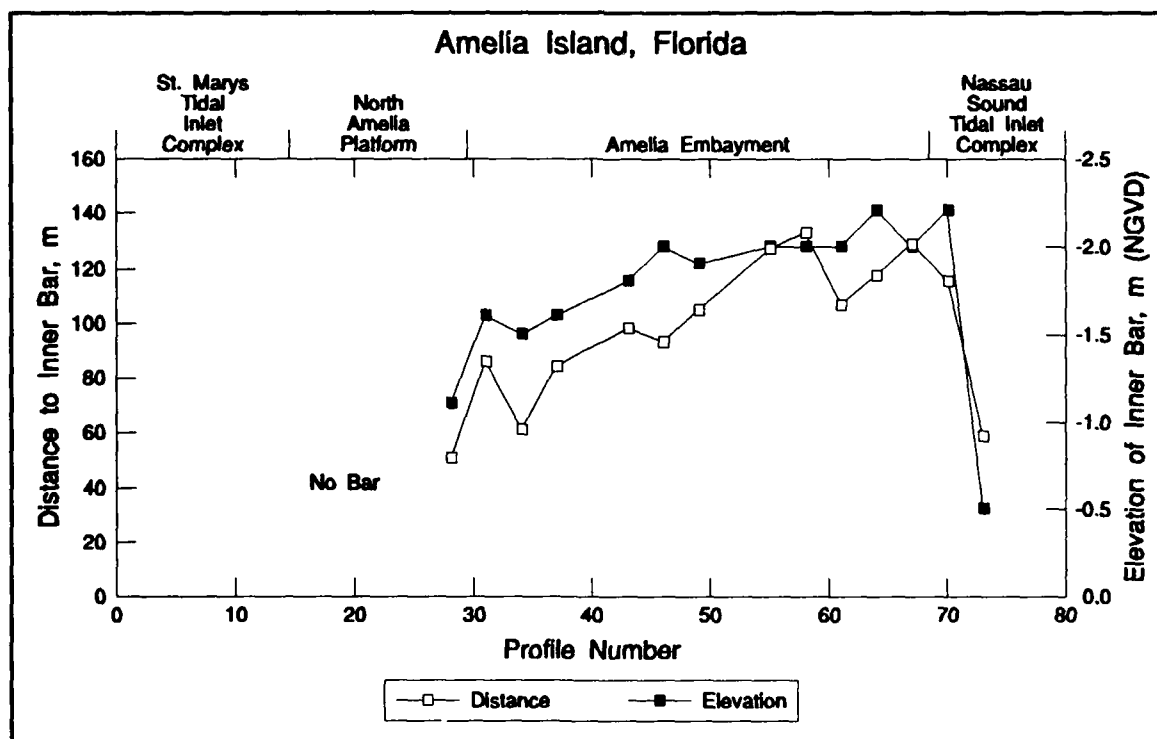


Figure 130. Distance to inner bar from elevation 0.0 m (NGVD) and inner bar elevation, Apr/May 1992, Amelia Island

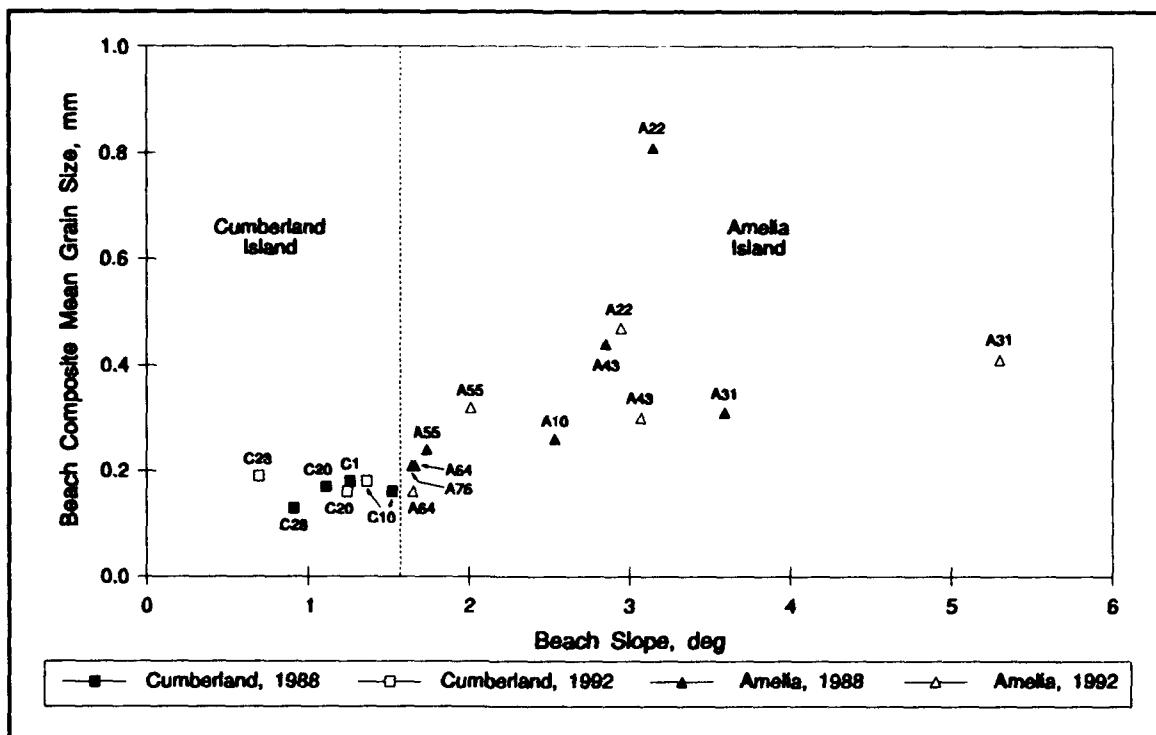


Figure 131. Mean grain size, mm, versus beach slope, deg

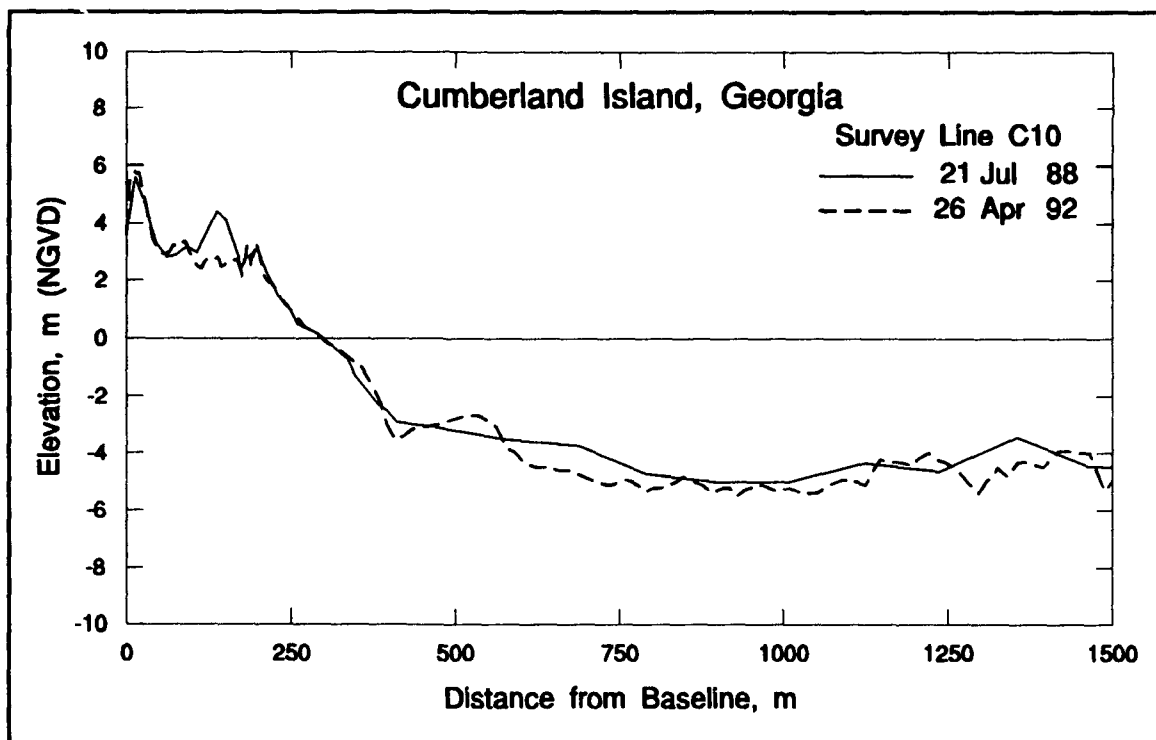


Figure 132. Representative profile comparison, Stafford Shoal

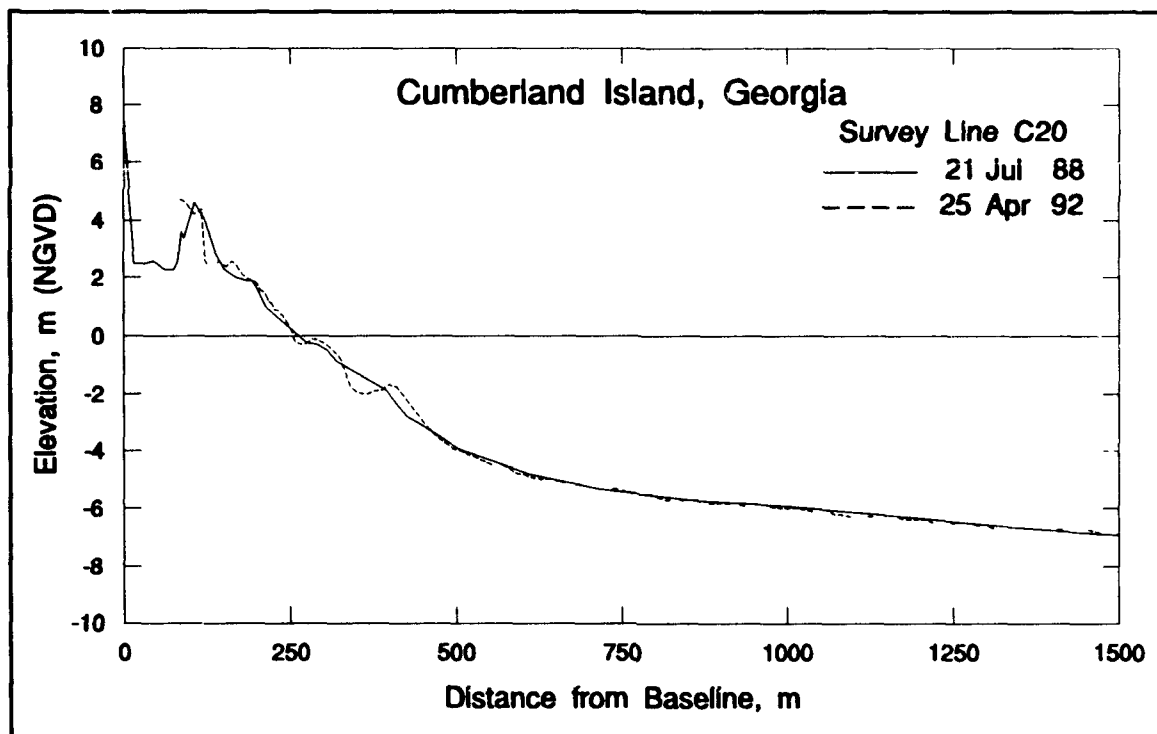


Figure 133. Representative profile comparison, Cumberland Embayment

the furthest offshore (averaging 123.0 m), has the deepest crest elevation (averaging -1.6 m, Table 31), and is also highly consistent throughout the compartment (Figure 129). Cumberland Embayment is characterized by a classical ridge and runnel morphology. The combination of a stable shore, gentle slopes, featureless bathymetry, fine-grained sediments, and an extensive shore-parallel inner bar ridge is frequently found along coasts which have a significant tidal range, but low wave energy (King 1972).

#### St. Marys Tidal Inlet Complex (Lines C27-C28 and A10-A13)

The fillet areas adjacent to and seaward of the north and south jetties on both islands comprise this compartment. The beach and surf zone morphology of this compartment is influenced by an abundant sediment supply, shallow offshore, and tidal inlet currents (Figures 134 and 135). The north fillet located on the updrift side of the Cumberland jetty is a fine-grained sandy beach (mean grain size averaging from 0.13 to 0.19 mm) with a broad (average beach width of 148.0 and 192.2 m), and flat beach face (slope of 0.7 to 0.9 deg) (Table 31). On Amelia Island, the southerly fillet, downdrift of the south jetty, is coarser grained (0.25 mm) (Table 32). The nearshore slope is flat and featureless both immediately north and south of the jettied entrance with average nearshore slopes of 0.6 and 0.7 deg for Cumberland and Amelia Islands, respectively.

In addition to natural changes, beach fill placements have further modified the local beach system along the northern Amelia Island shoreline. Although none of the recent beach fill operations included direct placement of material in this compartment (Table 27), significant quantities of material have been placed immediately south of Line A13. Any updrift (to the

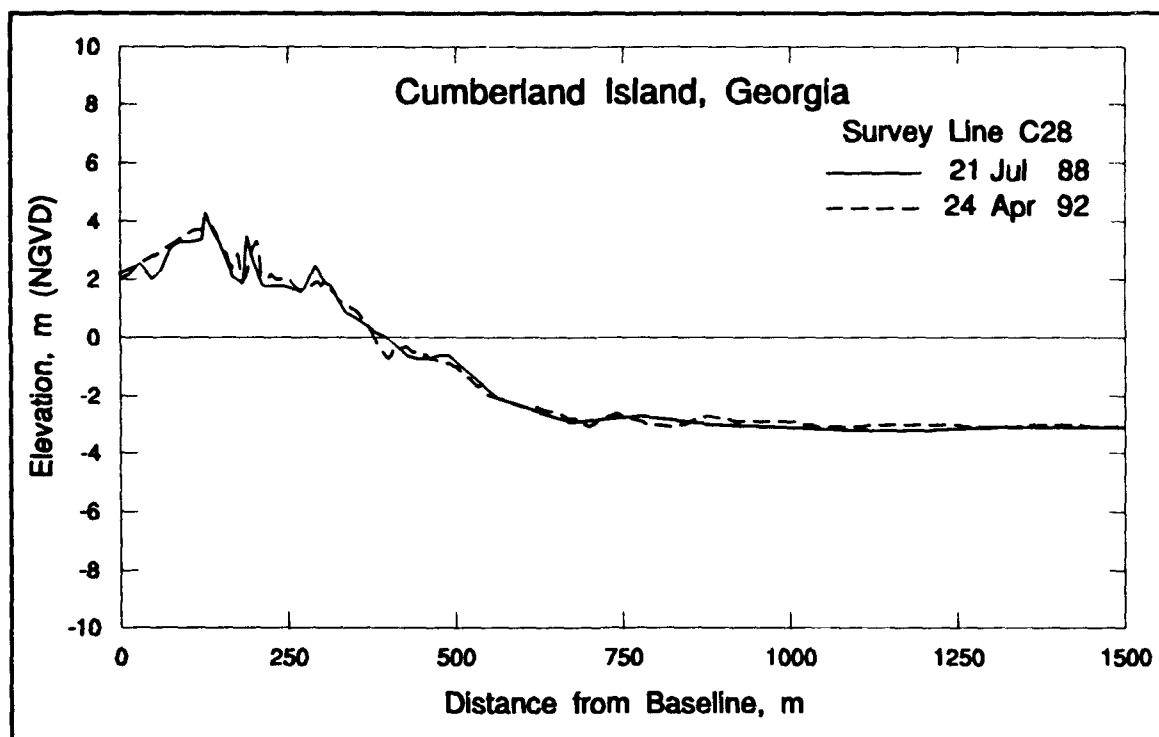


Figure 134. Representative profile comparison, north fillet of St. Marys Entrance

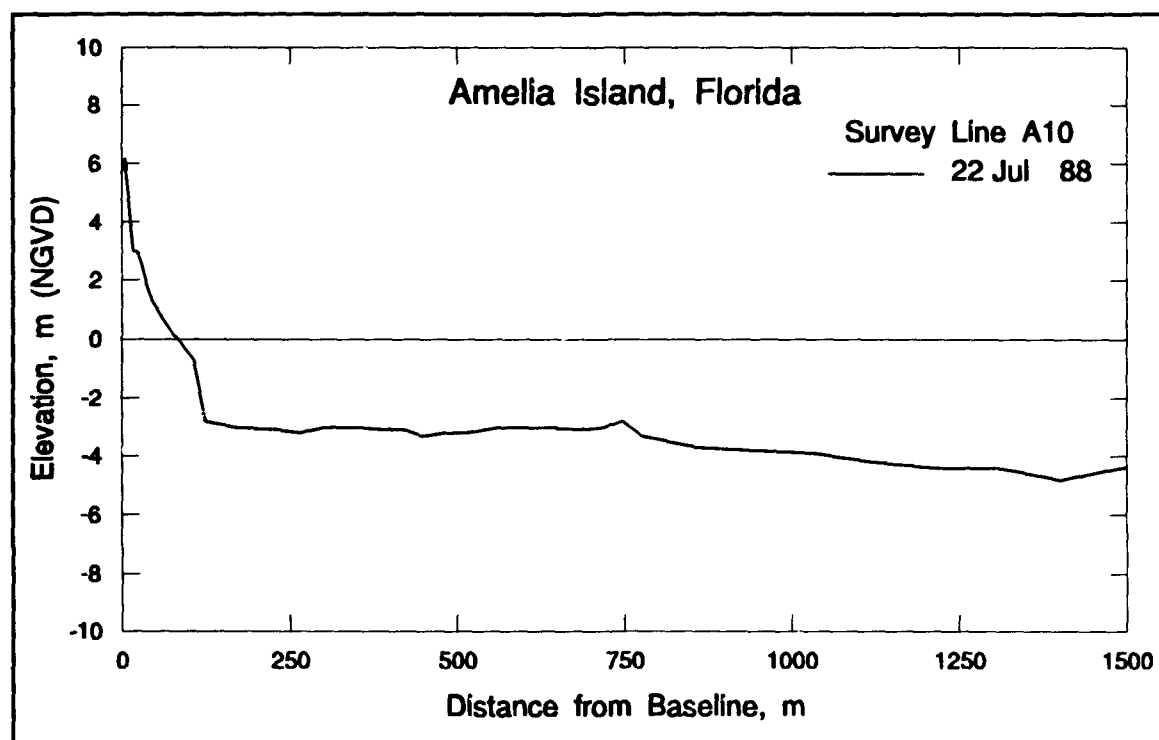


Figure 135. Representative profile, south fillet of St. Marys Entrance

north) transport of the placed material would be trapped in the Amelia Island fillet and would modify the beach topography and texture. Other contributors to the morphological character of this compartment are scour trenches along the flanks of each jetty and occasional shoals trapped near both jetties.

#### North Amelia Platform (Lines A16-A28)

North Amelia Platform is part of the historic ebb delta, and within the shadow of the modern ebb delta platform (Chapter 3). The shore is backed by 4.0-m-high vegetated dunes. The beach face is erosional and steep (slope of 3.4 to 4.1 deg) with medium-size sands (mean grain size 0.81 to 0.47 mm) (Table 32). This compartment includes the historically eroding section of shore which is 3 to 5 km south of the south jetty. In 1982, 302,000 cu m of dredged material were designated for beach disposal between Lines A19 and A25. During 1987 and 1988, an additional 693,370 cu m were designated for disposal along the entire length of the compartment (Table 27).

The beach width averages between 28.3 and 30.4 m give North Amelia Platform the narrowest beach of any compartment within the study area. The nearshore is flat (slope of 1.1 deg) with no distinctive inner bar over much of the compartment (Figure 136). An inner bar which is located fairly close to shore (50.6 m at Line A28) develops toward the southern end of the compartment.

#### Amelia Embayment (Lines A31-A67)

The central portion of Amelia Island, called Amelia Embayment, is characterized by medium-grained, narrow beaches with relatively steep offshore slopes (Figure 137). The average

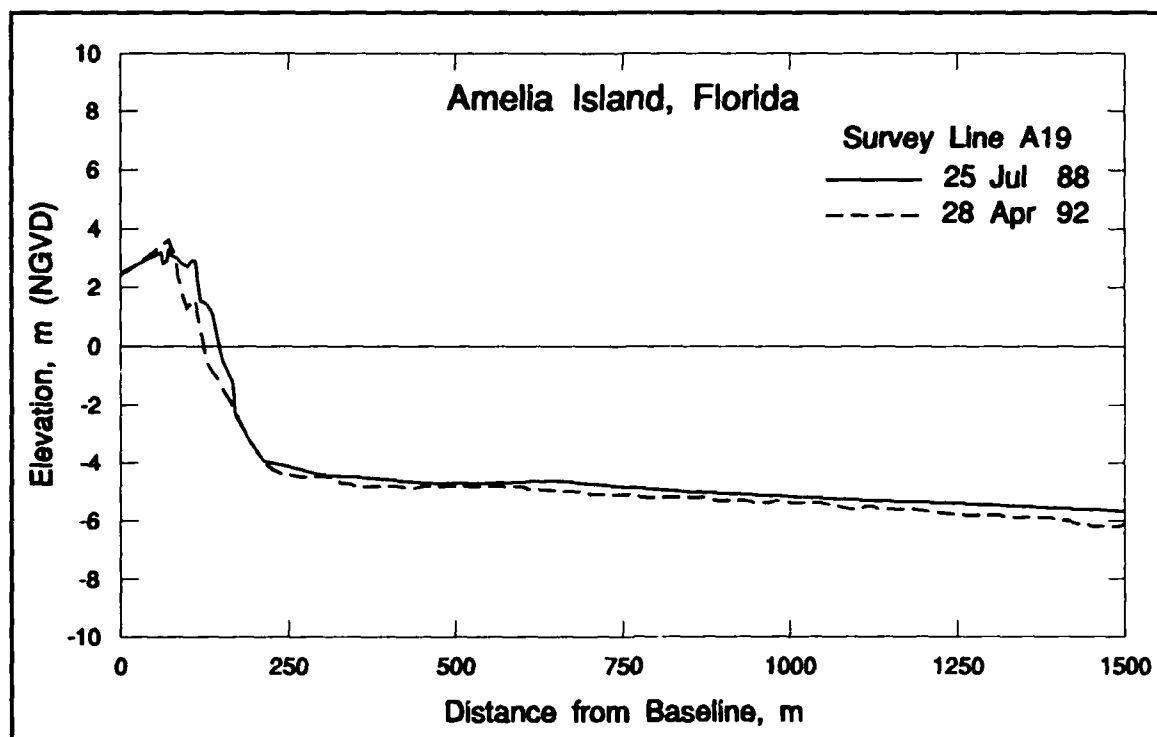


Figure 136. Representative profile comparison, North Amelia Platform

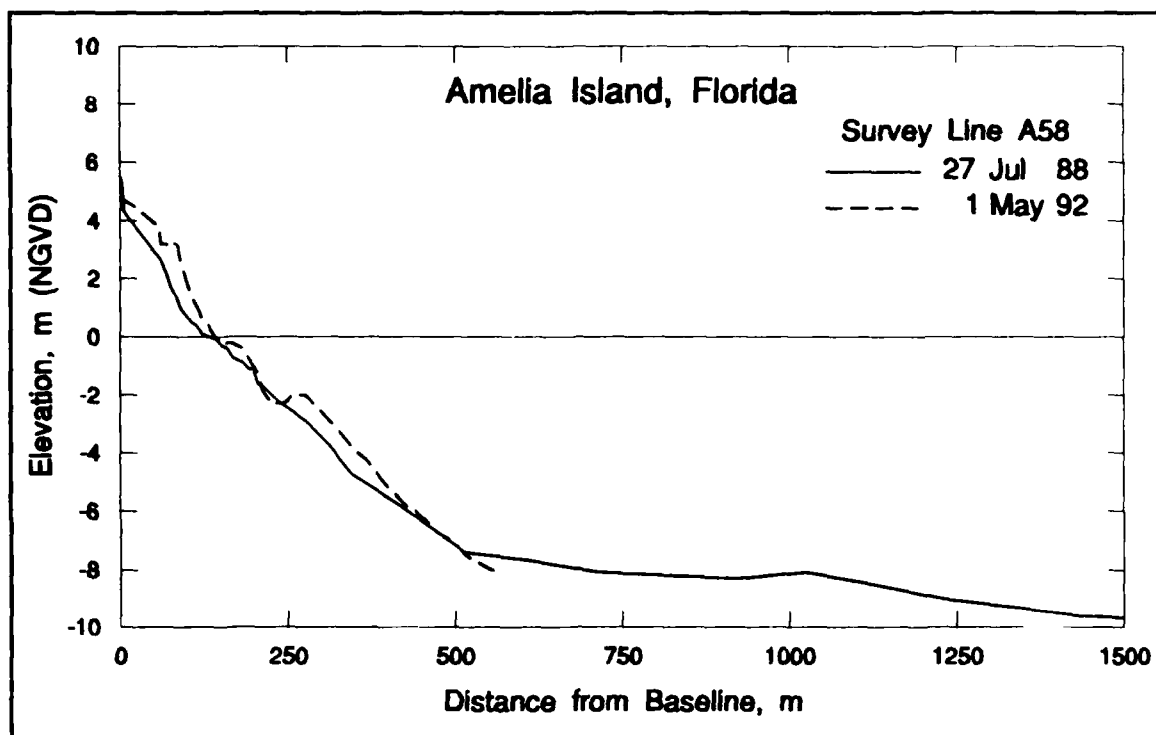


Figure 137. Representative profile comparison, Amelia Embayment

foreshore grain size is 0.30 mm and the beach slope gradient ranged from 2.2 to 2.8 deg (Table 32). A primary source of sediment for this compartment comes from the downdrift movement of beach fill material from the North Amelia Platform and the two major beach fill placement operations in this compartment immediately before and during the monitoring period (Table 27).

The nearshore bathymetry in this compartment is flat (0.6 deg) with no significant shoal features (Figure 137). The inner bar consistently increases in distance offshore of NGVD ranging between 60.9 and 133.0 m (Appendix D). Similarly, the bar crest follows the same trend, increasing in depth from 1.6 to 2.0 m (NGVD) (Appendix D) from Line A31 to Line A67 at the southern limits of Amelia Embayment (Figure 130).

#### Nassau Sound Tidal Inlet Complex (Lines A70-A79)

The southernmost compartment in the study area is part of, and strongly influenced by, inlet processes associated with Nassau Sound. The southern end of Amelia Island is dynamic, experiencing significant and frequent changes in both the dune/beach zone and across the offshore tidal shoal field (Figure 138). Dunes in this compartment are the highest on Amelia Island, with a maximum elevation of 8 m (NGVD) at Line A76. The littorally dominated northern end of this compartment (Lines A70-A76) is narrow, steep, and eroding (Figure 138). Toward the south (Lines A76-A79), the beach widens and the inner bar disappears to be replaced by tidal-dominated shallow and broad shoals (Figure 113).

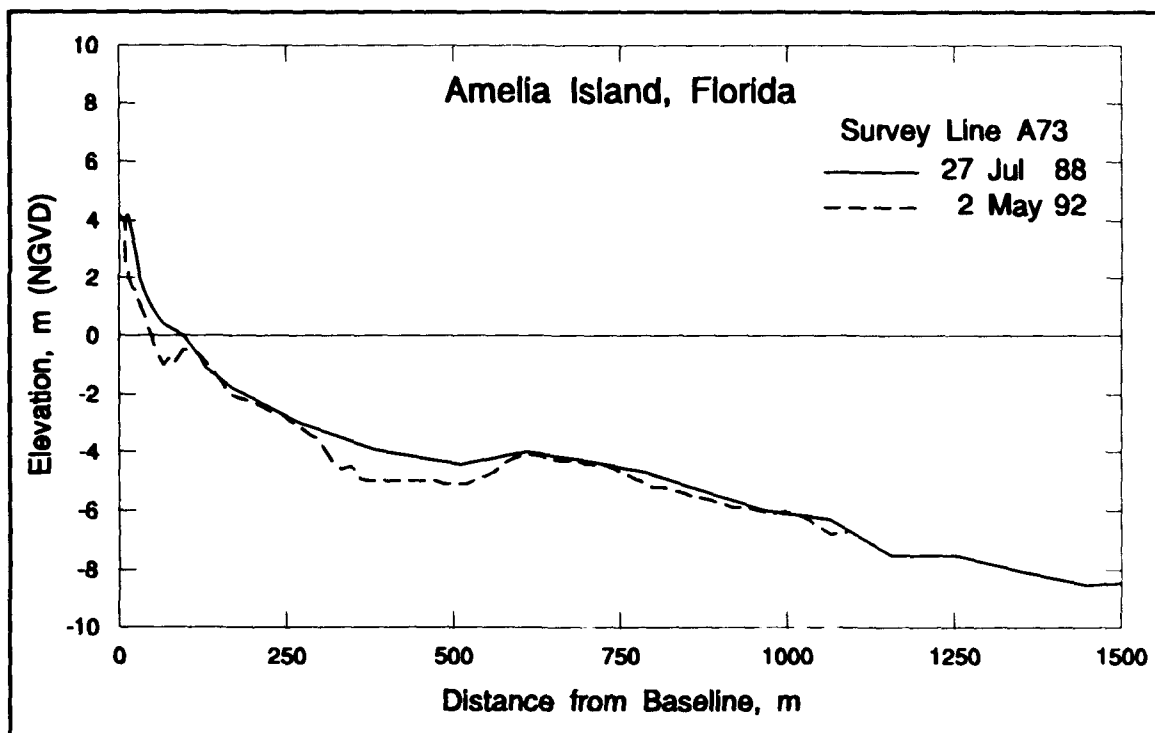


Figure 138. Representative profile comparison, Nassau Sound Tidal Inlet Complex

The beaches at the northern end of this compartment (Lines A70-A76) are narrow and steep, and frequently inundated by storm surges that can be enhanced by high tide. Winter storm waves frequently reach the base of the dunes resulting in scarping and cutback of the dunes. The foreshore has been altered by small-scale storm protection and erosion control work. Sand scraped from the lower beach area was placed at the dune toe in the 1970s and early 1980s (USAED, Jacksonville 1993). A privately funded beach fill was placed at the base of the dune line during the winter of 1984 (USAED, Jacksonville 1993). Recently, during the 1988-1990 period, sand fences were placed at the base of the dunes to reduce sand loss, and small privately funded beach fills were placed at the northern end of this compartment in 1989 and 1991.

South of Line A76, the profile is much more gently sloping with frequent shoal growth and migration due to tidal currents (Figure 113). Here, the inner bar disappears as tidal shoals associated with the Nassau Sound are exposed during low tide and dominate the local morphodynamics.

## Trend Analysis and Implications of Recent Engineering Activities

During the July 1988 - April/May 1992 monitoring period, no significant changes in the beach or nearshore evolutionary trends were found for Cumberland Island, relative to the long-term analysis described in Chapter 3. Spatial trends of shoreline movement and net volumetric change along Cumberland Island were relatively uniform throughout the monitoring period and within

each morphologic compartment. The historic trend of slight erosion continued to the north and accretion to the south about a transition zone between Lines C14 and C15 at Stafford Shoal. Overall, Cumberland Island beaches remained stable, with a slight trend of accretion (0.3 m/year from July 1988 through April/May 1992). However, considering the 13.6-m seasonal variability in shoreline position and other fluctuations within the coastal system (i.e. storm events), a 0.3-m/year change during this limited monitoring period is not a significant indication of the longer term shore response.

In contrast, the subaerial beach on Amelia Island varied both temporally and spatially, and exhibited some deviation from the long-term historical trends. Several major beach fills were placed just prior to and during the monitoring period, directly influencing beaches along approximately 17 km of Amelia Island. These fills dominated the observed pattern of beach change, obscuring the natural seasonal and longshore variability. In 1988, 480 m of the landward portion of the south jetty was sand tightened, reducing the permeability of this structure and possibly influencing the fillet at the northern end of Amelia Island. The historically stable trend for the central portion of Amelia Island (Chapter 3) changed to an accretionary trend (Figure 116). The beach area directly adjacent to the unstructured tidal inlet at Nassau Sound continued to be influenced by the dynamic ebb-delta complex morphology and sediment exchange patterns. These findings are based on the previously discussed analyses of individual survey measurements including shoreline position, cumulative net volume change, and surficial sediment samples.

The July 1988 - April/May 1992 monitoring program, consisting of beach profile surveys, bathymetric surveys, and sediment sampling, documents the character and variability of the study area beaches and nearshore. These data represent a temporal window of detailed information within the long-term evolution of this system. This particular data set includes the influences of short-term climatological variability, major beach fill operations on Amelia Island, sand-sealing of the south jetty, and Navy-sponsored TRIDENT channel deepening, widening, and lengthening. Based on these data and comparison to the historical trends, the following discussion of the implications of recent (post-1988) engineering activities on the morphological trends for each island has been developed.

### **Cumberland Island**

The planform of the shoreline, beach slope and volumetric change, and sediment grain-size trends for each compartment on Cumberland Island are consistent with the historical trends. Cumberland Island has been, and continues to be, stable to slightly accretionary. The morphology of Cumberland Island is characterized by high, fine-grained dunes along most of the coastline, except at the southern end where the dune field is recurved toward the soundside. In the Stafford Shoal compartment, dunes and periodic releases of sediments from the St. Andrew ebb delta complex are major sources for local beach sediments. Large, migrating sand shoals extend over a 72-sq-km area of the nearshore shelf, influencing the nearshore and beach processes of this compartment. Migration of the shoals and swales during the monitoring period was evident in the survey data. Along Cumberland Embayment, the beaches continue to be fine-grained with flat foreshore and nearshore slopes. The Cumberland Embayment shore, located in the lee of the Stafford Shoals complex, is arc-shaped with a morphology typical of a low-wave energy, moderate tidal range, and sheltered coast. Beach morphology and measured trends were consistent both spatially and temporally for this slightly accretionary shore. The southernmost compartment consists of a large fillet area with poorly sorted sands and broad, flat shoals adjacent

to the north jetty. Sediment migration through the north jetty into the inlet and the migration of tidal current-influenced shoals cause some variability in the pattern of erosion and accretion of the north fillet area.

A net sediment deficit of 14.2 cu m/m occurred across the active beach profile (defined as 2.5 to 0.0 m NGVD) in the Stafford Shoal compartment, while Cumberland Embayment had a net sediment gain of 28.4 cu m/m over the same profile zone (Table 25). Net accretion along the subaerial profile envelope continued to increase toward the south. The north fillet of St. Marys Entrance experienced an average volumetric gain of 35.8 cu m/m. The overall trend of net volumetric gain along the profile envelope increasing from north to south is repeated in the shoreline position change trends and is a continuum with the historical trends. The primary sediment supply to Cumberland Island is from the St. Andrew Sound inlet system to the north and the nearshore shoal complex. The Cumberland Island morphodynamic system exhibits no evidence of a dependency upon St. Marys Entrance for sediment supply.

### **Amelia Island**

Recent areas of erosion and accretion along Amelia Island are influenced by St. Marys Entrance, Nassau Sound, and beach fill operations. In general, Amelia Island has moderately high, vegetated, fine-grained dunes intermittently fronted (since the late 1970s) by a medium- to occasionally coarse-grained beach fill. Historically, the central section of the island (Amelia Embayment) has been relatively stable with a minor trend toward accretion, whereas the southern end of the island and a zone 3-5 km south of the south jetty have shown continuing patterns of erosion. Local sand supply for the Amelia Island beaches comes from adjacent dunes, updrift beaches, the offshore, and multiple beach fills.

The longshore pattern of beach volume and shoreline change throughout the monitoring period on Amelia Island was heteromorphic. The subaerial beach profile for Amelia Island was defined as 4.0 to 0.0 m (NGVD). The effect of beach fills, which were placed along central and southern Amelia Island as a high beach berm fronting the dunes, was examined using this subaerial beach data set. Despite placement of beach fills along Amelia Island (between Lines A13 and A22 and between Lines A53.7 and A71) during the monitoring period, there was only a slight net volume gain to the subaerial portion of the beach of 0.6 cu m/m (less than 0.2 cu m/m/year). Erosion occurred along the North Amelia Platform (44.3 cu m/m) and Nassau Sound Tidal Inlet Complex (79.3 cu m/m) compartments (Table 26). In order to understand this erosion, the response of the beach fills and their impact on Amelia Island during the monitoring period was evaluated in the context of recent trends.

In order to understand the behavior of the Amelia Island shore, the quantity, timing, and location of dredged material placed on the beach is compared to shoreline change rates. Since the first placement of dredged material (November 1978 - June 1979), the temporal and spatial pattern of shoreline change on Amelia Island has been a function of the sequence of beach fill operations. This section reviews the history of dredged material placements as beach fill both before and during the monitoring period and the subsequent shoreline response. The purpose of this analysis is to determine if the shoreline change pattern during the monitoring period provides any evidence of a potential impact associated with the deepening, widening, and lengthening of the entrance channel.

The pattern of beach fill placement on Amelia Island was used to identify five beach fill zones (called Zones A-E), and to illustrate the influences of the sequence of fill operations (Table 33). The quantity of fill reported (Tables 27 and 33) is the quantity dredged from the channel which was designated for beach disposal. No data are available on the actual volume of material placed on the beach, as disposal area profile surveys are not normally performed as part of navigation channel dredging projects. The actual quantity of beach fill is expected to be less than the reported volume, due to losses incurred during the dredging and placement operations. This discrepancy in the volume dredged from the channel and that which was placed on the beach is most significant in the case of the 825,770 cu m of fill which were dredged from July 1988 through July 1989 from an offshore disposal site and pumped onto the shore in Zone D. Narrative reports from local residents and USACE observers suggest that this material contained a higher percentage of fine sediment (silts and clays) than material which is dredged from the channel and placed directly on the beach. The density of beach-quality fill placed on the subaerial beach is therefore less than the 426 cu m/m calculated in Table 33.

**Table 33**  
**Comparison of Dredged Material Quantities Placed on Amelia Island to Net Beach Volume Change (Jul 1988 - Apr/May 1992)**

Beach Fill Zone	Morphologic Compartment	Profile Line	Length of Shore, m	Reported Volume Dredged, cu m	Total Reported Placement Density cu m/m	Measured Volume Change Density <sup>1</sup> cu m/m
A	St. Marys Tidal Inlet Complex North Amelia Platform	A13-A22	2,629	260,750 <sup>2</sup>	99	-70 <sup>3</sup>
B	North Amelia Platform Amelia Embayment	A22-A48	7,569	0	0	17
C	Amelia Embayment	A48-A53.7	1,630	0 <sup>4</sup>	0	-8
D	Amelia Embayment	A53.7-A60	1,938	825,770 <sup>5</sup>	426	96
E	Amelia Embayment Nassau Sound Tidal Inlet Complex	A60-A71	3,223	48,170	15	-37
Total			16,989	1,134,690		4

<sup>1</sup> Weighted average subaerial volume change density A16-A71 = 4 cu m/m.

Weighted average subaerial volume change density A16-A60 = 14 cu m/m.

<sup>2</sup> 693,370 cu m were placed 1987-1988 prior to the July 1988 survey between Lines A13-A22; the 260,750 cu m were placed between Lines A13-A16.

<sup>3</sup> Based on Lines A16-A22.

<sup>4</sup> 405,240 cu m were placed 1987-1988 prior to the July 1988 survey.

<sup>5</sup> Probably includes fine material from the nearshore disposal area; see main text.

The amount of dredged material designated for placement in each of the five beach fill zones (maximum potential fill) can be compared to both the measured subaerial beach volume change (4.0-0.0 m NGVD) (Table 33) and the shoreline change rate (Figure 139) during the monitoring period. This analysis procedure provides a mechanism for relating the significance of the documented beach change trends during the monitoring period to the prechannel modification period. As defined here, shoreline change rate is the landward or seaward movement of the 1.3-m NGVD elevation on the beach profile lines over the time between surveys. A qualitative comparison of shoreline change rates was performed to evaluate shoreline change during the monitoring period (1988-1992) which included beach fill and TRIDENT channel expansion operations, relative to pre-TRIDENT channel and beach fill-influenced trends from 1974 to 1988 (Figure 139).

The February 1974 and September/November 1981 shorelines are based on State of Florida DNR survey data sets and represent the prechannel modification, beach fill-influenced, baseline condition for Amelia Island. Shoreline (profile) data coverage for the prechannel modification condition is limited to only two complete surveys. In addition, due to baseline monument resets, not all profile data could be used (Appendix D). Therefore, beach fill Zones C and D are represented by one or fewer profile lines, and overall data density available for this analysis was greater than 1.4 km per survey line. The 1988 and 1992 shoreline positions were documented during the monitoring period and represent the post-channel modification period. Shoreline positions used in Figure 139 correspond to the high-water level of 1.3 m (NGVD) as extracted from profile survey data.

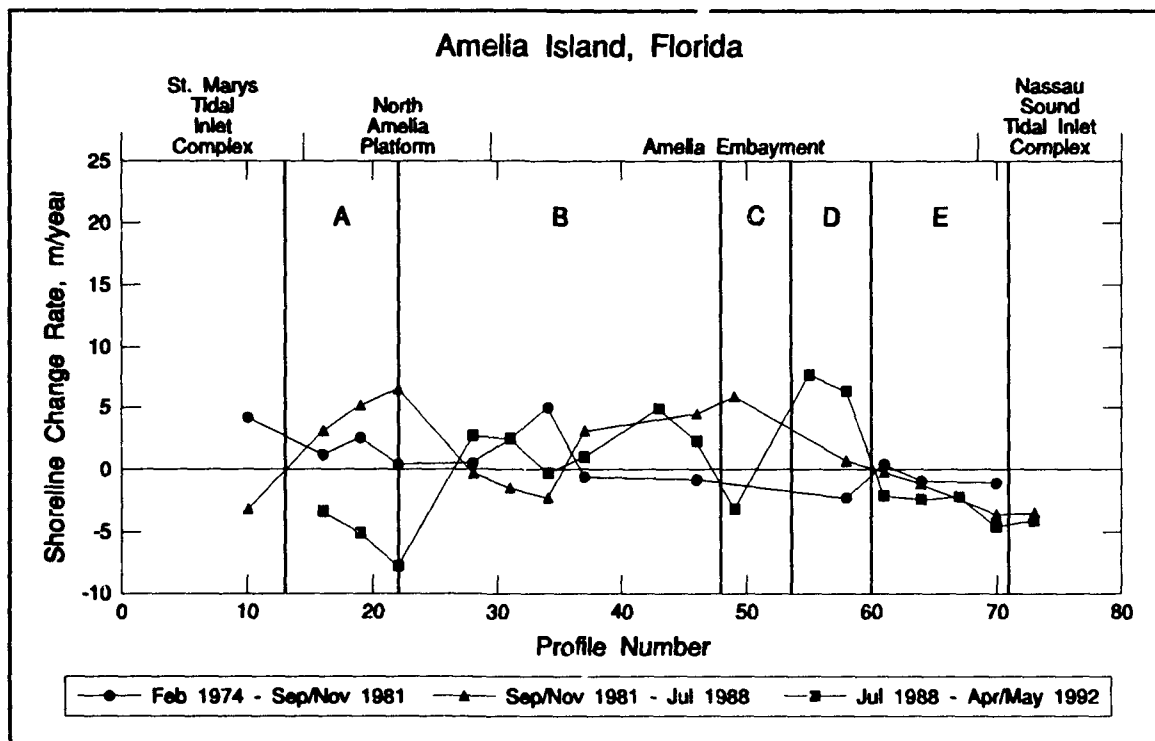


Figure 139. Comparison of shoreline change rates (Feb 1974 - Sep/Nov 1981, Sep/Nov 1981 - Jul 1988, and Jul 1988 - Apr/May 1992)

Zone A (Lines A13-22) was the site of the 693,370 cu m (June 1987 - February 1988) beach fill placed prior to the July 1988 survey. Consequently, a major beach fill construction berm perched on the subaerial portion of the profile was surveyed as the baseline condition for the monitoring period. An additional 260,750 cu m of dredged material were designated for beach placement in this zone in 1990 and 1992 (Tables 27 and 33). This zone lost 70 cu m/m from the subaerial beach during the monitoring period; this loss is an artifact of the recent beach fill construction and the timing of the baseline survey. The July 1988 survey was performed just after fill placement and therefore documented a beach in disequilibrium. Figure 140 illustrates the continuous erosion of the pre-July 1988 placed beach fill cross section throughout the monitoring period. This zone includes the area from 3 to 5 km south of the south jetty which has historically eroded. During the premonitoring period (1974-1988) 1,609,370 cu m (114,955 cu m/year) of beach fill were placed in this zone (Table 27). In contrast, during the monitoring period (1988-1992), only 260,750 cu m (65,187 cu m/year) were placed in Zone A. Figure 139, therefore, shows an accretionary shore for Zone A prior to the July 1988 survey, but an eroding shore for the monitoring period (1988-1992). The change in trend from accretionary to erosional is reasonable considering that less material was placed in this zone during the monitoring period than during the previous two periods (1974-1981 and 1981-1988).

No beach fill was placed in Zone B (Lines A22-A48) during the monitoring period. However, the shoreline advanced (Figure 139), and the subaerial beach profile increased in volume (17 cu m/m) (Table 33) during the period from July 1988 to April/May 1992. Profile lines in Zone B exhibit a pattern of accretion, with the more northerly profiles (Figure 141) experiencing the most growth from 1988 through 1989 and the more southerly profiles (Figure 142) accreting more during 1990 through 1992. The general trend of accretion in Zone B and the sequential

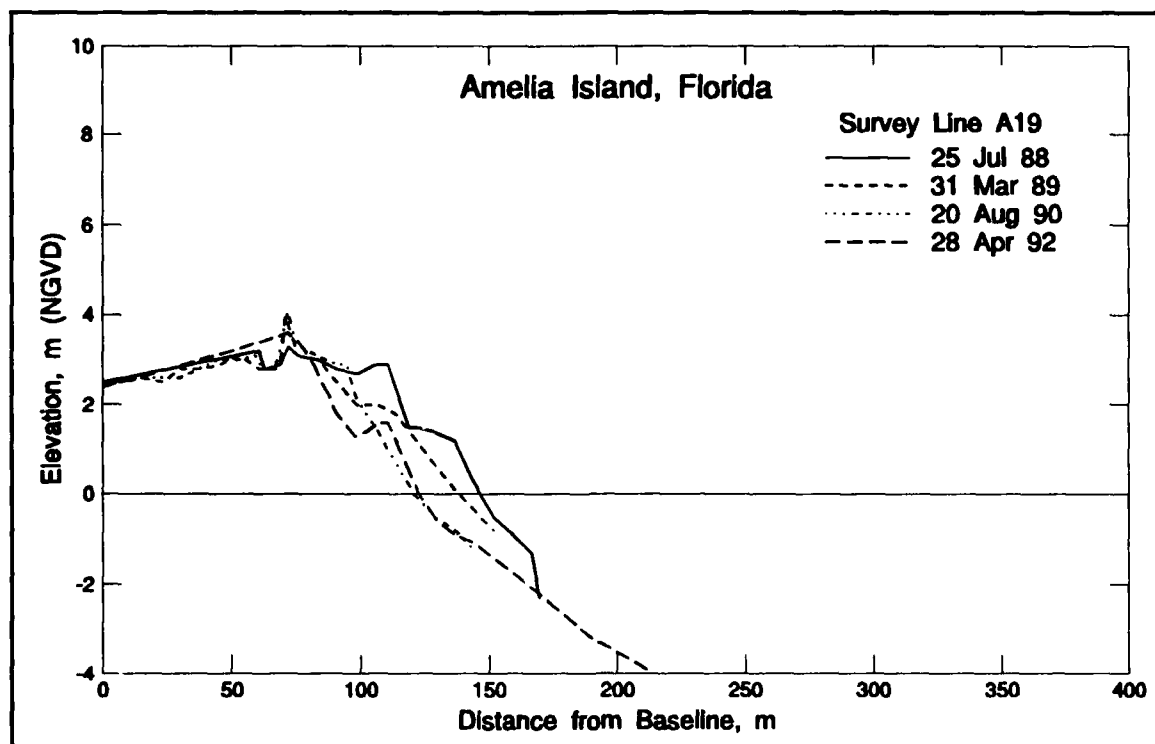


Figure 140. Profile comparison of Line A19 in beach fill Zone A illustrating the sequential retreat of the placed beach fill (Jul 1988) through the monitoring period

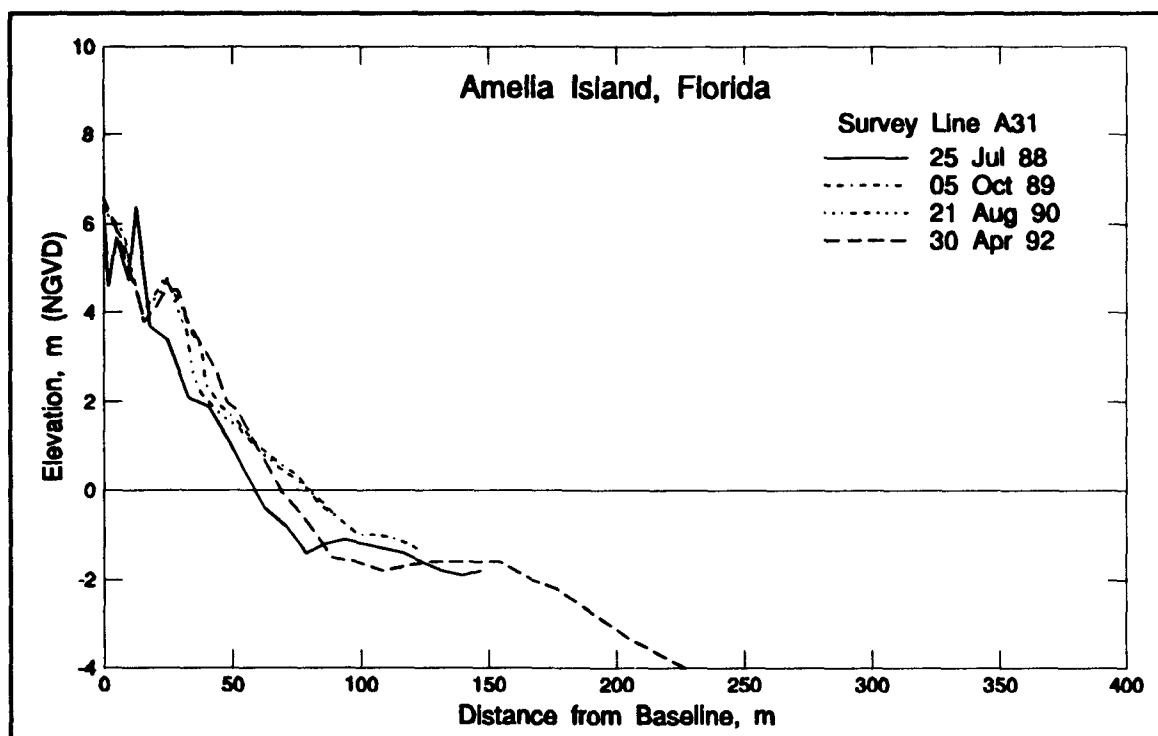


Figure 141. Profile comparison of Line A31 in the northern portion of beach fill Zone B illustrating profile accretion between Jul 1988 and Oct 1989

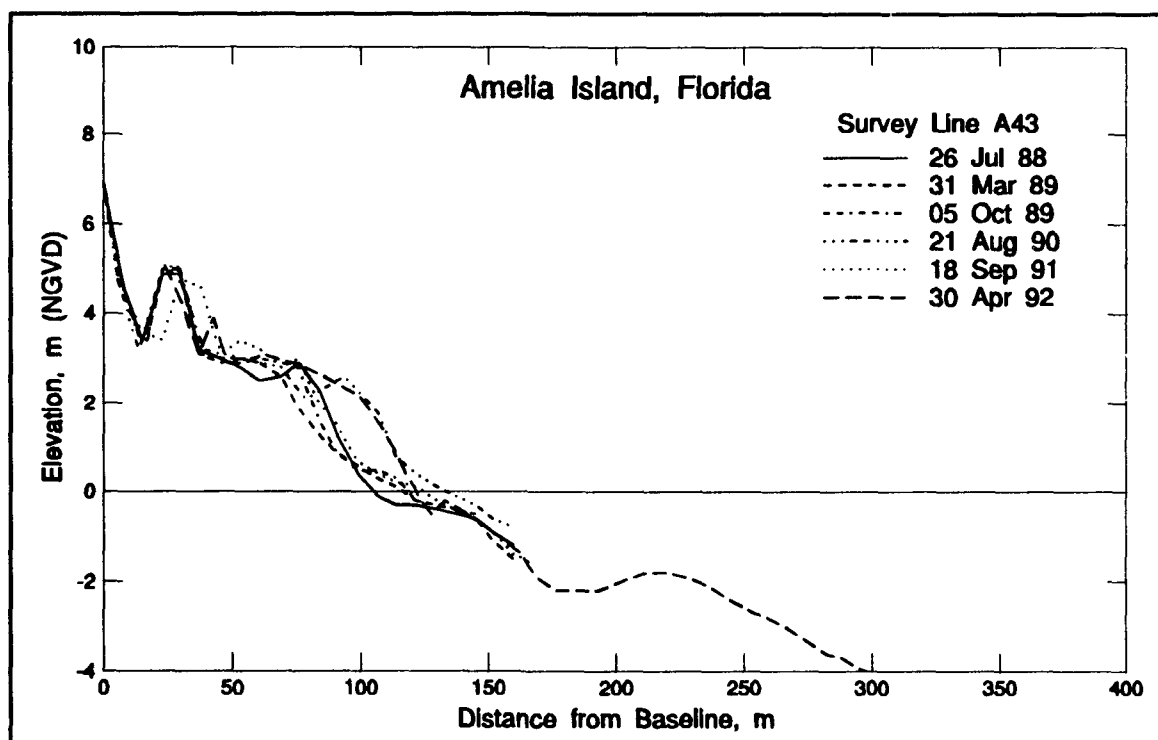


Figure 142. Profile comparison of Line A43 in the southern portion of beach fill Zone B illustrating profile accretion between Oct 1989 and Sep 1991

accretion from north to south appear to indicate that some of the fill placed in Zone A prior to the July 1988 survey was transported alongshore toward the south.

Zone C (Lines A48-A53.7) was filled with a substantial amount of material (405,240 cu m) between September 1987 and May 1988, just prior to the July 1988 survey. No fill was placed in this zone during the monitoring period (Figure 139, Table 33). This short (1.6-km-long) section of beach appears to be an exception to the general trend of shoreline advance and subaerial beach volume gain (Figures 111 and 116) which characterized Amelia Embayment during the monitoring period. The following discussion is based on limited data, as Line A49 is the only profile survey line in this short reach (Figure 143). As in the case of Zone A, the July 1988 baseline survey documented an unstable beach fill profile which lost 8 cu m/m of material during the monitoring period. However, Line A49 in Zone C did not exhibit the same dramatic profile retreat and loss of subaerial beach volume as did Zone A. This more limited loss may be due to the uncertainties associated with evaluating only one profile line. In addition, Zone C is south of the major 1987-1988 fill in Zone A and directly north of the major 1988-1989 fill placed in Zone D. The normal tendency for an unstable beach fill cross section to retreat may have been partially obscured in Zone C by an ample longshore sediment supply, regardless of transport direction. In addition, Figure 143 suggests that there has been some movement of material seaward of the 1.3-m NGVD elevation resulting in a redistribution of the placed fill as the underwater portion of the profile is built up.

Zone D (Lines A53.7-A60) received 73 percent (825,770 cu m) of the 1,134,690 cu m of beach fill which was placed on Amelia Island during the monitoring period. This is the single

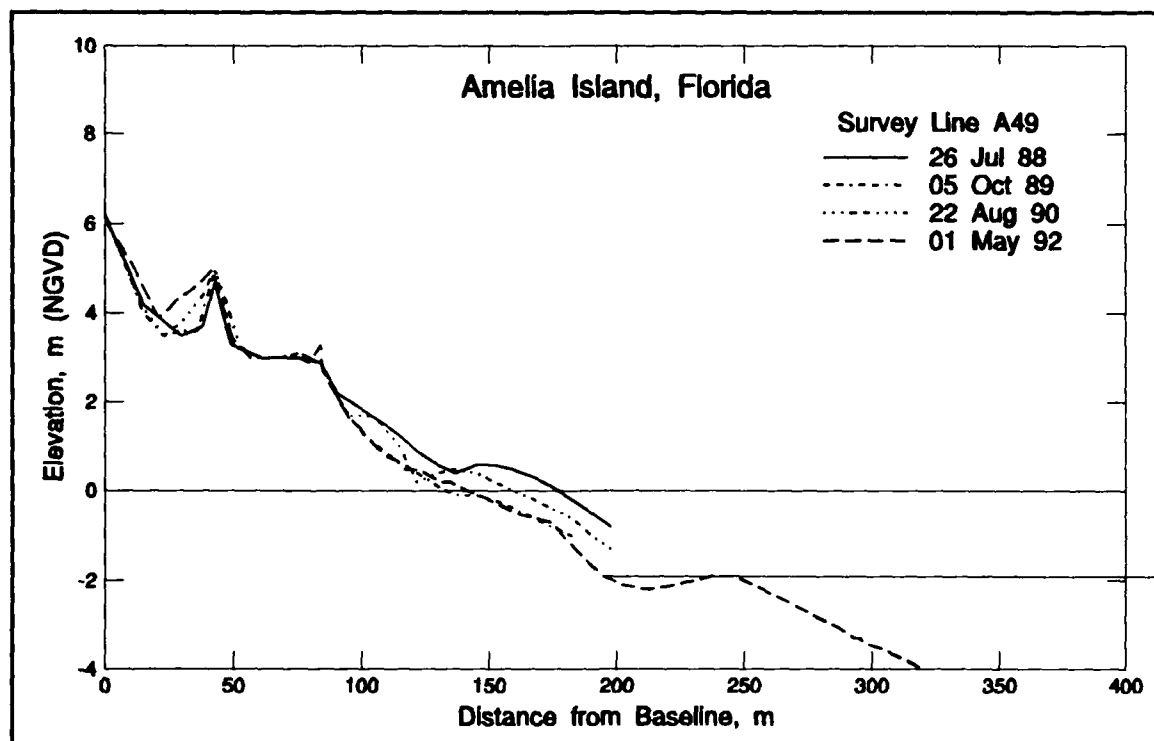


Figure 143. Profile comparison of Line A49 in beach fill Zone C illustrating the retreat of fill placed prior to the Jul 1988 survey

largest fill in the 14-year history of dredged material placement on Amelia Island. Consequently, this zone exhibited the most subaerial volume increase (96 cu m/m) and the greatest net seaward displacement of the shoreline (approximately 30 m) (Figures 111, 116, 117, and 139). As discussed previously, there is some question as to how much of the 825,770 cu m of stockpiled dredged material was beach quality and would remain stable on the subaerial beach. The potential placement density of 426 cu m/m is significantly greater than the 96 cu m/m volume change density (based on two profile lines) realized through the monitoring period (Table 33). However, the beach-fill cross section in this zone has been relatively stable since the October 1989 survey. At the northern end of Zone D, there has been some seaward displacement of the shoreline since the postplacement October 1989 survey (Figures 117 and 144); however, toward the south there has been minor erosion during the 3 years since fill placement (Figure 145). These data suggest that much of the material placed from July 1988 to July 1989 was lost from the subaerial beach in Zone D prior to the October 1989 survey, probably during placement.

Only a small quantity of non-Federally sponsored fill was placed at the southern end of Amelia Island in Zone E (Lines A60-71, Table 27). Private interests placed 48,170 cu m of fill along the back beach to reconstruct portions of the eroded dunes, resulting in a maximum potential fill density of 15 cu m/m. These minor fill operations were not sufficient to reverse the natural long-term trend of erosion which this area has experienced since 1924 (Figure 46). Although 38,230 cu m of beach fill were reportedly placed in December 1989, the August 1990 survey did not exhibit evidence of this fill operation in the subaerial beach (Figure 146). There was, however, some gain in the lower foreshore below the 1.3-m NGVD shoreline (October 1989 - August 1990). In addition, there was a temporary shoreline advance at Line A67 (October 1989) and further south (August 1990), suggesting some southerly sediment transport from the major

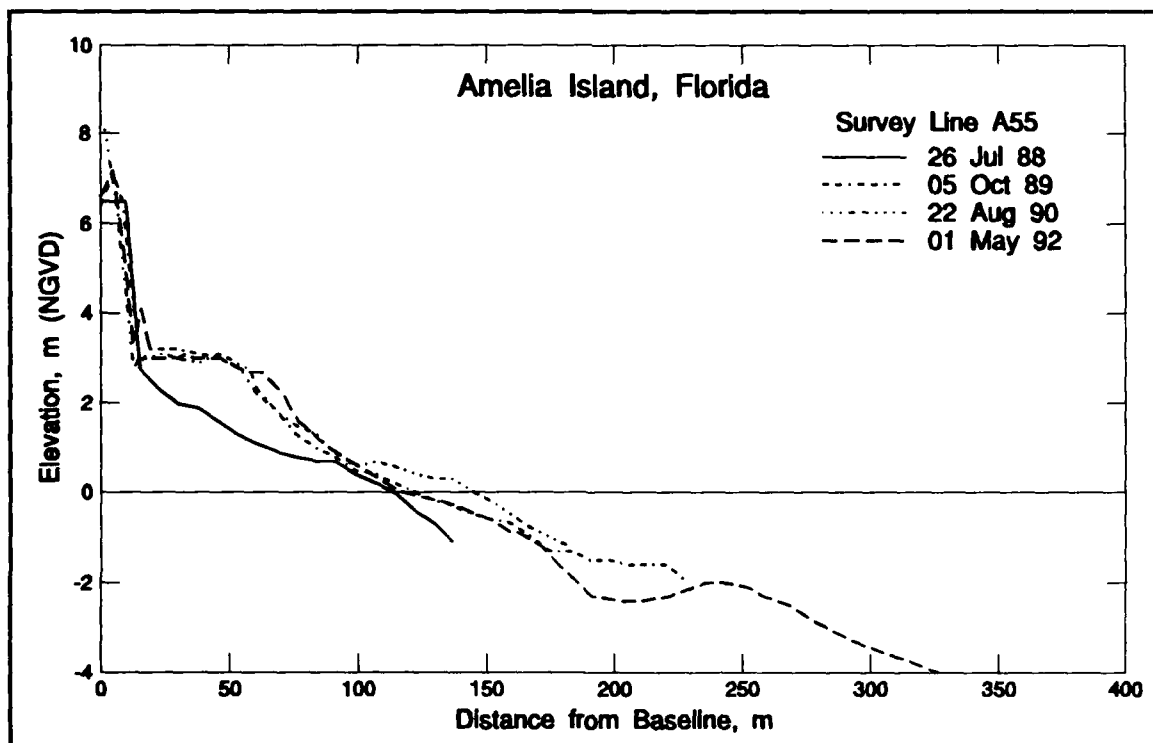


Figure 144. Profile comparison of Line A55 in the northern portion of beach fill Zone D illustrating the relative stability of the beach fill since Oct 1989

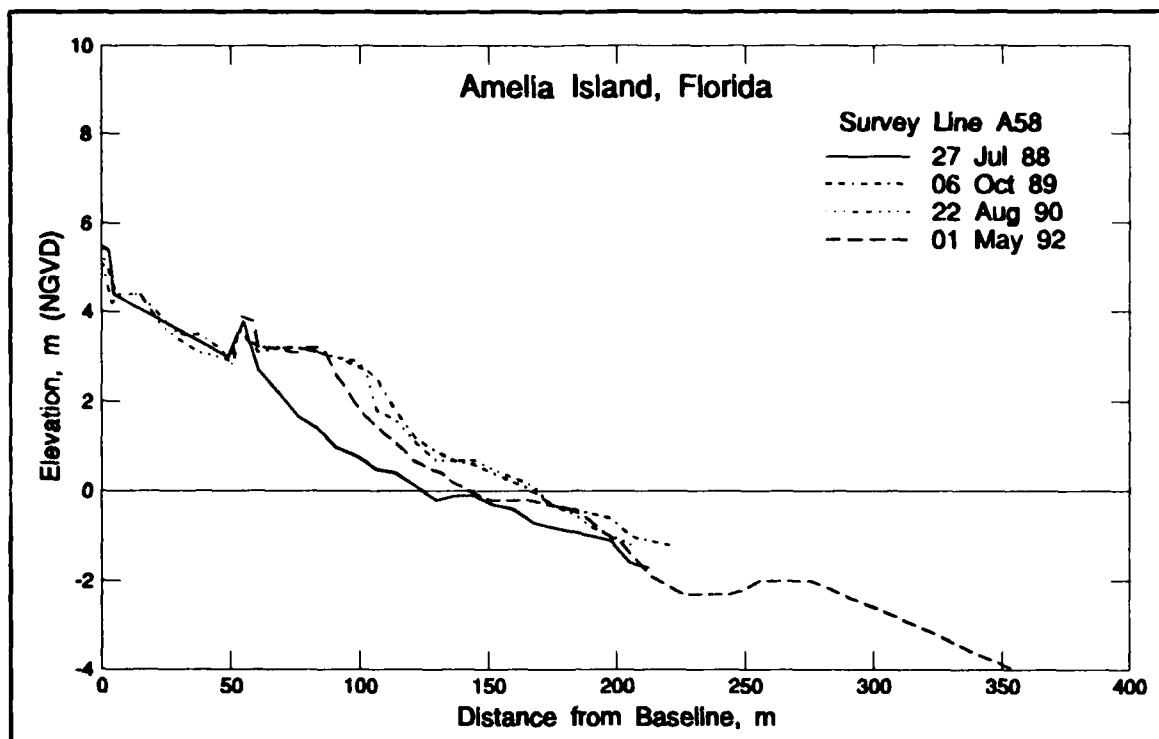


Figure 145. Profile comparison of Line A58 in the southern portion of beach fill Zone D illustrating minor erosion of the placed fill since Oct 1989

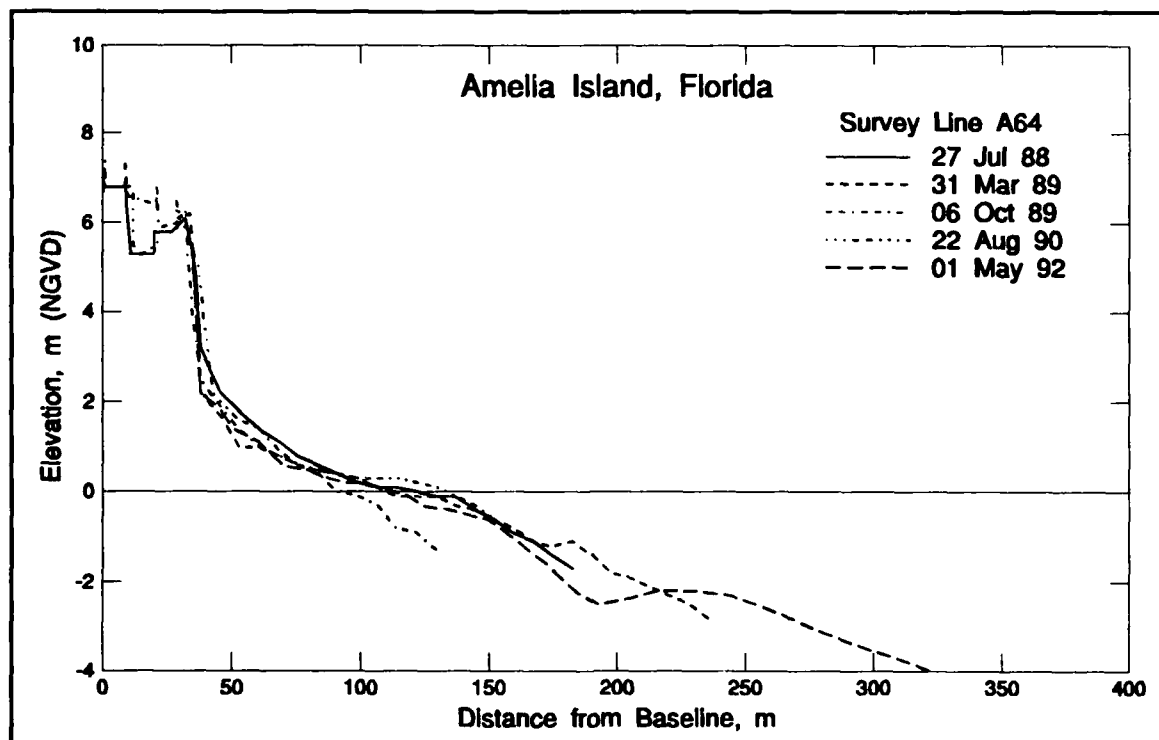


Figure 146. Profile comparison of Line A64 in beach fill Zone E. Note that there is no visible evidence of beach fill placement in the Aug 1990 profile

fill in Zone D (Figure 117). The historical trend of sediment loss continued throughout Zone E during the 1988-1992 period.

The prechannel expansion (1974-1981 and 1981-1988) versus postchannel expansion (1988-1992) shoreline change trends further illustrate the dominance of the beach-fill operations in modifying the beach conditions (Figure 139, Table 34). Figure 147 illustrates the sequence, quantity, and timing of each beach fill placement relative to the recent shoreline change history. The entire Amelia Island shoreline advanced 0.2 m/year over the 1988-1992 period, which is comparable to the 0.0 m/year change found for the 1974-1981 period (Table 34), although both values are well within the range of the natural variability in shoreline position. Yet, 1.5 times as much material was placed in the 1988-1992 period as during 1974-1981 (i.e., 1,134,690 versus 765,000 cu m). During 1981-1988, the 1.3-m (NGVD) shoreline on Amelia Island advanced significantly (1.9 m/year) when 1,462,150 cu m (or approximately 30 percent more material) was placed than during the monitoring period. Why did the Amelia Island shoreline advance so little during the monitoring period? This apparent discrepancy is examined in the following paragraphs.

**Table 34**  
**Shoreline Change Rates Per Beach-Fill Compartment for Amelia Island**

Beach-Fill Zone <sup>1</sup>	1974-1981		1981-1988		1988-1992		1974-1992	
	Shore Change Rate <sup>2</sup> m/year	Reported Fill Volume Dredged cu m	Shore Change Rate m/year	Reported Fill Volume Dredged cu m	Shore Change Rate m/year	Reported Fill Volume Dredged cu m	Shore Change Rate m/year	Reported Fill Volume Dredged cu m
A	1.7	765,000	5.0 <sup>5</sup>	844,370	-5.4 <sup>5</sup>	260,750	1.4	1,870,120
B	0.7	0	2.1	151,000	1.1	0	1.2	151,000
C	.. <sup>3</sup>	0	5.9 <sup>5</sup>	405,240	0.0 <sup>5</sup>	0	--	405,240
D	-2.1 <sup>4</sup>	0	0.6 <sup>4</sup>	0	6.2 <sup>5</sup>	825,770	0.5 <sup>4</sup>	825,770
E	-0.7	0	-1.7	61,540	-2.8	48,170	-1.5	109,710
Total	0.0	765,000	1.9	1,462,150	0.2	1,134,690	0.7	3,361,840

<sup>1</sup> See Table 33 for lengths of shoreline represented per beach-fill zone.

<sup>2</sup> Shoreline.

<sup>3</sup> No data available.

<sup>4</sup> Based on only one profile line within zone.

<sup>5</sup> Shoreline change contaminated by significant beach-fill placements immediately prior to survey.

Of the total 3,361,840 cu m of fill placed on Amelia Island during the last 18 years, 2,227,150 cu m (66 percent) of that material were placed prior to the July 1988 baseline survey of the monitoring period (Table 34). All beach-fill zones except Zone D received beach fill during the period 1981-1988, when 1.3 times as much fill was placed as during the monitoring period (Figure 147). Beach-fill quantities placed during the monitoring period are within the baseline supply rate which Amelia Island has experienced during the past 2 decades. The pre-1988 beach condition was one which had been influenced by numerous fill operations. Approximately 2.2 million cu m were placed during the 10 years prior to 1988, whereas 1.1 million cu m were placed during the 4 years since 1988 (or 0.22 million cu m/year pre-1988

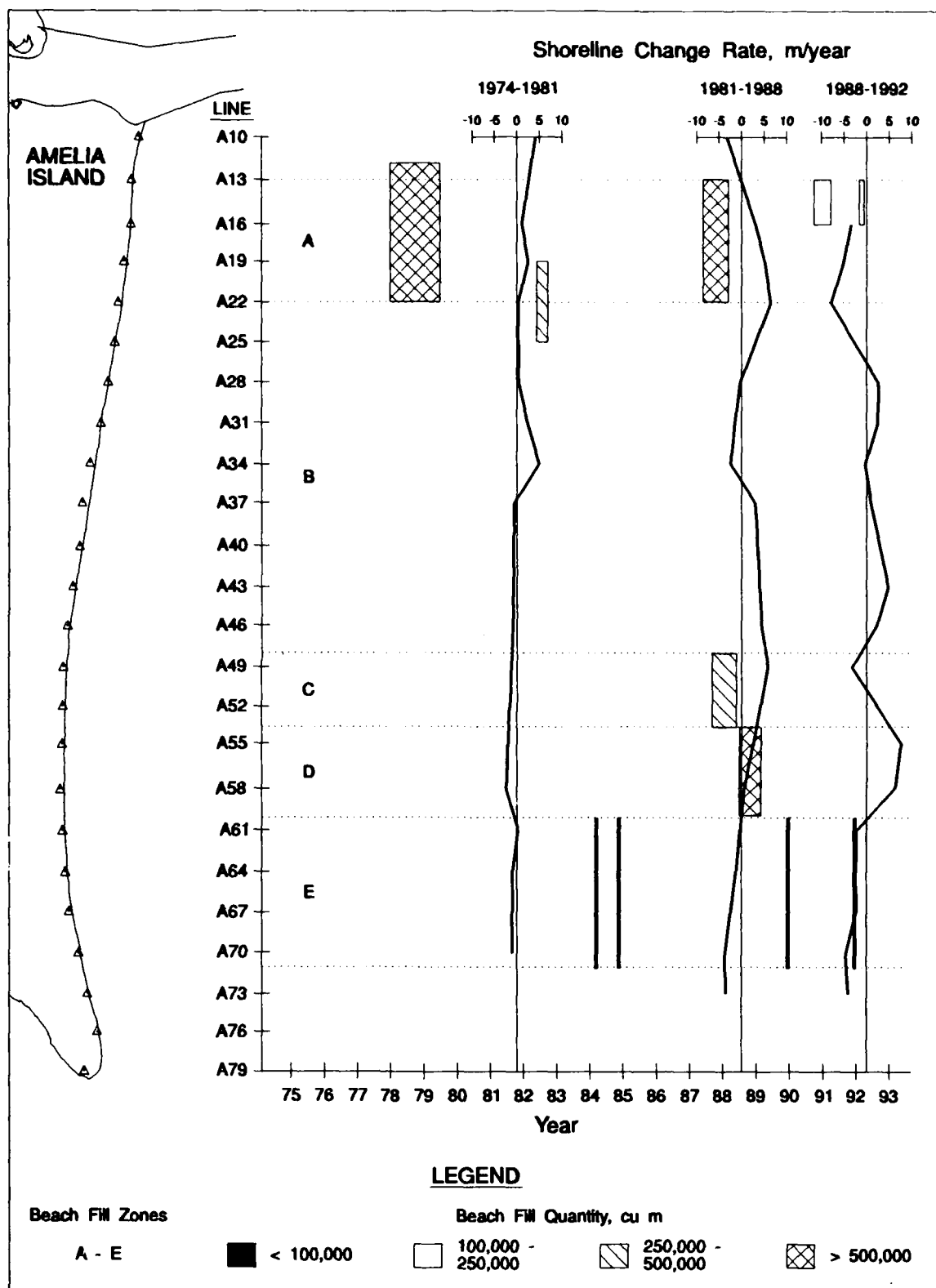


Figure 147. Recent shoreline change rate response as a function of Amelia Island beach-fill placement operations. Approximate width and location of beach-fill symbols represents the time frame of placement

versus 0.28 million cu m/year post-1988). A strict quantitative comparison of the shoreline change values presented in Table 34, relative to the quantity of fill placed, is not recommended as the surveys were taken during different seasons and the density of the data (particularly for the central part of the island, i.e., Zones C and D) is coarse relative to the length of the beach fill placement areas. However, a trend comparison of the shoreline change rates per compartment does show a relationship between the placement of fill and an advancement of the shore (Figure 147). Major fills in Zone A (1974-1981 and 1981-1988), Zone C (1981-1988), and Zone D (1988-1992) caused a local shore advancement for those zones on the order of 5-6 m/year (Figure 147, Table 34). Therefore, the quantity placed during the monitoring period was not a significant addition to the system relative to previous years (i.e., already a beach-fill-influenced system).

The relative timing of fill operations and surveys greatly influences the computed shoreline change rate. The highest computed rate of shoreline advance (1.9 m/year) for Amelia Island is for the 1981-1988 period, when 1,462,150 cu m were placed, 75 percent of which was placed during the year prior to the July 1988 survey. More beach fill was placed from June 1987 through May 1988 than during any other 1-year period. For example, the Zone A shoreline advanced 5.0 m/year between 1981 and 1988 in response to placement of 844,370 cu m (693,370 cu m of which were placed from July 1987 to February 1988). Yet, the Zone A shoreline only advanced 1.7 m/year between 1974 and 1981 when a similar quantity of material was placed (765,000 cu m) from November 1978 to June 1979. The significant difference in shoreline change between these two periods is related to the timing of the surveys relative to the placement period. In 1981-1988, the beach fill was placed immediately before the 1988 survey, whereas in 1974-1981, the fill was placed 2 to 3 years prior to the September/November 1981 survey, giving this fill sufficient time to adjust. Therefore, in the present comparisons, computed shoreline change is more a function of the timing of the survey relative to fill operations than to the actual quantity placed (i.e., importance of high initial losses from a disequilibrium fill).

Of the quantity of material reported to be available for placement as beach fill, 73 percent was dredged from an offshore disposal stockpile site by hopper dredge and pumped onto a less than 2-km section of shore (Zone D). The remaining 260,750 cu m of Federal fill placed during the monitoring period was dredged from the navigation channel and placed directly on the beach (Figure 147). There is narrative information that the placed fill contained finer grained material which dissipated during placement. In addition, there are performance data to support the hypothesis that there were higher-than-usual initial loss rates associated with this fill placement; the October 1989 survey (taken the Fall after placement) showed a narrower subaerial beach fill berm than the reported placement quantity should have created, the fill exhibited a steep berm face (suggesting some consolidation), and the post-October 1989 surveys exhibited minimal retreat during the remainder of the monitoring period. This combination of evidence suggests that some quantity less than the reported 825,770 cu m of dredged material was stable and remained on the subaerial beach.

Although the quantity placed on the beach is probably less than the quantity dredged and designated for this purpose, comparison of the fill density to the volume change density suggests that there has been loss of placed material from the subaerial beach (Table 33). Some fill was transported seaward of the 0.0-m NGVD offshore limit used in computing the volume change. A newly placed beach fill will quickly adjust toward an equilibrium slope, resulting in an offshore and longshore transport (Stauble and Hoel 1986). In addition, some of the placed fill was transported alongshore, both north toward St. Marys Inlet and south into Nassau Sound Inlet

complex. Longshore transport of fill is shown in the 17 cu m/m of volume increase (Table 33) and 1.1 m/year of shoreline advance (Table 34) in Zone B, where no fill was placed, and by the temporary period of accretion south of the Zone D fill in 1989 and 1990. In addition, Line A10, which crosses the fillet south of the south jetty, has exhibited a trend of continuing accretion since 1988 (Figure 148). These data support the premise that some fill material has migrated north of the north fill area into the south jetty fillet.

In summary, an examination of beach response relative to the timing and location of beach fill placements during the monitoring period and those of the previous 14 years indicates placement of 1,134,690 cu m of dredged material on the beach has only resulted in minor (0.2 m/year) shoreline advance. Possible reasons for the relatively small advance are:

- a. The 1974 through July 1988 data sets contain the influences of 2,227,150 cu m fill placement and are, therefore, not representative of a natural shoreline change rate.
- b. The July 1988 monitoring period baseline survey documented the recent placement of 1,098,610 cu m of fill and recorded the condition of a disequilibrium beach. The July 1988 survey was of an artificially advanced shoreline in Zones A and C.
- c. Of the 1,134,690 cu m of dredged material placed between 1988 and 1992, 825,770 cu m (73 percent) were placed within a single 1.9-km section of beach, resulting in a potential fill density of 426 cu m/m. The first postfill survey for this section (October 1989) only documented a 40- to 50-m-wide berm, which is only one-half as wide as the beach width this fill density could have supported. This relatively narrow berm suggests that there

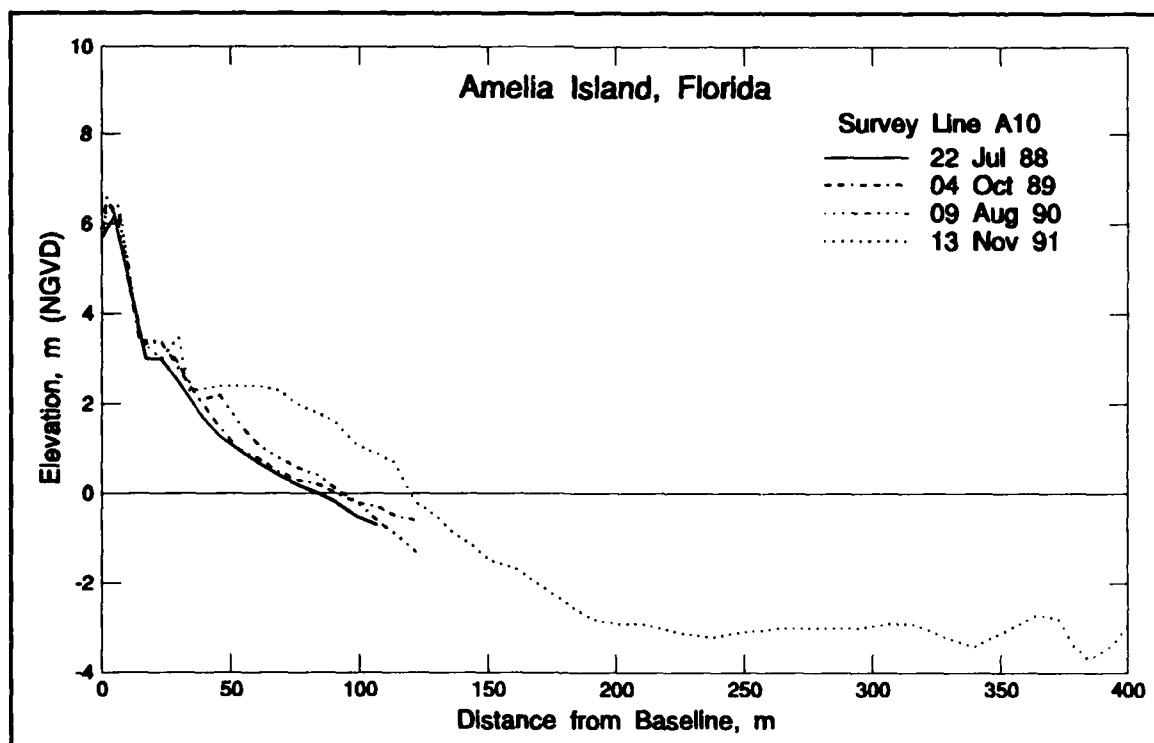
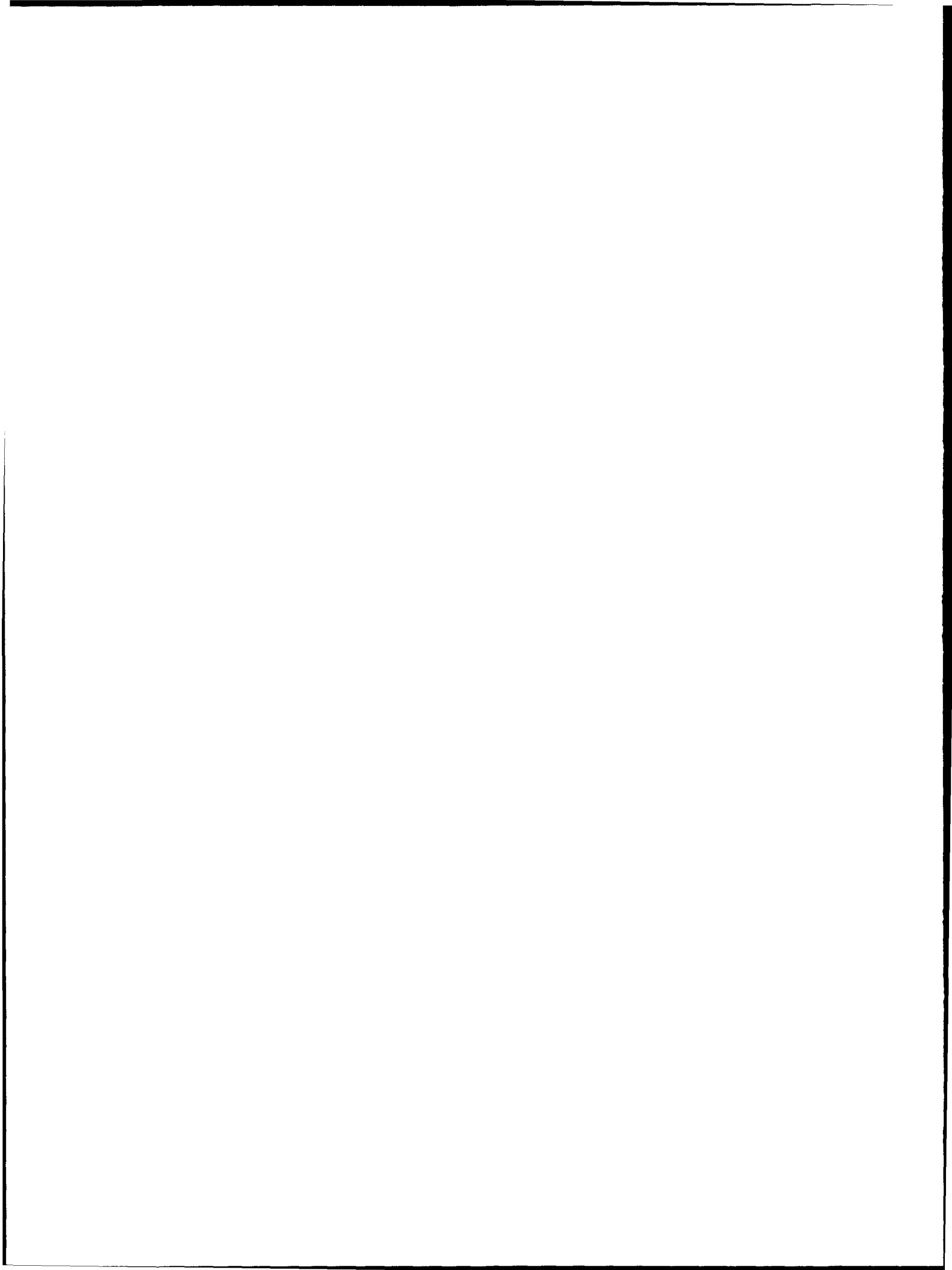


Figure 148. Profile comparison of Line A10 north of beach fill Zone A illustrating accretionary trend of the fillet south of the south jetty since Jul 1988

was offshore fill adjustment during placement. The 825,770 cu m placed between July 1988 and July 1989 were pumped from an offshore disposal area rather than from St. Marys Entrance channel as was the case with other beach fill operations. The excavated material probably contained more fine-grained sediments than that dredged from the entrance channel and placed directly on the beach.

- d.* A shoreline change rate of 0.2 m/year for the short monitoring period interval is insignificant relative to seasonal and other natural fluctuations in shoreline position.



# 6 Tides and Waves<sup>1</sup>

---

## Introduction

This chapter documents tidal and wave conditions measured in support of the coastal monitoring study. Tidal conditions in the project vicinity were evaluated using NOS tide data and data from several water-level gages both along the St. Marys Entrance channel and alongshore. The data were used to characterize variation in tidal amplitude and phase in the offshore directions, to the seaward end of the navigation channel, and parallel to Cumberland and Amelia Islands. Wave conditions were determined using three wave measurement systems. The three systems consisted of a wave buoy placed offshore near the entrance channel and two subsurface gages deployed nearshore along Amelia and Cumberland Islands. Data from each system were analyzed to provide important wave parameters at each location including wave height, period, direction, and wave energy spectra.

The importance of this information is to define the processes which occurred during the monitoring period. The tide data were used for datum control during the bathymetric surveys. Wave data documented storm conditions occurring during the monitoring period and were used in model calibration (Chapter 7).

## Tides

A monitoring study includes repetitive measurement and comparison of specific processes and conditions relative to an initial baseline to determine changes about the baseline. In the coastal zone, most processes and conditions must be measured relative to a known vertical datum such as MLW, and thus repetitive measurements must be made relative to the instantaneous water surface elevation in order to refer back to the vertical datum. The accurate, long-term measure of tides is a prerequisite in establishing the vertical datum, and an instantaneous determination of water surface elevation is a requisite when measuring processes and conditions. Inaccuracies in measuring instantaneous water surface elevation add random error to the measurements that may be the same order of magnitude as the anticipated change about the baseline.

---

<sup>1</sup> Written by John W. McCormick, William D. Corson, and Jeff W. Lillycrop.

Computation of astronomical tides from local water-level measurements,  $h(t)$ , is based upon the following equation (Harris 1981):

$$h(t) = h_0 + \sum_{n=1}^N A_n \cos(\sigma_n t - \theta_n) \quad (6)$$

where

$h(t)$  = tidal height at any time,  $t$

$h_0$  = height of local Mean Sea Level (MSL) datum above reference datum

$A_n$  = amplitude of constituent

$N$  = number of tidal constituents

$\sigma_n$  = frequencies determined from theory

$\theta_n$  = phases determined partly from theory and partly from measurements

Using the known harmonic constants of the tide, the amplitude  $A_n$  and the phase  $\theta_n$  of Equation (6) are determined empirically from the analysis of tide records.

### Previous studies

Several studies incorporated tidal analysis for the Fernandina Beach area and are reported in Vemulakonda et al. (1988) and Lillycrop et al. (1991). The first report describes a numerical modeling effort performed to study the effects of channel modifications on coastal processes near the inlet, especially channel shoaling rates. A system of models for tides, waves, wave-induced currents, and sediment transport was used. The WES Implicit Flooding Model was used to model tides. Tide data were collected by the USGS and WES between September and December 1982. Measurements were made within the inlet and throughout the estuary.

The Automated Real Time Tidal Elevation System (ARTTES) (Lillycrop et al. 1991) was developed as part of the Kings Bay channel deepening project to provide accurate real-time estimates of offshore water level to survey craft and dredges operating seaward of the jetties at St. Marys Entrance. Development of the system required water-level measurements along the navigation channel, seaward of the jetties. A permanent pressure sensor linked to a shore-based Remote Transmitting Unit and a mechanical gage coupled with a stilling well provided nearshore measurements. The absolute pressure measure from the underwater gage was adjusted using barometric pressure to provide a relative water level. Figure 149 shows the location of these and other tidal measurement instrumentation. Temporary Temperature-Depth Recorders (TDR's) were placed adjacent to the channel approximately 10 and 20 km offshore. Water surface levels were recorded every 6 min for the pressure sensor and TDR's and every 15 min for the stilling well. The data were processed by a least squares harmonic analysis routine to extract the tidal amplitude and phase for five tidal constituents, which are used in the ARTTES analysis procedure.

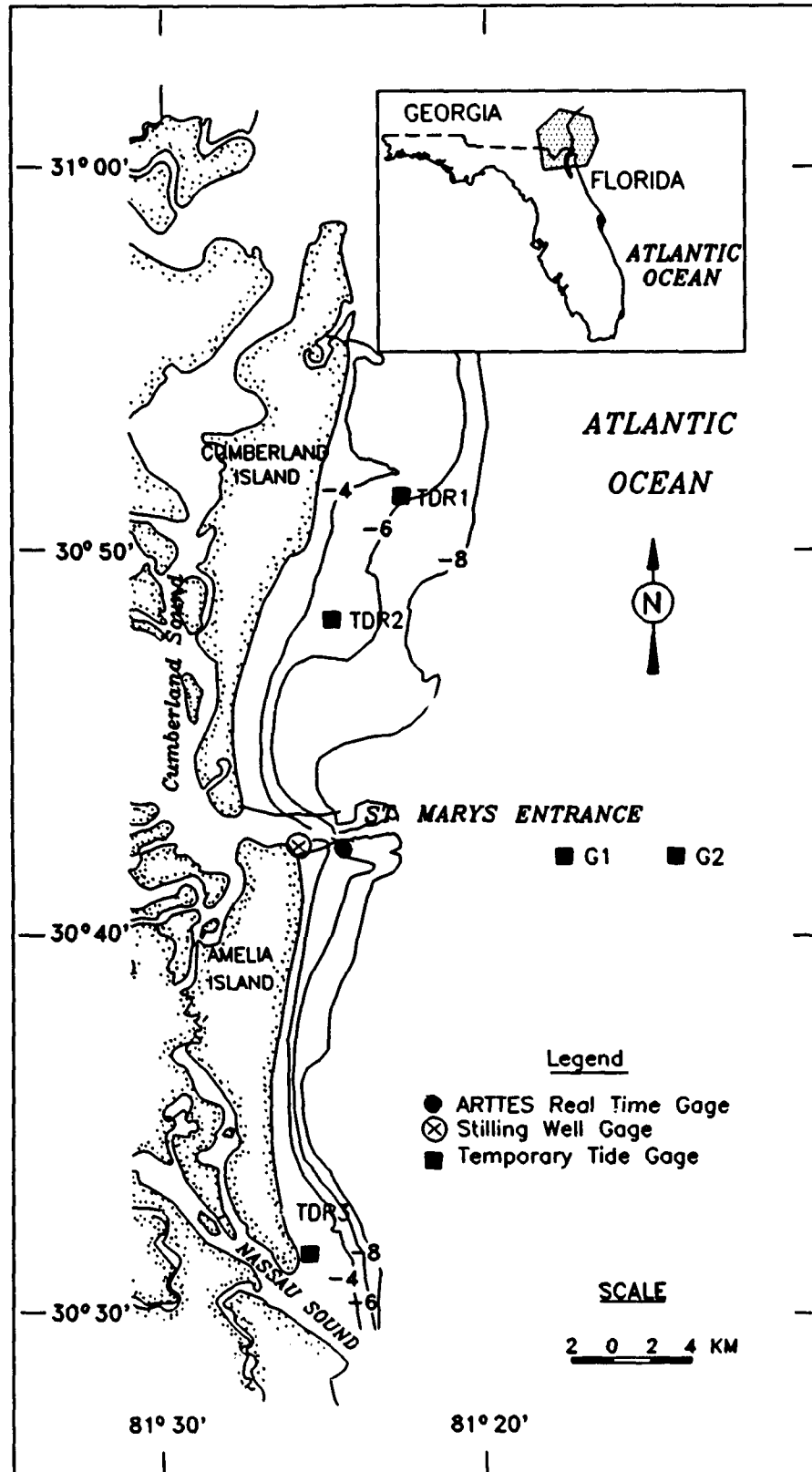


Figure 149. Kings Bay tide gage location map

A third study conducted as part of the Kings Bay Monitoring Study was to evaluate the use of ARTTES output for estimating tides along Cumberland and Amelia Islands as an aid to beach profiling operations. Three TDR's were installed, two along Cumberland Island, TDR1 and TDR2, and one on the south end of Amelia Island, TDR3. Results of this analysis are presented later in this section.

### Tide data

Tide data for the Kings Bay area and surrounding regions were obtained and analyzed to determine the tidal characteristics of the region. Regional tide data from Charleston, South Carolina, to Mayport, Florida, were obtained from Tide Tables, East Coast of North and South America (NOAA 1991b) to describe regional variations in tide range and phase along the East Coast. Tide data from the studies discussed above were used to describe local tide conditions and demonstrate local variations in tide.

**Regional tides.** Tides along the southeastern region of the United States are semidiurnal with ranges varying from approximately 1.5 to 2.5 m. The tide wave propagates from north to south with high tides occurring at Charleston, South Carolina, and Savannah, Georgia, approximately 16 and 13 min earlier than at Kings Bay/Fernandina Beach, respectively. Table 35 summarizes average tidal ranges for the region and presents phase differences for several locations relative to Fernandina Beach tides. The ocean and coastal tides are dominated by the lunar constituent  $M_2$  that alone accounts for the preponderance of annual water-level variance along this region. The greatest regional tidal ranges are experienced in locations where the continental shelf is widest, such as adjacent to the Georgia Bight where Savannah has one of the greater tide ranges in the southeast. Here, shallow water amplifies the tidal range.

**Tides at the monitoring site.** Tides along the Cumberland and Amelia Island open coast and within the Kings Bay navigation channel are semidiurnal (Figure 150), with a mean range of 1.8 m and spring range of 2.1 m. The primary tidal constituent is  $M_2$ , which, along with  $N_2$ ,  $S_2$ ,  $O_1$ , and  $K_1$ , account for over 90 percent of the astronomically driven water-level variance. Results of a least squares harmonic analysis performed on 31 days of data (28 June - 29 July 1989) for the ARTTES gage located outside of the inlet are presented in Table 36.  $M_2$  is the dominant constituent; its amplitude is over four times greater than any of the remaining constituents used in the analysis.

**Table 35**  
**Regional Tides**

Location	Phase Difference Relative to Fernandina min		Range m	
	High	Low	Mean	Spring
Charleston, SC	-16	-31	1.6	1.9
Savannah, GA	-13	-18	2.1	2.4
Fernandina Beach, FL (N. Jetty)	0	0	1.8	2.1
Mayport, FL	25	0	1.4	1.6

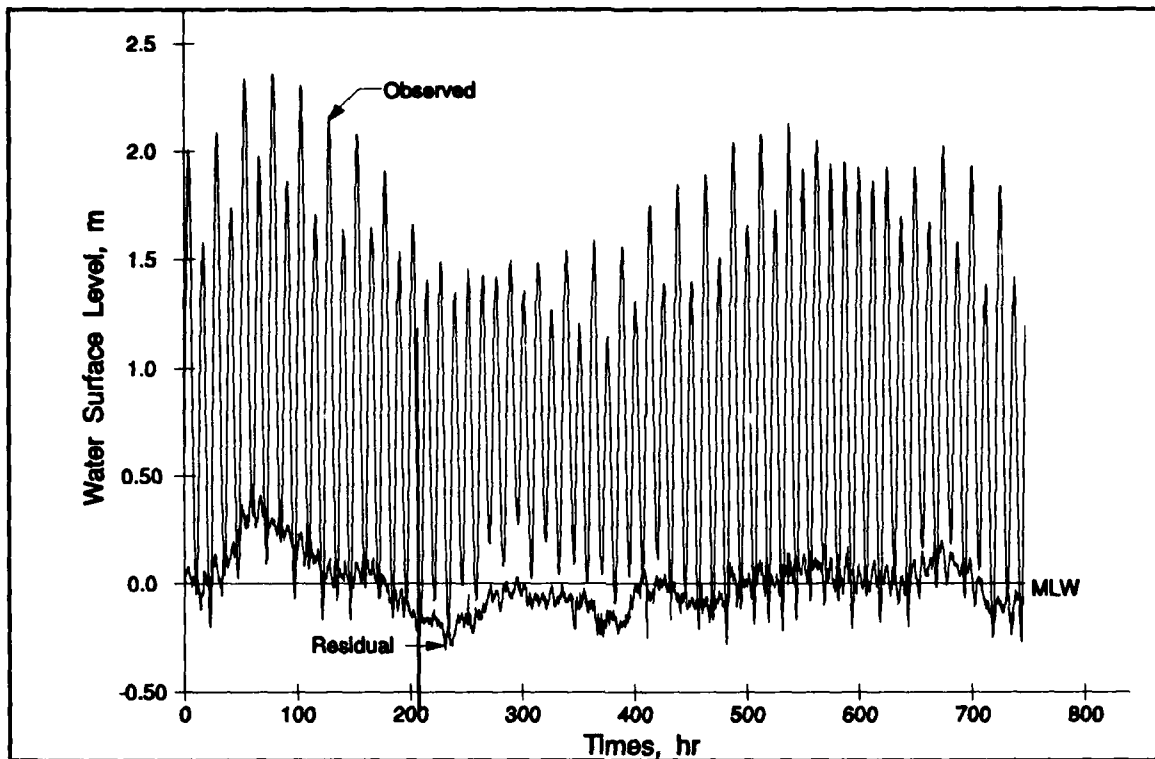


Figure 150. Kings Bay ARTTES observed tide and nonastronomical residual

**Table 36**  
**Tidal Constituents for ARTTES and Stilling Well Gage<sup>1</sup>**

Constituent		ARTTES Gage		Stilling Well Gage	
Symbol	Period, hr	Amp, m	Phase, deg	Amp, m	Phase, deg
M <sub>2</sub>	12.4206	0.85	107.7	0.87	118.1
N <sub>2</sub>	12.6583	0.19	104.2	0.08	145.3
S <sub>2</sub>	12.0000	0.15	236.2	0.13	243.8
K <sub>1</sub>	23.9345	0.11	118.3	0.11	119.3
O <sub>1</sub>	25.8193	0.10	20.9	0.09	23.0
K <sub>2</sub>	11.9672	0.08	42.2	0.06	38.0
ν <sub>2</sub>	12.6260	0.05	295.4	0.11	111.6
P <sub>1</sub>	24.0659	0.04	84.3	0.03	86.9
L <sub>2</sub>	12.1916	0.01	336.0	0.03	111.6
2N <sub>2</sub>	12.9054	0.01	32.2	0.01	4.7

<sup>1</sup> Computations were performed for the ARTTES data and for the concurrent stilling well gage data for 31 days following 1200 hr 28 June 1989 (EST).

The high percentage of variance accounted for by the harmonic analysis on the ARTTES gage means that water-level fluctuations at the monitoring site are primarily caused by astronomical forces. However, meteorological events also affect water surface elevations in this area. Figure 150 presents a 31-day (28 June - 29 July 1989) observed/measured tide record from the ARTTES and a residual element that is the calculated difference between the observed tide and the predicted astronomical tide. Note that early in the record, the residual, or nonastronomical water-level fluctuation reaches a third of a meter. During this period, measured tide elevations were greater than the purely astronomical predicted tide and were caused by a northeast wind that created a net setup in the coastal water surface elevation. A negative residual corresponds to a setdown in water surface elevation, typically caused by offshore winds. These meteorological events typically have high-frequency components associated with daily weather changes such as those caused by afternoon thunderstorms and a low-frequency component several times longer than astronomical periods associated with weather fronts, as seen in Figure 150.

**Tide variability.** Tide amplitude varies with position alongshore and along the navigation channel. Tide data collected for ARTTES were analyzed to illustrate differences between ARTTES and the stilling well, ARTTES and the temporary gages along the navigation channel, and ARTTES and temporary gages along Cumberland and Amelia Islands.

Table 36 also summarizes results of a least squares harmonic analysis performed on 31 days of data (28 June - 29 July 1989) for the stilling well gage and allows a comparison with ARTTES. Although the ARTTES and stilling well are only 600 m apart, a constituent analysis for the same time period yields slightly different values at the two locations. The difference is small, yet observable in the data for these two gages, and is due to the stilling well being inside the jetties versus ARTTES being located along the open coast.

Because the jetties are permeable, floodwaters enter the inlet through the navigation channel inlet opening, and over and through the jetties at sufficient rates to maintain a near constant water level between the inlet and the open coast. However, as the tide ebbs, flow through the inlet is channelized and constricted. This delays the withdrawal of tide waves from the estuary relative to the receding open coast tidal wave, resulting in a slight modulation of the tide within the inlet. Figure 151 illustrates the modulation by a slightly higher water surface elevation at the stilling well compared to the ARTTES open coast water surface elevation. On the flood stage of the tide, water levels are nearly equal, but during the ebb stage the tide at the stilling well lags the open coast tide by a few minutes.

**Offshore tide variation.** Tide amplitude varies with position along the entrance channel. Table 37 lists constituents calculated at ARTTES and a temporary gage located approximately 10 km to the east, labelled G1 in Figure 149. The temporary gage was originally installed in support of the ARTTES development program sponsored by USAED, Jacksonville. Note that the value of  $M_2$  is slightly larger at the offshore position; when these constituents are used to predict the tide, the offshore amplitude is greater than at the ARTTES gage during spring tide when semidiurnal constituents dominate (Figure 152). During neap tide, diurnal constituents dominate and the ARTTES amplitude is slightly greater than the offshore amplitude (Figure 153). This variability in elevation is likely a function of the local bathymetry.

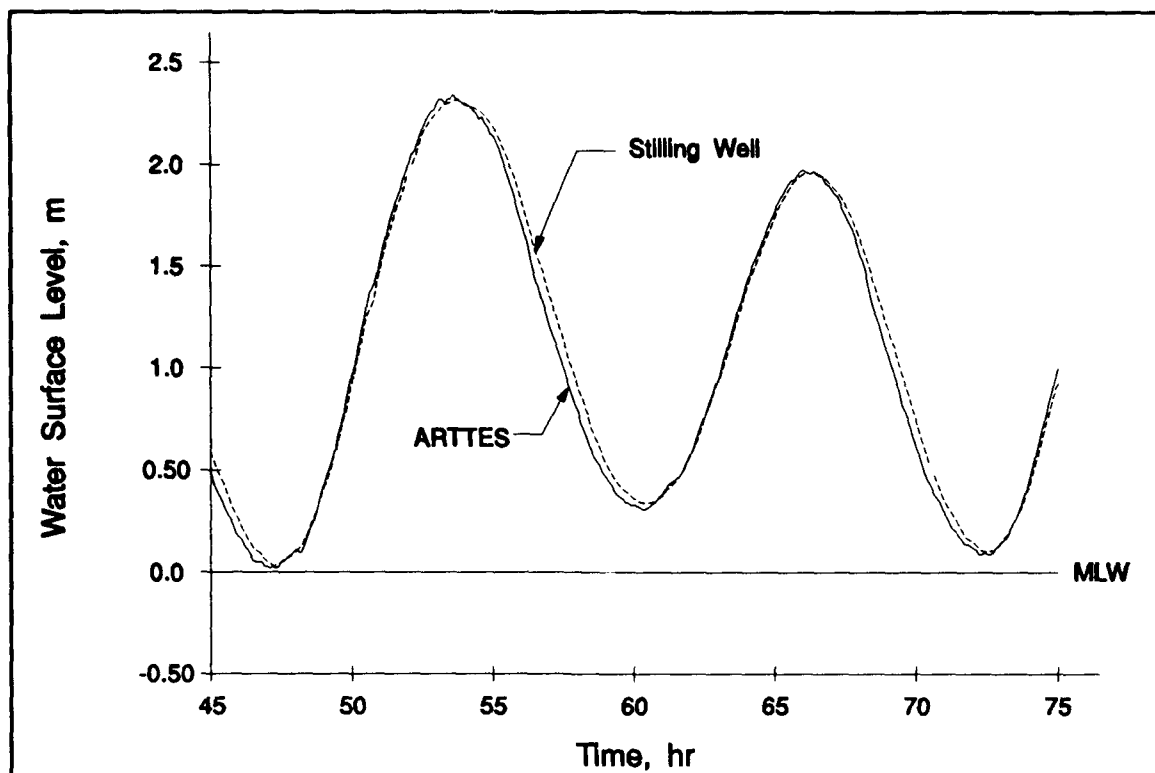


Figure 151. Comparison of ARTTES and stilling well gage measurements

**Table 37**  
**Tidal Constituents for ARTTES and Offshore Gage G1<sup>1</sup>**

Constituent		ARTTES Gage		Offshore Gage G1	
Symbol	Period, hr	Amp, m	Phase, deg	Amp, m	Phase, deg
M <sub>2</sub>	12.4206	0.82	359.6	0.84	351.8
N <sub>2</sub>	12.6583	0.17	253.3	0.21	0.9
S <sub>2</sub>	12.0000	0.17	265.1	0.18	245.0
K <sub>1</sub>	23.9345	0.09	131.6	0.09	89.7
O <sub>1</sub>	25.8193	0.07	260.1	0.07	261.1

<sup>1</sup> Computations were performed for the ARTTES data and for the concurrent offshore gage data during 1988. The phases have been normalized to 0000 hr 1 January 1988 (EST).

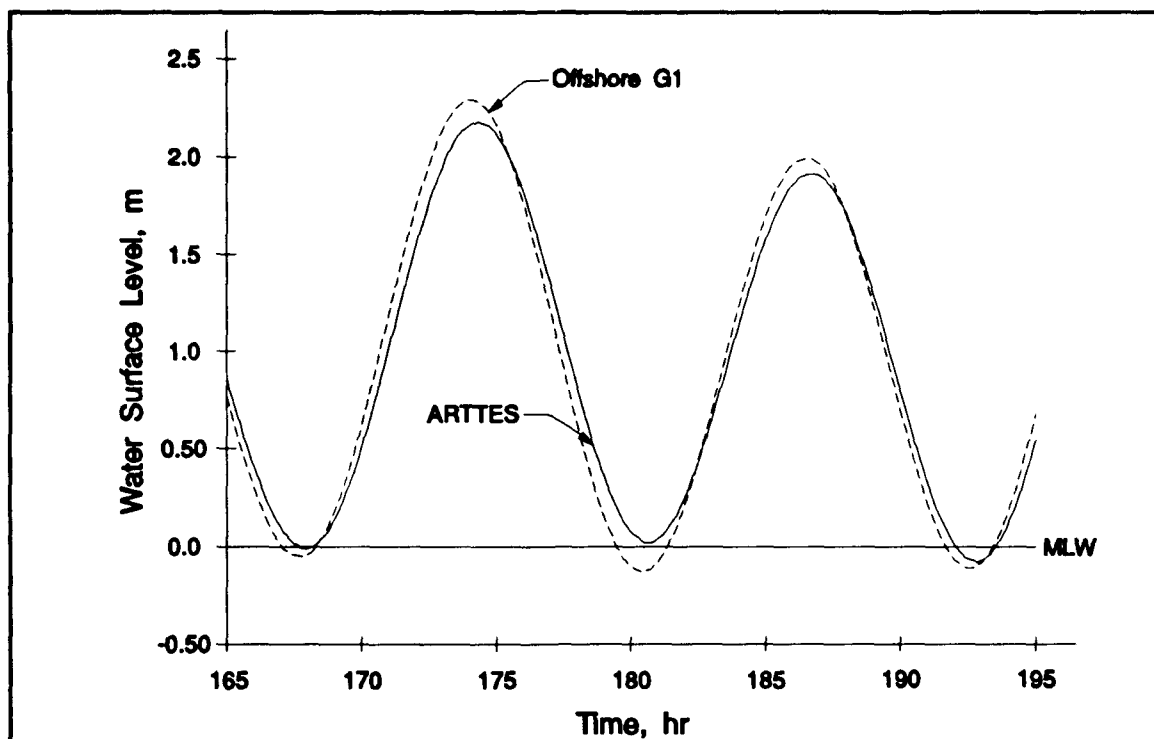


Figure 152. Comparison of ARTTES and offshore gage G1 during spring tide

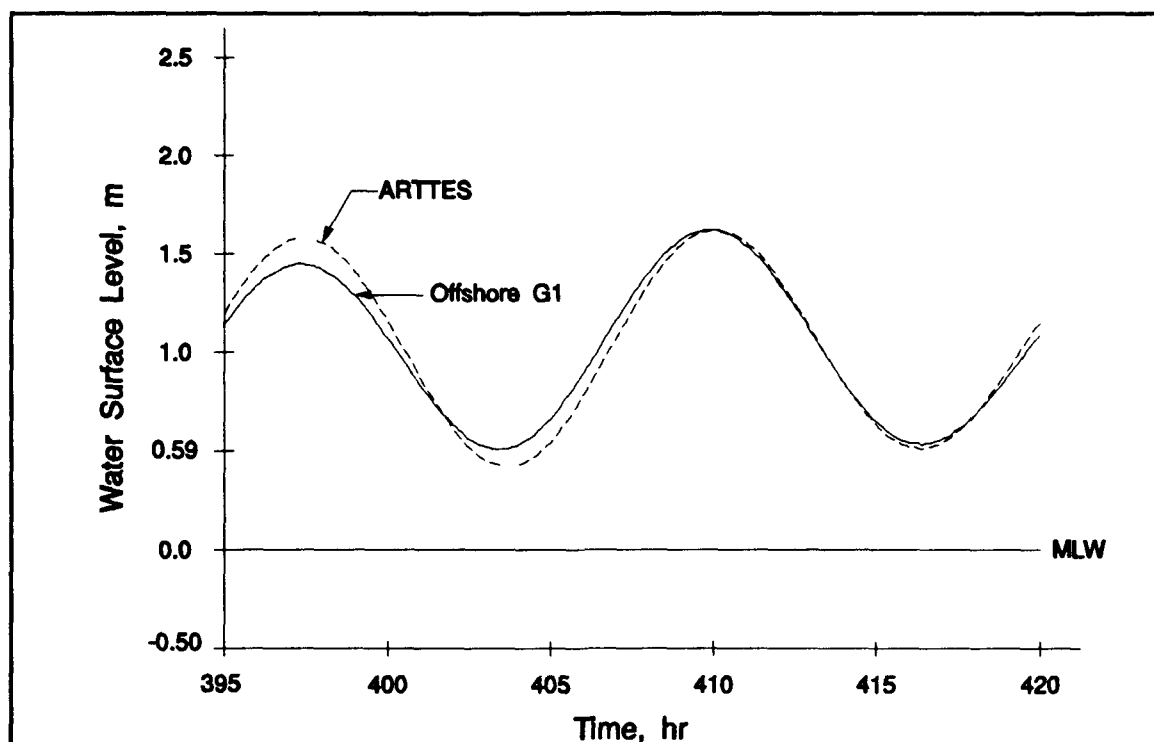


Figure 153. Comparison of ARTTES and offshore gage G1 during neap tide

**Alongshore tide variation.** In 1989, a need was identified to use ARTTES for determining tide elevation during times of beach profile surveys made in support of the monitoring effort. However, because ARTTES was neither designed nor intended for use other than along the seaward section of the St. Marys Entrance channel, there were no available data to perform an objective assessment of the adequacy of this system for such purposes.

To provide data for such an assessment, CERC established three temporary nearshore tide stations, two along Cumberland Island and one at the south end of Amelia Island (Figure 149). The bathymetry along Amelia Island is relatively uniform with parallel depth contours. Therefore, tide effects could be expected to vary approximately linearly with distance along the shore. A single temporary tide station, called TDR 3, was judged to be adequate to assess the alongshore variation. The bathymetry along Cumberland Island, however, is characterized by a crescent-shaped basin south of Stafford Shoal with a shallow shelf to the north. To determine tide characteristics in the two different bathymetric regimes, two temporary tide stations were installed, one at the northern perimeter of the basin, called TDR 1, and the other on the shelf, called TDR 2. Table 38 lists the inclusive dates when the three temporary gages were operating.

**Table 38**

**Temporary Tide Gage Locations and Dates of Operation**

Gage	Location	Dates of Operation
TDR 1	30°53.15'N; 81°22.69'W Middle Cumberland Island	August 1989 to November 1989
TDR 2	30°48.55'N; 81°24.49'W South Cumberland Island	August 1989 to November 1989
TDR 3	30°32.41'N; 81°25.80'W South Amelia Island	March 1991 to May 1991

Table 39 presents results from analyses of concurrent TDR 3 and ARTTES data for 29 days following 0000 hr 1 April 1991. The table suggests that the tides at south Amelia Island have a great similarity to those at Fernandina Beach. The dominant constituent  $M_2$ , which constitutes more than 90 percent of the tidal energy for both locations, shows only a 6-cm difference in amplitude and 5-deg difference in phase. The total astronomical tide along the coast from south Amelia Island to middle Cumberland Island has a maximum difference of about 15 cm from that at the ARTTES gage. The observed water levels at south Amelia Island have a maximum difference of about 20 cm from the observed water levels at the ARTTES gage. However, differences of 10 cm or less occur about 78 percent of the time (Table 40).

Table 41 summarizes the analyses for the ARTTES and concurrent TDR 1 and TDR 2 data for 29 days following 0000 hr 21 October 1989. Tidal characteristics at the three locations are almost identical during the period of observation. Differences between the  $M_2$  amplitudes are less than 5 cm and the phase less than 2 deg. Therefore, with the assumption that the mean water levels at the gages are the same during the observation period, it is expected that the water levels along Cumberland Island correlate better with ARTTES measurements than those along Amelia Island. However, surveys along both islands can be postcorrected to sufficient vertical accuracies using recorded ARTTES data.

**Table 39**  
**Tidal Constituents for South Amelia TDR 3 and ARTTES<sup>1</sup>**

Constituents		ARTTES		South Amelia Island TDR 3	
Symbol	Period hr	Amp m	Phase deg	Amp m	Phase deg
M <sub>2</sub>	12.4206	0.87	231.7	0.81	226.3
N <sub>2</sub>	12.6583	0.18	228.7	0.17	222.1
S <sub>2</sub>	12.0000	0.15	251.9	0.14	248.8
K <sub>1</sub>	23.9345	0.12	95.8	0.11	94.4
O <sub>1</sub>	25.8193	0.08	159.6	0.08	156.2
K <sub>2</sub>	11.9672	0.04	37.7	0.04	34.7
v <sub>2</sub>	12.6260	0.02	50.7	0.02	46.6
P <sub>1</sub>	24.0659	0.04	125.6	0.04	124.1
L <sub>2</sub>	12.1916	0.04	186.1	0.03	179.7
2N <sub>2</sub>	12.9054	0.02	225.2	0.02	217.4

<sup>1</sup> Computations were performed for the ARTTES data and for the concurrent TDR3 and TDR2 data for 29 days following 0000 hr 1 April 1991 (EST). The phases have been normalized to 0000 hr 1 January 1989 (EST).

**Table 40**  
**Observed Water-Level Differences Between South Amelia Island and Fernandina Beach**

Differences in Observed Water Level, cm	Percent of Data with a Smaller Difference
20	99.8
15	97.1
10	77.9

**Table 41**  
**Tidal Constituents for Cumberland Island TDR1 and 2 and ARTTES<sup>1</sup>**

Constituents		ARTTES		Middle Cumberland TDR 1		South Cumberland TDR 2	
Symbol	Period, hr	Amp, m	Phase, deg	Amp, m	Phase, deg	Amp, m	Phase, deg
M <sub>2</sub>	12.4206	0.82	74.3	0.87	72.7	0.84	74.0
N <sub>2</sub>	12.6583	0.20	248.2	0.22	246.8	0.21	248.4
S <sub>2</sub>	12.0000	0.15	251.9	0.17	255.3	0.16	256.8
K <sub>1</sub>	23.9345	0.09	120.0	0.10	111.7	0.10	112.2
O <sub>1</sub>	25.8193	0.07	349.2	0.07	350.8	0.07	352.0
K <sub>2</sub>	11.9672	0.04	42.5	0.04	46.3	0.04	47.8
v <sub>2</sub>	12.6260	0.02	102.8	0.02	100.8	0.02	102.0
P <sub>1</sub>	24.0659	0.03	145.8	0.03	138.3	0.03	138.8
L <sub>2</sub>	12.1916	0.04	42.3	0.04	41.0	0.04	42.5
2N <sub>2</sub>	12.9054	0.03	60.2	0.03	59.3	0.03	61.0

<sup>1</sup> Computations were performed for the ARTTES data and for the concurrent TDR1 and TDR2 data for 29 days following 0000 hr 21 October 1989 (EST). The phases have been normalized to 0000 hr 1 January 1989 (EST).

## Waves

### Introduction

Summaries of directional wave data are available for three wave measurement systems. To measure waves in the vicinity of Kings Bay, a buoy was placed approximately 30 km offshore in approximately 18 m of water (MLW), and two subsurface gages were deployed nearshore in a depth of approximately 10 m (Figure 154). The three systems are:

- CERC pressure (P) and velocity component (UV) wave gage. The PUV gage was deployed approximately 5 km offshore of the south end of Cumberland Island and approximately 3.5 km north of the north jetty of St. Marys Entrance (30.75 °N, 81.41 °W).
- CERC slope array (SA) wave gage. The SA was positioned approximately 1.5 km offshore of Amelia Island and approximately 8 km south of the St. Marys Entrance south jetty in approximately 10 m of water (30.63 °N, 81.42 °W).
- NDBC pitch-roll buoy #41008. The buoy was located approximately 30 km offshore directly east of the St. Marys Entrance (30.73 °N, 81.08 °W).

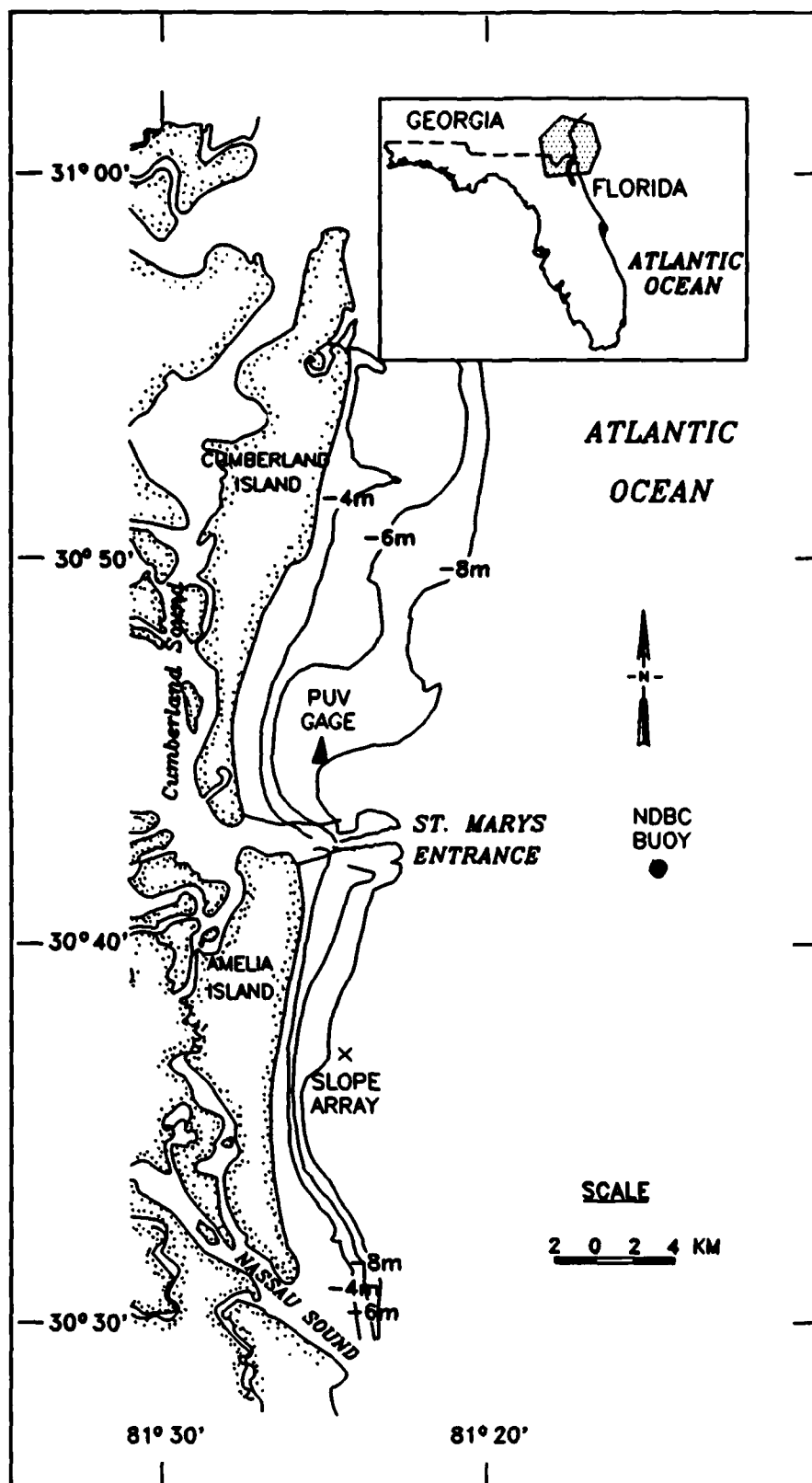


Figure 154. Location of wave gages relative to St. Marys Entrance

The wave parameters summarized in this report include:

- a. Wave height:  $H_{m_0}$ , where  $H_{m_0}$  is four times the square root of the wave energy in a sample (*Shore Protection Manual* (SPM) 1984) and approximately equal to the significant wave height if measured.
- b. Wave period:  $T_p$ , where  $T_p$  is the inverse of the value of the frequency band with the highest energy (*Shore Protection Manual* (SPM) 1984).
- c. Wave direction:  $\Theta_p$ , direction from which waves are incident relative to true north. Direction selected as direction of frequency band with highest wave energy.
- d. Wave energy spectra: wave energy and direction for each frequency band.

### Wave measurement systems

Each of the wave measurement systems is designed to provide directional wave spectra at selected time intervals for a specified sample length. Although sampling characteristics are different for each system, similar analysis techniques are used to reduce differences in the information obtained between systems that might arise through data processing. Because of the complexity of the measurement systems and the harsh coastal environment in which they are deployed, the data from each system were reviewed for unlikely output. For the PUV and SA gages, problems such as records of extreme pressure changes (spikes) beyond physical possibility were edited and the record either used, or not, depending on the percent of spikes in the record. Quality control of the NDBC buoys is discussed in Steele et al. (1990).

CERC's internal recording PUV gage was deployed for nearly a month (May 1989) when it was overturned by a trawler and became no longer useful. The PUV gage was placed to record nearshore waves north of the jetty. The 10-m depth is best for recording waves over a wide range of periods. If deployed in deeper water, it is difficult to determine shorter wave period energy levels, and, if deployed in shallower water, accuracy can be lost due to wave breaking over the sensor. A replacement system for the PUV was not deployed, because the SA was in place and a replacement system would have required additional funding. The PUV gage recorded data every 3 hr for bursts of 1024 sec at a rate of one sample per second (1 Hz). The data were originally recorded in EST, and local time was converted to Greenwich Mean Time (GMT) for comparison with the other measurement platforms. The PUV gage is composed of a near-bottom mounted pressure sensor and an electromagnetic current meter combined to give pressure (P) and components of the wave orbital velocities (U and V). Although the main purpose of the PUV was to measure waves, records of near-bottom currents measured during the May 1989 deployment of the PUV are available, but are not summarized in this report.

CERC's near-real-time-reporting SA was operated from April 1989 through June 1990. The SA recorded data hourly for April and May 1989; thereafter, it was converted to recording data every 4 hr for the remainder of the deployment. Bursts were for 1024 sec at 1 Hz. Instrumentation of the SA consists of three pressure sensors mounted near the bottom on a triangular pod. The SA was deployed about 8 km south of the south jetty to take advantage of the location of a pier for bringing cables ashore. Because the SA uses pressure sensors for wave calculations, the same depth restrictions apply as noted for the PUV gage.

Diver observations of the SA during maintenance in January 1990 and when it was retrieved later in March 1991, indicated that it had been struck (probably by a trawl net) and moved sometime prior to those observations. After the SA was moved, its orientation became unknown and wave direction data obtained from this gage are unreliable. However, in both instances, the SA had not been operating for some time prior to the diver observations. Considerable study of the data produced no evidence that the SA was struck during the time it was operational or that the recorded data were incorrect because the gage had moved. It seems likely that the SA was struck after it had already stopped transferring data. Therefore, the results presented in Appendix E are considered valid within expected ranges of gage accuracy. Investigations into the wave directions for the SA are presented in Appendix E of this report. The lack of more uninterrupted data sets from the SA can be attributed to two sources: the difficulty of maintaining a nearshore gage in an area that has intensive trawling activities, and logistical and fiscal constraints which delayed repairs.

The NDBC directional wave buoy includes heave, pitch, and roll sensors, and it provides (among other parameters) accelerometer-based measurements of surface elevation and slope. From these measurements, the NDBC calculates required information for directional wave spectra. The NDBC provided the data under contract to CERC. The location of buoy 41008 was selected to be near the location of WIS Station 57 (Corson et al. 1982). The NDBC buoy 41008 was deployed offshore of Kings Bay from June 1988 to March 1992. Data are recorded hourly in GMT for bursts of 1200 sec at a rate of 2 Hz. Further information on NDBC buoys can be found in Steele, Lau, and Hsu (1985) and Steele et al. (1990).

#### **Data summaries**

After all the wave data were acquired, several data products were prepared to provide summaries. Tables E1, E2, and E3 in Appendix E provide sample listings of data from each system. Data availability tables are also provided for the buoy and the SA (Tables E4 and E5). Monthly time-series plots of  $H_{m0}$ ,  $T_p$ , and  $\Theta_p$  are provided in Appendix E for each measurement system (Plates E1-E62). Inquiries about obtaining similar data products for all or part of the wave records should be directed to the Engineering Development Division of CERC. Water depths for the PUV and SA gages represent water depth at sensor and are not referenced to a datum. The reported depths have not been adjusted to account for variation in atmospheric pressure. The depth listed for the buoy is the nominal depth provided by NDBC and is not measured by the buoy.

Because the buoy has a relatively long deployment time, additional products are provided to summarize the obtained data:

a. Mean and largest wave height summary (Table 42) which provides:

- (1) Monthly and annual mean  $H_{m0}$  values.
- (2) Monthly largest  $H_{m0}$  values.
- (3) Overall mean  $H_{m0}$  and  $T_p$  values.
- (4) Most frequent direction band.

**Table 42**  
**Mean and Largest Wave Height Summary**

Year	Month												Mean
	Jan	Feb	Mar	Apr	May	Jun	Jul	Aug	Sep	Oct	Nov	Dec	
Mean $H_{m0}$ (Meters) by Month and Year NDBC Buoy 41008 (30.73N 81.08W)													
1988	-- <sup>1</sup>	--	1.0	0.9	--	0.9	0.9	0.9	1.0	1.2	1.1	0.9	1.0
1989	1.1	0.9	1.1	0.9	0.7	0.7	0.7	0.8	1.2	1.0	0.7	1.1	0.9
1990	0.8	1.2	1.1	1.0	0.8	0.7	0.8	0.6	0.9	1.3	1.1	1.1	1.0
1991	1.1	1.1	1.1	1.0	0.8	0.9	0.7	0.7	1.1	1.3	1.2	1.1	1.0
1992	1.0	1.0	0.9	--	--	--	--	--	--	--	--	--	1.0
Mean	1.0	1.1	1.1	0.9	0.8	0.8	0.8	0.7	1.1	1.2	1.1	1.1	
Largest $H_{m0}$ (Meters) by Month and Year NDBC Buoy 41008 (30.73N 81.08W)													
1988	--	--	1.7	1.7	--	2.2	2.3	2.2	2.9	2.4	2.8	3.1	
1989	4.6	2.9	2.8	2.2	2.2	1.5	1.5	2.3	3.2	2.5	1.4	2.8	
1990	2.0	2.7	2.9	3.0	1.9	1.6	2.2	1.2	1.7	3.1	3.5	2.2	
1991	2.7	2.7	3.0	2.5	1.9	2.8	1.7	1.9	2.6	3.3	2.9	2.7	
1992	2.8	2.8	2.5	--	--	--	--	--	--	--	--	--	
4-Year Statistics for NDBC Buoy 41008 (30.73N 81.08W)													
Mean significant wave height (meters)												1.0	
Mean peak wave period (seconds)												7.7	
Most frequent 22.5 (center) direction band (degrees)												90.0	
Standard deviation of $H_{m0}$ (meters)												0.5	
Standard deviation of $T_p$ (seconds)												2.6	
Largest $H_{m0}$ (meters)												4.6	
$T_p$ (seconds) associated with largest $H_{m0}$												11.1	
Peak direction (degrees associated with largest $H_{m0}$ )												102.0	
Date of largest $H_{m0}$ occurrence												89012301	
<sup>1</sup> No data available.													

(5) Standard deviation of  $H_{m0}$  and  $T_p$ .

(6) Overall largest  $H_{m0}$  with associated  $T_p$ ,  $\Theta_p$ , and date.

*b.* Percent occurrence tables (Appendix E).

The summary of the buoy data in Table 42 indicates a mean  $H_{m0}$  of 1.0 m and a mean  $T_p$  of 7.7 sec. Waves are most common from the east. Table 42 also shows that the largest  $H_{m0}$  recorded by the buoy was 4.6 m at 11.1 sec incident from 102 deg (east-southeast).

The percent occurrence tables provide summaries of the percent occurrence of waves in height and period ranges for specified direction bands and for all directions combined (Table E6). The direction bands are centered on 22.5-deg increments, such as 0.0, 22.5, 45.0, etc. (Table E7). The period ranges are derived from the frequency band available from the buoy data (Table E8).

The title lines of each percent occurrence table identify the buoy number, location, and direction band. The last line of each table presents the mean  $H_{m_0}$ , largest  $H_{m_0}$ , mean  $T_p$ , and number of cases for the selected direction band. The tables may be used to estimate the percent occurrence of selected wave conditions or simply to form an overview of the wave climate of the area. For example, the tables indicate that waves of 1.0 to 1.4 m and 8.1 to 9.5 sec from 90 deg (east) occur 2.4 percent of the time (Table E6). The same table indicates that waves from 90 deg of 1.0 to 1.4 m (for all wave periods) occurred 7.5 percent of the time. The table also indicates that the mean  $H_{m_0}$  from 90 deg was 0.9 m and the largest  $H_{m_0}$  from 90 deg was 4.4 m. The largest  $H_{m_0}$  recorded by the buoy was from the 112.5-deg band.

A sample plot of the directional spectra from all three systems for 0200 GMT, 4 May 1989, is presented in Figure 155. In this example, all systems measured significant wave energy from about 130 deg (south-southeast) at about 15 and 7 sec. Scatter in the plot of wave direction ( $\Theta_p$ ) by frequency band is mostly due to lack of energy in the regions of the spectra for wave periods shorter than 5 sec and longer than 20 sec (approximately).

Data from the NDBC Buoy presented in Appendix E were briefly analyzed to estimate the frequency of storm conditions throughout the monitoring period. A "Storm" was interpreted as the occurrence of wave heights greater than 2.0 m. A summary of storm conditions occurring during the monitoring period is presented in Figure 156. An increase in storm activity can be observed during the latter stages of the monitoring period, particularly during 1991, which included the three stormiest months (i.e., January, September, and October) of this record.

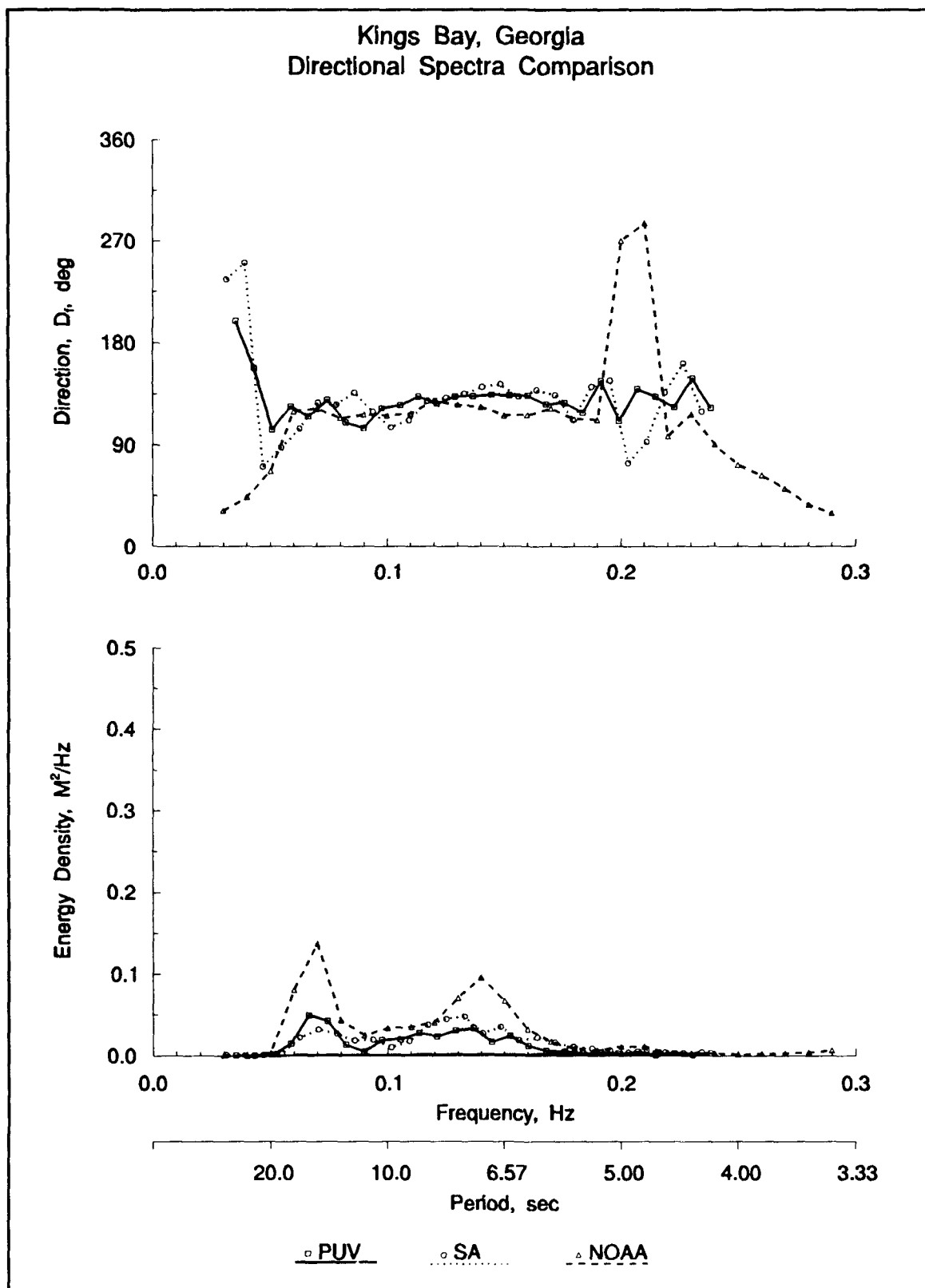


Figure 155. Plot of wave spectra for 4 May 1989 at 0200 Hr GMT

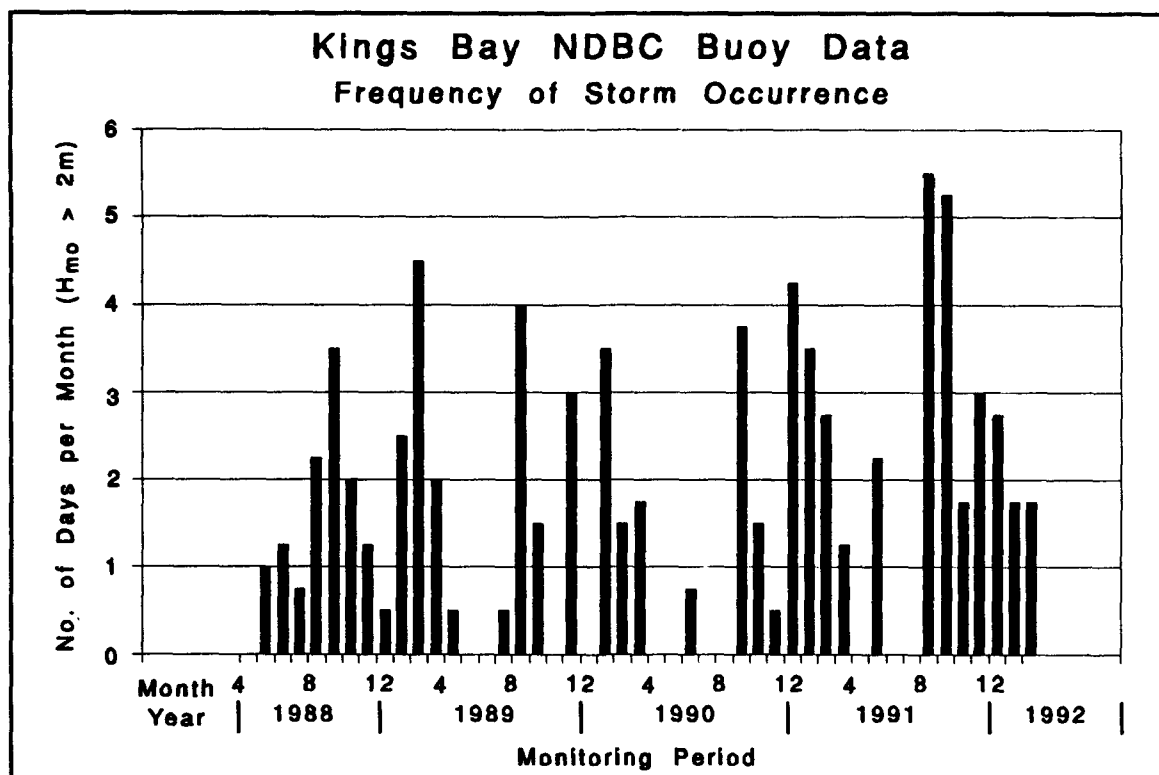


Figure 156. Number of days per month where wave heights exceeded 2 m based on NDBC buoy data (Appendix E)

# 7 Shoreline Change Extrapolation<sup>1</sup>

---

## General Approach

The objective of work described in this chapter is to make quantitative estimates of longshore sand transport rates and shoreline change along Cumberland and Amelia Islands. This portion of the study employs two numerical simulation models: STWAVE, a nearshore wave transformation model, and GENESIS, a shoreline change model. The models are calibrated and verified with measured wave and shoreline position data, respectively. The calibrated modeling system is applied to estimate longshore sand transport rates for historical bathymetric conditions of the 1870s and 1920s and to extrapolate shoreline conditions into the future. The magnitude of the effect of the dredged navigation channel on neighboring shorelines is assessed by comparing present-day sediment transport rates and resulting shoreline change rates with those that have historically occurred. Also, probable ranges of longshore sand transport rates are estimated by examining potential rates obtained for each year of a 20-year wave hindcast. Finally, an investigation is made through numerical simulation of the potential effect of the TRIDENT channel deepening on shoreline processes.

## Wave Database

To provide nearshore wave conditions that determine shoreline change, waves are transformed to the nearshore from deeper water. Wave conditions in deeper water are referred to as offshore wave conditions. This section describes the offshore wave data available for the shoreline change extrapolation study.

Offshore wave data were supplied from a CERC WIS Phase III hindcast specially performed for the Kings Bay project rather than use the standard regional-scale Phase III hindcast. The shoreline orientations in the study area render the standard Phase III hindcast data inappropriate for detailed calculations because the original hindcast was performed for a regional-scale coastal orientation. Information concerning the development of WIS wave hindcast data is given by Jensen (1983a).

The custom hindcast for the Kings Bay study provided improved offshore wave data to account for the specific shoreline orientations of Cumberland and Amelia Islands (7 and 4 deg,

---

<sup>1</sup> Written by William G. Grosskopf and Nicholas C. Kraus.

respectively, from true north). Sheltering by the Georgia coast to the north and by the Florida coast to the south also restricted onshore-directed waves to  $\pm 70$  deg from a shore-normal line. The custom hindcast produced an historical time series of wave height, period, and direction distribution at a depth of 18.6 m. This depth provides an appropriate offshore boundary location for finer scale wave transformation modeling over the irregular nearshore bathymetry.

In producing Phase III hindcast data, the WIS approach requires that bottom contours be straight and parallel and that sea and swell waves be independent. Sea waves are generated by local winds and exhibit short crests and broad spectra. Swell is generated by distant storms and has long wave crests with narrower frequency and directional spectra than sea waves. The hindcasts include normal storm conditions but not extreme hurricanes or tropical storms.

For the purpose of this study, the customized WIS Phase III hindcast produced the following:

- a. Time series of significant wave height, peak spectral wave period, and predominant wave direction at the spectral peak for both sea and swell at 3-hr intervals over the 20-year period from 1956 to 1975.
- b. Tables showing the joint frequency of occurrence of wave height and period for each direction band. The tables were compiled using the entire time series described above, for each year of the time series, for each of the four seasons, and for each calendar month.
- c. A record by magnitude and date of the 250 largest wave heights, with associated periods and directions, in the 20-year simulation period.

The significant wave height from the WIS hindcast is the zero-moment wave height determined from integration of the wave spectrum, rather than an average of the one-third highest waves in a time series. These quantities are virtually identical in deep water, but deviate in shallow water. The peak wave period is the period of highest energy concentration in the wave spectrum. The predominant wave direction is the mean direction at the period of highest energy concentration. The WIS-generated joint frequency tables contain both sea and swell components, and also include the average and largest significant wave height for each angle band.

The wave conditions produced by the customized WIS Phase III hindcast at Cumberland and Amelia Islands were similar, with minor differences produced by different shoreline orientations. A summary of results is presented in Appendix F. Wave angles were discretized into nine direction bands. The angle bands and the percentage of waves from each direction are shown in Table 43. The direction bands containing wave energy had a width of 22.5 deg. No waves occur in Bands 1 and 9 because of sheltering by adjacent coastlines.

The 20-year time series of data has an average significant wave height of 0.6 m and an average peak wave period of 7 sec. The largest and longest period waves arrive from nearly due east with winter storms. The largest average significant wave heights accompany storms from the ENE at Cumberland Island and from the NE at Amelia Island, with the largest average significant wave height occurring in the month of October at both islands. A maximum wave height of 4.7 m occurred during the March 1962 northeaster.

**Table 43**  
**WIS Hindcast Direction Bands and Percent Occurrence**

Band	Deg From True North	Percent Occurrence	
		Amelia	Cumberland
1	0.00 - 11.24	0.0	0.0
2	11.25 - 33.74	4.6	3.2
3	33.75 - 56.24	9.8	10.3
4	56.25 - 78.74	13.7	13.8
5	78.75 - 101.24	25.0	24.9
6	101.25 - 123.74	17.3	17.3
7	123.75 - 146.24	12.6	12.1
8	146.25 - 168.74	12.5	14.0
9	168.75 - 187.00	0.0	0.0

## Wave Model

To determine shoreline change produced by combinations of wave height, period, direction, nearshore bathymetry, and entrance channel/ebb-tidal shoal conditions, the custom Phase III data were transformed from a depth of 18.6 to 6.1 m according to standard procedures in application of the shoreline change model GENESIS (Hanson and Kraus 1989; Gravens, Kraus, and Hanson 1991). The sea bottom between these water depth contours is extremely irregular and varies considerably over the study area. The numerical spectral wave transformation model STWAVE (Resio 1987, 1988a, 1988b) was selected to model wave transformation over this irregular bottom. A monochromatic wave transformation model was tested initially for use in this study. The model was rejected, however, because the long-crested waves (several kilometers alongshore) propagating over a highly irregular bathymetry gave an unrealistically varying wave height and direction alongshore near the breaker line.

STWAVE numerically simulates wave refraction, shoaling, and bottom-induced diffraction of short-crested waves for mild bottom slopes, negligible wave reflection, and spatially homogeneous and steady offshore wave conditions. Surf-zone breaking was not of concern in the STWAVE simulation, because information from the simulation was stored seaward of breaking. Combinations of wave height, period, and direction were used to form a shallow-water spectrum called a TMA spectrum along the offshore boundary of the finite-difference grid. Directional spreading was specified as a  $\cos^n \theta$  function, where  $n$  is a number, and the spread in wave direction  $\theta$  and frequency resolution were chosen as a function of peak wave period, as described in Appendix F.

STWAVE was validated using field data collected for this project during a wave measurement program conducted in May 1989 (Chapter 6). Directional wave data were collected using an offshore pitch-roll buoy, a pressure gage-current meter (PUV gage) in the nearshore area of Cumberland Island, and a nearshore sea-surface slope array located off Amelia Island. Each

device measured sea surface wave height, direction, and period, including complete directional spectra. Measured wave height, period, and direction at the offshore buoy location were used to synthesize TMA spectra as an offshore boundary condition to the STWAVE model, which then transformed that wave condition to the site of the nearshore wave measurement (PUV or slope array) near Cumberland and Amelia Islands.

As described in Appendix F, the numerical model STWAVE wave transformations were validated by the field measurements within the accuracy of the wave measurement and analysis procedures. The field measurements tended to exhibit more scatter in wave direction and height than did the model calculations. Scatter was primarily attributed to tidal variations and local wind effects that are not included in the numerical simulations. The good overall comparison between measured and modeled wave heights and directions at nearshore gage locations indicated that the model can be used confidently to drive longshore sediment transport and shoreline change models such as GENESIS.

For further applications of STWAVE in this study, which include wave transformations over historical bathymetries and in the ebb shoal/entrance area, this model was configured to transform waves through three finite-difference grids shown schematically in Figure 157. The first grid, with 784 cells spaced at 1,854 m (1 n.m.) was used to transform waves from an 18.1- to a 9-m depth. The second grid, with 3,737 cells spaced at 457 m (1,500 ft), was used to transform waves from the 9- to 6.1-m water depth. The reason for selecting the 6.1-m depth was that the largest wave in the WIS time series did not break at this depth. Both the first and second grids covered the entire length of Cumberland and Amelia Islands. Contour plots of Grids 1 and 2 are presented in Figures 158 and 159a/159b, respectively. A 3-D perspective plot of Grid 2 is presented in Figure 160. A third grid, aligned obliquely to the other two grids, with 5,670 cells spaced at 91.4 m (300 ft), was used to transform waves from the 9- to 6.1-m water depth through the ebb-tidal shoal and channel area. This third grid was configured to simulate fine-scale wave transformations that would play a role in determining sediment transport patterns at the southern end of Cumberland Island and the northern end of Amelia Island. The third grid was extended sufficiently to the north and south where the bathymetry was less variable and where wave model results were similar to those produced in simulations using the coarser second grid. A contour plot of Grid 3 is presented in Figure 161, which displays the complicated bathymetry in the ebb-tidal shoal and channel area.

## Wave Transformation Analysis

Magnitude and direction of the longshore sand transport rate are dependent on the sine of the breaking wave angle with respect to the shore and on the breaking wave height raised to the  $5/2$  power. Therefore, accurate representation of the nearshore wave conditions is critical in modeling shoreline change.

The STWAVE model was configured to transform offshore wave conditions to the nearshore area through the three finite-difference grids described above. Execution of the wave transformation model for every offshore wave condition contained in the custom WIS time series

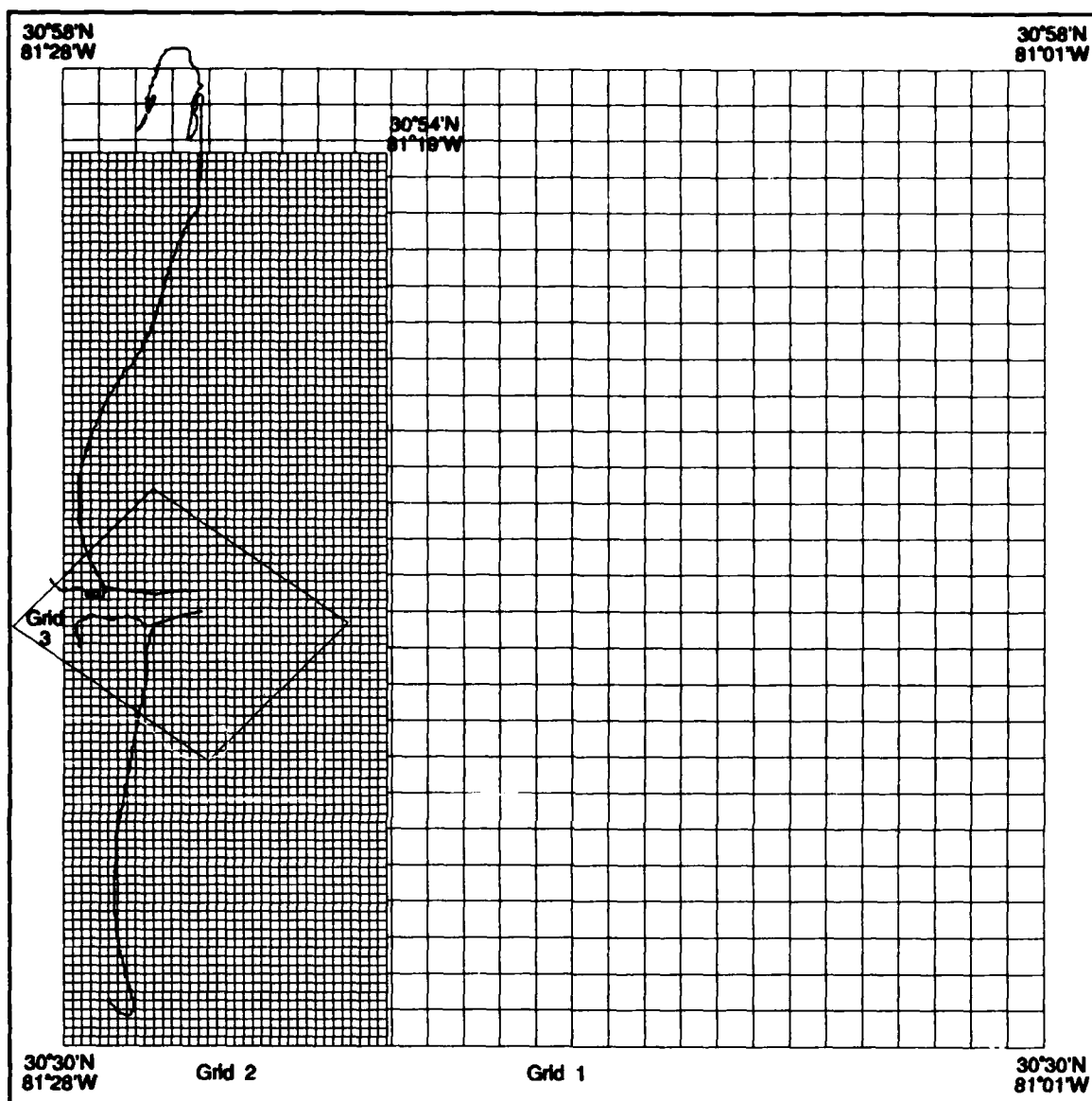


Figure 157. Location of nested grids used in STWAVE modeling

would require extensive computer resources and time, and was not justified given the level of accuracy and sophistication of the input data and the sediment transport model. Therefore, another approach was taken which is commonly used in regional-scale shoreline response studies performed by CERC (Kraus et al. 1988). In this approach, offshore wave data were separated into seven 22.5-deg angle bands and two 11.25-deg angle bands centered about the compass directions north northwest, northwest, west northwest, etc. An STWAVE model simulation was performed for wave periods from 3 to 16 sec in 2-sec increments in each angle band. An input wave-energy spectrum (called a boundary condition) was generated along the offshore boundary of Grid 1 using a JONSWAP/TMA spectral shape, a significant wave height of unity, and a peak wave period corresponding to each incremental case in each angle band. The standard CERC boundary condition generator was used to prepare the boundary spectra. Each spectral condition

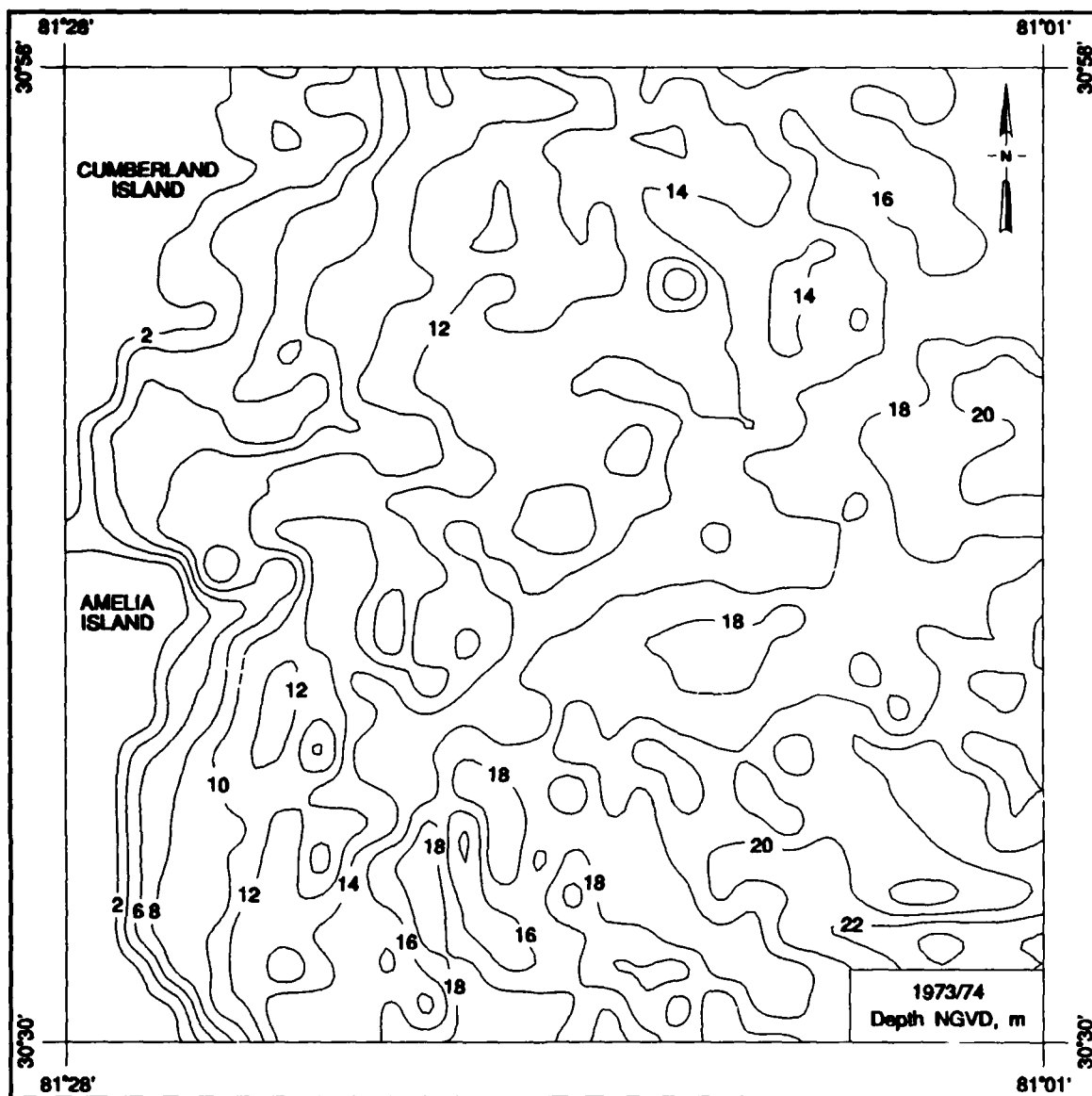
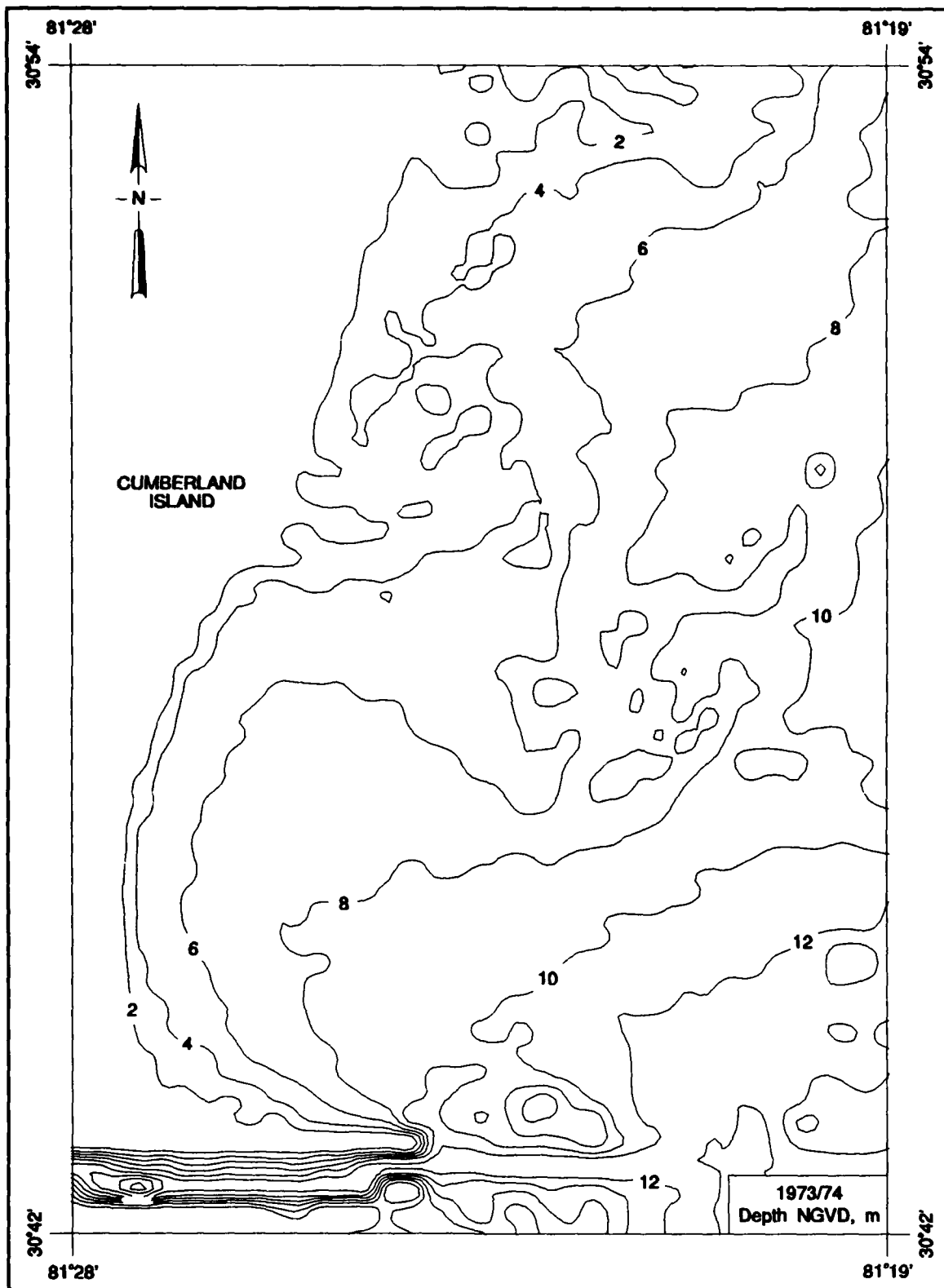


Figure 158. Contour map of Grid 1 (1,854 m) for STWAVE modeling

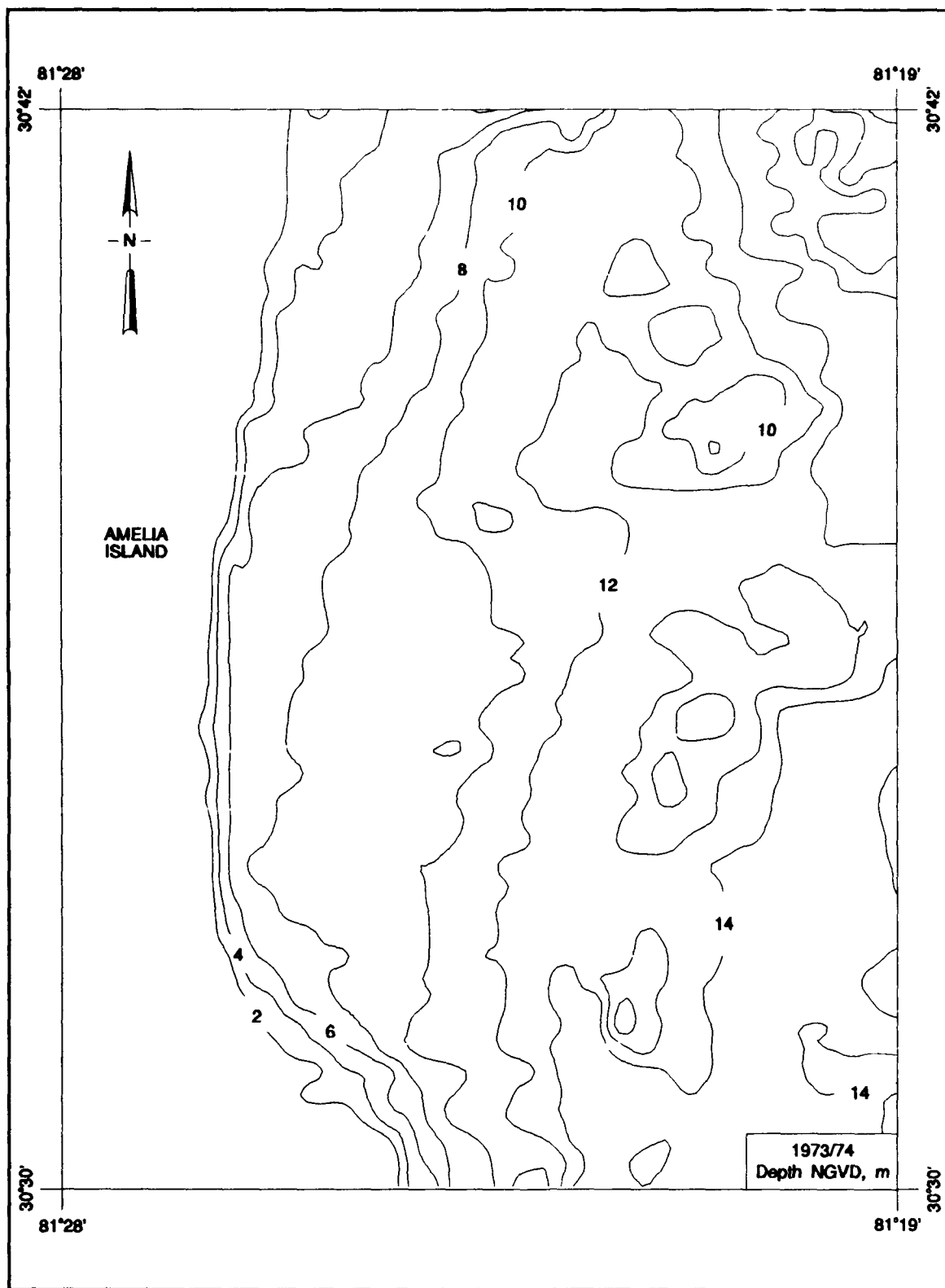
was transformed to the outer boundary of Grid 2. Transformed output spectra were stored at latitude 30.83 °N for further Cumberland Island wave modeling and at latitude 30.62 °N for further Amelia Island wave modeling. These output spectra then served as input to applications of STWAVE on Grid 2.

Once the boundary spectra were generated for the STWAVE model runs on Grid 2, each case was transformed to a nearshore water depth of 6.1 m. The transformed energy spectra were integrated to determine the nearshore wave height and mean wave angle for input to the shoreline change model, GENESIS. The 6.1-m water depth is also called the nearshore reference line for



a. Northern half

Figure 159. Contour map of Grid 2 (457 m) for STWAVE modeling (Continued)



b. Southern half

Figure 159. (Concluded)

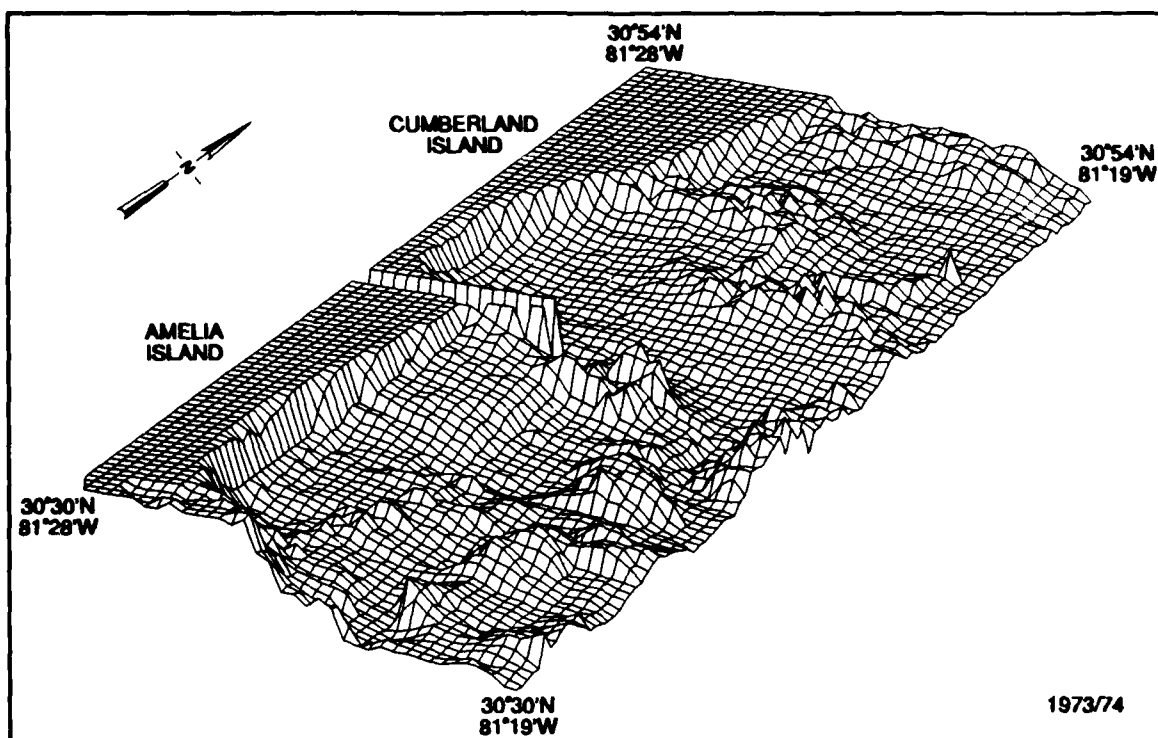


Figure 160. Three-dimensional perspective of Grid 2 (457 m) for STWAVE modeling

GENESIS modeling. The wave spectra at the center of the offshore boundaries of Grid 3 were stored for finer scale wave transformation modeling over the ebb-tidal delta and jetty areas. Wave transformation was accomplished in two ways. Waves incident and arriving on the southern end of Cumberland Island from the northeasterly quadrant were transformed by using the grid with the northeast boundary as the offshore boundary. Waves incident and arriving on the northern end of Amelia Island from the southeasterly quadrant were transformed by using the grid with the southeast boundary as the offshore boundary. Fine-scale characteristics of the ebb-tidal delta and dredged channel were resolved in this bathymetry. Only onshore-directed wave energies present in the directional wave spectra at the offshore boundaries of Grid 2 simulations were used for transforming the waves to the 6.1-m water depth. Results of finer grid transformations were then re-referenced to the latitude-longitude coordinate system used in the larger wave model grids and archived along the nearshore reference line for application with GENESIS, superseding the less-accurate wave transformations from the coarser Grid 2 at the southern end of Cumberland Island and the northern end of Amelia Island.

The wave transformation coefficient and nearshore wave angle were stored at a spacing of 457 m along the nearshore reference line. Results were written to a database and keyed to the offshore wave angle band and wave period used to generate them. This allowed the shoreline change model to read the offshore wave conditions at a specific time-step and to calculate a key based on the incident wave angle and period. The key was then used to identify the corresponding nearshore wave transformation coefficient and wave angle along the project coast. The use of STWAVE in this manner allowed the shoreline change model to account for major offshore bathymetric features which may cause convergence or divergence of wave energy along the coast.

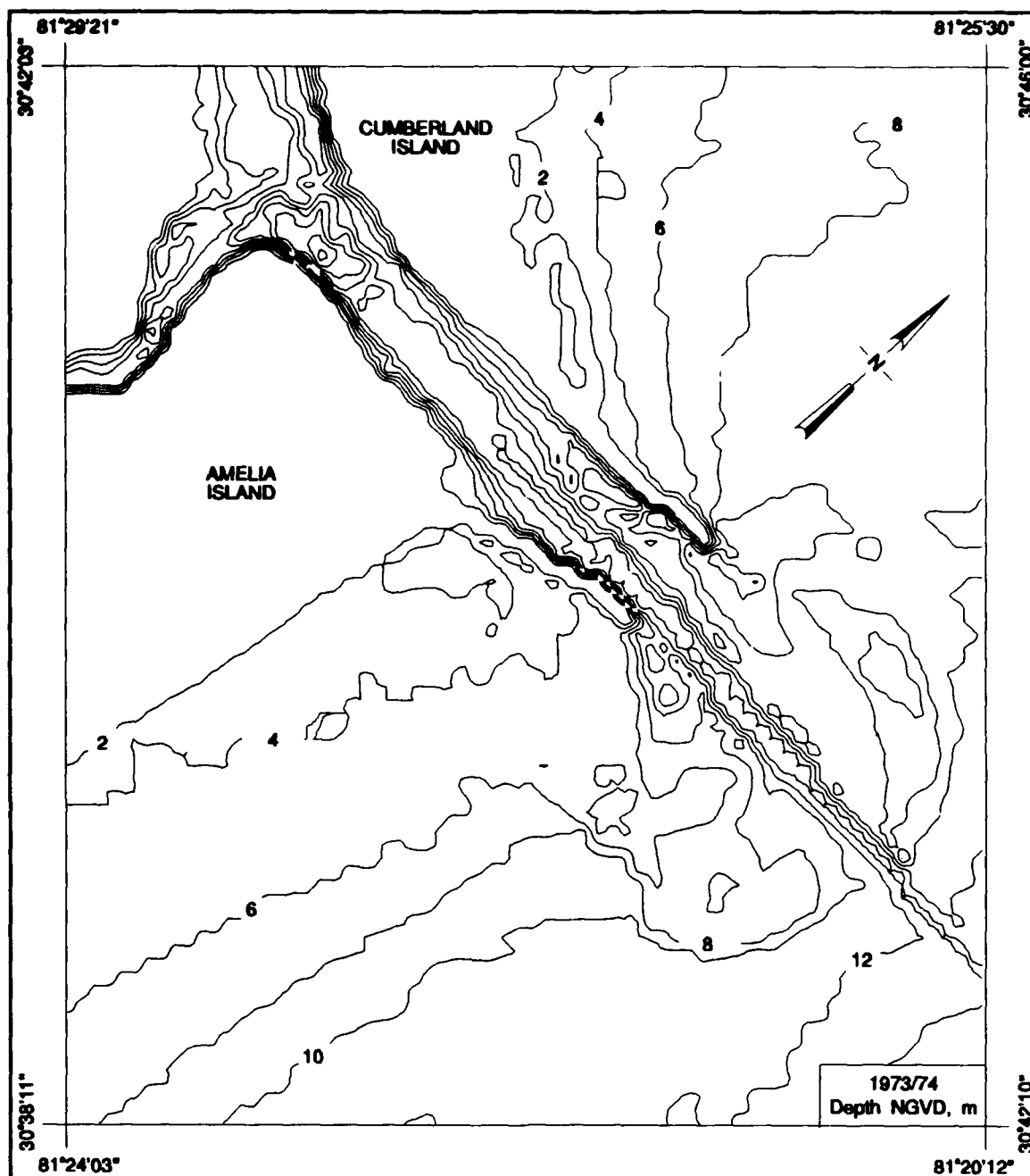


Figure 161. Contour map of Grid 3 (91.4 m) for STWAVE modeling

## Shoreline Change Model

### Overview of GENESIS

The shoreline change model GENESIS used in this study is described in detail in Hanson (1987, 1989) and Hanson and Kraus (1989), and will only be briefly reviewed here. GENESIS is an integrated system of numerical models and computer subroutines which allows simulation

of long-term shoreline change under a wide variety of user-specified wave, beach, coastal structure, and boundary conditions.

GENESIS calculates local wave breaking, longshore sand transport rate, and the resulting plan-shape evolution of the modeled coast. Natural features such as headlands, shore-protection structures such as seawalls and groins, and engineering activities such as beach fills, are represented in the model by modification of the local transport rate through boundary conditions and constraints. The diffraction effect of detached breakwaters and long jetties on the local wave climate also is represented around and behind these structures. Kraus (1989) summarizes the capabilities and limitations of GENESIS and compares it to other types of bathymetry change models.

The calculation flow for the shoreline change calculation is shown in Figure 162. Wave information can be entered in GENESIS in two ways, depending on the available data and degree of sophistication and computational effort required. If only a single offshore or deepwater wave condition is available, an internal wave transformation model will calculate breaking wave conditions along a modeled reach with straight and parallel bottom contours, and will account for local shoreline curvature. Alternatively, a more sophisticated wave transformation model (such as STWAVE) which describes wave propagation over the actual offshore bathymetry can be used to perform the required wave transformation. In this case, GENESIS retrieves nearshore wave characteristics (output from STWAVE) from a database and performs local refraction, diffraction, and shoaling calculations to obtain breaking wave height and angle at intervals alongshore. This study employed the more sophisticated wave transformation procedure provided via the model STWAVE as described in the previous section. In either case, once the breaking wave field along the modeled reach is available, longshore sand transport rates are calculated and the shoreline positions updated through time.

GENESIS calculates long-term changes in shoreline position associated with alongshore movement of sand. Offshore transport of sand caused by short-term events (for example, an intense short-duration storm) is not modeled. However, estimates of shoreline change resulting from these events could be superimposed on the shoreline position calculated by GENESIS to obtain a first approximation of the potential variation about the calculated shoreline position. Examples of calculations of short-term, storm-induced beach change performed at CERC are given by Larson and Kraus (1989) and Scheffner (1989). In practice, however, and as was done here, shoreline change is calculated over a longer time interval (several years) between the same seasons to average out the cyclical (short-term) influence of storms on shoreline position.

A shoreline change model must be applied where there is a long-term trend in shoreline behavior in order to separate and predict a clear signal of shoreline movement from cyclical and random movement in the beach produced by storms, seasonal changes in waves, and tidal fluctuations. In essence, the assumption of a clear trend in shoreline change implies that breaking waves and boundary conditions are the major factors controlling long-term beach change. This assumption is usually well satisfied for engineering projects involving long jetties, such as in the present situation. Specification of boundary conditions at natural inlets, such as is the case at the southern end of Amelia Island, is difficult owing to the complexity and varied scales of the acting physical processes present. In summary, standard assumptions of shoreline change modeling include the following:

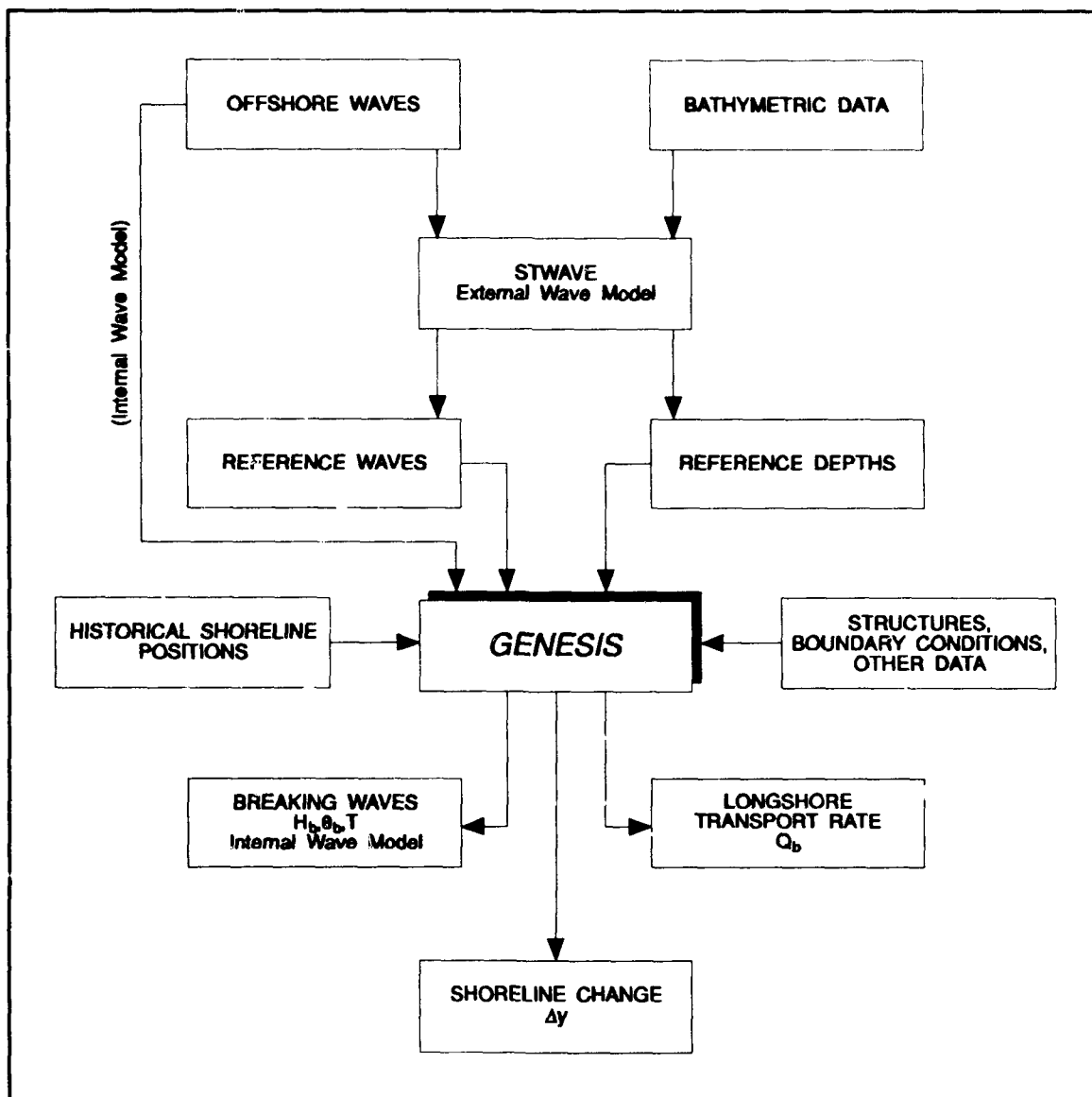


Figure 162. Flow of shoreline change calculation

- a. The beach profile shape is constant.
- b. The shoreward and seaward limits of the profile are constant.
- c. Sand is transported alongshore by the action of breaking waves.
- d. The detailed structure of the nearshore circulation can be ignored.

#### Governing equation for shoreline change

The partial differential equation governing shoreline change in the one-line model is formulated by conservation of sand volume under the above assumptions. Shoreline change in GENESIS is

calculated in a right-handed Cartesian coordinate system in which the y-axis points offshore and the x-axis is oriented parallel to the trend of the coast. The quantity y thus denotes shoreline position, and x denotes distance alongshore. The beach profile is assumed to translate seaward or shoreward along a section of coast without changing shape within a vertical extent defined by the berm elevation  $D_B$  and the closure depth  $D_C$ , both measured from the same vertical datum (in the present case, NGVD).

The change in volume of a shoreline segment alongshore is determined by the net amount of sand that enters or exits the segment laterally, from the beach, and from the offshore. In this project, contributions from cross-shore sinks and sources of sediment were not included, and further discussion and equations will not be given. With cross-shore contributions absent, the only contribution to beach volume change results from a difference in the longshore sand transport rate  $Q$  at the lateral sides of the segment. The governing equation for the rate of change of shoreline position becomes

$$\frac{\partial y}{\partial t} + \frac{1}{(D_B + D_C)} \frac{\partial Q}{\partial x} = 0 \quad (7)$$

where

$t$  = time

To solve Equation (7), the initial shoreline position over the full reach to be modeled, boundary conditions on each end of the beach, and values for  $Q$ ,  $D_B$ , and  $D_C$  must be given. These quantities, together with information on structure configurations, comprise the main data requirements for using GENESIS in this project, and further information on them is given below.

### Longshore sand transport rate

The empirical predictive formula for the longshore sand transport rate used in GENESIS is

$$Q = H_b^2 C_{gb} \left( a_1 \sin 2\theta_{bs} - a_2 \cos \theta_{bs} \frac{\partial H_b}{\partial x} \right) \quad (8)$$

where

$H$  = wave height, m

$C_g$  = wave group speed at breaking given by linear-wave theory, m/sec

$b$  = subscript denoting wave breaking condition

$\theta_{bs}$  = angle of breaking waves to the local shoreline

The nondimensional parameters  $a_1$  and  $a_2$  are given by

$$a_1 = \frac{K_1}{16(S - 1)(1 - p)} \quad (9)$$

$$a_2 = \frac{K_2}{8(S - 1)(1 - p)\tan\beta}$$

where

$K_1$  = empirical coefficient, treated as a calibration parameter

$S = \rho_s/\rho$

$\rho_s$  = density of sand (taken to be  $2.65 \cdot 10^3 \text{ kg/m}^3$  for quartz sand)

$\rho$  = density of water ( $1.03 \cdot 10^3 \text{ kg/m}^3$  for seawater)

$p$  = porosity of sand on the bed (taken to be 0.4)

$K_2$  = empirical coefficient, treated as a calibration parameter

$\tan\beta$  = average nearshore bottom slope

The first term in Equation (8) corresponds to the "Coastal Engineering Research Center (CERC) formula" described in the *Shore Protection Manual* (SPM) 1984)) and accounts for longshore sand transport produced by obliquely incident breaking waves. A value of  $K_1 = 0.77$  was originally determined by Komar and Inman (1970) from their sand tracer experiments, using root-mean-square (rms) wave height in the calculations. Kraus et al. (1982) recommended a decrease of  $K_1$  to 0.58 on the basis of their tracer experiments. Because these values of  $K_1$  are well-known in the literature, the standard engineering quantity of significant wave height entered in the data stream is converted to an rms value in GENESIS.

The second term in Equation (8) is not part of the CERC formula and describes another generating mechanism for longshore sand transport, the longshore gradient in breaking wave height,  $\partial H_b/\partial x$ . The contribution arising from the longshore gradient in wave height is usually much smaller than that from oblique wave incidence on an open coast. However, in the vicinity of structures, where diffraction produces a substantial change in breaking wave height over a considerable length of beach, inclusion of the second term provides an improved modeling result. The value of  $K_2$  is typically 0.5 to 1.0 times that of  $K_1$ .

Because of the many assumptions and approximations that have gone into formulation of the shoreline response model, to reproduce longshore sand transport and shoreline change along a given coast, the coefficients  $K_1$  and  $K_2$  are treated as calibration parameters. Their numerical values are determined by reproducing measured shoreline change and magnitude and direction of the longshore sand transport rate.

## Shoreline Response Model Application

### Review of physical setting

A short review of the physical aspects of the beach and nearshore specifically pertaining to the shoreline change modeling task is given in this section for completeness. Chapters 2 and 3 and relevant appendixes provide further information. St. Marys Entrance is located on the border of Georgia and Florida and separates Cumberland Island, Georgia, and Amelia Island, Florida. Cumberland Island is approximately 30 km long and is mostly undeveloped. In particular, the beach along Cumberland Island is in a pristine state. Amelia Island is approximately 20 km long and is developed along most of the shore. Fernandina Beach at the northern end and Amelia Island Plantation at the southern end are the principal areas of coastal development on the island.

Cumberland Island is characterized as having steep dunes and broad, gently sloping beaches with relatively shallow offshore bathymetry. The northern half of the island is generally stable or slightly eroding with a straight shoreline and some scarping at the toe of the large dunes. The beach slope gradually decreases from north to south. The southern half of the island is sheltered by Stafford Shoals and bounded by a jetty at St. Marys Entrance, contributing to an average shoreline advance in recent time of 2 to 3 m per year. The southern half of the island has the shape of a concave pocket beach, with a large impoundment fillet near the jetty. Beach profiles exhibit a 6- to 10-m-wide berm in the curved area between Stafford Shoals and the jetty, and a continued decrease in beach slope from north to south into the jetty impoundment fillet.

Amelia Island has a coastal topography with smaller, less stable dunes, and a steeper nearshore profile than Cumberland Island. The island curves gently concave between St. Marys Entrance and Nassau Sound. The northern end of the island, primarily the Fort Clinch area, is somewhat sheltered from northeasterly storm waves by a jetty and the ebb-tidal delta at St. Marys Entrance. The beach profile has a steep foreshore slope, and the shoreline is receding at a rate of 3 to 4 m per year. The beach profile slope remains steep through the city of Fernandina Beach, with little or no berm and very narrow dunes that are occasionally armored with scrap pieces of concrete. Approximately 7 km south of St. Marys Entrance, the beach profile begins to exhibit more extensive dunes, a steep foreshore, and a broad berm. The beach in this middle third of the island is generally stable or slightly accreting. The southern third of the island, from American Beach through Amelia Island Plantation to Nassau Sound, is eroding, as evidenced by crumbling, steep-faced dunes. The beach profile exhibits a low berm elevation and shear-faced dunes that have been eroded by wave and tidal energy. The southern tip of the island facing toward Nassau Sound returns to a flatter profile shape and low dunes because of protection from waves afforded by shoals at the mouth of the sound. Most of the island, including Fernandina Beach and Amelia Island Plantation, has seen numerous local shore-protection and beach nourishment projects in the past.

### Model application

Long-term coastal shoreline evolution on southern Cumberland Island and on Amelia Island was numerically simulated with the model GENESIS in separate applications. As described above, both the physical characteristics and the hydrodynamics of the coastal environment differ

significantly between the two islands. St. Marys Entrance, between the islands, provided an ideal boundary at which to divide the modeled area.

The southern half of Cumberland Island was simulated by the GENESIS model. This reach extended 12.8 km from the north jetty at St. Marys Entrance. The shoreline is a crenelate-shaped beach sheltered by Stafford Shoals to the northeast and by the St. Marys Entrance north jetty at the southern end of the island. Based on observation of historical shoreline surveys, the northern boundary of the model reach was assigned as a "pinned" or "fixed-beach" boundary condition. This boundary condition specified a uniform sand transport rate at the boundary which results in a fixed shoreline position at the boundary. The jetty was made as a long, permeable, diffracting structure. The implication of this boundary condition is that sand can move through the structure into St. Marys Entrance. Permeability of the jetty was varied between 0 and 100 percent during the calibration process to determine the best possible match to the measured shoreline position at the end of the calibration time period. No other constraints on sediment transport were imposed inside the modeled Cumberland Island reach.

The Amelia Island model reach included the northern 18.3 km of the island. The northern boundary of the Amelia Island model reach was the jetty on the south side of St. Marys Entrance. This structure was simulated as a long diffracting jetty. The southern boundary of the model reach was treated as a fixed-beach boundary condition. The jetty at the northern boundary was represented as impermeable. Although this condition is not accurate in a hydrodynamic sense, an impermeable jetty was found to produce the most reliable shoreline change in preliminary model testing. No other constraints on sediment transport were imposed inside the modeled Amelia Island reach.

## Shoreline Response Calibration/Verification

For southern Cumberland Island, the shoreline change model GENESIS was calibrated for the period 14 February 1957 to 6 April 1974. Reliable shoreline position data were not available for verification of the Cumberland Island model. For Amelia Island, the model was calibrated for the period 14 February 1957 to 1 November 1962 and was verified for the period 1 November 1962 to 6 April 1974. Shoreline data were digitized from maps and aerial photographs as described in Chapter 3 and by Knowles and Gorman (1991). The shoreline position survey data used in the calibration and verification activities were chosen based on availability of data, coincidence of surveys with the WIS time series (1956-1957), and greatest spread in time between surveys. The data were digitized into UTM coordinates or latitude/longitude and then transferred to the GENESIS coordinate system for each island. The shoreline was then interpolated to the 91.4-m cell spacing of the model using a cubic spline routine for input to GENESIS. The GENESIS grid origin in UTM coordinates for Cumberland Island simulations is 82°23'03" E and 20°59'45" N. The Amelia Island origin is 82°17'50" E and 20°55'42" N. The accuracy of the location of digitized high-water shorelines is estimated to be  $\pm 15$  m (Chapter 3). Figure 163 shows the model reaches used in the shoreline change simulations and plots the measured shorelines available for the calibration and verification.

GENESIS requires the specification of longshore transport coefficients which are determined through the model calibration process. The best performance of the model for south Cumberland

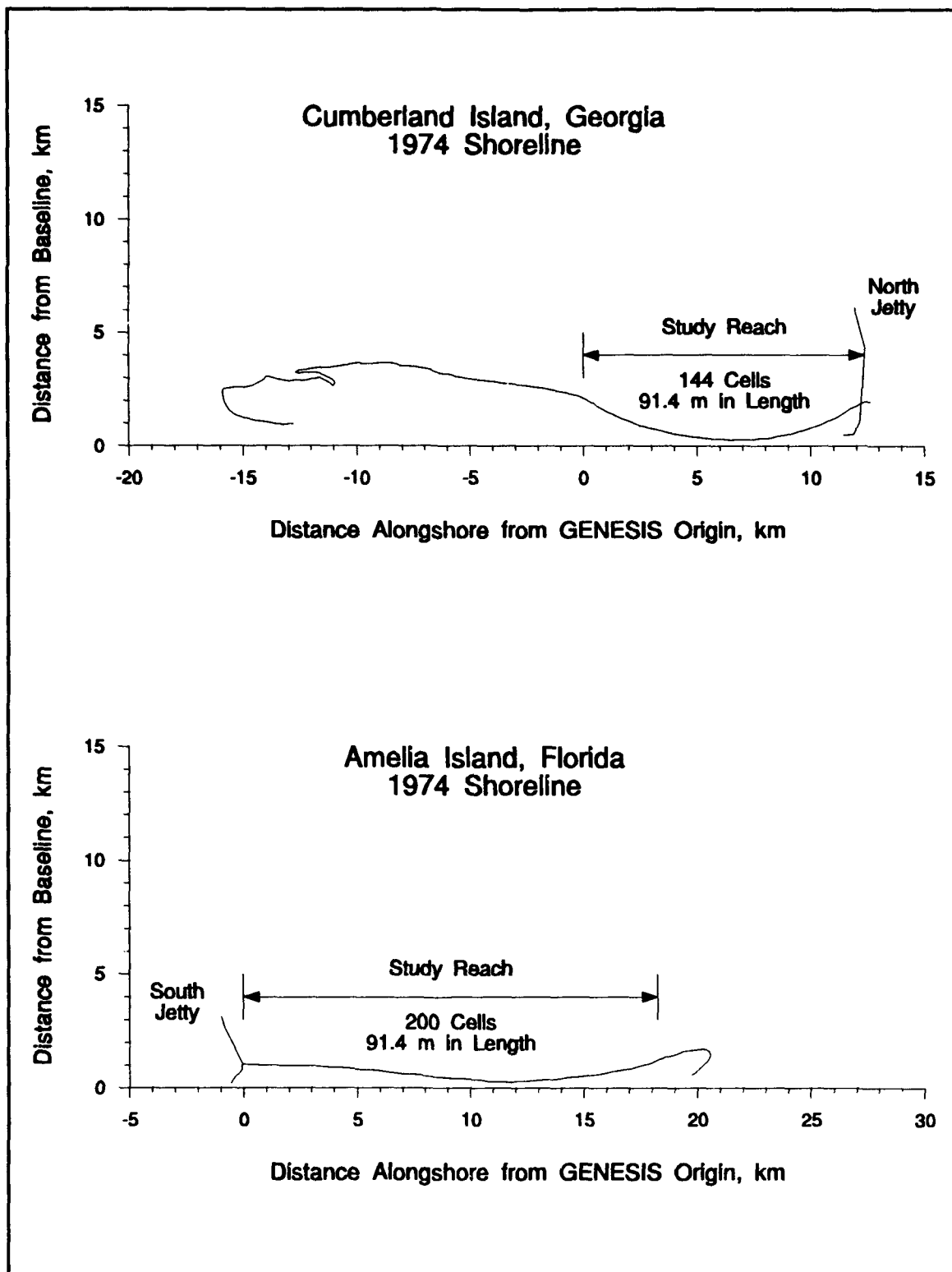


Figure 163. Shoreline model reaches and grids

and Amelia Islands for the calibration and verification time periods resulted from using a  $K_1$  value of 0.58. This value is in the typical range found in GENESIS field and laboratory studies for fine- to medium-grained sand (Hanson and Kraus 1989, 1991). Testing of the model with the calibration grids and input waves for this study indicated that shoreline change predictions were not sensitive to reasonable variations in  $K_2$ . Based upon typical values of the coefficient used in other GENESIS applications, a value  $K_2 = 0.3$  was used in the final calibration and verification runs for Cumberland and Amelia Islands.

The shoreline evolution model requires specification of an effective sand grain size, taken to be the median grain size. Appendix D summarizes previous sediment sampling studies and the sediment grain-size data collected from July 1988 to April/May 1992 for this study. Previous studies indicate that southern Cumberland Island exhibited a median grain size of 0.12 to 0.18 mm and that Amelia Island exhibited a median grain size of 0.20 to 0.25 mm. In the previous data sets, Amelia Island also evidenced progressively finer material to the south. The 1988-1992 data set shows a mean size of 0.18 mm along southern Cumberland Island, and coarser material with a mean size of 0.34 mm along northern Amelia Island. The recent sediment data for Amelia Island exhibit much more variability in grain size, with generally finer material (with a median size of approximately 0.25 mm) to the south. Hanson and Kraus (1989) present templates that can be used to estimate the effective grain size for GENESIS by comparing beach profile shapes with the template curves. Cumberland Island profiles, which are very gently sloping and shallow, indicate an effective grain size of 0.14 mm. A similar approach using Amelia Island profiles indicates an effective grain size of 0.25 mm. These values were used in model application. They compare favorably with field-derived grain sizes for older data sets and with recently collected samples. In many cases, however, recent data show areas on Amelia Island where median grain size exceeds 0.50 mm and approaches 0.75 mm. Numerous beach fills on Amelia Island have contributed to the high variability in grain size along the island. In addition, other coastal projects have been undertaken throughout the past decades that are not well-documented and therefore not modeled in this study. Because the numerical model GENESIS uses a single effective grain size for the entire island and can only simulate well-documented construction projects, some variability between model and measured shoreline changes can be expected.

Shoreline evolution also depends upon the total height of the active beach profile, extending from the average beach berm height to the depth of closure. Early work in the project (Knowles and Gorman 1991), and more recent field data suggest that profile closure depth was between 6 and 7 m NGVD. A depth of 6.4 m was chosen for both islands. The Cumberland Island shoreline exhibits much more variability in beach profile shape, especially offshore, with much shallower beach slopes and irregular bottom features than off Amelia Island. A review of beach profile data for Cumberland Island resulted in a selection of a berm elevation of 2.1 m. A natural berm elevation of 1.3 m NGVD was specified for Amelia Island, although the berm elevation can be as much as 1.5 m higher in artificially filled areas.

Several model simulations were performed for Cumberland and Amelia Islands in order to determine appropriate calibration parameters. The calibration of the GENESIS model for Cumberland Island was started with the February 1957 shoreline. The calculated April 1974 shoreline position was then plotted with the 1974 surveyed shoreline for comparison. In addition, the calculated longshore sand transport rates were monitored and compared with independent estimates of transport rates on Cumberland Island.

The calibration results for Cumberland Island are given in Figure 164. The scale of the plot (Figure 164a) is distorted to better illustrate the agreement between modeled and measured shoreline positions. The dotted line in Figure 164a represents the initial shoreline position (February 1957 surveyed shoreline position) and the dashed and solid lines represent the April 1974 surveyed and calculated shoreline positions, respectively. Results may also be compared in Figure 164b, which plots the difference between calculated and measured final shoreline positions. The model tended to simulate trends in erosion and accretion very well over most of the island, with a slight underprediction of accretion between alongshore coordinates 40 and 55. The permeability of the jetty was varied and a value of 0.85 was found to provide the best fit with the measured shorelines. This value, at first inspection, seems high; however, the jetty is awash during high water, indicating that overtopping and sediment transport likely occur over a significant portion of the tidal cycle. In addition, periods of superelevated water levels and coincident winds (i.e. storm conditions) will almost certainly bring high southerly sand transport rates and almost continual overtopping of the jetty. Generally, the model results for Cumberland Island are considered satisfactory, given that the measured shoreline positions have an accuracy of  $\pm 15$  m.

Longshore sand transport rates for Cumberland Island during the calibration period are presented in Figure 165. The average annual net transport rate decreased from a value of about 270,000 cu m/year at the northern end of the modeled reach to a value of approximately 45,000 cu m/year at the southern end of the island. The estimated annual maintenance dredging in the inlet during the 1954-1973 time period (which overlaps with 17 years of the calibration period) was 74,000 cu m/year (Appendix C). This order of agreement between the calculated transport rate at the southern end of the island with the maintenance dredging quantity is considered to be good and provides an independent check of model results.

The calibration results for Amelia Island are given in Figure 166a. Again, the scale of the plot is distorted to better illustrate the comparison. The dotted line in Figure 166 represents the initial shoreline position (February 1957 shoreline survey) and the dashed and solid lines represent the November 1962 surveyed and calculated shoreline positions, respectively. The model tended to simulate trends in erosion and accretion along the island well, with some deviation attributed to the placement of periodic beach fills and attempts at coastal protection measures, groins in particular, during the time period.

Longshore sand transport rates during the calibration period on Amelia Island are presented in Figure 167. The average annual net transport rate varied from a northerly transport rate near St. Marys Entrance of approximately 115,000 cu m/year, to zero about 2.8 km to the south, to between 40,000 and 75,000 cu m/year to the south along most of the remaining model reach extending south another 15.8 km.

The calibrated GENESIS model for Amelia Island was verified for another time period, from November 1962 to April 1974. The results of the model verification are presented in Figure 168. As before, the dotted line in Figure 168 represents initial shoreline position and the dashed and solid lines represent the April 1974 surveyed and calculated shoreline positions, respectively. Although the agreement between calculated and surveyed shoreline positions is not as close for the verification as for the calibration, overall measured change in shoreline position is reproduced and considered acceptable. The largest discrepancies between calculated and surveyed shoreline

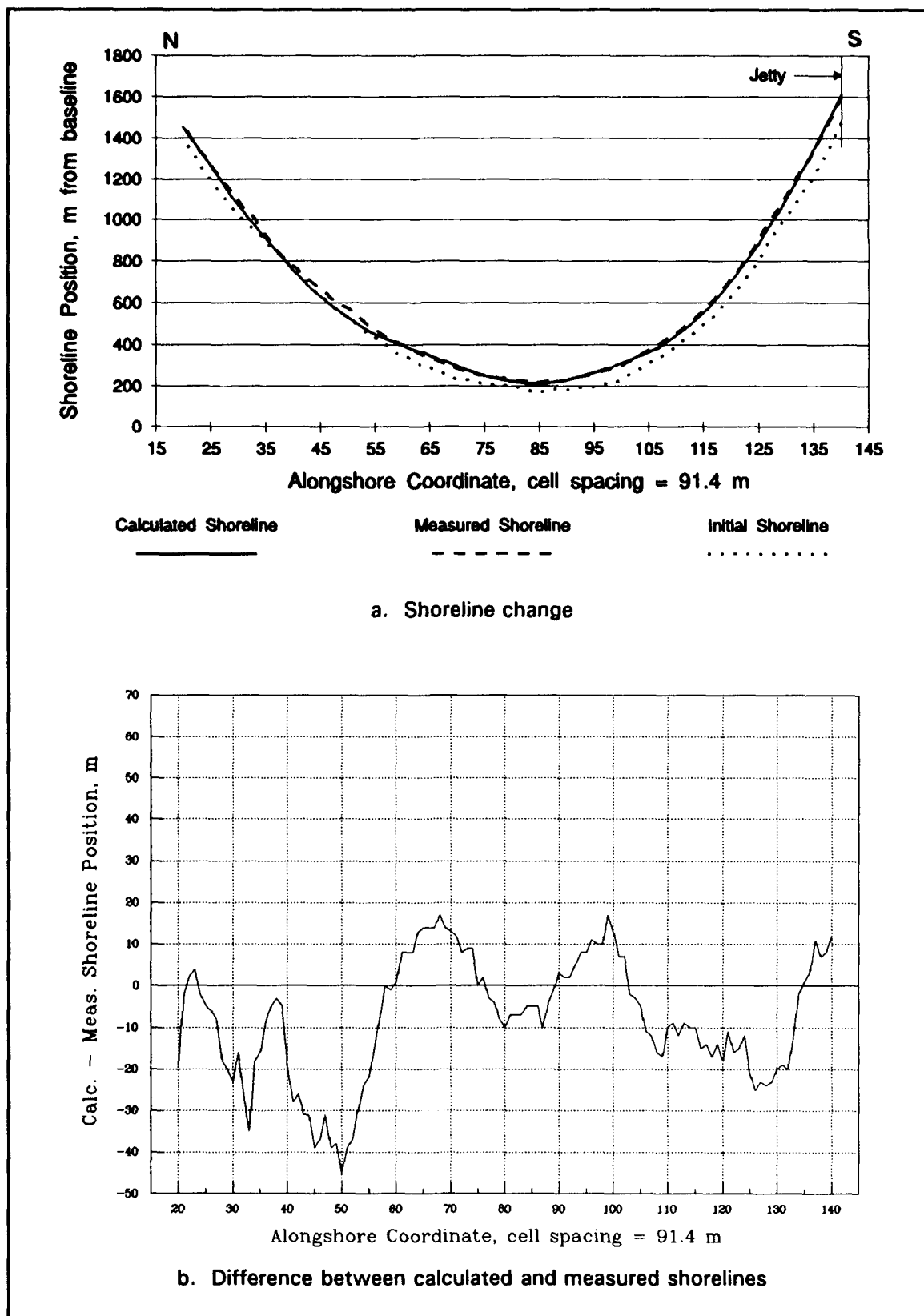


Figure 164. Cumberland Island model shoreline change calibration results

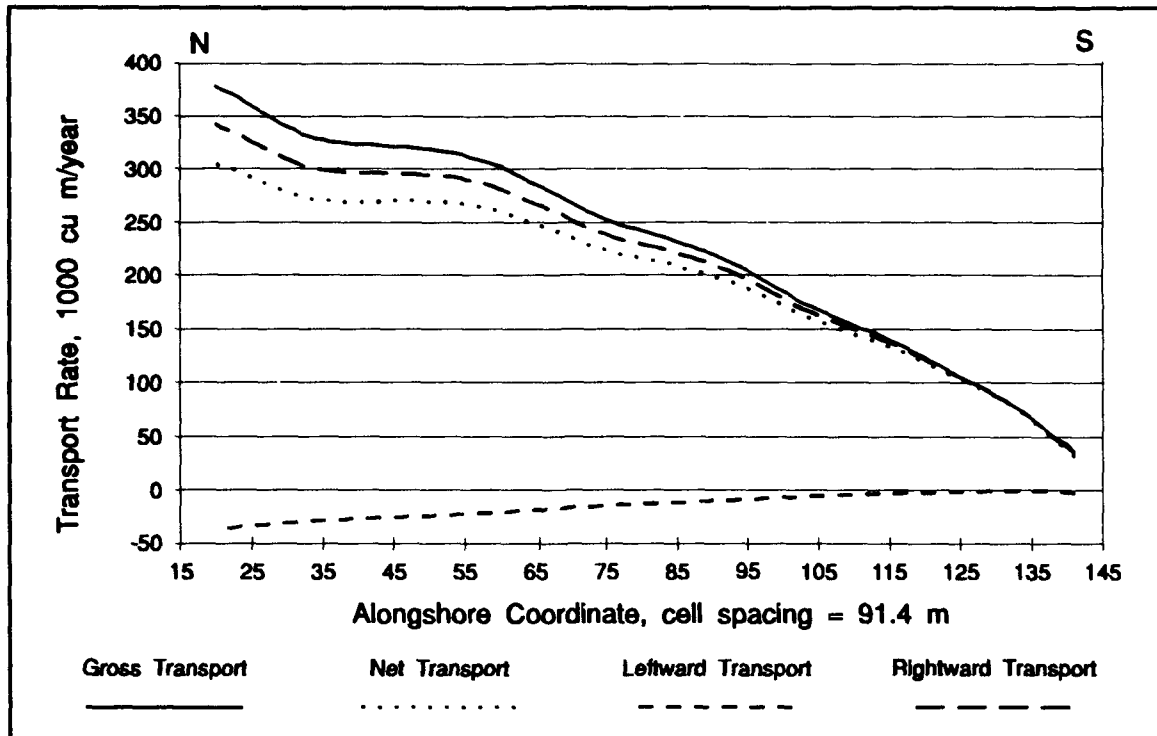


Figure 165. Sand transport rates for Cumberland Island during calibration period

positions occur adjacent to the jetty, near the southern boundary of the model, and at an isolated area near alongshore coordinates 100 to 120. Shoreline configuration adjacent to the jetty exhibits a shape that is not reproduced by the model, but the model simulates the general trend of shoreline recession and erosion quantities occurring in that region. The model predicts the shoreline near the southern boundary to be accreting whereas the measurements show the shoreline to be slightly eroding. This discrepancy is attributed to the limited applicability of the pinned-beach boundary condition for this area believed to be influenced by non-wave-related processes associated with Nassau Sound. The lack of agreement between model and measurements results between coordinates 100 and 120 appears to be the possible result of undocumented beach fill placement in that area. Figure 169 presents longshore transport calculations for the verification period. Trends and magnitudes for the verification are similar to those described for the calibration results.

## Shoreline Position Extrapolation

The purpose of this task was to estimate trends that may have occurred if the TRIDENT channel deepening had not taken place. For the shoreline extrapolation, the same wave data sets available from the Cumberland Island shoreline change calibration (17 years) and Amelia Island shoreline change verification (11 years) were used.

Shoreline change on southern Cumberland Island was extrapolated with the calibrated GENESIS model for 17 years beyond the April 1974 surveyed shoreline. The extrapolation

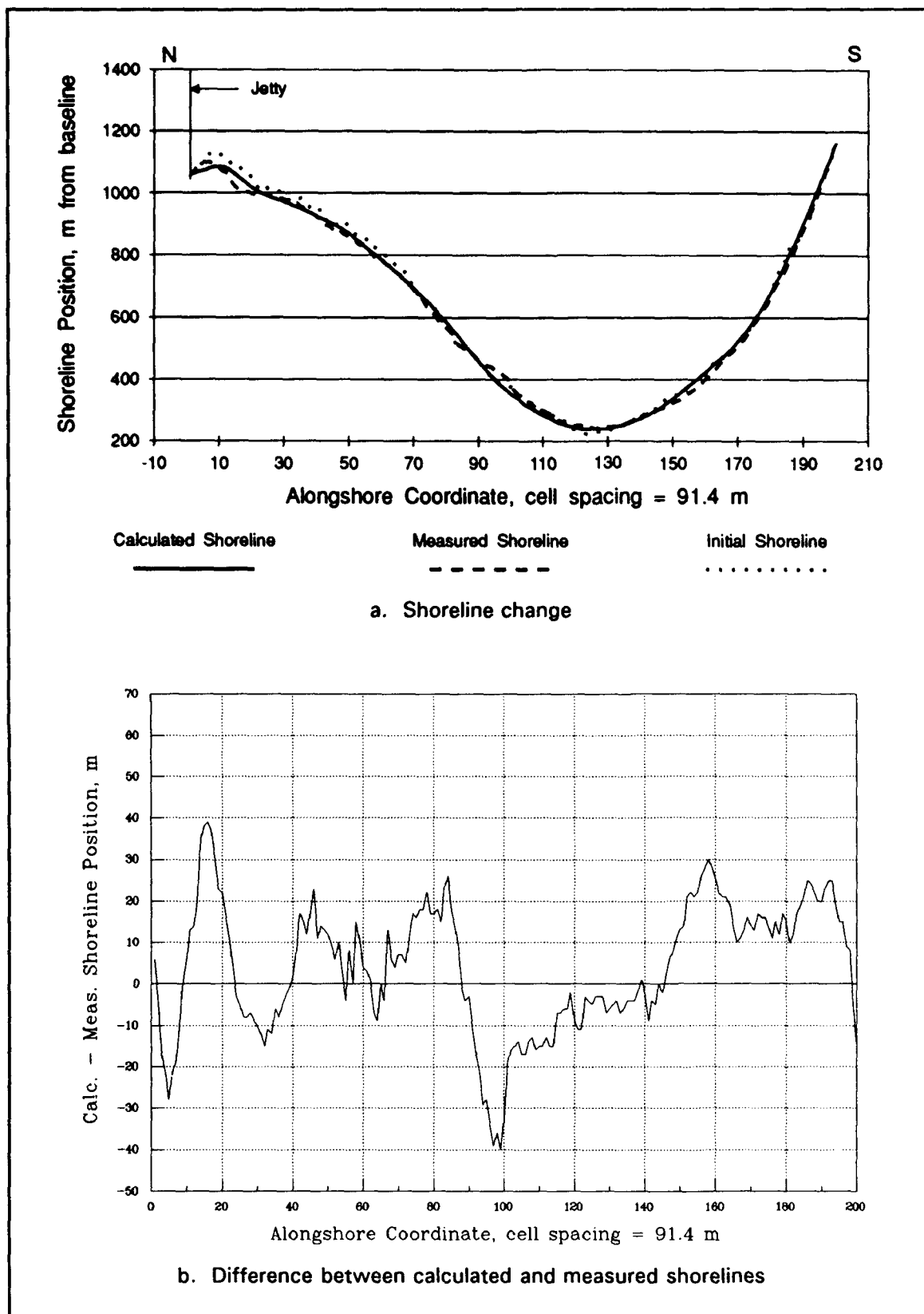


Figure 166. Amelia Island model shoreline change calibration results

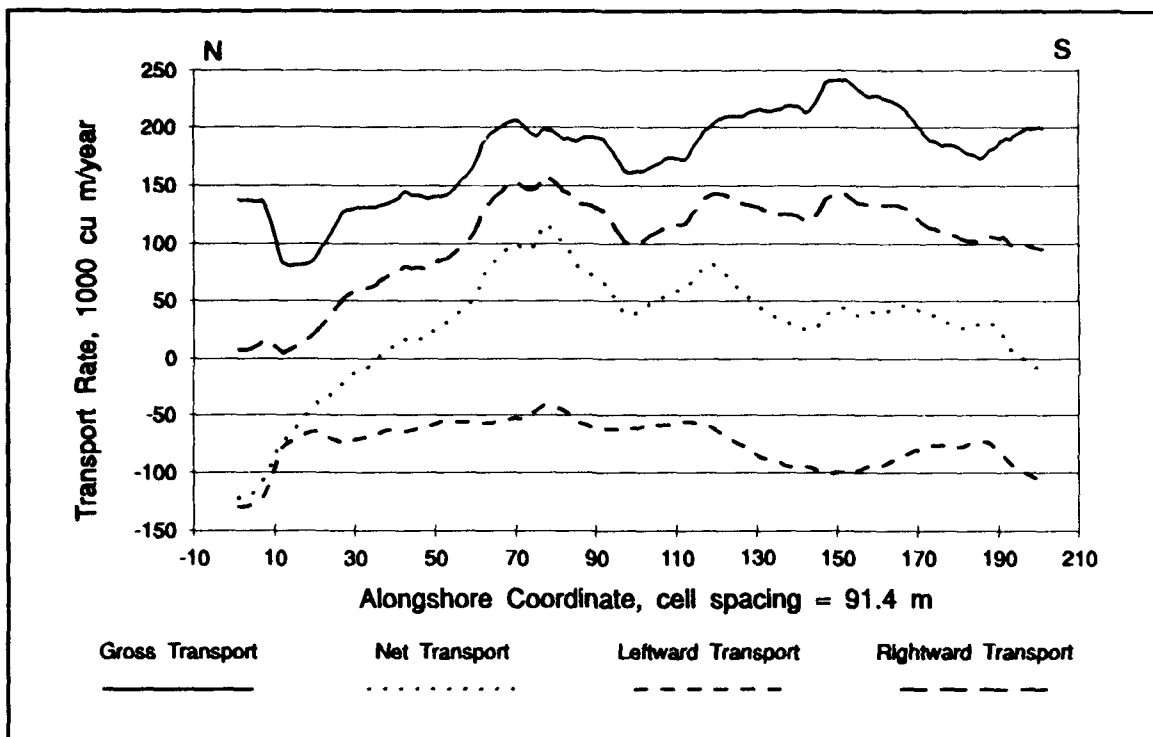


Figure 167. Sand transport rates for Amelia Island during calibration period

results are presented in Figure 170. The calculation gave accretion over the modeled area, with a seaward building of the shoreline near the jetty of 120 m, and a decreased but still significant building for almost 8 km to the north.

The calibrated and verified GENESIS model for Amelia Island was applied to extrapolate shoreline for 11 years beyond the April 1974 surveyed shoreline. The extrapolation is presented in Figure 171. The results show continued erosion over the northern 5.5 km of the island, with generally stable or slightly accretionary conditions to the south. Predicted accretion to the south does not agree with the observed recent trend of erosion, as described in Chapters 3 and 5; the discrepancy is due to lack of capability of imposing a realistic boundary condition on the southern end of the island, which is, in part, under the influence of Nassau Sound.

## Historical Sand Transport Rates

### GENESIS simulations

Bathymetry data for calibrating and verifying the shoreline change model were taken from the most recent and comprehensive data set of 1974. Offshore bathymetric data, which were also used in this analysis, extended over the southern 5.5 km of Cumberland Island and the northern 5.5 km of Amelia Island. These data extended offshore approximately 9.3 km to just beyond the present ebb-tidal delta. Historical bathymetries were spliced into the present day bathymetry used

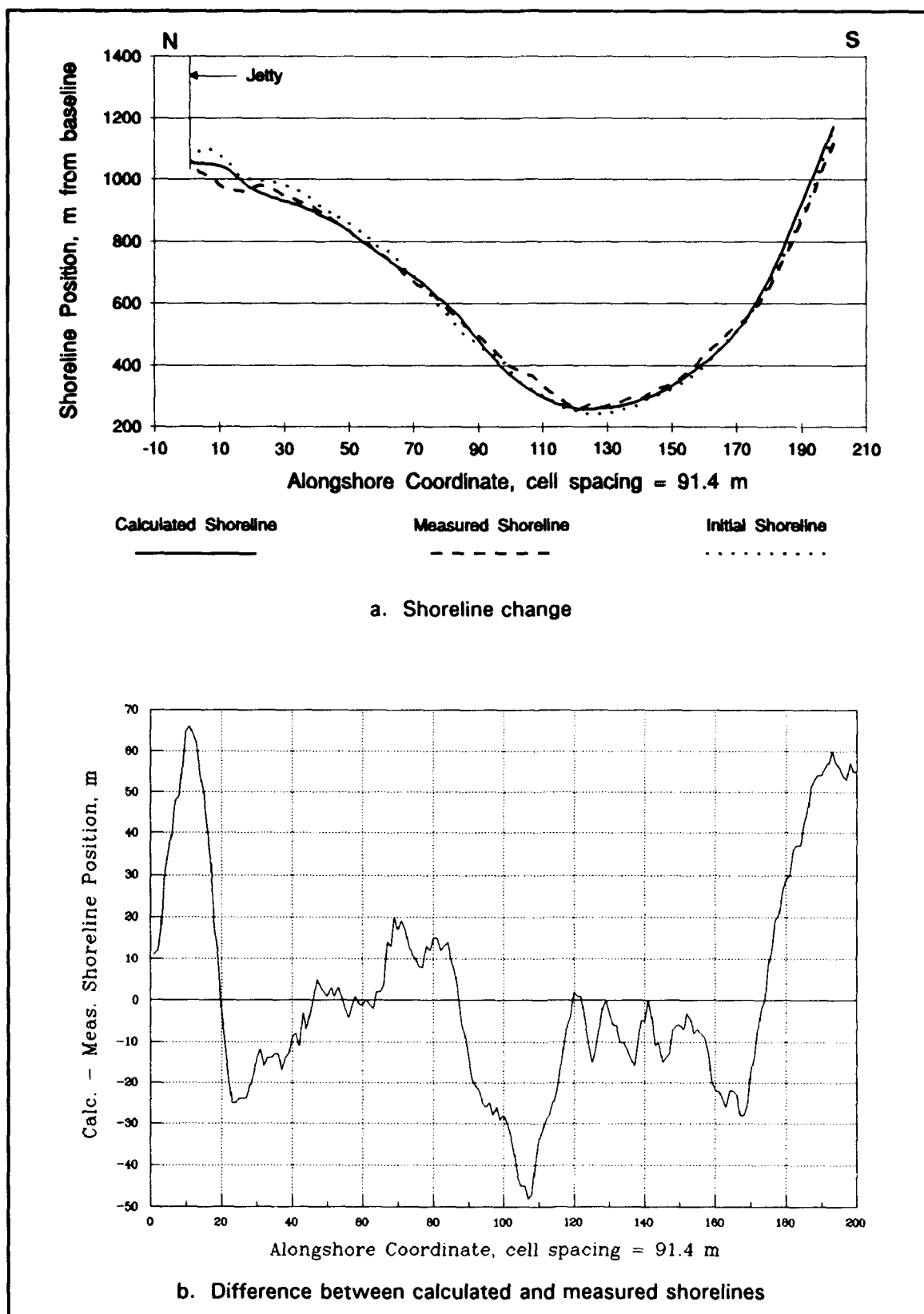


Figure 168. Amelia Island model shoreline change verification results

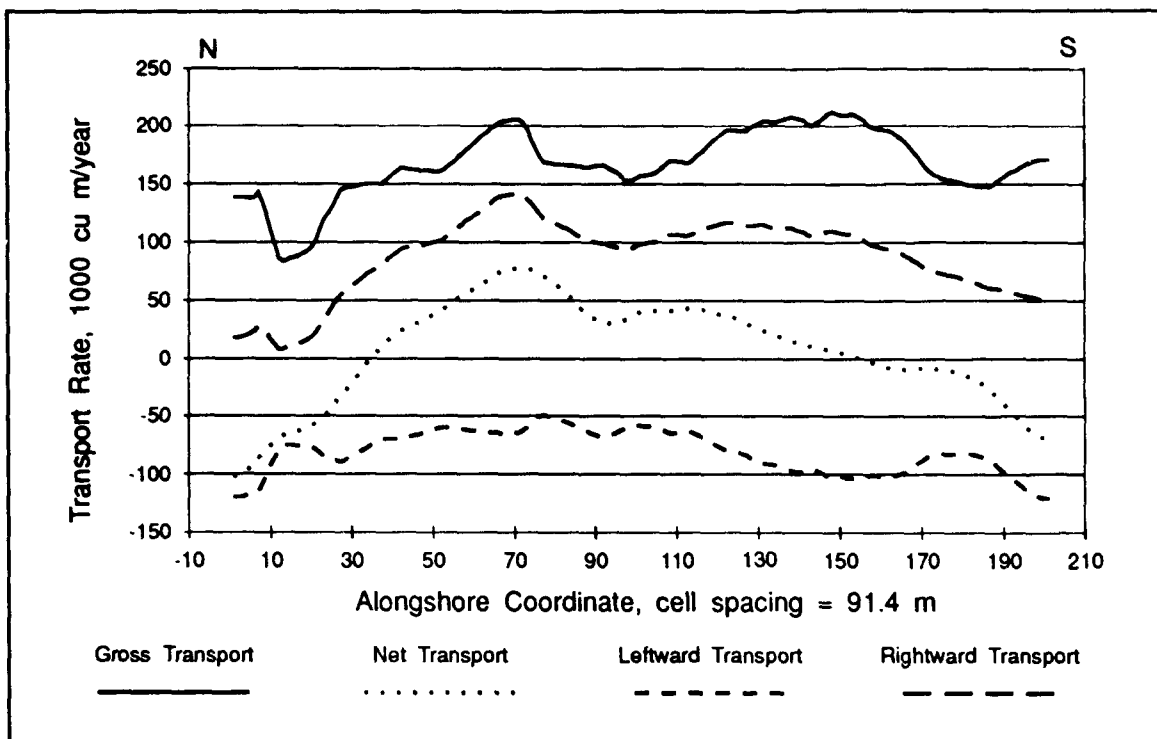


Figure 169. Transport rates for Amelia Island verification period

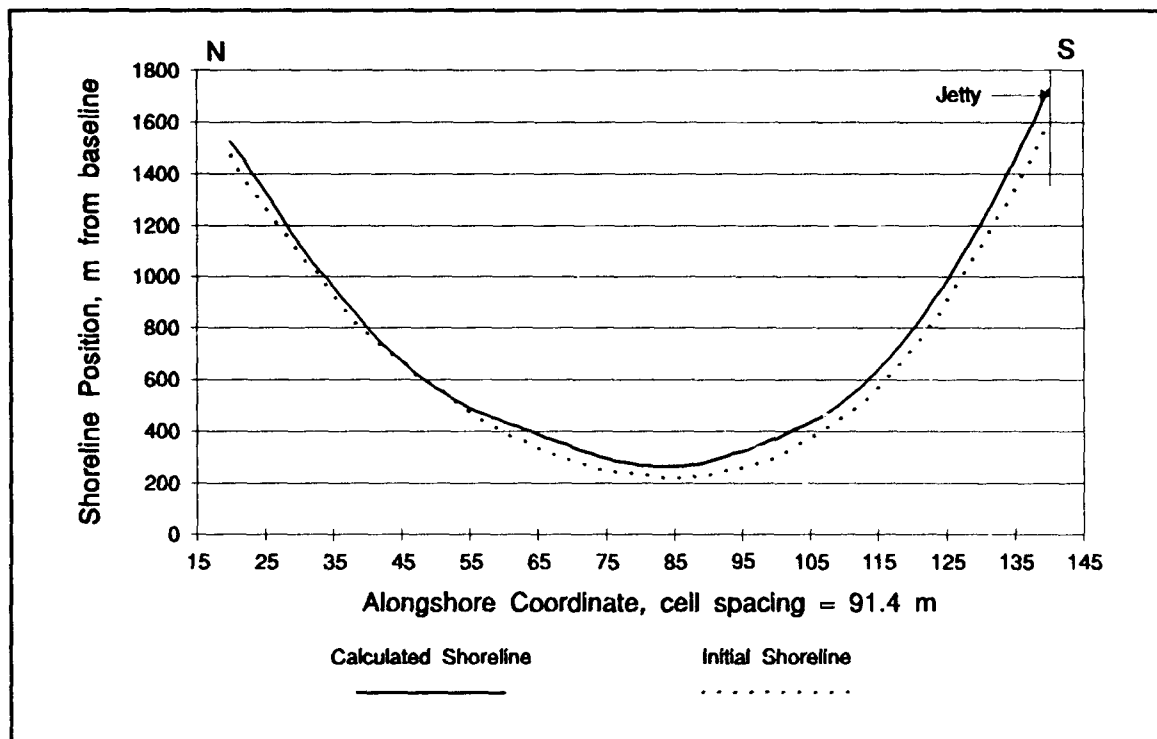


Figure 170. Cumberland Island shoreline 17-year extrapolation, 1974-1991

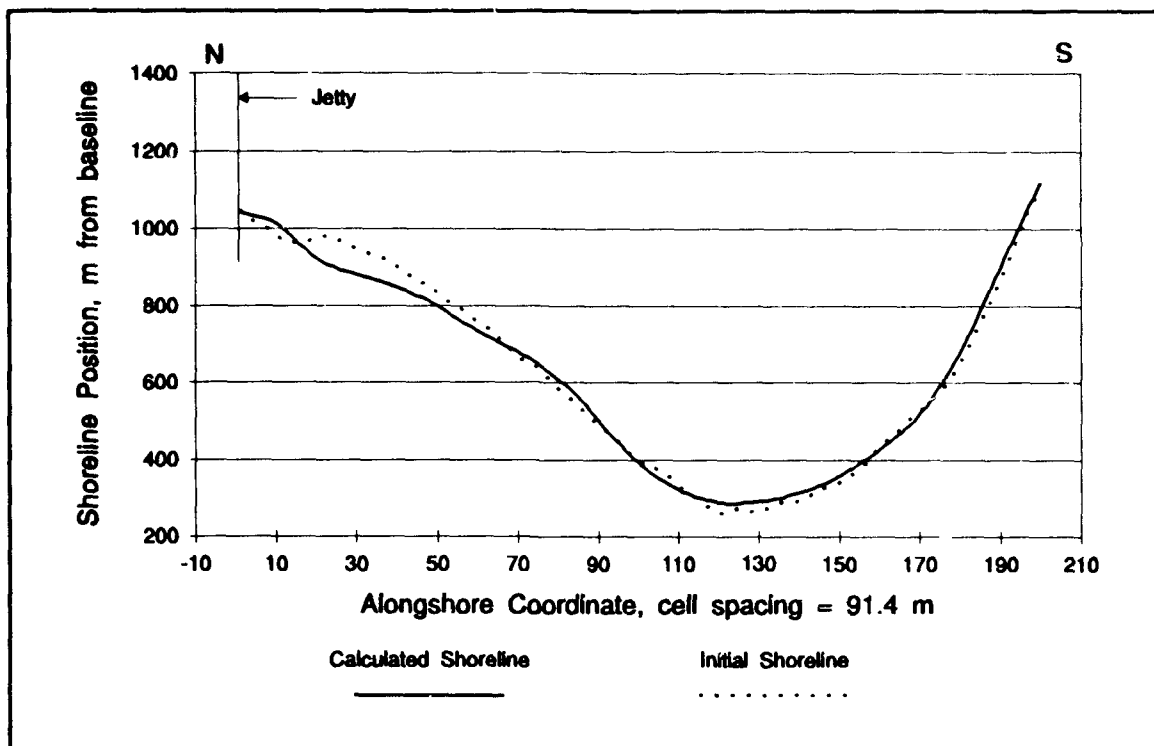


Figure 171. Amelia Island shoreline 11-year extrapolation, 1974-1985

in the calibration and verification phases of this study. Nearshore wave transformation files were developed and GENESIS simulations run for each epoch and each island. The Cumberland Island simulations used the offshore wave data from the calibration period, 17 years. The Amelia Island simulations used validation wave data extending over 11 years.

The Cumberland Island results are presented in Figures 172 and 173. Because the historical bathymetries extended 5.5 km to the north of the inlet, the pertinent area of comparison between epochs is between alongshore coordinates 80 and 140. The model results show that the net longshore transport rate near coordinate 80 is approximately 250,000 cu m/year during the two historical epochs and in the calibration run. The calculated annual net transport between coordinates 110 and 140 is directed toward the south, and the annual rates range between 75,000 and 270,000 cu m in the 1870s, 170,000 and 270,000 cu m in the 1920s, and 45,000 and 150,000 cu m for the calibration period 1950s to 1970s.

The Amelia Island results are presented in Figures 174 and 175. Because the historical bathymetries extended 5.5 km to the south of the inlet, the pertinent area of comparison between epochs is between alongshore coordinates 1 and 60. The model results show that the maximum net longshore transport rate in the region was approximately 300,000 cu m/year to the north in the 1870s and decreased to 185,000 cu m/year in the 1920s with the location of the maximum varying between time periods. By the 1950s to 1970s time period (Amelia Island verification period), the maximum net annual transport rate in the area decreased to about 125,000 cu m to the north.

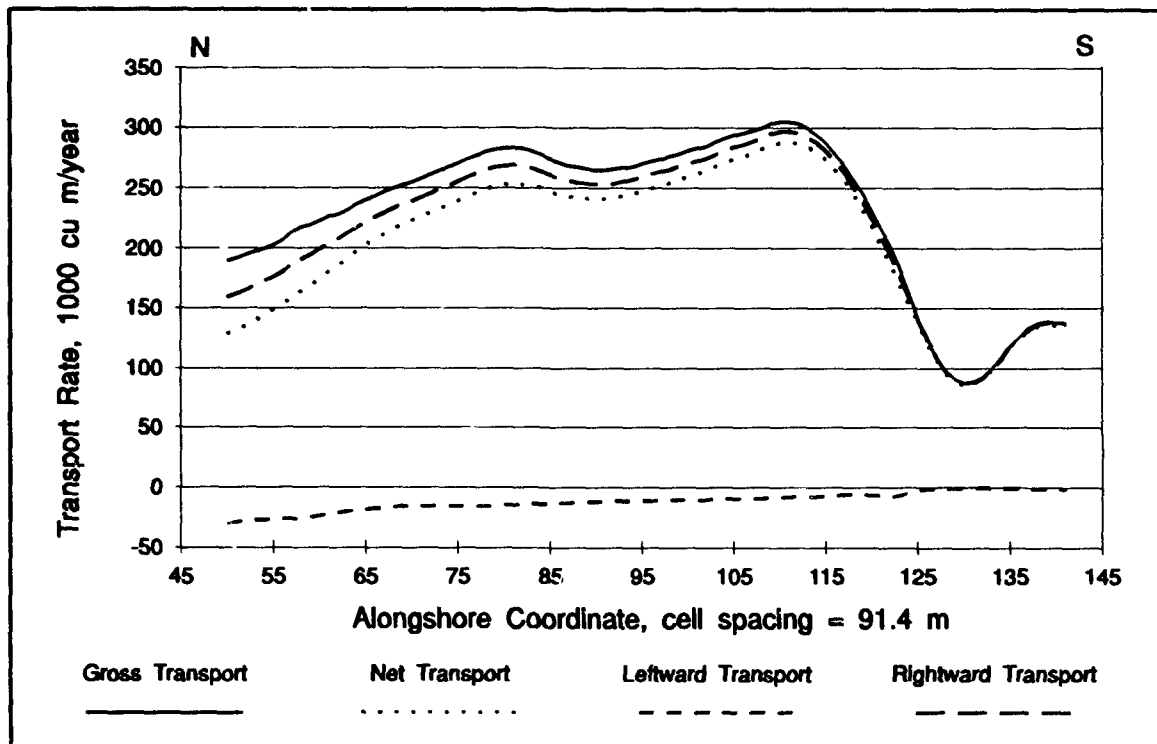


Figure 172. Cumberland Island sand transport rates during the 1870s

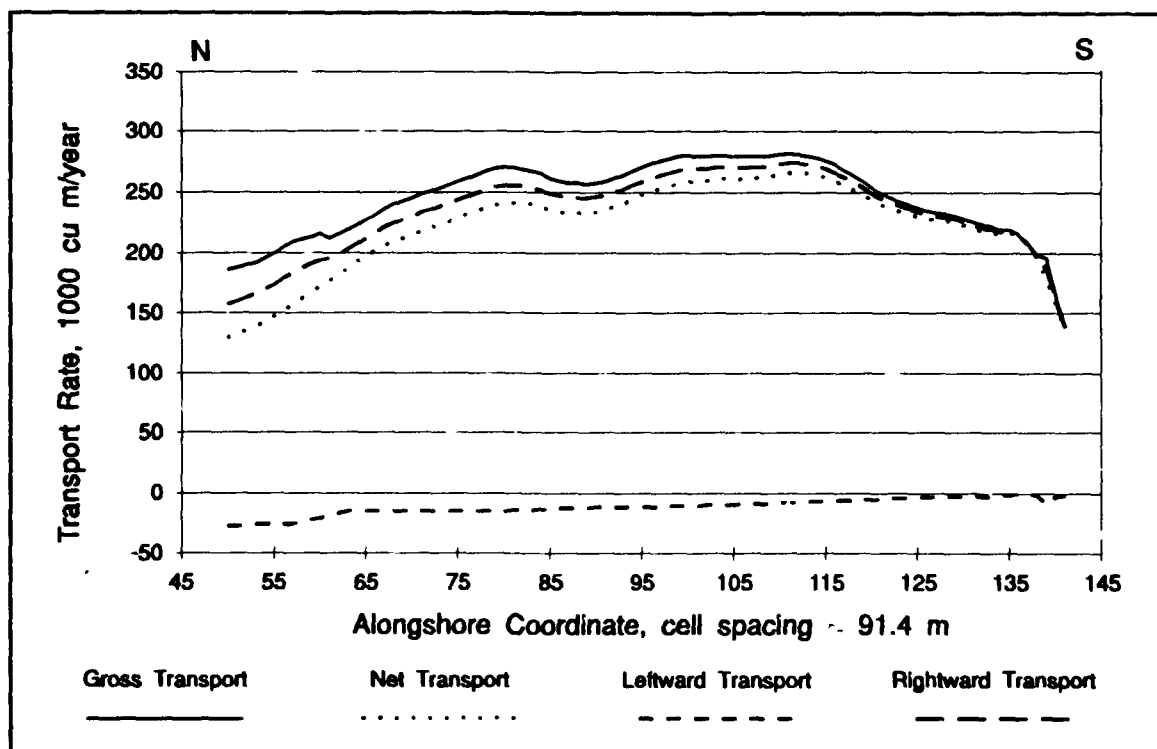


Figure 173. Cumberland Island sand transport rates during the 1920s

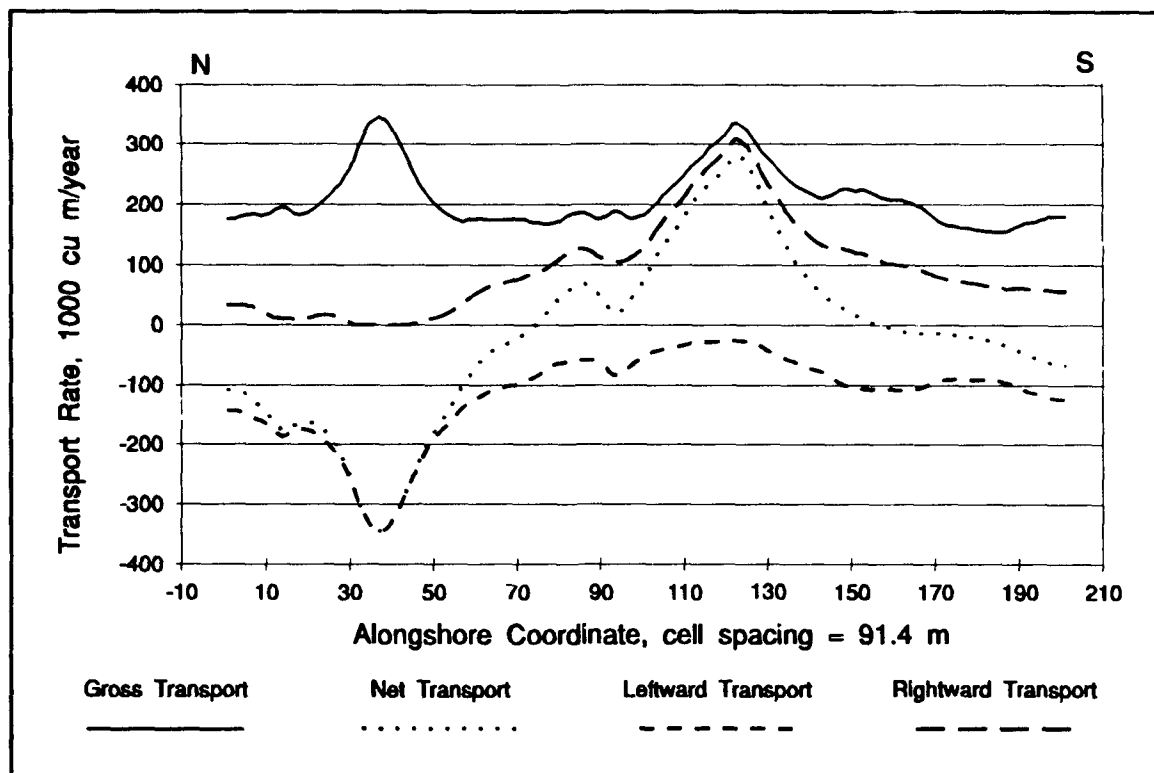


Figure 174. Amelia Island sand transport rates during the 1870s

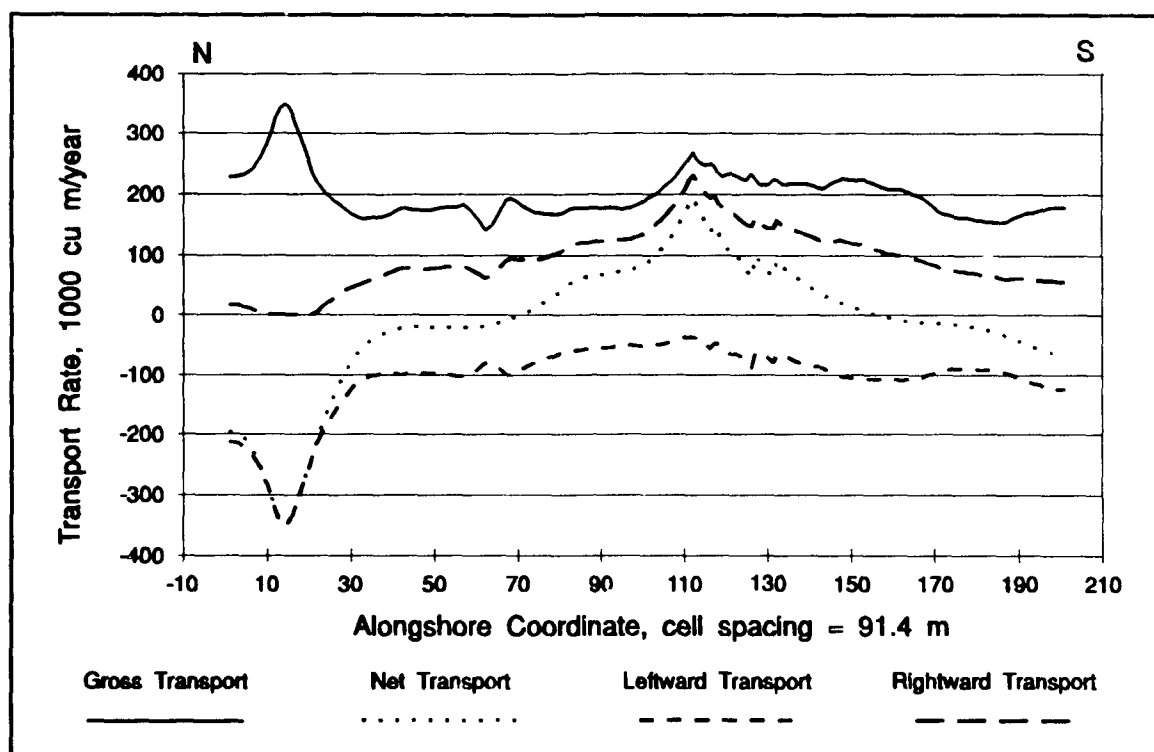


Figure 175. Amelia Island sand transport rates during the 1920s

Analysis of potential longshore transport rates on Cumberland and Amelia Islands for the historical time periods indicates that the rate can change by as much as 200,000 cu m/year over a 50-year time period due solely to natural changes in the nearshore bathymetry.

### **Transport rate variability**

Year-to-year variability in wave-induced longshore transport rates was estimated by analyzing predictions obtained with the 20-year WIS time series of GENESIS simulations for the two islands. The estimate by this procedure includes variations produced by seasonal and longer time weather cycles, as well as shoreline curvature and offshore bathymetric influence on wave transformation.

In order to simplify the longshore transport analysis, the island shorelines were divided into 1.8-km-long segments (1 n.m.). The average annual gross, net, leftward, and rightward longshore sand transport rates were calculated over each segment for each of the 20 years of record. This provided seven longshore segments on Cumberland Island and ten longshore segments on Amelia Island. The maximum, minimum, and average annual transport rates, and the standard deviation were calculated for each segment for the gross, net, leftward, and rightward rates.

Table 44 presents longshore transport results for Cumberland Island. Longshore segments are numbered from north to south along the island shoreline. The transport rates are larger than those computed for Amelia Island and decrease from north to south along the modeled reach, primarily due to shoreline orientation and wave refraction. The annual net transport rates on Cumberland Island are less variable than on Amelia Island with the standard deviation being about one-third of the average net annual transport rate. Maximum annual rates do not exceed the average by more than 100 percent. At the southern end of the island (segments 6 and 7), the average transport rate over the 20-year hindcast lies in the range of 85,000 to 210,000 cu m/year, a range corresponding well with the historical transport rates computed during the model calibration for the corresponding alongshore coordinates 80 to 140. The large magnitude of the year-to-year change in net longshore sediment transport rate and in its direction are primarily a result of annual changes in wave climatology.

Similar analysis of the longshore transport rates for Amelia Island is presented in Table 45. Longshore segments are numbered from north to south along the island shoreline. The analysis indicates that gross annual transport rates are not extremely variable overall (as indicated by the relatively small standard deviation), with the variation reaching  $\pm 50$  percent around the mean rate during the period of record. Variability in the net transport rate is much greater, with changes in the direction in net transport from year to year and maximum net rates that are 200 to 300 percent greater than the annual average. Average net transport in segments 1 and 2 is to the north (i.e., toward the jetty and the entrance).

## **Effect of TRIDENT-Related Channel Deepening**

The numerical simulations described above demonstrate the variability in annual longshore sediment transport rate along shorelines adjacent to the St. Marys Entrance. Naturally occurring

**Table 44**  
**Annual Transport Rates (1,000 cu m/year) at 1.8-km-Long (1-n.m.) Increments**  
**Along Cumberland Island Based Upon a 20-Year Wave Hindcast**

Segment	1	2	3	4	5	6	7
Max. Gross	607	602	542	468	367	267	156
Min. Gross	183	182	159	141	112	84	45
Avg. Gross	384	370	339	289	232	164	91
S.D. Gross	116	110	107	89	71	51	28
Max. Net	482	493	459	409	333	252	152
Min. Net	145	149	134	123	102	79	44
Avg. Net	304	302	287	253	211	155	87
S.D. Net	92	90	91	78	64	48	28
Max. Left	-19	-16	-12	-9	-5	-2	-1
Min. Left	-63	-55	-42	-29	-17	-8	-2
Avg. Left	-40	-34	-26	-18	-11	-5	-1
S.D. Left	12	10	8	6	3	1	0
Max. Right	545	548	501	438	350	260	154
Min. Right	164	165	147	132	107	81	44
Avg. Right	344	336	313	271	222	159	89
S.D. Right	104	100	99	83	68	49	28
Note: Transport to the left indicates sediment transport to the north and is denoted by negative values. Transport to the right indicates sediment transport to the south and is denoted by positive values.							

long-term changes in offshore bathymetry and variability in annual wave climate have contributed to the variability in sediment transport patterns. These natural variations in sediment transport help put into perspective the effects of TRIDENT-related channel deepening performed during the 1980s.

The St. Marys Entrance channel depth was increased by 3.3 m during the 1980s. It increased from a pre-TRIDENT authorized depth of 12.2 m in 1979 to the TRIDENT depth of 15.5 m in 1988. The channel deepening also resulted in an increase in channel width of 30 m. Although the effect of the small increase in channel width on adjacent shorelines could not be assessed using the models employed in this study because of the horizontal resolution of model grids, the effect of the channel deepening could be examined by modifying the depths used in the bathymetric inputs to the models.

In order to examine the effect of the TRIDENT-related deepening of the entrance channel on the adjacent shorelines of Cumberland and Amelia Islands, the channel depths used in the numerical modeling described in previous sections of this chapter were decreased by 3.3 m. The

**Table 45**  
**Annual Transport Rates (1,000 cu m/year) at 1.8-km-Long (1-n.m.) Increments**  
**Along Amelia Island Based Upon a 20-Year Wave Hindcast**

Segment	1	2	3	4	5	6	7	8	9	10
Max. Gross	176	217	264	314	250	261	308	318	262	244
Min. Gross	59	68	80	89	81	83	99	103	88	81
Avg. Gross	123	153	180	202	176	185	218	224	185	171
S.D. Gross	33	39	47	54	43	45	53	55	45	43
Max. Net	-34	39	127	170	118	122	114	78	46	11
Min. Net	-129	-63	-16	4	5	-4	-17	-32	-45	-83
Avg. Net	-81	-23	38	67	43	38	21	-1	-17	-47
S.D. Net	27	25	37	44	30	32	32	29	23	24
Max. Left	-46	-39	-31	-30	-29	-32	-45	-53	-48	-50
Min. Left	-152	-132	-106	-98	-96	-107	-143	-165	-145	-162
Avg. Left	-102	-88	-71	-67	-66	-73	-98	-112	-101	-109
S.D. Left	29	25	21	20	20	20	26	30	27	405
Max. Right	43	106	179	235	171	174	191	176	138	103
Min. Right	8	29	49	59	52	50	53	50	37	26
Avg. Right	20	65	109	135	109	111	120	111	84	62
S.D. Right	8	21	36	45	31	34	35	32	24	17

Note: Transport to the left indicates sediment transport to the north and is denoted by negative values.  
Transport to the right indicates sediment transport to the south and is denoted by positive values.

wave modeling and GENESIS simulations described thus far included a channel with a depth of 14.6 m. This was the depth surveyed in 1990 in the channel area and reported on the bathymetric chart used to develop the input data for the numerical modeling. A combination of infilling and dredging error could account for the difference between the 15.5-m depth dredged in 1988 and the 14.6-m depth reported on the bathymetric chart. The numerical modeling procedures described earlier in the chapter using a channel depth of 14.6 m were repeated for a pre-TRIDENT channel condition with a channel depth of 11.3 m (14.6 m less 3.3 m).

STWAVE wave simulations were performed to transform offshore wave conditions to the near-shore area through the three finite difference grids shown in Figures 157-161 with a channel depth of 11.3 m. The transformed energy spectra were integrated to determine the nearshore wave height and mean wave angle along the nearshore reference line for the GENESIS model. The resulting wave conditions along the nearshore reference line were found to be the same as those calculated for the deeper (14.6 m) channel except for very small differences in wave height and angle along the southern 1,371 m of Cumberland Island and the northern 1,371 m of Amelia Island. The largest of these changes was 0.04 m for unit input wave height and 0.05 deg in wave angle. Wave data for input to GENESIS are retained to an accuracy of 0.1 m in wave height and

0.1 deg in wave angle (Hanson and Kraus 1989). A priori, then, it was expected that the shoreline simulations would not be influenced by changes in waves caused by alterations to channel depth. Simulations with GENESIS indeed showed that longshore sediment transport rates and shoreline change patterns calculated over the model calibration periods were the same for the shallower (pre-TRIDENT) channel as those shown earlier in this chapter for the TRIDENT channel.

The effect of channel deepening on neighboring shorelines was found to be negligible because the nearshore wave conditions that produce shoreline change were not appreciably changed. The nearshore wave conditions were not significantly changed because:

- a. The change in channel depth was negligible when compared to the variations in bathymetry surrounding the channel which dominate wave transformations in the ebb tidal delta area. Figures 160 and 161 illustrate the complex bathymetry through which the relatively narrow entrance channel passes.
- b. The spectral wave model tends to realistically diffuse wave energy broadly in the lee of shoal features, thereby reducing the likelihood of localized or significant changes to nearshore waves due to small changes to bathymetry<sup>1</sup> (Resio 1988a).

Based upon the results described in this chapter obtained with the most advanced tools presently available for coastal assessments of this type, it is apparent that the magnitudes and variability of longshore sediment transport and shoreline change along Cumberland and Amelia Islands have been dominated by offshore wave conditions and the bathymetry over which the waves propagate. Variability in both the bathymetry and offshore wave climate over short- and long-term time scales dominates shoreline processes in comparison to existing dredged channel depths.

---

<sup>1</sup> Grosskopf, W. G., and Resio, D. T. February, 1987. The Impact of Dredging Offshore Shoals on the Nearshore Environment at Ocean City, Maryland, Text -- Volume I of III. Report submitted to USAED, Baltimore, Maryland.

## 8 Conclusions<sup>1</sup>

---

This chapter summarizes the essential engineering and coastal processes conclusions addressing the coastal study objective. The conclusions are based on analyses of historical shoreline position and bathymetry change for various time intervals starting from 1855/75, measurements made during the study monitoring program conducted from 1988 to 1992, and numerical simulations of longshore sand transport and shoreline change from the 1950s to the present. The numerical simulations also incorporated historical bathymetry to estimate longshore sediment transport variability. Conclusions are drawn from detailed material contained in the preceding chapters and appendices of this report. Where possible, consistency of the various independent estimates made in the study of different physical processes is discussed as a means of judging reliability of the conclusions.

Major changes in large-scale morphology such as the ebb-tidal shoals occur over time periods on the order of decades to centuries. The 4-year monitoring (1988-1992) effort conducted in this study was aimed at documenting and understanding existing morphologic conditions and short-term changes that occur in the study area. These monitoring results were combined with the substantial, more than 100-year-long historic record of shoreline and bathymetry data available for St. Marys Entrance and surrounding shores, and enabled a regional assessment of large-scale morphology change valid to present.

### Study Background

The objective of the coastal study, part of a more comprehensive investigation that included monitoring and modeling of the estuarine areas of the project site, was to assess the impacts of Navy-sponsored navigation channel modification and maintenance activities conducted over 1985-1992 on the shoreline in the vicinity of the inlet traditionally called St. Marys Entrance. This inlet, separating Cumberland Island, Georgia, to the north, and Amelia Island, Florida, to the south, contains a large estuary, a commercial and recreational port, Fernandina Harbor, Florida, and, since the 1970s, a U.S. Navy submarine base located at Kings Bay, Georgia. Cumberland Island is bounded on the north by St. Andrew Sound, and Amelia Island is bounded on the south by Nassau Sound.

Chapters 1 through 7 of this report and the associated appendices present results of a multi-component study of the coastal area in the vicinity of St. Marys Entrance. The three technical

---

<sup>1</sup> Written by Nicholas C. Kraus and Mark R. Byrnes.

components were: (a) review of historical data and previous studies; (b) numerical simulation of waves, longshore sand transport, and shoreline change; and (c) monitoring of waves, water level, shoreline position, beach profile and sediments, and ebb-tidal delta bathymetry. The effective field data collection period of this study ran from March 1988 through April 1992.

Prior to 1881 and commencement of jetty construction, St. Marys ebb-tidal delta consisted of a bifurcated channel system and a large delta and swash platform extending 6.5 km alongshore (Figure 28). The maximum depth of the primary channel was 5.8 m MLW. Since 1881, engineering modifications to provide for commercial and military navigation have significantly changed the position and shape of the ebb-tidal delta and altered the shoreline configuration on adjacent beaches. Two large rubble-mound jetties constructed at St. Marys Entrance over the period 1881 to 1905 are an engineering work of major significance to coastal processes at the study site. The north and south jetties are 5,841 and 3,416 m long, respectively. The elevation of the jetties was raised over the period 1905 to 1923, and, in modern times as well as in the past, the jetties are submerged during high tide. The shoreward end of the south jetty was sand-tightened in 1988 and 1989 to prevent sand from Amelia Island from moving into the St. Marys Entrance navigation channel. The inlet entrance channel has been realigned three times (1902 and 1916 as shown in Figure 30, and in 1955 -- the present channel) as part of stabilization work to prevent channel migration to the south. A chronology of engineering events is contained in Table 6.

After jetty construction, substantial accretion took place on the shorelines of Cumberland Island and Amelia Island for about 3 km immediately adjacent to each of the jetties. The shoreline of the southern half of the 30-km-long Cumberland Island, that portion that might be expected to be impacted by U.S. Navy modifications to the channel, is stable to accretionary. The shoreline of the 20-km-long Amelia Island away from the area of the jetty contains sections that range between mildly accretionary and erosional. The area within 3 km of the south jetty has experienced net accretion from 1857 to 1991; however, between March 1957 and April 1974 that shoreline receded, possibly due to Hurricane Dora in 1964. Shoreline position along Amelia Island has been virtually stable near the jetty from April 1974 to October 1991. The southern 4 km of Amelia Island have been eroding since 1857 (Figure 44). Most significant change in shoreline position took place between 1857/71 and 1924 (after jetty construction). Shoreline change rates are summarized in Tables 15 and 16 and Figures 47 to 61.

The St. Marys Entrance navigation channel has served both commercial and military needs. The channel has been deepened, widened, and lengthened since dredging began following completion of initial jetty construction around 1905. There were notable increases in dredged volume and channel dimensions in the 1950s for commercial traffic, in the mid-1970s to accommodate POSEIDON missile-carrying submarines, and in the late 1980s to accommodate TRIDENT (Ohio-Class) submarines. The present study addresses possible adverse impacts to the beaches on Cumberland Island and Amelia Island due to TRIDENT-related channel modifications performed by the U.S. Navy since 1985 (since 1982 in Cumberland Sound).

The present civil-works-authorized channel is 122 m wide and 9.8 m deep (with respect to MLW; the depth is 10.6 m with respect to NGVD), and ends at the 9.8-m-depth (NGVD) contour (Figure 2). The authorized military portion of the channel widened the civil works channel by 30 m and increased its depth to 15.5 m (MLW) for the recent (post-1985) modifications. The civil-works-authorized channel extends 8.3 km offshore, and the authorized military channel extends seaward of this contour for a total length of 22.2 km, of which the shoreward 19.8 km

have required dredging to reach the naturally existing depth contour of 15.5 m. The channel is dredged on an as-needed basis, and, in maintenance operations funded by the Navy, dredged sediment is placed at upland disposal sites, offshore sites, and in the nearshore off of central Amelia Island or on the beaches of Amelia Island, which lie on the predominant downdrift side of St. Marys Entrance.

A navigation channel and associated dredging have the potential to alter coastal sediment processes and shoreline evolution in several ways. First, a channel can trap sediment moving alongshore in the littoral zone that might otherwise bypass the inlet entrance and move downdrift to adjacent shores. Second, a channel can modify the nearshore pattern of incident waves and the longshore sediment transport produced by waves. Both mechanisms were investigated in this study. The sediment trapping function of the navigation channel was examined through study of the change in the ebb-tidal delta, dredging records, and in the shoreline and cross-shore profile of adjacent beaches. Wave transformation and longshore sand transport rates were numerically simulated from hindcast offshore wave conditions to estimate potential changes in the nearshore wave pattern expected to occur due to migration and natural changes in the ebb-tidal shoal and by channel modifications.

In a third mechanism, a channel may alter the growth of the ebb-tidal delta by promoting offshore movement of jetted material and by side-slope adjustment that would tend to fill the channel and require dredging. In a fourth mechanism, a shoal on which dredging occurs may be deflated if the amount of material removed exceeds the naturally occurring accumulation that created and maintains the shoal. Reduction in shoal volume would potentially reduce protective wave sheltering in its lee and the capacity to bypass sediment to downdrift shores. In this study, shoal volume change through time was calculated from both the historical and monitoring period bathymetric data, and the wave field modification potential of the channel was evaluated by performing sensitivity tests with a random wave propagation model verified with wave gage data obtained during the monitoring program.

The permeable jetties allow sediment to enter St. Marys Entrance and channel, from where a portion of the sediment is carried offshore by the ebb-tidal flow. The jetties have focused the ebb-tidal current, and the original ebb-tidal delta of the inlet in the natural (pre-jetty) state has therefore been displaced approximately 4 km seaward and has continued to grow (Figure 79). Through similar analysis of bathymetry change as performed here, Olsen (1977) concluded that St. Marys Entrance has become a complete littoral trap, and the more rigorous and comprehensive bathymetric change component of the present study confirmed this conclusion.

## Conclusions

The conclusions listed below were reached based on analysis of historical data and previous findings, data obtained during the monitoring program, and numerical simulations of longshore sand transport and shoreline change. The following is a summary of the assessment made in this study of U.S. Navy navigation channel modification and maintenance activities at St. Marys Entrance and their possible impacts on the shores of Cumberland Island and Amelia Island.

*From a regional and long-term (100-plus years) perspective, the entire 60-km-long coastal barrier island and inlet system has shown remarkable stability*

*despite major engineering modifications to the inlet entrance. Jetty construction has been responsible for progradation of the shoreline along southern Cumberland Island and northern Amelia Island, and translation of the ebb-tidal delta seaward. The Cumberland Island shoreline has been stable to accretionary for the length of record (1857/70 to 1991). Recession of the previously (1857 to 1957) prograding shoreline on Amelia Island along the beach 3 to 5 km south of the jetty occurred during the period from March 1957 to April 1974, prior to channel modifications by the U.S. Navy. The jetties have contributed to localized erosion on Amelia Island by reducing the longshore sand supply. From February 1974 to April 1991, the Amelia Island shoreline position was accretionary, due to beach replenishment (Table 34). The southernmost 6 km of shoreline of Amelia Island have exhibited net retreat for the period of record. Nassau Sound appears to exert significant control over shoreline position along its banks, which includes the southern terminus of Amelia Island. The rate of shoreline retreat has increased irrespective of the magnitude, timing, and location of channel modifications at St. Marys Entrance (Figures 45 and 46, Table 16).*

*No adverse impact on the beaches of Cumberland Island and Amelia Island by U.S. Navy navigation channel modification and maintenance at St. Marys Entrance could be detected in any of the analyses or monitoring performed in this or any other published study. Because no adverse impacts were found in this study, there was no basis for extrapolating such impacts into the future.*

Detailed findings and conclusions of this study are as follows:

- a. As has been found in previous studies, there is net southerly movement of littoral and shelf sediments along the 60-km-long coast from St. Andrew Sound, Georgia, to Nassau Sound, Florida. This long-term trend of southerly movement is evident by the skewness in nearshore morphology and its change (Figures 75 and 79).
- b. Longshore sand transport as calculated with calibrated shoreline change numerical models for Cumberland Island and Amelia Island showed net transport to the south for all years of the 20-year wave hindcast used as input to drive the model (Tables 44 and 45). Annual variability in the magnitude of the longshore sand transport rate, arising through natural fluctuations in the offshore wave climate and morphologic changes in the ebb-tidal delta, was on the order of 100 percent of the average net transport rate. This is a typical variability for an open-ocean coast. Changes in the nearshore wave climate caused by recent deepening of the channel are negligible and much smaller than the capability to either measure or hindcast wave conditions. Any corresponding change in longshore transport rate as produced by the channel-modified wave field was to lie far below the capability to measure or calculate longshore sediment transport in an absolute sense, and was judged to be insignificant in comparison to natural variability of coastal sediment processes.

- c. Dredging records, grab samples, and core data document a material shoaling trend where sand is trapped landward of Station 210+00 and silt and clay occur seaward of Station 230+00 in the St. Marys Entrance Channel (Figures 102 and 103). During Epoch 6 (1974-1987) 272,000 cu m/year were removed during maintenance dredging which extended to Station 260+00. Most of this quantity (for all location-documented dredging events except one) was located landward of Station 215+00 in the sand shoaling section of channel. During Epoch 7 (1988-1992), 616,000 cu m/year maintenance dredging was performed over the entire length of the Entrance Channel. Seventy-one percent (437,000 cu m/year) of the 1988-1992 maintenance dredging consisted of silt and clay removed from the extension of the channel seaward of Station 210+00. Twenty-four percent (149,000 cu m/year) of the 1988-1992 quantity was sandy material removed landward of Station 225+00. Based on the clear distinction in location of sand and of silts and clays occurring in the vicinity of Station 230+00, there is no evidence of an increase in the amount of littoral-transported sand trapped in the channel since the 1987-1988 deepening. The increased quantity of maintenance dredged volume is a result of additional dredging of fine-grained (non-littoral) sediments in the outer one-third of the ebb-tidal shoal and seaward extension of the longer channel.
- d. Pre-project numerical simulations of channel shoaling rates of non-cohesive sediments gave an estimate of 603,000 cu m/year (Vemulakonda et al. 1988), and the Kings Bay Environmental Impact Statement (1966) specifies an estimated maximum required annual dredging volume of 1.032 million cu m. The actual maintenance dredged volume (paragraph c.) for the U.S. Navy-modified channel thus falls below preproject estimates.
- e. Regionally, the Cumberland Island shoreline has been stable to accretionary for the length of record (1857/70 to 1991) (Tables 12 and 15, Figure 51). There has been slight erosion of the headland behind Stafford Shoal (Figures 41 and 51), which is considered to be a local, shoal-dependent process, and the southern embayment has had an increasing rate of accretion with approach to the jetty. The shoreline at the southern terminus of Cumberland Island has prograded approximately 1.5 km since the north jetty was completed in 1924 (Figure 42).
- f. Based on the profile survey data from the monitoring program from July 1988 to April 1992, the shoreline along Cumberland Island prograded an average of 0.3 m per year (Table 28), consistent with the long-term trend. The morphologic record and longshore sand transport calculations show no dependence of the Cumberland Island coast on sediment supply from the south and from St. Marys Entrance.
- g. Regionally, the Amelia Island shoreline has shown net accretion for the length of record (1857/71 to 1991) (Tables 13 and 16), although the southern end has been receding (Figure 44). The northern terminus of Amelia Island has prograded approximately 1.1 km from the time of jetty construction to present (Figure 78). An approximately 2-km-long nodal reach of longshore sediment transport divergence, located 3 to 5 km south of the jetty near Fernandina Beach, retreated rapidly between 1857 and 1924 in response to the jetties. The central embayment shoreline has been stable to slightly accretionary (Figures 47 to 51). The southernmost 6 km of shoreline of Amelia Island that includes Amelia Island Plantation has exhibited net retreat for the period of record (Item h).

- h.* Based on the profile survey data from the monitoring program from July 1988 to April 1992, the shoreline along Amelia Island experienced minor advance in shoreline position (calculated as 0.2 m per year, with interpolation and distance weighting for missing profile survey lines and excluding the northern accretionary reach for which survey control markers could not be located). However, an increase in storm activity in the autumn of 1991 that continued into 1992, including the severe "Halloween" storm on 30 October 1991 (Figure 155), removed survey markers and severely eroded the cliffs on the southern end of Amelia Island.
- i.* The shoreline along the southern terminus of Amelia Island receded 645 m to the north between 1871 and 1924 (Table 14, Figure 44), and shoreline surveys made in August to October 1924 and in October 1991 show that the same area receded 15 m over the 67-year period. Jetty construction and modification took place from 1871 to 1924, but possible jetty-induced changes in shoreline position at the southern terminus of Amelia Island cannot be distinguished from naturally occurring morphologic change at Nassau Sound, of which the southern terminus is a major component. As a pristine inlet, Nassau Sound undergoes cyclical and random morphologic change that will dominate the shape and evolution of the shores directly adjacent to it. Investigation of processes related to Nassau Sound (and St. Andrew Sound) was not part of this study.
- j.* The location of the 6-m-depth (NGVD) contour has remained effectively unchanged over the period of record (1855/75 to 1954/79) for the Cumberland Embayment and Amelia Embayment (Figure 76). The 6-m depth (NGVD) was independently determined to be the depth of closure in the morphologic change study and shoreline change simulation study. Adjacent to the north jetty, the location of the 6-m-depth contour has remained constant. Along the Northern Amelia Platform, the 6-m-depth contour moved shoreward approximately 1 km because of degradation of the original ebb-tidal shoal after jetty construction. Confinement of littoral processes to within a long-term depth of closure of 6 m (NGVD) indicates that maintenance of the civil works channel to 10.6-m depth (NGVD) traps littoral sediments and exposes them to ebb-tidal flow that moves and deposits sediment on the shelf, seaward of the littoral zone. The U.S. Navy modifications to the channel have not changed the capability of the channel to trap littoral sediment. Therefore, the sediment trapping capacity and subsequent impacts on the shorelines of Cumberland Island and Amelia Island by U.S. Navy modifications of the channel are inconsequential compared to those of the pre-existing commercial channel.
- k.* The 9-m-depth (NGVD) contour along Stafford Shoal in the Cumberland Embayment has moved to the south, due to southerly migration of the shoal. The 9-m (NGVD) contour along the Amelia Embayment has moved landward approximately 1 km over the period of record (compare Figures 73 and 75). In the vicinity of St. Mary's Entrance, the 9- and 12-m-depth (NGVD) contours moved seaward as a result of growth of the modern (postjetty) ebb-tidal delta. Seaward growth of these contours indicates continued sand capture by the modern delta. Movement of the 9- and 12-m (NGVD) contours along the open coast and away from inlet deltas is believed to be related to sediment transport by nearshore shelf (deepwater) currents. Such movement occurs much more slowly than that caused by sediment-transport-related processes in the littoral zone.
- l.* For the 120-year period from 1870/75 to 1992, the ebb-tidal delta at St. Marys Entrance has been a sink of littoral sediment (Figure 98). Immediately after jetty construction,

sediment deposition offshore increased when a delta began to develop approximately 2 to 3 km seaward of the original delta. Since 1934/55, the ebb-tidal delta has experienced a relatively small annual volume increase, 171,000 cu m, as compared to 828,000 cu m annual increase for the period 1910/24 to 1934/55 (Table 21, Figure 99). The northern and southern lobes of the ebb-tidal delta have shown a trend of accretion since 1934/55 (Figure 94), whereas the region of the ebb delta occupied by the channel has lost volume since 1934/55 (Table 22, Figure 99). In the future, the southerly growth of the ebb-delta lobe, although difficult to extrapolate, may provide additional wave protection and shoreline stability for northern Amelia Island. The shoal presently shelters both the southern end of Cumberland Island and the northern end of Amelia Island.

## Consistency of Results

The observation-based studies, involving historical and monitoring data, and the simulation study, involving numerical modeling of shoreline change, were performed in parallel by different investigators and from different perspectives. The main commonality between these two types of studies is a subset of the total-project offshore bathymetry and recent shoreline position data sets. The shoreline change modeling depends directly on a wave hindcast not related to the observation-based studies and on boundary conditions imposed by the modelers based on interpretation of coastal sediment processes in the area.

Confidence in the conclusions listed above is increased by identifying consistency among the independent methodologies. The following properties or observations showed consistency in results:

- a. Analysis of the regional morphology indicates net movement of sand to the south on Cumberland Island and Amelia Island (Figure 79). Similarly, the coupled wave hindcast and shoreline change modeling produced net longshore sand transport directed to the south on both islands, except for a local trend of transport to the north on the northern end of Amelia Island (Tables 44 and 45). This trend, produced by entrapment of material by the jetty during periods of northerly transport, is also observed in the bathymetric and shoreline change.
- b. The estimated annual average maintenance dredged volume for the entrance channel (excluding Cumberland Sound) during the period from 1954 to 1973 was 81,000 cu m (Figure 100). At the north jetty, the calibrated shoreline change model for Cumberland Island gave an average net longshore transport rate of 87,000 cu m per year directed south (Table 44), and, at the south jetty, the calibrated model for Amelia Island gave 47,000 cu m per year directed north (Table 45). Not all of the material directed toward the inlet will pass through or around the jetties to enter the maintenance dredging prism. Agreement within a factor of two of the average annual maintenance dredged volume and the sediment volume that may potentially enter the inlet laterally supports the correctness of the order of magnitude of the estimated longshore transport rate. In addition, the bathymetric change analysis for the period 1934/55 to 1953/79 for the region covered by the 1988 and 1992 bathymetric surveys (which exclude the channel landward and between the jetties) gave an annual volume change of 155,000 cu m for the St. Marys Tidal Inlet

Complex (Table 21). This annual volume change agrees well with the gross (north and south-directed) transport obtained in the shoreline change simulation model.

- c. The calibrated shoreline change model for Cumberland Island produced net average annual deposition of 217,000 cu m for the Cumberland Island Embayment (the full model reach, Table 44), which compares favorably with the net increase calculated for the bathymetric change analysis Polygons 5 and 8 of 185,000 cu m/year for the period 1924 to 1954/79.
- d. Along the northern end of Amelia Island, the calibrated shoreline change model predicted an average annual deposition of 81,000 cu m (Table 45), which compares favorably with 116,000 cu m (for the period 1924 to 1954/79, Table 18) obtained in the morphology change analysis for Polygon 10. However, the shoreline change model gave net average annual deposition of 68,000 cu m along the Amelia Embayment (Segments 4-8 in Table 18) as compared to a loss of 41,000 cu m for Polygon 13. This difference is attributed to the lack of an accurate boundary condition on the southern side of the shoreline change model, a region that is probably dominated by tidal inlet processes at Nassau Sound.
- e. The predicted depth of closure for the littoral zone was approximately 6 m (NGVD) based on the hindcast wave climate. The bathymetric change analysis for the period of record 1855/75 to 1954/79 (Figure 76) showed that the 6-m depth was stable along the Cumberland Island and the Amelia Island Embayments.

No discrepancies between the two methodologies, morphology change analysis and shoreline change numerical modeling, were noted except at the southern half of Amelia Island. An accurate and general boundary condition in this area dominated by tidal inlet processes at Nassau Sound could not be imposed in the shoreline change model. Predictions of the model are considered reliable except for this region, for which the morphologic change analysis is definitive.

# References

---

- Abel, C. E., Tracy, B. A., Vincent, C. L., and Jensen, R. E. (1989). "Hurricane hindcast methodology and wave statistics for Atlantic and Gulf hurricanes from 1956-1975," WIS Report 19, U.S. Army Engineer Waterways Experiment Station, Coastal Engineering Research Center, Vicksburg, MS.
- Adams, K. T. (1942). "Hydrographic manual," U.S. Coast and Geodetic Survey, Washington, DC.
- Anders, F. J., and Byrnes, M. R. (1991). "Accuracy of shoreline change rates as determined from maps and aerial photographs," *Shore and Beach* 59(1), 17-26.
- Anders, F. J., Reed, D. W., and Meisburger, E. P. (1990). "Shoreline movements, Report 2: Tybee Island, Georgia, to Cape Fear, North Carolina, 1851-1983," Technical Report CERC-83-1, U.S. Army Engineer Waterways Experiment Station, Coastal Engineering Research Center, Vicksburg, MS.
- Anderson, T. W., and Sclove, S. L. (1978). *An introduction to statistical analysis of data*. Houghton Mifflin Company, Boston, MA.
- Aubrey, D. G., McSherry, T., and Spencer, W. (1990). "Sedimentation study: Environmental monitoring and operations guidance system (EMOGS), Kings Bay, Georgia, and Florida, 1988-1990," Final Report for the U.S. Navy, Report No. WHOI-91-17, Woods Hole Oceanographic Institution, Woods Hole, MA.
- Barnett, T. P. (1983). "Recent changes in sea level and their possible causes," *Climatic Change* 5, 15-38.
- \_\_\_\_\_. (1984). "The estimation of "global" sea level change: A problem of uniqueness," *Journal of Geophysical Research* 89, 7980-88.
- Barwis, J. H. (1978). "Sedimentology of some South Carolina tidal creek point bars and a comparison with their fluvial counterparts." *Proceedings Calgary Fluvial Conference*. Calgary, Alberta, Canada.
- Bascom, W. N. (1959). "The relationship between sand size and beach-face slope," *American Geophysical Union Transaction* 32(6), 866-74.

- Birkemeier, W. A. (1984). "The interactive survey reduction program: User's manual of ISRP," Instruction Report CERC-84-1, U.S. Army Engineer Waterways Experiment Station, Coastal Engineering Research Center, Vicksburg, MS.
- Bludgett, J. W. (1956). "A preliminary investigation of some depositional features between St. Augustine and Fernandina Beach, Florida," *Bulletin of the Georgia Academy of Science* 14(3), 63-68.
- Bouws, E., Günther, H., Rosenthal, W., and Vincent, C. L. (1985). "Similarity of the wind wave spectrum in finite depth water: 1. Spectral form.," *Journal of Geophysical Research* 90(C1), 975-86.
- Bowie, W. (1928). "The triangulation of North America," *The Geographical Journal* 72, 348-56.
- Braatz, B. V., and Aubrey, D. G. (1987). "Recent relative sea-level change in eastern North America." *Sea-level fluctuation and coastal evolution*. D. Nummedal, O. H. Pilkey, and J. D. Howard, ed., Society of Economic Paleontologists and Mineralogists, Tulsa, OK, 29-46.
- Brown, P. J. (1977). "Variations in South Carolina coastal morphology." *Beaches and barriers of the central South Carolina Coast, field trip guidebook*. D. Nummedal, ed., Department of Geology, University of South Carolina, Columbia, SC, 11-24.
- Bruun, P. (1954). "Coast erosion and the development of beach profiles," Technical Memorandum No. 44, Beach Erosion Board, U.S. Army Engineer Waterways Experiment Station, Vicksburg, MS.
- Byrnes, M. R., and Patnaik, P. "Automated shoreline analysis program (ASAP)," In preparation.
- Byrnes, M. R., McBride, R. A., and Hiland, M. W. (1991). "Accuracy standards and development of a national shoreline change data base." *Proceedings Coastal Sediments '91*. American Society of Civil Engineers, New York, NY, 1027-42.
- \_\_\_\_\_. (1994). "Quantifying changes in shoreline position: standard procedures for accurate data capture and analysis," Technical Report, Center for Coastal, Energy, and Environmental Resources, Louisiana State University, Baton Rouge, LA.
- Byrnes, M. R., McBride, R. A., Penland, S., Hiland, M. W., and Westphal, K. A. (1991). "Historical changes in shoreline position along the Mississippi Sound barrier islands." *GCS-SEPM 12<sup>th</sup> Annual Research Conference*, Coastal Depositional Systems in the Gulf of Mexico: Quaternary Framework and Environmental Issues, 43-55.
- Caldwell, J. M. (1966). "Coastal processes and beach erosion," *Journal of the Society of Civil Engineers* 53(2), London, UK, 142-57.
- Church, M. (1920). "Triangulation in Rhode Island 9," Special Publication No. 62, U.S. Coast and Geodetic Survey, Rockville, MD.

- Cialone, M. A., Mark, D. J., Chou, L. W., Leenknecht, D. A., Davis, J. E., Lillycrop, L. S., and Jensen, R. E. (1992). "Coastal modeling system (CMS) user's manual, Supplement 1 to September 1991 manual," Instruction Report CERC-91-1, U.S. Army Engineer Waterways Experiment Station, Vicksburg, MS.
- Clausner, J. E., Birkemeier, W. A., and Clark, G. R. (1986). "Field comparison of four nearshore survey systems," Miscellaneous Paper CERC-86-6, U.S. Army Engineer Waterways Experiment Station, Coastal Engineering Research Center, Vicksburg, MS.
- Cofer-Shabica, S. V., and Hargrove, W. (1991). "Automated remote meteorological stations for climatic water budget determination at Cumberland Island, GA, USA." *Proceedings Coastal Zone '91, Biological and Physical Aspects of Dredging, Kings Bay, Georgia*. American Society of Civil Engineers, New York, NY, 118-31.
- Cooke, C. W. (1943). "Geology of the Coastal Plain of Georgia," Bulletin No. 941, U. S. Geological Survey, Washington, DC.
- \_\_\_\_\_. (1945). "Geology of Florida," Bulletin No. 29, Florida Geological Survey, Tallahassee, FL.
- Corson, W. D., and McKinney, J. P. (1991). "Summary of directional wave data from 3 different monitoring systems deployed offshore of St. Marys Entrance, Georgia." *Proceedings Coastal Zone '91, Biological and Physical Aspects of Dredging, Kings Bay, GA*. American Society of Civil Engineers, New York, NY, 132-42.
- Corson, W. D., Resio, D. T., Brooks, R. M., Ebersole, B. A., Jensen, R. E., Ragsdale, D. S., and Tracy, B. A. (1982). "Atlantic coast hindcast, Phase II wave information," WIS Report 6, U.S. Army Engineer Waterways Experiment Station, Coastal Engineering Research Center, Vicksburg, MS.
- Crowell, M., Leatherman, S. P., and Buckley, M. K. (1991). "Historical shoreline change: Error analysis and mapping accuracy," *Journal of Coastal Research* 7(3), 839-52.
- Davies, J. L. (1973). *Geographical Variation in Coastal Development*. Hafner, New York, NY.
- Davis, J. E., Smith, J. M., and Vincent, C. L. (1991). "Parametric description for a wave energy spectrum in the surf zone," Miscellaneous Paper CERC-91-11, U.S. Army Engineer Waterways Experiment Station, Coastal Engineering Research Center, Vicksburg, MS.
- Davis, R. A., Jr. (1989). "Texture, composition and provenance of beach sands, Victoria, Australia," *Journal of Coastal Research* 5(1), 37-47.
- Dean, R. G. (1977). "Equilibrium beach profiles: U.S. Atlantic and Gulf Coasts," Ocean Engineering Report No. 12, Department of Civil Engineering, University of Delaware, Newark, DE.

- Dean, R. G. (1988). "Sediment interaction at modified coastal inlets: Processes and policies." *Lecture Notes on Coastal and Estuarine Studies. Symposium on Hydrodynamics and Sediment Dynamics of Tidal Inlets* 29. D. G. Aubrey and L. Weishar, ed., Springer-Verlag, New York, NY.
- Dean, R. G., and Grant, J. (1989). "Development of methodology for 30-year shoreline projections in the vicinity of beach nourishment projects," Florida Department of Natural Resources.
- Dean, R. G., and Walton, T. L. (1973). "Sediment transport processes in the vicinity of inlets with special reference to sand trapping." *Proceedings International Estuarine Research Federation Conference*. L. E. Cronin, ed., Academic Press, New York, NY, 129-49.
- DePratter, C. B., and Howard, J. D. (1977). "History of shoreline changes determined by archaeological dating: Georgia coast, U.S.A." *Transactions-Gulf Coast Association of Geological Societies* 26. 252-58.
- Dolan, R., Hayden, B. P., May, P., and May, S. (1980). "Reliability of shoreline change measurements from aerial photographs," *Shore and Beach* 48(4), 22-29.
- Dolan, R., Hayden, B. P., Rea, C. C., and Heywood, J. (1979). "Shoreline erosion rates along the middle Atlantic coast of the United States," *Geology* 7, 602-06.
- Doyle, D. R., and Dewhurst, W. T. (1989). "North American datum of 1983," *Arc News* 11(4).
- Ebersole, B. A., Cialone, M. A., and Prater, M. D. (1986). "Regional coastal processes numerical modeling system; Report 1, RCPWAVE - a linear wave propagation model for engineering use," Technical Report CERC-86-4, U.S. Army Engineer Waterways Experiment Station, Vicksburg, MS.
- Ellis, M. Y. (1978). *Coastal mapping handbook*. U.S. Department of the Interior, Geological Survey, U.S. Department of Commerce, National Ocean Service, U.S. Government Printing Office, Washington, DC.
- Emery, K. O. 1961. "A simple method of measuring beach profiles," *Limnology and Oceanography* 6, 90-93.
- Everts, C. H., Battley, J. P., and Gibson, P. N. (1983). "Shoreline movements; Report 1, Cape Henry, Virginia, to Cape Hatteras, North Carolina, 1849-1980," Technical Report CERC-83-1, U.S. Army Engineer Waterways Experiment Station, Coastal Engineering Research Center, Vicksburg, MS.
- Fagerburg, T. L., Coleman, C. J., and Parman, J. W. (1991a). "Cumberland Sound monitoring; Report 1, 1988 data collection report," Technical Report HL-91-4, U.S. Army Engineer Waterways Experiment Station, Hydraulics Laboratory, Vicksburg, MS.

Fagerburg, T. L., Coleman, C. J., and Parman, J. W. (1991b). "Cumberland Sound monitoring; Report 2, 1989 data collection report," Technical Report HL-91-4, U.S. Army Engineer Waterways Experiment Station, Hydraulics Laboratory, Vicksburg, MS.

Fagerburg, T. L., Knowles, S. C., Benson, H. A., and Fisackerly, G. M. (1992). "Hydrodynamic data collection for Kings Bay, Cumberland Sound," Technical Report HL-92-4, U.S. Army Engineer Waterways Experiment Station, Hydraulics Laboratory, Vicksburg, MS.

Fisackerly, G. M., Fagerburg, T. L., and Knowles, S. C. (1991). "Estuarine dynamics at Cumberland Sound, Georgia, USA." *Proceedings Coastal Zone '91, Biological and Physical Aspects of Dredging, Kings Bay, Georgia*. American Society of Civil Engineers, New York, NY, 143-56.

Fisher, J. J. (1968). "Barrier island formation: Discussion," *Bulletin of the Geological Society of America* 79, 1421-26.

Fisher, J. J., and Simpson, E. J. (1979). "Washover and tidal sedimentation rates as environmental factors in development of a transgressive barrier shoreline." *Barrier Islands from the Gulf of St. Lawrence to the Gulf of Mexico*. S. P. Leatherman, ed., Academic Press, New York, NY, 127-48.

FitzGerald, D. M. (1986). "Shoreline erosional-depositional process associated with tidal inlets." *Lecture Notes on Coastal and Estuarine Studies. Symposium on Hydrodynamics and Sediment Dynamics of Tidal Inlets* 29. D. G. Aubrey and L. Weishar, ed., Springer-Verlag, New York, NY, 186-225.

\_\_\_\_\_. (1988). "Shoreline erosional-depositional process associated with tidal inlets." *Lecture Notes on Coastal and Estuarine Studies. Symposium on Hydrodynamics and Sediment Dynamics of Tidal Inlets* 29. D. G. Aubrey and L. Weishar, ed., Springer-Verlag, New York, NY, 364-81.

FitzGerald, D. M., and Hayes, M. O. (1980). "Tidal inlet effects on barrier island management." *Proceedings Coastal Zone '80*. American Society of Civil Engineers, New York, NY, 2355-79.

FitzGerald, D. M., and Nummedal, D. (1983). "Response characteristics of an ebb-dominated tidal inlet channel," *Journal of Sedimentary Petrology* 53, 833-45.

FitzGerald, D. M., Hubbard, D. K., and Nummedal, D. (1978). "Shoreline changes associated with tidal inlets along the South Carolina coast." *Proceedings Coastal Zone '78, Symposium on Technical, Environmental, Socioeconomic, and Regulatory Aspects of Coastal Zone Management 1973-1974*. American Society of Civil Engineers, New York, NY.

Flint, R. F. (1964). *Glacial and Quaternary geology*. John Wiley and Sons, Inc., New York, NY.

- Florida Coastal Engineers, Inc. (1976). "Beach erosion control study Nassau County, Florida," U.S. Army Engineer District, Jacksonville, FL.
- Folk, R. L. (1974). *Petrology of sedimentary rock*. Hemphill Publishing Company, Austin, TX.
- Folk, R. L., and Ward, W. C. (1957). "Brazos River bar: A study in the significance of grain size parameters," *Journal of Sedimentary Petrology* 27, 3-26.
- Frey, R. W., and Basan, P. B. (1985). "Coastal marshes." *Coastal Sedimentary Environments*. R. A. Davis, Jr., ed., Springer-Verlag, New York, NY.
- Friedman, G. M., and Sanders, J. E. (1978). *Principles of sedimentology*. John Wiley & Sons, New York, NY.
- Garcia, A. W., Jarvinen, B. R., and Schuck-Kolben, R. E. (1990). "Storm surge observations and model hindcast comparison for Hurricane Hugo," *Shore and Beach* 58(4), 15-21.
- Giles, R. T., and Pilkey, O. H. (1965). "Atlantic beach and dune sediments of the southern United States," *Journal of Sedimentary Petrology* 35(4), 900-10.
- Gorman, L. T. (1991). "Assessment of the nearshore zone at St. Marys Inlet, Florida." *Proceedings Coastal Zone '91, Biological and Physical Aspects of Dredging, Kings Bay, Georgia*. American Society of Civil Engineers, New York, NY, 169-79.
- Gornitz, V., and Seeber, L. (1990). "Vertical crustal movements along the east coast, North America, from historic and late Holocene sea-level data," *Tectonophysics* 178, 127-50.
- Gornitz, V., Lebedeff, S., and Hansen, J. (1982). "Global sea level trend in the past century," *Science* 215, 1611-14.
- Granat, M. A. (1990). "Numerical model predictions of Cumberland Sound sediment redistribution associated with TRIDENT channel expansion," Miscellaneous Paper HL-90-3, U.S. Army Engineer Waterways Experiment Station, Hydraulics Laboratory, Vicksburg, MS.
- Granat, M. A., Brogdon, N. J., Cartwright, J. T., and McAnally, W. J., Jr. (1989). "Hydrodynamic and sediment transport hybrid modeling of Cumberland Sound and Kings Bay navigation channel, Georgia: Verification and basic plan testing," Technical Report HL-89-14, U.S. Army Engineer Waterways Experiment Station, Hydraulics Laboratory, Vicksburg, MS.
- Gravens, M. B., Kraus, N. C., and Hanson, H. (1991). "GENESIS: Generalized model for simulating shoreline change; Report 2, workbook and system user's manual," Technical Report CERC-89-19, U.S. Army Engineer Waterways Experiment Station, Coastal Engineering Research Center, Vicksburg, MS.

- Griffin, M. M., and Henry, V. J. (1984). "Historical changes in the mean high water shoreline of Georgia, 1857-1982," Bulletin 98, Georgia Geological Survey, Atlanta, GA.
- Grosskopf, W. G., Aubrey, D. G., Mattie, M. G., and Mathiesen, M. (1983). "Field intercomparison of nearshore directional wave sensors," *IEEE Journal of Oceanic Engineering* OE-8(4), 254-71.
- Hails, J. R., and Hoyt, J. H. (1968). "Barrier development on submerged coasts: Problems of sea-level changes from a study of the Atlantic coastal plain of Georgia, U.S.A. and parts of the east Australian coast," *Zeitschrift für Geomorphologie*, Suppl. 7, 24-55.
- Hallermier, R. J. (1981). "A profile zonation for seasonal sand beaches from wave climate," *Journal of Coastal Engineering* 4, 253-77.
- Hands, E. B. (1976). "Observations of barred coastal profiles under the influence of rising water levels, eastern Lake Michigan, 1967-71," Technical Report 76-1, U.S. Army Engineer Waterways Experiment Station, Coastal Engineering Research Center, Vicksburg, MS.
- Hands, E. B. (1980). "Prediction of shore retreat and nearshore profile adjustments to rising water levels on the Great Lakes," Technical Paper 80-7, U.S. Army Engineer Waterways Experiment Station, Coastal Engineering Research Center, Vicksburg, MS.
- Hansen, J., Johnson, D., Lacis, A., Lebedeff, S., Lee, P., Rind, D., and Russell, G. (1981). "Climate impact of increasing atmospheric carbon dioxide," *Science* 219, 996-97.
- Hansen, M., and Knowles, S. C. (1988). "Ebb-tidal delta response to jetty construction at three South Carolina inlets." *Lecture Notes on Coastal and Estuarine Studies. Symposium on Hydrodynamics and Sediment Dynamics of Tidal Inlets* 29. D. G. Aubrey and L. Weishar, ed., Springer-Verlag, New York, NY, 364-81.
- Hanson, H. (1987). "GENESIS, a generalized shoreline change model for engineering use," Report No. 1007, Department of Water Resources Engineering, University of Lund, Lund, Sweden.
- \_\_\_\_\_. (1989). "GENESIS, a generalized shoreline change numerical model," *Journal of Coastal Research* 5(1), 1-27.
- Hanson, H., and Kraus, N. C. (1989). "GENESIS, a generalized model for simulating shoreline change; Report 1: Reference," Technical Report CERC-89-19, U.S. Army Engineer Waterways Experiment Station, Coastal Engineering Research Center, Vicksburg, MS.
- \_\_\_\_\_. (1991). "Comparison of shoreline change obtained with physical and numerical models." *Proceedings Coastal Sediments '91*. American Society of Civil Engineers, New York, NY, 1785-1813.

- Harris, D. L. (1981). "Tides and tidal datums in the United States," Special Report No. 7, U.S. Army Engineer Waterways Experiment Station, Coastal Engineering Research Center, Vicksburg, MS.
- Hayes, M. O. (1975). "Morphology and sand accumulation in estuaries." *Estuarine Research*. L. E. Cronin, ed., Academic Press, New York, NY, 3-22.
- \_\_\_\_\_. (1977). "Development of Kiawah Island, South Carolina." *Proceedings Coastal Sediments '77*. American Society of Civil Engineers, New York, NY, 828-47.
- \_\_\_\_\_. (1979). "Barrier island morphology as a function of tidal and wave regime." *Barrier Islands: From the Gulf of St. Lawrence to the Gulf of Mexico*. S. P. Leatherman, ed., Academic Press, New York, NY.
- \_\_\_\_\_. (1980). "General morphology and sediment patterns in tidal inlets," *Sedimentary Geology* 26, 139-56.
- \_\_\_\_\_. (1991). "Geomorphology and sedimentation patterns of tidal inlets: A review," N. C. Kraus, K. J. Gingerich, and D. L. Kriebel, ed., *Proceedings Coastal Sediments '91*. American Society of Civil Engineers, New York, NY, 1343-55.
- Hayes, M. O., and Kana, T. W. (1976). "Terrigenous clastic depositional environments," Technical Report CRD-11, Department of Geology, University of South Carolina, Columbia, SC.
- Hayes, M. O., Goldsmith, V., and Hobbs III, C. H. (1970). "Offset coastal inlets." *Proceedings 12th Coastal Engineering Conference*, American Society of Civil Engineers, New York, NY, 1187-1200.
- Headland, J. R., Vallianos, L., and She'don, J. G. (1987). "Coastal processes at Wallops Island, Virginia." *Proceedings Coastal Sediments '87*. American Society of Civil Engineers, New York, NY, 1305-20.
- Henry, V. J., Jr., and Kellam, J. A. (1988). "Seismic investigation of the phosphate-bearing, Miocene-age strata of the continental shelf of Georgia," Bulletin 109, Georgia Geological Survey, Atlanta, GA.
- Herndon, J. G., and Cofer-Shabica, S. V. (1991). "Potential for seawater encroachment near Cumberland Island, GA." *Proceedings Coastal Zone '91, Biological and Physical Aspects of Dredging, Kings Bay, Georgia*. American Society of Civil Engineers, New York, NY, 88-102.
- Herrick, S. M., and Vorhis, R. C. (1963). "Subsurface geology of the Georgia coastal plain," Information Circular 25, Georgia Geological Survey, Atlanta, GA.
- Hillestad, H. O., Bozeman, J. R., Johnson, A. S., Berisford, C. W., and Richardson, J. I. (1975). "Ecology of the Cumberland Island National Seashore, Camden County, Georgia," Technical Report 75-5, Marine Science Center, Savannah, GA.

- Hosier, P. E., and Cleary, W. J. (1977). "Cyclic geomorphic patterns of washover on a barrier island in southeastern North Carolina," *Environmental Geology* 2, 23-31.
- Howard, J. D., DePratter, C. B., and Frey, R. W. (1980). "Physical and biogenic processes in Georgia estuaries; I, coastal setting and subtidal facies." *Sedimentary processes and animal-sediment relationships in tidal environments*. S. B. McCann, ed., 153-82.
- Hoyt, J. H., Henry, V. J., Jr., and Weimer, R. J. 1968. "Age of late-Pleistocene shoreline deposits, coastal Georgia," *Means of Correlation of Quaternary Successions* 8, Congress of International Association for Quaternary Research, 381-93.
- Hubbard, D. K., Barwis, J. H., and Nummedal, D. (1977). "Sediment transport in four South Carolina inlets." *Proceedings Coastal Sediments '77*. American Society of Civil Engineers, New York, NY, 734-53.
- Hubertz, J. M., Brooks, R. M., Brandon, W. A., and Tracy, B. A. (1992). "Hindcast wave information for the U.S. Atlantic Coast," WIS Report 30, U.S. Army Engineer Waterways Experiment Station, Coastal Engineering Research Center, Vicksburg, MS.
- Huddlestun, P. F. (1988). "A revision of the lithostratigraphic units of the coastal plain of Georgia: the Miocene through Holocene," Bulletin 104, Georgia Geological Survey, Atlanta, GA.
- Hunt, C. B. (1974). *Natural regions of the United States and Canada*. W. H. Freeman and Company, San Francisco, CA.
- Intergraph Corporation. (1992). "MGE/SX Reference Manual," Publication Number 0JA051180, Intergraph Corporation, Huntsville, AL.
- Jensen, R. E. (1983a). "Atlantic Coast hindcast, shallow-water significant wave information," WIS Report 9, U.S. Army Engineer Waterways Experiment Station, Hydraulics Laboratory, Vicksburg, MS.
- \_\_\_\_\_. (1983b). "Methodology for the calculation of a shallow-water wave climate," WIS Report 8, U.S. Army Engineer Waterways Experiment Station, Coastal Engineering Research Center, Vicksburg, MS.
- Kana, T. W. (1977). "Suspended sediment transport at Price Inlet, SC." *Proceedings Coastal Sediments '77*. American Society of Civil Engineers, New York, NY, 366-82.
- \_\_\_\_\_. (1989). "The South Carolina coast; I, natural processes and erosion." *Barrier islands: Process and management*. D. K. Stauble, ed., American Society of Civil Engineers, New York, NY.
- Kana, T. W., and Mason, J. E. (1988). "Evolution of an ebb-tidal delta after an inlet relocation." *Lecture Notes on Coastal and Estuarine Studies. Symposium on Hydrodynamics and Sediment Dynamics of Tidal Inlets* 29. D. G. Aubrey and L. Weishar, ed., Springer-Verlag, New York, NY, 382-411.

- Kellam, J. A., and Henry, V. J. (1986). "Interpretation of the seismic stratigraphy of the phosphatic middle Miocene on the Georgia continental shelf," Geological Atlas 4, Georgia Geological Survey, Atlanta, GA.
- Keulegan, G. H. (1948). "An experimental study of submarine sand bars," TR-3, Beach Erosion Board, Washington, DC.
- King, C. A. M. (1972). *Beaches and coasts*. St. Martins Press, New York, NY.
- Knowles, S. C., and Gorman, L. T. (1991). "Historical coastal morphodynamics at St. Marys entrance and vicinity, Florida, U.S.A." *Proceedings Coastal Sediments '91*. American Society of Civil Engineers, New York, NY, 1447-61.
- Komar, P. D., and Inman, D. L. (1970). "Longshore sand transport on beaches," *Journal of Geophysical Research* 75(30), 5914-27.
- Korte, G. B. (1991). *GIS 1991: A practitioner's handbook*. Design Strategies, Chamisal, NM.
- Kraus, N. C. (1989). "Beach change modeling and the coastal planning process." *Proceedings Coastal Zone '89*. American Society of Civil Engineers, New York, NY, 553-67.
- Kraus, N. C., and Harikai, S. (1983). "Numerical model of the shoreline change at Oarai Beach." *Coastal Engineering* 7(1), 1-28.
- Kraus, N. C., Isobe, M., Igarashi, H., Sasaki, T., and Horikawa, K. (1982). "Field experiments on longshore sand transport in the surf zone." *Proceedings 18th Coastal Engineering Conference*. American Society of Civil Engineers, 969-88.
- Kraus, N. C., Scheffner, N. W., Chou, L. W., Cialone, M. A., Smith, J. M., and Hardy, T. A. (1988). "Coastal processes at Sea Bright to Ocean Township, New Jersey, Volume 1: Main text and Appendix A," Miscellaneous Paper CEK-88-12, U.S. Army Engineer Waterways Experiment Station, Coastal Engineering Research Center, Vicksburg, MS.
- Kruczynski, L. R., and Lange, A. F. (1990). "Geographic information systems and the GPS Pathfinder System: Differential accuracy of point location data," Trimble Navigation Study Report, Sunnyvale, CA, 7 pp.
- Lai, R. J., Lee, W. T., and Silver, A. L. (1988). "Nearshore wave climatology at Kings Bay, Georgia, and Cape Canaveral, Florida," DTRC/SHD-1190-03, David Taylor Research Center, Bethesda, MD.
- Langfelder, L. J., Stafford, D. B., and Amein, M. (1970). "Coastal erosion in North Carolina," *Journal of Waterways and Harbors Division* 96(WW2), American Society of Civil Engineers, New York, NY, 531-45.

- Larson, M., and Kraus, N. C. (1989). "SBEACH: Numerical model for simulating storm-induced beach change," Technical Report CERC-89-9, U.S. Army Engineer Waterways Experiment Station, Coastal Engineering Research Center, Vicksburg, MS.
- Larson, M., Kraus, N. C., and Byrnes, M. R. (1990). "SBEACH: Numerical modeling for simulating storm-induced beach change," Technical Report CERC-89-9, U.S. Army Engineer Waterways Experiment Station, Coastal Engineering Research Center, Vicksburg, MS.
- Leatherman, S. P. (1979). "Migration of Assateague Island, Maryland, by inlet and overwash processes," *Geology* 7, 104-07.
- \_\_\_\_\_. (1983a). "Barrier dynamics and landward migration with Holocene sea level rise," *Nature* 301(5899), 415-18.
- \_\_\_\_\_. (1983b). "Shoreline mapping: A comparison of techniques," *Shore and Beach* 51, 28-33.
- \_\_\_\_\_. (1984). "Shoreline evolution of north Assateague Island, Maryland," *Shore and Beach* 52, 3-10.
- Leenknecht, D. A., Szuwalski, A., and Sherlock, A. R. (1992). "Automated coastal engineering system, user's guide," U.S. Army Engineer Waterways Experiment Station, Coastal Engineering Research Center, Vicksburg, MS.
- Leick, A. (1990). *GPS satellite surveying*. John Wiley and Sons, New York, NY.
- Leve, G. W. (1961). "Reconnaissance of the ground water resources of the Fernandina area, Nassau County, Florida," Information Circular 28, Florida Geological Survey, Tallahassee, FL.
- \_\_\_\_\_. (1966). "Ground water in Duval and Nassau Counties, Florida," Report of Investigation 43, Florida Geological Survey, Tallahassee, FL.
- Lewis, D. W. (1984). *Practical sedimentology*. Hutchinson Ross Publishing Company, Stroudsburg, PA, 68-79.
- Lillycrop, W. J., Garcia, A. W., Howell, G. L., and Grogg, W. E. (1991). "An automated real time tidal elevation system for offshore dredging operations." *Tidal hydrodynamics*. B. B. Parker, ed., John Wiley and Sons, New York, NY.
- Lisitzin, E. (1974). *Sea level changes*. Elsevier, NY.
- List, J. H., Jaffe, B. E., and Sallenger, A. H. (1991). "Large-scale coastal evolution of Louisiana's barrier islands." *Coastal Sediments '91*. N. C. Kraus, K. J. Gingerich, and D. L. Kriebel, ed., American Society of Civil Engineers, New York, NY, 1532-46.

- Longuet-Higgins, M. S., Cartwright, D. E., and Smith, N. D. (1963). "Observations of the directional spectrum of sea waves using the motions of a floating buoy." *Ocean wave spectra*. Prentice-Hall, Englewood Cliffs, NJ, 111-36.
- Lyles, S. D., Hickman, L. E., Jr., and Debaugh, H. A., Jr. (1988). *Sea level variations for the United States 1855-1986*. U.S. Dept. of Commerce, National Oceanic and Atmospheric Administration, Rockville, MD.
- Marino, J. N., and Mehta, A. J. (1988). "Sediment trapping at Florida's East Coast inlets." *Lecture Notes on Coastal and Estuarine Studies. Symposium on Hydrodynamics and Sediment Dynamics of Tidal Inlets* 29. D. G. Aubrey and L. Weishar, ed., Springer-Verlag, New York, NY, 284-96.
- Markewich, H. W., Hacke, C. M., and Huddleston, P. F. (1992). "Emergent Pliocene sediments of southeastern Georgia: An anomalous, fossil-poor, clastic section," *Quaternary Coasts of the United States: Marine and Lacustrine Systems*, Society of Sedimentary Geology Special Publication No. 48, 173-89.
- Martens, J. H. C. (1935). "Beach sands between Charleston, South Carolina, and Miami, Florida," *Bulletin of the Geological Society of America* 48, 1563-96.
- McBride, R. A. (1989). "Accurate computer mapping of coastal change: Bayou Lafourche shoreline, Louisiana, USA." *Proceedings Coastal Zone '89*. American Society of Civil Engineers, New York, NY, 707-19.
- McBride, R. A., and Moslow, T. F. (1991). "Origin, evolution, and distribution of shoreface sand ridges, Atlantic inner shelf, U.S.A.," *Marine Geology* 97, 57-85.
- McBride, R. A., Hiland, M. W., Penland, S., Williams, S. J., Byrnes, M. R., Westphal, K. A., Jaffe, B., and Sallenger, Jr., A. H. (1991). "Mapping barrier island changes in Louisiana: Techniques, accuracy, and results." *Proceedings Coastal Sediments '91*. American Society of Civil Engineers, New York, NY, 1011-26.
- McLemore, W. H., Swann, C. T., Wigley, P. B., Turlington, M. C., Henry, V. J., Nash, G. J., Martinez, J., Carver, R. E., and Thurmon, J. T. (1981). "Geology as applied to land-use management on Cumberland Island, Georgia," Georgia Geological Survey, Atlanta, GA.
- Meisburger, E. P., and Field, M. E. (1975). "Geomorphology, shallow structure, and sediments of the Florida inner continental shelf, Cape Canaveral to Georgia," Technical Report 54, U.S. Army Engineer Waterways Experiment Station, Coastal Engineering Research Center, Vicksburg, MS.
- Merchant, D. C. (1987). "Spatial accuracy specification for large scale topographic maps," *Photogrammetric Engineering and Remote Sensing* 53, 958-61.
- Milliman, J. E., Pilkey, O. H., and Ross, D. A. (1972). "Sediments of the continental margin off the eastern United States," *Bulletin of the Geological Society America* 83, 1315-34.

- Moody, D. W. (1964). "Coastal morphology and processes in relation to the development of submarine sand ridges off Bethany Beach, Delaware," Ph.D. diss., Johns Hopkins University, Baltimore, MD.
- Moore, B. (1982). "Beach profile evolution in response to changes in water level and wave height," M.S. thesis, Department of Civil Engineering, University of Delaware, Newark, DE.
- Morgan, J. G. (1987). "The North American datum of 1983." *Geophysics: The leading edge of exploration*. 27-33.
- Morgan, J. P., and Larimore, P. B. (1957). "Changes in the Louisiana shoreline," *Transactions, Gulf Coast Association of Geological Societies* 7, 303-10.
- Morton, R. A. (1979). "Temporal and spatial variations in shoreline changes and their implications, examples from the Texas Gulf Coast," *Journal of Sedimentary Petrology* 49, 1101-12.
- Nash, G. J. (1977). "Historical changes in the mean high water shorelines and nearshore bathymetry of south Georgia and north Florida," unpublished M.S. thesis, University of Georgia, Athens, GA.
- National Academy of Sciences. (1971). *North American datum*. National Geodetic Information Center, National Oceanic and Atmospheric Administration, Rockville, MD.
- National Oceanic and Atmospheric Administration. (1976). "Climate of Fernandina Beach, Florida," *Climatology of the United States* 20, National Climatic Center, Asheville, NC.
- \_\_\_\_\_. (1982). "Monthly normals of temperature, precipitation, and heating and cooling degree days 1951-80," *Climatology of the United States* 18, U.S. Department of Commerce, National Climatic Center, Asheville, NC.
- \_\_\_\_\_. (1987a). "Climatological data annual summary, Florida," 91(13), U.S. Department of Commerce, National Climatic Center, Asheville, NC.
- \_\_\_\_\_. (1987b). "Tropical cyclones of the North Atlantic Ocean, 1871-1987," U.S. Department of Commerce, National Climatic Center, Asheville, NC.
- \_\_\_\_\_. (1991a). "Tidal current tables 1988, Atlantic coast of North America," U.S. Department of Commerce, Rockville, MD.
- \_\_\_\_\_. (1991b). "Tide tables 1992, high and low water predictions; East coast of North and South America," U.S. Department of Commerce, Rockville, MD.
- National Research Council. (1987). *Responding to changes in sea level; engineering implications*. National Academy Press, Washington, DC.

- Nummedal, D., Oertel, G. F., Hubbard, D. K., and Hine, A. C. (1977). "Tidal inlet variability: Cape Hatteras to Cape Canaveral." *Proceedings Coastal Sediments '77*. American Society of Civil Engineers, New York, NY, 543-62.
- Oertel, G. F. (1988). "Processes of sediment exchange between tidal inlets, ebb deltas, and barrier islands." *Lecture Notes on Coastal and Estuarine Studies. Symposium on Hydrodynamics and Sediment Dynamics of Tidal Inlets* 29. D. G. Aubrey and L. Weishar, ed., Springer-Verlag, New York, NY.
- Oertel, G. F., and Howard, J. D. (1972). "Water circulation and sedimentation at estuary entrances on the Georgia coast." *Shelf sediment transport*. D. J. P. Swift, D. P. Duane, and O. H. Pilkey, ed., Dowden, Hutchinson, and Ross, Inc., Stroudsburg, PA, 411-27.
- Olsen Associates, Inc. (1990). "Feasibility study for comprehensive beach and dune preservation, Amelia Plantation, Amelia Island, Florida." Submitted to Amelia Island Plantation Community Association, Jacksonville, FL.
- Olsen, E. J. (1977). "A study of effects of inlet stabilization at St. Marys Entrance, Florida." *Proceedings Coastal Sediments '77*. American Society of Civil Engineers, New York, NY, 616-31.
- Parchure, T. M. (1982). "St. Marys Entrance: Glossary of inlets," Report No. 11, University of Florida, Department of Coastal and Oceanographic Engineering, Gainesville, FL.
- Pierce, J. W. (1969). "Sediment budget along a barrier island chain," *Journal of Sedimentary Geology* 3, 5-16.
- Pilkey, O. H., and Field, M. E. (1972). "Offshore transport of the continental shelf sediment, Atlantic Southeastern United States." *Shelf sediment transport*. Dowden, Hutchinson and Ross, Stroudsburg, PA.
- Pilkey, O. H., Blackwelder, B. W., Doyle, L. J., Estes, E., and Terlecky, P. M. (1969). "Aspects of carbonate sedimentation on the Atlantic Continental Shelf off the southern United States," *Journal of Sedimentary Petrology* 39(2), 744-68.
- Pope, J. (1991). "Ebb delta and shoreline response to inlet stabilization, examples from the southeast Atlantic Coast." *Proceedings Coastal Zone '91, Biological and Physical Aspects of Dredging, Kings Bay, Georgia*. American Society of Civil Engineers, New York, NY, 157-68.
- Radtke, D. B. (1985). "Sediment sources and transport in Kings Bay and vicinity, Georgia and Florida, July 8-16, 1982," Professional Paper No. 1347, U.S. Geological Survey, Washington, DC.
- Redfield, A. C. (1967). "Postglacial change in sea level in the western North Atlantic Ocean," *Science* 157, 687-92.

- Resio, D. T. (1987). "Shallow-water waves; I, theory," *Journal of Waterways, Port, Coastal, and Ocean Engineering* 113(3), American Society of Civil Engineers, New York, NY, 264-81.
- \_\_\_\_\_. (1988a). "A steady-state wave model for coastal applications." *Proceedings 21st Coastal Engineering Conference* 114(1). American Society of Civil Engineers, New York, NY, 929-40.
- \_\_\_\_\_. (1988b). "Shallow-water waves; II, Data comparisons," *Journal of Waterways, Port, Coastal, and Ocean Engineering* 114(1), American Society of Civil Engineers, New York, NY, 50-65.
- \_\_\_\_\_. (1993). "Program STWAVE: Wave propagation simulation theory, testing, and application," draft report, U.S. Army Engineering Waterways Experiment Station, Coastal Engineering Research Center, Vicksburg, MS.
- Richards, D. R., and Clausner, J. E. (1988). "Feasibility of sand bypassing systems for reducing maintenance dredging in the St. Marys River Entrance channel, Florida," Miscellaneous Paper HL-88-9, U.S. Army Engineer Waterways Experiment Station, Hydraulics Laboratory, Vicksburg, MS.
- Roberts, J. W. (1975). "Geologic evolution of the south end of Cumberland Island, Georgia," unpublished M.S. thesis, Smith College, North Hampton, MA.
- Sargent, F. E. (1988). "Case histories of Corps breakwater and jetty structures; Report 2, South Atlantic Division," Technical Report REMR-CO-3, U.S. Army Engineer Waterways Experiment Station, Coastal Engineering Research Center, Vicksburg, MS.
- Savage, R. J. (1991). "Predicted storm probabilities and dune erosion." *Proceedings Fourth Annual National Beach Preservation Technology Conference, preserving and enhancing our beach environment*. Tallahassee, FL, 355-67.
- Savage, R. J., and Birkemeier, W. A. (1987). Storm erosion data from the U.S. Atlantic Coast. *Proceedings Coastal Sediments '87*. American Society of Civil Engineers, New York, NY, 1445-59.
- Scheffner, N. W. (1989). "Dune erosion-frequency of storm occurrence relationships." *Proceedings Coastal Zone '89*. American Society of Civil Engineers, New York, NY, 596-606.
- Scholl, D. W., and Stuvier, M. (1967). "Recent submergence of southern Florida: A comparison with adjacent coasts and other eustatic data," *Bulletin of the Geological Society of America* 78, 437-54.
- Shalowitz, A. L. (1964). "Shoreline and sea boundaries," U.S. Department of Commerce Publication 10-1, U.S. Coast and Geodetic Survey, U.S. Government Printing Office, Washington, DC.

- Shore protection manual (SPM)*. (1984). 4th ed., 2 Vol, U.S. Army Engineer Waterways Experiment Station, Coastal Engineering Research Center, U.S. Government Printing Office, Washington, DC.
- Short, A. D. (1991). "Macro-meso tidal beach morphodynamics - an overview," *Journal of Coastal Research* 7(2), 417-36.
- Shows, E. W. (1978). "Florida's coastal setback line - an effort to regulate beach front development," *Journal of Coastal Zone Management* 4(1/2), 151-64.
- Smith, J. M., and Vincent, C. L. (1992). "Shoaling and decay of two wave trains on a beach," *Journal of Waterway, Port, Coastal and Ocean Engineering* 118(5).
- Snyder, J. P. (1987). "Map Projections - a working manual," Professional Paper No. 1395, U.S. Geological Survey, U.S. Government Printing Office, Washington, DC.
- Stafford, D. B., and Langfelder, J. (1971). "Air photo survey of coastal erosion," *Journal of Photogrammetric Engineering* 35, 565-75.
- Stauble, D. K., and Hoel, J. (1986). "Guidelines for beach restoration projects; Part II, Engineering," SGR-77, Florida Sea Grant College, Gainesville, FL.
- Stauble, D. K., and Warnke, D. A. (1974). "The bathymetry and sedimentation of Cape San Blas shoals and shelf off St. Joseph Spit, Florida," *Journal of Sedimentary Petrology* 44, 1037-51.
- Stauble, D. K., Pitchford, K. R., Livingston, C., and Gorman, L. T. "Shoreline change analysis and sediment distributions: Glynn County," Georgia Beach Erosion Control and Hurricane Flooding Damage Reduction Project, in preparation, U.S. Army Engineer Waterways Experiment Station, Coastal Engineering Research Center, Vicksburg, MS.
- Steele, K. E., Lau, J. C., and Hsu, Y. L. (1985). "Theory and application of calibration techniques for an NDBC directional wave measurements buoy," *Journal of Oceanic Engineering* OE-10(4), Institute of Electrical and Electronic Engineers, 382-94.
- Steele, K. E., Wang, D. W., Teng, C., and Lang, N. C. (1990). "Directional wave measurements with NDBC 3-meter discus buoys," U.S. Department of Commerce, National Oceanic and Atmospheric Administration, National Data Buoy Center, Stennis Space Center, MS.
- Stevenson, J. C., Ward, L. G., and Kearney, M. S. (1986). "Vertical accretion in marshes with varying rates of sea level rise." *Estuarine variability*. Academic Press, New York, NY, 233-65.
- Stringfield, V. T. (1966). "Artesian water in Tertiary limestone in the Southeastern States," Professional Paper No. 517, U.S. Geological Survey, Washington, DC.
- Swinburne, S. R. (1981). "Cumberland Island - a walk across a barrier island," *Underwater Naturalist* 13(2).

- Tanner, W. F., ed. (1978). "Standards for measuring shoreline changes: A study of the precision obtainable and needed in making measurements of changes (erosion and accretion)." *Proceedings of a workshop*. Florida State University, Tallahassee, FL.
- U.S. Army Corps of Engineers. (1948). "Fernandina Harbor, Florida." House Document No. 662, 80th Congress, 2nd Session, U.S. Government Printing Office, Washington, DC.
- \_\_\_\_\_. (1961). "Amelia Island, Florida, beach erosion control study." House Document No. 200, 87th Congress, 1st Session, U.S. Government Printing Office, Washington, DC.
- \_\_\_\_\_. (1991). "Hydrographic surveying," Engineer Manual 1110-2-1003, Washington, DC.
- U.S. Army Engineer District, Jacksonville. (1984a). "Feasibility report with environmental impact statement for beach erosion control Nassau County, Florida," (Amelia Island), Jacksonville, FL.
- \_\_\_\_\_. (1984b). "Section 103, detailed project report, Fort Clinch, Nassau County, Florida," Jacksonville, FL.
- \_\_\_\_\_. (1993). "Nassau County, Florida, Fernandina Harbor, section 933 study," Jacksonville, FL.
- U.S. Army Engineer Waterways Experiment Station. (1960). "The Unified Soil Classification System," Technical Memorandum 3-357, reprinted 1967, 1976, 1980, Vicksburg, MS.
- U.S. Coast and Geodetic Survey. (1957). *Horizontal control data 15*. Special Publication No. 227, Washington, DC.
- \_\_\_\_\_. (1985). "Datum differences - Atlantic, Gulf, and Pacific Coasts, United States," Washington, DC.
- U.S. Department of the Army. (1970). "Geodetic and topographic surveying," Technical Manual 5-441, Washington, DC.
- U.S. Department of the Interior, U.S. Geological Survey. (1978). *Coastal mapping handbook*. M. Y. Ellis, ed., U.S. Department of Commerce, National Ocean Service, U.S. Government Printing Office, Washington, DC.
- U.S. Study Commission, Southeast River Basins. (1963). "Plan for development of the land and water resources of the Southeast River Basins, Appendix 4, Satilla-St. Marys Basins." United States Study Commission Southeast River Basins, Atlanta, GA.
- Vemulakonda, S. R., and Scheffner, N. W. (1987). "Application of CIP modeling to St. Marys Inlet, Florida." *Proceedings Coastal Zone '87*. American Society of Civil Engineers, New York, NY, 616-31.

- Vemulakonda, S. R., Scheffner, N. W., Earickson, J. A., and Chou, L. W. (1988). "Kings Bay coastal processes numerical model," Technical Report CERC-88-3, U.S. Army Engineer Waterways Experiment Station, Coastal Engineering Research Center, Vicksburg, MS.
- Vincent, C. L., and Lichy, D. E. (1981). "Wave measurement in ARSLOE." *Proceedings Conference on Directional Wave Spectra Applications*. American Society of Civil Engineers, 71-85.
- Wade, E. B. (1986). "Impact of North American datum of 1983," *Journal of Surveying Engineering* 112(1), 49-62.
- Walton, T. L., and Adams, W. D. (1976). Capacity of inlet outer bars to store sand. *Proceedings 15th Coastal Engineering Conference*. American Society of Civil Engineers, New York, NY, 1919-37.
- Weimer, R. J., and Hoyt, John H. 1964. "Burrows of *Callianassa major* say, (McIntosh County) geologic indications of littoral and shallow neretic environments," *Journal of Paleontology* 38(4), 761-67.
- Wilson, S. K., Rose, S., and Cofer-Shabica, S. V. (1991). "Hydrogeochemistry of Southern Cumberland Island, GA." *Proceedings Coastal Zone '91, Biological and Physical Aspects of Dredging, Kings Bay, Georgia*. American Society of Civil Engineers, New York, NY, 103-17.
- Woolsey, J. R. (1977). "Neogene stratigraphy of the Georgia coast and inner continental shelf," Ph.D. diss , University of Georgia, Athens, GA.
- Wright, L. D., and Short, A. D. (1983). "Morphodynamics of beaches and surf zones in Australia." *Handbook of coastal processes and erosion*. CRC Press, Boca Raton, FL, 35-64.

# Appendix A

## Notation

---

$a$	Semimajor axis of the earth, m
$a_1$	Longshore sand transport parameter (contains $K_1$ ; see below)
$a_2$	Longshore sand transport parameter (contains $K_2$ ; see below)
$A$	Equilibrium profile shape parameter, $m^{1/3}$
$b$	Semiminor axis of the earth, m
$b$	Subscript denoting condition at wave breaking
$C_{gb}$	Wave group speed at breaking, m/sec
$d_i$	Seaward limiting depth for initiation of sand
$d_l$	Seaward limiting depth for significant sand transport, m
$d_{50}$	Median sand grain size, mm
$D_B$	Average berm height, m
$D_c$	Depth of closure
$f$	Flattening ratio (used in cartographic calculations)
$g$	Acceleration due to gravity, $m/sec^2$
$H$	Wave height, m
$H_b$	Breaking wave height, m
$H_{m0}$	Zero-moment spectral wave height
$i$	Subscript denoting grid cell number
$K_1$	Longshore transport rate calibration parameter
$K_2$	Longshore transport rate calibration parameter
$n$	Number controlling wave directional spreading
$Q$	Longshore sand transport rate, $m^3/sec$
$t$	Time, sec
$T_p$	Spectral peak wave period, sec
$x$	Longshore coordinate, m
$y$	Shoreline position, m
$\tan\beta$	Average nearshore bottom slope, deg
$\gamma$	Wave breaking proportionality constant

$\Delta y$	Change in shoreline position, m
$\theta$	Angle of wave crest to depth contour, deg
$\theta_b$	Angle of breaking wave crests to x-axis, deg
$\theta_{br}$	Angle of breaking wave crests to the shoreline, deg
$\rho$	Density of water, kg/m <sup>3</sup>
$\rho_s$	Density of sediment, kg/m <sup>3</sup>
$\phi$	Phi

REPORT DOCUMENTATION PAGE			Form Approved OMB No. 0704-0188	
<small>Public reporting burden for this collection of information is estimated to average 1 hour per response, including the time for reviewing instructions, searching existing data sources, gathering and maintaining the data needed, and completing and reviewing the collection of information. Send comments regarding this burden estimate or any other aspect of this collection of information, including suggestions for reducing this burden, to Washington Headquarters Services, Directorate for Information Operations and Reports, 1215 Jefferson Davis Highway, Suite 1204, Arlington, VA 22202-4302, and to the Office of Management and Budget, Paperwork Reduction Project (0704-0188), Washington, DC 20503.</small>				
1. AGENCY USE ONLY (Leave blank)		2. REPORT DATE August 1994		3. REPORT TYPE AND DATES COVERED Final report
4. TITLE AND SUBTITLE Kings Bay Coastal and Estuarine Physical Monitoring and Evaluation Program: Coastal Studies; Volume I: Main Text and Appendix A			5. FUNDING NUMBERS	
6. AUTHOR(S) Nicholas C. Kraus, Laurel T. Gorman, Joan Pope				
7. PERFORMING ORGANIZATION NAME(S) AND ADDRESS(ES) U.S. Army Engineer Waterways Experiment Station 3909 Halls Ferry Road, Vicksburg, MS 39180-6199			8. PERFORMING ORGANIZATION REPORT NUMBER  Technical Report CERC-94-9	
9. SPONSORING / MONITORING AGENCY NAME(S) AND ADDRESS(ES)  Office of the Chief of Naval Operations Alexandria, VA 22332			10. SPONSORING / MONITORING AGENCY REPORT NUMBER	
11. SUPPLEMENTARY NOTES Available from National Technical Information Service, 5285 Port Royal Road, Springfield, VA 22161.				
12a. DISTRIBUTION / AVAILABILITY STATEMENT  Approved for public release; distribution is unlimited.			12b. DISTRIBUTION CODE	
13. ABSTRACT (Maximum 200 words)  <p>The objective of this study was to assess the impacts of U.S. Navy-sponsored navigation channel modification and maintenance activities conducted from 1985-1992 on the shoreline in the vicinity of the traditionally called St. Marys Entrance. This inlet, separating Cumberland Island, Georgia, to the north and Amelia Island, Florida, to the south contains a large estuary, a commercial and recreational port, Fernandina Harbor, Florida, and, since the 1970s, a U.S. Navy submarine base located at Kings Bay, Georgia. A study of the coastal area included the following components:</p> <ul style="list-style-type: none"> <li>a. Review of historical data and previous studies.</li> <li>b. Numerical simulation of waves and shoreline change.</li> <li>c. Monitoring of waves, water level, shoreline position, beach profile and sediments, and ebb-tidal bathymetry over the period 1988-1992.</li> </ul> <p>No adverse impact on the beaches of Cumberland Island and Amelia Island by U.S. Navy navigation channel modification and maintenance at St. Marys Entrance could be detected in any of the analyses or monitoring performed in this study.</p>				
14. SUBJECT TERMS  See reverse.			15. NUMBER OF PAGES 310	
			16. PRICE CODE	
17. SECURITY CLASSIFICATION OF REPORT  UNCLASSIFIED	18. SECURITY CLASSIFICATION OF THIS PAGE  UNCLASSIFIED	19. SECURITY CLASSIFICATION OF ABSTRACT	20. LIMITATION OF ABSTRACT	

**14. (Concluded).**

**Amelia Island  
Channel deepening  
Coastal monitoring**

**Coastal surveying  
Kings Bay  
Navigation impacts**

**Shoreline change  
St. Marys**